PL-TR-96-2038
Special Reports, No. 277

PROCEEDINGS OF AIR FORCE OFFICE OF SCIENTIFIC RESEARCH AND PHILLIPS LABORATORY WORKSHOP ON SPRITES AND BLUE JETS

Editor:
L. Jeong

30 January 1996

APPROVED FOR PUBLIC RELEASE; DISTRIBUTION UNLIMITED

19960220 077



PHILLIPS LABORATORY
Directorate of Geophysics
AIR FORCE MATERIEL COMMAND
HANSCOM AFB, MA 01731-3010

"This technical report has been reviewed and is approved for publication"

Dr. WILLIAM A.M. BLUMBERG, Chief
Simulation Branch
Optical Environment Division

Dr. ROGER A. VAN TASSEL, Director
Optical Environment Division

This report has been reviewed by the ESC Public Affairs Office (PA) and is releasable to the National Technical Information Service (NTIS).

Qualified requesters may obtain additional copies from the Defense Technical Information Center (DTIC). All others should apply to the National Technical Information Service (NTIS).

If your address has changed, if you wish to be removed from the mailing list, or if the addressee is no longer employed by your organization, please notify PL/IM, 29 Randolph Road, Hanscom AFB, MA 01731-3010. This will assist us in maintaining a current mailing list.

Do not return copies of this report unless contractual obligations or notices on a specific document require that it be returned.

REPORT DOCUMENTATION PAGE

Form Approved
OMB No. 0704-0188

Public reporting burden for this collection of information is estimated to average 1 hour per response, including the time for reviewing instructions, searching existing data sources, gathering and maintaining the data needed, and completing and reviewing the collection of information. Send comments regarding this burden estimate or any other aspect of this collection of information, including suggestions for reducing this burden, to Washington Headquarters Services, Directorate for Information Operations and Reports, 1215 Jefferson Davis Highway, Suite 1204, Arlington, VA 22202-4302, and to the Office of Management and Budget, Paperwork Reduction Project (0704-0188), Washington, DC 20503.

1. AGENCY USE ONLY *(Leave blank)*	2. REPORT DATE	3. REPORT TYPE AND DATES COVERED
	30 January 1996	Scientific Interim

4. TITLE AND SUBTITLE
Proceedings of Air Force Office of Scientific Research and Phillips Laboratory Workshop on Sprites and Blue Jets

5. FUNDING NUMBERS
PR 3054
TA GD
WU 01

6. AUTHOR(S)
Editor, L.S. Jeong

7. PERFORMING ORGANIZATION NAME(S) AND ADDRESS(ES)
Phillips Laboratory/GPOS
Geophysics Directorate
29 Randolph Road
Hanscom AFB, MA 01731-3010

8. PERFORMING ORGANIZATION REPORT NUMBER
PL-TR-96-2038
SR, No. 277

9. SPONSORING/MONITORING AGENCY NAME(S) AND ADDRESS(ES)

10. SPONSORING/MONITORING AGENCY REPORT NUMBER

11. SUPPLEMENTARY NOTES

12a. DISTRIBUTION/AVAILABILITY STATEMENT
Approved for public release; distribution unlimited

12b. DISTRIBUTION CODE

13. ABSTRACT *(Maximum 200 words)*

This report contains the viewgraphs presented at the AFOSR-PL Workshop on Sprites and Blue Jets held at the Phillips Laboratory, Geophysics Directorate, Hanscom AFB, MA, 18-19 October 1995.

14. SUBJECT TERMS
Blue Jets; High-Altitude Discharges; Sprites; Upward Lightning

15. NUMBER OF PAGES
412

16. PRICE CODE

17. SECURITY CLASSIFICATION OF REPORT	18. SECURITY CLASSIFICATION OF THIS PAGE	19. SECURITY CLASSIFICATION OF ABSTRACT	20. LIMITATION OF ABSTRACT
UNCLASSIFIED	UNCLASSIFIED	UNCLASSIFIED	SAR

Air Force Office of Scientific Research
and
Phillips Laboratory
Workshop on Sprites and Blue Jets
18-19 October 1995
Hanscom Air Force Base, MA

Agenda

Wednesday, 18 October

8:30 AM - 8:40 AM Welcome
Dr. Herb Carlson, Deputy Chief Scientist
Geophysics Directorate, Phillips Laboratory

8:40 AM - 8:50 AM Opening Remarks
Major J. Kroll, AFOSR
L. Jeong, Phillips Laboratory

8:50 AM - 9:10 AM The Colorado SPRITES '95 Campaign: Initial Results
W.A. Lyons, ASTER Division, Mission Research Corp.

9:10 AM - 9:30 AM Red Sprite and Blue Jet Campaigns of the University of Alaska
D. Sentman and E. Westcott, University of Alaska

9:30 AM - 9:50 AM Spectral and Spatial Properties of Sprites
S.B. Mende, Lockheed Martin Palo Alto Research Laboratory

9:50 AM - 10:05 AM Evidence for Ionization in Sprites - N_2^+ 427.8 First Negative Emission Measured in SPRITES '95 Campaign
R.A. Armstrong and J. Shorter, Mission Research Corp.
W.A. Lyons, ASTER Division, Mission Research Corp.

10:05 AM -10:20 AM Fast Imaging of High Altitude Atmospheric Flashes (Sprites)
J.D. Molitoris, Lawrence Livermore National Laboratory
J.F. Arens, University of CA Berkeley
C. Price, Tel Aviv University
W. Lyons, ASTER Division, Mission Research Corp.

10:20 AM - 10:40 AM Break

10:40 AM - 10:50 AM Short Wavelength Infrared Images of Sprites
P.A. Bernhardt and J.A. Antoniades, Naval Research Laboratory

10:50 AM - 11:05 AM Topside Views of Lightning and Sprites
W.L. Boeck, Niagara University
O.H. Vaughan, Jr. and R. Blakeslee, NASA Marshall Space Flight Center

11:05 AM - 11:20 AM Observations of Electric Field and X-Rays Above Thunderstorms: Relevant to Optical Sprites?
K.B. Eack, W.H. Beasley, and M. Stolzenburg, University of Oklahoma
W.D. Rust, National Severe Storms Laboratory
T.C. Marshall, University of Mississippi

11:20 AM - 11:30 AM US/Russian Joint Lightning Experiments
S. Voss and E. Symbalisty, Los Alamos National Laboratory

11:30 AM - 11:40 AM Measurements of Lightning-Generated Electric Fields in the Nighttime D-Region
C.L. Siefring, Naval Research Laboratory

11:40 AM - 12:00 AM Space-Borne Observations of Intense Gamma-Ray Flashes Above Thunderstorms
G.J. Fishman, NASA Space Flight Center

12:00 AM - 1:00 PM Lunch

1:00 PM - 1:15 PM Electromagnetic Fields of Red Sprites
L.Hale and L. Marshall, Penn State University

1:15 PM - 1:35 PM Mesoscale Origin of Sprites and Schumann Resonance Methods for their Location on a Global Scale
E. Williams, Massachusetts Institute of Technology

1:35 PM - 1:55 PM Sprites, Blue Jets, and High Altitude Optical Flashes Produced by Quasi-Electrostatic Thundercloud Fields and Lightning EMP
U.S. Inan, Stanford University

1:55 PM - 2:05 PM VLF Observations of the Ionospheric Effects of Lightning in East Coast Summer Storms
J.V. Rodriguez and K.M. Groves, Phillips Laboratory

2:05 PM - 2:25 PM Measurements of Sprites and Blue Jets with High-Frequency Diagnostics
F. T. Djuth, Geospace Research Inc.

2:25 PM - 2:40 PM RF Measurements of Lightning-Induced Ionospheric Effects
K.M. Groves, J.V. Rodrriguez, P.J. Erickson, J.M. Quinn, T. Arce, and M. Cox, Phillips Laboratory

2:40 PM - 3:00 PM Break

3:00 PM - 3:15 PM Pulsed Radar Investigations of Red Sprites
R.T.Tsunoda, SRI International

3:15 PM - 3:35 PM On Runaway Breakdown and Upward Propagating Discharges
R. Roussel-Dupre and Y. Taranenko, Los Alamos National Laboratory
A.V. Gurevich, Lebedev Institute of Physics

3:35 PM - 3:50 PM Numerical Simulations of Lower Ionospheric Breakdown Caused by Lightning-Generated Electric Fields
H.L. Rowland, R.F. Fernsler, C.L. Siefring, and P.A. Bernhardt, Naval Research Laboratory

3:50 PM - 4:00 PM Runaway Breakdown in the Presence of a Magnetic Field
G.M. Milikh, K. Papadopoulos, and J. Valdivia, University of Maryland
A.V. Gurevich, Lebedev Institute of Physics

4:00 PM - 4:10 PM On the Fine Structure of the Red Sprites
K. Papadopoulos, G.M. Milikh, and J. Valdivia, University of Maryland

4:10 PM - 4:30 PM Nonequilibrium Infrared Radiative Modeling - Application to Sprites
R.H. Picard, J.R. Winick, Phillips Laboratory
P.P. Wintersteiner, ARCON Corp.
R.A. Armstrong and J. Shorter, Mission Research Corp.

Thursday, 19 October

8:30 AM - 9:00 AM Overview of Air Force Program Plans
Major J. Kroll, AFOSR
L. Jeong, Phillips Laboratory

9:00 AM - 9:30 AM Overview of NASA Sprite Activities
R. Howard, NASA Headquarters

9:30 AM - 10:00 AM Overview of Air Force ARES Aircraft Program
P. Kupferman, Aerospace Corp.

10:00 AM - 12:00 AM Summary and Discussion of Major Research Issues

12:00 AM - 1:00 PM Lunch

1:00 PM - 5:00 PM	Discussion of Major Research Issues (continued) Discussion of Experiments for SPRITES '96 Campaign
5:00 PM	End of Meeting

PROCEEDINGS OF

AIR FORCE OFFICE OF SCIENTIFIC RESEARCH

AND

PHILLIPS LABORATORY

WORKSHOP ON SPRITES AND BLUE JETS

18-19 OCTOBER 1995

HANSCOM AIR FORCE BASE, MA

THE SPRITES'95 CAMPAIGN

Our Guiding Principles.....

Cooperation

Coordination

Correlation

ASTeR, Inc.
Yucca Ridge Field Station
46050 Weld County Road 13
Ft. Collins, CO 80524
(voice) 970-568-7664
(fax) 970-482-8627
(e-mail) lyonsccm@csn.org

SPRITES'95

§ § § § § §

A Large Scale
Multi-Agency, Multi-Disciplinary
Research Effort Seeded by the
NASA KSC SBIR Phase II Project

= = = = = = = = =

18 Teams of Investigators
(US, Japan, New Zealand)

46 Scientists and Support Staff

45 Day Intensive Field Program [CO]

Optical
[visible, infrared, ultraviolet, all sky OH and narrow band]
Spectra (Narrow and Broad-Band)
In-situ Electric Field Measurements
ELF, VLF
VHF
Radar
Acoustic (Infrasound)
Satellite

ASTER, Inc. SPRITE-RELATED PUBLICATIONS/PRESENTATIONS

Publications

Lyons, W.A., 1996: The SPRITES'95 field campaign: Initial results - characteristics of sprites and the mesoscale convective systems that produce them, Preprints, 18th Conf. on Severe Local Storms, AMS, San Francisco, 5 pp.

Lyons, W.A. and T.E. Nelson, 1996: Processing, integrating and displaying disparate data sources from the SPRITES'95 field program. Preprints, 12th IIIPS for Meteor., Oceanog. and Hydrol., AMS, Atlanta, 6 pp.

Fukunishi, H., Y. Takahashi, M. Kubota, K. Sakanoi, U.S. Inan and W.A. Lyons, 1996: Elves: Lightning-induced transient luminous events in the lower ionosphere. Nature (in press).

Dowden, R.L., J.B. Brundell and W.A. Lyons, 1996: Are VLF RORDs and optical sprites produced by the same cloud-to-ionosphere discharge? J. Geophys. Res., (in preparation).

Mende, S.B., R.L. Rairden, G.R. Swenson and W.A. Lyons, 1995: Sprite spectra: N_2 First Positive Band Identification. Geophys. Res. Lett., 22, 2633-2636.

Winckler, J.R., W.A. Lyons, T. E. Nelson and R.J. Nemzek, 1995: New high-resolution ground based studies of sprites. J. Geophysical Res. (submitted).

Inan, U.S., T.F. Bell, V. Pasko, D. Sentman, E. Wescott and W. Lyons, 1995: VLF signatures of red sprites. Geophys. Res. Lett. (submitted).

Boccippio, D.J., E.R. Williams, W.A. Lyons, I. Baker and R. Boldi, 1995: Sprites, ELF transients and positive ground strokes. Science, 269, 1088-1091.

Lyons, W.A., 1995: The relationship of large luminous stratospheric events to the anvil structure and cloud-to-ground discharges of their parent mesoscale convective system. Preprints, Conf. on Cloud Physics, AMS, Dallas, 541-546.

Lyons, W.A., 1994: Characteristics of luminous structures in the stratosphere above thunderstorms as imaged by low-light video. Geophysical Research Letters, 21, 875-878.

Lyons, W.A. and E.R. Williams, 1994: Some characteristics of cloud-to-stratosphere "lightning" and consideration for its detection. Preprints, Symposium on the Global Electrical Circuit, Global Change and the Meteorological Applications of Lightning Information, AMS, Nashville, 8 pp.

Lyons, W.A., 1994: Low-light video observations of frequent luminous structures in the stratosphere above thunderstorms. Mon. Wea. Rev., 122, 1940-1946.

Lyons, W.A. and E.R. Williams, 1993: Preliminary investigations of the phenomenology of cloud-to-stratosphere lightning discharges. Preprints, Conference on Atmospheric Electricity, American Meteorological Society, St. Louis, 8 pp.

Presentations

Lyons, W.A., 1996: Coordinated RF and optical measurements of sprites, jets and elves in the Colorado SPRITES'95 campaign. National Radio Science Meeting, Boulder, CO. (abstract only).

Armstrong, R.A., J. Shorter, W.A. Lyons, L. Jeong and W.A.M. Blumberg, 1995: Evidence for ionization in sprites - N2+ 478.8 first negative emission measured in SPRITES'95 campaign. AGU winter meeting, San Francisco, EOS (abstract only).

Lyons, W.A. and T.E. Nelson, 1995: The Colorado SPRITES'95 Campaign: Initial results. AGU winter meeting, San Francisco, EOS (abstract only).

Rairden, R.L., S.B. Mende G.R. Swenson and W.A. Lyons, 1995: Ground based observations of airglow above thunderstorms. AGU winter meeting, San Francisco, EOS (abstract only).

Takahashi, Y., M. Kubota, K. Sakanoi, H. Fukunishi, U.S. Inan, and W.A. Lyons, 1995: Spatial and temporal relationships between lower ionospheric flashes and sprites. AGU winter meeting, San Francisco, EOS (abstract only).

Dowden, R.L., J. Brundell, W.A. Lyons and T. Nelson, 1995: RORDs and sprites. AGU winter meeting, San Francisco, EOS (abstract only).

Williams, E., D. Boccippio, C. Wong, W. Lyons, M. Ishii and W. Koshak, 1995: The physical origin of Schumann resonance excitation. AGU winter meeting, San Francisco, EOS (abstract only).

Inan, U.S., S.C. Reising, V.P. Pasko and W.A. Lyons, 1995: VLF signatures of ionospheric disturbances associated with sprites. AGU winter meeting, San Francisco, EOS (abstract only).

Lyons, W.A., I.T Baker, T.E. Nelson, R. Armstrong, J. Shorter, J. R. Winckler, R.J. Nemzek, P R.. Malcolm and E.R. Williams, 1995: Sprite Observations above the U.S. High Plains. Preprints, IUGG, Boulder, CO (poster, abstract only).

Lyons, W.A., 1995: Observations of sprites above intense thunderstorms during the 1994 Colorado Sprite Campaign. URSI, National Radio Science Meeting. (abstract only)

Lyons, W.A., I.T. Baker, T.E. Nelson, J.R. Winckler, R.J. Nemzek, P.R. Malcolm, E.R. Williams and D. Boccippio, 1994: The 1994 Colorado SPRITE Campaign (abstract), EOS, 75, vol. 44, p. 108.

Lyons, W.A., I.T. Baker, T.E. Nelson, J.R. Winckler, R.J. Nemzek, E.R. Williams, D. Boccippio and P.R. Malcolm, 1994: New observations of luminous stratospheric and ionospheric events above intense thunderstorms (abstract). EOS , 75, vol. 44, p. 108.

Winckler, J.R., W.A. Lyons, T. Nelson and R.J. Nemzek, 1994: New high-resolution ground-based studies of cloud-ionosphere discharges (abstract). EOS, 75, vol. 44, p 107.

Boccippio, D., E. Williams, W. A. Lyons, I. T. Baker and R. Boldi, 1994: Sprites, Q-bursts and positive ground flashes (abstract). EOS, 75, vol. 44, p. 108.

1995 COLORADO SPRITE CAMPAIGN

DATES (UTC) WITH IMAGED SPRITES

§ § § § §

19 June
20 June
21 June
23 June
25 June
27 June
04 July
07 July
08 July
12 July
13 July
15 July
16 July
20 July
21 July
22 July
23 July
24 July
25 July
26 July
27 July
31 July
3 August
4 August
6 August

THE YUCCA RIDGE FIELD STATION

- 24 hour operation; 80 acres for deployment
- 1000 km radius of operations for optical (areal coverage 400,000 km^2)
- 3 year sprite archive
- available now
- culturally quiet for RF
- can "guarantee" sprites 25-50 nights per warm season (ideal storms and viewing conditions)
- have meteorological data acquisition infrastructure in place
- convenient to other related facilities
- low overhead

FROM THE YUCCA RIDGE FIELD STATION...

SOME INITIAL ACCOMPLISHMENTS

NAS10-12113 and Cooperating Groups

- Confirmed high frequency of spites above high plains MCSs
- Relationship of sprites to large positive CGs
- Relationships between Sprites, +CGs and Q-bursts
- Multi-channel high speed photometry identified lower ionospheric flash as separate entity (ELVES)
- Stereo imaging confirms sprites/+CG proximity
- More evidence for "blue" jets
- Developed sprite forecasting tools for mesoscale convective systems
- Coordinated optical and RF measurements of specific sprite events
- Confirmed presence of "VLF sprites"
- Multiple ELF Q-burst measurements, confirmed relationship w/ sprites
- Obtained numerous spectra
- Evidence of significant ionization in sprites and or elves
- Initial calculations of impact upon upper atmospheric chemistry
- High speed infrared optical and infrared measurements (IROCS)
- Active probing of sprites using radar
- Vectored balloon-borne electric-field measurements above Kansas
- Imaged gravity waves emanating from sprite producing storm system and evidence of other luminous phenomena

EMERGING SCIENTIFIC QUESTIONS

- How are sprites, elves and jets different from each other?
- What is the entire spectrum of each phenomena [UV-visible-IR] ?
- What other phenomena are present above thunderstorms?
- What don't large negative CG apparently produce sprites?
- Why do only some large positive CGs produce sprites and elves?
- What actually triggers a sprite, jet or elve?
- What is the cause of the fine structure/tendrils in sprites?
- So sprites illuminate pre-existing atmospheric structure?
- What role, if any, do storm-generated gravity waves play in sprite structure?
- What is the direction of propagation for sprites and elves?
- Why do some mature storms wait several hours before generating sprites?
- Do sprites, jet and elves also occur during the day?
- Are sprites induced by large "spider" lightning discharges?
- Relationship to x-rays, gamma rays and TIPPS/SIPPS?
- What is the structure of the ENTIRE lightning discharge producing sprites?
- Can sprites generate acoustic waves?
- What is the electric field above the parent thunderstorms?
- Can we use ELF/VLF measurements for global detection and location?
- What are their roles in the global circuit?
- Relationship to whistlers/trimpis ?
- What is the global temporal and spatial climatology of sprites, jets and elves?
- What are the atmospheric chemistry impacts of sprites, elves and jets?
- Do they pose a hazard to aerospace navigation between 20 -110 km altitude?

CREATURES IN THE MESOSPHERIC ZOO....

SPRITES

BLUE JETS

ELVES

AIRGLOW WAVES

GNOMES

SPRITES

Stratospheric/mesospheric

Perturbations

Resulting from

Intense

Thunderstorm

Electrification

ELVES

Emissions of

Light and

VLF perturbations from

EMP

EventS

(Singular: ELVE ?)

GNOMES

Goofy

Nocturnal

Optical

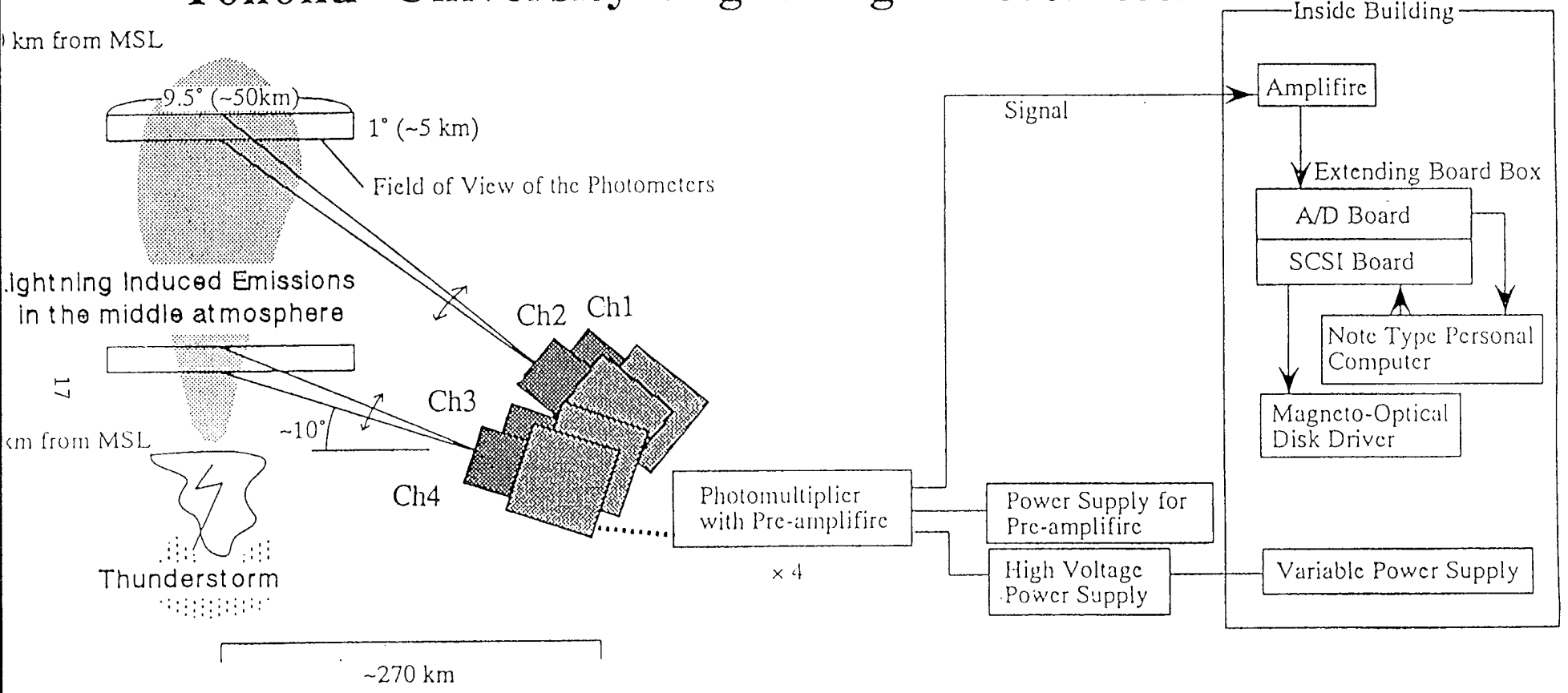
Mesospheric

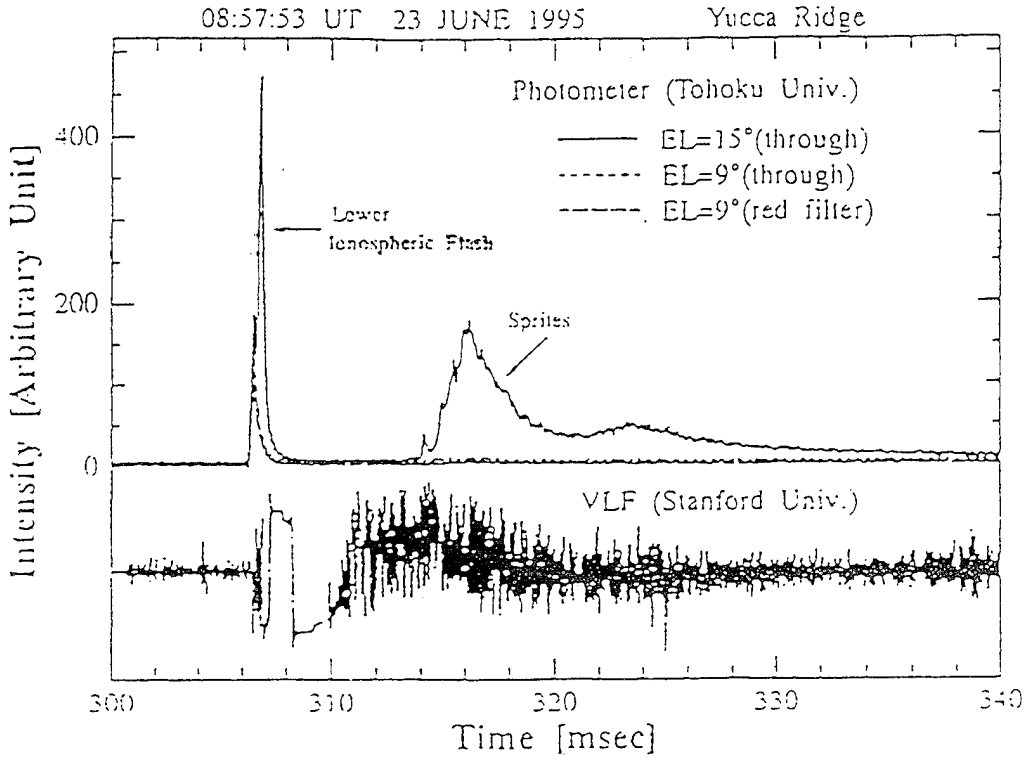
EmissionS

This is a "holding category" for the various other phenomena which are yet to be identified and named. It is not proposed to be used in formal publications.

Tohoku University
Sendai, Miyagi, 980-77 Japan

Tohoku University Lightning Photometer




08:57:53 UT 23 JUNE 1995
Yucca Ridge
Photometer (Tohoku Univ.)
EL=15°(through)
EL=9°(through)
EL=9°(red filter)
Lower Ionospheric Flash
Sprites
VLF (Stanford Univ.)
Intensity [Arbitrary Unit]
400
200
0
300
310
320
330
340
Time [msec]

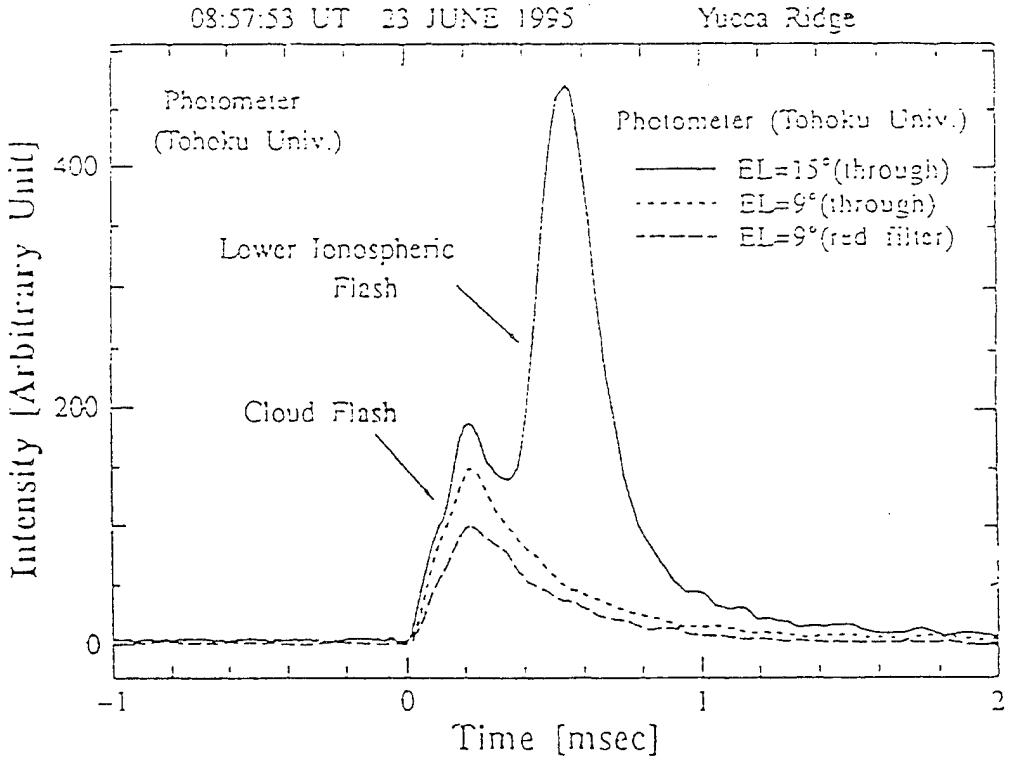

08:57:53 UT 23 JUNE 1995
Yucca Ridge
Photometer (Tohoku Univ.)
Photometer (Tohoku Univ.)
EL=15°(through)
EL=9°(through)
EL=9°(red filter)
Lower Ionospheric Flash
Cloud Flash
Intensity [Arbitrary Unit]
400
200
0
-1
0
1
2
Time [msec]

Fig. 1

Aster, Inc.

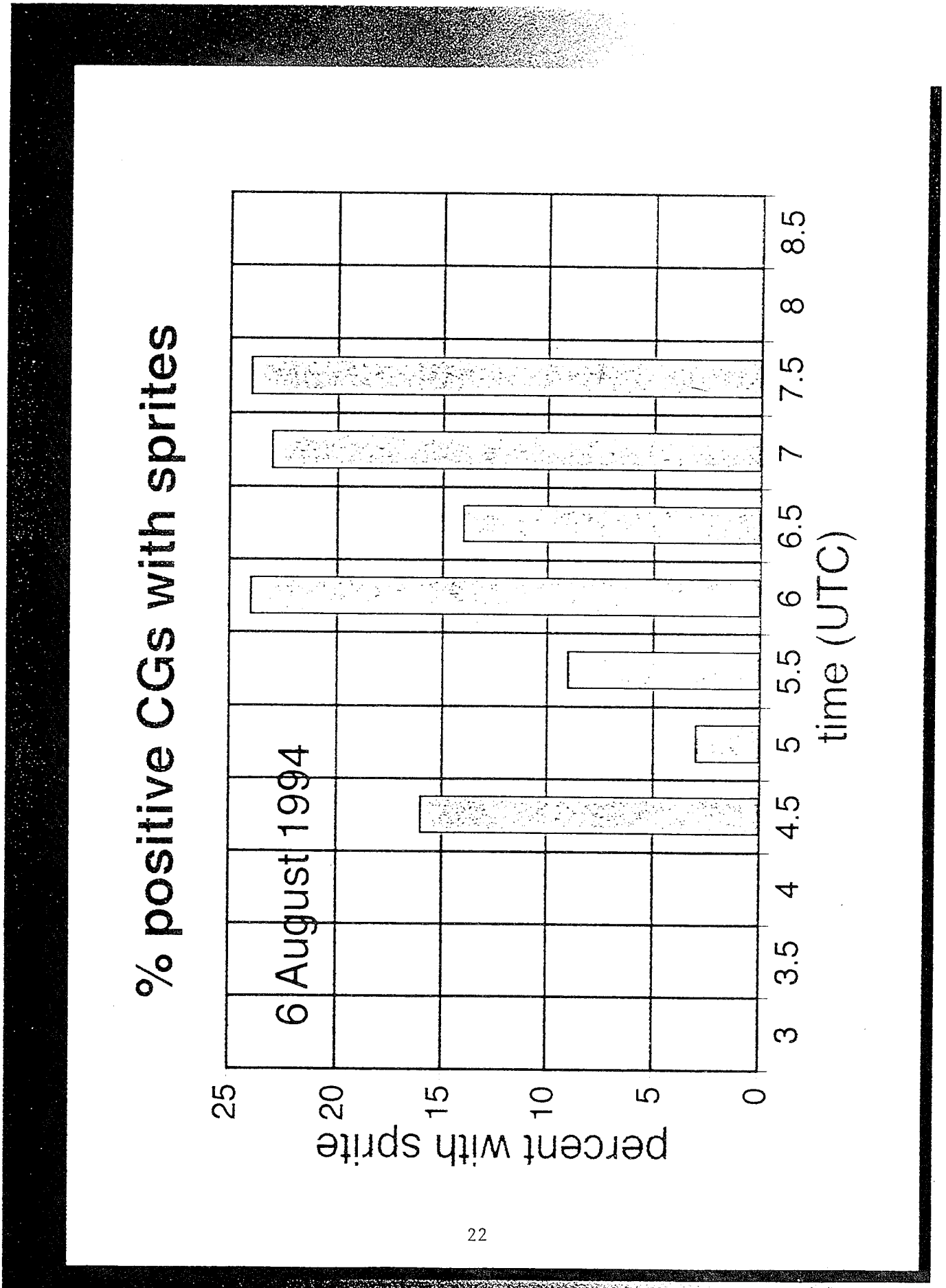
APPARENT LOWER IONOSPHERIC FLASH ASSOCIATED WITH A 213 KILOAMP POSITIVE CG IN NORTHEASTERN NEW MEXICO. NO SPRITE WAS IMAGED WITH THIS EVENT. 25 JUNE 1995.

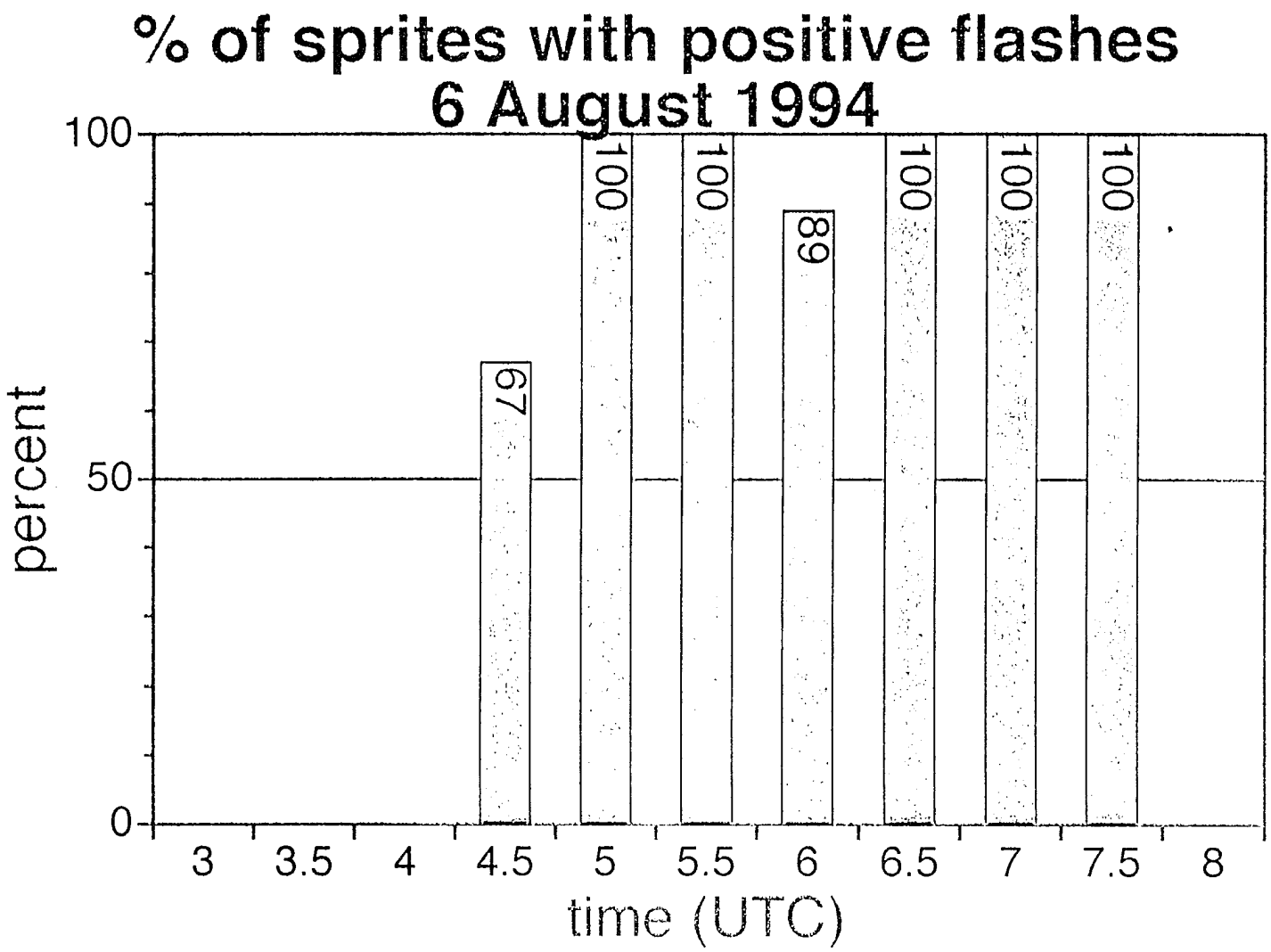


24 July 1995

Sprites and elves both result from large positive CG events - but elves seem to be associated with the largest of the +CG flashes.

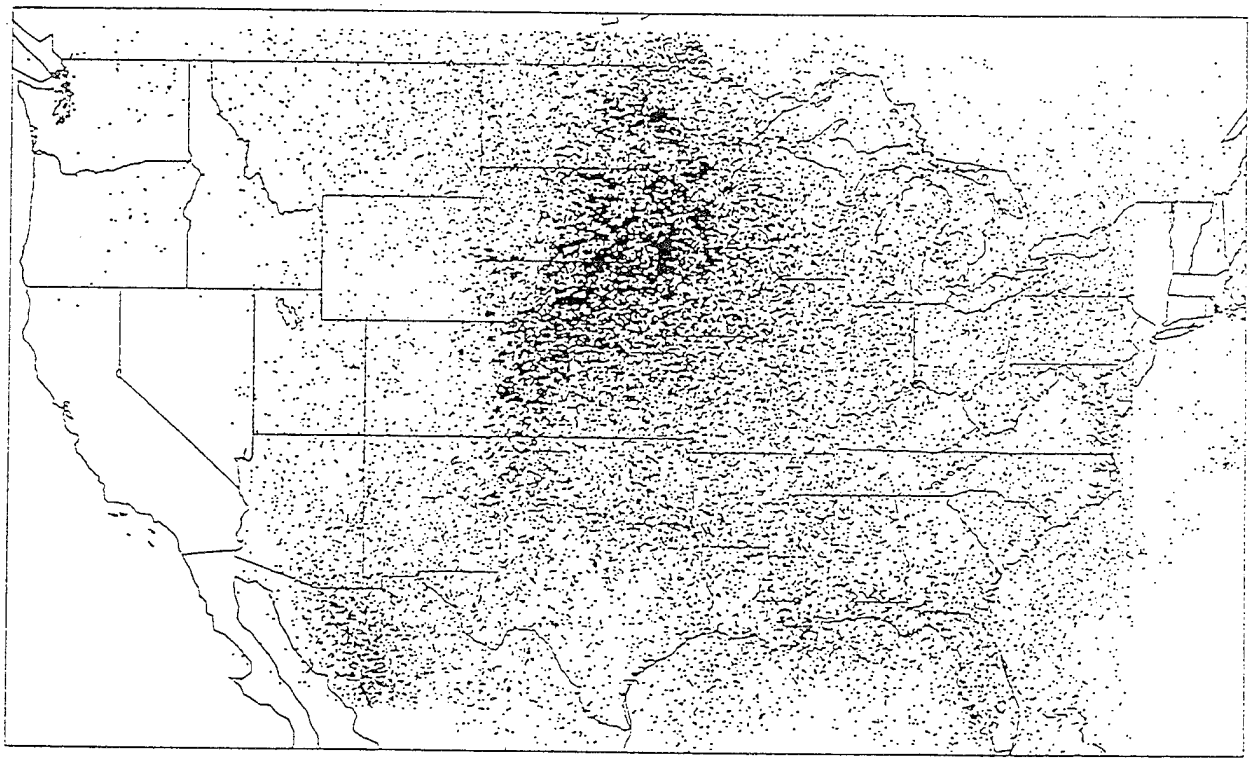
Phenomena	Number	Avg Peak Current	Largest
SPRITES	68	58 kamp	113 kamp
ELVES	14	104 kamp	200 kamp


% positive CGs with sprites
6 August 1994
percent with sprite
time (UTC)
0
5
10
15
20
25
3
3.5
4
4.5
5
5.5
6
6.5
7
7.5
8
8.5

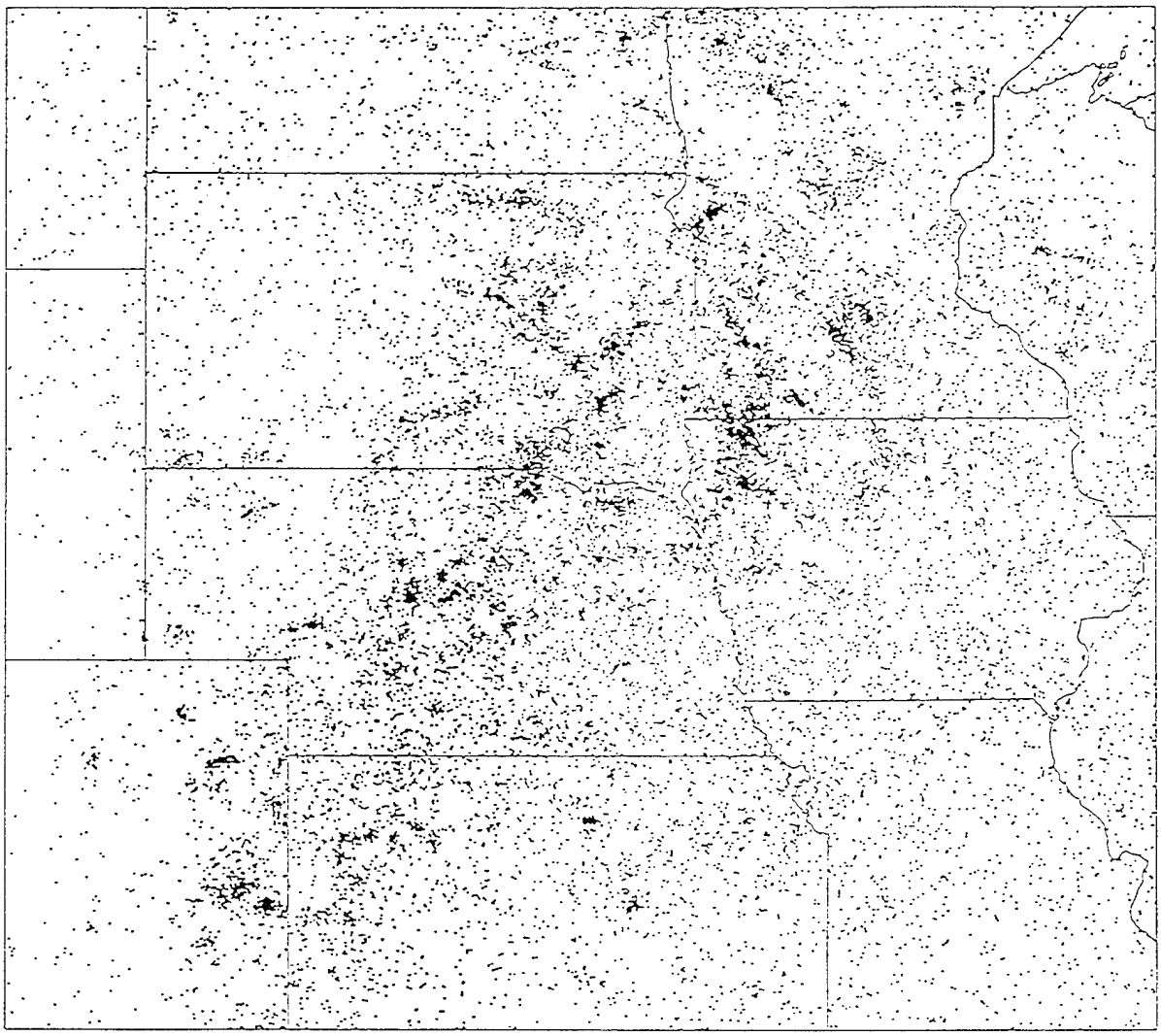

% of sprites with positive flashes
6 August 1994
100
50
0
percent
67
100
100
89
100
100
100
3
3.5
4
4.5
5
5.5
6
6.5
7
7.5
8
time (UTC)

CLIMATOLOGY OF LARGE POSTIVES

JUL–AUG 93, JUN–SEP 94

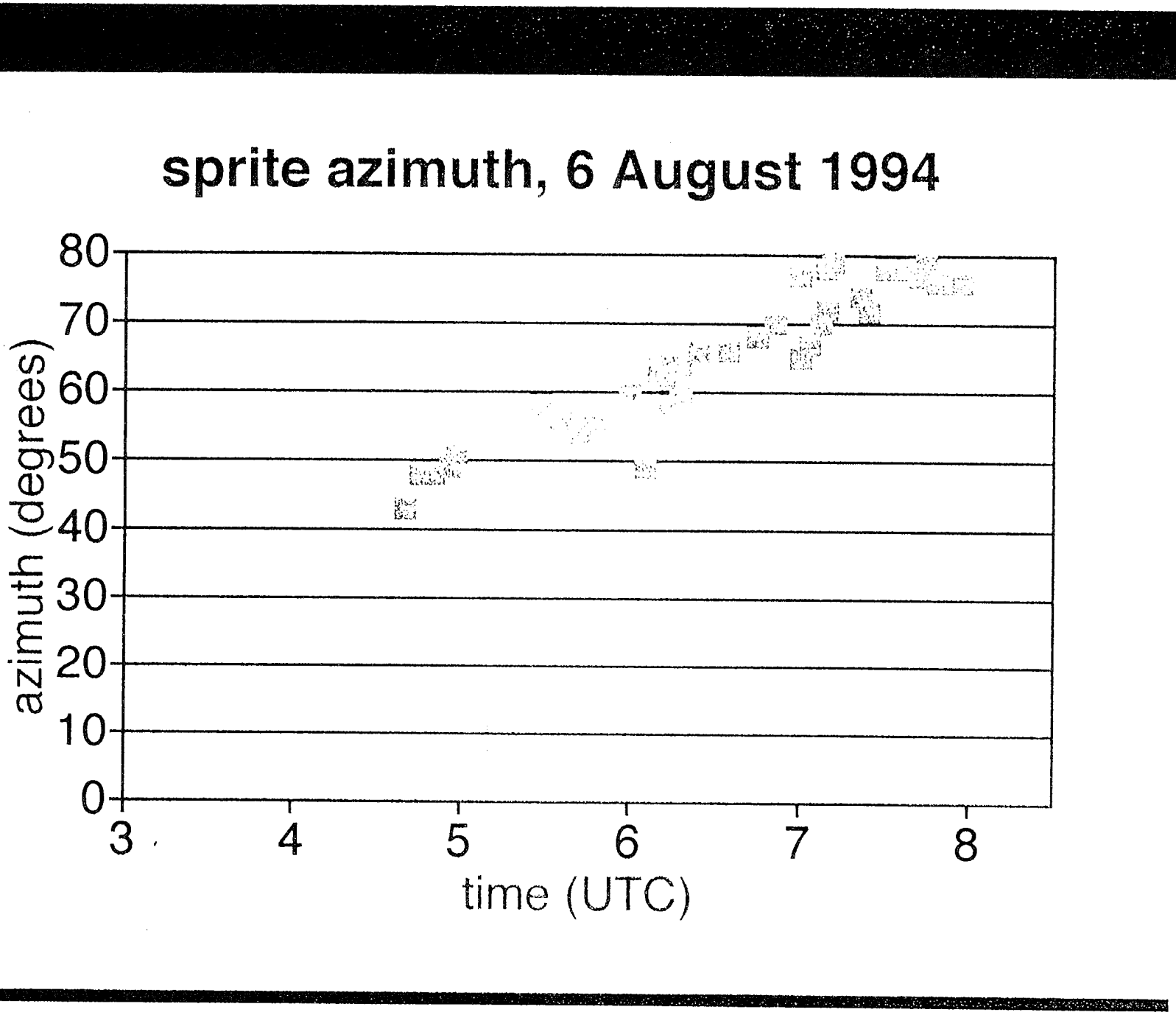


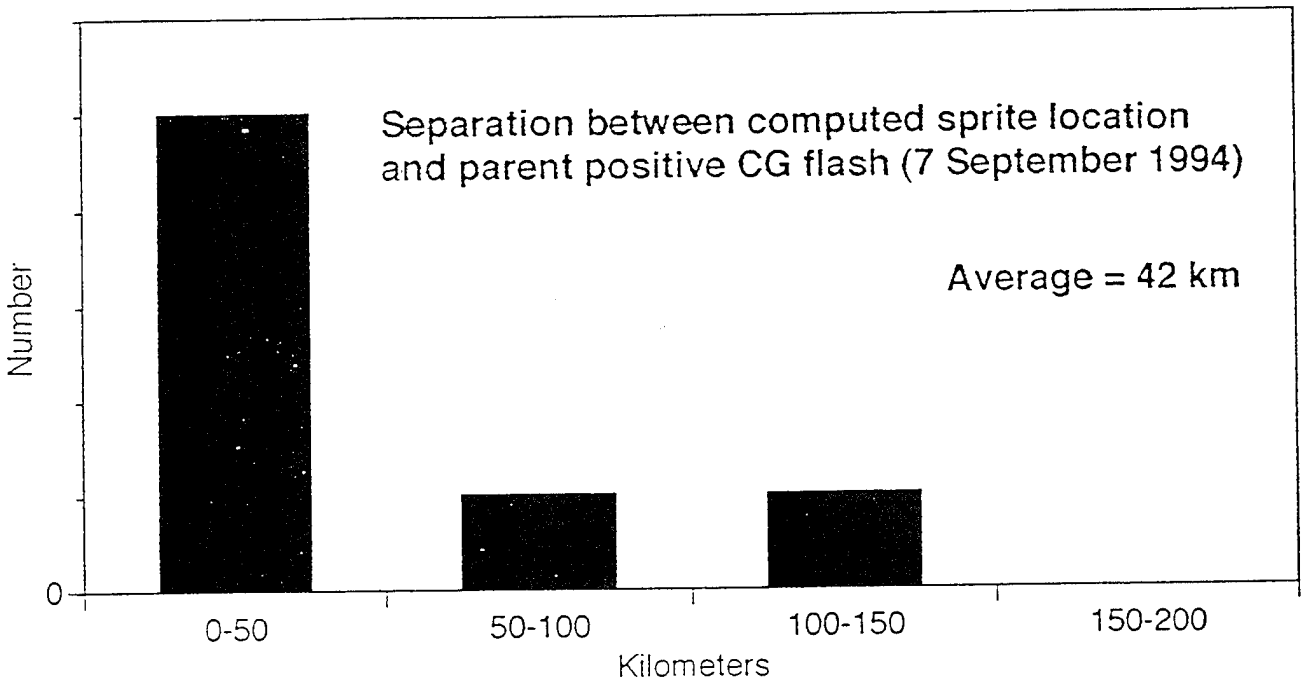
CLIMATOLOGY OF LARGE POSTIVES

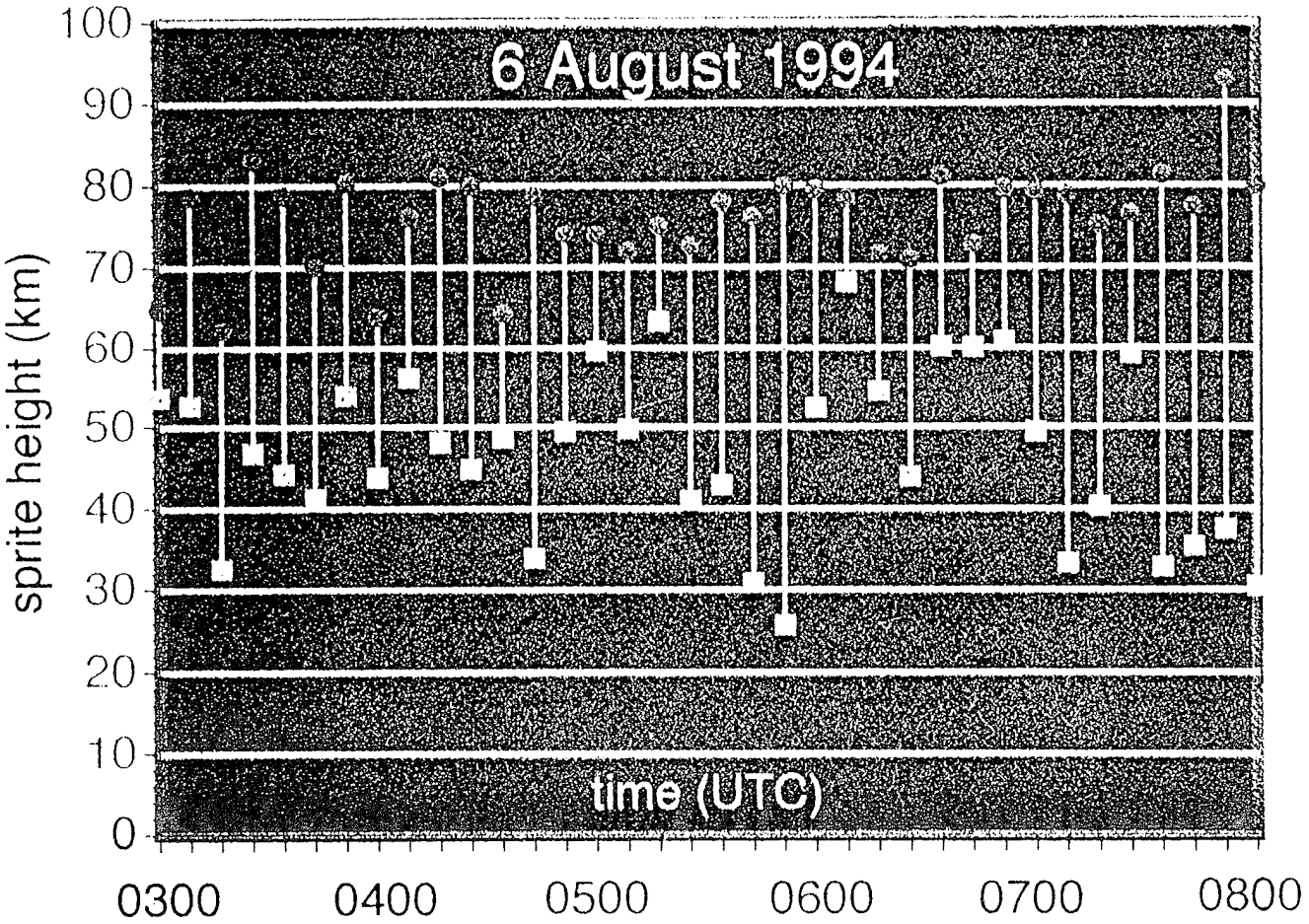


JUL–AUG 1993, JUN–SEP 1994

All strikes larger than 100kA


sprite azimuth, 6 August 1994
azimuth (degrees)
80
70
60
50
40
30
20
10
0
3
4
5
6
7
8
time (UTC)


Separation between computed sprite location
and parent positive CG flash (7 September 1994)
Average = 42 km
Number
0
0-50
50-100
100-150
150-200
Kilometers

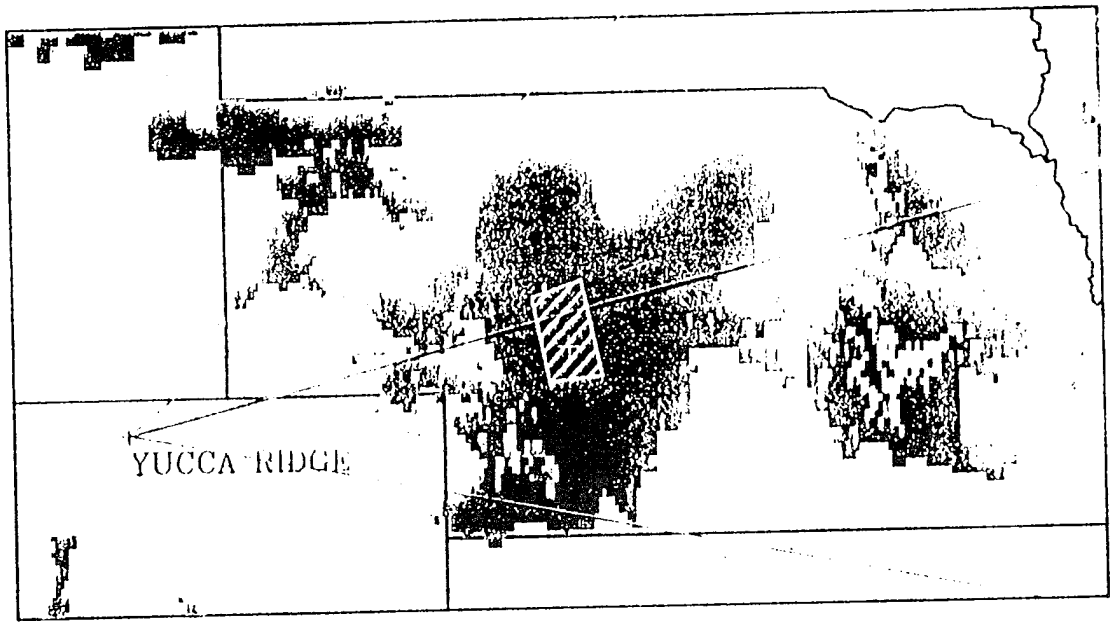

6 August 1994
sprite height (km)
100
90
80
70
60
50
40
30
20
10
0
time (UTC)
0300
0400
0500
0600
0700
0800

LIGHTNING STRIKES - RADAR SPRITES

Box represents calculated sprite location

08 06 94

[illegible] TO [illegible] PT

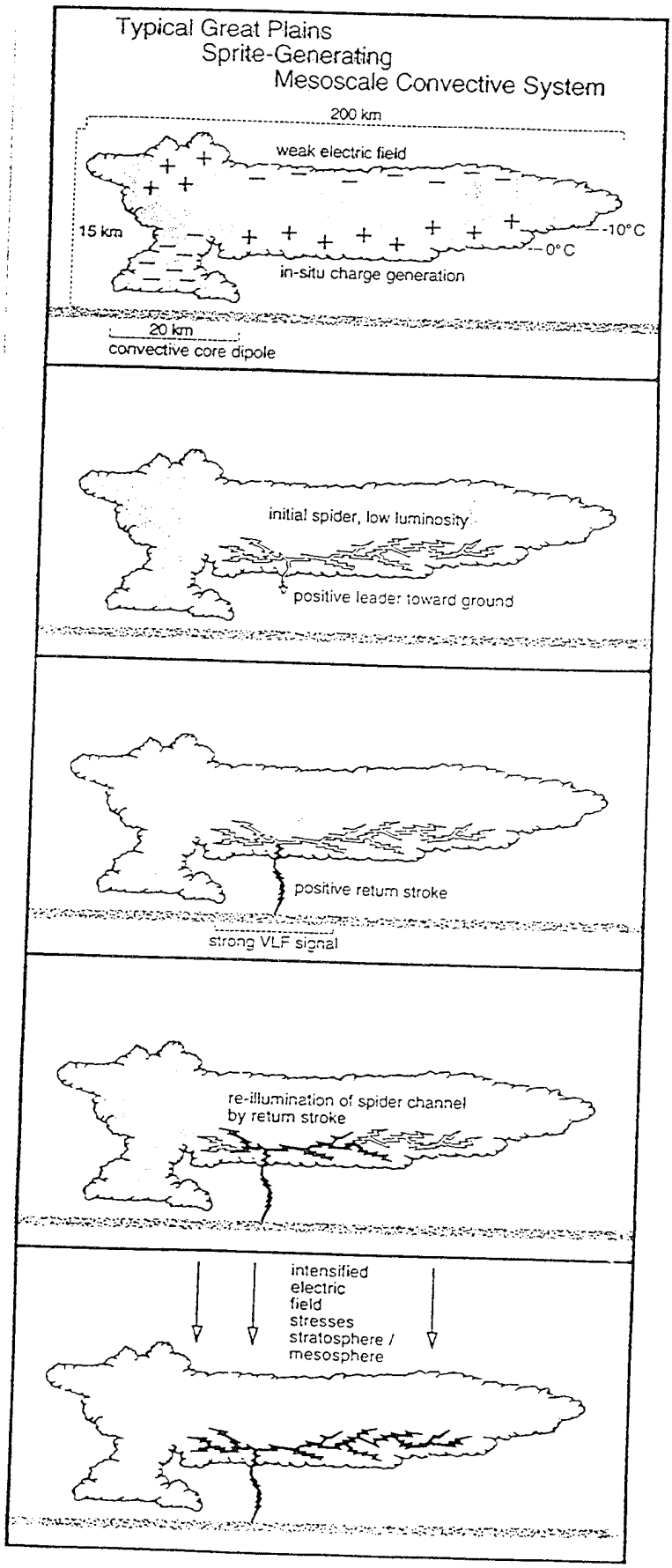


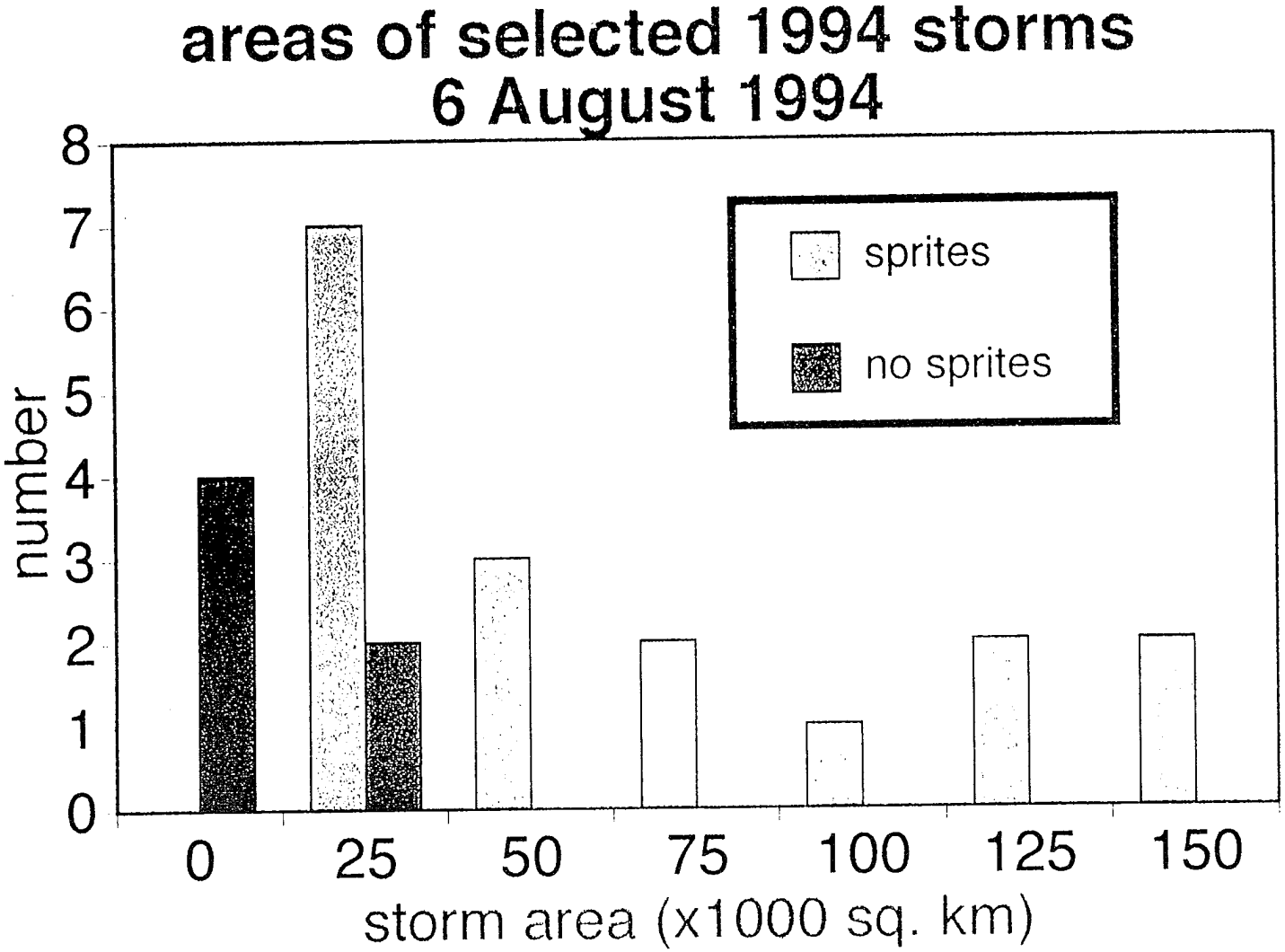
CAMERA AZIMUTH 076.0 DEGREES

SPRITE AZIMUTH 072.5 TO 084.0 DEGREES

SPRITE RANGE 325.0 TO 368.0 KILOMETERS

positive strikes ( ) 0 negative strikes (0)


Typical Great Plains
Sprite-Generating
Mesoscale Convective System
200 km
weak electric field
15 km
-10°C
0°C
in-situ charge generation
20 km
convective core dipole
initial spider, low luminosity
positive leader toward ground
positive return stroke
strong VLF signal
re-illumination of spider channel
by return stroke
intensified
electric
field
stresses
stratosphere /
mesosphere


areas of selected 1994 storms
6 August 1994
number
0
1
2
3
4
5
6
7
8
sprites
no sprites
0
25
50
75
100
125
150
storm area (x1000 sq. km)

(HIGH PLAINS) FORECAST ACCURACY

1995

25 Sprite Nights

100% Correctly Forecasted

*** ASTeR, Inc.**
Atmospheric Simulation, Testing & Research
46050 Weld County Road 13 • Ft. Collins, CO 80522 • 970-568-7664

DATE: 31 October 1995
FROM: Walt Lyons
RE: SPRITES '95 Project Participants

The following is the updated roster of direct and indirect participants for the SPRITES '95 Campaign in Colorado. Please inform us if there are any errors in this information and/or yoyu wish to provide additional information.

ASTeR, Inc.		
Participants: Walt Lyons, Tom Nelson, Liv Lyons	970-568-7664	voice
Yucca Ridge Field Station	970-482-8627	fax
46050 Weld County Road 13		
Ft. Collins, CO 80524	lyonsccm@csn.org	e-mail
Mission Research Corporation		
Participants: Dr. Russ Armstrong, Dr. Jeff Shorter	603-891-0070, x203	voice
One Tara Blvd., Suite 302	603-891-0088	fax
Nashua, NH 03062-2801	@lanl.gov:rarmstrong@mrcnh.com	e-mail
Lawrence Livermore National Lab		
Participants: Dr. John Molitoris/Dr. Colin Price	510-423-3496	voice (JM)
Regional Atmospheric Sciences Div.	510-423-2300	voice (CP)
7000 East Avenue	520-422-5844	fax
PO Box 808, MS/L-262	molitoris1@llnl.gov	e-mail
STAR Lab, Stanford University		
Participants: Prof. Umran Inan, Steve Reising,	415-723-4994	voice
Bill Trabucco, Alexander Slingeland	415-723-1461	voice
Durand 321, MC-4055	415-723-9251	fax
Stanford University	inan@nova.stanford.edu	e-mail
Stanford CA 94305	scr@nova.stanford.edu	e-mail
	trabucco@nova.stanford.edu	e-mail
Tohoku University		
Participants: Profs. Yukihiro Takahashi, M. Kubota and		
Prof.Hiroshi Fukunish	011+81 22 217 6537	voice
Dept. of Astrophysics & Geophysics	011+81 22 217 6739	fax
Sendai, Miyagi 980-77, Japan	yukihiro@stpp2.geophys.tohoku.ac.jp	e-mail
University of Otago		
Participant: Prof. Richard L. Dowden	011+64 03 479 7752	voice
Department of Physics	011+64 03 479 0964	fax
PO Box 56	dowden@newton.otago.ac.nz	e-mail
Dunedin, New Zealand		
Utah State University	801-797-0491 (PM), 797-3919 (MT)	voice
Participants: Prof. Michael Taylor, Peter Mace	801-797-4044	fax
Space Dynamics Laboratory	petermace@cc.usu.edu	e-mail
Logan, Utah 84322-4145	taylor@psi.sci.sdl.usu.edu	e-mail
Lockheed Space and Missile		
Participants: Stephen Mende, Rick Rairden	415-424-3282	voice
Dept. 91-20, Building 252	415-424-3333	fax
3251 Hanover Street	rairden@lockhd.space.lockeed.com	e-mail
Palo Alto, CA 94304	mende@sag.space.lockheed.com	e-mail

Pennsylvania State University
Participants: Les Hale, Lee Marshall
780 Suzanne Ave.
Las Cruces, NM 88005

505-647-0104 voice (LH)
505-642-1906 voice (LH)
814-863-8457 fax(LM)
814-867-8077 voice [LM]

SRI International
Participant: Dr. Roland T. Tsunoda, John Buonacore
Geoscience & Engineering Center
333 Ravenswood Avenue
Menlo Park, CA 94025

415-859-3124 voice
415-322-2318 fax
tsunoda@unix.sri.com e-mail

Massachusetts Institute of Technology
Participants: Dr. Earle Williams, Charles Wong
Lincoln Lab, Group 43, Weather Systems
Cambridge, MA

617-253-2459 voice (MIT)
617-981-7430 voice (LL)
617-253-4689 voice (CW)
617-981- fax
401-397-8982 (V-RI SR site)

Los Alamos National Laboratory
Participant: Dr. Robert Franz, Dave Smith
LANL
MS D466
Los Alamos NM 87545

505-665-3331 voice(RF)
505-667-1055 voice (DS)
505-665-2483 fax
rfranz@lanl.gov e-mail
smithda@lanl.gov. e-mail
505-665-7395 fax(DS)

University of Minnesota
Participant: Prof. John Winckler
2012 Irving Avenue South
Minneapolis, MN 55405

612-374-5722 voice

Dr. Robert Nemzek
4226 C Alabama Avenue
Los Alamos, NM 87544

505-662-7621 (home)
nemzek@delphi.com e-mail

National Severe Storms Laboratory
Participants: Dr. W. David Rust,
Dr. Thomas Marshall (U of Miss)
1313 Halley Circle
Norman, OK 73069

405-366-0404 voice
405-366-0472 fax
rust@nssl.uoknor.edu e-mail
405-498-3735 pager

GeoSpace Research, Inc.
Participants: Frank T. Djuth, Matthew Cox, Ken Williams
550 N. Continenrtal Blvd.
Suite 110
El Segundo, CA 90245

310-322-1160 voice
310--322-2596 fax
djuth@netcom.com e-mail

US Air Force Academy
Participants: Maj. Perry Malcolm,
Maj. Geoff McHarg, Maj. Scott Dudley
HQ USAFA/DFP
2354 Fairchild Drive, Suite 2A42
USAF Academy, CO 80840-6254

719-472-2579 voice (PM)
malcolmpr%dfp%usafa@dfmail.usafa.af.mil e-mail
719-472-3055 voice (GM)
719-481-8543 voice (GM) (home)
grahm@nord.usafa.af.mil e-mail (GM)
719-472-3055 voice (SD)
dudleysc%dfp%usafa@dfmail.usafa.af.mil e-mail

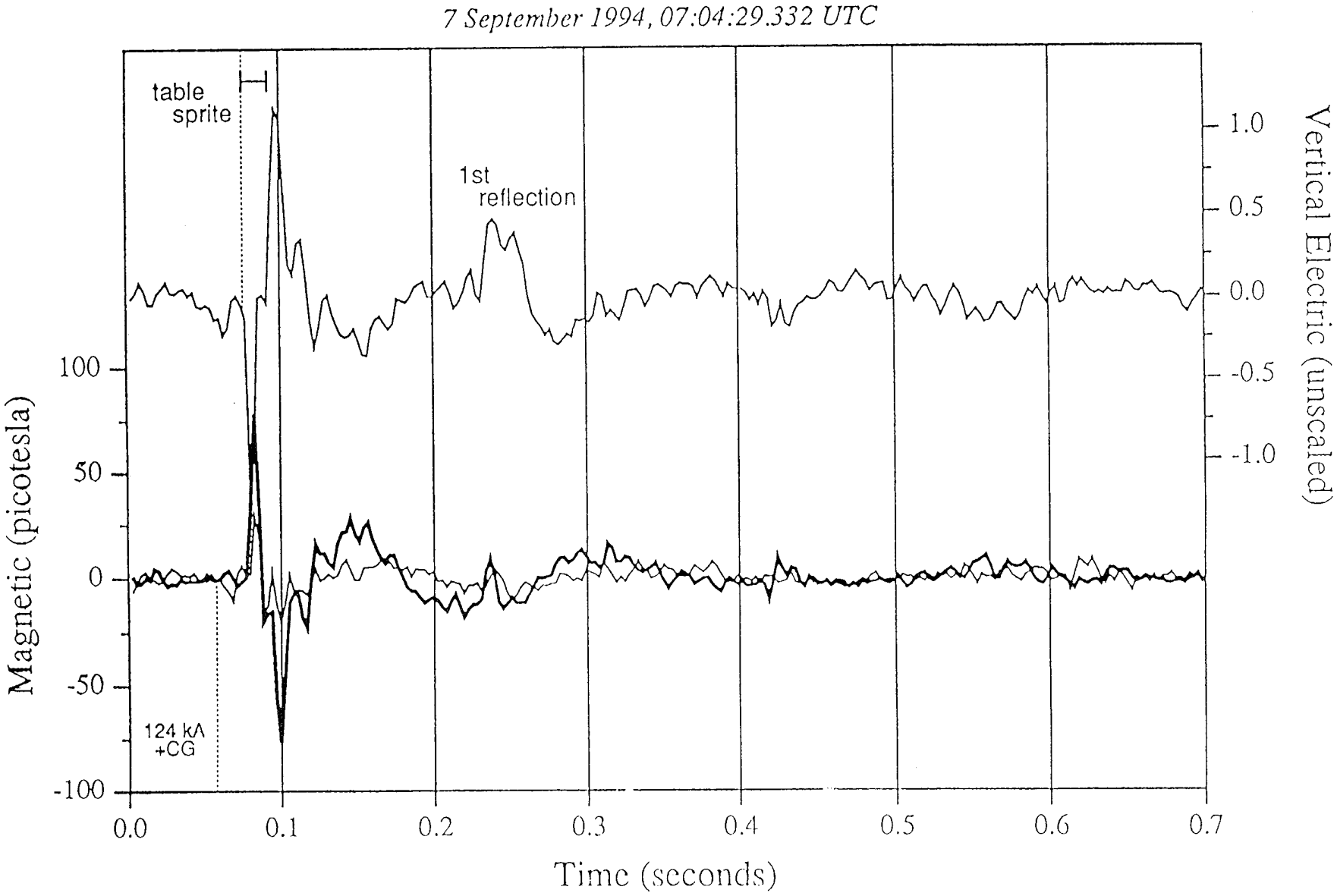

7 September 1994, 07:04:29.332 UTC
table sprite
1st reflection
124 kA +CG
Magnetic (picotesla)
100
50
0
-50
-100
Vertical Electric (unscaled)
1.0
0.5
0.0
-0.5
-1.0
0.0
0.1
0.2
0.3
0.4
0.5
0.6
0.7
Time (seconds)

Figure 2

18th Conf. on Severe Local Storms
American Meteorological Society
San Francisco, CA 19-23 February 1996

THE SPRITES ' 95 FIELD CAMPAIGN: INITIAL RESULTS - CHARACTERISTICS OF SPRITES AND THE MESOSCALE CONVECTIVE SYSTEMS THAT PRODUCE THEM

Walter A. Lyons

ASTeR, Inc.
Ft. Collins, CO 80524

1. INTRODUCTION

Anecdotal reports of unusual "lightning" discharging upward into the stratosphere or beyond have been reported for over a century (Toynbee and Mackenzie 1886) and were theoretically postulated by Wilson (1956). Little import was accorded such "cloud-to-space" lightning reports until 1989 when a chance observation from a low-light video system documented a transient (<33 ms) luminous structure extending 30-40 km above a thunderstorm top (Franz et al. 1990) ignited interest in this subject. Subsequently, similar features were discovered in low-light video images of storm systems taken onboard the Space Shuttle (Boeck et al. 1995). Low-light video imaging from the Yucca Ridge Field Station (YRFS) in Colorado since 1993 (Lyons 1994 a,b) have confirmed over 1500 of these large, luminous structures, now called sprites, in the stratosphere and mesosphere above mesoscale convective systems (MCS). Sprite rates as high as once per two minutes have been found with the most active systems. Sprites can extend from above the cloud tops to almost 100 km altitude and can be many tens of kilometers wide (Fig. 1). The detectable optical emissions may last 20 to 200 ms. They clearly appear to be related to electrical discharges within the storm. Concern that such a potentially energetic event occurs within portions of the upper atmosphere routinely traversed by aerospace vehicles, in particular the Space Shuttle, led NASA to fund a multi-year research effort. Among the goals of this current program are to determine the predictability of such events. This implies understanding the characteristics of the parent thunderstorms and their lightning discharges which result in sprites.

2. THE SPRITES'95 CAMPAIGN

A NASA-KSC funded field program was conducted at the Yucca Ridge Field Station, located some 20 km northeast of Ft. Collins, CO during the summer of 1995 (10 June - 6 August). This site has a panoramic view of the nocturnal thunderstorms which form over the High Plains. Low-light video systems have detected sprites at ranges up to 1000 km from YRFS. In addition to ASTeR's base experiments of low-light video monitoring and coincident VLF and ELF measurements, coordinated observations were made by numerous organizations in 1995 (Table 1). Additional optical measurements using special CCD sensors and photometers were made by Lawrence Livermore National Lab, Tohoku University, the University of Alaska and Mission Research Corporation. Coordination of measurements allowed for Mende et al. (1995) to obtain optical spectra indicating the presence of the N_2 1 PG bands, confirmatory of the red coloration of the sprites reported by Sentman et al. (1995). A suite of ELF and VLF measurements during sprite events were taken by MIT, Stanford University (STAR Labs) and the University of Otago (New Zealand). Other VHF propagation data were collected by GeoSpace Research, Inc. The National Severe Storms Laboratory and the University of Mississippi (Dave Rust and Tom Marshall) deployed an instrumented van (video, electric field) beneath the MCS anvils and made balloon soundings of electric fields in the stratosphere above anvils of sprite-producing MCS.

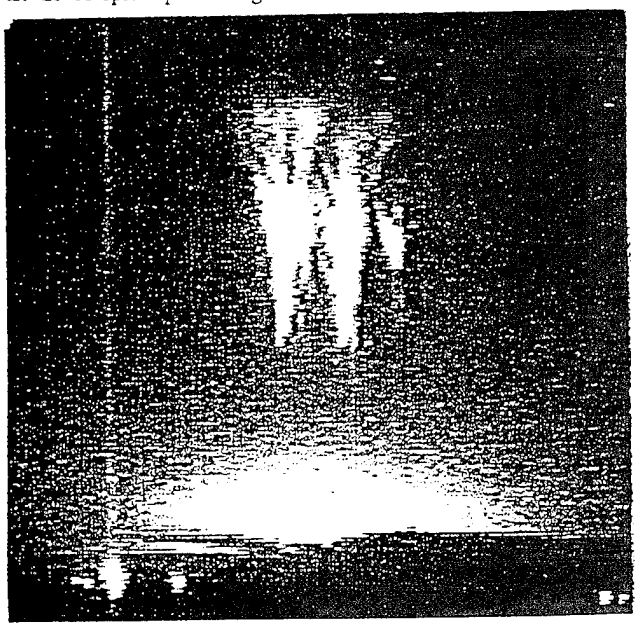


Fig. 1 Large sprite cluster, some 325 km NNE of the YRFS low-light camera site (0620 UTC 26 July 1995). The glow above the distant storm top is the from the parent lightning. The vertical striping is an artifact of the imager. (Courtesy of Steve Mende and Rick Rairden, Lockheed Space and Missile).

Corresponding author address: Walter A. Lyons, CCM, ASTeR, Inc., 46050 Weld County Road 13, Ft. Collins, CO 80524, (Voice) 970-568-7664; (Fax) 970-482-8627; e-mail: lyonsccm@csn.org

Table 1. Participants in SPRITES'95

ASTeR, Inc., Fort Collins, Colorado,
Walter Lyons, Project Director; Tom Nelson
dual Xybion ISS-255 low light imagers • ELF and VLF measurements • photometer • meteorological data

Tohoku University, Sendai, Japan
Hiroshi Fukunishi, Yukihiro Takahashi, Minoru Kubota
multiple (4) high speed 1°x10° FOV photometers

University of Otago, Dunedin, New Zealand
Richard Dowden - OMNIPAL VLF interferometry (3 sites)

STAR Laboratory, Stanford University
Umran Inan, Steve Reising, Bill Trabucco, Alex Slingeland
narrowband VLF from mobile van • VLF narrowband and broadband (0-30 kHz) VLF at YR • VLF observations in conjugate region (Palmer station)

GeoSpace Research, Inc.
Frank Djuth, Matt Cox, Ken Williams - bi-static propagation (WWV at 2.5, 5, 10, 15 and 20 mHz and 28 mHz transmissions)

Utah State University, Space Dynamics Lab
Michael Taylor, Peter Mace
all sky airglow camera • highly sensitive low-light vidicon and SIT cameras (filtered)

Lawrence Livermore National Laboratory
John Molitoris, Colin Price
IROCS - infrared optical camera system • fast optical imager • large format optical imager

Massachusetts Institute of Technology
Earle Williams, Charles Wong, Bob Boldi
Schumann Resonance/Q-bursts at Rhode Island and YR sites

NOAA, National Severe Storms Laboratory
David Rust, Thomas Marshall
lightning video and balloon-borne electric field mill

Pennsylvania State University
Les Hale, Lee Marshall
ELF and VLF measurements

Los Alamos National Laboratory
Robert Franz, Dave Smith
measurements of TIPPS and SIPPS

Mission Research Corporation, Nashua, NH,
Russ Armstrong, Jeff Shorter
CCD cameras system and photometer

Lockheed Space and Missile
Steve Mende, Rick Rairden
imaging spectrometer and low-light video

SRI International
Roland Tsunoda, John Buonocore
tunable radar system (2-30 mHz)

NASA Kennedy Space Center & MSFC
Carl Lennon, Launa Maier, Otha Vaughan, Jr.
LDAR • ELF/Q-burst measurements • OTD

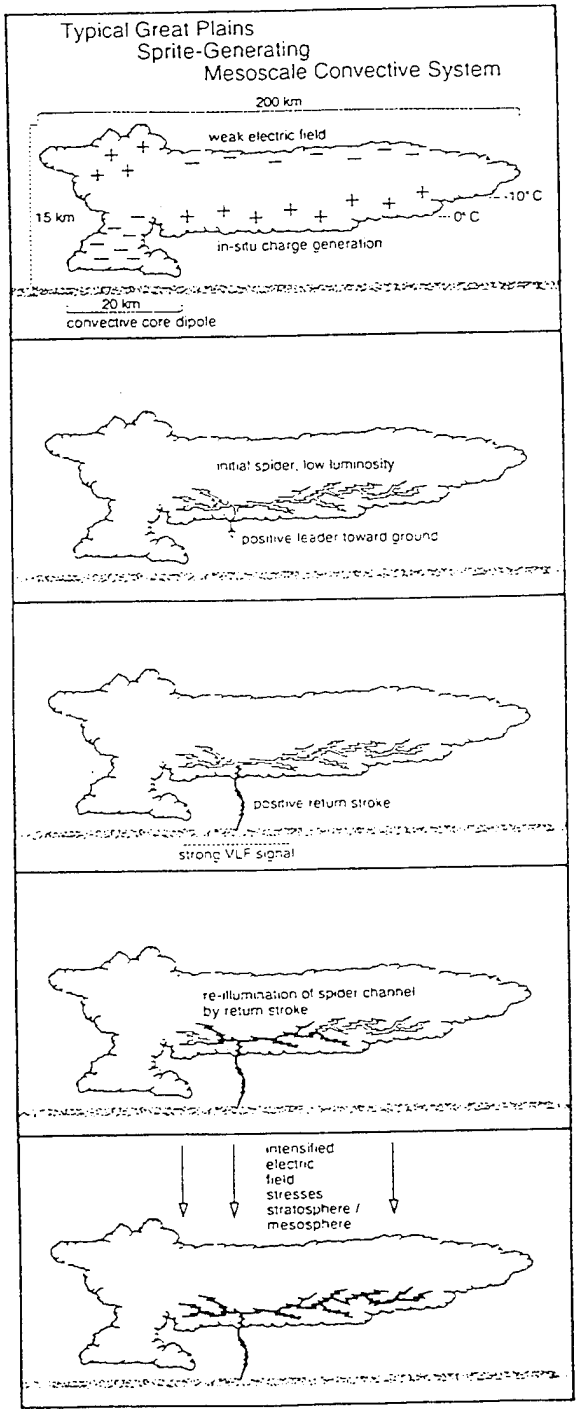


Fig. 2. A schematic of the hypothesized cloud morphology and electrical discharge mechanisms believed to be responsible for the sprite phenomenon in the stratosphere and mesosphere due to the quasi-electrostatic mechanism. This model is appropriate for midwestern mesoscale convective systems but may not be globally valid.

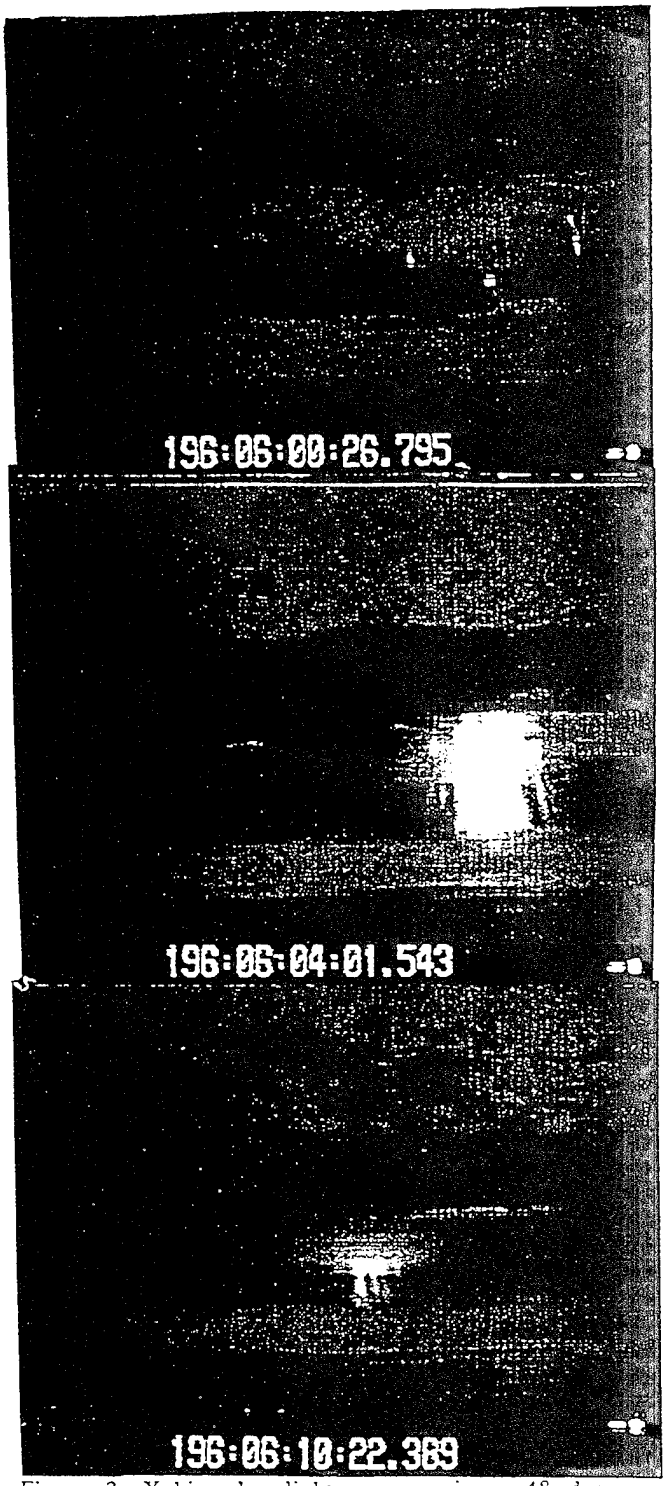


Figure 3. Xybion low-light camera views, 48 degree horizontal field of view, looking east from YRFS, 15 July 1995 (a) 06:00:26.795 UTC showing apparent blue jet (center) surrounded by ring of several small sprites, (b) 06:04:01.543 UTC, large sprite partially obscured by clouds, and (c) 06:10:22.383, elve (horizontal glow) and sprite (vertical tendrils) occurring during same 117 ms video field.

The focus of this paper is to begin quantification of the types of storms that generate sprites above the U.S. High Plains. Previous experience (Lyons 1995) has suggested that only the larger MCS (radar precipitation area >25,000 km^2) generate sprites, and only if they also possess significant numbers of high peak current, positive polarity cloud-to-ground (CG) discharges detected by the National Lightning Detection Network (NLDN), preferably in a bi-polar pattern. During 1995, we monitored a wide variety of convective storm types demonstrating a variety of CG lightning characteristics in order to confirm or revise our working hypothesis. Initial results suggest that the above criteria were essentially correct, though some slightly smaller systems (on the order of 20,000 km^2) could also generate a few sprites. On 25 nights during the 1995 experiment, both storm characteristics and viewing conditions were deemed conducive to sprite observations. On all of these 25 nights, at least one sprite was detected. Numerous smaller (sometimes severe) convective storms were also monitored, but without evidence of sprites. It has been previously demonstrated that sprites are uniquely associated with powerful cloud-to-ground (CG) flashes having positive polarity (Lyons 1995; Boccippio et al. 1995). Do sprites occur systematically over any special type(s) of convective systems? A working hypothesis (Fig. 2) suggests that an extensive mesoscale stratiform precipitation region is required. This allows for horizontally extensive in-cloud lightning discharges (sometimes called dendritic or "spider" lightning) in association with a large +CG flash. Balloon-born field mills have demonstrated the presence of large regions of positively charged anvil cloud (Marshall et al. 1995). It is suspected that the transfer of large quantities of charge within the broad anvil in association with the +CG event is a critical aspect of the sprite formation process.

A large MCS developed over eastern Colorado and Kansas after 0100 UTC 15 July 1995. Low clouds along the Front Range prevented viewing until shortly before 0600 UTC. However, as clouds cleared, in one eleven minute period, three distinct types of mesospheric luminous transient events were noted. A "blue jet," first identified by Wescott et al. (1995) rose upwards from behind a cloud bank over a six video field period (100 ms). It was characterized by a bright leading front and a glowing trail (rather like a roman candle). It was oriented about 25 degrees off the vertical, and subtended an angle of approximately 10 degrees. During the forth video field (50-67 ms into the event) a "ring" of small sprites appeared around the ascending jet (Fig. 3a). These sprites lasted only for one video field. The event was most likely related to a 36 kamp +CG flash at 0600.26.650 UTC at 89° azimuth and 326 km from YRFS. At 0604.01 UTC a very large and bright sprite, displaying downward diverging tendrils, was imaged (Fig. 3b). It was most likely associated with a 116 kamp +CG occurring at 0604.01.526 UTC at a 93° azimuth and 290 km range. The next event (Fig. 3c), at 0610.22 UTC, included an example of another recently identified phenomena called "elves." This is most likely the bright, very transient disk-shaped enhancement of the airglow layer seen in Space Shuttle video reported by Boeck et al. (1992). Similar disk-shaped glows were noted by Lyons et al. (1994). Fukunishi et al. (1995) confirmed that elves and sprites were distinct phenomena using a fast response (15 μs) photometer operated in conjunction with the low-light video

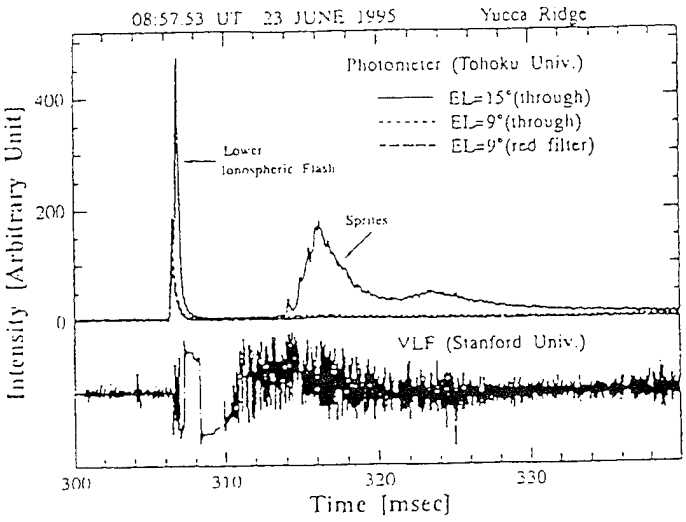
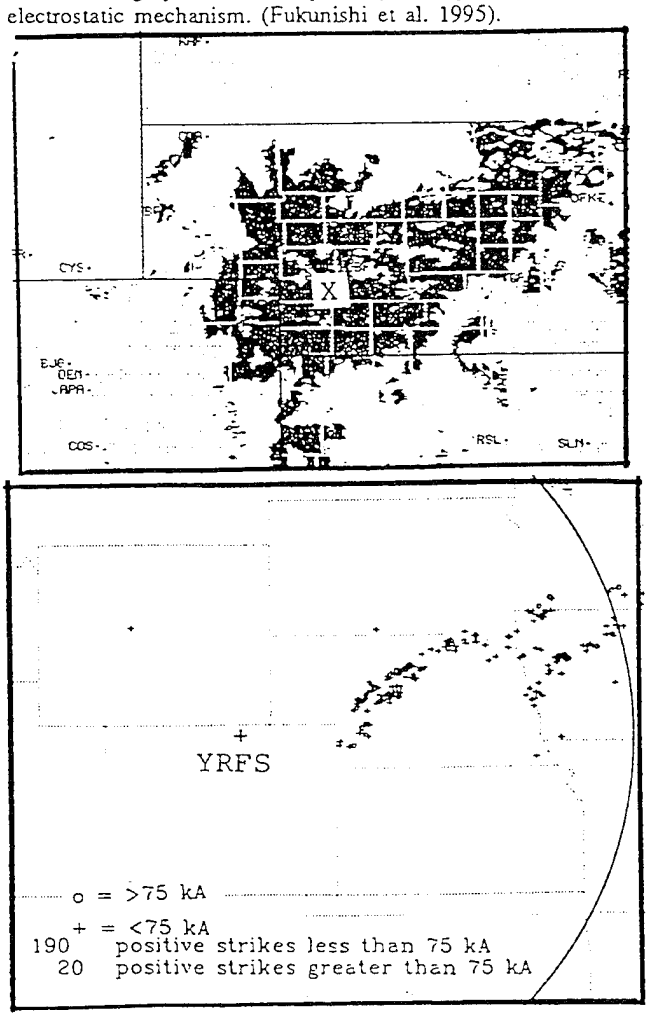


Fig. 4. High speed photometer traces revealing that a broad disk shaped glowing region and vertically oriented sprite-like tendrils were two separate events. The first (an elve) lasted less than 1 ms and was likely a response to the lightning CG's EMP whereas the dimmer but much longer lasting sprite occurred roughly 10 ms later, possibly in response to a quasi-electrostatic mechanism. (Fukunishi et al. 1995).



systems at YRFS (Fig. 4). Numerous cases of a broad, disk-shaped glows at altitudes (85-105 km) slightly higher than the sprites lasting less than 1 ms were noted, some with and many without associated sprites (the sprites generally occurring 5 to 30 ms after the elve). The +CG associated with the sprite/elve combination occurring at 0610.22.387 UTC, was located at 83° azimuth and 325 km range, and had a very high peak current of 185 kamp.

By 0600 UTC, the MCS had developed a region of radar reflectivity of 140,000 km^2 (Fig. 5). NLDN data revealed a large number of large +CG events within the system (Fig. 6). Many more sprites may have occurred than were detected by the YRFS cameras due to the patchy intervening cloud cover. During the 660 seconds spanning the three events shown here, there were a total of 282 CGs (26 flash/min rate). Of these, 24 CGs (8.5%) were positive in polarity. The average peak current for -CGs was 27 kamp, for +CGs (without sprites or elves) was 37 kamp, and for the 3 +CGs having sprites, jets or elves, 112 kamp. The tendency of sprite-related +CGs to have substantially higher reported peak currents as detected by the NLDN was noted by Boccippio et al. (1995). For the night of 24 July 1995, preliminary analysis shows that +CGs associated with sprites (64 cases) averaged 58 kamp, whereas those associated with elves or elves and sprites combined were even stronger, averaging 104 kamp for 14 cases (Earle Williams, personal communication). Thus very preliminary analysis suggests that jets, sprites and elves all are associated with +CG events, but that those producing elves may have, on the average, the strongest peak currents. The "X" in Fig. 5 marks the approximate location of the three +CGs apparently involved in the events shown in Fig. 3. As has been noted in previous analyses, these electrical discharges are located within the large stratiform region rather than directly above the high reflectivity core of the MCS. Stereo sprite images from Yucca Ridge and the USAF Academy 250 km to the south indicated that sprites were typically centered within ±25 km of their parent +CG event (Perry Malcolm, personal communication). This allows reasonable estimates of the vertical and horizontal sprite dimensions using single image photogrammetry using the NLDN-provided range to the sprite as well as relating sprites to the underlying storm structure. It is hypothesized that the sprite is in some way induced by extremely large and complex electrical discharges within the MCS anvil. Such horizontal anvil discharges are known to extend for over 100 km. The +CG may be part of this complex discharge. On a number of occasions sprites have been noted "dancing" in sync with cloud flashes propagating within extensive anvil canopies. All of the hard physical data obtained during SPRITES'95 are being assembled in part to begin testing the various theoretical models of sprites and elves of which Pasko et al. (1995) is an example.

Fig. 5 (left middle) Radar reflectivity chart (6 DVIP levels) from the national composite radar map at 0600 UTC 15 July 1995. "X" marks the general location of the several events shown in Fig. 3

Fig. 6. (left lower) NLDN lighting flash data from 0600-0700 UTC 15 July showing only positive CG events, with peak current amplitudes of greater than and less than 75 kamp indicated.

4. FUTURE RESEARCH REQUIREMENTS

Future activities should in part center of establishing the relationship between the in-cloud electrical processes and the sprite, jet and elve phenomena. This would include the coordination of ground-based and airborne remote sensing using a variety of optical and RF sensors, using the fixed base installation to guide aircraft reconnaissance. Ideally such a program would include the deployment of a system, such as the LDAR developed at the Kennedy Space Center, which is capable of three-dimensional mapping of the entire electrical discharge within the MCS. Coordination of such measurements with overflights of the Optical Transient Detector (OTD) now being tested by NASA would further assist in obtaining an integrated picture of the interrelationship of sprites and the electrical discharges within their parent cloud. Finally, a combination of low stratospheric balloon-borne field mills (and other sensors), along with a station-keeping instrumented UAV (unmanned aerospace vehicle) would complete the sensing suite for an ideal experiment.

5. ACKNOWLEDGMENTS

This work was supported under an SBIR Phase II contract (NAS10-12113) from the NASA Kennedy Space Center. We acknowledge the contributions of many including Carl Lennon, Launa Maier and Ron Bentti (NASA KSC), O. H. Vaughan, Jr. (NASA MSFC), John R. Winckler (University of Minnesota), Robert J. Nemzek (Los Alamos, NM), Perry R. Malcolm (U.S. Air Force Academy), Earle Williams, Charles Wong, Robert Boldi and Dennis Boccippio (MIT), William Sturz (Xybion Electronics Corp.), John Molitoris and Colin Price (Lawrence Livermore National Lab), Russ Armstrong, Ian Baker and Jeff Shorter (Mission Research Corp.), Michael Taylor and Peter Mace (Utah State Univ.), David Rust and Thomas Marshall (NSSL/Univ. of Mississippi), Umran Inan, Bill Trabucco, Alex Slingeland and Steve Reising (STAR Lab, Stanford University), Y, Fukunishi, Y. Takahashi and M. Kubota (Tohoku University), Richard Dowden (University of Otago), Stephen Mende and Rick Rairden (Lockheed), Les Hale and Lee Marshall (Pennsylvania State Univ.), Frank Djuth (GeoScience, Inc.), Roland Tsunoda (SRI International), Davis Sentman and Eugene Wescott (University of Alaska) and especially Thomas Nelson and Liv Lyons (ASTeR).

6. REFERENCES

Boccippio, D.J., E.R. Williams, W.A. Lyons, I. Baker and R. Boldi, 1995: Sprites, Q-bursts and positive ground strokes. Science, 269, 1088-1091.

Boeck, W.L., O.H. Vaughan, Jr., R.J. Blakeslee, B. Vonnegut and M. Brook, 1992: Lightning induced brightening of the airglow layer. Geophys. Res. Lett., 19, 99-102.

Boeck, W.L., O.H. Vaughan, Jr., R.L. Blakeslee, B. Vonnegut, M. Brook and J. McKune 1995: Observations of lightning in the stratosphere. J. Geophys. Res., 100, 11465-1475.

Franz, R.C., R. J. Nemzek and J.R. Winckler, 1990: Television image of a large upward electrical discharge above a thunderstorm system. Science, 249, 48-51.

Fukunishi, H., Y. Takahashi, M. Kubota, K. Sakanoi, U.S. Inan and W.A. Lyons, 1996: Elves: Lightning-induced transient luminous events in the lower ionosphere. Nature (in press).

Inan, U.S., T.F. Bell, V. Pasko, D.D. Sentman, E.M. Wescott, and W.A. Lyons, 1995: VLF signatures of ionospheric disturbances associated with sprites. Geophys. Res. Lett., (in press).

Lyons, W.A., 1995: The relationship of large luminous stratospheric events to the anvil structure and cloud-to-ground discharges of their parent mesoscale convective system. Preprints, Conf. on Cloud Physics, AMS, Dallas, 541-546.

Lyons, W.A., I.T. Baker, T.E. Nelson, J.R. Winckler, R.J. Nemzek, P.R. Malcolm, E.R. Williams and D. Boccippio, 1994: The 1994 Colorado SPRITE Campaign (abstract), EOS, 75, vol. 44, p. 108. Also a 20 minute video tape, available from ASTeR, Inc.

Lyons, W.A., 1994: Characteristics of luminous structures in the stratosphere above thunderstorms as imaged by low-light video. Geophysical Research Letters, 21, 875-878.

Lyons, W.A. and E.R. Williams, 1994: Some characteristics of cloud-to-stratosphere "lightning" and consideration for its detection. Preprints, Symposium on the Global Electrical Circuit, Global Change and the Meteorological Applications of Lightning Information, AMS, Nashville, 8 pp.

Lyons, W.A., 1994: Low-light video observations of frequent luminous structures in the stratosphere above thunderstorms. Mon. Wea. Rev., 122, 1940-1946.

Marshall, T.C., W.D. Rust and M. Stolzenburg, 1995: Electrical structure and updraft speeds in thunderstorms over the southern Great Plains. J. Geophys. Res., 100, 1001-1015.

Mende, S.B., R.L. Rairden, G.R. Swenson and W.A. Lyons, 1995: Sprite spectra: N_2 first positive band identification. Geophys. Res. Lett. 22, 2633-2636.

Pasko, V. P., U.S. Inan, Y. N. Taranenko and T.F. Bell, 1995: Heating, ionization and upward discharges in the mesosphere due to intense quasi-electrostatic thunderstorm fields. Geophys. Res. Letts., 22, 365-368.

Toynbee, H. and T. Mackenzie, 1886: title unknown. Nature, 33, p. 245.

Sentman, D.D., E.M. Wescott, D. L. Osborne, D. L. Hampton and M.J. Heavner, 1995: Preliminary results from the Sprites94 aircraft campaign 1. Red sprites. Geophys. Res. Lett., 22, 1205-1208.

Wescott, E.M., D. Sentman, D. Osborne, D. Hampton and M. Heavner, 1995: Preliminary results from the Sprites94 aircraft campaign: 2, Blue jets. Geophys. Res. Lett., 22, 1209-1212.

Wilson, C.T.R., 1956: A theory of thundercloud electricity, Proc. Royal Soc. London, 236, 297-317

Winckler, J.R., W.A. Lyons, T. E. Nelson and R.J. Nemzek, 1995: New high-resolution ground based studies of sprites, J. Geophysical Res. (submitted).

12th IIPS for Meteor., Oceanog. and Hydrology
American Meteorological Society
Atlanta, GA 28 Jan. - 2 Feb. 1996

PROCESSING, INTEGRATING AND DISPLAYING DISPARATE DATA SOURCES FROM THE SPRITES '95 FIELD PROGRAM

Walter A. Lyons and Thomas E. Nelson

ASTeR, Inc./FMA, Inc.
Ft. Collins, CO 80524

1. INTRODUCTION

Rarely during a career is one in the position of designing and conducting a major field measurement program for a phenomenon the existence of which was suspect, its characteristics unknown, and for which no proper names even yet existed. The SPRITES'95 field campaign was indeed the culmination of such an endeavor. While anecdotal reports of unusual "lightning" discharging upward into the stratosphere or beyond have been reported for over a century (Toynbee and Mackenzie 1886) and were theoretically postulated by Wilson (1956), little import was accorded such "cloud-to-space" lightning reports. Indeed, if known at all to atmospheric scientists, it was through Corliss (1977) who also included tales of turtles encased in hailstones and half-meter wide snowflakes, not to mention accounts of spontaneous human combustion. But the atmospheric science community was galvanized by a chance 1989 observation from a low-light video system which documented a huge, transient (<33 ms) luminous structure extending 30-40 km above a thunderstorm top (Franz et al. 1990). Subsequently, similar features were suspected after reviews of low-light video images of distant storm systems taken onboard the Space Shuttle (Vaughan et al., 1992). These new observations, combined with a detailed literature search (Lyons and Williams, 1993 and 1994) suggested these luminous events, now generally called sprites (Fig. 1), occur with some regularity and were not a totally rare or "freak" event. Concern that such a potentially energetic event occurs within layers of the upper atmosphere routinely traversed by aerospace vehicles, in particular the Space Shuttle, led to NASA funding a multi-year research effort. The goal was to document how frequently such sprites occurred, how they might be detected, and thereafter what their potential impacts might be. The initial observation phase of the study was conducted at the Yucca Ridge Field Station, located 20 km northeast of Ft. Collins, CO. This site has a panoramic view of the deep convection which develops over the U.S. High Plains, often during the night hours (Fig. 2). The challenge of the project: how to study a phenomenon only a few fleeting glimpses of which had ever been obtained and about which virtually no information existed as to its frequency, phenomenology or physical characteristics. The initial approach selected (Lyons, 1994 a,b) deployed low-light video camera systems which, it has proven, can detect sprite events to distances approaching 1000 km. On a single night (7 July 1993) as many as 240 sprites were detected from the Yucca Ridge site. Far from being rare, at least over the U.S. High Plains, the sprite is a common event above mesoscale convective systems (MCS).

Corresponding author address: Walter A. Lyons, CCM, ASTeR, Inc./FMA Inc., 46050 Weld County Road 13, Ft. Collins, CO 80524, (Voice) 970-568-7664; (Fax) 970-482-8627; e-mail: lyonsccm@csn.org

2. THE 1995 SPRITE CAMPAIGN

Given that the sprite was a frequent summer occurrence above the central U.S., how best to characterize its structure and its impacts? Do sprites occur systematically over any special type(s) of convective systems? Can they be predicted? What are their optical spectra? Do they have signatures in the UV and infrared? Were they associated with perturbations in RF signals at various frequencies?

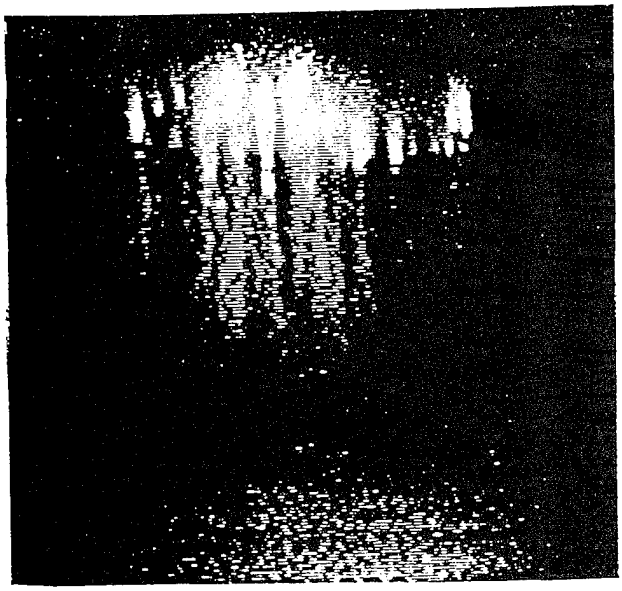
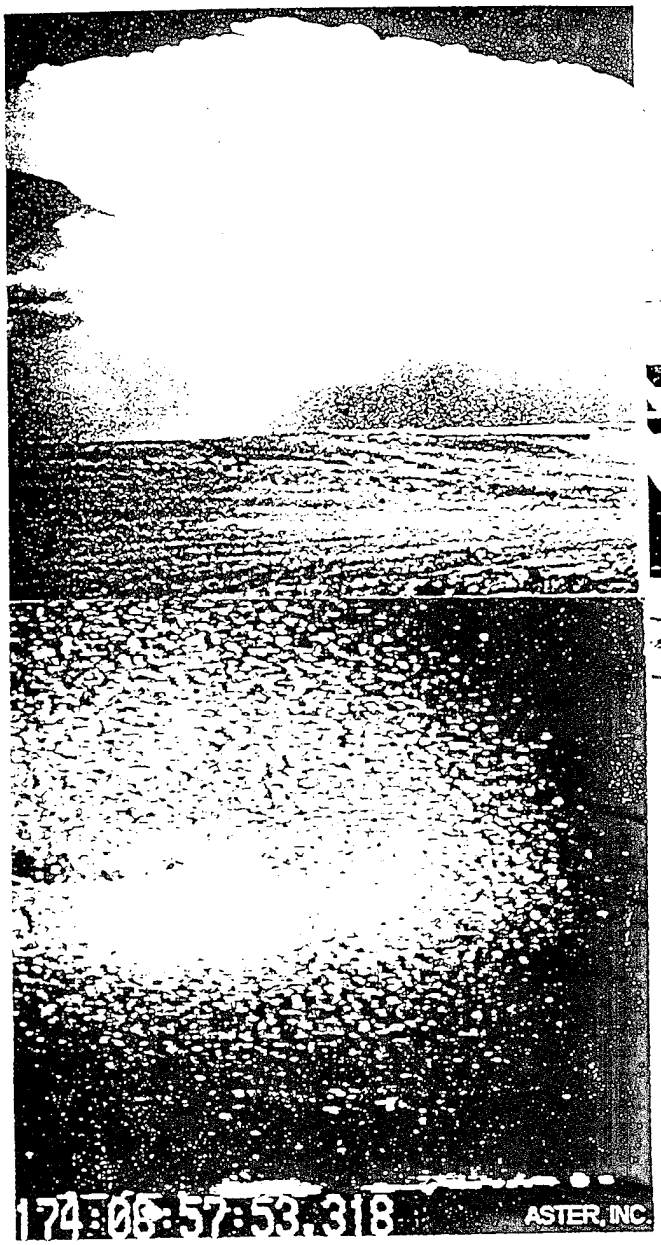


Fig. 1 A large sprite extending to 92 km altitude, 400 km east of the low-light camera site. The glow above the horizon is the parent CG lightning in the distant storm.



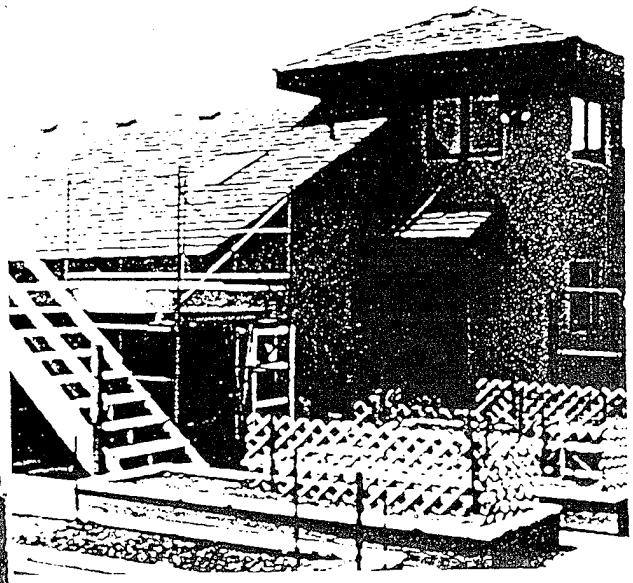


Fig. 2 (top) Panoramic view of mesoscale convective systems as viewed from Yucca Ridge Field Station near Ft. Collins, CO and the instrumentation platform built at the site to collocate the various cameras and optical systems.

Fig. 3. (bottom) Single video field (16.7 ms) from Xybion low-light camera showing both a sprite (bright spot) and the brightening of the airglow layer, an amorphous ionospheric glow, now tentatively called elves.

Can they be detected by radar? These are some of the questions that needed to be addressed in order to assess their potential impact on the middle and atmosphere. The SPRITES'95 campaign was designed to deploy as many different types of passive and active remote sensing systems as possible in a coordinated study of individual sprite events as well as their parent storms. Table 1 summarizes the participating organizations and sensors deployed during a two month period (June through early August) at Yucca Ridge. A key objective was to coordinate observations in space and time. Since preliminary studies (Winckler et al. 1995) had shown the sprite time scales to be on the order of 10-100 ms, precise time coordination was a requisite. This was accomplished by use of GPS time (2 μs nominal accuracy) for all systems. When possible, video cameras were further electronically synched so each 17 ms video field record would be temporally coincident. Selected RF signals were continuously recorded on the four-channel audio of the SVHS tapes, and also digitally sampled at 40 kHz and 200 kHz using LabView on a Pentium-based PC in 1500 ms segments coincident with sprites. RF receivers included a 1-10 kHz system suitable for whistler detection, broader bandwidth VLF systems (1-50 and 1-100 kHz), and narrow band receivers at selected frequencies. In addition, coordinated measurements of ELF signals (3-30 Hz) were made at the Rhode Island Schumann resonance station of the Massachusetts Institute of Technology (Williams 1992). Initial results from 1994 tests and the full 1995 field program, in which large and disparate data sets were collected and integrated, have already begun to yield significant results. In addition to sprites, we have confirmed from ground-based sensors the presence of brief (≈ 1 ms) brightenings of the airglow layer (tentatively called "elves") as a distinct phenomenon (Fig. 3). This was made possible by the use of high speed pointing photometers with 15 μsec resolution. A video field (Fig 3) shows a sprite which is surrounded by a broad amorphous glowing region. The high temporal resolution photometer traces revealed that this single 17 ms video

Table 1. Participants in SPRITES'95

ASTeR, Inc., Fort Collins, Colorado.
Walter Lyons, Project Director; Tom Nelson
dual Xybion ISS-255 low light imagers • ELF and VLF measurements • photometer • meteorological data

Tohoku University, Sendai, Japan
Hiroshi Fukunishi, Yukihiro Takahashi, Minoru Kubota
multiple (4) high speed 1°x10° FOV photometers

University of Otago, Dunedin, New Zealand
Richard Dowden - OMNIPAL VLF interferometry (3 sites)

STAR Laboratory, Stanford University
Umran Inan, Steve Reising, Bill Trabucco, Alex Slingeland
narrowband VLF from mobile van • VLF narrowband and broadband (0-30 kHz) VLF at YR • VLF observations in conjugate region (Palmer station)

GeoSpace Research, Inc.
Frank Djuth, Matt Cox, Ken Williams - bi-static propagation (WWV at 2.5, 5, 10, 15 and 20 mHz and 28 mHz transmissions)

Utah State University, Space Dynamics Lab
Michael Taylor, Peter Mace
all sky airglow camera • highly sensitive low-light vidicon and SIT cameras (filtered)

Lawrence Livermore National Laboratory
John Molitoris, Colin Price
IROCS - infrared optical camera system • fast optical imager • large format optical imager

Massachusetts Institute of Technology
Earle Williams, Charles Wong, Bob Boldi
Schumann Resonance/Q-bursts at Rhode Island and YR sites

NOAA, National Severe Storms Laboratory
David Rust, Thomas Marshall
lightning video and balloon-borne electric field mill

Pennsylvania State University
Les Hale, Lee Marshall
ELF and VLF measurements

Los Alamos National Laboratory
Robert Franz, Dave Smith
measurements of TIPPS and SIPPS

Mission Research Corporation, Nashua, NH.
Russ Armstrong, Jeff Shorter
CCD cameras system and photometer

Lockheed Space and Missile
Steve Mende, Rick Rairden
imaging spectrometer and low-light video

SRI International
Roland Tsunoda, John Buonocore
tunable radar system (2-30 mHz)

NASA Kennedy Space Center & MSFC
Carl Lennon, Launa Maier, Otha Vaughan, Jr.
LDAR • ELF/Q-burst measurements • OTD

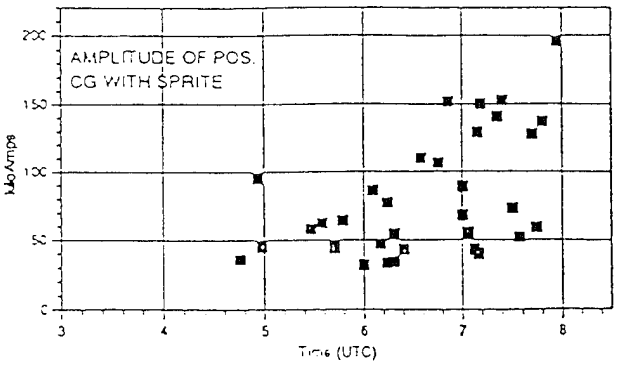


Fig. 4. The peak current (kiloamps) of each +CG associated with a sprite plotted versus time for the night of 6 August 1994.

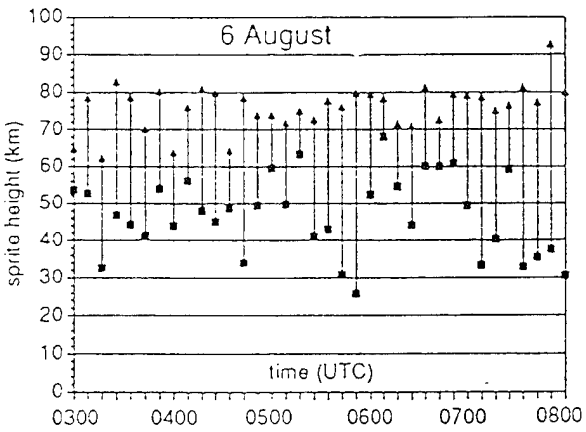


Fig. 5. Estimated altitude of the top and base of the sprite as a function of time. Single image photogrammetry assumes that the sprite is centered above its parent +CG.

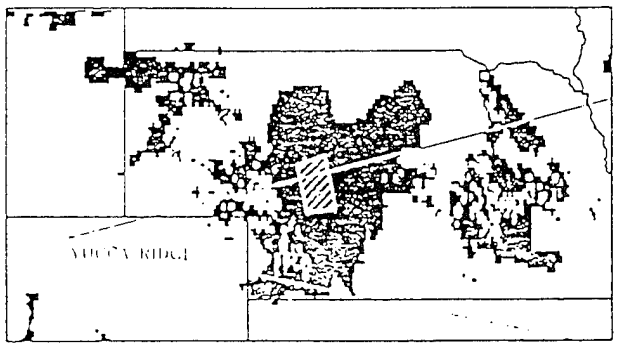


Fig. 6. Combined workstation display showing radar reflectivity, the field-of-view of the low-light camera and the estimated location of the sprite based upon its observed azimuth (video) and range (assumed the same as the associated +CG flash).

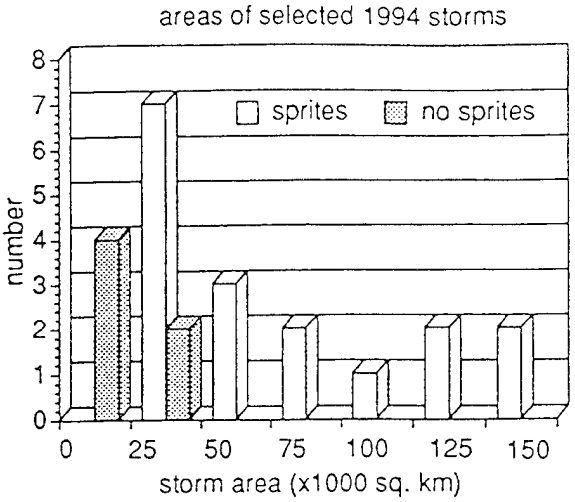


Fig. 7. Areas of storms that did and did not generate sprites, based upon areal reflectivity from composite digital national radar, suggesting a minimum critical anvil size for a sprite-producing storm.

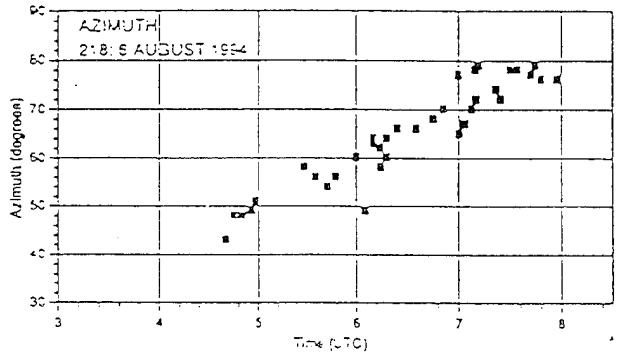


Fig. 8. The azimuth (degrees) of the center of each sprite observed on a given night plotted as a function of time, illustrating the clustering of sprites in a relatively small portion of the anvil.

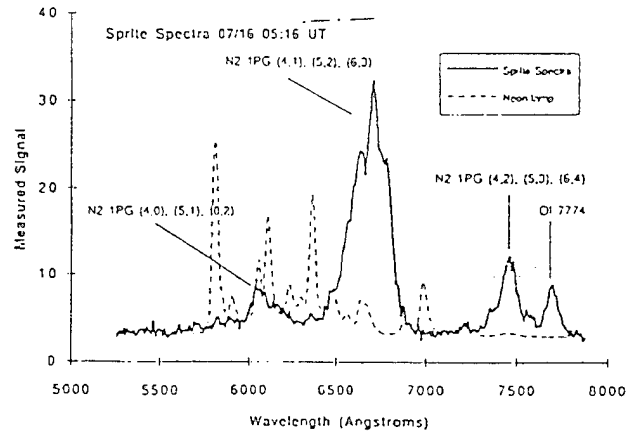


Fig. 9. Optical spectra of a sprite showing the N_2 first positive bands (Mende et al., 1995), an observation made possible by coordinating low-light video imagers and pointing spectrometers.

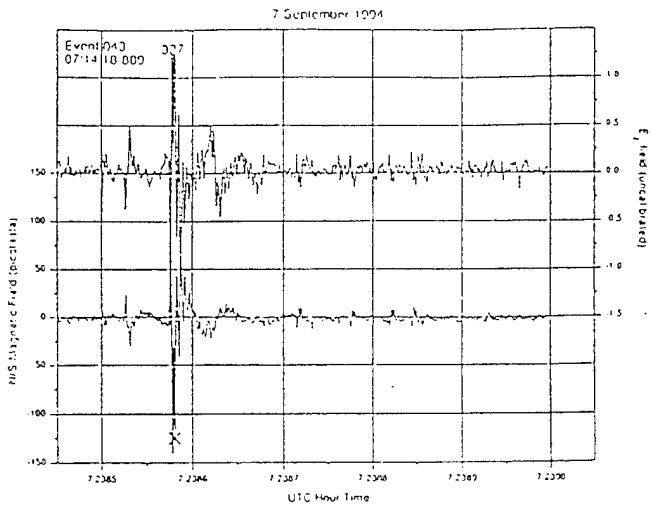


Fig. 10. Q-bursts signature in the ELF Schumann resonance bands which is coincident with the occurrence of a very large +CG flash measured by the NLDN (Boccippio et al., 1995). This pattern suggests Q-bursts serve as a diagnostic for sprite events.

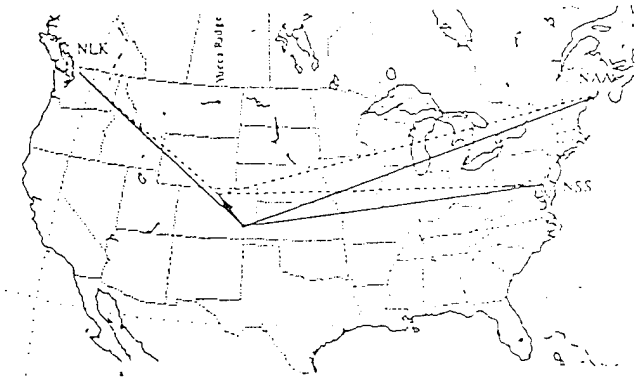


Fig. 11. Location of three VLF transmitters, the Yucca Ridge Omnipal receiver (point of arrow) and the sprite (small circle, 300 km SE), the same event as shown in Fig. 3. (Dowden, personal communication).

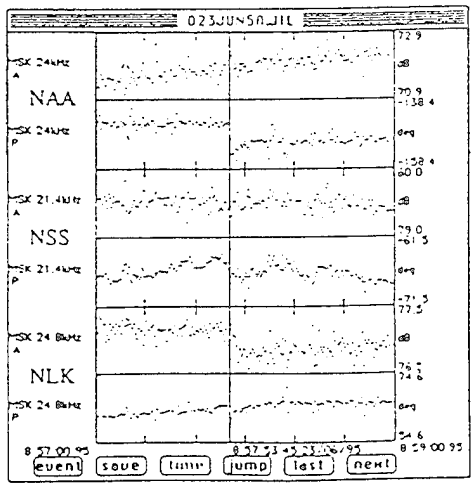


Fig. 12. Changes in phase and amplitude of Navy VLF transmissions due to the sprite discussed in Figs. 3 and 11. (Dowden, personal communication).

field contains two distinct phenomena: the 1 ms elve event followed about 10 ms later by the onset of the sprite, which then lasted for several more video fields. Cloud-to-ground (CG) flash data from the National Lightning Detection Network (NLDN) were compared (using millisecond timing coincidences) with the sprite events. It was immediately discovered (Lyons, 1995) that sprites were almost uniquely correlated with positive CG events, often with amplitudes substantially larger than the average for such events (Fig. 4). Stereo sprite images from Yucca Ridge and the USAF Academy 250 km to the south indicated that sprites were typically centered within ±25 km of their parent +CG event. This allows reasonable estimates of the vertical and horizontal sprite dimensions using single image photogrammetry using the NLDN-provided range to the sprite (Fig. 5). Combining the NLDN CG data, the estimated sprite locations and regional radar reflectivity composites at 4 km resolution (from Kavouras, Inc.) revealed that the sprite occurred not over the high reflectivity core but rather in the large stratiform precipitation region associated with the MCS anvil. This was accomplished by integrating and displaying these data using an IBM RS/6000 workstation and NCAR graphics (Fig. 6). Successive case studies showed that not only were sprites associated with unusually energetic +CG events, but that the parent storm required a precipitation area generally >20,000 km^2 (Fig. 7). These two simple forecast rules resulted in a virtual 100% forecast accuracy for sprite storms during the 1995 campaign. Detailed study of the sprite location in the video images also revealed that the sprites tended to concentrate in relatively small portions of the MCS anvil. The tight clustering of sprite azimuths viewed by the Yucca Ridge cameras (Fig. 8) typifies this behavior. Aside from raising interesting questions about the sprite-generating mechanism itself, it also suggests that once sprites are detected, close-up views can be attained by pointing telescopic systems at distant storms. This allowed us to acquire numerous optical spectra (Fig. 9) from storms as distant at 500-600 km (Mende et al. 1995). The ability to detect sprites and associate them with their parent CG lightning has resulted in a variety of discoveries relating sprites to VLF and ELF radio propagation. Boccippio et al. (1995) found a strong correlation between sprites, large +CGs and a global ELF phenomenon called the Q-burst. It has long been assumed that the background "hum" of natural radio at frequencies below 100 Hz was due to the integrated effect of all the planet's lightning discharges. Occasional large excursions (Fig. 10) called Q-bursts remained something of a mystery. Apparently the intense RF emissions from sprite-producing +CGs are the source of this ringing of the earth-ionospheric cavity on a global scale. At higher frequencies (20 kHz), researchers from the University of Otago (New Zealand) have found that continuous VLF transmissions from several U.S. Navy sites are distorted both in phase and amplitude as shown in Figs. 11 and 12 (R. Dowden, personal communication, 1995). By comparing these time-tagged perturbations with the corresponding low-light videos, it will be possible to verify whether this effect can be used as the basis of an automated sprite detection system that would work during cloudy conditions and daylight, when low-light video systems are unsuitable.

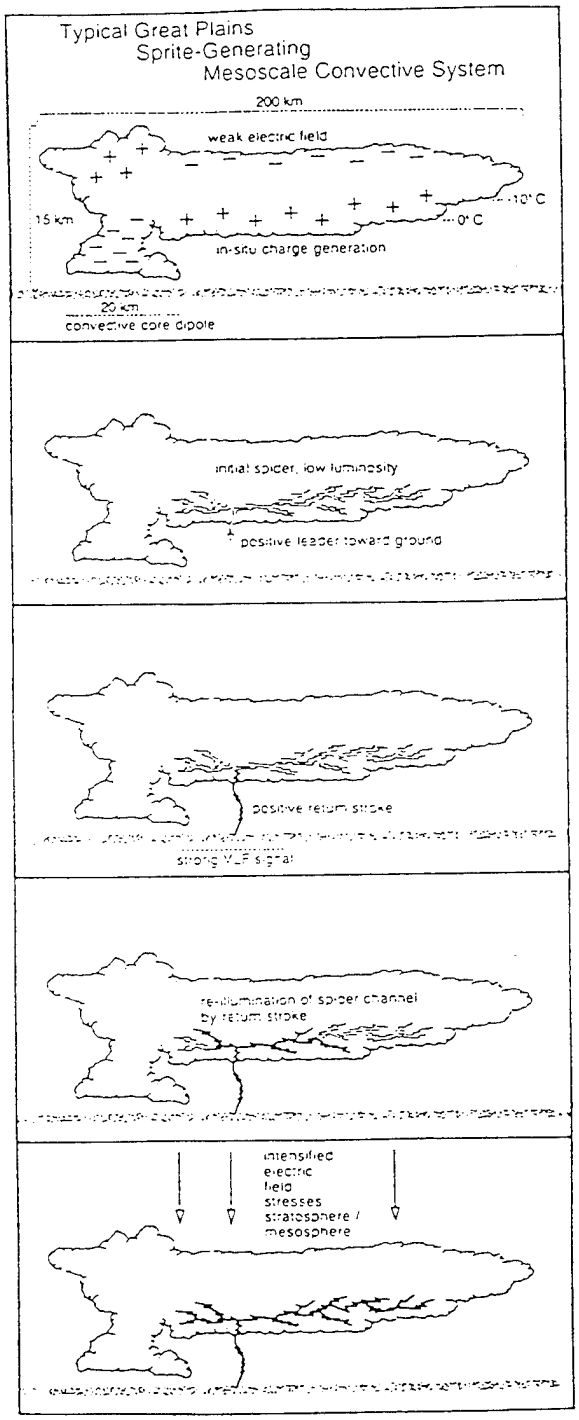


Fig. 13. A schematic of the hypothesized cloud morphology and electrical discharge mechanisms believed to be responsible for the sprite phenomenon in the stratosphere and mesosphere above midwestern mesoscale convective systems.

3. CONCLUSIONS

The collection of various optical and RF data types using common GPS-time bases has already yielded extensive results. The use of a common precision time base may also allow for coordination with other field programs operating at the same time, such as mountain-top measurements similar to those described by Sentman et al. (1995). The variety of coordinated observations has already permitted a physical model of the sprite-generating mechanism in large MCS storms to emerge (Lyons, 1995) (Fig. 13). The sprites appear associated spatially and temporally with positive CG events, often of much larger than average peak current amplitude and multiplicity. It is hypothesized that the sprite is in some way induced by extremely large and complex electrical discharges within the MCS anvil. Such horizontal anvil discharges are known to extend for over 100 km. The +CG may be part of this complex discharge. On a number of occasions sprites have been noted "dancing" in sync with cloud flashes propagating within extensive anvil canopies. Hard physical data are being assembled against which various theoretical models of sprites can be tested (Pasko et al., 1995). Future activities may include the coordination of ground-based and airborne sprite imaging (Sentman et al., 1995). Ongoing analyses will continue integrating NLDN lightning, digital radar and GOES data for comprehensive studies of sprite storms. The morphology of sprites and elves are being investigated using new digital, non-linear video editing systems which allow motion studies while maintaining perfect synch with the simultaneously recorded 4-channel audio of the various VLF signals.

4. ACKNOWLEDGMENTS

This work was supported under an SBIR Phase II contract (NAS10-12113) from the NASA Kennedy Space Center. We acknowledge the contributions of many including Carl Lennon, Launa Maier and Ron Bentti (NASA KSC), O. H. Vaughan, Jr. (NASA MSFC), John R. Winckler (University of Minnesota), Robert J. Nemzek (Los Alamos, NM), Perry R. Malcolm (U.S. Air Force Academy), Earle Williams, Charles Wong, Robert Boldi and Dennis Boccippio (MIT), William Sturz (Xybion Electronics Corp.), John Molitoris and Colin Price (Lawrence Livermore National Lab), Russ Armstrong, Ian Baker and Jeff Shorter (Mission Research Corp.), Michael Taylor and Peter Mace (Utah State Univ.), David Rust and Thomas Marshall (NSSL/Univ. of Mississippi), Umran Inan, Bill Trabucco, Alex Slingeland and Steve Reising (STAR Lab, Stanford University), Y. Fukunishi, Y. Takahashi and M. Kubota (Tohoku University), Richard Dowden (University of Otago), Stephen Mende and Rick Rairden (Lockheed), Les Hale and Lee Marshall (Pennsylvania State Univ.), Frank Djuth (GeoScience, Inc.), Roland Tsunoda (SRI International), and Liv Lyons (ASTeR).

5. REFERENCES

Boccippio, D.J., E.R. Williams, W.A. Lyons, I. Baker and R. Boldi, 1995: Sprites, Q-bursts and positive ground strokes. Science, in press.

Corliss, W.L., 1977: Handbook of Unusual Natural Phenomena. The Source Book Project, Glen Arm, MD 21057

Franz, R.C., R. J. Nemzek and J.R. Winckler, 1990: Television image of a large upward electrical discharge above a thunderstorm system. Science, 249, 48-51.

Lyons, W.A., 1995: The relationship of large luminous stratospheric events to the anvil structure and cloud-to-ground discharges of their parent mesoscale convective system. Preprints, Conf. on Cloud Physics, AMS, Dallas, 541-546.

Lyons, W.A., 1994: Characteristics of luminous structures in the stratosphere above thunderstorms as imaged by low-light video. Geophysical Research Letters, 21, 875-878.

Lyons, W.A. and E.R. Williams, 1994: Some characteristics of cloud-to-stratosphere "lightning" and consideration for its detection. Preprints, Symposium on the Global Electrical Circuit, Global Change and the Meteorological Applications of Lightning Information, AMS, Nashville, 8 pp.

Lyons, W.A., 1994: Low-light video observations of frequent luminous structures in the stratosphere above thunderstorms. Mon. Wea. Rev., 122, 1940-1946.

Lyons, W.A. and E.R. Williams, 1993: Preliminary investigations of the phenomenology of cloud-to-stratosphere lightning discharges. Preprints, Conference on Atmospheric Electricity, American Meteorological Society, St. Louis, 8 pp.

Mende, S.B., R.L. Rairden, G.R. Swenson and W.A. Lyons, 1995: Sprite spectra: N_2 first positive band identification. Geophys. Res. Lett. (submitted).

Pasko, V. P., U.S. Inan, Y. N. Taranenko and T.F. Bell, 1995: Heating, ionization and upward discharges in the mesosphere due to intense quasi-electrostatic thunderstorm fields. Geophys. Res. Letts., 22, 365-368.

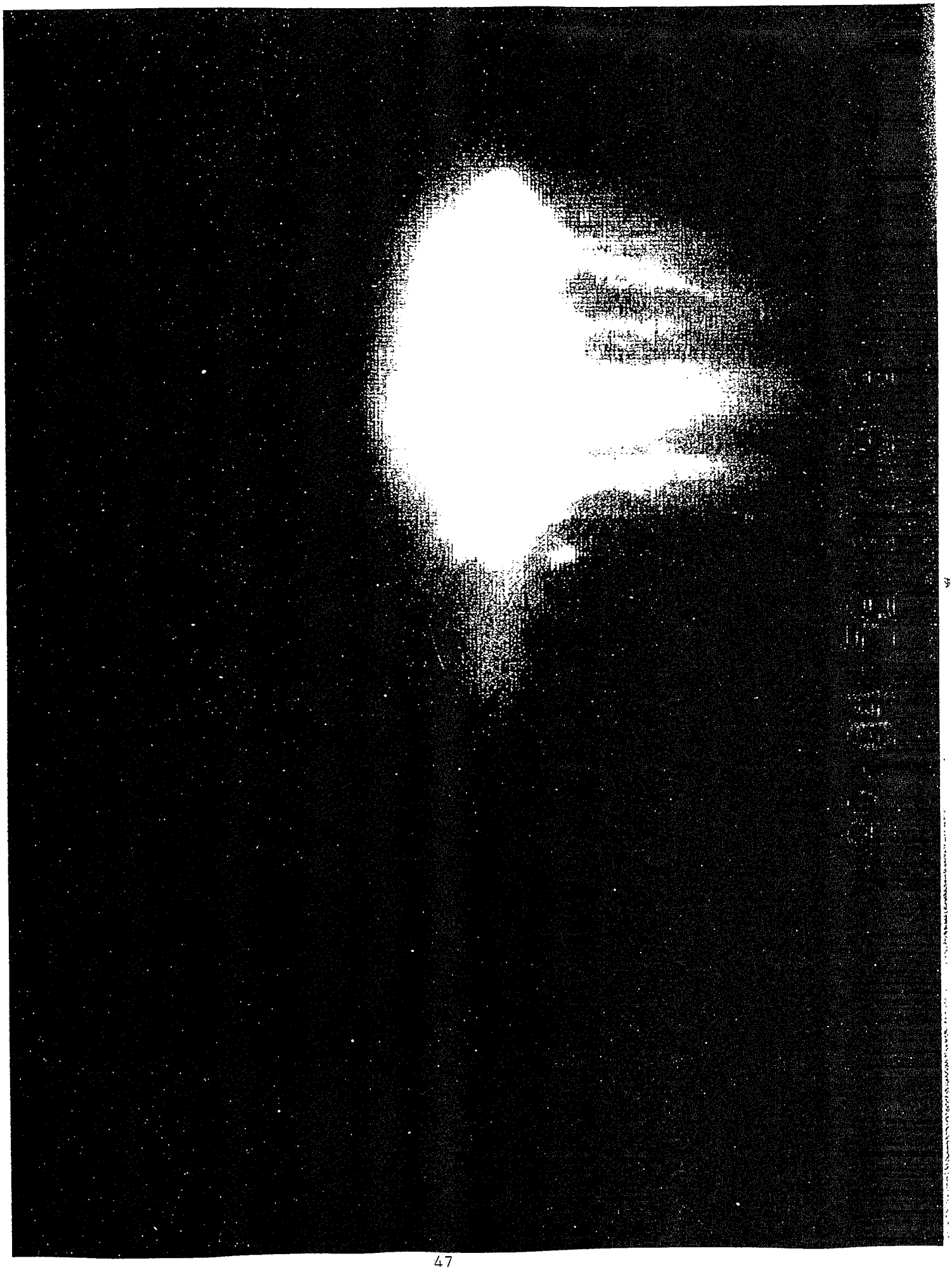
Toynbee, H. and T. Mackenzie, 1886: title unknown. Nature, 33, p. 245.

Sentman, D.D., E.M. Wescott, D. L. Osborne, D. L. Hampton and M.J. Heavner, 1995: Preliminary results from the Sprites94 aircraft campaign 1. Red sprites. Geophys. Res. Lett., 22, 1205-1208.

Williams, E.R., 1992: The Schumann Resonance: A global tropical thermometer. Science, 256, 1184-1187.

Wilson, C.T.R., 1956: A theory of thundercloud electricity, Proc. Royal Soc. London, 236, 297-317

Winckler, J.R., W.A. Lyons, T. E. Nelson and R.J. Nemzek, 1995: New high-resolution ground based studies of sprites, J. Geophysical Res. (submitted).

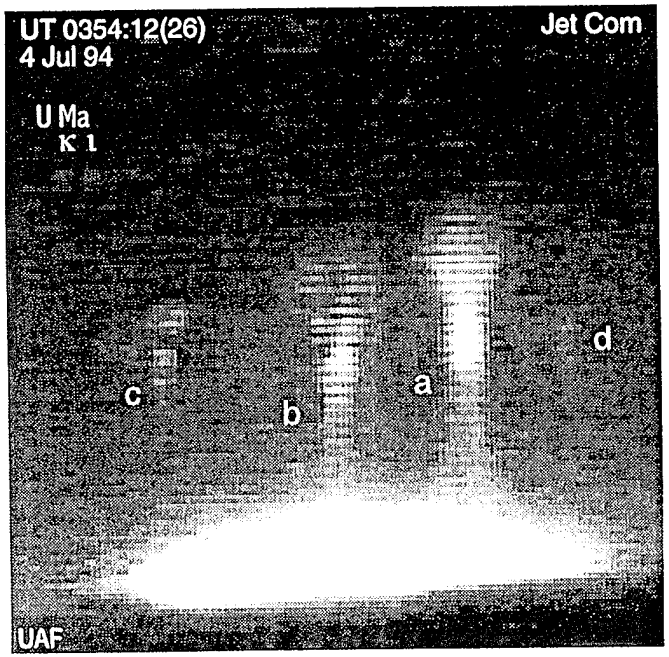


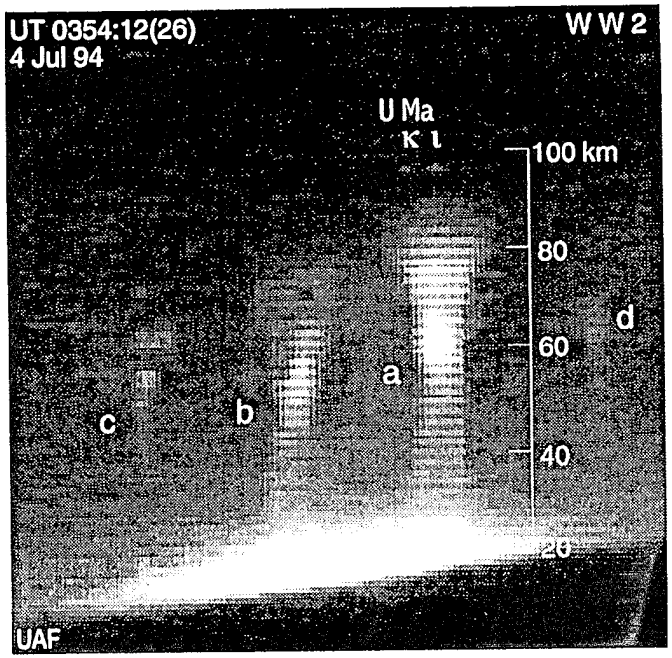
University of Alaska Aircraft and Ground Campaigns to Observe Red Sprites and Blue Jets

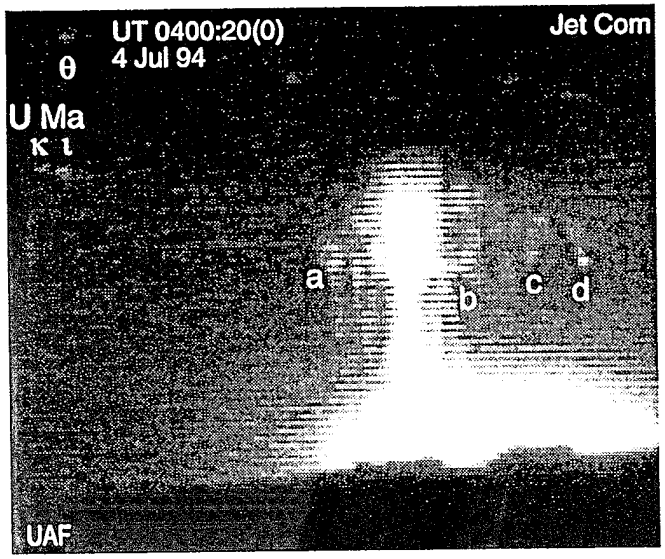
D.D. Sentman and E.M Wescott

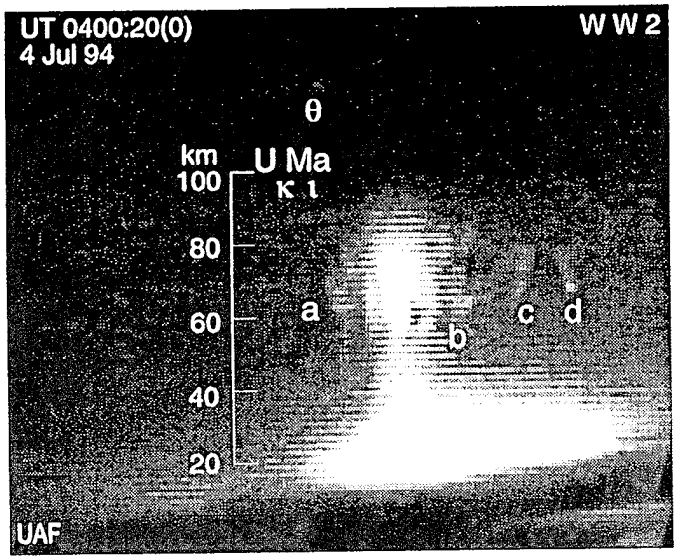
- Brazil93 A/C Campaign: Andes/Amazon
- Sprites94 A/C Campaign: Midwest Low/High Plains
- Peru95 A/C Campaign: Peru, Brazil, Bolivia
- Panama95 A/C Campaign: Central America, Colombia
- Gasp95 Ground Campaign: Colorado, High Plains

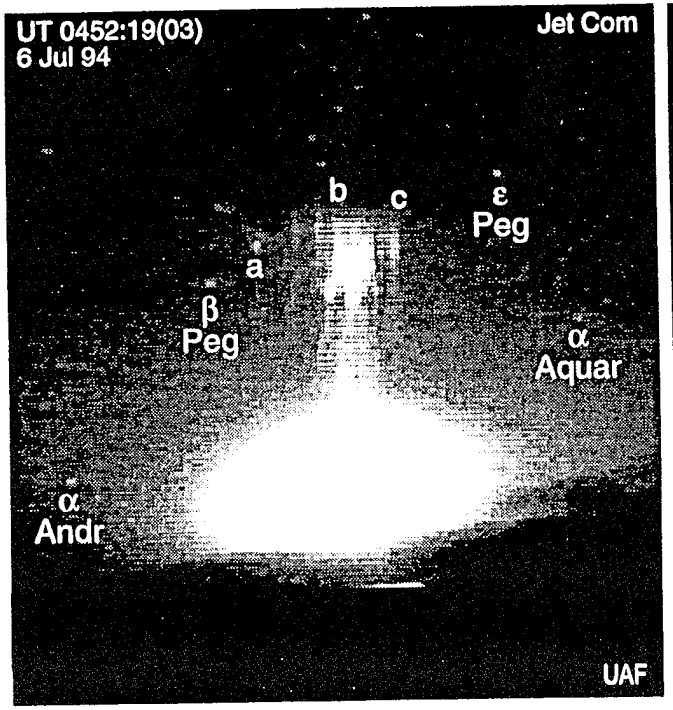
Sprites94 Aircraft Campaign

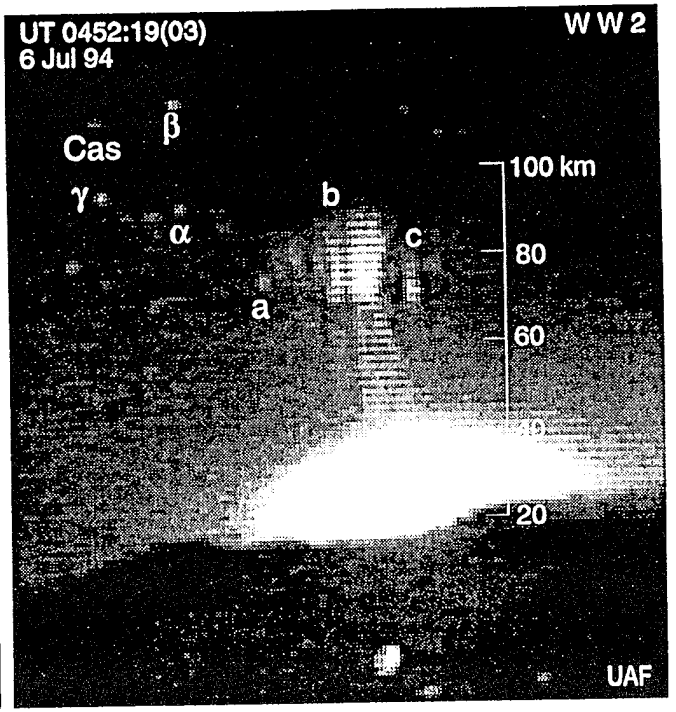

UT 0354:12(26)
4 Jul 94
Jet Com
U Ma
κ ι
a
b
c
d
UAF

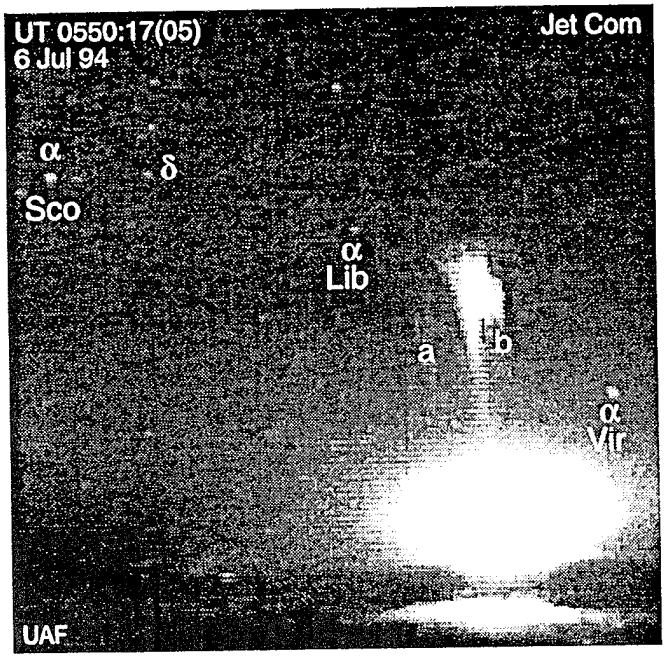

UT 0354:12(26)
4 Jul 94
W W 2
U Ma
κ ι
100 km
80
60
40
20
a
b
c
d
UAF

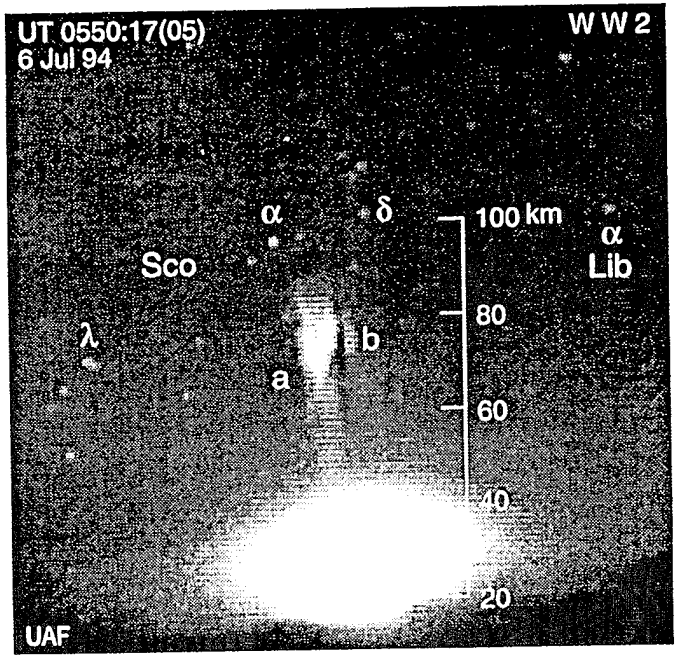

UT 0400:20(0)
4 Jul 94
Jet Com
θ
U Ma
κ ι
a
b
c
d
UAF

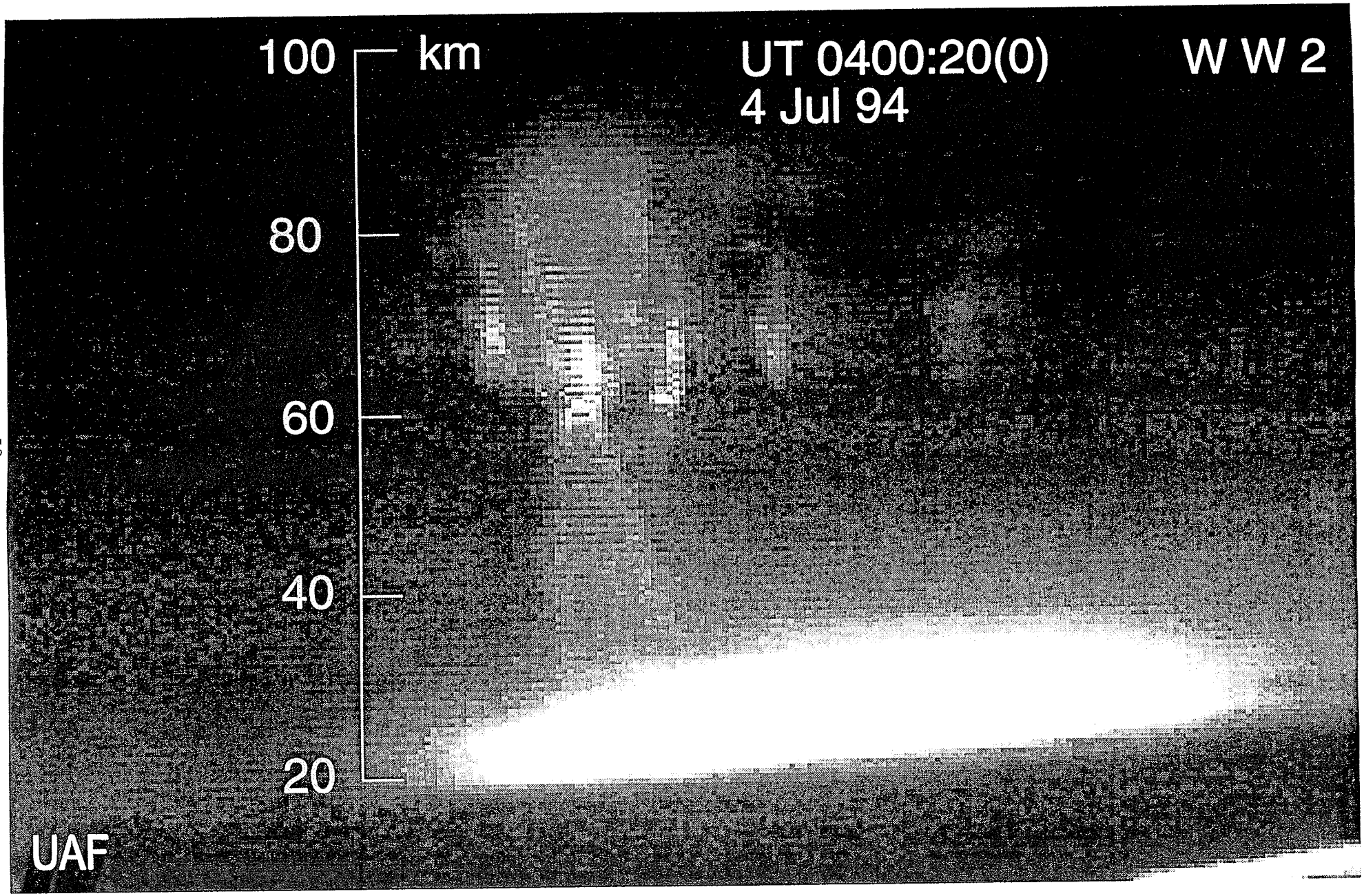

UT 0400:20(0)
4 Jul 94
W W 2
θ
km
100
80
60
40
20
U Ma
κ ι
a
b
c
d
UAF

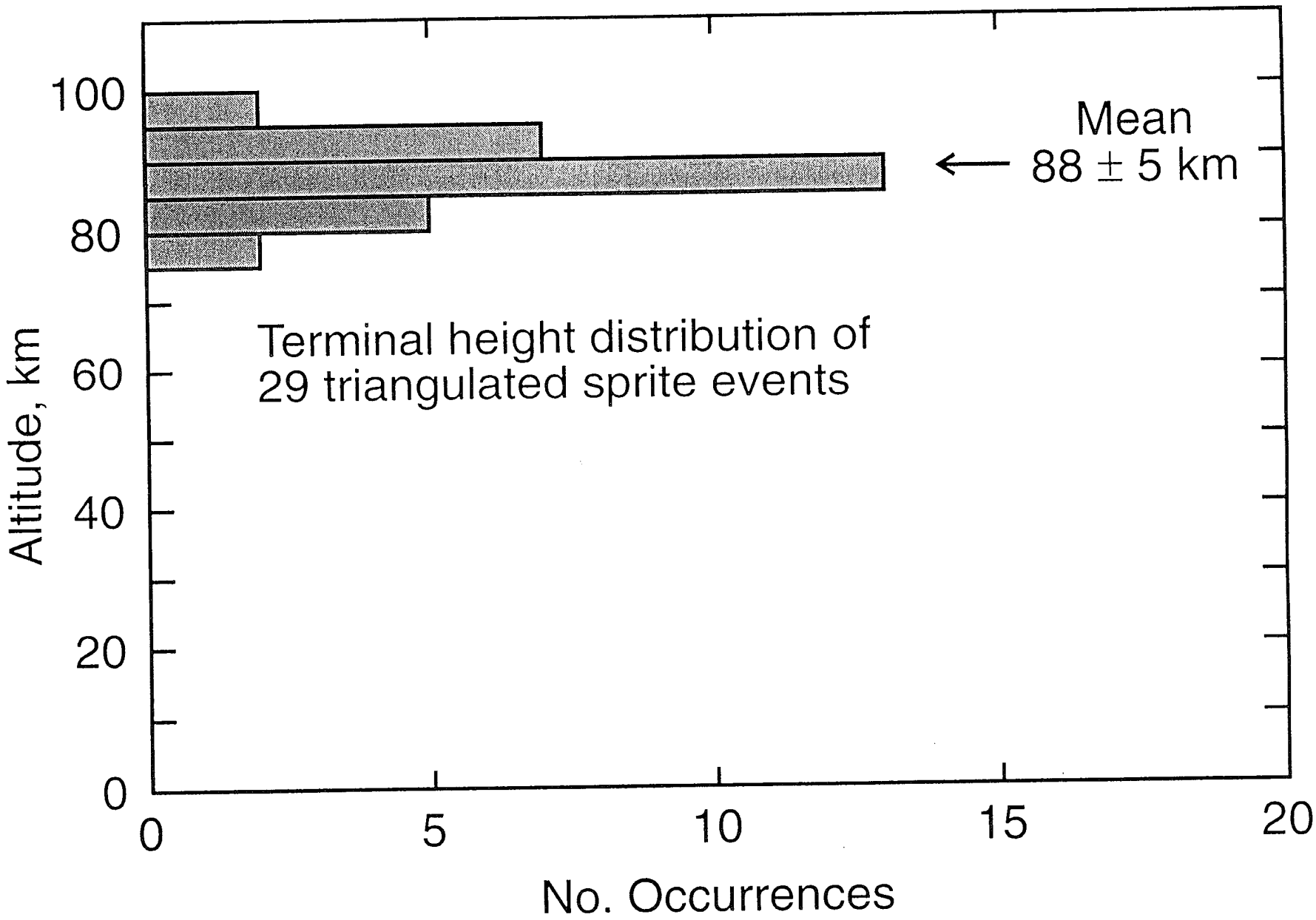

UT 0452:19(03)
6 Jul 94
Jet Com
b
c
ε
Peg
a
β
Peg
α
Aquar
α
Andr
UAF

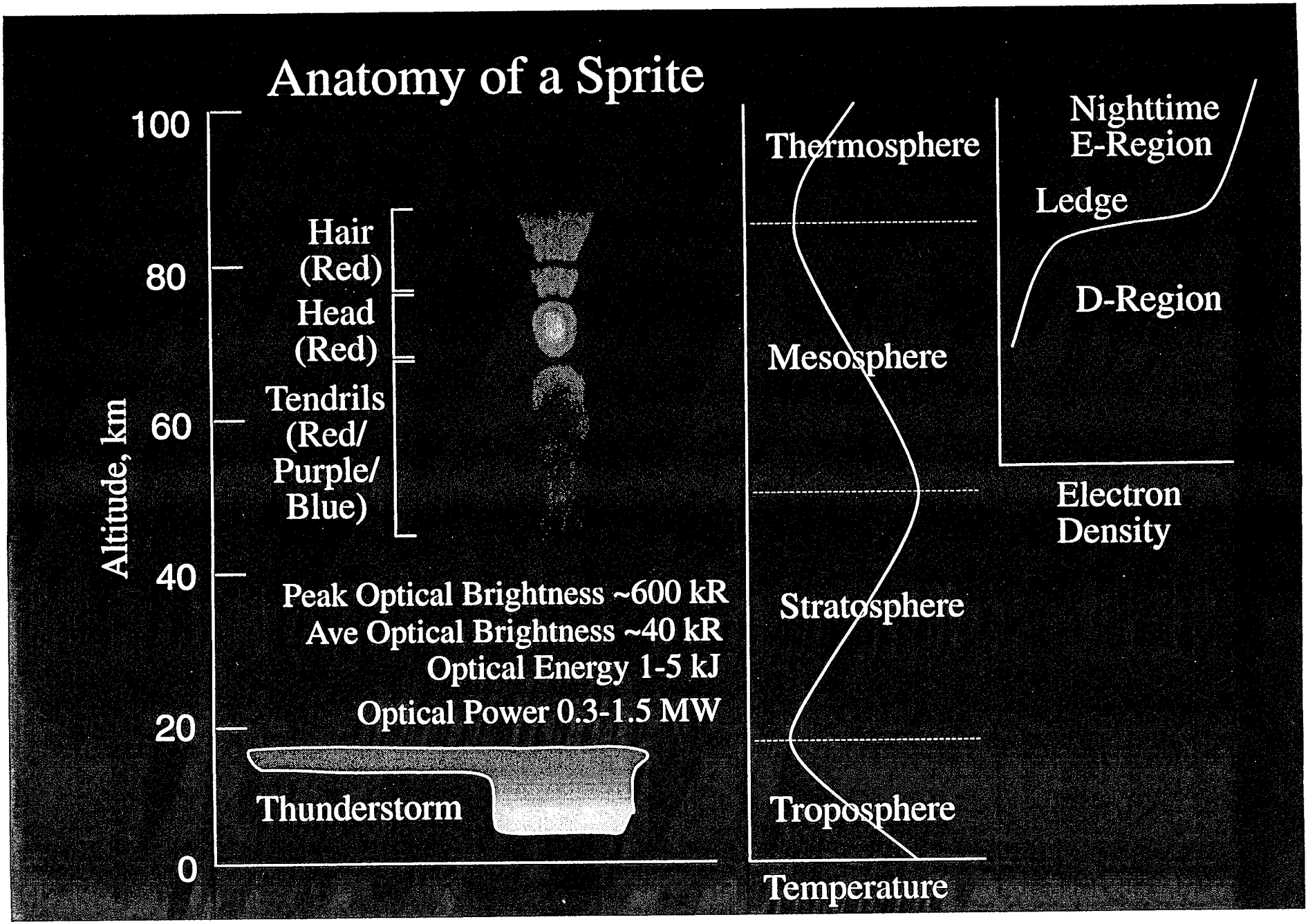

UT 0452:19(03)
6 Jul 94
W W 2
β
Cas
γ
α
b
c
a
100 km
80
60
20
UAF

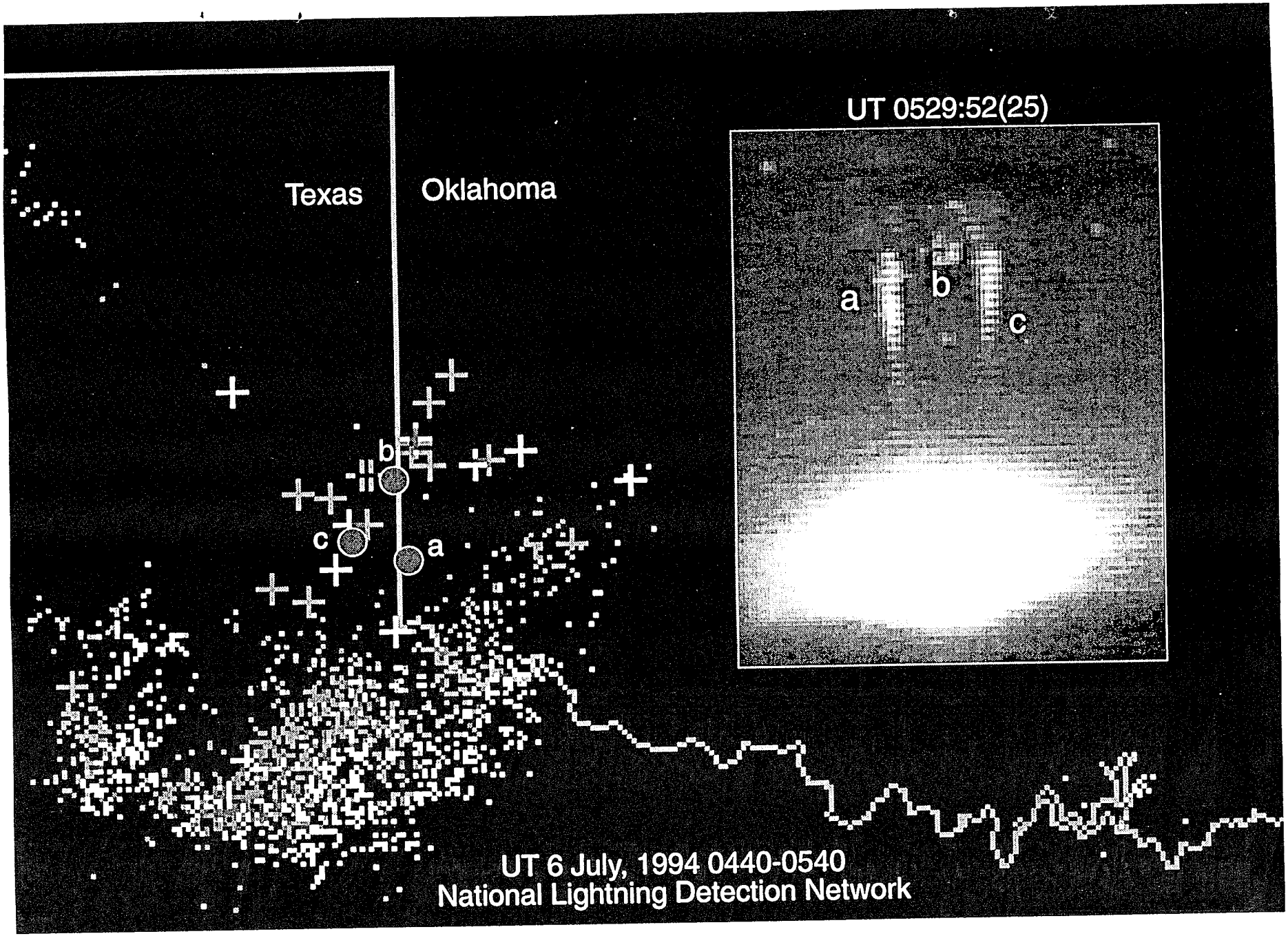

UT 0550:17(05)
6 Jul 94
Jet Com
α
δ
Sco
α
Lib
a
b
α
Vir
UAF


UT 0550:17(05)
6 Jul 94
W W 2
α
δ
Sco
100 km
α
Lib
λ
a
b
80
60
40
20
UAF


100
km
80
60
40
20
UT 0400:20(0)
4 Jul 94
W W 2
UAF


Mean
88 ± 5 km
Terminal height distribution of
29 triangulated sprite events
Altitude, km
100
80
60
40
20
0
0
5
10
15
20
No. Occurrences


Anatomy of a Sprite
100
80
60
40
20
0
Altitude, km
Hair (Red)
Head (Red)
Tendrils (Red/ Purple/ Blue)
Peak Optical Brightness ~600 kR
Ave Optical Brightness ~40 kR
Optical Energy 1-5 kJ
Optical Power 0.3-1.5 MW
Thunderstorm
Thermosphere
Mesosphere
Stratosphere
Troposphere
Temperature
Nighttime E-Region
Ledge
D-Region
Electron Density


Texas
Oklahoma
UT 0529:52(25)
a
b
c
a
b
c
UT 6 July, 1994 0440-0540
National Lightning Detection Network

Perú95

Aircraft Observations of Sprites Over Western Amazonia

University of Alaska Sprite Observation Campaign

Rationale for the Peru95 Sprites Campaign

Using low light level television systems, more than 1000 instances of upper atmospheric optical emissions (red sprites and blue jets) were recorded above thunderstorms in the American plains states in the summers of 1993 and 1994. Each observation of sprites and jets was accompanied by simultaneous intense lightning activity in a thunderstorm below. However, it is believed the bulk of Earth's atmospheric lightning takes place in equatorial thunderstorm systems, principally in the Amazon basin, the Congo basin, and the extreme western Pacific. Given the differences in the manner in which storm systems evolve in equatorial and midlatitude regions, it is therefore of interest to know if equatorial storms are also the globally dominant sources of sprites and blue jets.

During the Peru95 Aircraft Campaign we investigated sprites over storms in the thunderstorm region believed to be globally dominant. The goals of the Peru95 Aircraft Campaign were to:

- Investigate the occurrence of sprites and blue jets (upper and middle atmospheric optical emissions) above equatorial thunderstorm systems.
- Determine the optical structure and color of sprites and blue jets, and compare with midlatitude observations.
- Obtain optical spectra.
- Investigate their correlation with size and height of thunderstorm systems.
- Investigate possible effects of the equatorial ionospheric magnetic field.

Peru95 Sprites Campaign

- Observing Platform

Westwind 2 corporate jet aircraft, operated by Aero Air, Inc., Hillsboro, OR
Typical operating altitude: 39,000-45,000 ft
Cruise speed: 425 knots
Modifications to accommodate instruments
    Factory new plastic windows for left/right side viewing ports, aircraft equipment racks, 400-60 Hz power converters, lightning strike finder

- Instruments

Wide angle low light level monochrome television camera system
    Dage Model MTI VE-1000 SIT camera
    92 x 68 deg field of view
Intensified color television camera system
    Ikegami Model HL-51S, 3 separate red, green and blue SIT subsystems
Intensified slit spectrograph television camera system

Peru95 Sprites Campaign Summary

Data Flights (evenings, Local Time)

- 18 Feb 95 In transit from Brownsville, TX to Lima, Peru. Desultory lightning observed 1 hr north of Lima over Andes. No sprites detected.
- 20 Feb 95 Storms along Andes spine north and south of Lima. No sprites detected.
- 21 Feb 95 Storms in Amazon basin near Iquitos, Peru. No sprites detected.
- 24 Feb 95 Storms between Lima, Peru and Chilean border. No sprites detected.
- 25 Feb 95 Storms in Amazon basin in north-eastern Peru near Ecuador. Three groups of sprites observed.
- 26 Feb 95 Storms over Amazon basin in Peru, Colombia and Brazil. No sprites detected.
- 28 Feb 95 Storms over central Peru north of Lima. Fourteen groups of sprites observed.
- 1 Mar 95 Storms over Amazon basin in Peru and Brazil. No sprites detected.
- 2 Mar 95 Storms over central Bolivia. Three groups of sprites observed.

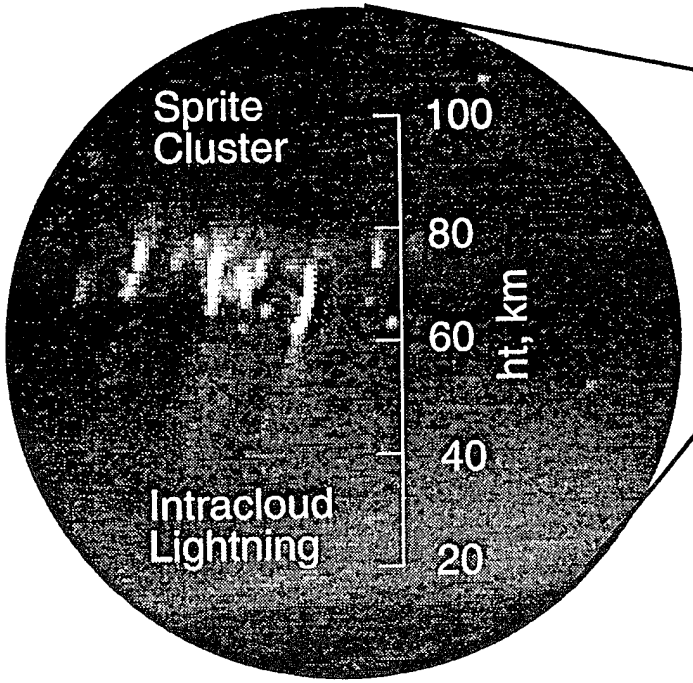
26 February 1995

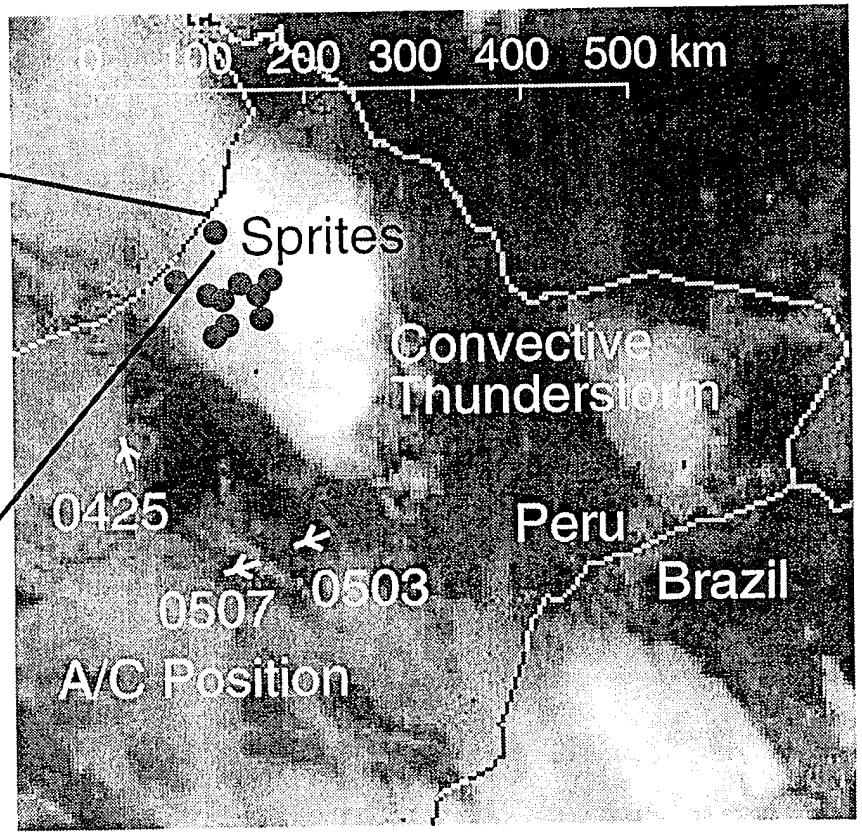
- The right hand figure shows the region of aircraft operation during an interval when images of 3 groups of sprites were captured, superimposed on a GOES 8 11 micron temperature map of storms in the area, on the first night sprites were observed during the Peru95 aircraft campaign. Dark blue corresponds to +25 C, and white to the approximately -70 C temperature of cloud tops. Regions of thunderstorm activity show up as white blobs. The positions of the sprites, assuming their terminal altitude to be 88 km, are indicated by red dots. The sprites were associated with a moderate sized convective storm system about 200 km diameter in northeast Peru near the border with Ecuador.

- The left hand figure shows a single frame from the low light level TV sequence that captured a cluster of sprites. . The cluster of sprites has a spatial distribution reminiscent of similar clusters of sprites observed over the American midwestern states. Here, the altitude scale has been set to correspond to previously triangulated sprites. Note that the horizontal extent of the cluster is about 50 km.

Aircraft View
UT 0425:53(16)

Goes 8 View
0344 UT, 26 Feb 95
11 micron IR Temperature





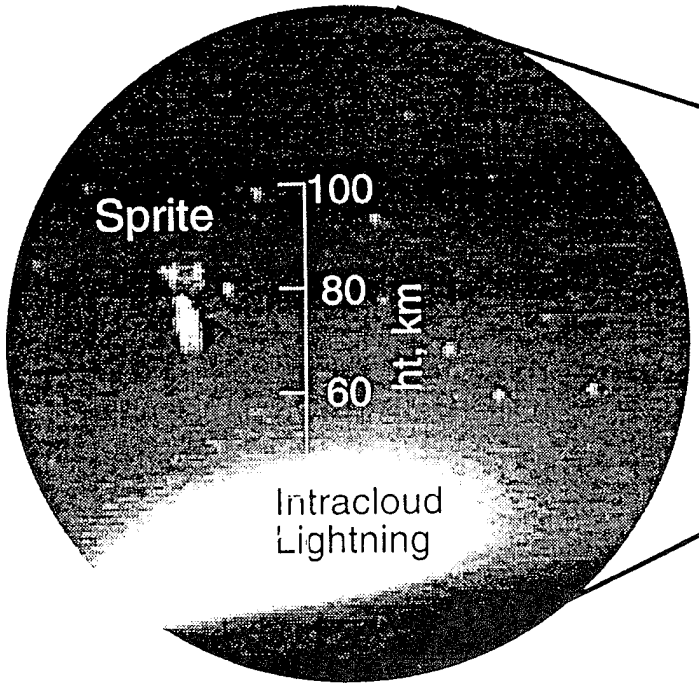
1 March 1995

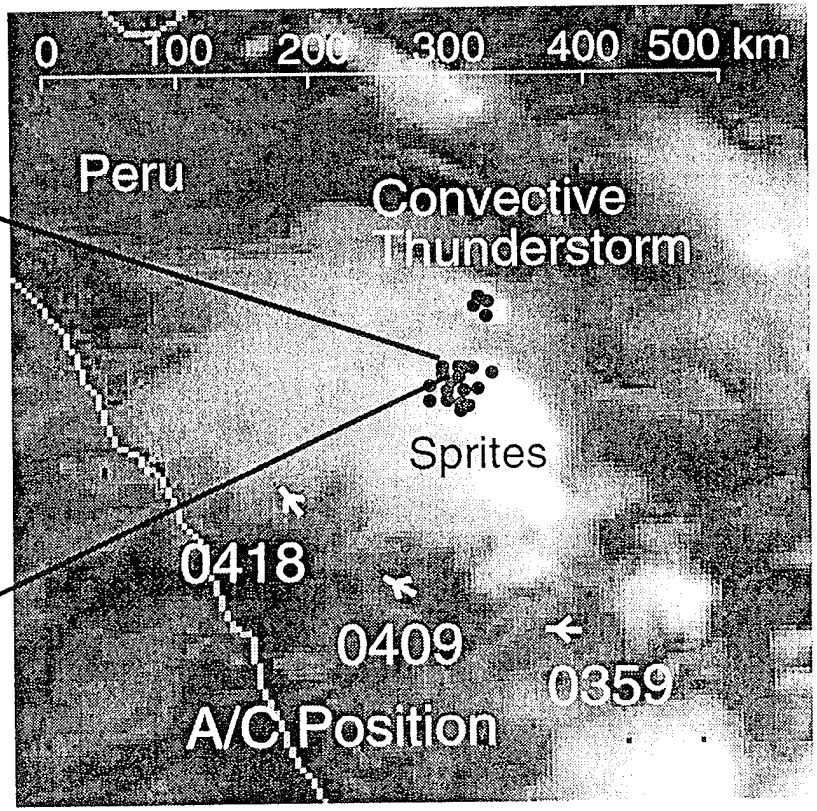
- The figure on the right shows the region of aircraft operation north of Lima during an interval when sprite images were captured. The image is from GOES 8 11 micron temperature data. Dark blue corresponds to +25 C, and white to the approximately -70 C temperature of cloud tops. Regions of thunderstorm activity show up as white blobs. The positions of the sprites are indicated by red dots. The sprites were observed from two separate regions. The larger region is a convective system about 100-150 km diameter. The smaller convection region has a diameter of about 50 km, much smaller than the minimum size previously thought to be a necessary condition for sprites to occur.

- The figure on the left shows an expanded portion of a single TV sequence that captured a sprite. Note the bright lower part separated from the upper part by a dark band. The altitude scale has been set in the same fashion as in the previous figure.

Aircraft View
UT 0405:58(13)

Goes 8 View
0344 UT, 1 Mar 95
11 micron IR Temperature



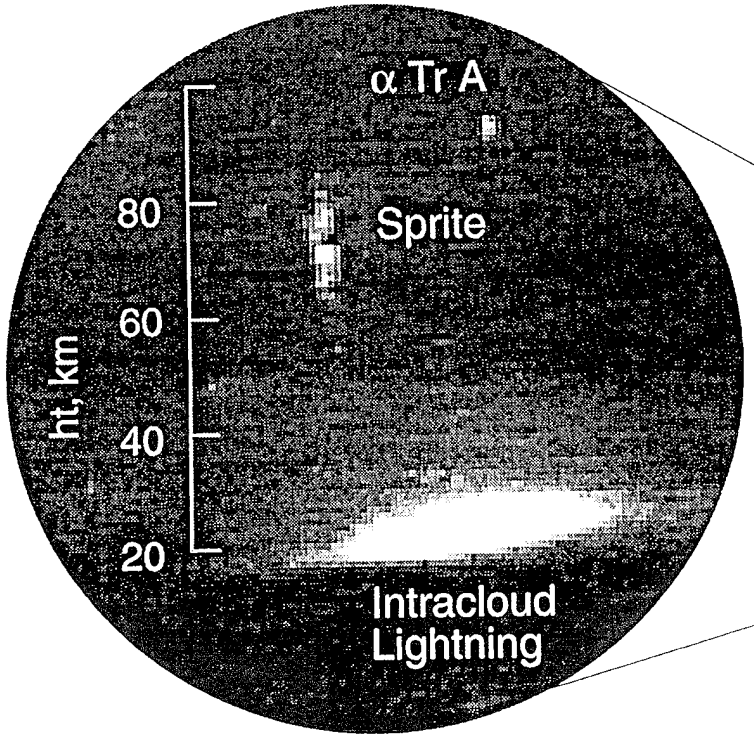


3 March 1995

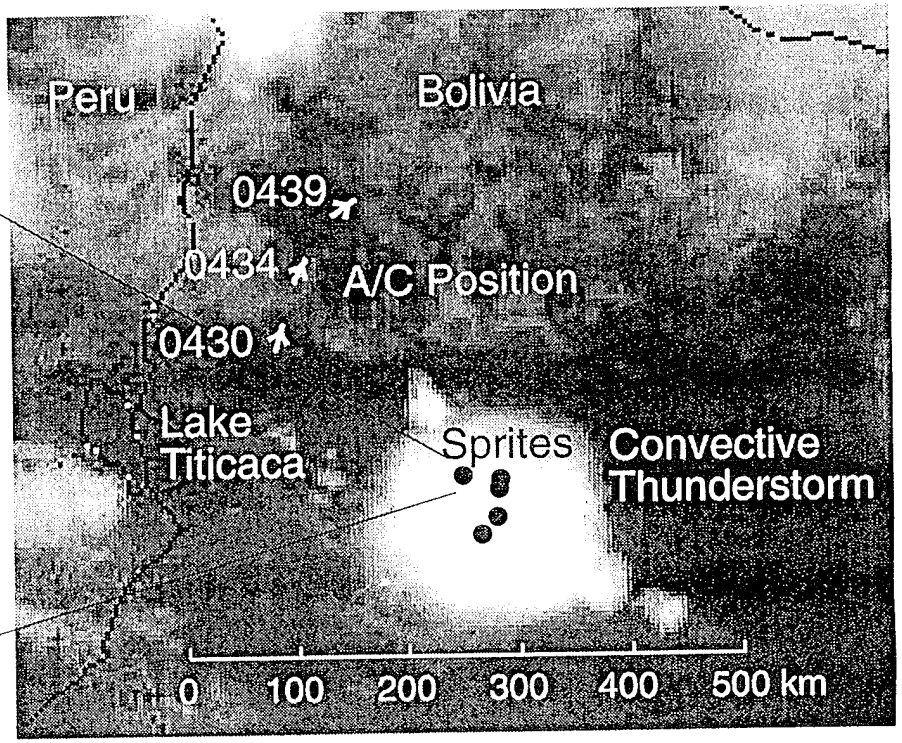
- The right hand figure shows a scan from the GOES 8 11 micron infrared channel that covered southern Peru and west-central Bolivia for the indicated scan time. Coincidentally, we studied the single convective storm system present in this image. The storm system was stationary and nearly circular, with a diameter of approximately 200 km. Here we show the region of aircraft operation superimposed on the infrared weather image. The positions of the sprites are indicated by red dots and are approximately centered on the storm.

- The left hand figure shows a frame from the low light level TV sequence that captured a very tight cluster of sprites. The star labeled here is Alpha Triangulum Australus. The altitude scale has been set in the same fashion as in the previous figures.

Aircraft View
UT 0439:13(28)



Goes 8 View
0400 UT, 3 Mar 95
11 micron IR Temperature



Conclusions - Peru95 Campaign

- Sprites occur over tropical-equatorial convective thunderstorms, which may be as small as ~50 km in diameter. The sprites appear in coincidence with large lightning discharges in the thunderstorm below.

- South American sprites resemble in color, shape, duration and probable altitude structure the sprites observed over summer thunderstorm systems in the continental U.S. They are also similar in average brightness for the storms studied during Peru95, but none were as bright as some of the very large, tight clusters seen over the continental U.S.

- There does not seem to be any readily apparent effect of the quasi-horizontal orientation of the magnetic field on the vertical structure of the sprites.

- No sprites were detected during five of the eight research flights launched from Lima, although there was lightning in the storms investigated. The rate of sprite occurrence seemed to be much less, relative to the background lightning flash rate, than midwestern thunderstorms.

- No blue jets were detected.

The University of Alaska Gasp95 Sprite Observation Campaign

- Purpose was to measure optical line spectra of sprites.
- Operated slit spectrograph and high resolution, low light level scene camera from top of Mt. Evans, Colorado.
- Principal results: In late June, obtained first sprite spectra. High quality spectra were measured for about a dozen events. The red color of sprites comes from the 1st positive bands of neutral N2.

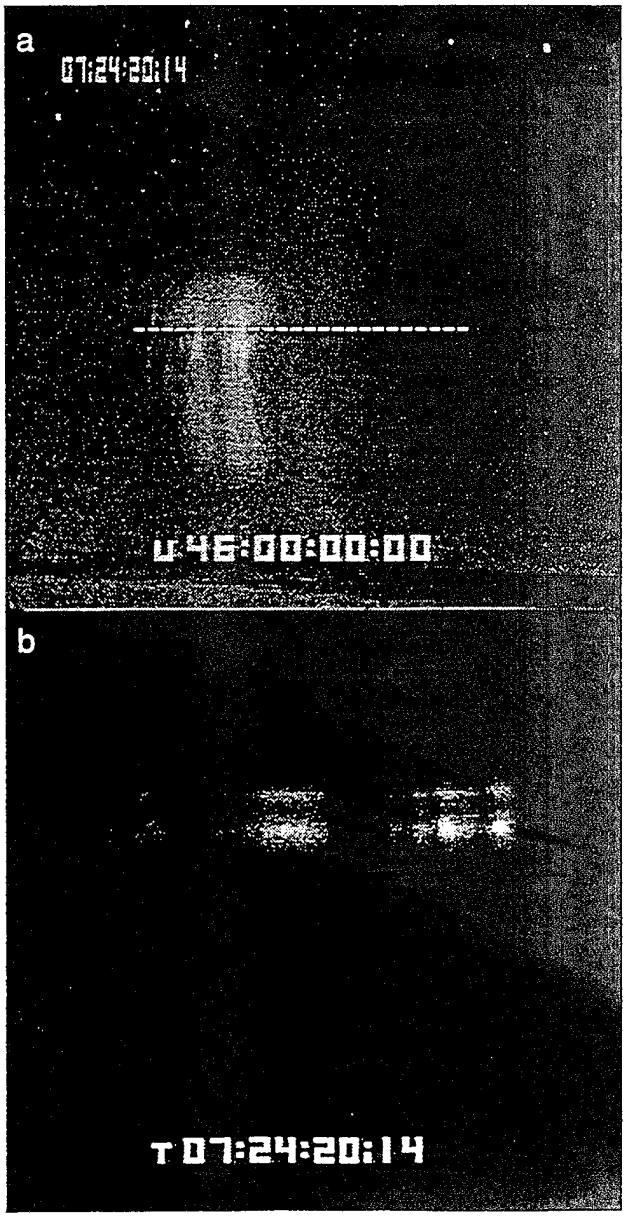


Figure 2. Raw digitized video images of (a) the scene camera and (b) the spectrograph. Note the spectrograph image is rotated, in that the slit direction is vertical.

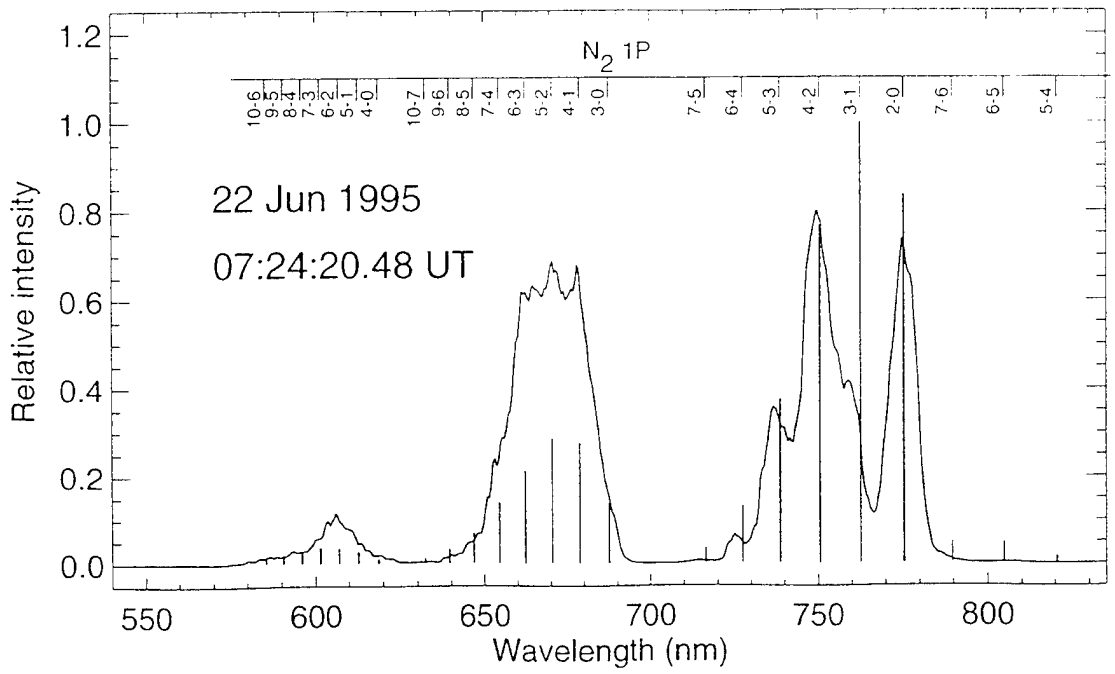


Figure 3. Reduced spectrum from 07:24:20;14 UT. The wavelengths for the band heads for different transitions of the first positive bands of N_2 are marked at top. The vertical lines show the auroral intensities of these transitions

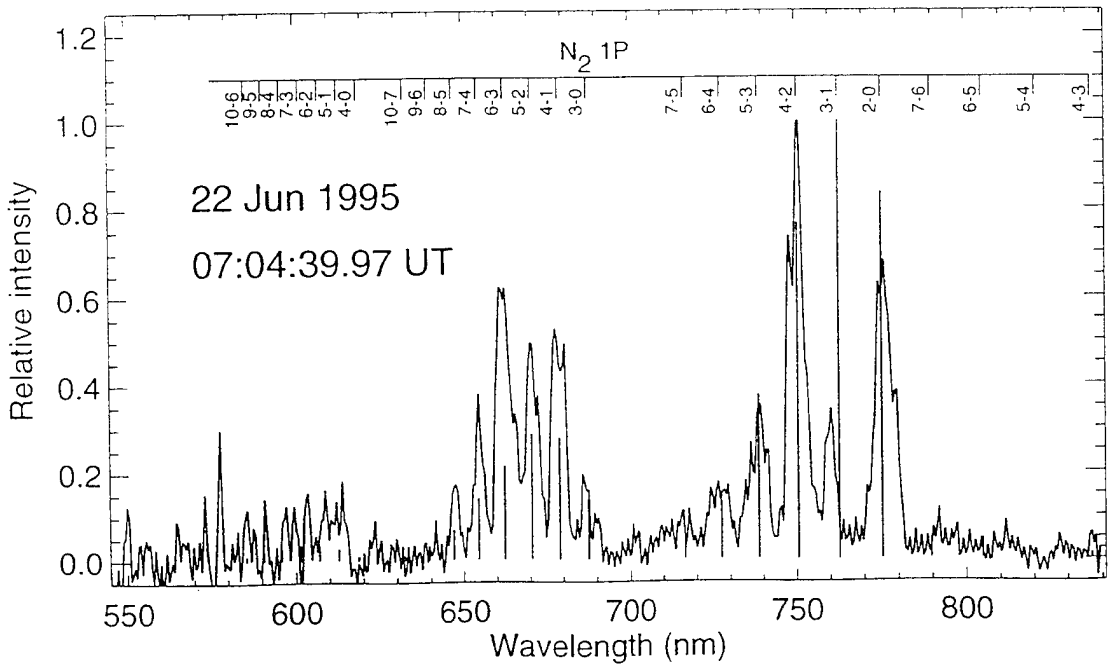
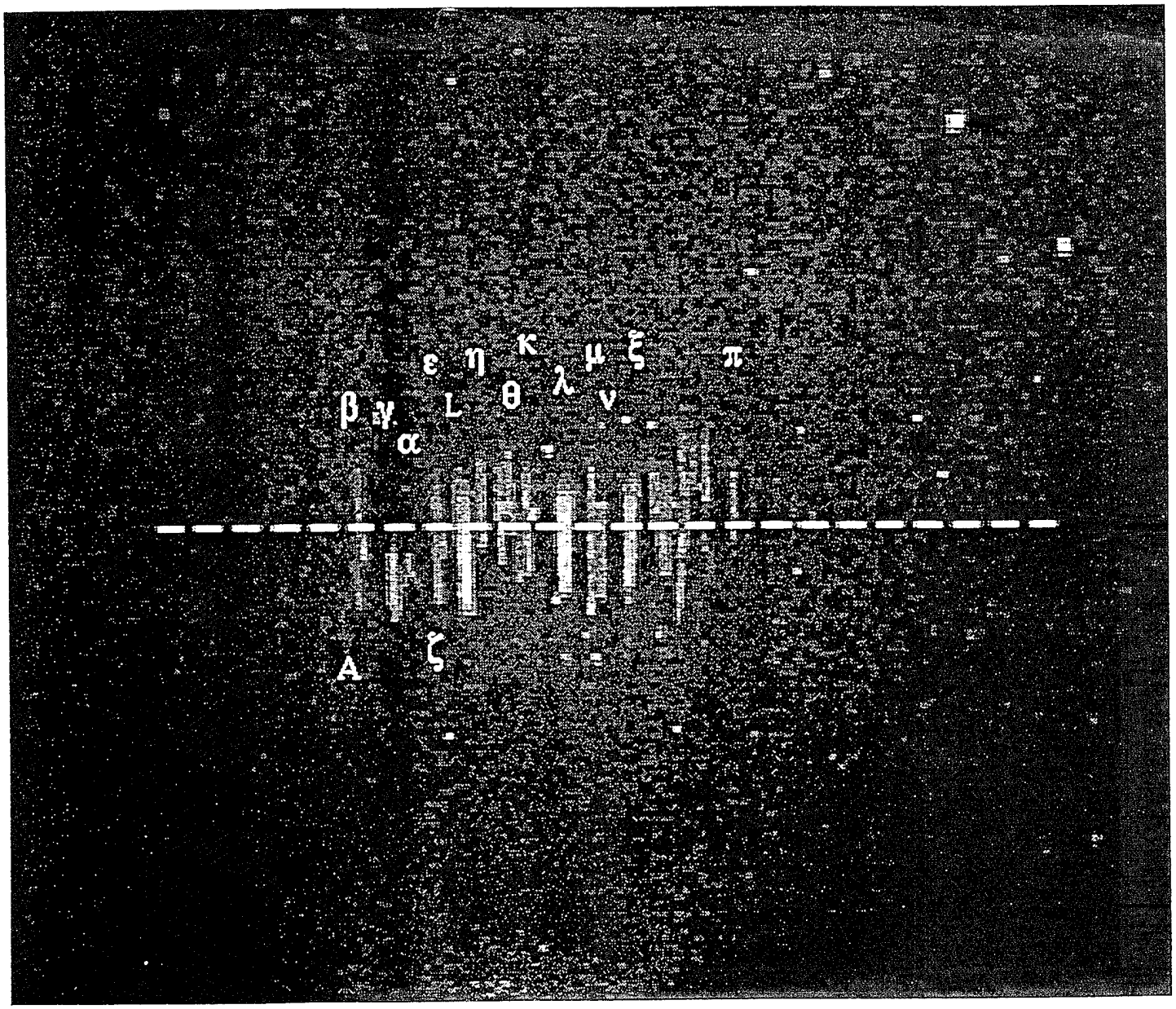


Figure 4. Reduced spectrum from 07:04:39;29 UT. The format is the same as that in Figure 3.



High resolution TV picture, June 19, 1995 from Mount Evans, Colorado showing a group of a different type of sprite. The sprites appear to be very thin (less than 1 km horizontal cross section), and generally seem to be higher than the classic sprite. Tops are at 86.4 $\pm$1.9 km and the bottoms are at 76.14 $\pm$ 1.4 km from 14 triangulated elements.



High resolution TV picture of a large group of sprites which show very clearly that the tendrils show fine dendridic structures, branching downwards. This is proof that the sprites propagate downwards from the core. There is no way that the dendridic structures would start from below and join together as they propagated upward.

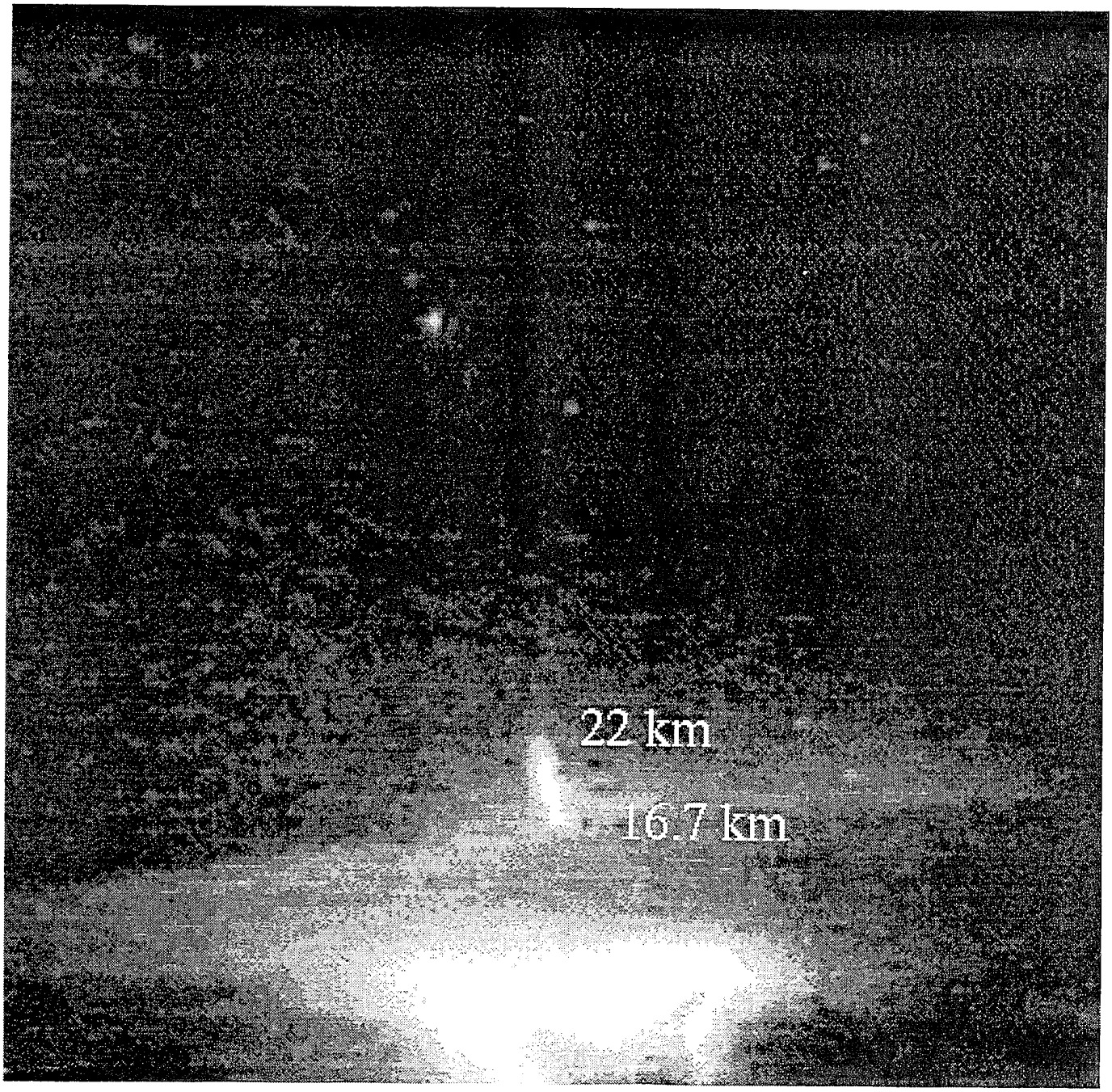


Another high resolution TV picture of a large group of sprites which show very clearly that the tendrils show fine dendridic structures, branching downwards.

Blue Jets and Blue Starters

Twenty-seven events were recorded from both aircraft during the five minute period 03:04:16.47 to 03:09:29.97 UT. Many were just barely visible above the apparent cloud The locations of thirteen of the blue starters have been triangulated. Twelve of them arose from one small area near 33.670N, 94.453W with a σ of radius about 3.7 km The other triangulated blue starter occurred within 1 km of Texarkana.

None of the blue starters was associated with a positive stroke as measured by the lightning network. There were no simultaneous or close in time negative cloud to ground strokes associated with the blue starters either. We have examined this possibility by comparing the distance from the blue starter to the nearest previous stroke in time.



This shows a 46° by 35° portion of a monochrome SIT TV frame at 03:07:55.27 UT of a blue starter which extended upward to 22 km (72,000 ft). The pillar of light is 7.5° off the vertical.

Blue Jets

- Color: primarily blue.
- Narrowly collimated ($\sim$ 15 $\pm$ 7.5°) with an apparent fan out near the top (40 to 50 km).
- Apparent vertical propagation speed: $\sim$ 100 km/s.
- The angle of propagation varies slightly from the vertical, and does not correspond to the magnetic field direction.
- Their apparent source duration is $\sim$ 200 ms at the base of the jet.
- The overall brightness decays simultaneously along the jet beginning at about 200 to 300 ms.
- The estimated brightness near the base ranges up to near 800 kR assuming emissions from the first negative bands of N_2^+ and from the second positive bands of N_2.
- They are often observed to follow blue starters.
- There is a faint hemispherical "shock" observed beyond the terminus of some jets travelling at the same speed as the earlier rising portion of the jet. If it were a sonic shock it would be at Mach 300.
- The average occurrence rate was $\sim$ 2.8/min in the July 1, 1994 storm during the first 22 minutes of observation.
- The estimated energy deposited is about 30 MJ.
- They are not associated with positive cloud to ground strokes, they occur with negative cloud to ground strokes.
- During the Arkansas storm hail 2.75 inches in diameter was observed in the area of the blue starters and jets during the 22 minutes.

Blue Jets

Outstanding questions

- What are the actual spectral emissions, optical, IR and UV?
- Is there any detailed structure to the jets not evident in the wide angle images available?
- What is the production mechanism?
  - Cloud to cloud, cloud to ground, d.c. field effect?
  - Particle (electron, ion) beam?
  - Ion fountain?
  - Optical bleaching?
- What is the nature and energetics of the "shock wave"?
- Are there associated ULF/ELF/VLF emissions?
- Are blue jets associated with gamma rays and TIPPS detected from satellites?
- Secondary effects:
  - Stratospheric chemistry?
  - Danger to aircraft?
- Are Blue jets related to the VHS radar echoes reported by *Rumi* [1957]?
- What are the meteorological conditions for creating blue jets, and what is the occurrence rate of blue jets compared to red sprites?

VHF radar echoes from blue jets.

Rumi [1956,1957] described VHF echoes whose characteristics are similar to the optical observations of blue jets. He was operating a 27.85 MHz radar pointed north from Cornell, in a study of auroras, meteors and lightning funded by the U. S. Signal Corps. His observations were limited to the Fall of 1955. Detailed analysis of amplitude vs time displays led him to dissociate many of the echoes from meteors or auroras. He attributed these echoes to "upward discharges" although no correlation with thunderstorms or lightning strokes was made. *Rumi,* [1956] was also operating a 106.6 Mhz radar which was used to deal with lightning strokes. He could clearly distinguish lightning strokes separately. *Rumi*[private communication, 1995] wrote that there was considerable lightning activity north of Ithaca during the Fall of 1955.

Rumi [1957] listed the characteristics of the 27.85 MHz echoes as:

1. They are discrete and generally last less than 500 ms.
2. They show no preferred range, the maximum in the absence of aurora was around 900 km.
3. They sometime rise from noise level to maximum in two repetition periods of the radar, or 40 ms. Calculations of the velocity to produce the first Fresnell zone of a column of ionization gives values in some cases greater than 100 km/s. (Meteors with their origin within the solar system have a maximum velocity of 72 km/s.)
4. They usually decay very rapidly in 100 ms. The decay is not exponential (as expected from meteors).
5. They sometimes show a tendency to repeat themselves at the same range.
6. They generally occurred for two hours around midnight, but did not occur every night. During the months of September, October, and November, 1955, they occurred on more than half the nights. Very few were observed during December. As many as 400 echoes in one hour were seen.
7. The columns of ionization do not present a preferred direction (indeed they do not show a preferred range) and disappear at a height of about 50 km.
8. The peak of activity was in October, but there was no correlation with any meteor showers.
9. The appearance of the echoes was not a regular one; nights of complete absence were randomly alternated with very active nights.

University of Alaska campaign results reported to date include:

Sentman, D.D., and E.M. Wescott, Video observations of upper atmospheric optical flashes recorded from an aircraft, *Geophys. Res. Lett.*, **20**, 2857, 1993.

Sentman, D.D., E.M. Wescott, D.L Osborne, D.L. Hampton, and M.J. Heavner, Preliminary results from the Sprites94 aircraft campaign: 1. Red sprites, *Geophys. Res. Lett.,* **22**, 1205, 1995.

Sentman, D. D. and E.M., Wescott, Red sprites and blue jets: Thunderstorm-excited optical emissions in the stratosphere, mesosphere, and ionosphere, *Phys. Plasmas*, **2**, 2415, 1995.

Wescott, E.M., D.D. Sentman, , D.L Osborne, D.L. Hampton, and M.J. Heavner, Preliminary results from the Sprites94 aircraft campaign: 2. Blue jets, *Geophys. Res. Lett.,* **22**, 1205, 1995.

Hampton, D.L., M.J. Heavner, E.M. Wescott, and D.D. Sentman, Optical spectra of sprites, *Geophys. Res. Lett.*, (in press), 1995.

Inan, U.S., T.F. Bell, V.P Pasko, D.D. Sentman, E.M. Wescott, and W.A. Lyons, VLF signatures of ionospheric disturbances associated with sprites, *Geophys. Res. Lett.*, (in press), 1995.

Spectral and spatial properties of SPRITE-s

Lockheed

S. B. Mende

Abstract

S. B. Mende, (Lockheed Martin Palo Alto Research Laboratory, 3251 Hanover St., Palo Alto CA 94304; 415-424-3282; MENDE@SAG.SPACE.LOCKHEED.COM)

Imagery and spectra of high altitude luminous flashes, otherwise known as Sprites, occurring in the stratosphere/mesosphere above electrically active cumulonimbus clouds were acquired in the month of July, 1995 from an observation site near Ft. Collins, CO. The spectra, resolved from ~4500-8000 included four spectral features in the 6000-7600 region which have been identified as N2 1PG system with dv=2,3, and 4 from the v=2,4,5,6 vibrational levels of the $B^3\Pi g$ state. The spectra were lacking in other features such as the N_2^+ Meinel or the N_2^+ 1st neg system indicating that the electron energy causing the excitation is quite low. The absence of other emissions and the spectral profile of the N2 first positive emissions suggests that the observed Sprite did not produce hard electrons. This observation therefore does not support the explanation that Sprites are responsible for generating energetic electrons above thunderstorms. Our spectral observations confirm the previous reports that the Sprites appear red in color. During these experiments images of several sprites were recorded with the wide field imaging camera. Most of the sprites exhibited multiple columns or channels. Light entering the CCD-s frame transfer register showed artifacts on the images which could be used in measuring the temporal behavior of the observed sprites. Evidence was also obtained for short lived broad diffuse airglow enhancements above thunderstorms. The duration of the observed enhancements are less than a single television frame. The enhancements sometimes occur simultaneously with SPRITES detected from the same site. These enhancements are expected to be the same phenomena that was reported from the space shuttle camera observations. Planned future ground aircraft and spacecraft based observations will also be reviewed.

Spectral and spatial properties of SPRITE-s

S. B. Mende

- Lockheed has participated in the Sprites 95 campaign.

- Images were recorded with high detail. Narrow channels seemingly connecting adjacent sprites. Triangulation is needed

- Spectra were recorded and published. The energy content of the sprites are low. Agrees with theoretical predictions of electric field excited discharge.

- High time resolution imaging paper was submitted. Measurments of time interval between lightning and sprite. Duration and timing of adjacent columns.

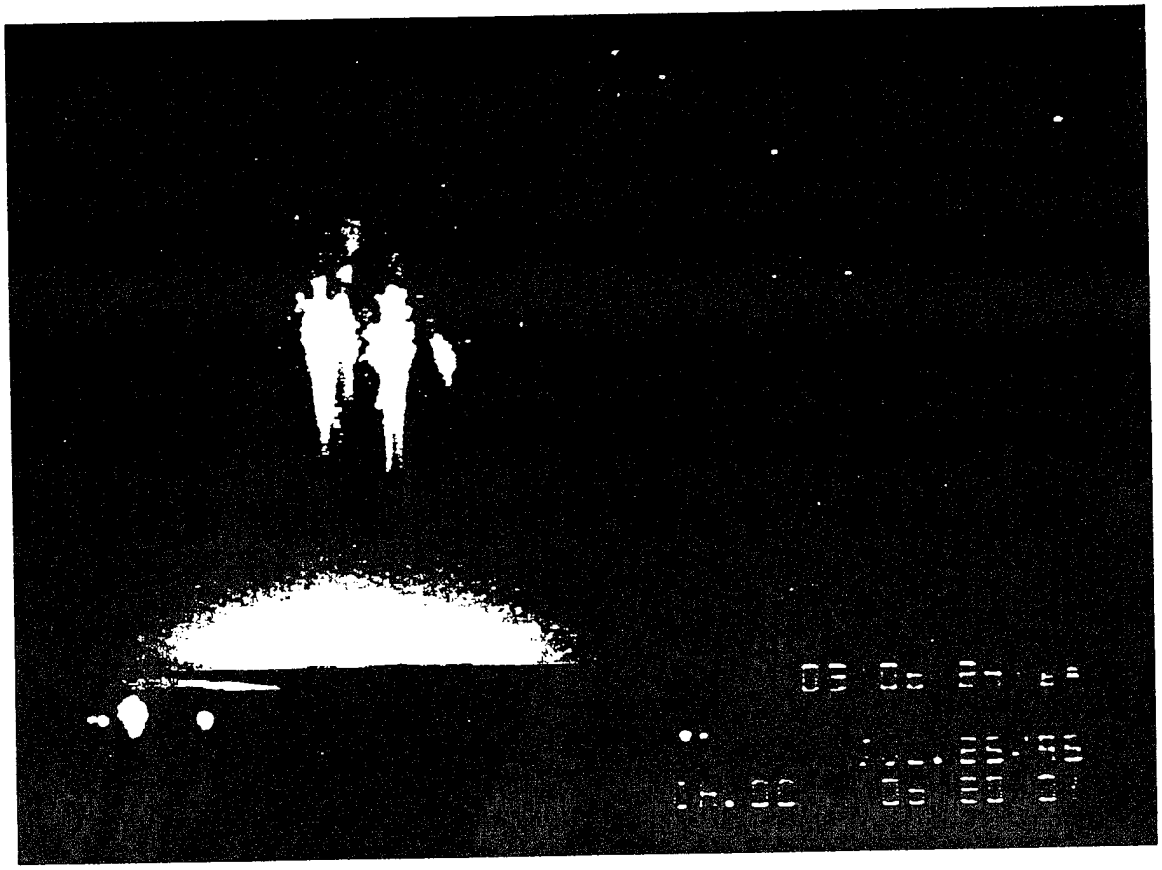
- Airglow enhancements are being studies. What are the connections between airglow enhancements and sprites?

Space based measurements.

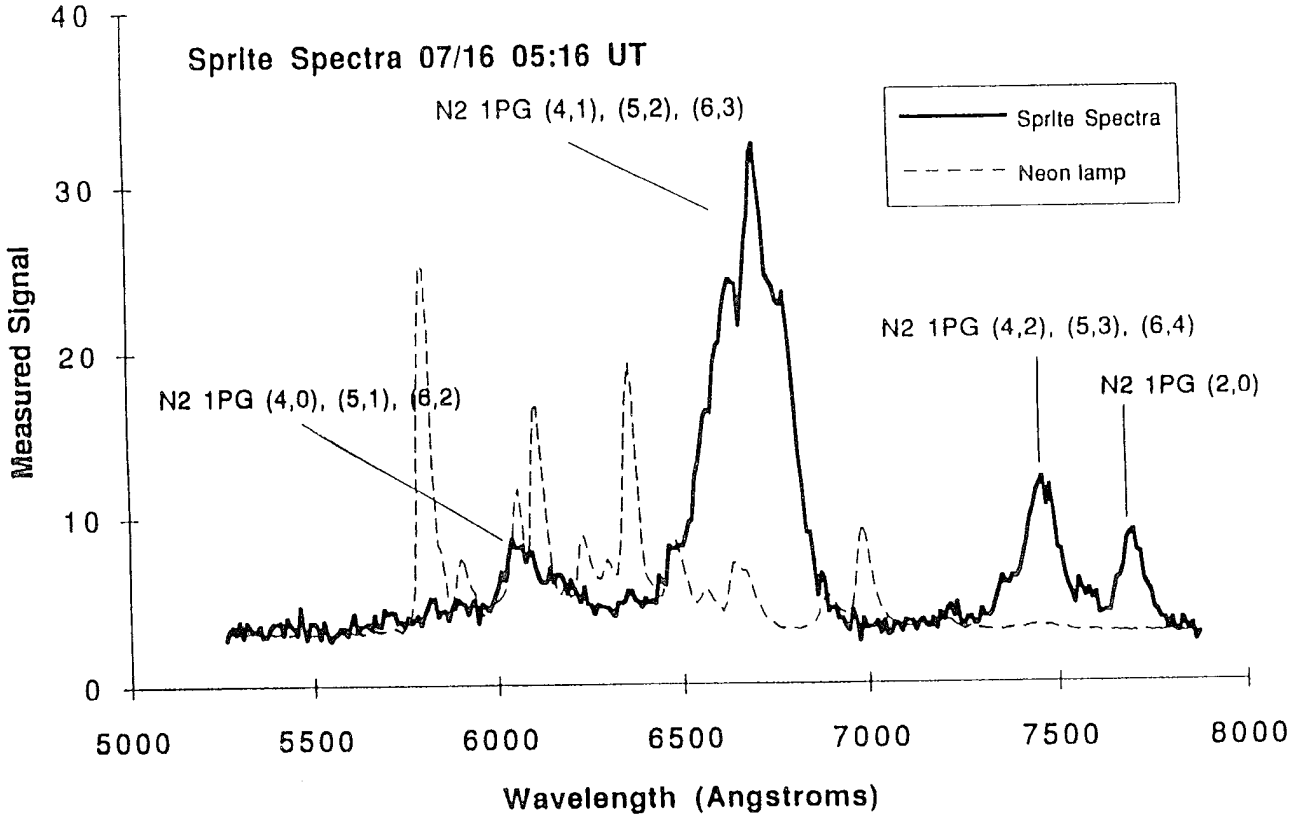
Reasons for space based measurments:
Latitude longitude survey associattion with thunderstorm types.
Wide spectral range UV/IR
Accelerated particles, X rays etc.

Tether Optical Phenomena (TOP) experiment flight in February 1996
Repeat are proposed flights. These flights are somewhat similar to the Philips Lab sponsored APE shuttle experiments

Image showing the narrow filamentary structure of some Sprites



Spectrum of the Sprite showing enhancement in the N_2 1 PG system only



Spectral and spatial properties of SPRITE-s

Lockheed

S. B. Mende

One of the cameras during the Sprites 95 campaign had a light leak into the transfer registers. From the measurement of the resulting ghost streaks the timing of the sprites could be derived.

The following conclusions were derived from this study.

1. The onset of the Sprites occurs 1.5 - 4 ms after the positive lighning flash pre-cursor
2. Each element of a Sprite cluster is initiated within 1 ms of each other.
3. The brightest "core" gains full intensity strength within a period of .3 msec. It generally lasts for 5-10 msec with a decay which is also 5-10 msec.

Tasks ahead:

- Analyze current data

- Repeat observations with improvements:
  "Tune up" spectrometer
  Bore sight photometer
  Triangulated data multiple sights
  Measurement of altitude propagation
  Obtain temperature of N2 1st positive
  Observe in N2 2nd positive

Spectral and spatial properties of SPRITE-s

S. B. Mende

Space based measurements.

Reasons for space based measurments:

- Latitude longitude survey associattion with thunderstorm types.
- Wide spectral range UV/IR
- Accelerated particles, X rays etc.

Tether Optical Phenomena (TOP) experiment flight in February 1996

Repeat flights which are specifically optimized for studying sprite phenomena are proposed.

The U.S. Government is authorized to reproduce and sell this report.
Permission for further reproduction by others must be obtained from
the copyright owner.

GEOPHYSICAL RESEARCH LETTERS, VOL. 22, NO. 19, PAGES 2633-2636, OCTOBER 1, 1995

Sprite Spectra; N_2 1 PG band identification

S. B. Mende, R. L. Rairden, and G. R. Swenson
Lockheed Martin Palo Alto Research Laboratory, Palo Alto, California

W. A. Lyons
ASTeR, Inc., Fort Collins, Colorado

Abstract. Imagery and spectra of high altitude luminous flashes, otherwise known as sprites, occurring in the stratosphere/mesosphere above electrically active cumulonimbus clouds were acquired on July 16, 1995 from an observation site near Ft. Collins, Colorado. The spectra, resolved from ~4500-8000 Å included four spectral features in the 6000-7600 Å region which have been identified as N_2 1PG system with Δv=2,3, and 4 from the v=2,4,5,6 vibrational levels of the $B^3\pi_g$ state. The spectra were lacking in other features such as the N_2^+ Meinel or the N_2^+ 1st neg system indicating that the electron energy causing the excitation is quite low.

Introduction

Direct evidence for coupling from lightning events to the upper atmosphere is found in the optical observation and recording of cloud-ionosphere (CI) discharges or sprites from thunderstorm regions [Franz et al., 1990; Winckler et al., 1993; Sentman and Wescott, 1993; Lyons, 1994; Sentman et al., 1995]. The images of these CI discharges were obtained by ground and aircraft-based, low light level television systems. Morphologically there are probably several distinct types of upward luminous phenomena associated with thunderstorms, the most common of which are the so-called red sprites [Sentman et al., 1995] which have been observed by red sensitive low light level television cameras from the ground and from aircraft. A second class of phenomena, "blue jets", which do not propagate beyond the stratosphere [Wescott et al., 1995] have also been identified. There are however no published spectral measurement of these type of events. Spectral measurements are exceedingly important because they can provide a remote sensing characterization of the physical and chemical processes resulting in the emission. In this paper we are reporting one of the first sets of spectral observations of upward discharge phenomena.

Observations

The instrument used in our observation is illustrated schematically in Figure 1 from a top view. It consisted of two channel bore sighted intensified CCD video camera system. The optics of the spectrometer channel is a copy of the transmission grating spectrometers used in the shuttle borne aurora and airglow investigations e.g. Mende et al., [1993]. The spectrograph consisted of an objective lens L1 (f=85 mm F/1.4) which projected the image of the scene on a plate which had a 25 mm long vertically oriented open slit. The slit was widened for the sprite observations and the slit width was approximately 0.3 mm producing an equivalent spectral resolution of about 9 nm. The light from the lens was collimated by L2, a 50 mm F/1.2 lens and diffracted by a transmission grating mounted on the back side of the prism. The prism grating combination (Grism) split the light into divergent beams into a horizontal fan according to wavelength. In Figure 1 three different monochromatic wavelength regions are illustrated as being focused at different part of the detector as λ_1, λ_2 and λ_3. An imaging lens L3 (50 mm F/1.2), focused parallel light rays on the intensifier photo cathode, therefore a given wavelength of light, appeared along a vertical line on the image intensifier photo cathode. The prism was used mainly to steer the light beam back to the center so that the center wavelength of the first order spectra appeared in the center of the image. Note, that the system is an imaging spectrometer and the distribution of luminosity of the image in the direction parallel to the vertical slit is preserved providing true vertical intensity profiles of the observed phenomena. The second optical channel the imaging camera was a simple low light level intensified CCD camera with a 50 mm F/1.4 photographic lens producing an approximately 20x15 degree field of view image on a 25 mm image intensifier. Both cameras had second generation image intensifiers with extended red S-20 photo cathodes. The image intensifiers were fiber optically coupled to the CCD-s. Both video cameras were scanned at standard video rates at 30 frames per second. The video signals were recorded on VHS video tape with suitable time codes marked on each video frame. The spectral responses of both channels were determined through calibration using light sources of known spectral profile. The imager sensitivity peaked at 490 nm dropping off uniformly and quite rapidly towards the blue/UV region to reach 25% sensitivity at about 400 nm. Towards the red it dropped off more gradually reaching the 25% sensitivity point at around 800 nm. The spectrometer had a similar S-20 detector but the grating blaze favored the red region putting the overall sensitivity peak at around 630 nm. The response dropped off quite symmetrically in either direction reaching 25% of peak sensitivity at 450 and 760 nm.

Both instruments were mounted on an azimuth and elevation mount. The bore sighting of the camera and spectrograph were pre calibrated using star images. This allowed the precise determination of the spatial position of the spectrograph slit in the imaging camera field of view and accurate real time pointing of the spectrometer through the imaging camera. This technique also permitted the recording of the two

Copyright 1995 by the American Geophysical Union.

Paper number 95GL02827
0094-8534/95/95GL-02827$03.00

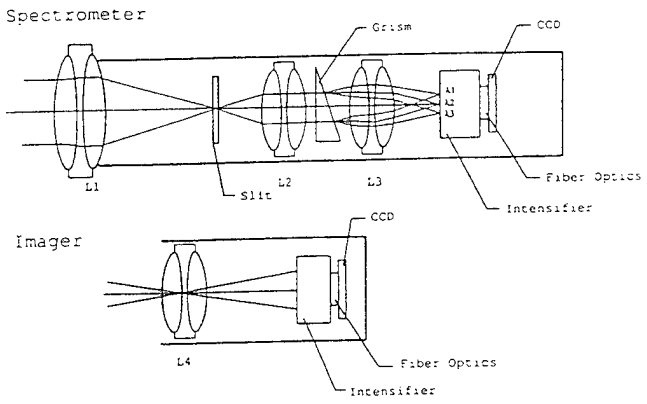


Figure 1. Instrument block diagram of the boresighted imager and spectrograph for Sprite Observations.

dimensional image of the sprite simultaneously with the sprite spectra.

The system was operated at the Yucca Ridge Field Station, operated by ASTeR, Inc. 20 km northeast of Ft. Collins, Colorado. This site provides for nearly unobstructed viewing of sprites and related phenomena to distances as great as 1000 km over the U. S. High Plains (approximately from northwest clockwise through directly south). Several sprite events were detected. On July 16, 1995 conditions were favorable for the observation of sprites although the storms were at some distance from Yucca Ridge. A sprite occurred at 05:16:48.534 UT and a sequence of video frames depicting the sprite is shown on Figure 2. To minimize unwanted backgrounds and nonuniformities a common background frame taken prior to each sprite set was subtracted from each image presented here. The onset of the sprite luminosity was coincident with the start of the underlying cloud illumination and continued for 3 video frames (33 msec each). The first two frames were the brightest with rapid decay in the third frame. The data shows an apparent motion of the luminosity in the westerly direction (towards the left). The far left feature for example on the third frame is actually brighter on the third frame than on the first two.

The storm under surveillance was located near Rapid City, SD, on an azimuth of roughly 25 degrees, and spanned a range from about 400 to 450 km. The radar derived precipitation area associated with the cell was approximately 25,000 km^2. Given the storm's size, and the presence of positive cloud to ground (CG) lightning flashes, it met the criteria found by Lyons [1995] for mesoscale convective systems over the US High Plains to begin generating sprites.

The sprite morphology was typical of the many observed during the campaign. It exhibited a curtain of smaller vertical striations (8-10) with the brightest portion near the top of the structure with less intense tendrils extending downward. From the star field present in the raw images the angular extent of the sprite could be measured accurately. The horizontal extent was 6.5 degrees, and at the estimated range of 450 km (based on the location of the parent positive CG) this implies a horizontal dimension of 51 km. The upper portion of the sprite extended to about 9.2 degree elevation, and locating the sprite within 25 km of the parent positive CG implies the highest extent to be 90 km. The bottom end of the same sprite was at 74 km. No indication of vertical propagation could be obtained from our low-light level video system operating at 16.7 ms field rate.

The spectral slit was vertical and located very close to the brightest event near the center of the image. On Figure 3 we present the spectrum which was observed simultaneously with the imager of Figure 2. Figure 3 is a spectrum in which the left edge of the image represents the 850 nm infrared region and the right edge corresponds to the blue cut off of the instrument at approximately at 430 nm. In the entire spectral range there were only four features. It is important to note that outside of these features there were no other discernible enhancements in the entire spectral range covered by the instrument. The region, which contained some discernible signal, was digitized. In Figure 3 a white frame marks this region. A spectral plot (Figure 4) was produced by summing vertically across the luminous features of Figure 3 and plotting the results along a horizontal (wavelength) axis. To facilitate wavelength calibration we have superimposed the spectra of a neon calibration light source taken while the instrument was still in position at the field site. Using the features of the neon gas a wavelength scale was determined and added to the figure. The wavelength scale permits the recognition of the major features of the sprite spectra.

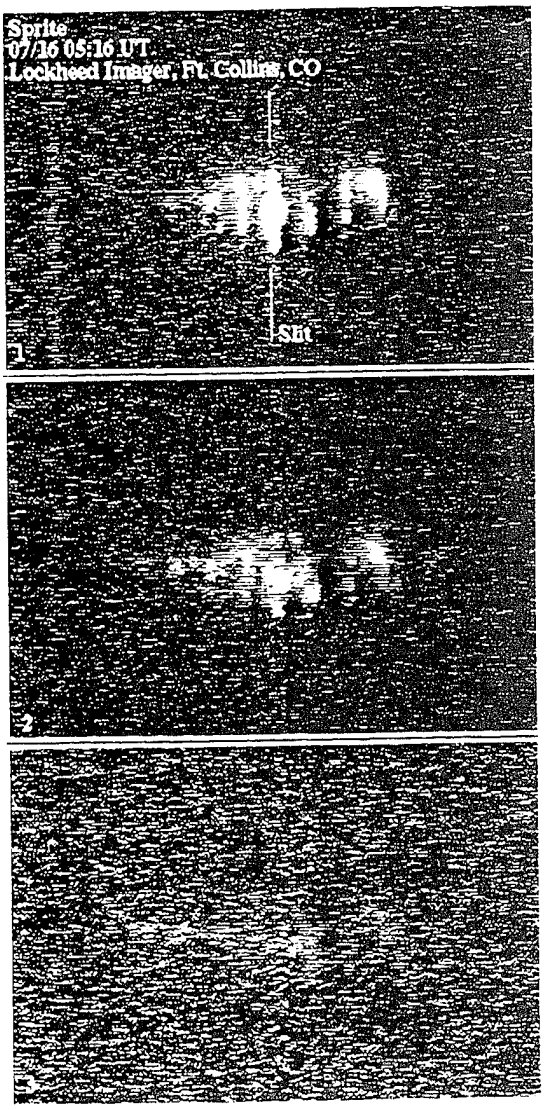


Figure 2. Three consecutive TV frames of the sprite observed with the imaging camera on the 16th of July at 05:16:48.534 UT.

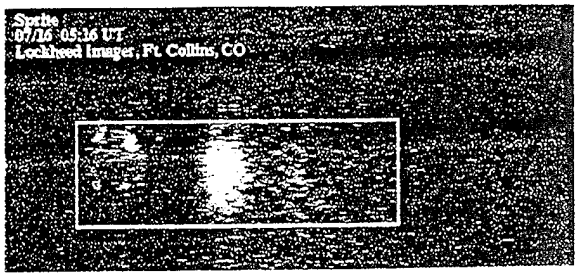


Figure 3. Spectral image or spectrogram of the Sprite event occurring at 05:16 UT. The image covers the wavelength range from 850 nm (left) to 430 nm (right). White frame shows area of detectable signal selected for display on Figure 4.

Discussion

The processes leading to emissions in the atmosphere by energetic electrons accelerated by electric fields in thunderstorms should be greatly similar to auroral light production. Auroras however do not generally penetrate to 90 km and light in sprites is generally produced at this altitude or lower. Although the atmospheric composition is not drastically different at these lower altitudes increased collision frequencies will quench long lifetime auroral emissions. Thus we expect to see only the fast, permitted transitions. The theory of optical excitation of the atmosphere above thunderstorms and the generation of sprites by quasi electrostatic fields has been discussed by Taranenko et al., [1993] and by Pasko et al., [1995] respectively. Taranenko et al. [1993] have predicted that the N_2 1PG system is the brightest emission feature to occur in lightning stimulated upper atmospheric emissions.

The N_2 1PG system was been positively identified in our sprite spectrum and is shown in Figure 4. Between 760 and 770 the (3,1) component of N_2 1PG is strongly attenuated due to absorption by O_2 at 762 nm at slant path. It should be noted that the instrumental spectral response was not applied to the data presented in Figure 4. The N_2 1PG system is a well investigated emission associated with electron bombardment of the atmosphere by auroral electrons is largely the result of secondary electron impact on atmospheric N_2 as described by Vallance Jones [1974] and Strickland [1976]. Chutjian et al.

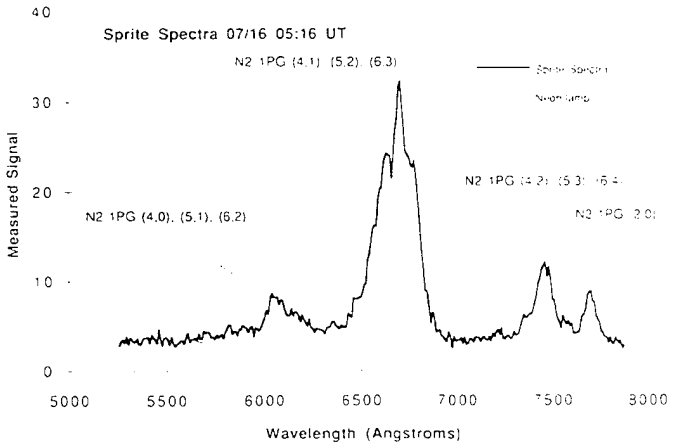


Figure 4. Spectral scan of the image shown in Figure 3. The thick trace represents the spectra of the sprite while the thin trace shows the spectra of a calibration neon light.

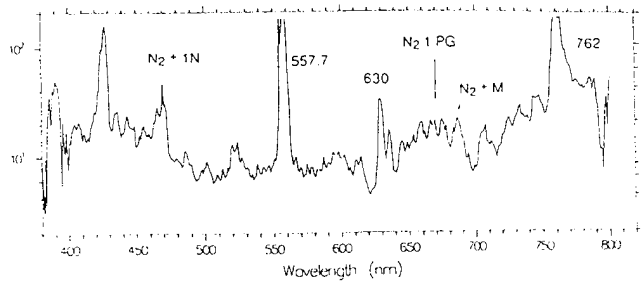


Figure 5. Auroral spectrum taken from the space shuttle. The spectrum was taken with a similar transmission grating image intensified instrument system.

shown the peak of excitation to be near 10 eV with a fast drop off to higher energy with the cross section decreasing by a factor of 15 at 100 eV. In the aurora, it is the large population of secondary electrons produced by primary (keV) electrons which produces the N_2 1PG emission. It is well established that the lifetime is 6-8 μs [Nicholls, 1969], and that with known quenching rates, the emission is not visible below ~50 km as a result of the collisional frequency with known quenching species [Vallance Jones, 1974].

In the case of the sprite spectra, the N_2 1PG system was the only emission detected. In the spectral range of the instrument (430 - 850 nm) no other features were detected above instrument noise background. If electrons with energies higher than 20 eV had been produced by the sprite, then N_2^+ emissions would have been present. For example in aurora where higher energy electrons are available several N_2^+ emissions features are significant. Some of these emissions have very short lifetimes and would not be quenched significantly at sprite altitudes down to 50-60 km. In auroral spectra at about 690 nm there is a strong contribution of the N_2^+ (3,0) Meinel band (See for example spectra presented by Vallance Jones [1974 page 83]). This feature is missing from the spectra presented in Figure 4. The absence of this feature indicates that the electrons in the sprite had insufficient energy to efficiently ionize the nitrogen. Several other features were also missing from the sprite spectra which are characteristic of normal auroral spectra. The same type of instrument was flown on the space shuttle and several auroral spectra had been taken for example on mission STS-45. We have included one of these spectra for comparison as Figure 5. These spectra give us direct one to one comparison between the Sprite spectra and the auroral spectra as observed by the same instrument type. If the sprite had contained hard electrons of several keV then we would expect some of the auroral fast transitions to take place. The shuttle based instrument detected strong 427.8 and 470.9 N_2^+ emissions. Although 427.8 nm emissions was just outside of the wavelength range of the ground based instrument one would have expected to see N_2^+ first negative at 470.9 nm which, when observed in aurora is stronger than the N_2 1PG bands in the 650 and 680 nm range. In Figure 5, apart form the well known auroral features such as 427.8, 557.7, 630 and 636.4 and the 762 airglow band, we can distinguish four peaks between 650 and 700 nm. The three on the left are the N_2 1PG (4,1),(5,2) and (6,3) components. The fourth peak is a combination of the N_2 1PG (3,0) and the N_2^+ Meinel (3,0) where most of the intensity is produced by the ionized Meinel contribution in aurora suggesting the absence of such emission in the sprite. Note that the O_2 atmospheric (0,0)

band at 762 nm is a strong emission band in the topside auroral spectra whereas it is a dark absorption feature in the ground based sprite spectra. The relatively poor signal to noise ratio of our measured spectra coupled with the decreasing sensitivity of the instrument and the larger scattering of the slant range atmosphere in the blue spectral region probably accounts for the absence of the N_2 2nd positive bands in our spectra. Our observations therefore could be consistent with the intensity ratio of 7 between the two bands as predicted by Taranenko et al. [1993] There remain a number of controversial issues regarding the details of N_2 1PG excitation in sprites. Just as in auroras these emissions can be produced from possible interactions with other N_2 states or $N(^4S)$ [see Partridge et al. 1988 and Vallance Jones, 1974]. These issues may be enlightened regarding the excitation in sprites through spectral observations in the UV and IR, but the likeliest conclusion is that the electrons in the sprite discharge have energies <100 eV.

Conclusions

During these experiments several sprite images were recorded with the wide field imaging camera. These sprites were quite similar in appearance to the one described above. Most of the observed sprites exhibited multiple columns or channels similar to the image presented in Figure 2. It should be also noted that there appeared to be a spatial drift of the Sprite phenomena. Most sprites observed by our instrument showed that after the first bright frame the images in the weaker frames were seen to be substantially displaced spatially. Assuming that the range was 450 km the event shown on Figure 2 appears to be displace by a distance of about 50 km in 1 or 2 TV frames. Thus the speed of propagation of this phenomena was of the order of about 1500 km/sec in the plane normal to the viewing direction.

A bore sighted imaging camera and imaging spectrograph observed sprite events and recorded their spectra. The spectra contains N_2 first positive bands without any discernible contribution from other emissions. The observed spectrum is consistent with predictions of Taranenko et al. [1993] regarding the relative intensity of optical emissions created in this altitude regime. The absence of other emissions in the sensitivity range of the instrument and the spectral profile of the N_2 first positive emissions suggest that the efficiency of hard electron production in the observed Sprite was low. This observation therefore does not support the attempt of Chang and Price [1995] in explaining the observations of energetic electrons above thunderstorms [Fishman et al., 1994]. Our spectral observations confirm the previous reports that the sprites appear red in color.

Acknowledgments. The authors are indebted to R. Armstrong of Mission Research for valuable discussions and for assistance in the operation of the instrument during the observation of the reported sprites. The authors are also grateful to Mr. T. Nelson of ASTeR Inc. for providing assistance during the field operations. The Lockheed observations and data handling were supported by a Lockheed Independent Research Program. ASTeR's coordination of the SPRITE'95 project was funded by NASA Kennedy Space Center, SBIR Phase II Contract NAS10-12113.

References

Chang B., and C. Price, Can gamma radiation be produced in the electrical environment above thunderstorms?, *Geophys. Res. Lett.*, 22, 1117-1120, 1995.

Chutjian, A., D. C. Cartwright, and S. Trajmar, Excitation of the $W^3\Delta_u$, $w^1\Delta_u$, $B'^3\Sigma_u^-$, and $a'^1\Sigma_u^-$ states of N_2 by electron impact, *Phys. Rev. Lett.*, 30, 195, 1973.

Fishman, et al., Discovery of intense gamma-ray flashes of atmospheric origin, *Science*, 264, 1313-1316, 1994.

Franz, R. C., R. J. Nemzek, R. J. Winckler, Television image of a large upward electrical discharge above a thunderstorm system, *Science*, 249, 48-51, 1990.

Lyons, W. A., Characteristics of luminous structures in the stratosphere above thunderstorms as imaged by low-light video, *Geophys. Res. Lett.*, 21, 875-878, 1994

Lyons, W. A., The relationship of large, luminous stratospheric events to the anvil structure and cloud to ground discharges of their mesoscale convective system. *Conference on Cloud Physics*, American Meteorological Society, Dallas, Tex., 1995.

Mende, S.B., G.R. Swenson, S.P. Geller, R.A. Viereck, E. Murad, and C.P. Pike, Limb view spectrum of the earth airglow, *J. Geophys. Res.*, 98, 19,117-19,125, 1993.

Nicholls, R. W., Aeronomically important Transition Probability Data, *Can. J. Chem.*, 47, 1847, 1969.

Partridge, H., S. R. Langhoff, C. W. Bauschlicher, Jr., and D. W. Schwenke, Theoretical study of the $A^{'5}\Sigma_g^+$ and $C^{''5}\Pi_u$ states of N_2: Implications of Afterglow, *J. Chem. Phys.*, 88, 3174-3186, 1988.

Pasko, V. P., U. S. Inan, Y. N. Taranenko, T. F. Bell, Heating, ionization and upward discharges in the mesopshere due to intense quasi-electrostatic thundercloud fields, *Geophys. Res. Lett.*, 22, 365-368, 1995.

Sentman, D. D., E. Westcott, Observations of upper atmospheric optical flashes recorded from an aircraft. *Geophys. Res. Lett.*, 20, 2857, 1993.

Sentman, D. D., E. M. Wescott, D. L. Osborne, D. L. Hampton and M. J. Heavner, Preliminary results from the sprites 94 aircraft campaign, 1, Red sprites, *Geophys. Res. Lett.*, 22, 1205-1208, 1995.

Strickland, D. J., Transport equation techniques for the deposition of auroral electrons, *J. Geophys. Res.*, 81, 2755-2764, 1976.

Taranenko, Y. N., U. S. Inan, and T. F. Bell, The interaction with lower ionosphere electromagnetic pulses from lightning: excitation of optical emissions. *Geophys. Res. Lett.*, 20, 2675, 1993.

Vallance Jones, Alister, *Aurora*, D. Reidel, Hingham, Mass., 1974.

Westcott, E. M., D. Sentman, D. Osborne, D. Hampton and M. Heavner, Preliminary results from the sprites 94 aircraft campaign: 2. Blue jets, *Geophys. Res. Lett.*, 22, 1209-1212, 1995.

Winckler, J. R, R. C. Franz, R. J. Nemzek, Fast low-level light pulses from the night sky observed with the SKYFLASH program, *J. Geophys. Res.*, 98, 8775, 1993.

W.A. Lyons, ASTeR, Inc, 46050 Weld County Road 13, Fort Collins, CO 80524.

S.B. Mende, R.L. Rairden and G.R. Swenson, Lockheed Martin Palo Alto Research Laboratory, Dept. 91-20, Bldg. 252, 3251 Hanover Street, Palo Alto, CA 94304. (email:internet:: mende@sag.space.lockheed.com; rairden@lockhd.span.nasa.gov; swenson@lockhd.span.nasa.gov)

(Received July 31, 1995; revised September 1, 1995; accepted September 8, 1995.)

EVIDENCE FOR IONIZATION IN SPRITES

N_2^+(1N) 4278A EMISSION IN SPRITES '95 CAMPAIGN

IMPLICATIONS FOR CHEMICAL DYNAMICS AND RADIANCE

RUSS ARMSTRONG, JEFF SHORTER
MISSION RESEARCH CORPORATION, NASHUA, NH

WALT LYONS
MRC/ASTeR DIVISION, FORT COLLINS, CO

BILL BLUMBERG, LAILA JEONG
PHILLIPS LABORATORY, HANSCOM AFB, MA

PRESENTATION AT THE WORKSHOP ON SPRITES AND BLUE JETS

PHILLIPS LABORATORY, HANSCOM AFB, MA

18-19 OCTOBER 1995



Mission Research Corporation

CHARACTERISTICS OF SPRITES

ARE SPRITES IMPORTANT FOR CHEMICAL DYNAMICS AND RADIANCE IN THE MIDDLE ATMOSPHERE?

- EMISSION FROM $N_2^+(1N)$ DETERMINES IONIZATION LEVELS AND RESULTING CHEMICAL DYNAMICS
- CHEMICAL DYNAMICS DETERMINES LEVEL AND PERSISTENCE OF STRUCTURED RADIANCE
- PHOTOMETRIC CHARACTERIZATION ALONG WITH SPECTRAL/SPATIAL INFORMATION REQUIRED
- "QUICK-LOOK" IN SPRITES '95 CAMPAIGN IS THE FIRST PHOTOMETRIC EVIDENCE OF IONIZATION
- RESULTS HAVE IMPLICATIONS FOR INTERPRETATION OF OTHER EXPERIMENTAL FINDINGS
- PRESENTATION OF PRELIMINARY FINDINGS - ANALYSIS IN PROGRESS - SUGGESTIONS WELCOME

SOURCES OF OPTICAL EMISSION IN ELECTRIC FIELD INDUCED CS EVENTS

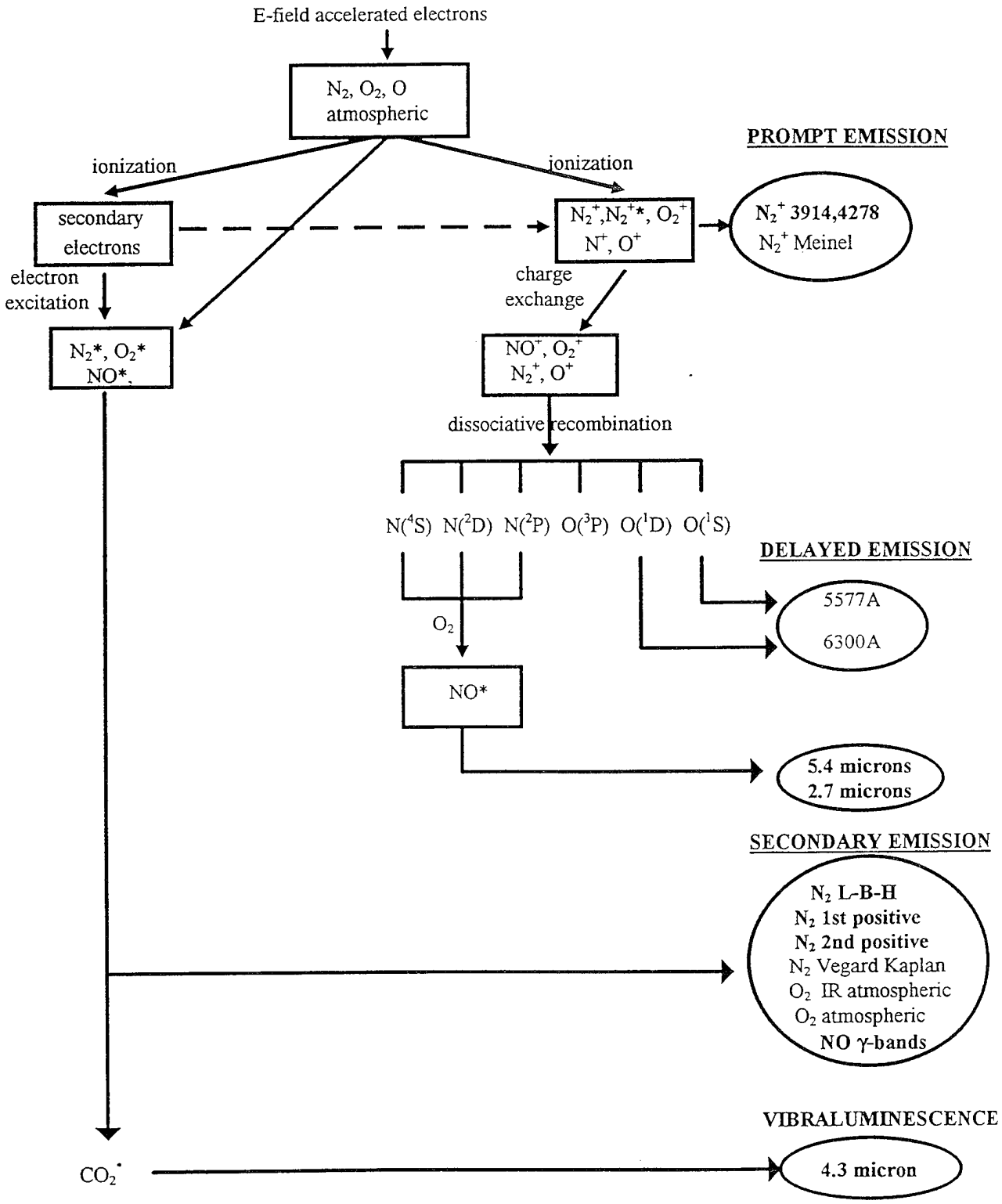


Table 1.
Characteristic Emission Features for Energized Atmosphere
(Molecular Band Characteristic Wavelength Refers to (v',v''=0,0) band origin)

Species System	Characteristic Transition	Characteristic Wavelength	Radiative Lifetime (s)
$O(^1D)$ Red Line	$^1D \rightarrow {}^3P$	6300A	148
$O(^1S)$ Green Line	$^1S \rightarrow {}^1D$	5577A	0.8
$O_2(^1\Sigma)$ Atmospheric	$b^1\Sigma \rightarrow X^3\Sigma$	7619A	11.76
$O_2(^1\Delta)$ IR Atmospheric	$a^1\Delta \rightarrow X^3\Sigma$	1.269μm	3.9×10^{3}
$O_2(^3\Sigma)$ Herzberg	$A^3\Sigma \rightarrow X^3\Sigma$	2856A	3.0×10^{-2}
$O_2(^3\Sigma)$ Schumann-Runge	$B^3\Sigma \rightarrow X^3\Sigma$	2030A	4.2×10^{-8}
$N_2^+(^2\Sigma)$1st Negative	$B^2\Sigma \rightarrow X^2\Sigma$	3914A, 4278A(0,1)	7.1×10^{-8}
$N_2^+(^2\Pi)$ Meinel	$A^2\Pi \rightarrow X^2\Sigma$	7200A	1.7×10^{-5}
$N_2(^3\Sigma)$ Vegard Kaplan	$A^3\Sigma \rightarrow X^1\Sigma$	2600A	1.9
$N_2(^3\Pi)$ First Positive	$B^3\Pi \rightarrow A^3\Sigma$	6700A	8.9×10^{-6}
$N_2(^3\Pi)$ Second Positive	$C^3\Pi \rightarrow B^3\Pi$	4000A	3.7×10^{-8}
$N_2(a^1\Pi)$ L-B-H	$a^1\Pi \rightarrow X^1\Sigma$	2000A	1.5×10^{-4}
$NO(A^2\Sigma)$ γ-bands	$A^2\Sigma \rightarrow X^2\Pi$	2275A	2.0×10^{-7}

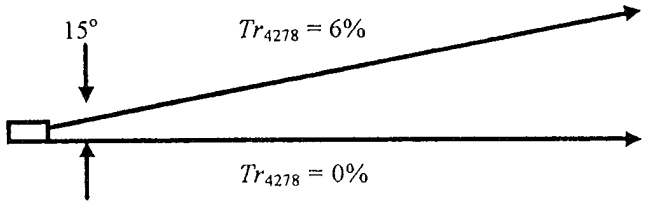


Mission Research Corporation

(BACK-UP)

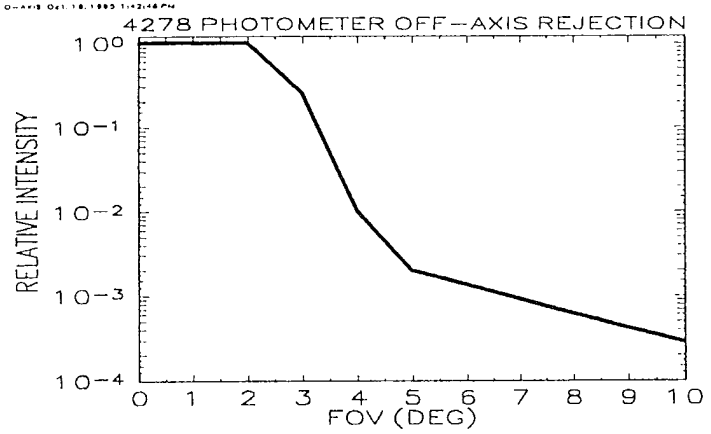
CHARACTERISTICS OF SPRITES

DESCRIPTION OF PHOTOMETER MEASUREMENTS



ELEVATION ANGLE PUTS C/L AT ≈ 80 KM FOR 300 KM RANGE

PHOTOMETER FOV=6° - FOOTPRINT ≈10 KM PER 100 KM RANGE



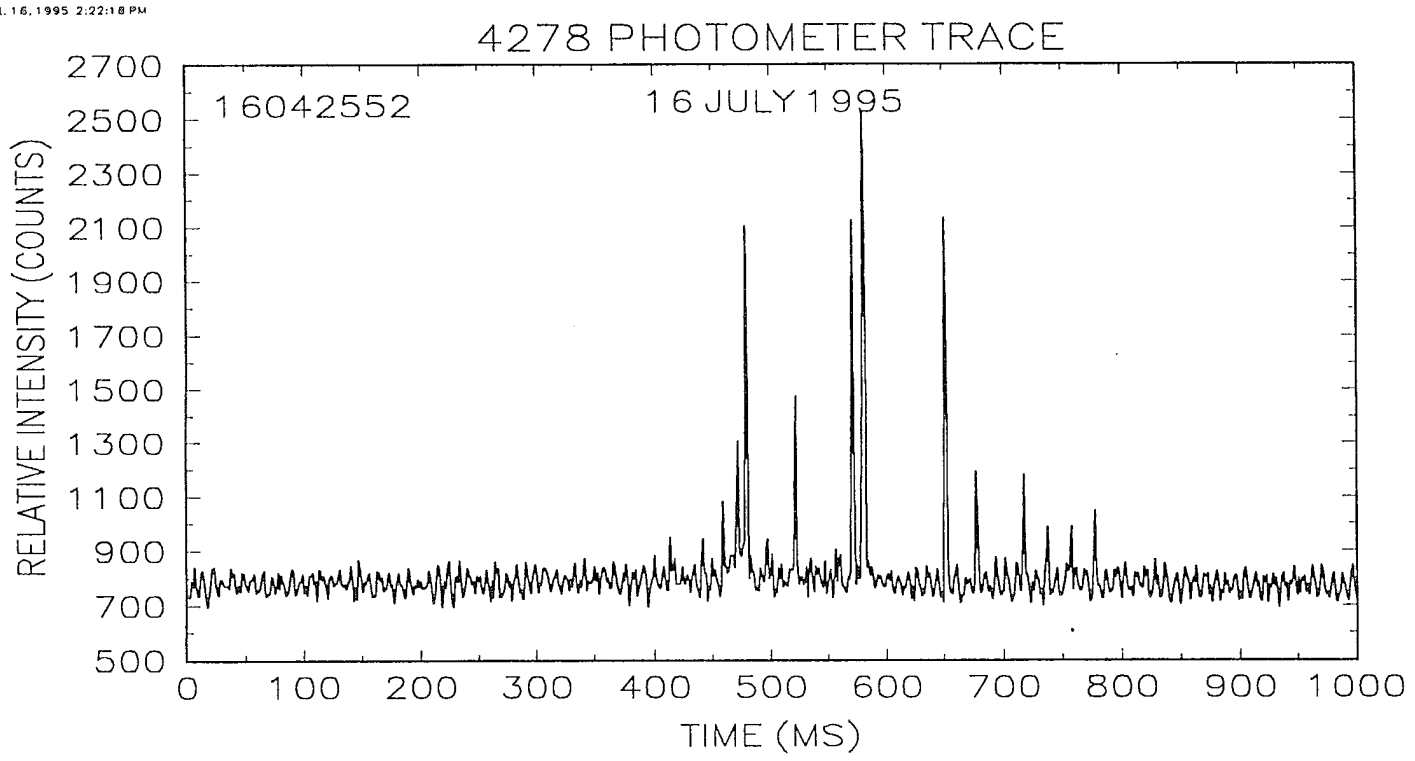
- PHOTOMETER DESIGNED FOR PL EXCEDE III
- APERTURE = 4.458 CM^2 , $A\Omega = 8.559X10^{-5}$ CM^2-SR
- DETECTOR RESPONSE N, TIME CONSTANT 80 nS
- DARK NOISE 10 COUNTS S^{-1}
- QUANTUM EFFICIENCY @ 4278A ≈ 17%
- FILTER 4317A CENTER AT ≈ 50%, FWHM 106A
- SAMPLE FREQUENCY - 700 Hz

Mission Research Corporation

CHARACTERISTICS OF SPRITES

4278A PHOTOMETER RESULTS FOR SPRITES

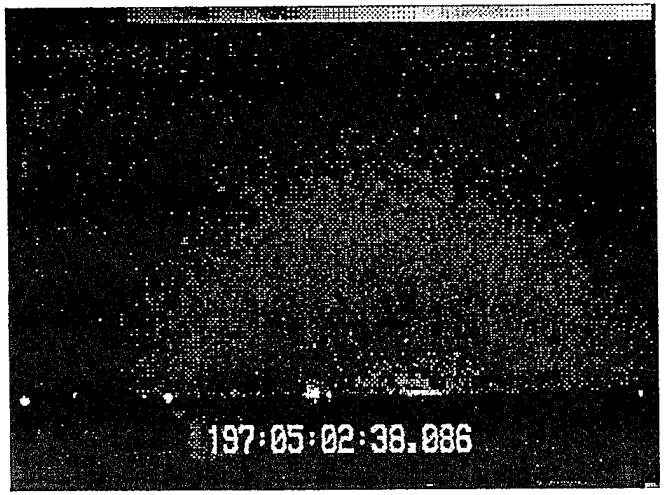
NORMAL CG/CC LIGHTNING TO SOUTH

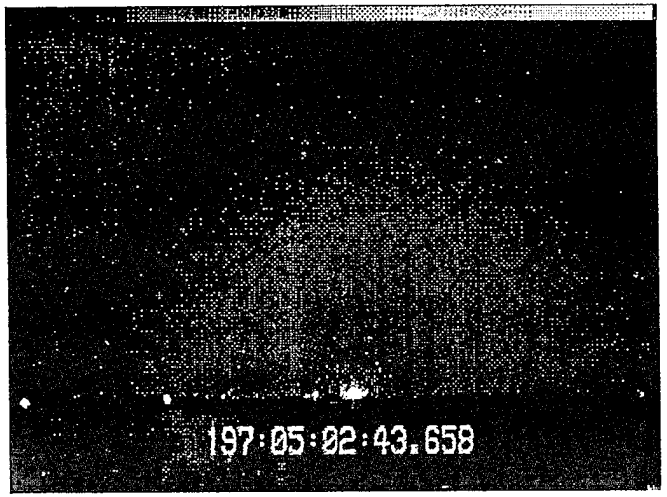


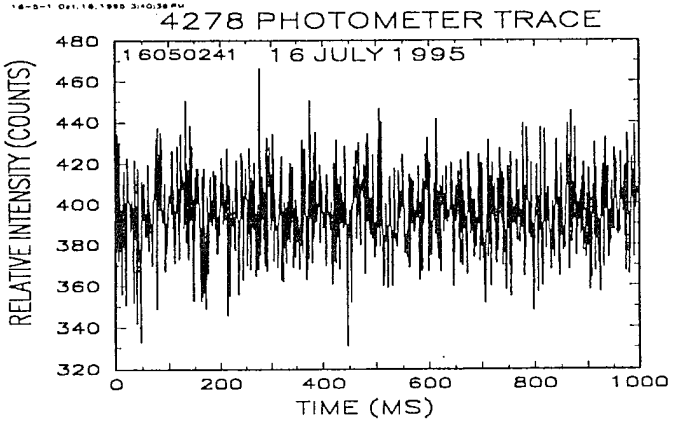
Mission Research Corporation

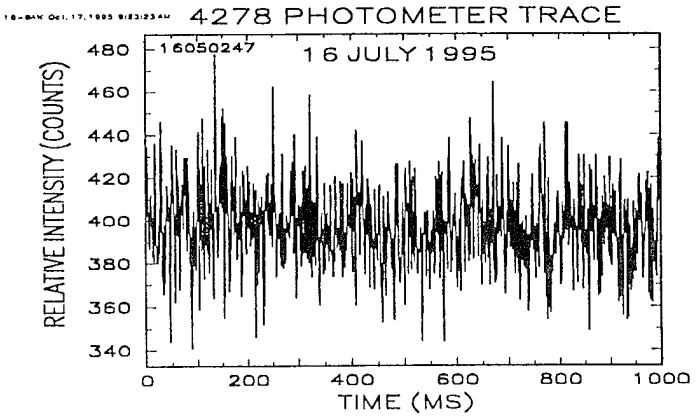
CHARACTERISTICS OF SPRITES

4278A PHOTOMETER RESULTS FOR SPRITES









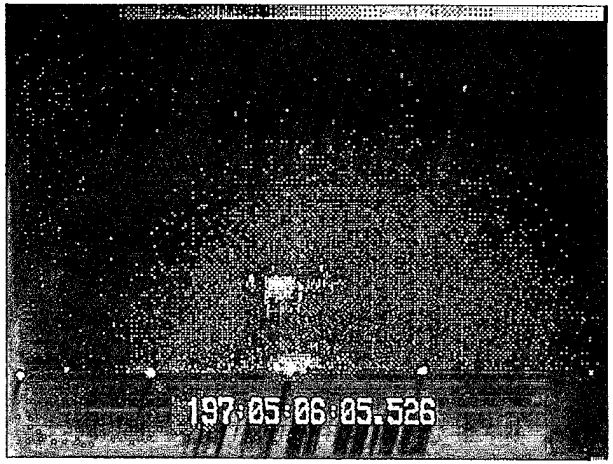
BACKGROUND LIGHTNING DOES NOT YIELD SIGNAL

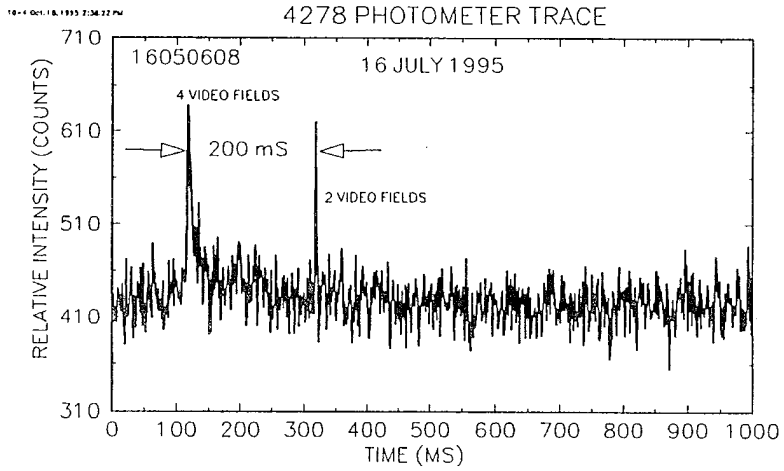
Mission Research Corporation

CHARACTERISTICS OF SPRITES

4278A PHOTOMETER RESULTS FOR SPRITES



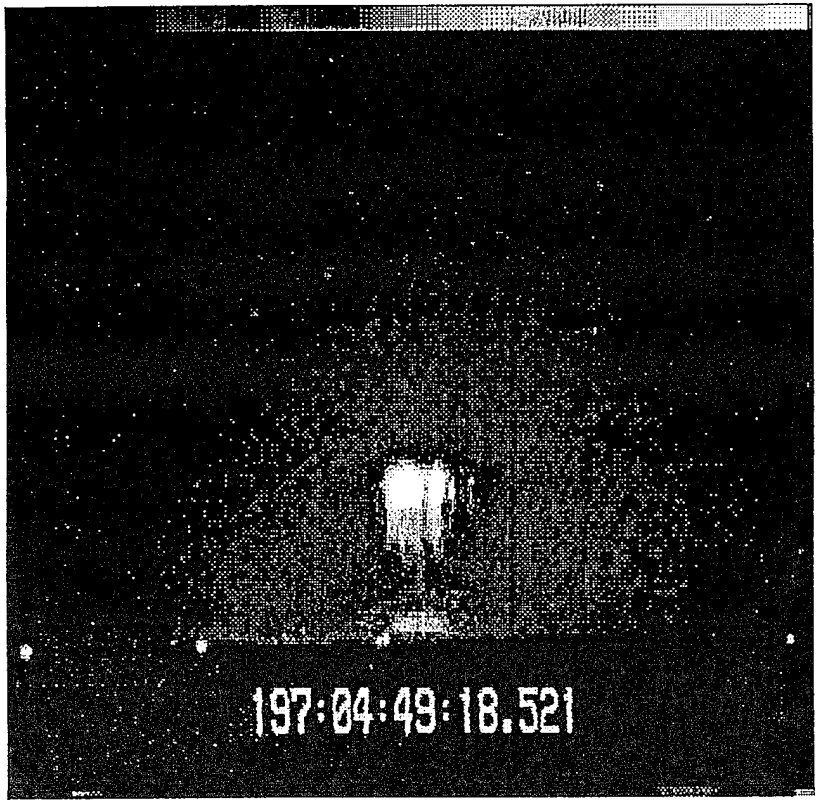


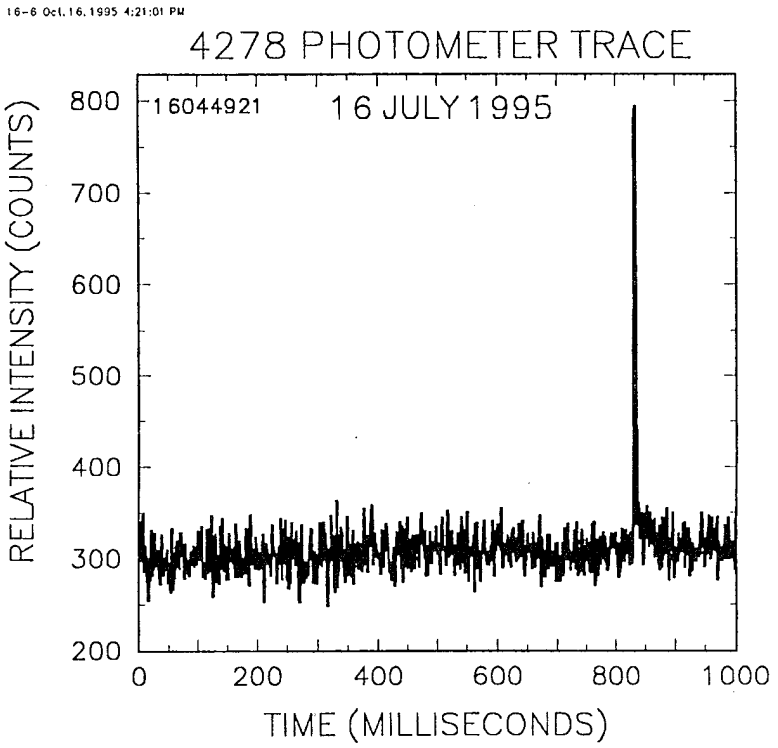


TYPICAL SIGNATURE FROM SPRITE WITHOUT WELL-DEVELOPED TENDRIL STRUCTURE

CHARACTERISTICS OF SPRITES

4278A PHOTOMETER RESULTS FOR SPRITES



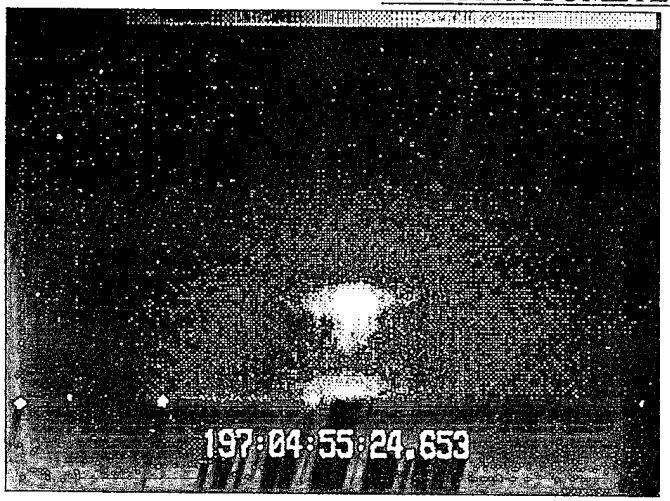


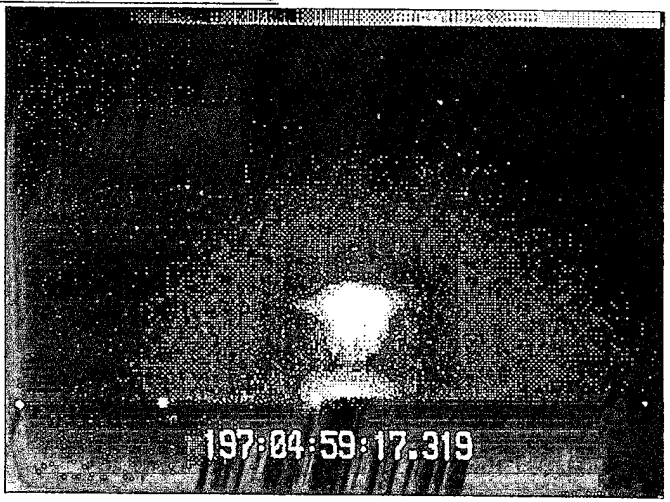
TYPICAL SIGNAL FROM SPRITE WITH WELL-DEVELOPED TENDRIL STRUCTURE

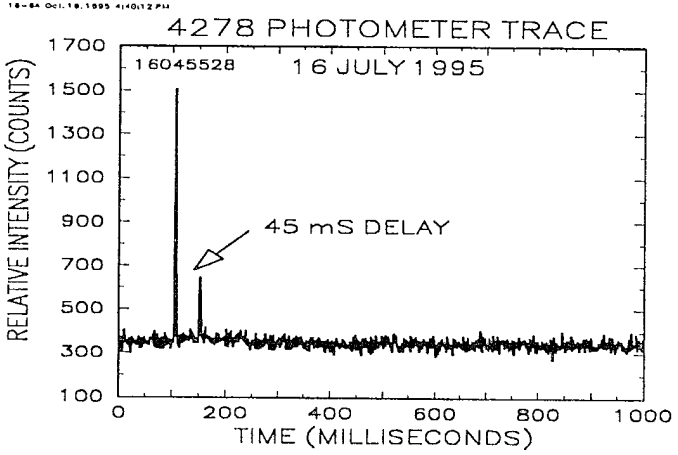
Mission Research Corporation

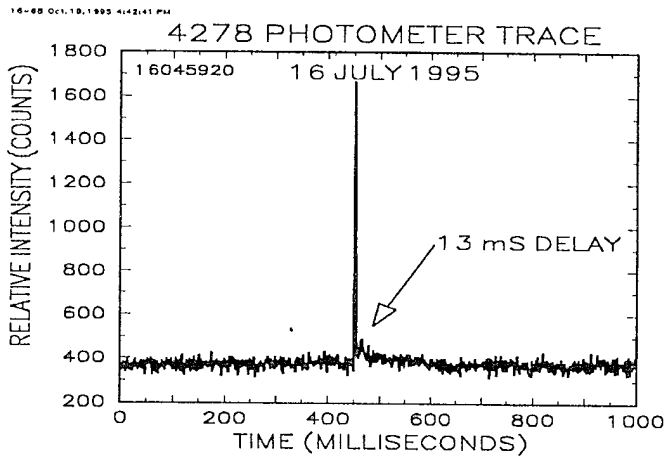
CHARACTERISTICS OF SPRITES

4278A PHOTOMETER RESULTS FOR SPRITES







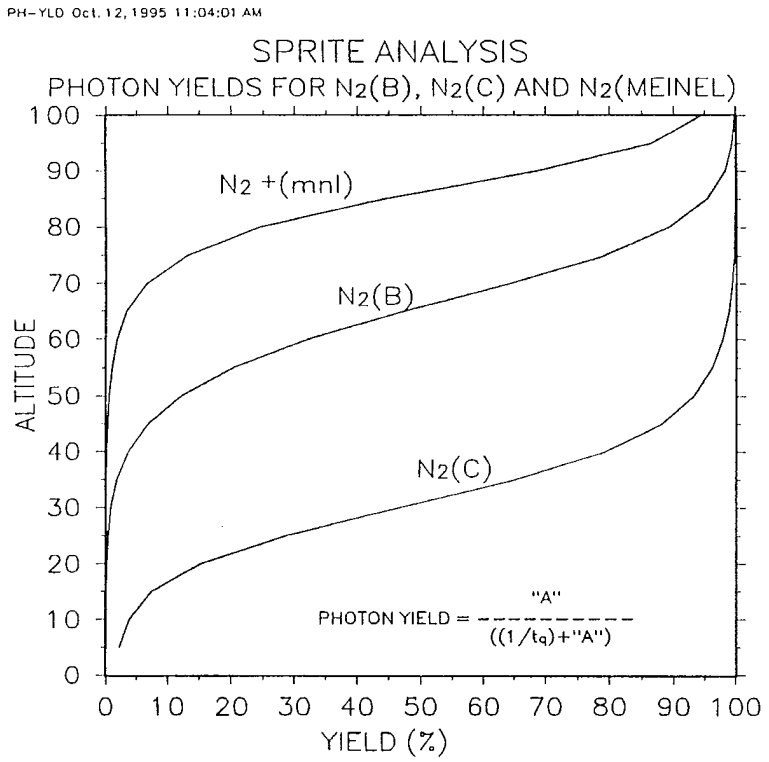


TYPICAL SIGNAL FROM SPRITE WITH WELL-DEVELOPED TENDRIL STRUCTURE AND ELF

Mission Research Corporation

CHARACTERISTICS OF SPRITES

ATMOSPHERIC QUENCHING CAN BE IMPORTANT



ANALYSIS BY ANALOGY WITH AURORA HELPFUL

BUT

ATMOSPHERIC QUENCHING AND SCATTERING CAN PLAY AN IMPORTANT ROLE

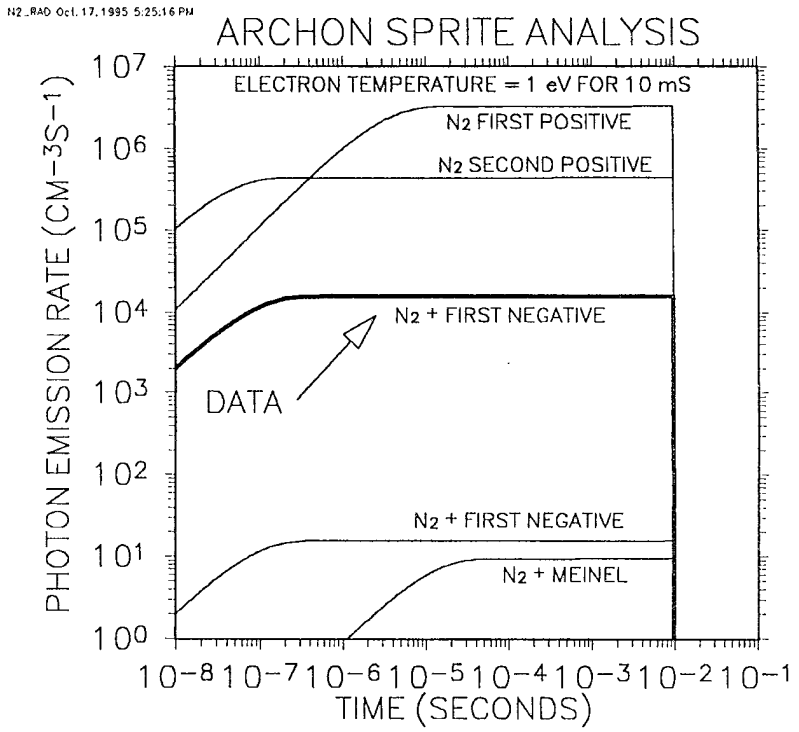
THIS MAY EXPLAIN WHY $N_2(1P)$ NOT DOMINANT AT LOWER ALTITUDES

BUT

THIS DOES NOT EXPLAIN WHY $N_2(2P)$ NOT IMPORTANT AT HIGHER ALTITUDES

CHARACTERISTICS OF SPRITES

ANALYSIS OF "RED" PART OF SPRITE



QUESTION: CAN LOW ENERGY ELECTRONS MAKE 600 kR $N_2(1P)$?

MAGIC HAPPENS → ELECTRONS DETACH TO DAYTIME VALUES (10^3 CM^{-3}) AND HEAT TO 1eV

TIME-DEPENDENT ELECTRON IMPACT EXCITATION AND COLLISIONAL - RADIATIVE QUENCHING

ANSWER: YES - BUT THIS MODEL DOESN'T MAKE PHYSICAL SENSE
REALITY IS MORE COMPLEX

CAVEATS:

(1) IGNORES ENERGY INPUT
(2) E- SPECTRUM NOT LIKELY MAXWELLIAN
(3) E- "BITE-OUT"

CHARACTERISTICS OF SPRITES

SPRITE MORPHOLOGY (ÁLA SENTMAN)



(Lyons - 1993)

- ELF - LOWER IONOSPHERIC HEATING - FEW mS PULSE, MEGA-RALEIGH (FUKUNISHI) HIGHLY ENERGETIC APPARENTLY RED AND BLUE
- UPPER PART OF SPRITE (RED) IDENTIFIED AS $N_2(1^{ST}$ POSITIVE) (MENDE, SENTMAN) CAN POSSIBLY (?) BE EXPLAINED WITH LOW ENERGY/LOW DENSITY ELECTRON IMPACT EXCITATION
- LOWER PART OF SPRITE, BLUE TENDRILS, NOT SPECTRALLY IDENTIFIED - HIGHER ENERGY (PERHAPS "DISCHARGE") - INTENSITY NOT YET DETERMINED
- BLUE JETS IN THIS REGION HIGHLY ENERGETIC ESTIMATED TO BE 500 kR $N_2(1^{ST}$ NEGATIVE) (WESCOTT)

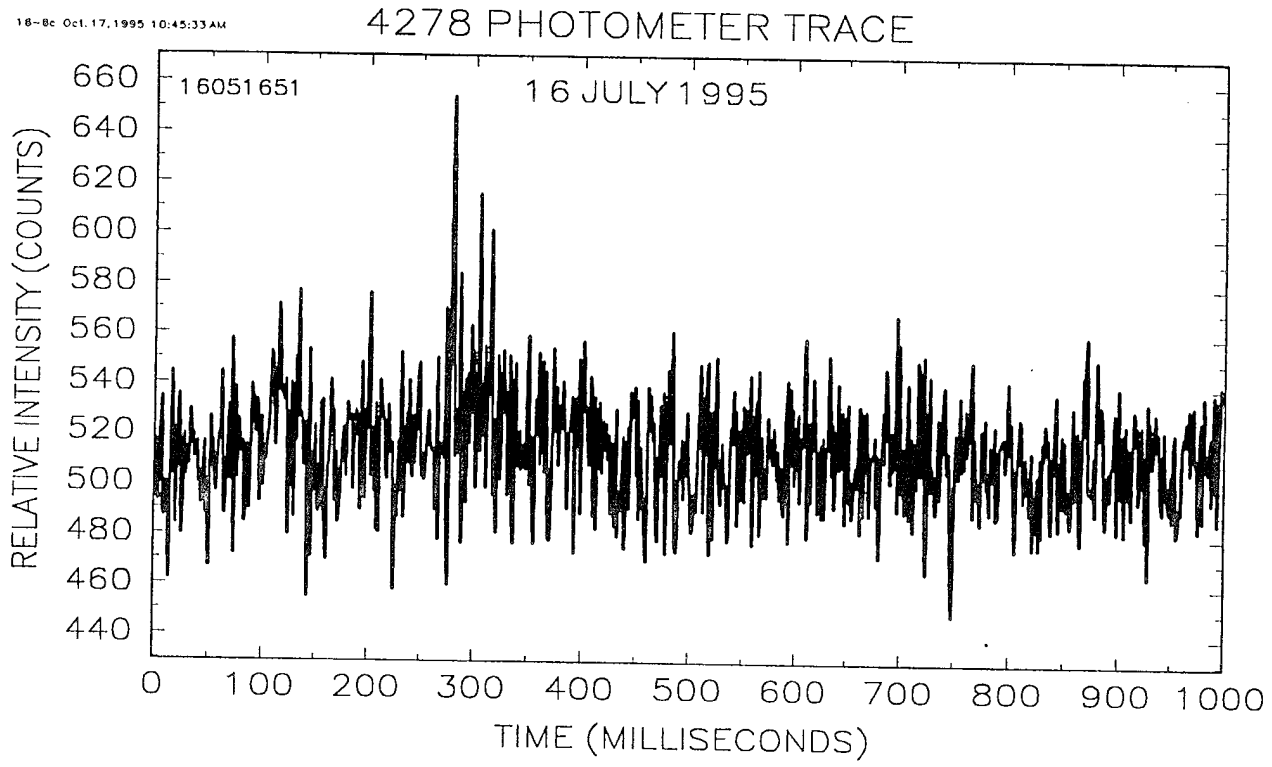
IMPLICATIONS FOR CHEMISTRY

THIS SUGGESTS MOST ENERGETIC PROCESSES AT LOWER ALTITUDES WITH RELATED BUT SEPARATE IONOSPHERIC HEATING (TARANENKO, INAN, et. al.)

CHARACTERISTICS OF SPRITES

4278A PHOTOMETER RESULTS FOR SPRITES

PHOTOMETER SIGNAL CORRESPONDING TO MENDE'S SPECTRUM

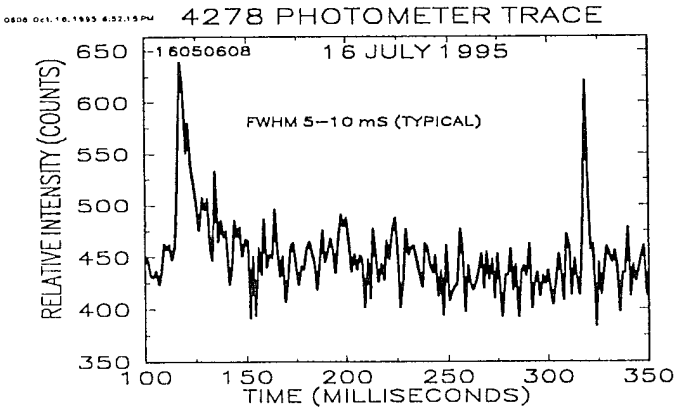


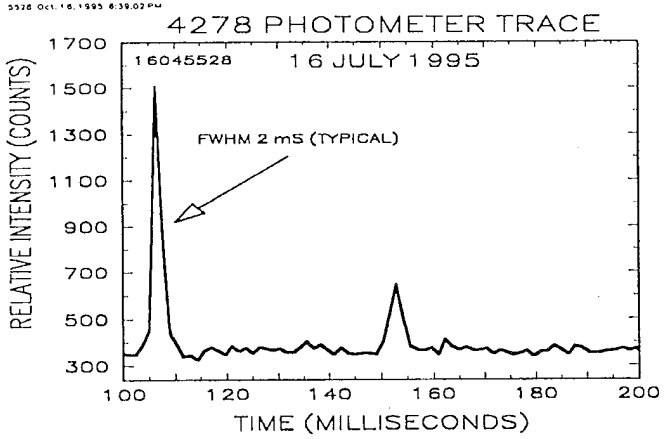
PHOTOMETER POINTING SLIGHTLY TO NORTH - PICKED UP "EDGE" OF SPRITE

Mission Research Corporation

CHARACTERISTICS OF SPRITES

SUMMARY OF 4278A PHOTOMETER RESULTS FOR SPRITES





- FIRST DIRECT EVIDENCE OF IONIZATION IN SPRITES

SUMMARY OF FINDINGS:

- SPRITES WITHOUT TENDRILS ≈ 200-400 COUNTS
- SPRITES WITH DEVELOPED TENDRILS ≈ 800 COUNTS
- "ELVES" SIGNATURE CHARACTERISTICS CONSISTENT WITH FINDINGS OF FUKUNISHI, 1200-2000 COUNTS
- OPTICAL SCATTERING AND QUENCHING IMPORTANT

WHAT'S NEXT?

- CO-ALIGNED PHOTOMETER WITH VIDEO
- SPECTRAL IDENTIFICATION REQUIRED



Plasma Physics Division

Optical Instruments Available From NRL

Carl L. Siefring, Paul A. Bernhardt, John A. Antoniadies

The NRL Plasma Physics Division has two low-light level optical systems that may be of use in ground based studies of Sprite, Elves, and Blue Jets.

1) Is a low-light level Near-IR imager ideally suited for monitoring OH emissions. This camera can be used to monitor atmospheric density and temperature changes due to gravity waves and Sprites.

2) Is a modular low-light level spectral imager (PHILLS) which covers the entire visible range plus a portion of the NIR and UV. This camera can be useds as either a spectrograph or as a streak camera.

NEAR INFRARED CAMERA AVAILABLE FOR OBSERVING SPRITES AND RELATED PHENOMENA

P.A. Bernhardt, J.A. Antoniades, and C. Siefring
Plasma Physics Division
Naval Research Laboratory
Washington, DC 20375-5320

Air Force Workshop on Sprites and Blue Jets
18-19 October 1995
Hanscom Air Force Base, MA

OBSERVATION OBJECTIVES

- Modulation of OH ($\Delta v = 2$) Nightglow During Lightning
  - Atmospheric Heating
  - Gravity Waves
- Excitation of Stratospheric and Mesospheric OH During Sprite Events
- Survey of Near Infrared in the Stratosphere/Mesosphere Over Storms

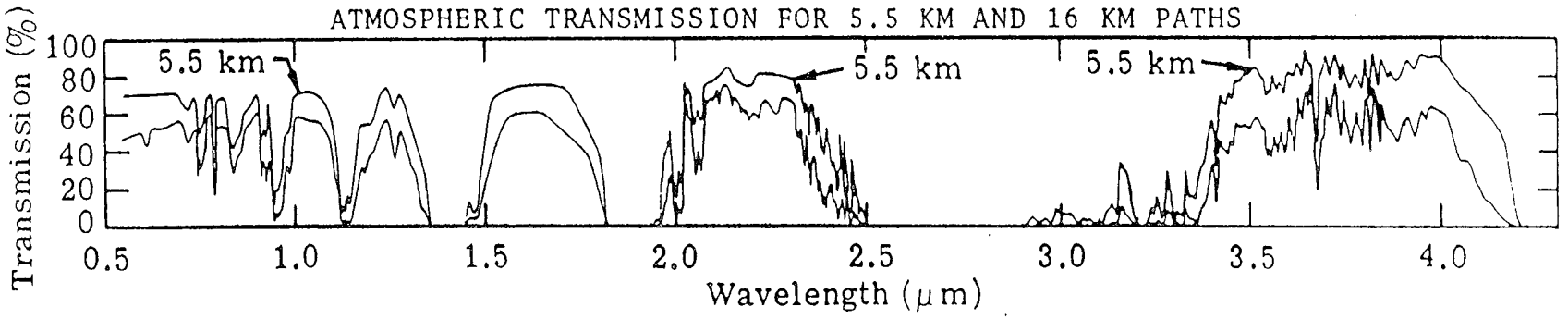
OH MOLECULAR BAND EMISSIONS

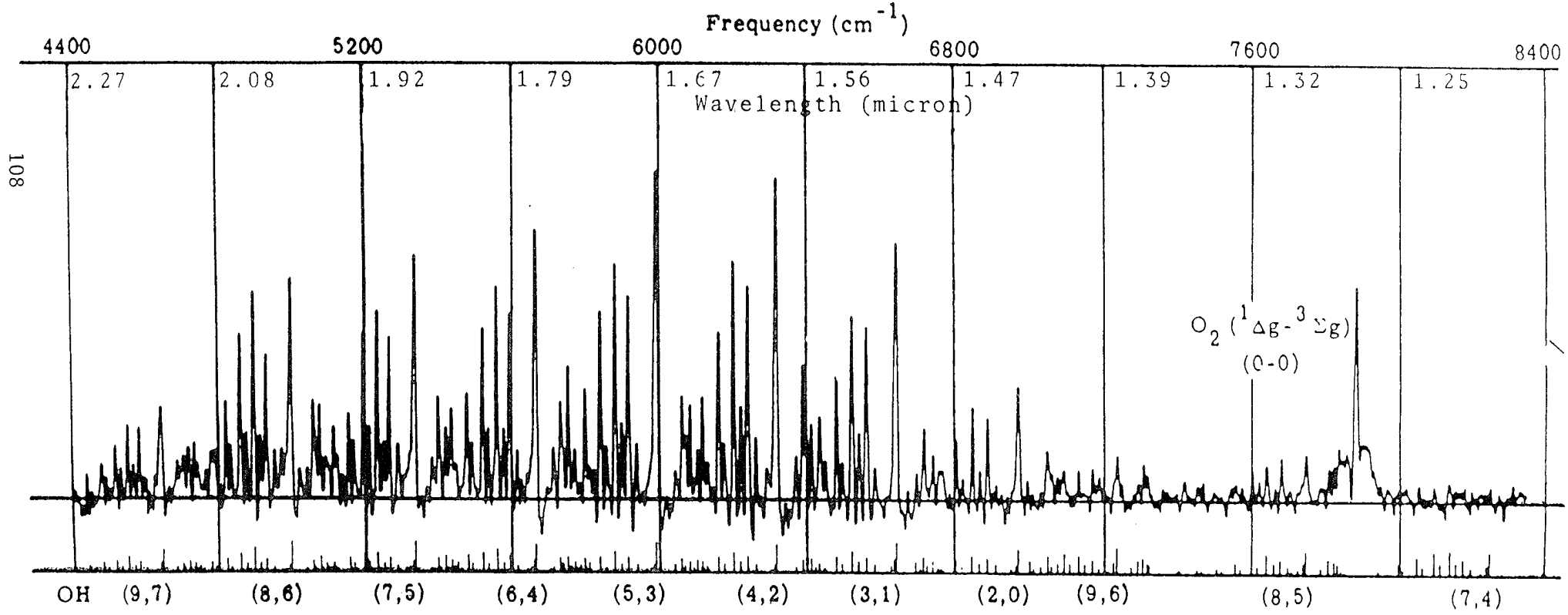
$$H + O_3 \rightarrow OH\ (v' \leq 9) + 0_2 + 3.3\ eV$$

Peak Emission Altitude 85 to 90 km (Mesosphere)

Strong 100 kR band near 1.5 μm

Spatial and Temporal Variations from Acoustic Gravity Waves





Spectrum of night airglow observed from an altitude of about 80,000 feet.

InGaAs Focal Plane Array Camera (IFPAC)

Unique Capabilities

1 to 1.7 μm Near Infrared Sensitivity

Room Temperature Operation

Small, Portable System Available for Aircraft

Both Imaging and Spectroscopy Configurations

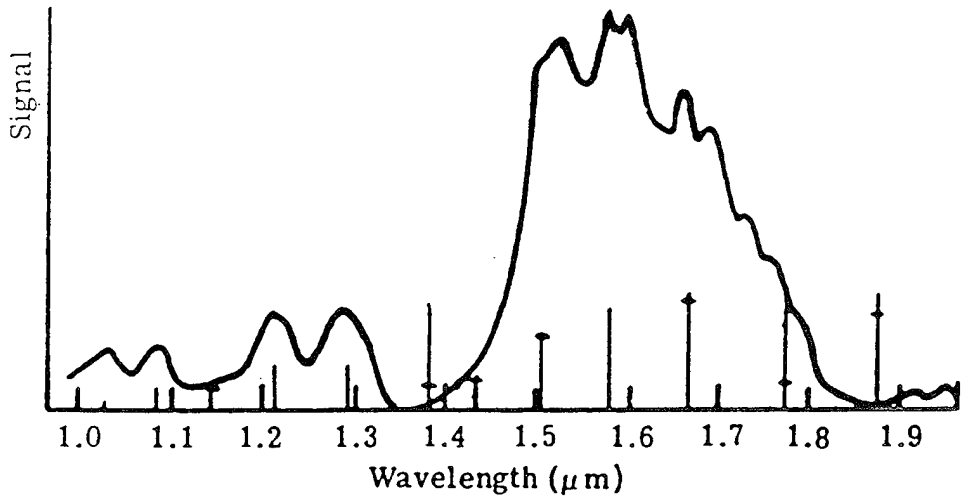
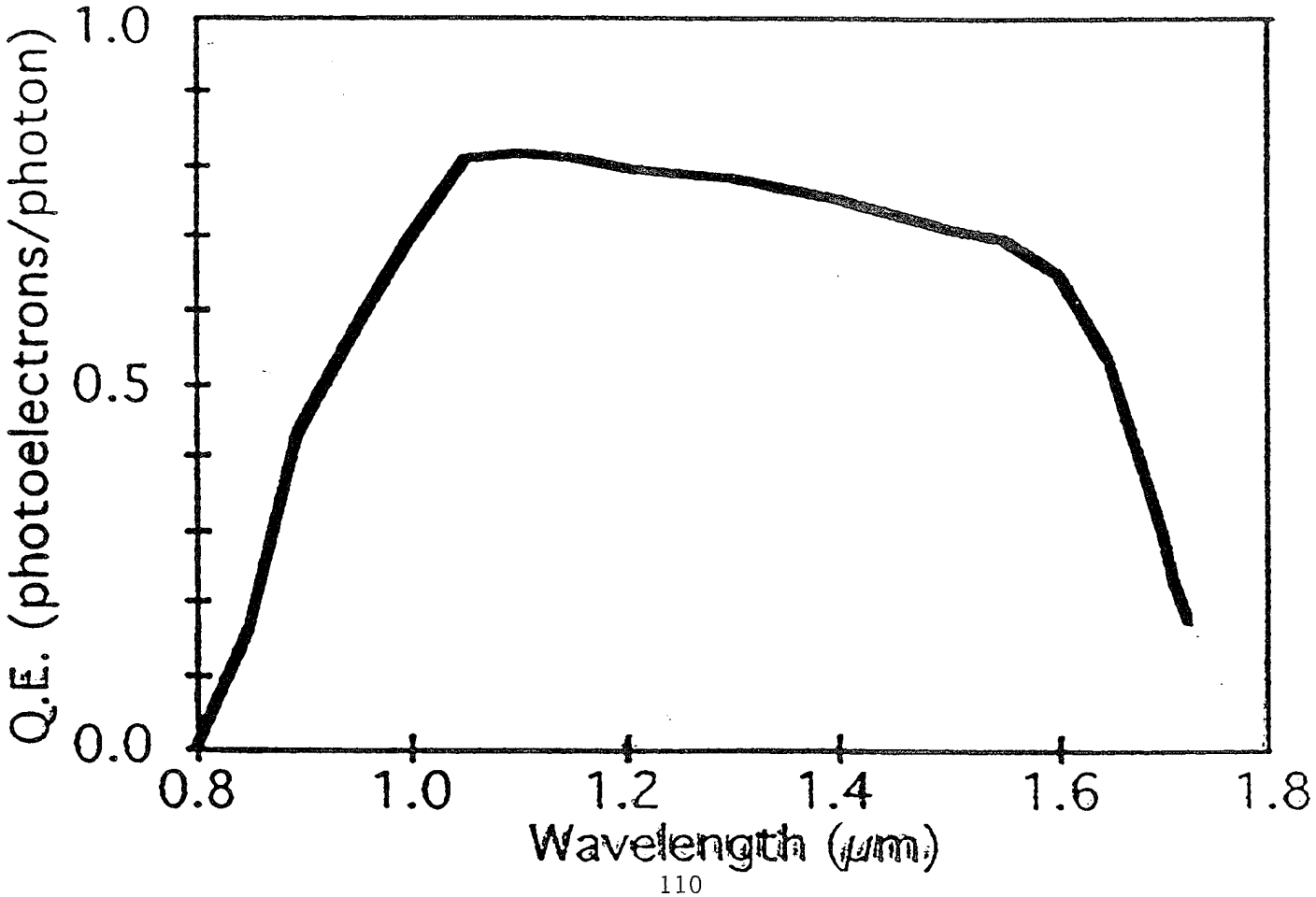
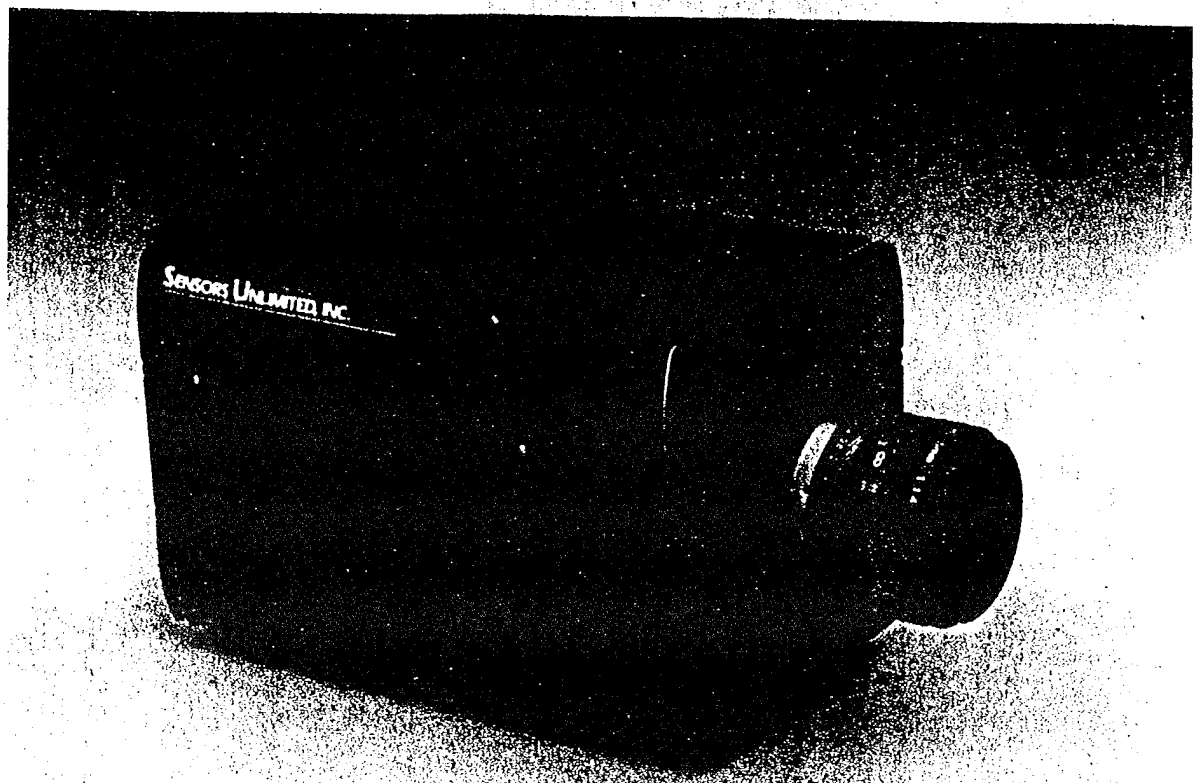


Fig. 3.41 Nightglow spectrum. It is obtained with a scanning spectrometer (projecting slit width of 200 Å). The origins and expected intensities of OH bands are shown by vertical lines; the horizontal strokes indicate the reduction due to water vapor.[80]





SHORT WAVELENGTH INFRARED CAMERA

InGaAs Photodiode Array (128 by 128)

Thermoelectrically Cooled to -30 C

200 IMAGES/S 12 BITS/PIXEL



Plasma Physics Division

PHILLS

Carl L. Siefring, John A. Antoniadies

PHILLS is a modular low-light level spectral imager which covers the entire visible range plus a portion of the NIR and UV.

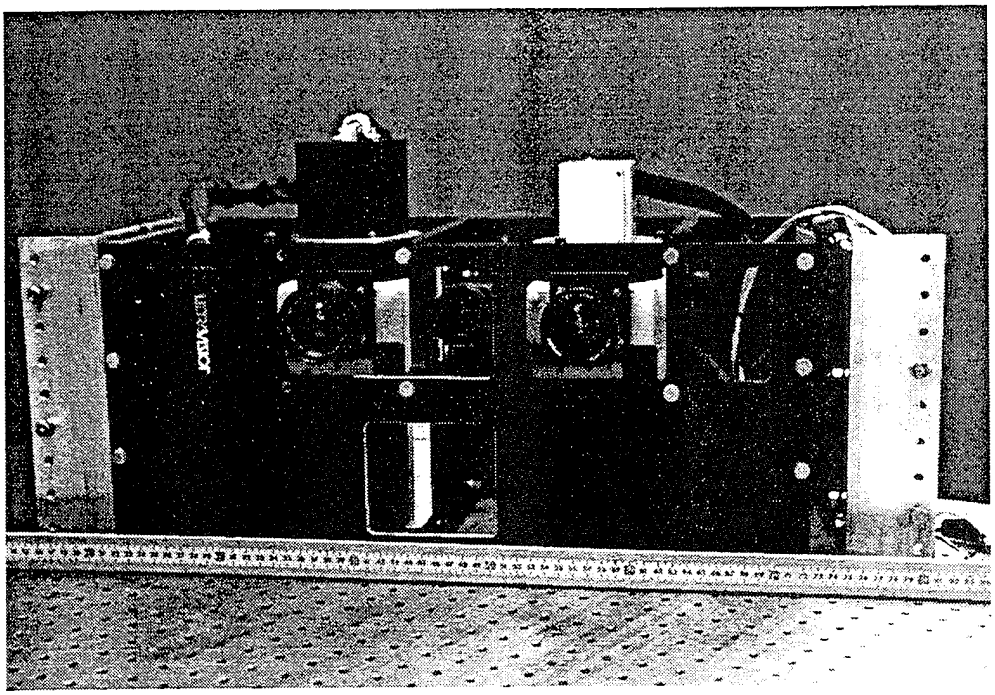
The camera can be used as a spectrograph to measure the optical spectra of Sprites and Blue Jets.

Or like a streak camera to measure the time/altitude history of the Sprite optical emissions.

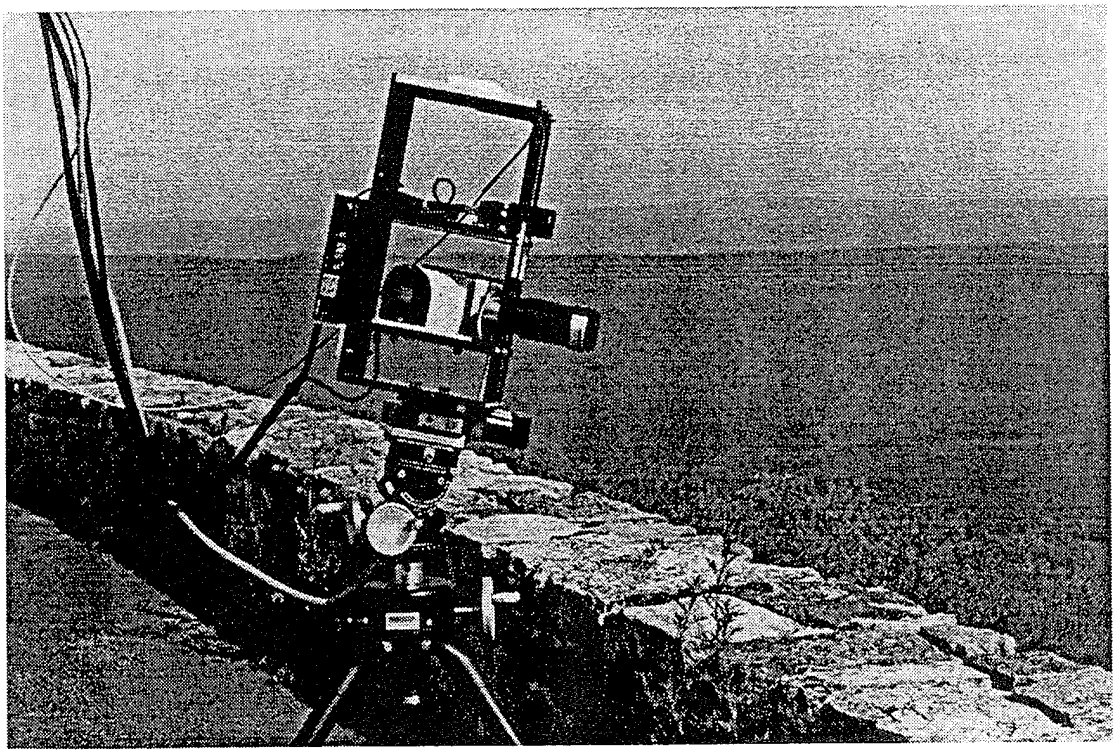
PHILLS Sensor Modules

- Light, Compact Device Ruggedized for Airborne or Field Operation
- Modular Design for Customized Sensor Configuration
- ≥ 0.2 nm Resolution, ≥ 500 bands / module, 1-72 deg Field of View
- Integrated Video Viewfinder for Precise Pointing
- Integrated GPS Tracking and Recording
- Multiple Modules
  - Analog: RS-170 Tape Output, up to 10 bits/pixel, 2hr Continuous Recording, Multiple Cameras, 300-950 nm intensified
  - High Speed Digital: (12 bits or 16 bits/pixel, up to 200 frames/sec with 256000 pixels/frame)
- Intensified modules for Low Light Operation

NRL PHILLS Sensor Assemblies

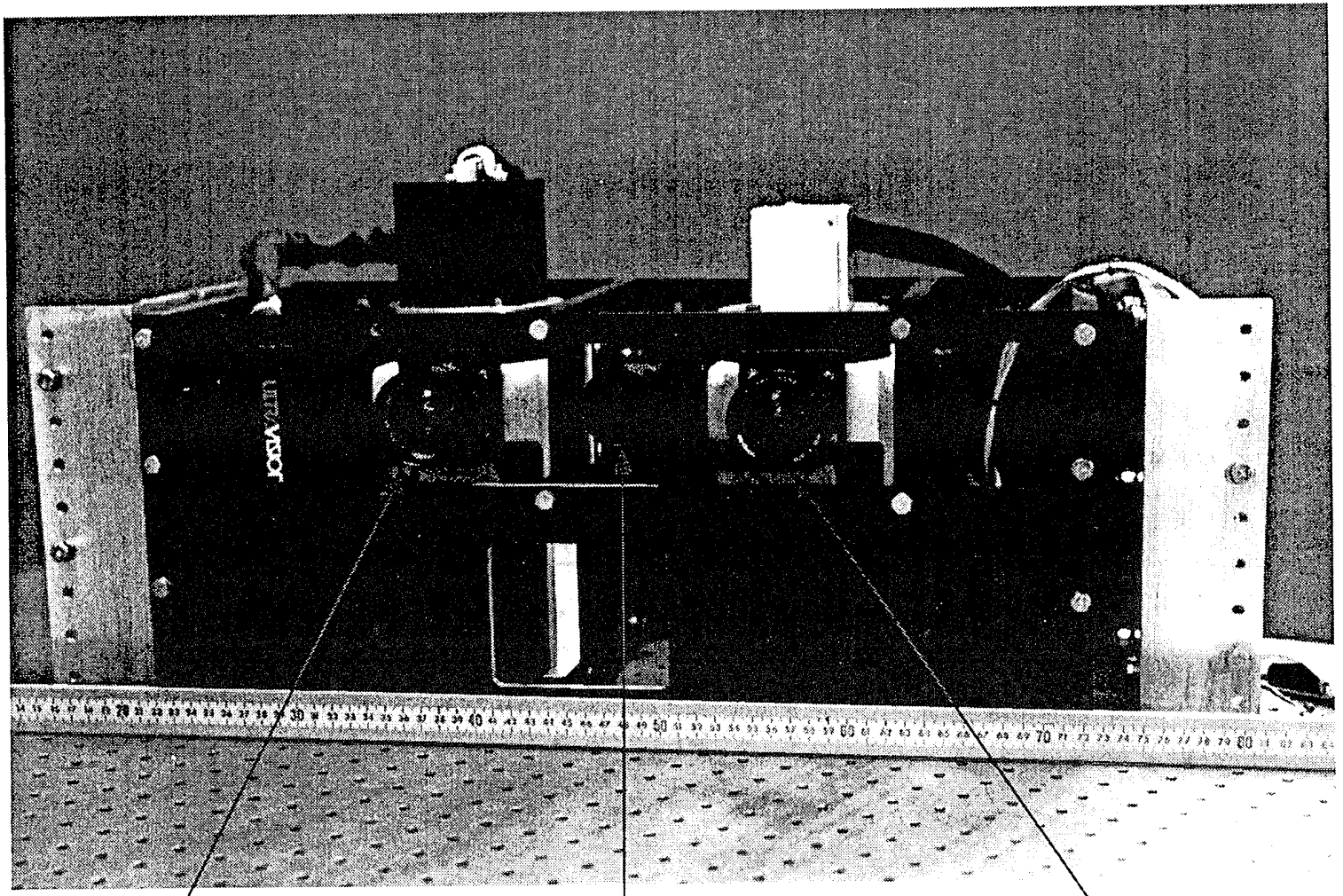


PHILLS sensor assembly deployed on NRL's P-3 589 for the Florida Keys Mapping expedition in October, 1994. The sensor assembly includes the intensified UV/VIS CCD and the VIS/NIR intensified hyperspectral imaging modules and the color CCD viewfinder.



PHILLS ground based deployment at Skyline Drive, Virginia. The photograph depicts the 16 bit digital, UV-NIR module. The sensor assembly includes the hyperspectral imager, the 3-CCD color viewfinder camera, the GPS antenna and the computerized scanning mount (360 degree rotation in 50 μrad steps).

Portable Hyperspectral Imager for Low Light Spectroscopy (PHILLS)



Near Infared (NIR) Spectrometer (500nm to 950nm, 420 bands)

3-CCD Color Viewfinder Camera

Visible Wavelength Spectrometer (330nm to 670nm, 610 bands)

Hyperspectral Imaging System

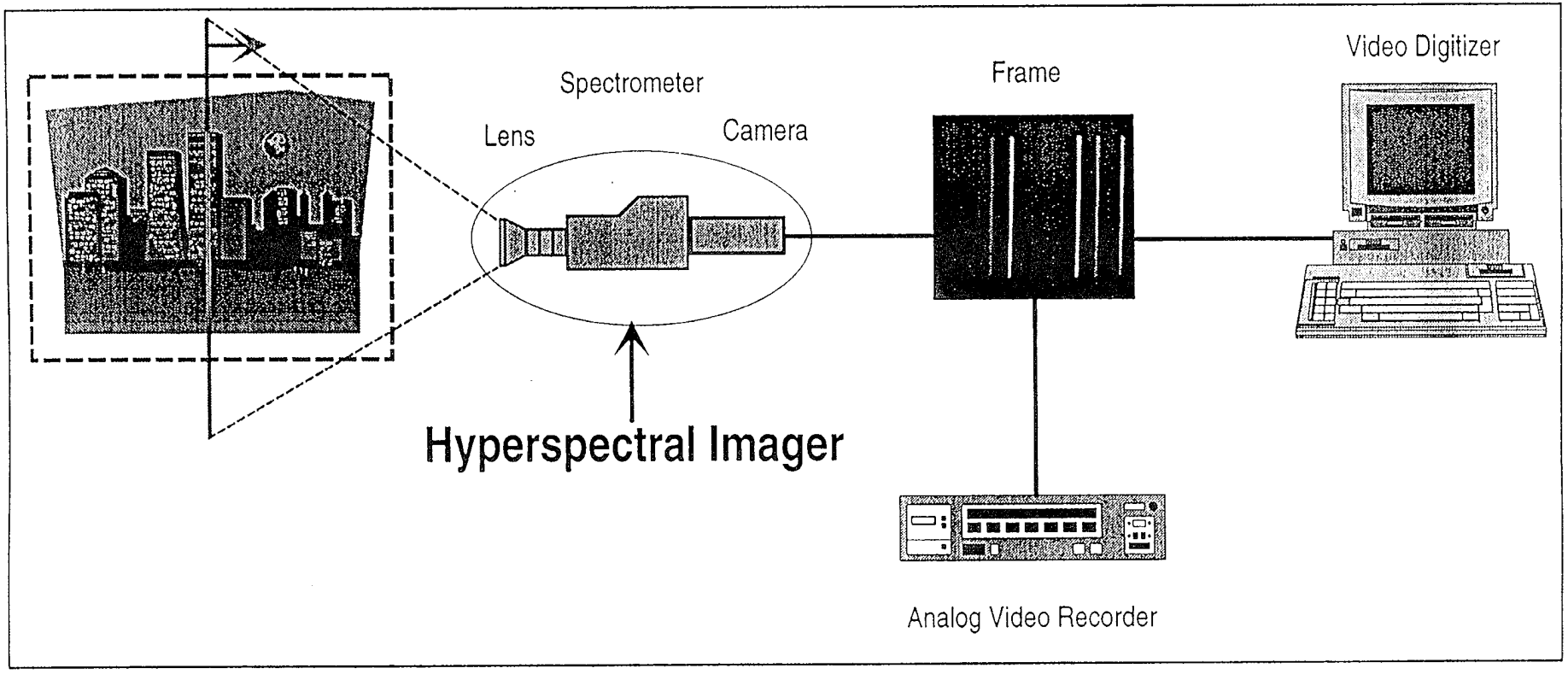
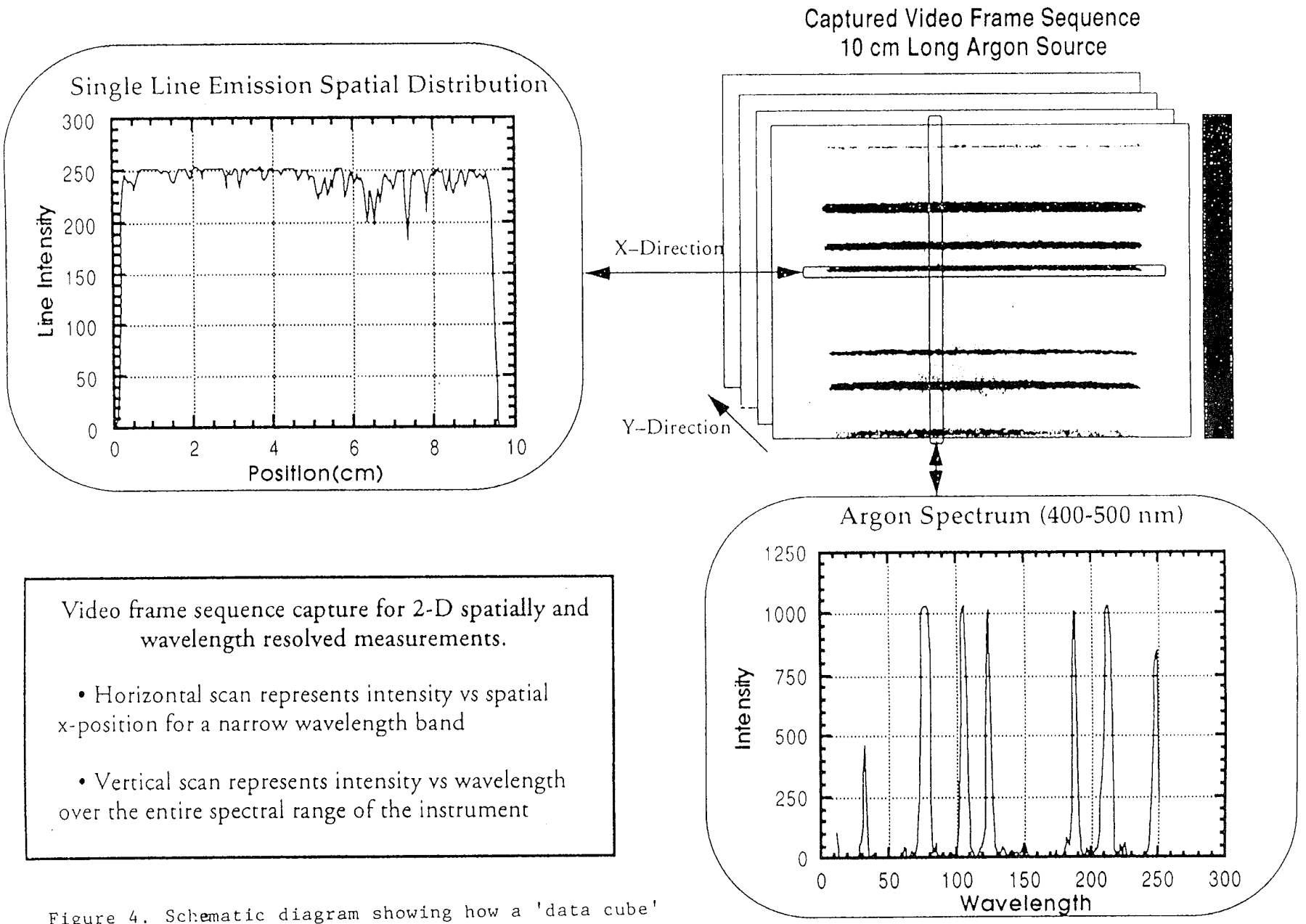


Figure 3. Basic components of a Hyperspectral Imaging System

Sample Analysis of 2-D Spatially Resolved Hyperspectral Images



Video frame sequence capture for 2-D spatially and wavelength resolved measurements.

- Horizontal scan represents intensity vs spatial x-position for a narrow wavelength band
- Vertical scan represents intensity vs wavelength over the entire spectral range of the instrument

Figure 4. Schematic diagram showing how a 'data cube' is formed from video frames.

PHILLS

Portable Hyperspectral Imager for Low Light Spectroscopy

Instrument Capabilities

- Modular Multisensor Imaging Instrument
- Highly Intensified CCD Detectors(<10 R*sec min Illumination for S/N=1, 10^{-8} fc sensitivity)
- Auto or Manual Gain, Gate and Iris (>10^{11} total dynamic range)
- 5.5-700 mm Focal Length Input Optics
- Remote Iris, Focus and Zoom Lens control
- High Throughput (f2.8 spectrograph)
- 300-1050 nm Coverage in >1100 Spectral Bands
- ≥0.3 nm Resolution with intensification
- 275 Spatial bands for UV/VIS, 488 for VIS/NIR
- 15 min max operation with real time (30 fps) full frame digital acquisition
- 2 hrs continuous acquisition with Hi8 tape
- 8-bit gray scale arbitrarily extensible with built-in frame accumulation operation
- RS-170 Output, 30 fps for Hi8 or SVHS tape
- Real Time Digital Frame Capture with up to 3 cameras
- SMPTE, RC or GPS Time and position tagging

Instrument Components

- Standard TV (C-mount) or 35 mm Input Optics
- Flat Field Holographic Grating Spectrographs with Interchangeable Gratings
- Extended Red GEN III ICCD Camera(VIS/NIR module)
- GEN II ICCD Camera (UV/VIS)
- Integrated Computer Controlled Programmable Scanning Mount (6 arc*sec resolution)
- PentiumPC based Real Time Image Acquisition and Processing
- Real Time Frame Grabber for Digital Capture
- Hi8 Tape Recorders
- Color or Monochrome Viewfinder Video Camera

Spectrograph Specifications

- Concave Holographic Flat Field Spectrograph (200 mm fl, 25x8 mm image) with Interchangeable Gratings
- Interchangeable Slits (25-1000 μm wide x 8 mm high)
- 24-70 nm/mm Dispersion

ICCD Camera Specifications

- Gated ICCD Camera (≥100 ns gate)
- 25 mm GEN III Intensifier
- 18 mm GEN II Intensifier
- 16-bit Digital Slow Scan CCD Camera
- 600 TV Line Resolution, RS 170 output
- Remote Operation via Camera Controller
- Genlock Sync

Scanning Mount Specifications[1]

- Stepper Motor Controlled Rotary Table
- 55 lbs load, 6 arcsec Resolution, 72 deg/sec max
- Computer Programmable Controller with up to 99 program memory+Hand Held Terminal
- RS-232 Mount Control Interface

Digital Frame Acquisition[1]

- EISA Bus Frame Grabber
- 30 fps full frame Real Time Acquisition, Processing and Display
- On-Board Graphics Accelerator
- 40 MPixel/sec Monochrome Data Acquisition
- Simultaneous Grab of up to 3 Synchronized Monochrome Inputs

Digital Data Acquisition System[1]

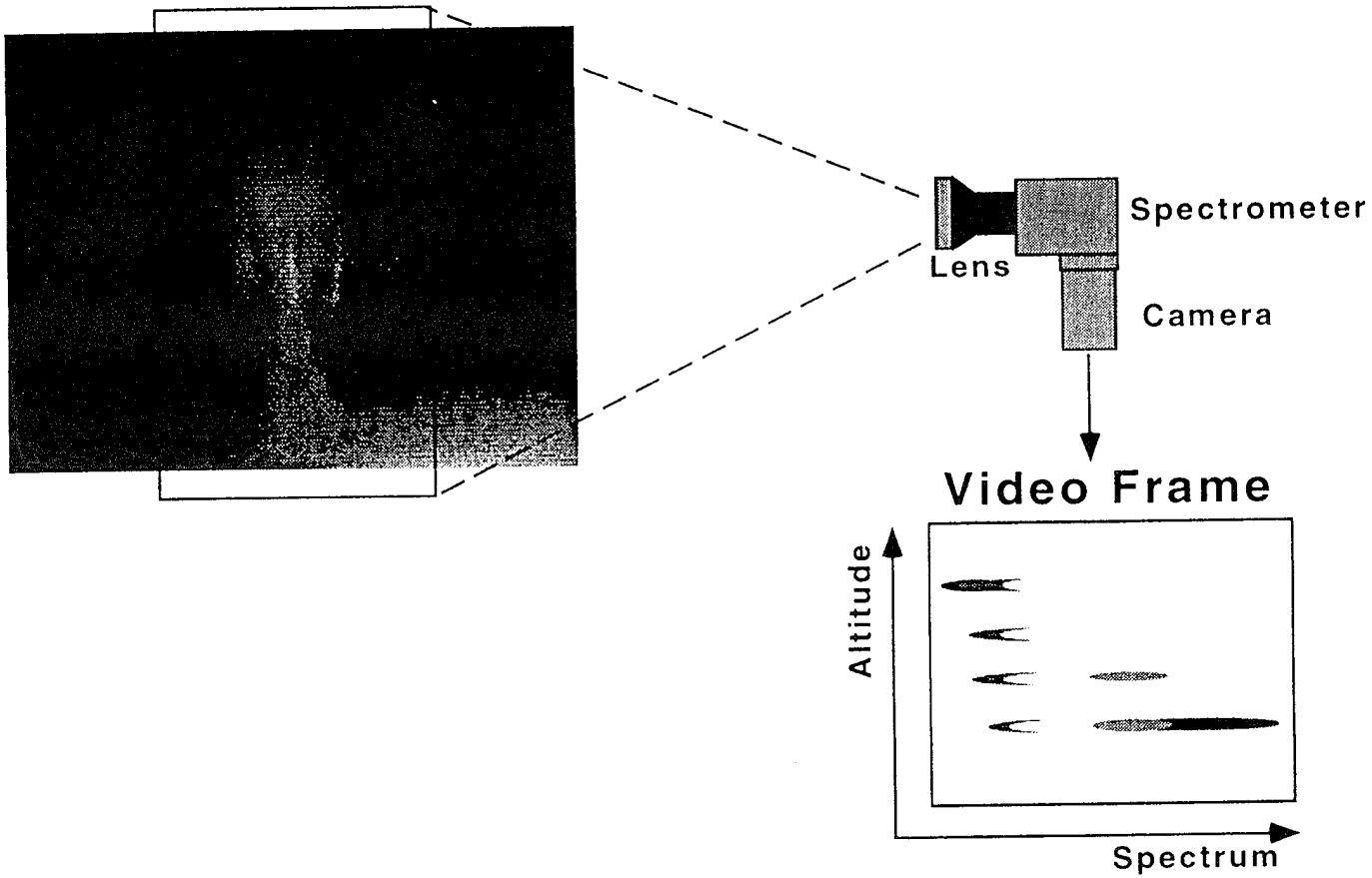
- 90 MHz Pentium Multi-processor System
- 6 GB Fast and Wide SCSI-2 Disk Array
- 96 MB Memory
- Fast Ethernet Adapter

Modes of Operation

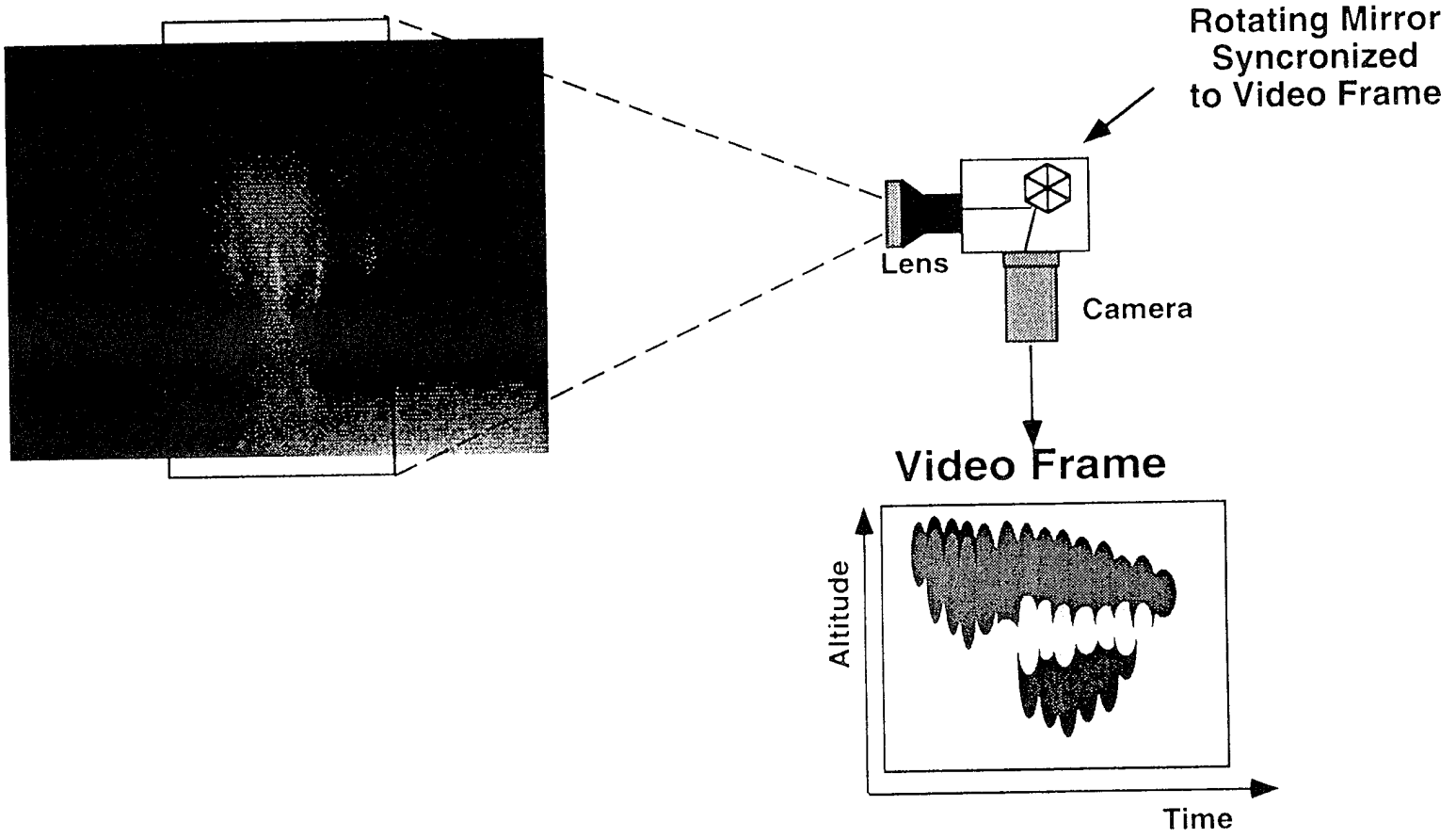
1. Analog Tape Acquisition
   Hi8 Tape Format (2 hrs/tape maximum)
2. Real-time Fast-Scan Digital Acquisition
   30 fps Acquisition Limited By Disk Space and Memory (15 MB/sec max)
   8-bits/pixel
3. Extended Dynamic Range Mode
   Real-time Frame Accumulation for Extended Sensitivity and Dynamic Range
4. Ultra High Sensitivity, Reduced Resolution Mode
   Arbitrary Pixel Binning in both directions
   Non-Contiguouss, Variable Width Band Selection

Table 1. Specifications for PHILLS Instrument as presently configured.

PHILLS Module
used as a Sprite Spectrometer



PHILLS Module
used Like a Streak Camera



TOPSIDE VIEWS OF LIGHTNING AND SPRITES

W. L. Boeck
Niagara University
and
O. H. Vaughan Jr. and R. Blakeslee
NASA Marshall Space Flight Center

For many years Vaughan and Vonnegut have gathered and published pilots reports of unusual sightings above lightning storms. The first video image of a sprite by Winckler showed the sprite but not the causative lightning flash. Trees in the foreground blocked the view of the horizon and the storm. Images obtained from space platforms view these phenomena from the topside.

In the following years, 17 images of sprites were found in the MLE video archives of lightning storm observations from the Space Shuttle. These images established: a strong causal link between a very bright lightning flash under a cloud anvil and a sprite in the mesosphere above the anvil; a fraction of a second time delay between the onset of cloud lightning activity and the appearance of the sprite; that the cloud source of the sprite is characterized by a low lightning flash rate(a few flashs /min) and that sprites are found over North and South America, Africa and Australia, the Atlantic and Pacific Oceans.

The one North American sprite was associated with a positive cloud to ground strike. The other lightning flashs in the scene were associated with negative CG and TRIMPI events. Measurements in the American Mid West demonstrated that the early estimated of height and frequency were much too small.

MLE also recorded the first images of rocket lightning a.k.a. "Blue Jet" on October 21, 1989. The Australian storm differed in several ways from a typical sprite producing storm. The most notable characteristic is the high lightning flash rate (greater than 50/min) and an optically thick anvil cloud. There is some evidence that an overshooting cloud turret is present when "jets" are observed.

In addition to luminous phenomena in the stratosphere and mesosphere, there is the first observation of a lightning flash simultaneous with a flash at the airglow layer. This phenomena is distinguished by the absence of a sprite or other visible event in the clear air below the airglow layer. The example was found during the STS-41 mission on October 7, 1990. The causal storm was over the Atlantic Ocean off the coast of South America. The cloud had a flash rate of less than 1 per minute. The airglow flash appear promptly along with the causal flash. Theories explain this observation as the prompt heating of the ionosphere due to the EMP produced by lightning. Other observations of this phenomena confirm that the production of a luminous disc of several hundred kilometers diameter occurs within 1 ms of the lightning discharge and well before any sprite activity.

Observations of Electric Field and X-rays Above Thunderstorms: Relevant to Optical Sprites?

K.B. Eack, Department of Physics and Astronomy, University of Oklahoma, Norman, OK.

W.H. Beasley, School of Meteorology, University of Oklahoma, Norman, OK.

W.D. Rust, NOAA - National Severe Storms Laboratory (NSSL), Norman, OK.

M. Stolzenburg, Cooperative Institute for Mesoscale Meteorology / NSSL, Norman, OK.

T.C. Marshall, Department of Physics and Astronomy, University of Mississippi, University, MS.

During the Spring of 1995, X-ray detectors were flown on four balloon flights into the stratiform regions of four mesoscale convective systems (MCS). The X-ray instrument uses a sodium iodide scintillation detector. A three-channel (30 to 60, 60 to 90 and 90 to 120 keV) X-ray spectrum is acquired every 0.25 seconds. In addition to the X-ray detector, an electric-field mill and a meteorological radiosonde are also flown on the balloon (Figure 1).

The original motivation for this work was to verify the hypothesis of C.T.R Wilson (1925) that thunderstorm electric fields should be able to produce energetic electrons, and to extend the measurements made by Parks et. al. (1981) and McCarthy and Parks (1985) of X-ray production in thunderstorms. In two of the four flights made, we did observe X-rays associated with the strong electric field region inside the cloud. The fourth and final flight of the season was made on June 29, 1995 from a launch site east of Guymon in the Oklahoma Panhandle. The detector was modified from the previous three flights in that it looked up rather than down. The complete X-ray and electric-field soundings for this flight are shown in Figure 2. Although no X-ray events were detected in the cloud, three pulses with a duration of about 1 second were observed above the cloud near 15 km MSL with a measured atmospheric pressure of 127 mb (Figure 3). Each step in Figure 3 is 0.25 seconds wide. The electric field strength measured at the balloon at the time of the pulses was about -0.5 kV/m (negative meaning the field lines directed downward).

The pulses occurred at 06:54:50, 06:55:24 and 06:55:26 UTC. From the NLDN (National Lightning Detection Network) ground-strike data, no cloud-to-ground lightning occurred at these times within 50 miles of the launch point. However during a period of 5 minutes on either side of the pulses there were 5 flashes within the 50 mile radius, all but one were positive, with one of the positives having a reported current of 103 kA. Expanding the search radius, we found that there were two positive flashes that occurred two seconds apart, but according to NLDN, were offset two seconds earlier than the observed X-ray pulses. A systematic timing error of 2 seconds is possible given the methods used to synchronize the time to a satellite clock, but would probably be on the outer edge of the error margin. The flashes occurred at 06:55:22 and 06:55:24 with currents of 73 kA and 74 kA. The first flash was 100 miles from the balloon's position, while the second was 64 miles distant. In addition, at the time of the X-ray pulses, we observed a large horizontal lightning discharge from the launch site.

References

Wilson, C.T.R, *Proc. Cambr. Phil. Soc.*, **22**, 534-538, 1925.
Parks, G.K. B.H. Mauk, R. Spiger, and J. Chin, *Geophys. Res. Lett.*, **8**, 1176-1179, 1981.
McCarthy, M., and G.K. Parks, *Geophys. Res. Lett.*, **12**, 393-396, 1985.

Acknowledgements

This work was supported by grant ATM-9414122 from the Physical Meteorology Program of the NSF. Field work was supported in part by NOAA/NSSL.

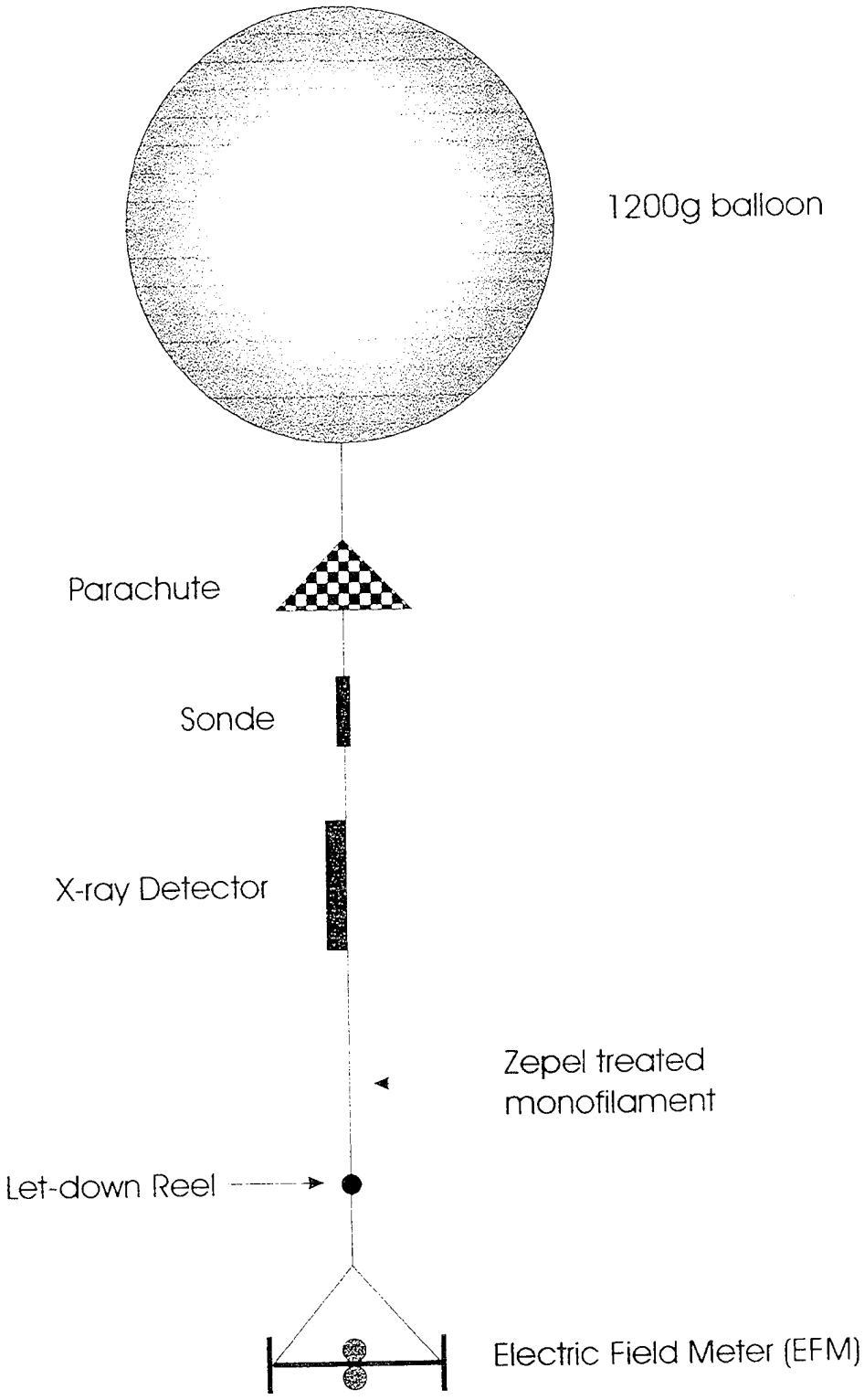


Figure 1. Typical configuration of balloon instrumentation for X-ray measurements.

Figure 2. X-ray and electric-field soundings 29 June 1995

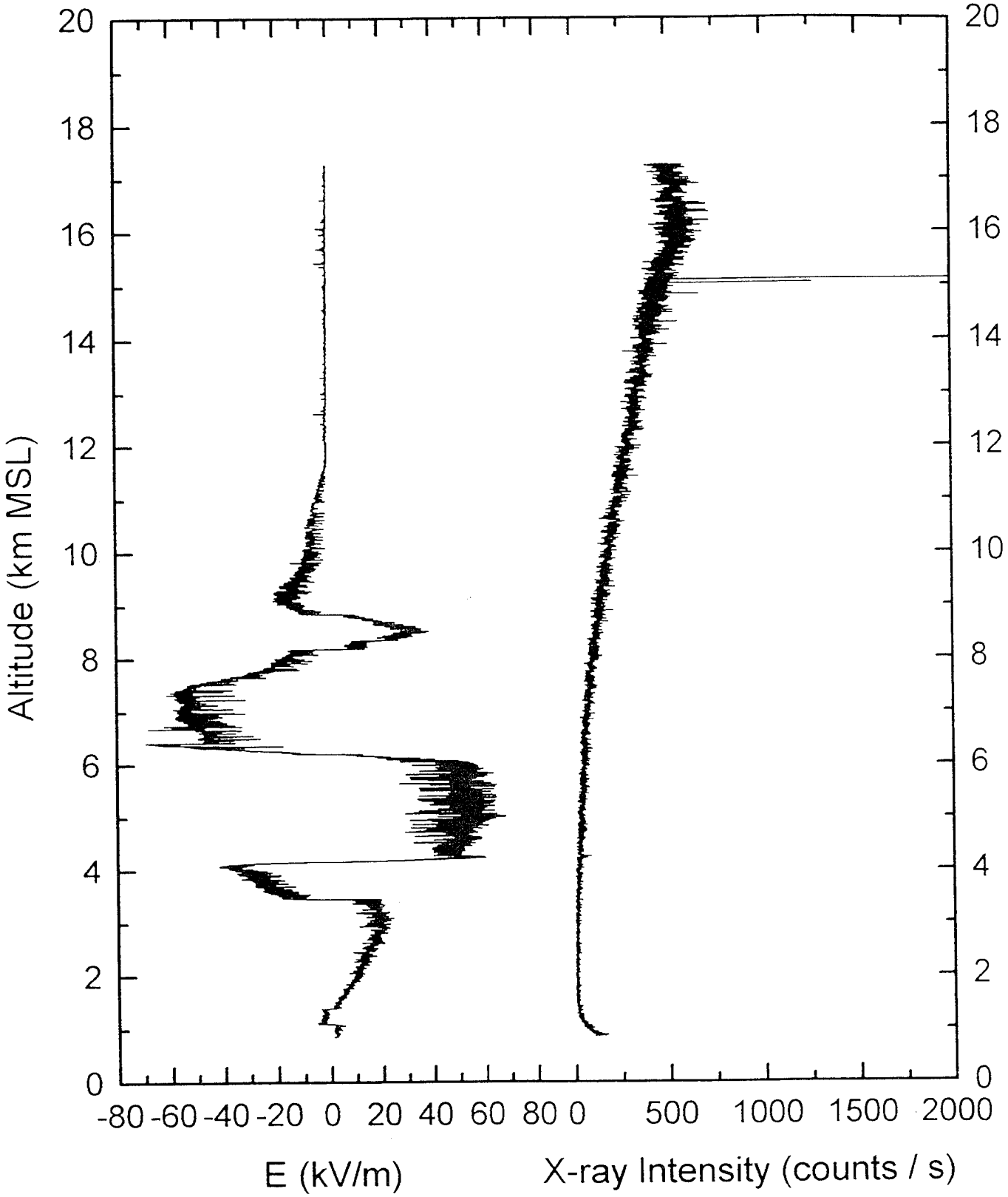
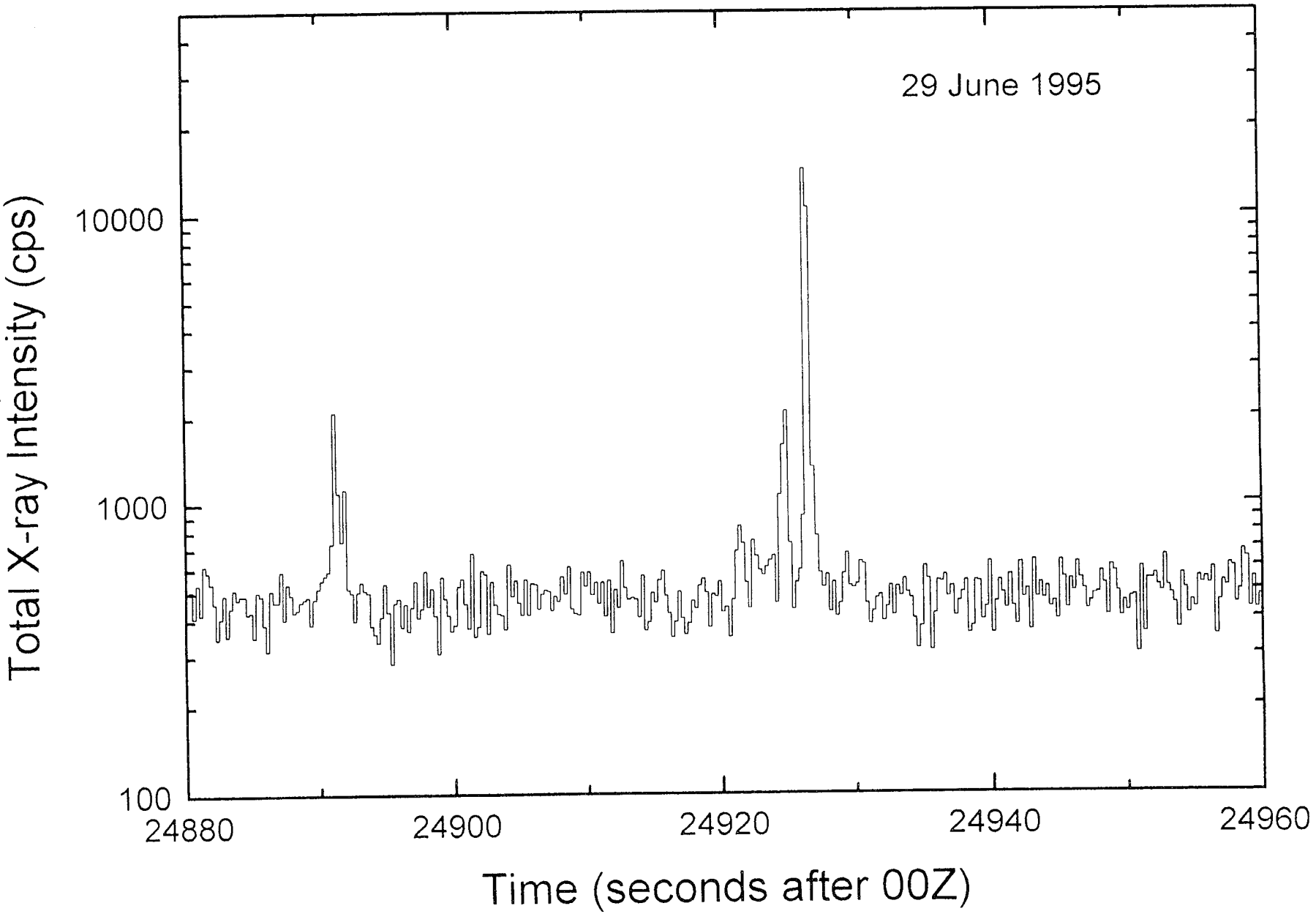


Figure 3. Detail of X-ray pulses at 15km MSL.



Joint US/Russian Lightning Experiments

Susan Voss and Eugene Symbalisty
Los Alamos National Laboratory
Space and Atmospheric Group

Presented at:

Phillips Laboratory Workshop on Sprites
and Blue Jets
October 18, 1995
Hanscom AFB, MA

Project Overview

- Los Alamos, in conjunction with two Russian Institutes, Arzamas-16 and Lebedev, are proposing to conduct joint experiments to obtain a better understanding of upward lightning.

- Four experiments have been proposed - the first of which was completed at the end of FY95 with the support of the AFPL Balloon Operations group in Albuquerque.

- US funding for FY95 was obtained in-house at Los Alamos and the Phillips Laboratory. A request has been submitted to DOE for FY96 project funds.

- Russian funding has been requested from the International Science and Technology Center (ISTC) in Moscow.

Test Objectives

The four primary objectives and their corresponding experiment are presented:

1. Determine if Trans-Ionospheric Pulse Pairs (TIPPs) could be caused by the reflection of RF off the ground.

   The experiment was completed September 28, 1995 with the support of the AFPL balloon experiments group. A Marx generator was used to produce RF pulses on a high altitude balloon. Data is currently being analyzed.

2. Determine if there is the predicted correlation between the optical signal produced by upward lightning, gamma-ray bursts and TIPPs. Compare to the predicted signals from the proposed theoretical relativistic-electron breakdown avalanche (Roussel-Dupre and Gurivich).

   Diagnostics to be carried on a high-altitude balloon (25 km) or the manned Odyssey flight during the summer of 1996. Payload: gamma detectors, digital cameras, RF receivers and field mills.

Test Objectives -

3. Generate an electric field in the absence of thunderstorm activity to test the proposed theoretical relativistic-electron breakdown avalanche (Roussel-Dupre and Gurivich).

   Fly an electron or ion generator on a low altitude (~5 km) tethered balloon to produce a uniform electric field. Diagnostic on the balloon: gamma detector and electric field mills. Diagnostic on the ground: gamma detectors, digital cameras, RF receivers and field mills.

4. Study the upward lightning tie to the ionosphere (preliminary planning stages). Experiment to be performed in Russia.

   Two options currently being examined are a Russian high-altitude balloon launch or a suborbital launch on a Russian SS-19. A magnetocumulative generator (MCG) is being considered as the primary payload.

Progress

- Developed a US and Russian team. Definition of roles and responsibilities.
- Developing our goals/objectives, experiment configuration and diagnostic requirements.
- Expansion of theoretical basis to experimental requirements.
- Requests for US and Russian funding.
- AFPL support - completion of the first proposed experiment.
- Examining Russian options for FY97 experiment.

Measurements of Lightning-Generated Electric Fields in the Nighttime D-Region

Dr. Carl L. Siefring

Naval Research Laboratory
Plasma Physics Division

The NASA
1981 Thunderstorm Campaign

Led By Cornell University

Designed to Study the Upward Coupling of of Lightning Generated-Electric Fields

Three Sounding Rockets, a Balloon and Ground Based Instrumentation

Published Results:

Siefring, C. L. and M. C. Kelley, Lightning transients in the ionosphere, mesosphere, stratosphere and on the ground, Paper 3.6, Seventh International Conference on Atmospheric Electricity, American Meteorological Society, Boston, MA, 1984.

Holzworth, R. H., M. C. Kelley, C. L. Siefring, L. C. Hale, and J. D. Mitchell, Electrical measurements in the atmosphere and ionosphere above a thunderstorm: 2. Direct Current electric fields and conductivity, J. Geophys. Res., 90, 9824, 1985.

Kelley, M. C., C. L. Siefring, R. F. Pfaff, P. M. Kintner, M. Larsen, R. Green, R. H. Holzworth, L. C. Hale, J. D. Mitchell, and D. LeVine, Electrical measurements in the atmosphere and ionosphere above a thunderstorm: 1. Campaign overview and initial ionospheric results, J. Geophys. Res., 90, 9815, 1985.

Siefring, C. L., Upward Propagating Electric Fields from Thunderstorms and VLF Transmitters, PH.D. thesis, Cornell University, Ithaca, N.Y. (Available: Univ. Microfilms Intl., Ann Arbor, MI), 1987.

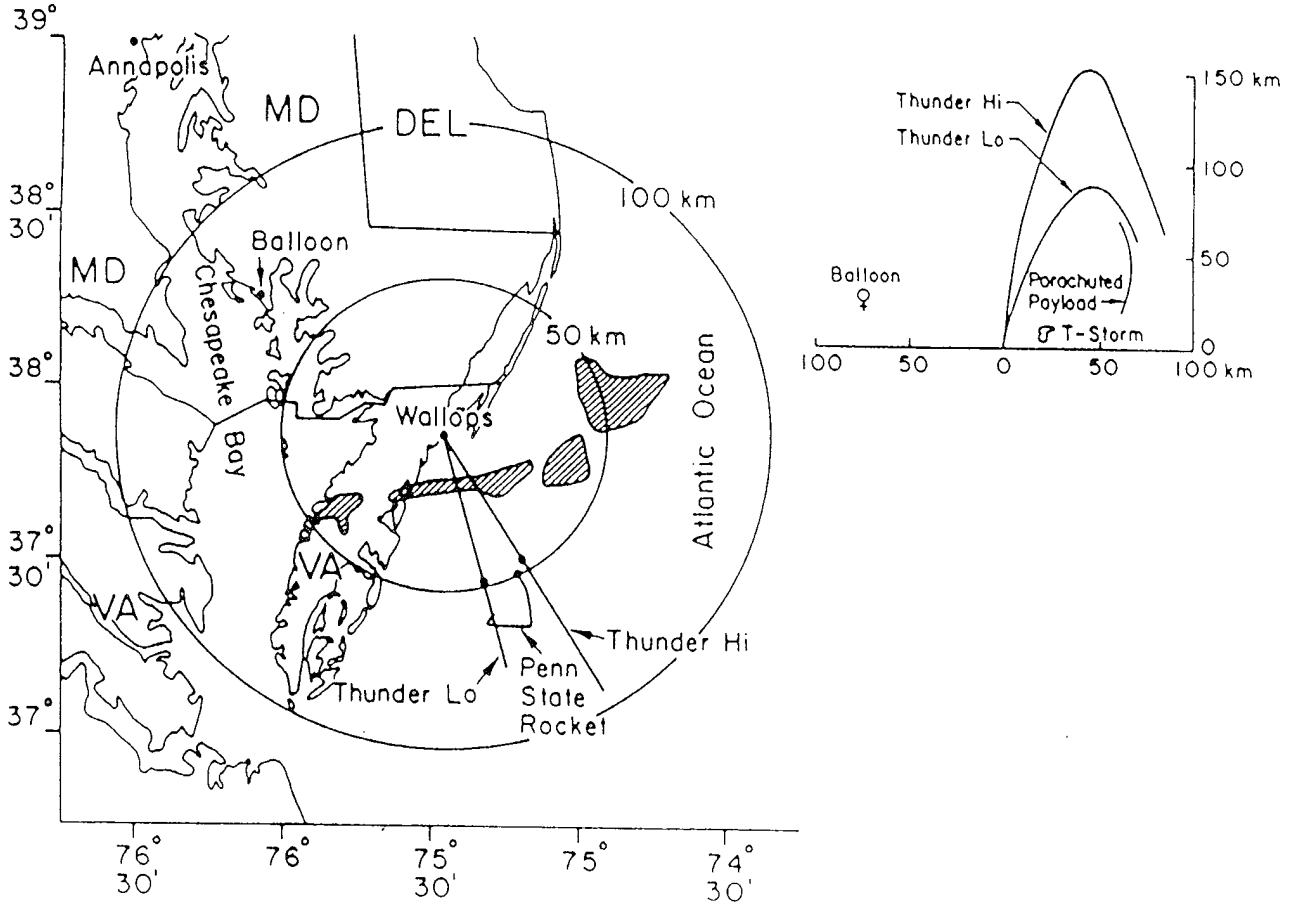
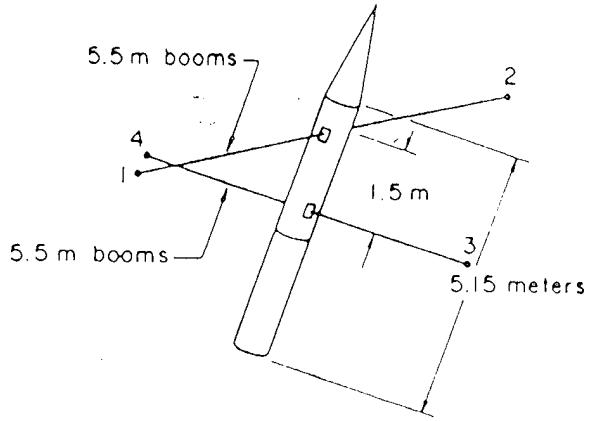


Figure 2.2 Map showing the location of the four thunderstorm cells and the balloon at the launch time of Thunder Lo. The ground tracks of the rocket payloads are also indicated. A vertical schematic of the thunderstorm and experiment trajectories is shown on the right-hand side.

Table 2.1: The instrumentation used during the thunderstorm electric field campaign, with the altitude ranges and operating institutions.

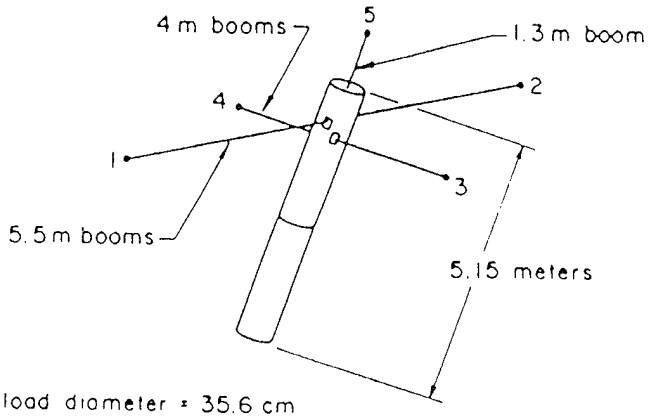
Experiment	Altitude Range	Institution
Ionospheric Rocket (Thunder Hi)	85 km - 154 km	Cornell University
Mesospheric Rocket (Thunder Lo)	60 km - 88 km	Cornell University
Rocket Released Parachute-Borne Payload	25 km - 75 km	Pennsylvania State University
Stratospheric Balloon	24 km - 30 km	University of Washington
Flat Plate Antenna	Ground Based	NASA/Goddard Space Flight Center
Meterological Radar (SPANDAR)	Ground Based	NASA/Wallops Flight Facility
Lightning Locating System (LDAR)	Ground Based	NASA/Wallops Flight Facility
Ionosonde	Ground Based	NASA/Wallops Flight Facility

Thunderstorm Electric Field Campaign
Wallops Island, Virginia
August 9, 1981



payload diameter = 35.6 cm
sphere diameter = 4.4 cm

Thunder - Hi
154 km Apogee
Taurus - Orion



payload diameter = 35.6 cm
sphere diameter = 4.4 cm

Thunder - Lo
89 km Apogee
Nike - Orion

Figure 2.1 Electric field measurement configuration for Thunder Hi (33.022) and Thunder Lo (31.022).

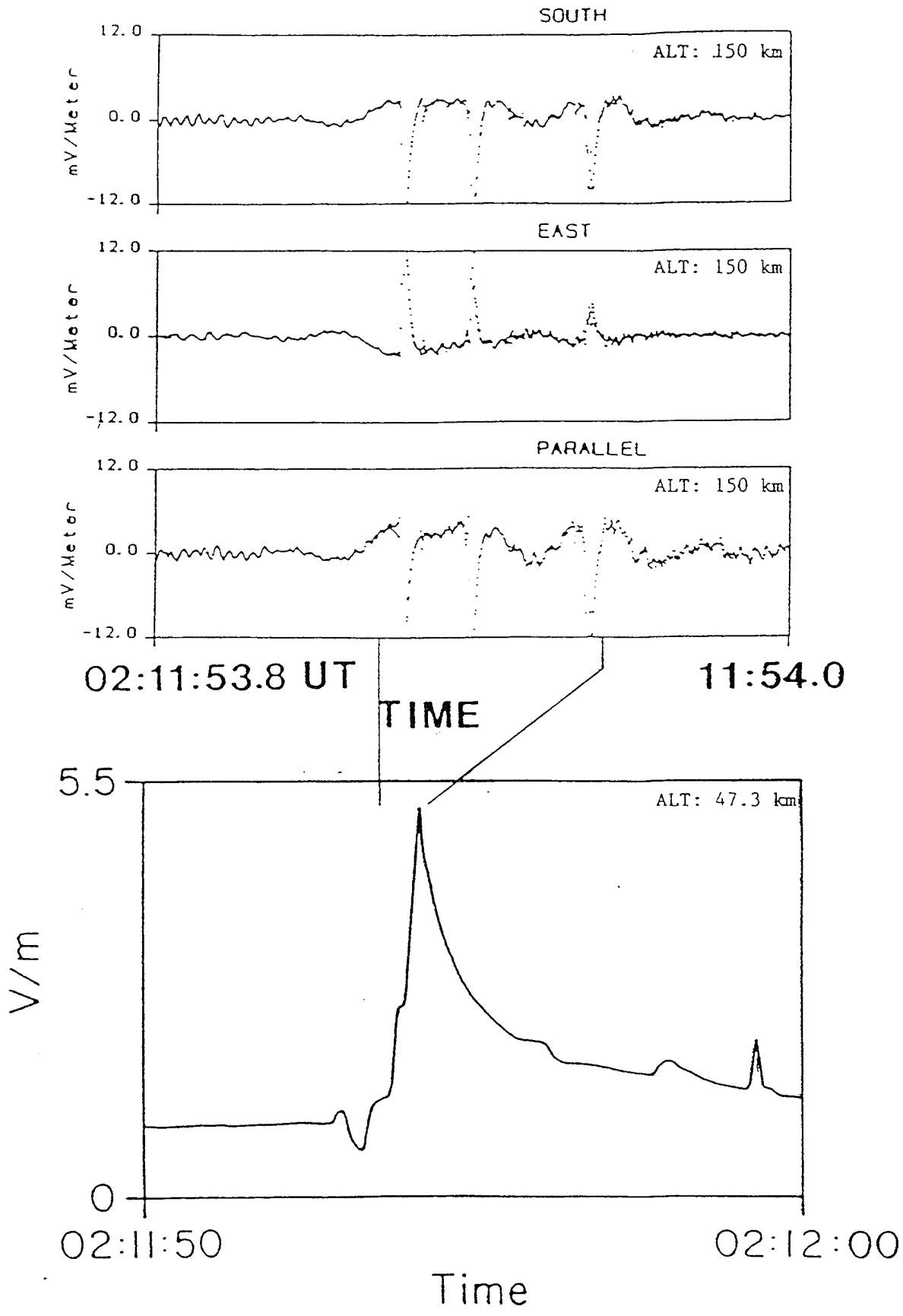


Figure 1. Lightning Induced Electric Fields in the Mesosphere and Ionosphere.

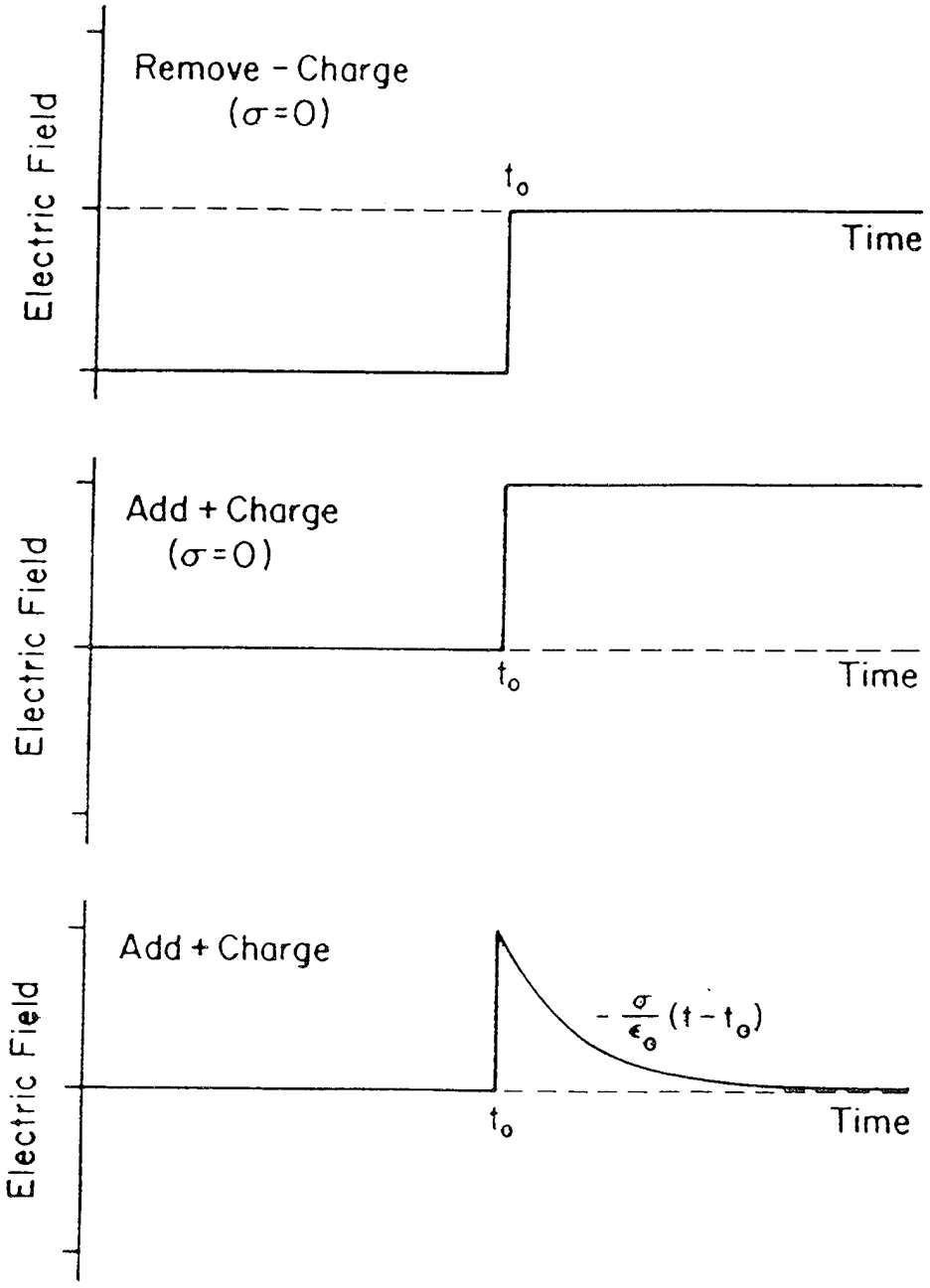


Figure 4.11 Electric field changes produced by: a) removing a negative charge from a perfect dielectric; b) adding a positive charge to a perfect dielectric; c) adding a positive charge to a conductor.

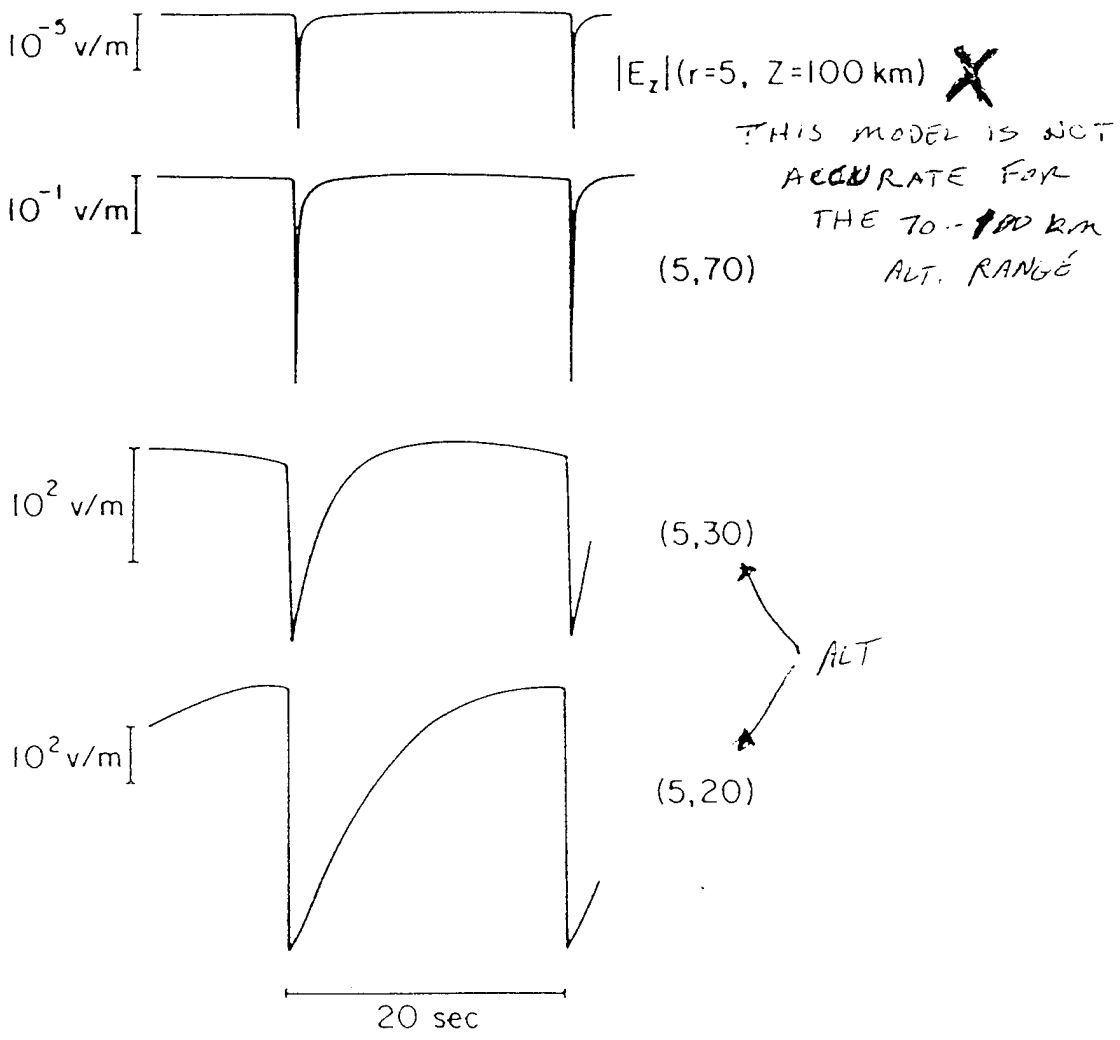


Figure 4.13 Plots of the vertical electric field (E_z) for a lightning flash as modelled by Dejnakarintra and Park [1974] at a horizontal distance r=5 km and selected altitudes (z).

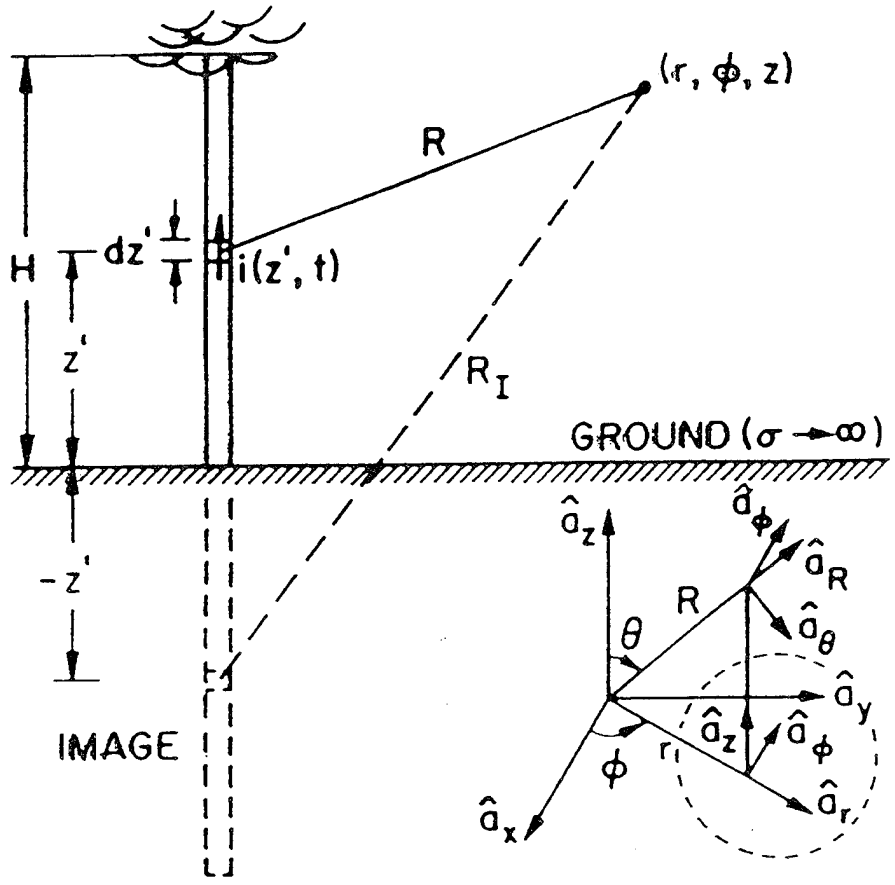


Figure 4.10 Geometry of the travelling-wave antenna model for lightning return strokes. Note: the fields are calculated in a cylindrical coordinate system.

the relationship between the currents and the electric fields they produce.

$$d\underline{E}(r,\phi,z,t) = \frac{dz'}{4\pi\epsilon_o}\left[\frac{3r(z-z')}{R^5}\overbrace{\int_o^t i(z',\tau-R/c)d\tau}^{①\ \text{ELECTROSTATIC SOURCE TERM}} + \overbrace{\frac{3r(z-z')}{cR^4}i(z',t-R/c)}^{②\ \text{INDUCTIVE}} + \overbrace{\frac{r(z-z')}{c^2R^3}\frac{\partial i(z',t-R/c)}{\partial t}}^{③\ \text{RADIATIVE}}\right]\hat{a}_r$$

$$+\frac{dz'}{4\pi\epsilon_o}\left[\overbrace{\frac{2(z-z')^2-r^2}{R^5}\int_o^t i(z',\tau-R/c)d\tau}^{①} + \overbrace{\frac{2(z-z')^2-r^2}{cR^4}i(z',t-R/c)}^{②} - \overbrace{\frac{r^2}{c^2R^3}\frac{\partial i(z',t-R/c)}{\partial t}}^{③}\right]\hat{a}_z \qquad (4.5)$$

$$d\underline{B}(r,\phi,z,t) = \frac{\mu_o\,dz'}{4\pi}\left[\overbrace{\frac{r}{R^3}i(z',t-R/c)}^{②} + \overbrace{\frac{r}{cR^2}\frac{\partial i(z',t-R/c)}{\partial t}}^{③}\right]\hat{a}_\phi \qquad (4.6)$$

There are three source terms in Equation (4.5) for the electric field produced by the travelling-wave antenna, while there are only two source terms in the magnetic field equation. We have labelled these terms in Equations (4.5) and (4.6) and will discuss each of them separately.

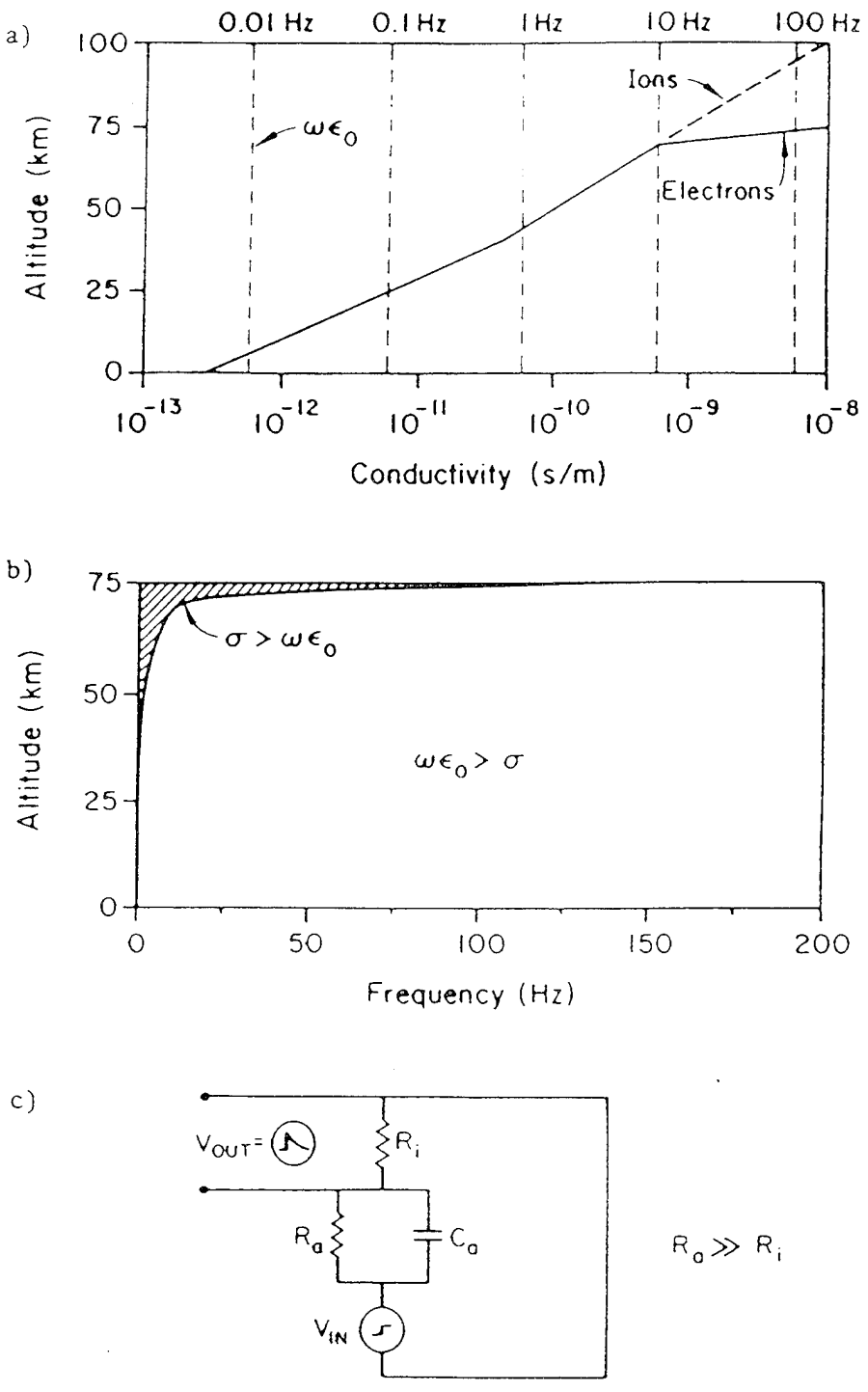


Figure 4.14 a) Conductivity profile derived from measurements shown in Figure 3.1. Conductivity is estimated above 75 km. b) Altitude where the conduction current equals the displacement current ($\sigma=\omega\epsilon_0$). In the shaded region the atmosphere can be considered a resistive medium. c) Equivalent circuit for the stratified atmosphere.

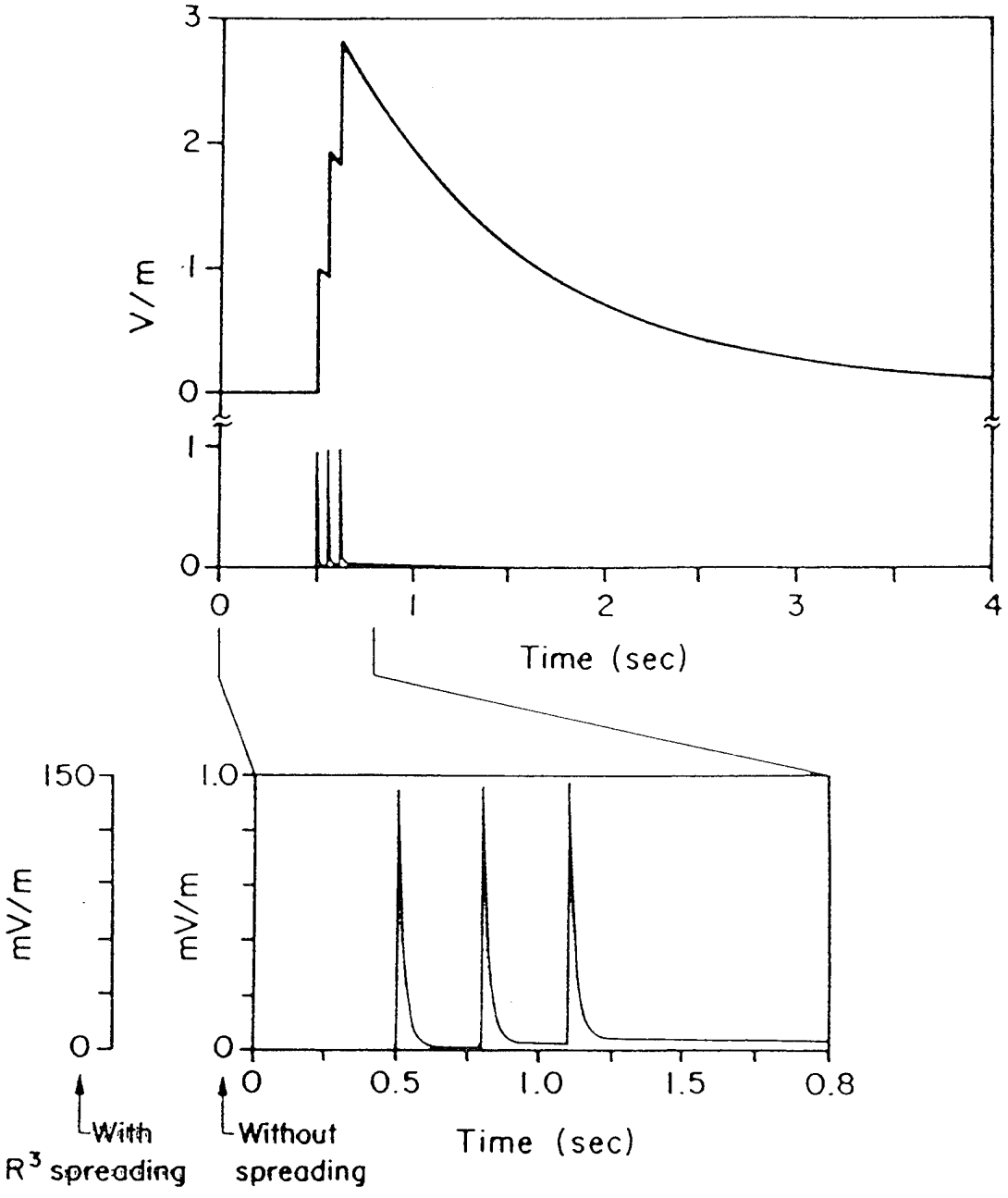
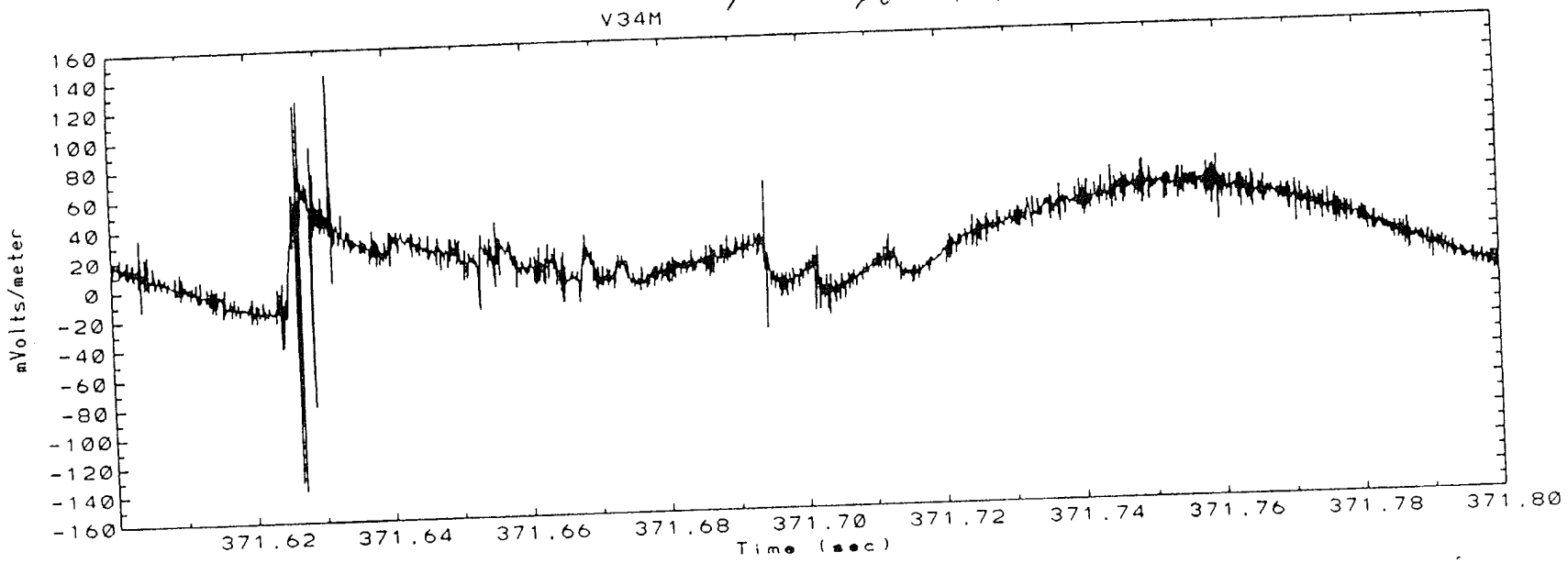


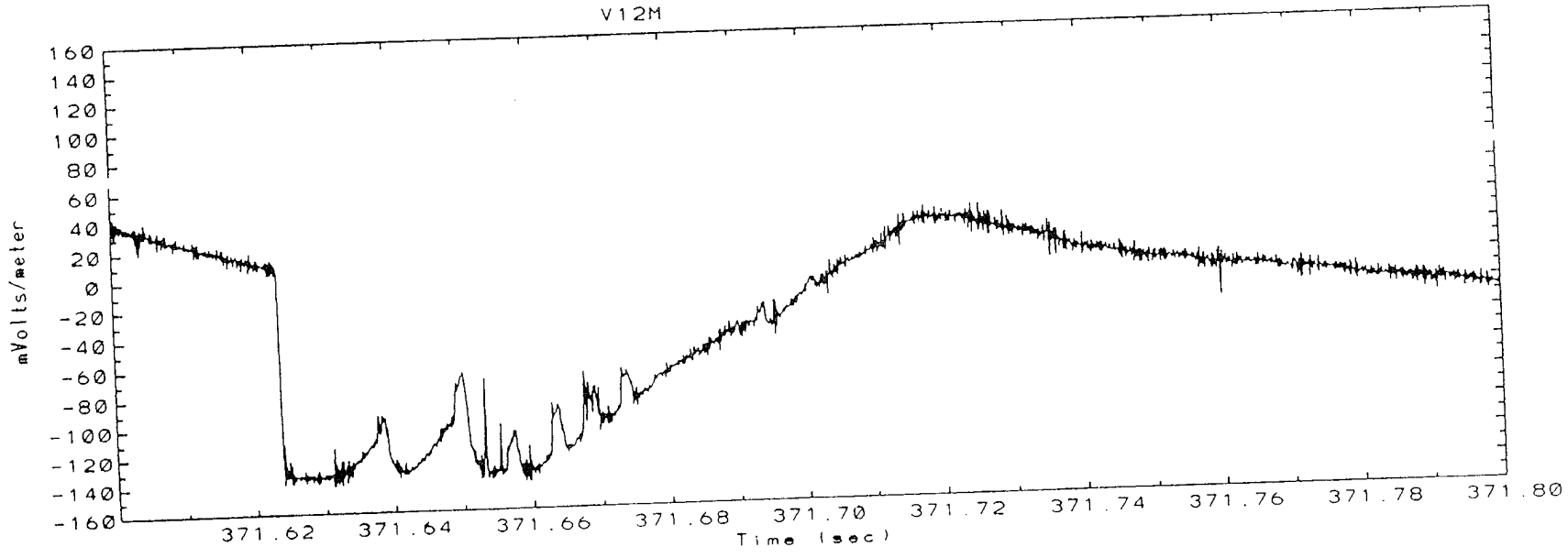
Figure 4.16 (Top panel) Model of electric fields measured in the upper atmosphere due to a lightning flash consisting of three return strokes and the result when the transfer function (with no spreading) is applied. (Cutout) Expanded section shows the expected up-going electric fields at 75 km. Two scales are given for the case with no spreading and for the case with R^3 spreading.

A SERIES OF ELECTRIC FIELD MEASUREMENTS FROM THE 1987

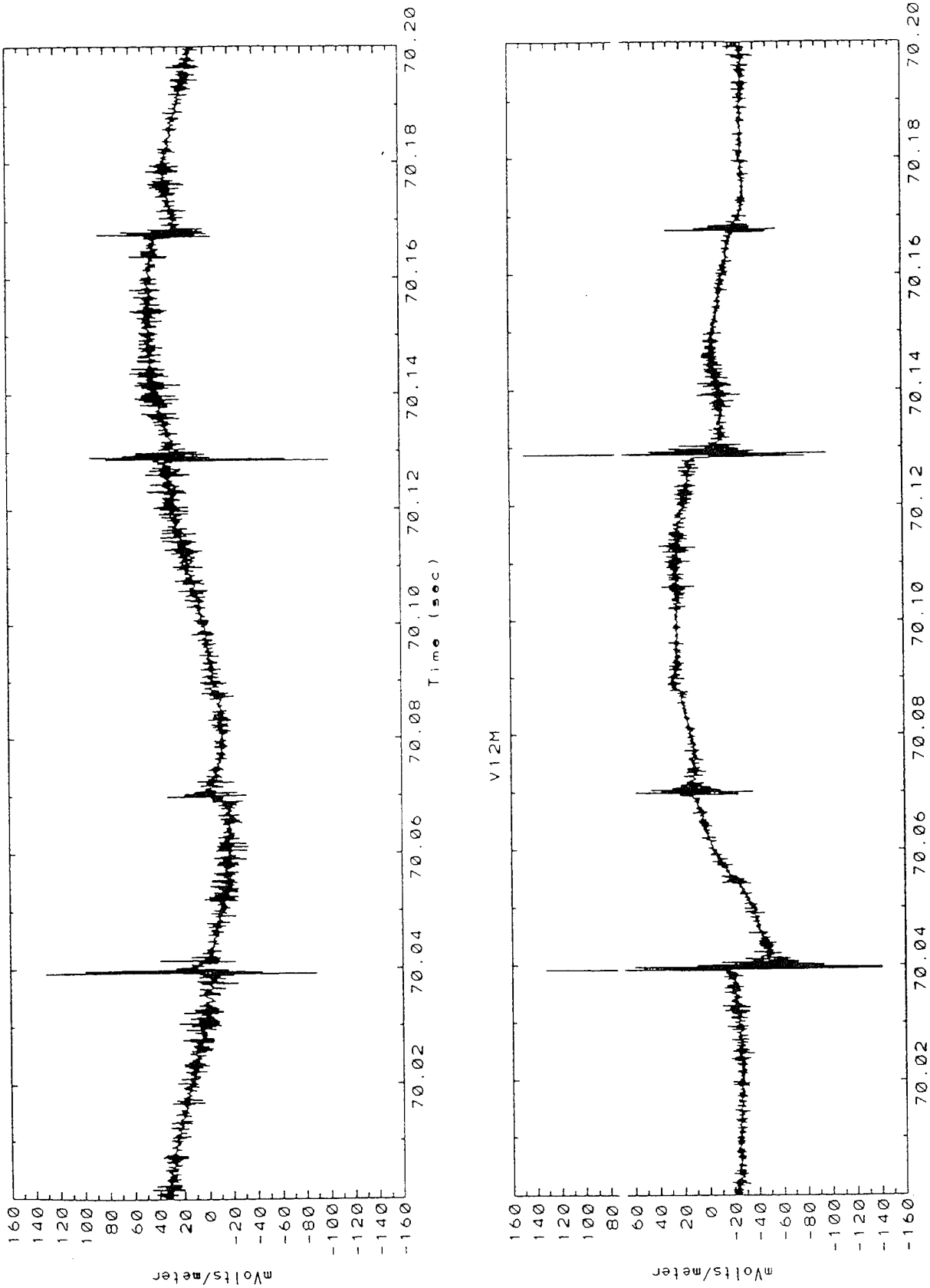
WIPP Campaign Rocket 33.053 -- Alt=73.0 km

NOTE: DECAY TIME VERSUS ALTITUDE

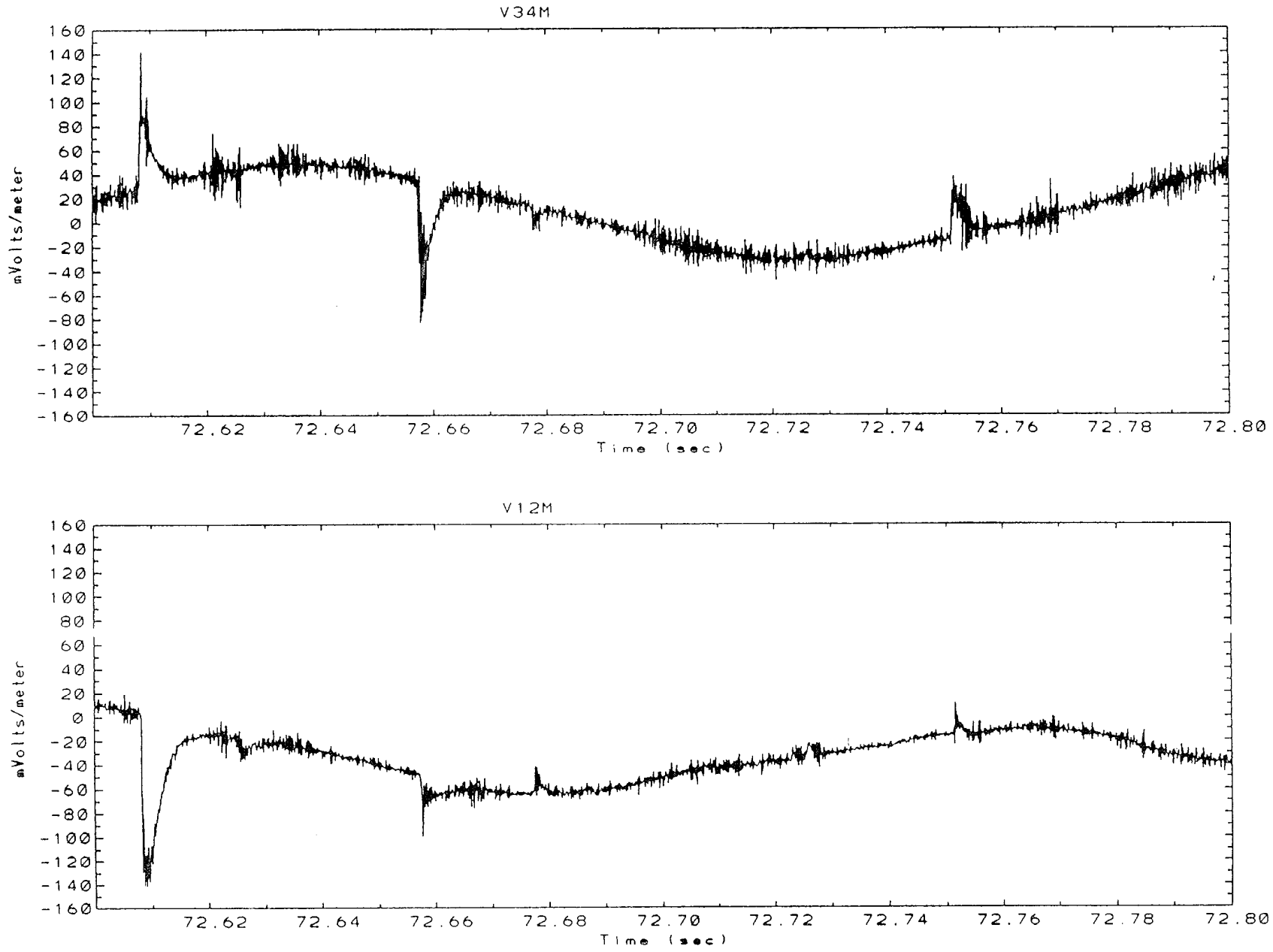




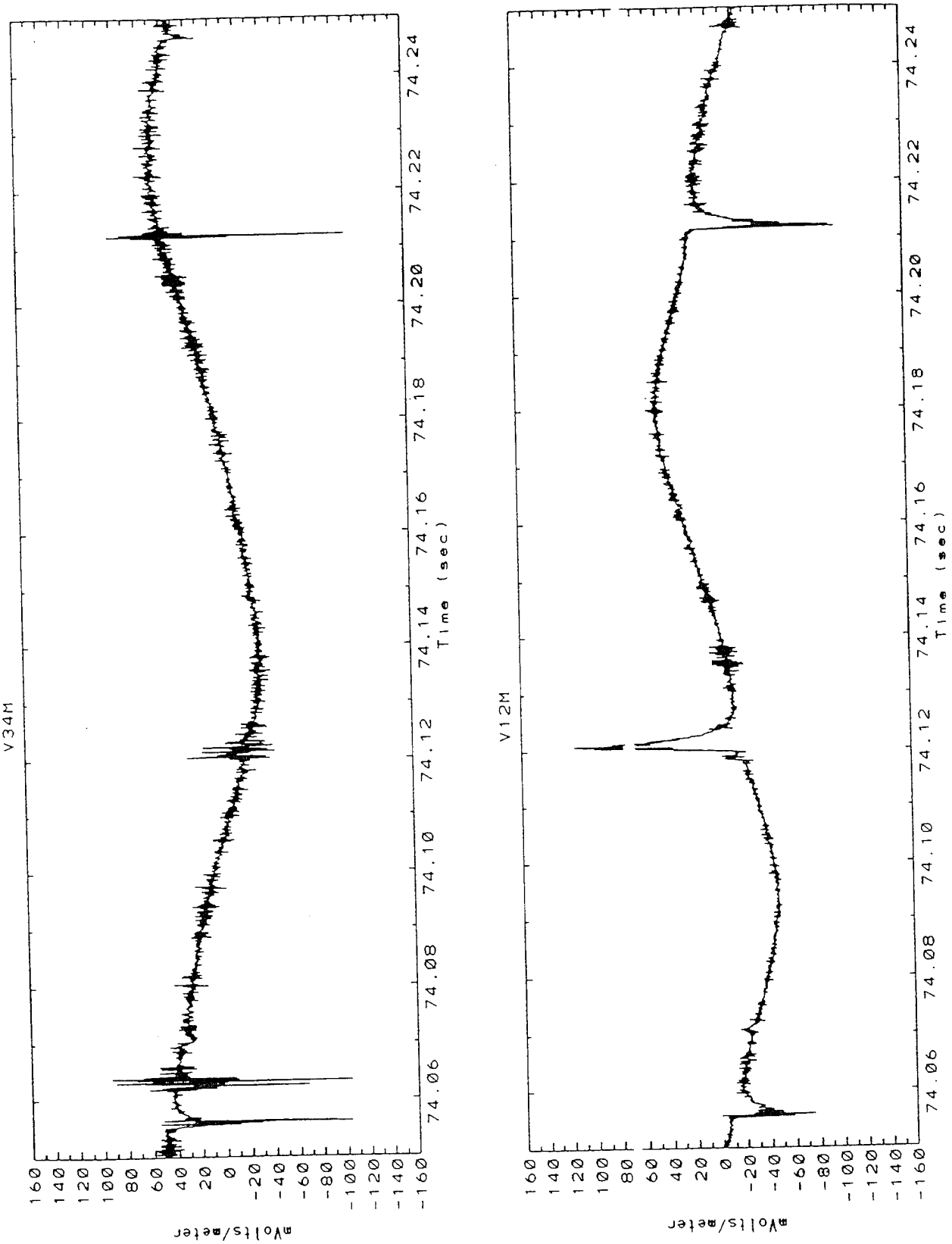
WIPP Campaign Rocket 33.053 -- Alt=84.1 km

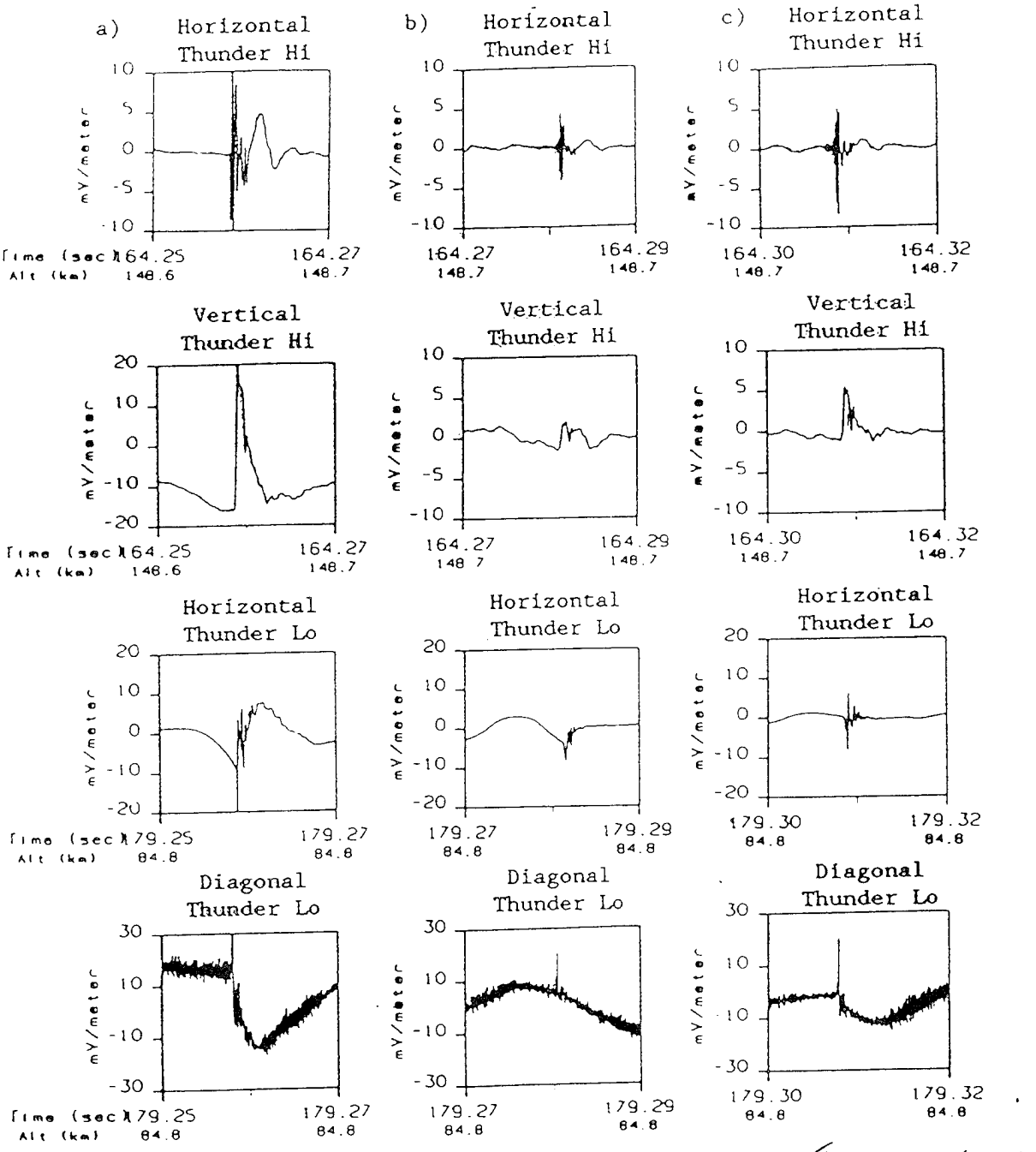


WIPP Campaign Rocket 33.053 -- Alt=87.6 km



WIPP Campaign Rocket 33.053 -- Alt=89.6 km

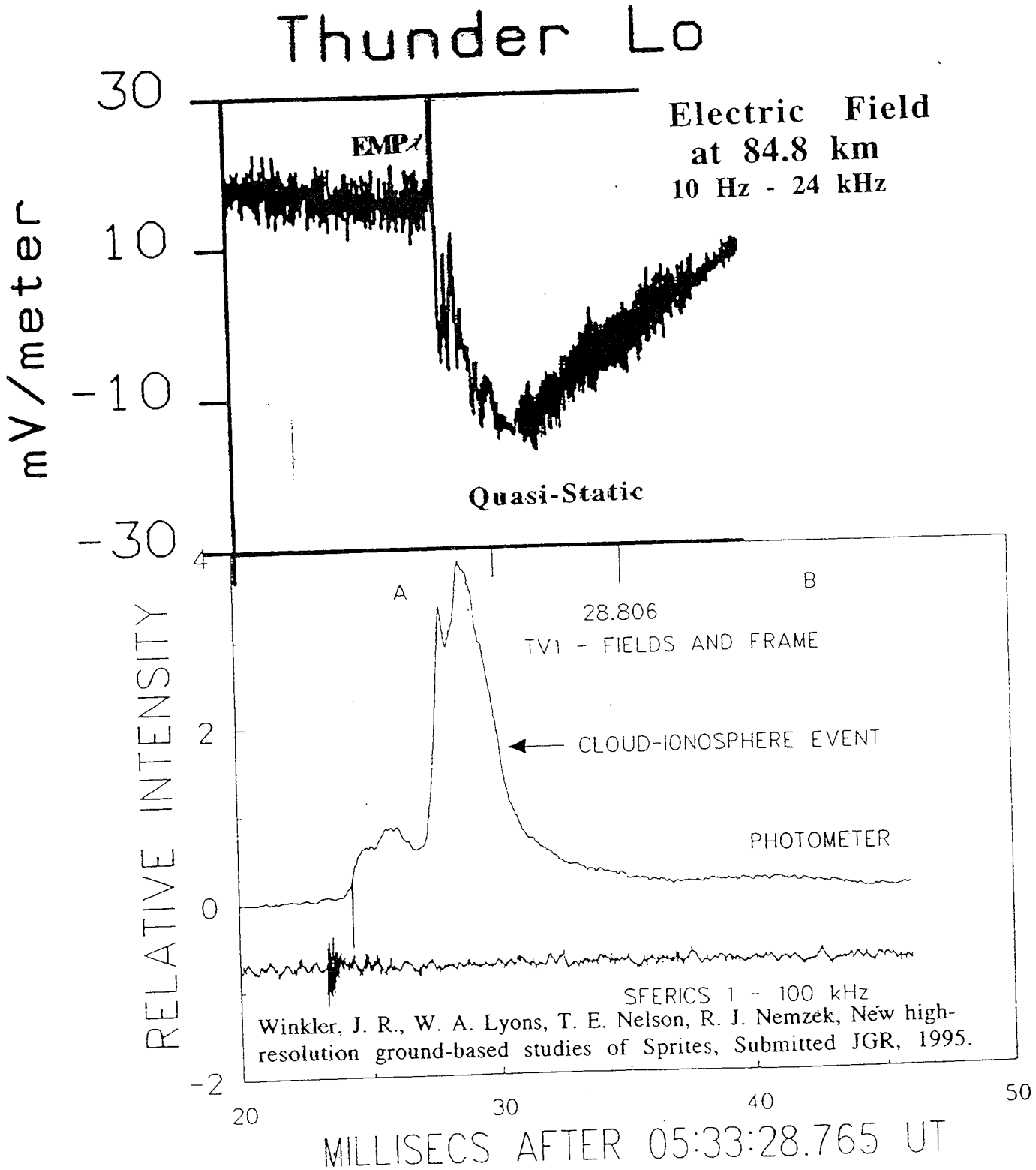




IN IONOSPHERE IN MESOSPHERE

Figure 4.6 Electric field data from both Thunder Hi and Thunder Lo. The data is for three strokes of the same lightning flash.

COMPARISON OF TIME SCALES FOR TYPICAL MESOSPHERIC E-FIELD AND SPRITE OPTICAL INTENSITY.



Winkler, J. R., W. A. Lyons, T. E. Nelson, R. J. Nemzek, New high-resolution ground-based studies of Sprites, Submitted JGR, 1995.

Table 4.1 Statistics for lightning-induced electric field transients.

Instrument	Number of Transients	Length of Data Period	Average Amplitude	Rise Time	Decay Time
Flat-Plate Antenna	11[1]	300 s	*[4]	*[4]	~10 s
Balloon	13[1] (721)[1]	300 s (3 hr)	~100mV/m	0.1 s[5]	~10 s
Parachute-Borne Payload	2[1] (8)[1]	300 s (11 min)	~5V/m	0.1 s[5,6]	1-2 s[8] 5-7 s
Thunder Lo	35[2]	120 s	~40mV/m	*[7]	30 ms[7,9]
Thunder Hi	70[2]	300 s	~15mV/m	0.2 ms[5]	3-5ms
33.050					
Below 150 km	45[1]	124 s	~35mV/m	0.2 ms[5]	>3 ms
Above 150 km	19[1,3]	179 s	~25mV/m[3]	0.2 ms[5]	>3 ms

[1] Corresponds to the number of lightning flashes that induced a transient.
[2] Corresponds to the number of lightning strokes that induced a transient.
[3] Signal-to-Noise ratio limited resolution to signals >10 mV/m.
[4] Instrument calibration not available.
[5] Measurement is limited by frequency response of instrument.
[6] Measurement somewhat limited by telemetry degradation due to lightning.
[7] Signals did not show a clear rise-time and decay.
[8] Data is fit best by two time constants. A fast time constant for the first portion of the transient (1 to 2 e-folds) and a 'tail' with a slower decay.
[9] Signals did not show a clear decay-time. The time given corresponds to the duration of the lightning induced signals.

D-Region Electric Field Measurements and Sprites

-Lightning-generated electric fields have been measured directly over thunderstorms in the nighttime D-region (although not many cases published).

-Field strengths are much lower than required for local breakdown 10-100 mV/m versus a few V/m (at 90 km) or 100 V/m (at 70 km).

-In the past entire field (EMP and Quasi-Static) has not been measured.
-Highest frequency response limited to about 24kHz, thus a large fraction of the EMP fields are unmeasured.

-Time scale of the Quasi-static field ~10 ms is close to Sprite duration while the EMP is consistent with short duration large area airglow.

-Previous measurements are from average sized east coast thunderstorms.
-There are no indications that large lightning discharges or positive cloud-to-ground discharges have ever been measured.

The upward coupling of the 'quasi-static' fields in the 70 -100 km altitude range is not well understood.

$$\overline{\overline{\sigma}} = \begin{pmatrix} \sigma_P & \sigma_H & 0 \\ -\sigma_H & \sigma_P & 0 \\ 0 & 0 & \sigma_{\parallel} \end{pmatrix}$$

$$\sigma_{\parallel} = parallel, \sigma_P = Pedersen, \sigma_H = Hall$$

Parallel fields ($E \parallel B$) should couple as at lower altitudes with $E \propto \sigma_{\parallel}^{-1}$.

Perpendicular fields are more complicated.

The 'quasi-static' electric field is driving currents in the atmosphere which are then converting to electromagnetic waves.

The Hall term in the conductivity allows the fields to penetrate much further in a whistler mode (i.e., $J \perp E$ is energy not absorbed in the medium).

Picture is further complicated by wave reflection and destructive interference in this region.

Most models have ignored Hall term.

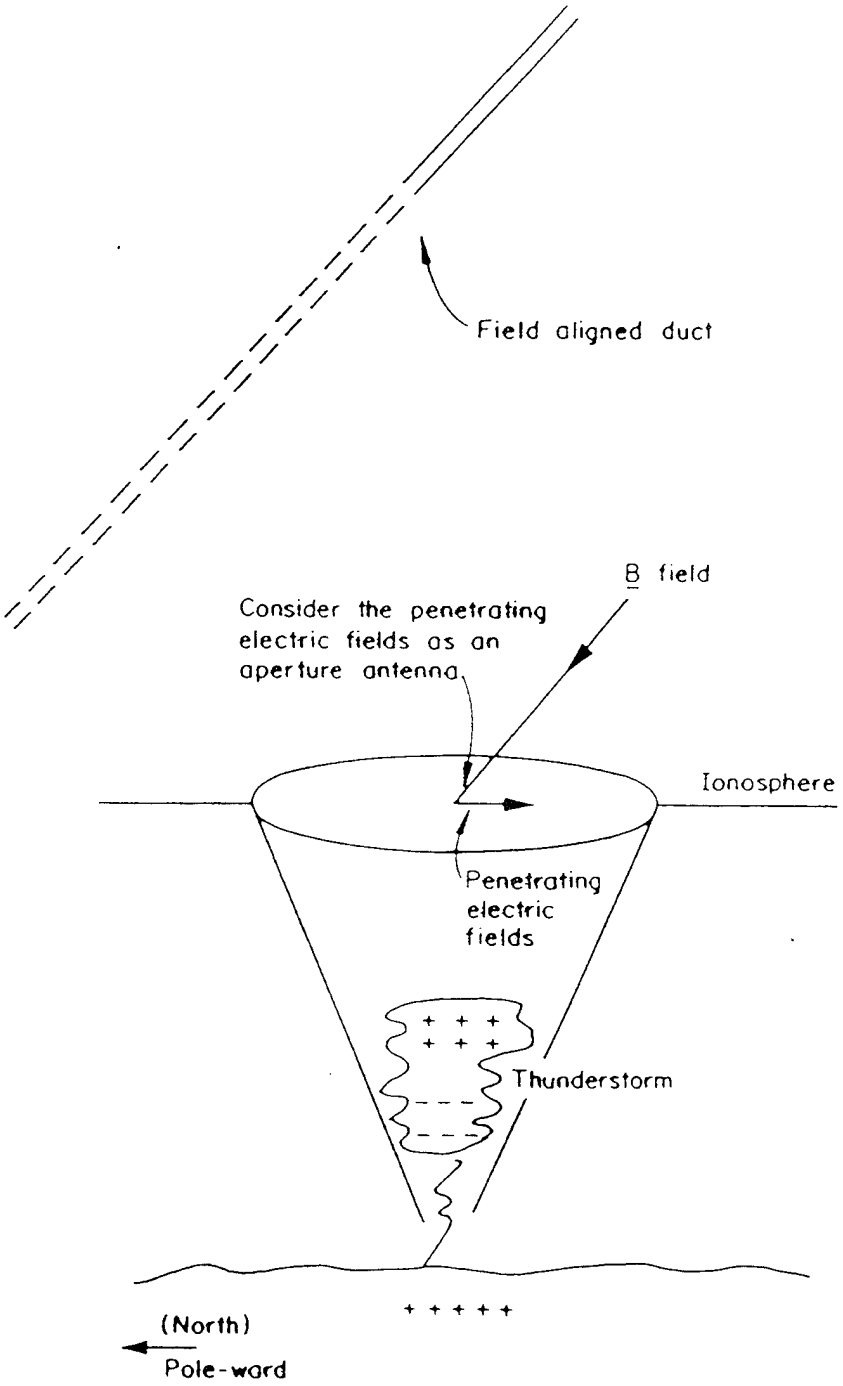


Figure 4.17 Schematic diagram of a new whistler generation model.

What to do next?

Fly rockets over a large storm that is producing both positive and negative cloud-to-ground flashes.

Wallops Island is not a good location.
White Sands Missile Range, New Mexico?
Eglin AFB, Florida?
Puerto Rico in 1997?
Others?

Measure full vector electric field (EMP and Quasi-Static) with high frequency response 0 - 100 KHz (? MHz).

Have high time resolution ground-based measurements to determine Q, I, $\delta I/\delta t$ so we can scale fields for the largest of lightning strokes.

Measure the response of the D-region to the applied fields (electron energy distribution, density enhancements, etc.).

Sprites Workshop
Phillips Laboratories
Hanscom AFB
Bedford, Mass.
October 18-19, 1995

SPACE-BORNE OBSERVATIONS OF GAMMA-RAY FLASHES ABOVE THUNDERSTORMS

G.J. Fishman, R. Mallozzi[1], J.M. Horack
Space Sciences Laboratory
NASA- Marshall Space Flight Center
Huntsville, AL 35812

Abstract

Intense flashes of MeV photons have been observed with space-borne detectors above thunderstorms. These flashes must originate at altitudes above 30 km, in order to be observable by orbiting detectors. At least fifty events have been detected over the past four years by the Burst and Transient Source Experiment (BATSE) aboard the Compton Gamma-Ray Observatory (CGRO). The most likely origin of these high-energy photons is bremsstrahlung from electrons, presumably from high altitude electrical discharges above thunderstorm regions. As a discharge phenomenon they are likely related to jets and sprites, although a coincident event has not yet been observed due to sporadic global coverage of both phenomena.

[1]also University of Alabama, Huntsville

Introduction

The Compton Gamma-Ray Observatory (CGRO) was launched in April 1991 to perform observations of celestial gamma-ray sources. The Burst and Transient Source Experiment (BATSE) is one of four experiments on the observatory. It serves as an all-sky monitor, detecting cosmic gamma-ray bursts, hard x-ray transients, persistent x-ray sources and solar flares. In addition to these celestial sources, on rare occasions BATSE has seen gamma-ray flashes from the earth's atmosphere.

The terrestrial gamma-ray flashes discovered by BATSE must originate at altitudes above at least 30 km in order to be observable by orbiting detectors. At least fifty events have been detected over the past four and a half years. Several of the events are seen to come from the direction of large weather systems, although concurrent weather images are not available in most cases. The energy spectra from the events are consistent with bremsstrahlung from energetic (MeV) electrons.

The BATSE Detector System

BATSE consists of an array of eight detector modules located at the corners of the observatory, arranged to provide maximum unobstructed sky coverage (Figure 1). The scintillation detectors are sensitive to photons with energies above 20 keV. The geometry of the array results in sources being usually observed by four detectors. Data from the detectors are processed on-board by a data system which sorts the data into several data types with differing temporal and spectral resolution.

The BATSE data type with high time resolution used to study the gamma-ray flashes reported here is the time-tagged event (TTE) data. These data are usually recorded whenever the on-board trigger system is enabled. However, sometimes these data are overwritten or otherwise unavailable due to telemetry gaps. In these cases, only data with 64 ms time resolution are available. The TTE data consist of up to 32,000 individual scintillation detector events that are identified by the detector module that recorded it, the energy channel (one of four channels) and the arrival time (recorded to 2μs relative accuracy). The four energy channels are approximately 20-50 keV, 50-100 keV, 100-300 keV and >300 keV. A continuously operating ring buffer allows the recording of approximately 8,000 events prior to the time of the trigger recognition. These "pre-trigger" data have been essential in these studies of short timescale phenomena such as these events.

Observations

The initial paper describing twelve of over fifty of these events was published last year (Ref.1). A world map of the spacecraft location at the time of these twelve events, along

with the global distribution of thunderstorms is shown in Figure 2 (from Ref. 1). Note that the 28.5 degree inclination of the spacecraft orbit confines the observatory primarily to tropical regions. The general similarity of the two distributions is apparent, along with the scarcity of events over the large ocean regions of the world, where few mesoscale thunderstorms form.

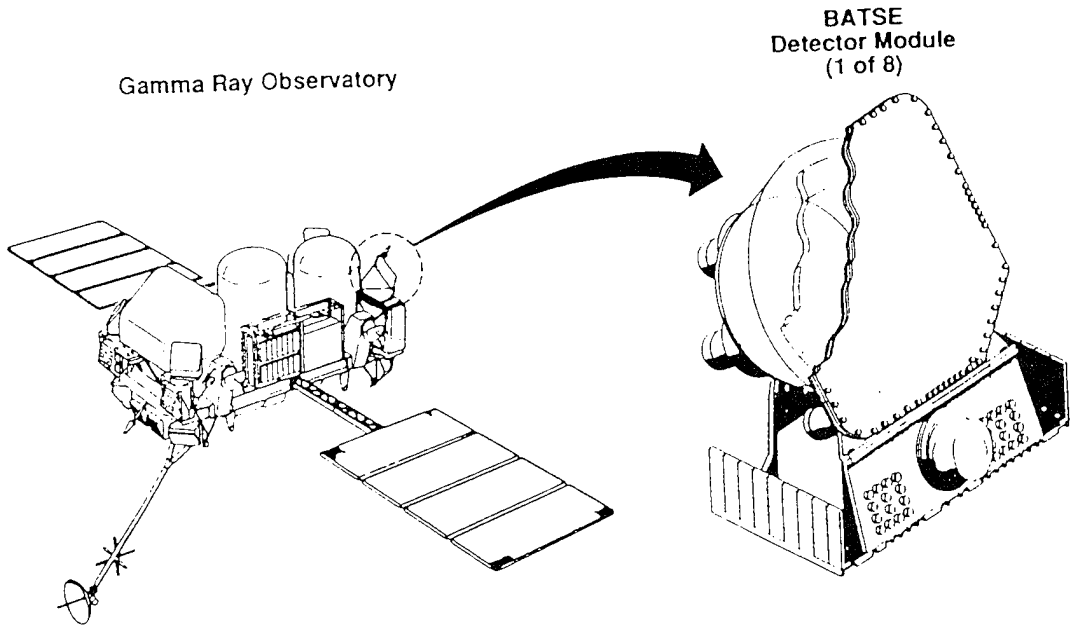


Figure 1. The BATSE experiment on the Compton Gamma-Ray Observatory

Two unique characteristics of these events are their extremely hard spectra and their short duration. These features are very distinct from other events which have triggered the BATSE detectors such as gamma-ray bursts, solar flares, fluctuations of other known hard x-ray and gamma-ray sources, and bremsstrahlung from precipitating magnetospheric electrons. Most of these events are seen by more than four detectors, as there is considerable scattering of photons in the spacecraft and transmission through the rear of the detector modules. However, the observed counting rate ratios of the detectors are consistent with the source of these events originating from a large distance relative to the spacecraft dimensions. Furthermore, these events are located by the BATSE detectors as emanating from below the local horizon. Other, independent detectors from another experiment on the Compton Observatory confirm these events. It is likely that many other, weaker events of similar origin go undetected due to the trigger criteria implemented by BATSE. In particular, the minimum sampling time for triggering the BATSE burst mode is 64ms, over ten times longer than the duration of most of these events. Estimates of the direction to the sources of the flashes can be made by comparing the relative responses of the eight BATSE detectors which view different directions.

However, the directions thus derived are rather imprecise due to the penetrating nature of these photons. Typically, the azimuth and elevation direction sectors are derived with uncertainties of from 30 to 60 degrees.

It is believed that prior instrumentation and experiments were incapable of detecting the events reported here for various reasons, or these events were overlooked as being

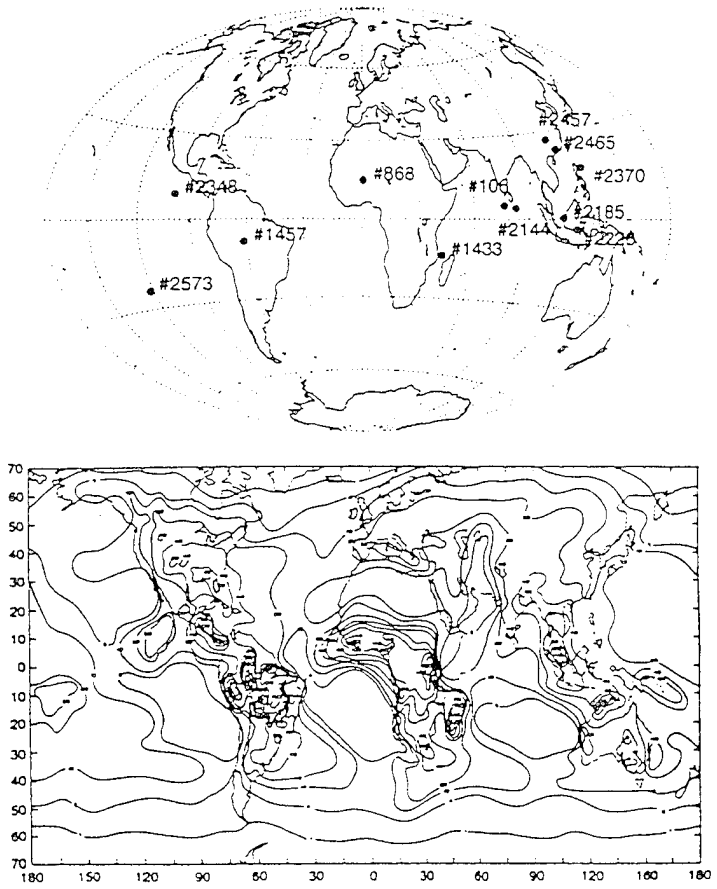


Figure 2. The global distribution of 12 of the events compared with that of thunderstorm regions.

spurious. The temporal resolution of most experiments would not have been able to respond to these very brief events and/or would have had poor signal to noise when sampled with coarser time resolution.

Many of the events have multiple pulses and, in a few events, the pulses seem to overlap. Durations of the majority of events are from 1ms to 6ms, although durations as short as 0.5ms and as long as 10ms have been seen. The time profile of an event detected on September 22, 1995 is shown in Figure 3. Here the detected photons in two detectors are

plotted in 100μs bins. The event duration was about 5ms and consisted of multiple of peaks, some of which are unresolved in the later stages of the event. All of the peaks have characteristic rise-times and fall-times of 100-200μs.

No prior references to gamma radiation from atmospheric electrical discharges or from electrons precipitating from the magnetosphere have been found in the literature. Because of the new and unique nature of these events, the lack of correlated observations in other spectral regions, and the paucity of concurrent weather data, the exact cause of the

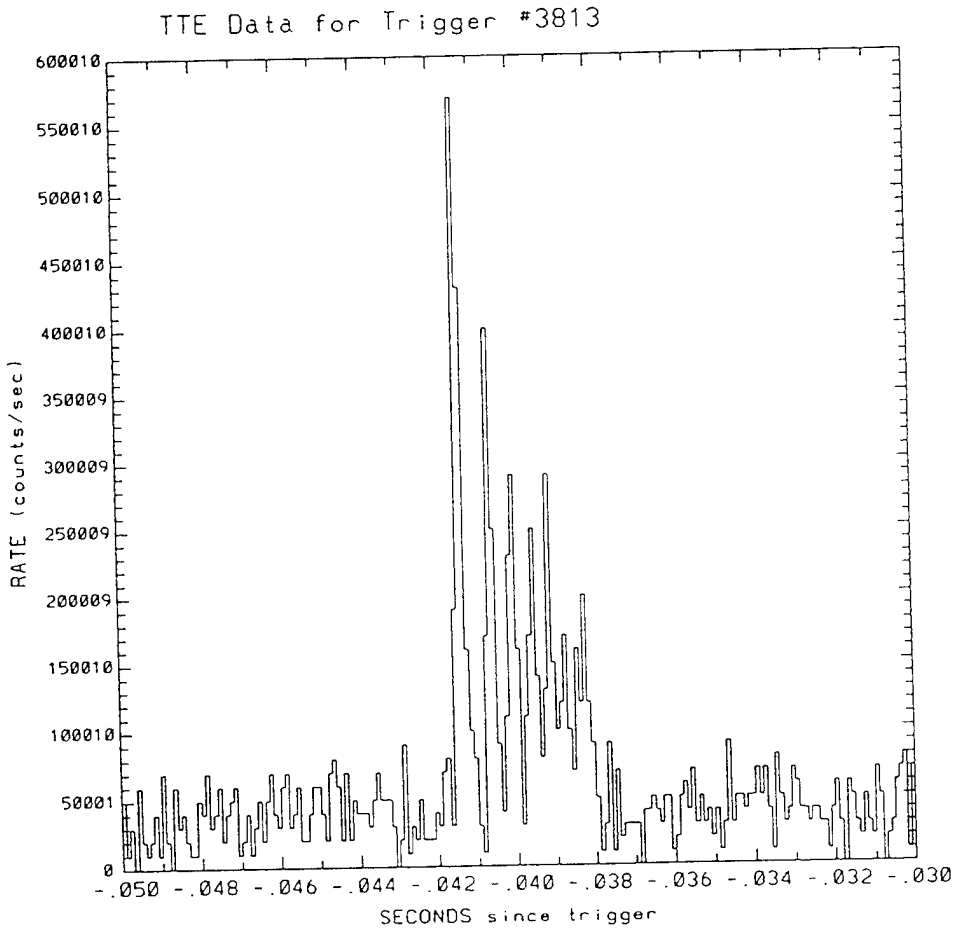


Figure 3. The time profile of a recent event (see text).

phenomenon must await further study. However, recent observations by Inan, et al. (priv. comm.) show evidence for at least one of these events being associated with intense spherics from thunderstorms off the western coast of Mexico.

Spectral Characteristics of the Terrestrial Gamma-ray Flashes

The terrestrial gamma-ray flashes (TGF's) seen by the BATSE experiment all have characteristic hard spectra that are unlike any other spectra observed by BATSE from either a geophysical or an astrophysical source. For example, the spectra produced by precipitating geomagnetically-trapped electrons are often seen by BATSE in the geomagnetic regions above L=1.0. These photons have a relatively soft spectra, with few observed photons above 300 keV. Most galactic neutron star and black hole sources observed by BATSE have spectra that are characteristic of radiation produced by optically-thin thermal bremsstrahlung (OTTB), with typical characteristic temperatures between 10 keV and 50 keV.

It has been difficult to deconvolve the spectra of the TGF's due to: 1) The penetrating nature of their spectra makes a unique deconvolution difficult, since only partial energy losses from the photons are usually recorded in the detectors and 2) The TGF's produce only a limited number of detected photons during the brief appearance of the event.

In Figure 4, we show a plot of individual photons (or, more correctly, counts) from one of the TGF events. Plotted here are the detected energy deposits of single photons in the eight BATSE spectroscopy detectors (SD's). Each photon is indicated by its arrival time and energy loss in the detector. The cluster of photons around 0.019s before the trigger of the on-board burst system clearly distinguishes the TGF from the isolated background events (mainly secondary cosmic-ray photons). The detectors are operated at different

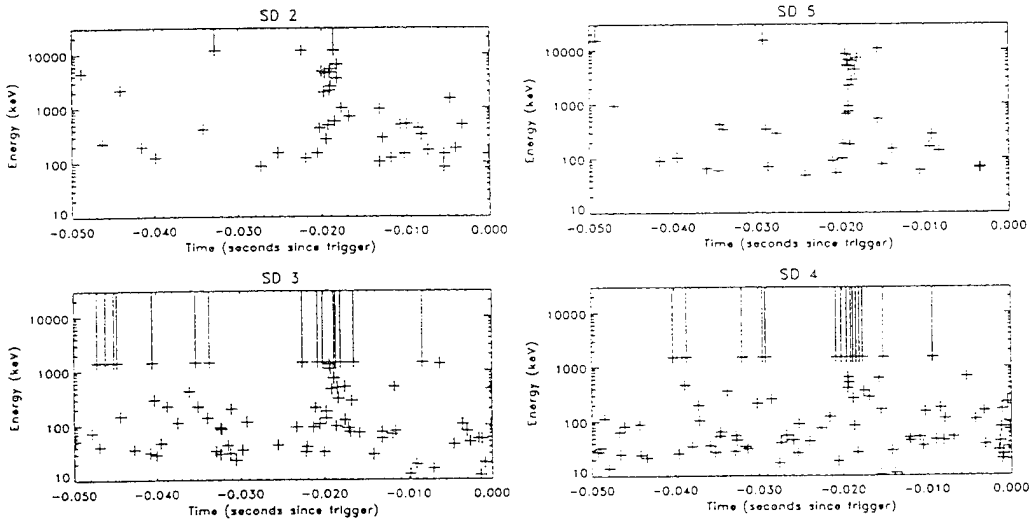


Figure 4. A plot of the arrival time and energy of photons from four of the eight BATSE spectroscopy detectors (SD's), from event #868, detected on October 5, 1991.

gains and thus have different energy ranges. Many of the events in the BATSE spectroscopy detectors no. 3 and 4 are above the upper range of the detectors (about 1.5 MeV), as indicated by an upward line from the cross at each event. The incident photon energies of these events are likely to be considerably higher than this lower limit.

Future Work

The Compton Gamma Ray Observatory will continue observations for at least another five years. The current interest in Sprite observations should allow numerous opportunities for coordinated observations of the gamma-ray phenomena and high-altitude discharges above thunderstorms. Work is currently in progress to improve the determination of the spectra of these events.

Reference

1. Fishman, G.J.; Bhat, P.N.; Mallozzi, R.; Horack, J.M., et al., "Discovery of Intense Gamma-ray Flashes of Atmospheric Origin", *Science*, 27 May 1994, Vol.*264*, (no.5163):1313-16.

ELECTROMAGNETIC FIELDS OF RED SPRITES

Les Hale and Lee Marshall
Communications and Space Sciences Laboratory
Penn State University, University Park, PA 16802
Tel: (814) 865-2361; FAX: (814) 863-8457; e-mail: Les Hale@PSU.EDU

The time-dependent electromagnetic (E and H) fields of several dozen "red sprites" (visually identified by Walt Lyons of Ft. Collins, CO) were measured in Central Pennsylvania. Battery-powered equipment at a low-noise site away from power lines was used to avoid 60 Hz and harmonics, although a 60 Hz notch filter was still necessary for the magnetic field data.

Unexpectedly, the sprites-related data were easily distinguishable from other events, which occurred much more frequently. This was due to a characteristic polarity (related to "positive" lightning), a greater pulse width, and other characteristics, including detailed structure related to the "visual" sprite. The power spectra of the sprites were primarily at ELF above the Schumann resonance range, at about 100-300 Hz. However, the EM energy was so large (about a megajoule) that they could be detected over a broader range of frequencies, and are probably large IR sources.

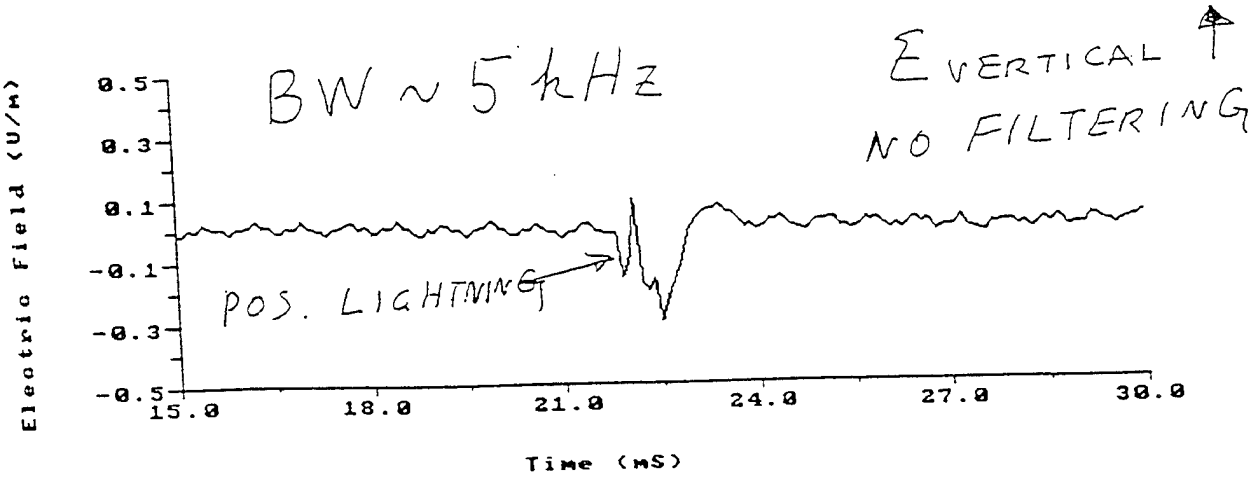
The characteristic shape of the waveforms was such that it would appear to be possible to build an electronic "sprite detector," which in conjunction with lightning locator data could provide a "sprite mapper" which would function independently of visual observations.

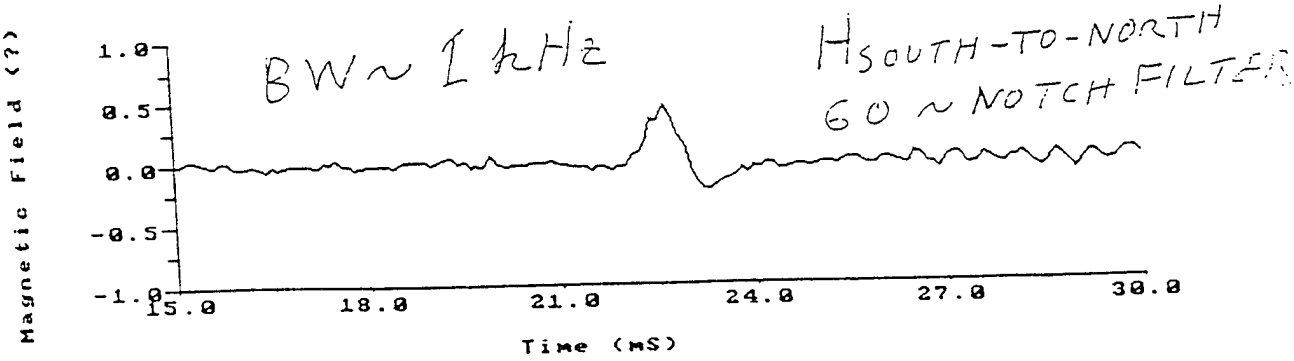
The original abstract is above. What was presented at the workshop follows below:

We show in the following figures electric and magnetic field data related to "sprites" and "airglow events identified by Walt Lyons on the date of July 24, 1995. The magnetic field has not yet been accurately calibrated but is believed to be related to the electric field by $E_z = 377 H_\phi$, which is consistent with the "radial TEM" or zero mode of propagation. The bandwidth of the electric field measurement was about 5 kHz and the magnetic field about 1 kHz. Note that the electric field consequently shows much more structure due to faster events but the lower frequency "filtered" magnetic field, which could also be generated by filtering of the electric field, shows a more consistent structure. This indicates that the ELF signal in the roughly 100 Hz to 1 kHz range could be used in constructing a "sprite monitor" with a range of thousands of kilometers (but ~5 Hz to ~50 kHz should be used to study basic physical processes, in conjunction with optical measurements, in future campaigns).

d:\rs724\064040.DAT

"SPRITE"

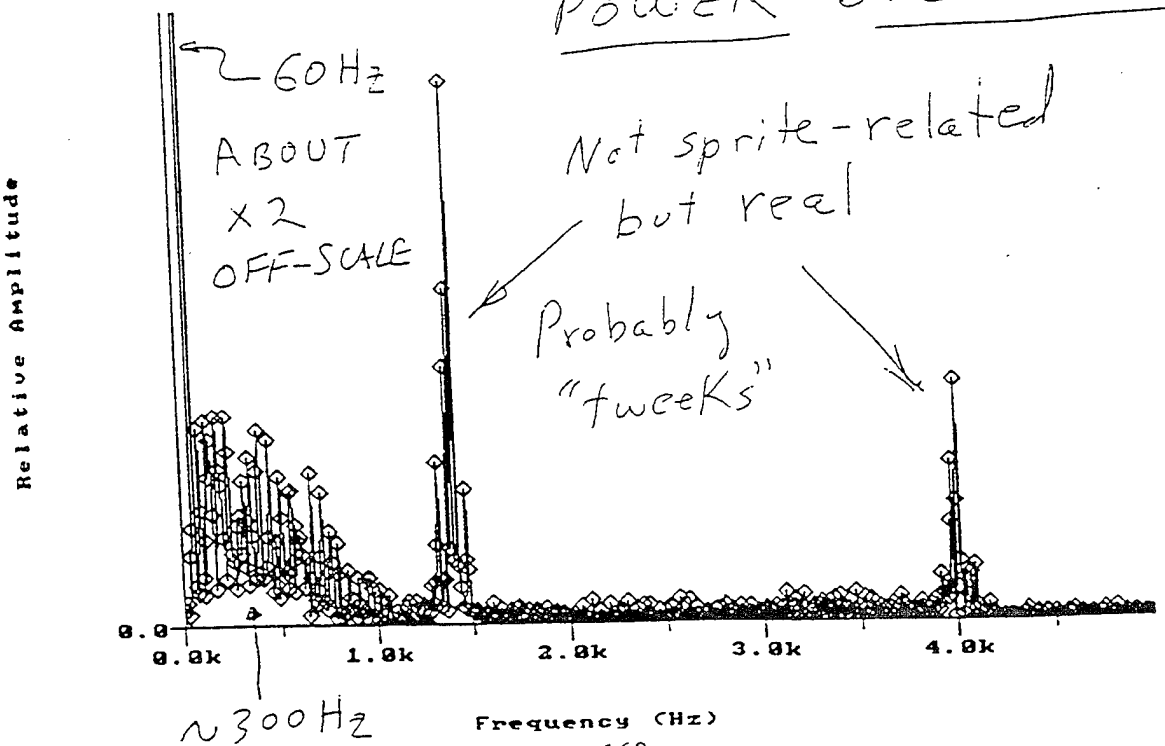




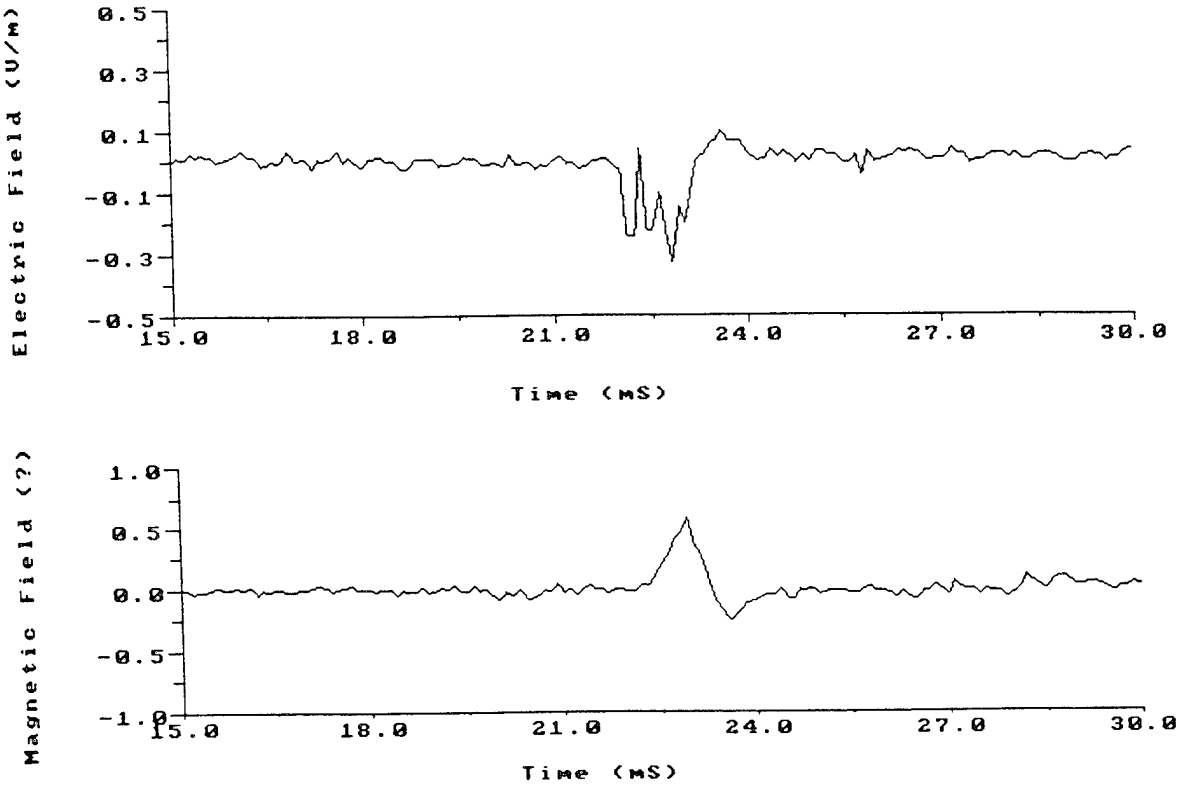
d:\rs724\064040.DAT

ELECTRIC PSD

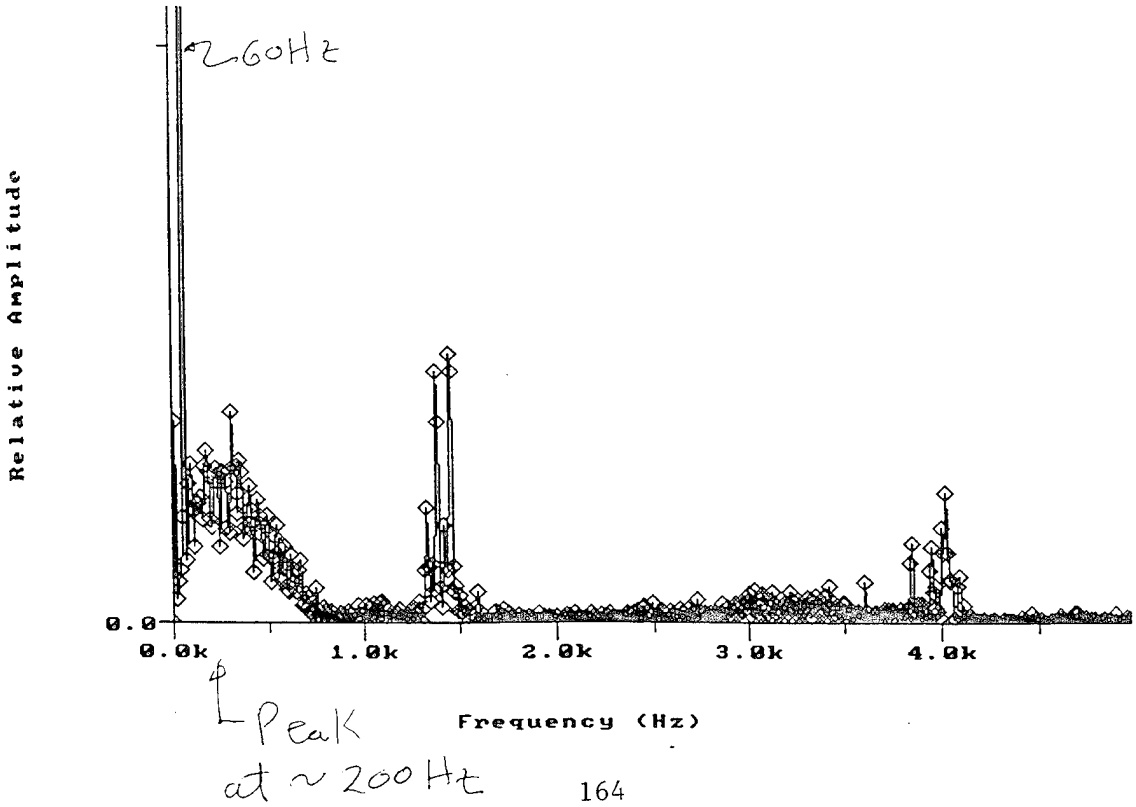
POWER SPECTRUM

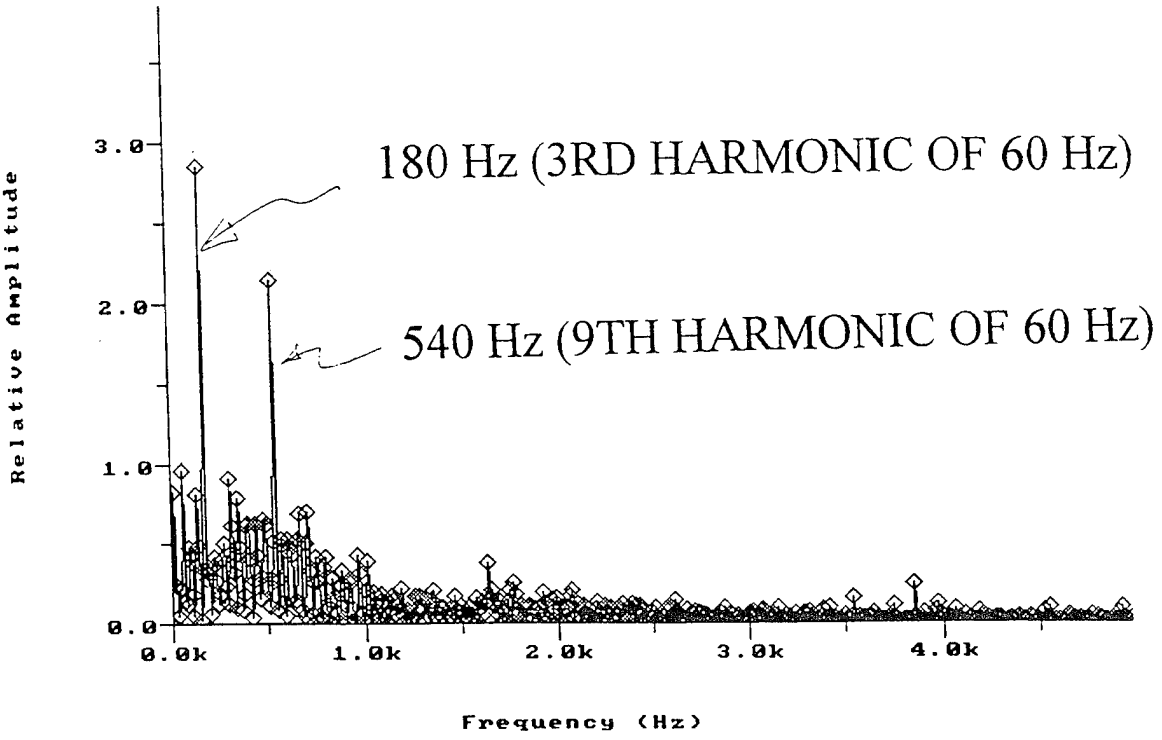


"SPRITE"

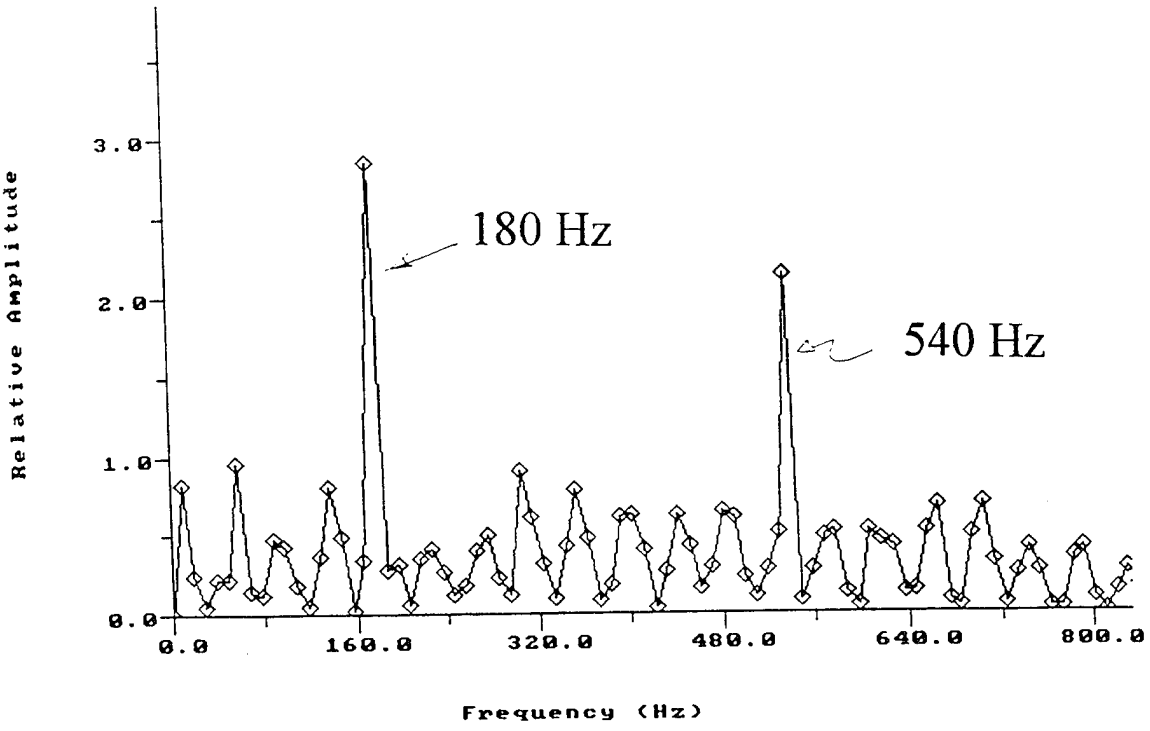


d:\rs724\065138.DAT ELECTRIC PSD



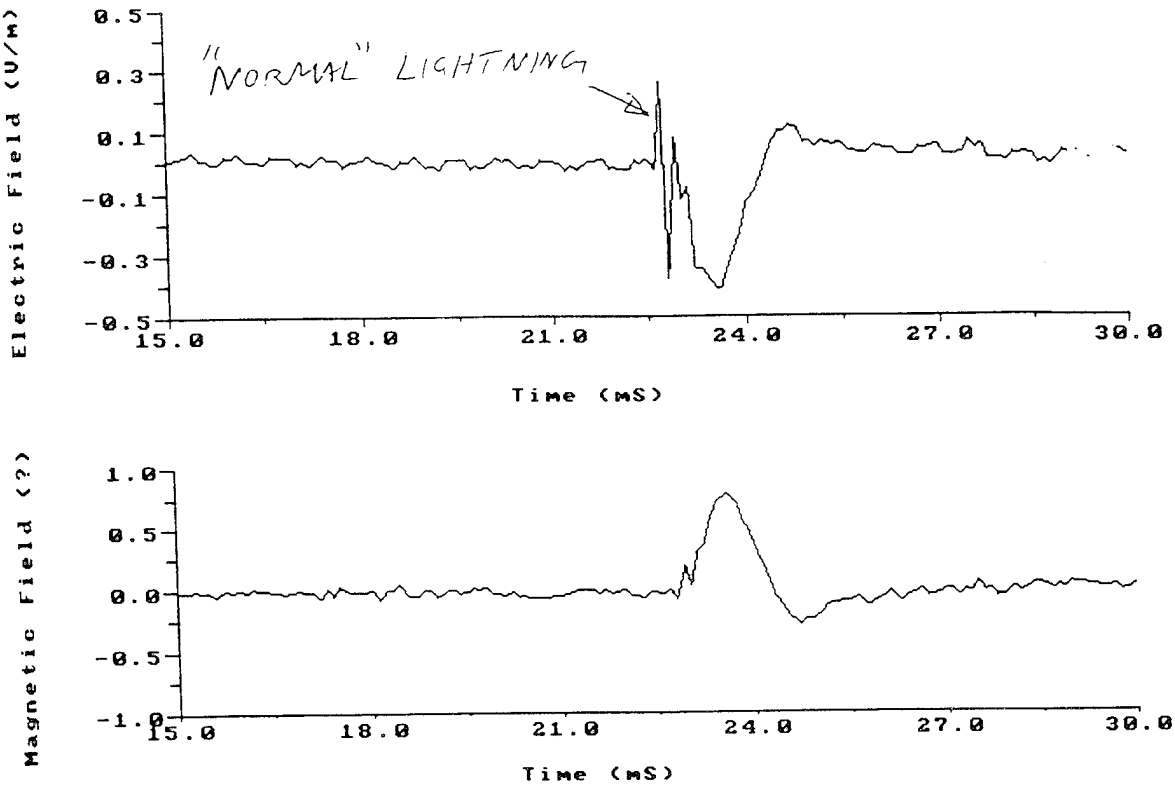


d:\rs724\065138.DAT MAGNETIC PSD

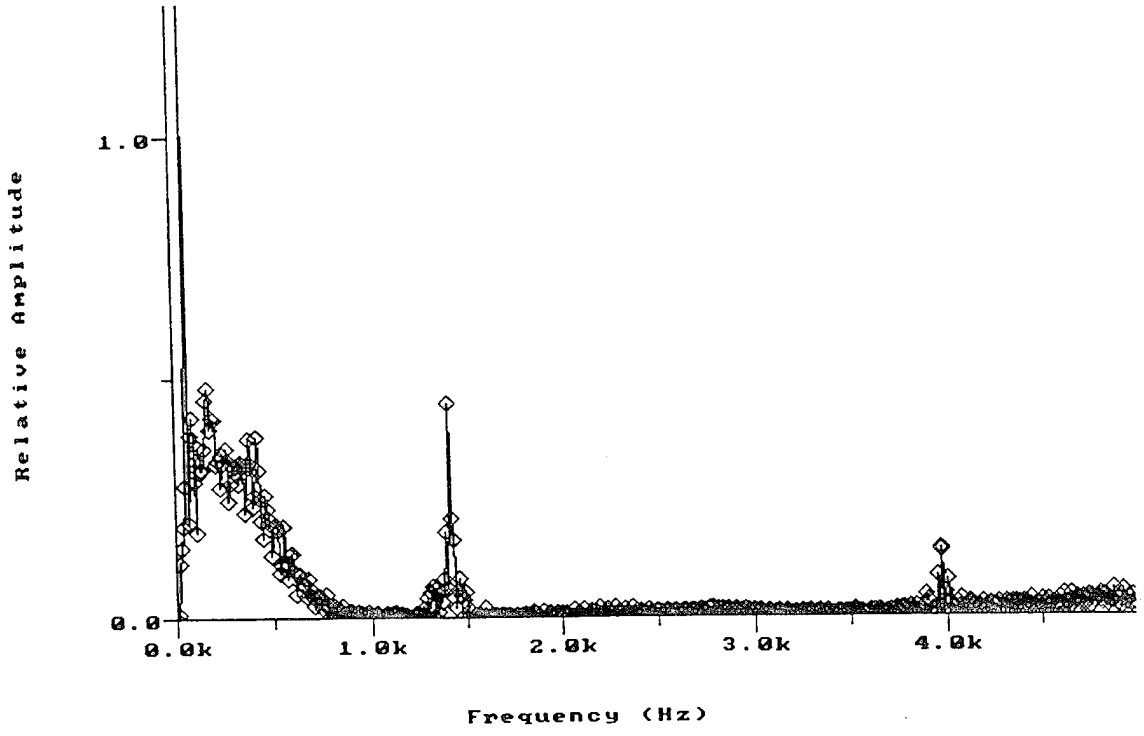


d:\rs724\065753.DAT

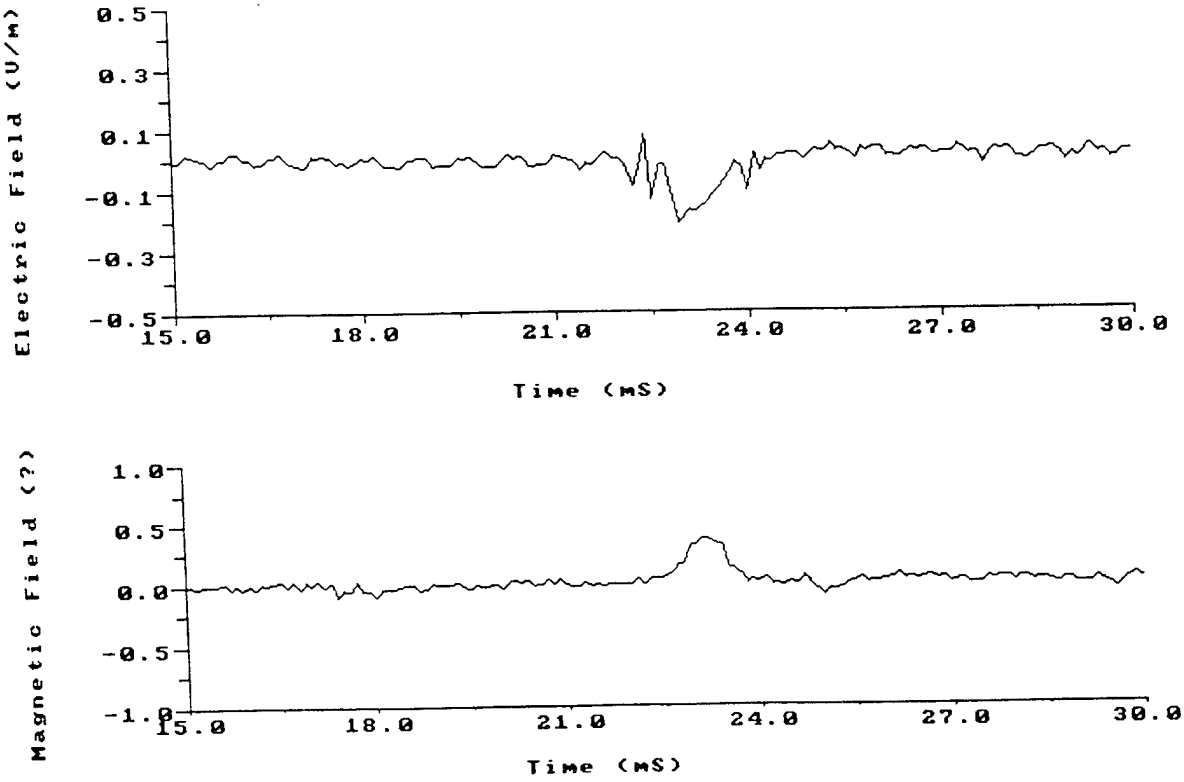
"AIRGLOW EVENT"



d:\rs724\065753.DAT ELECTRIC PSD

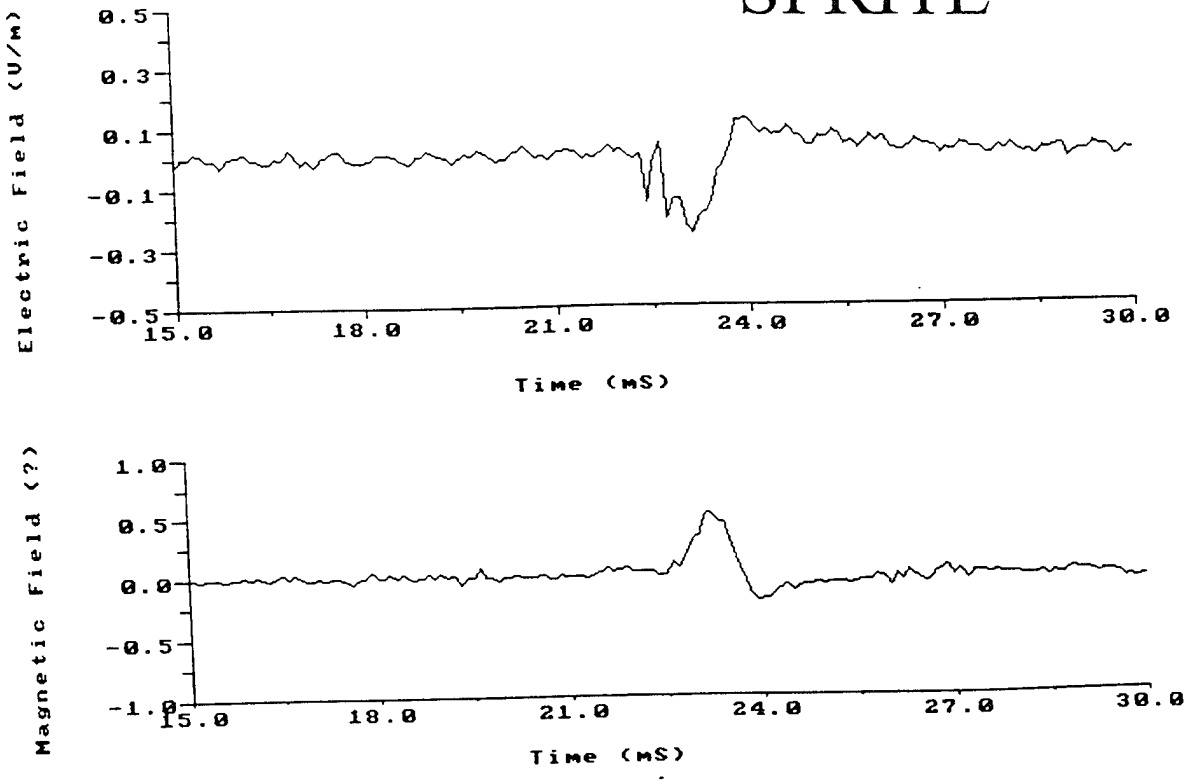


"SPRITE"



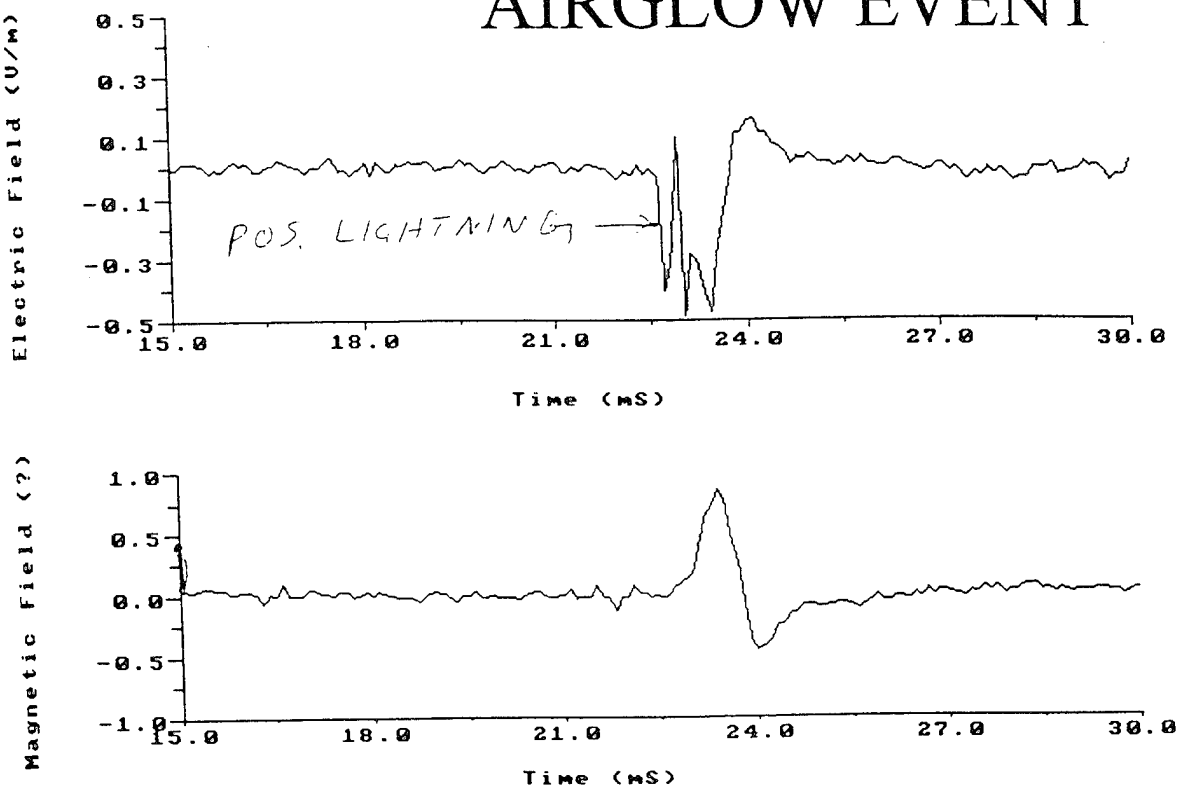
d:\rs724\071632.DAT

"SPRITE"



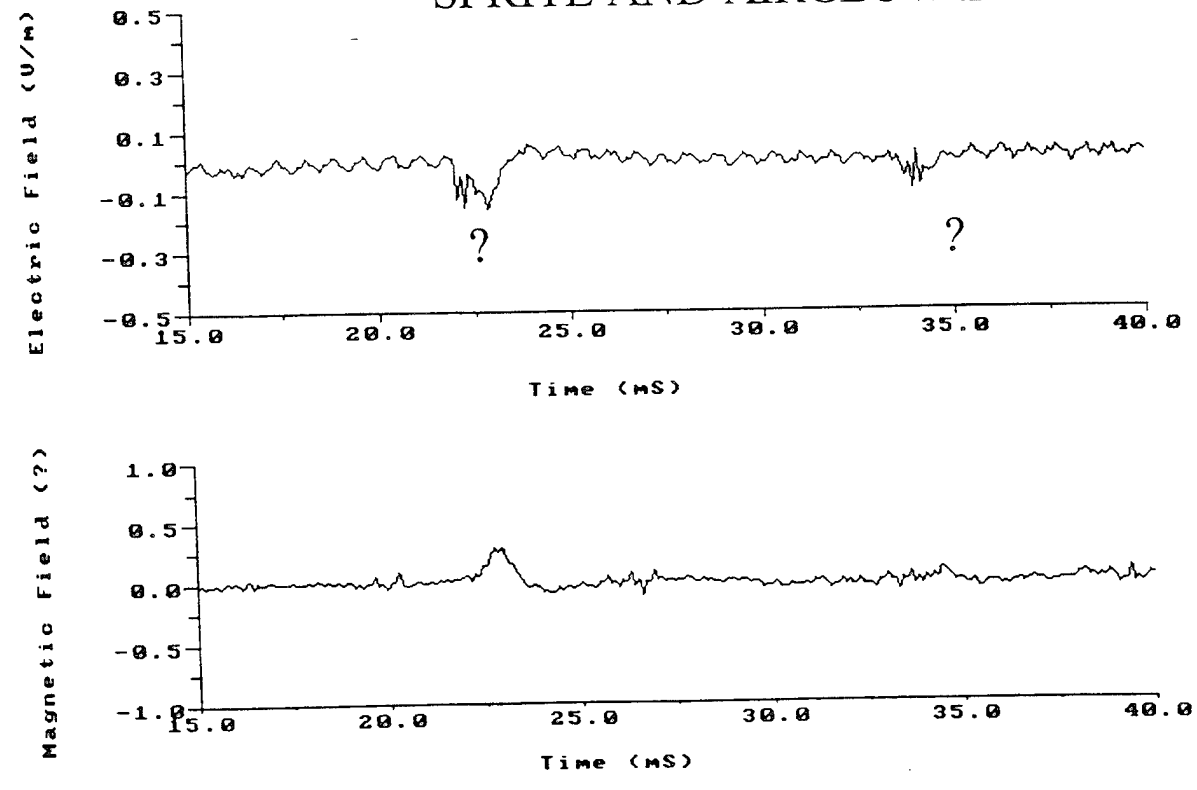
d:\rs724\070539.DAT

"AIRGLOW EVENT"

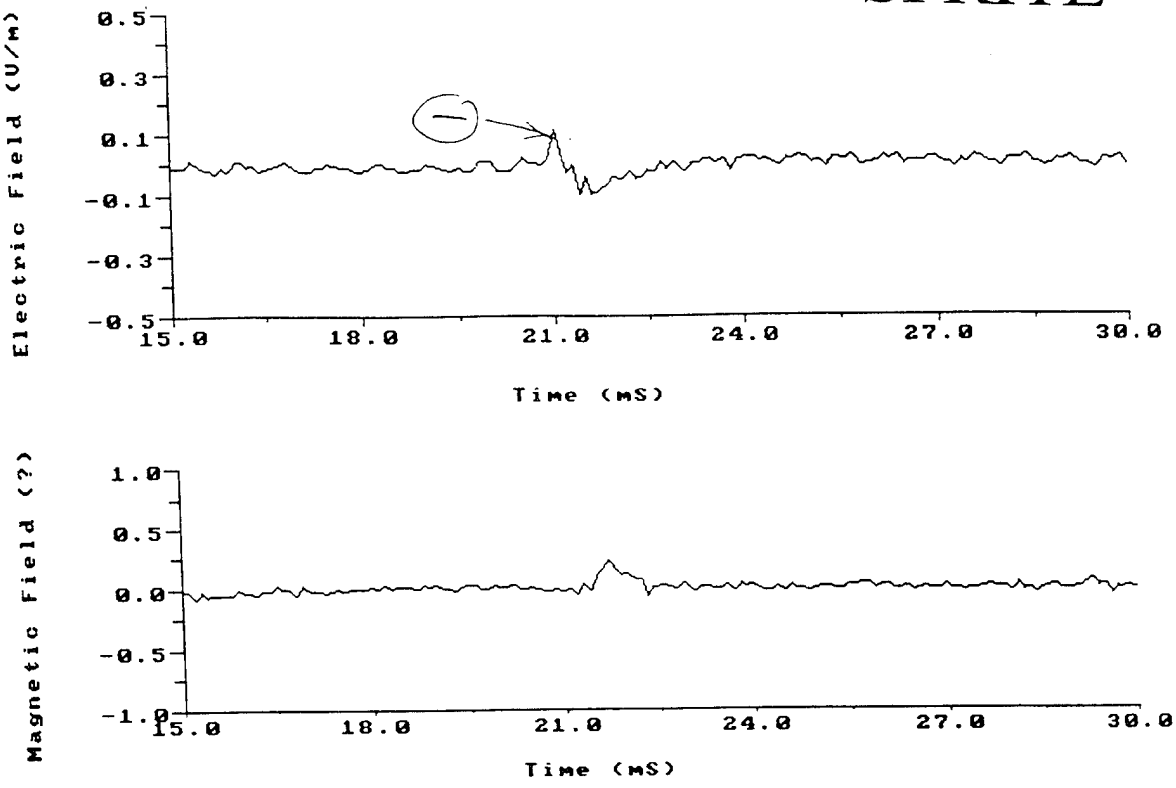


d:\rs724\070546.DAT

"SPRITE AND AIRGLOW EVENT"

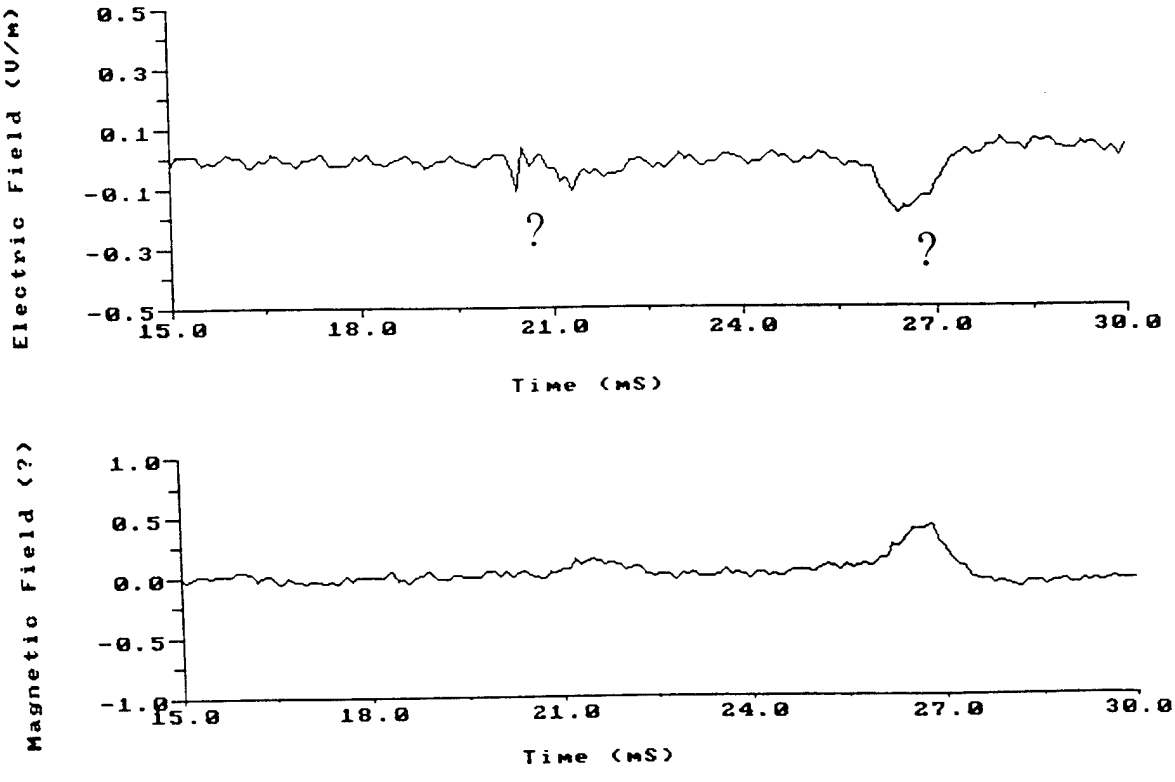


"SPRITE"

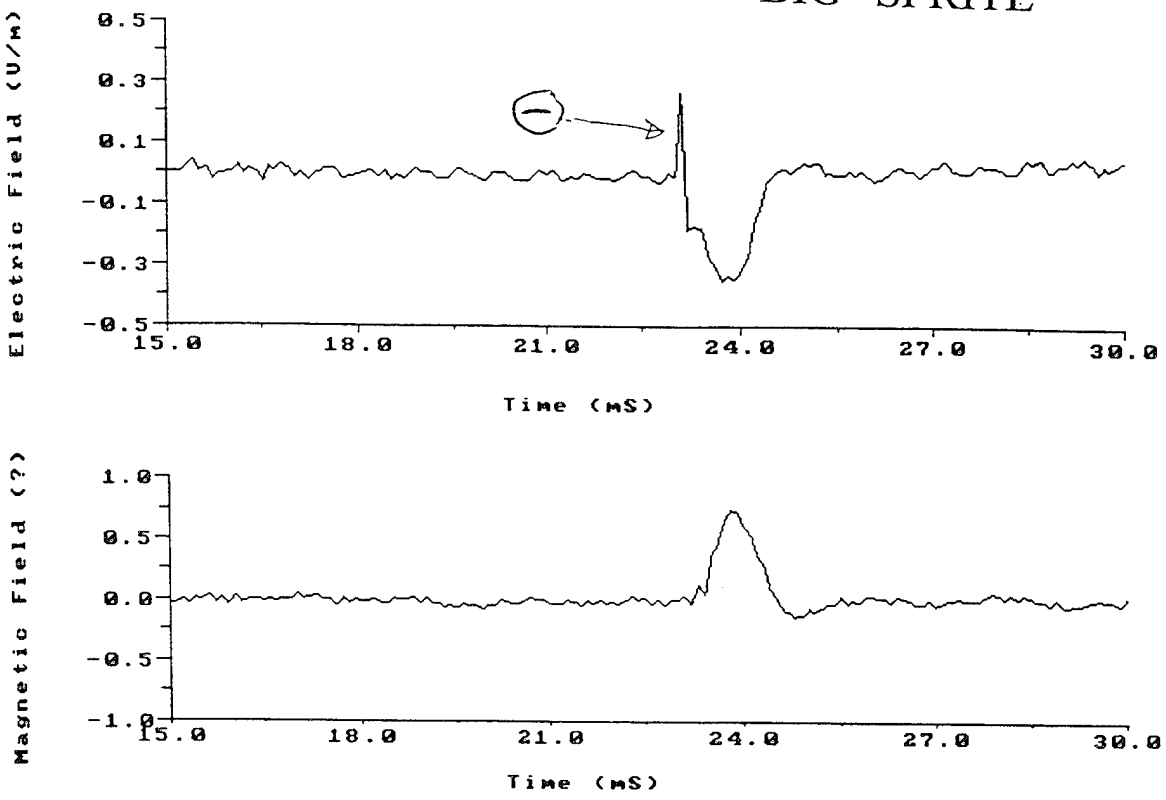


d:\rs724\080034.DAT

"SPRITE"

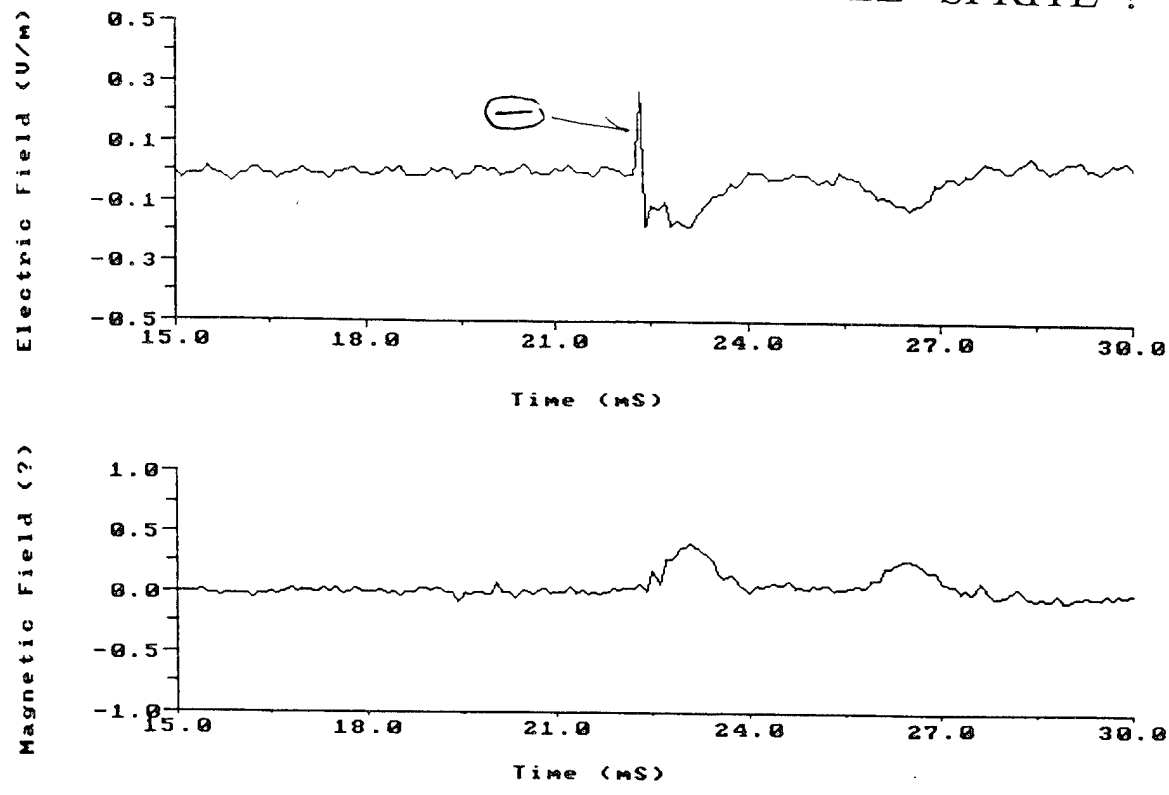


BIG "SPRITE"



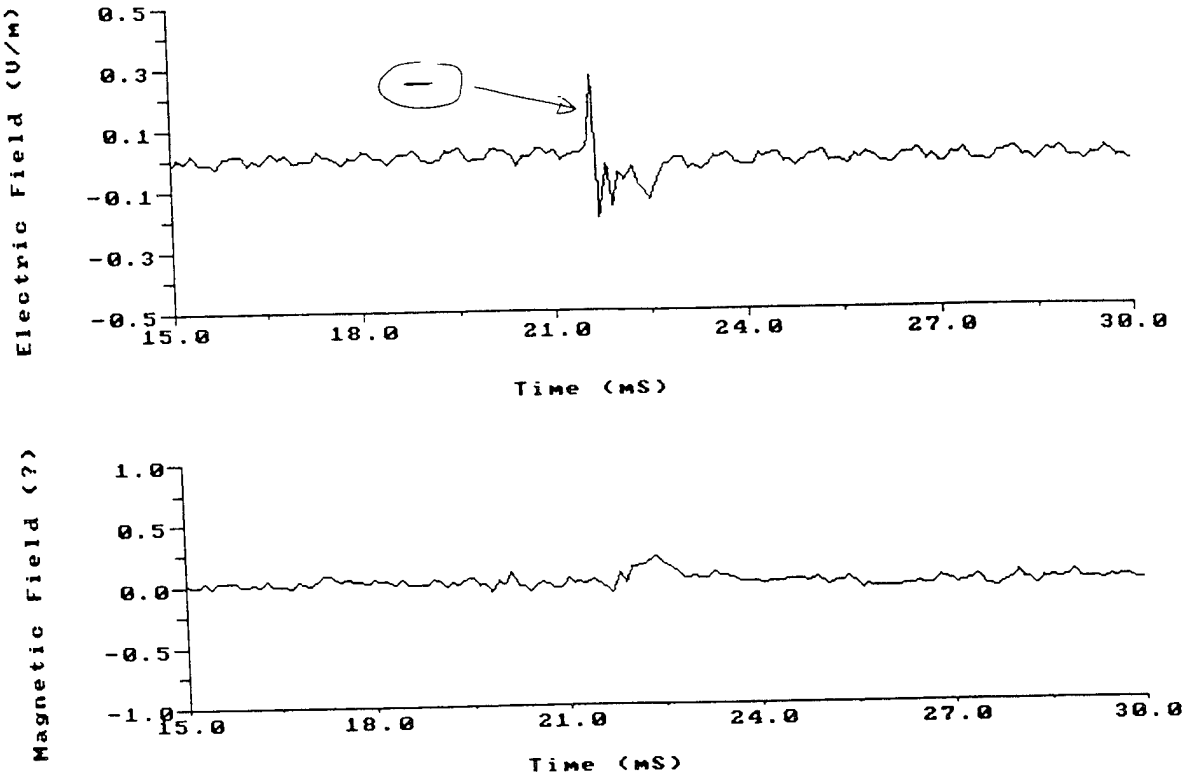
d:\rs724\081549.DAT

DOUBLE "SPRITE"?



d:\rs724\080118.DAT

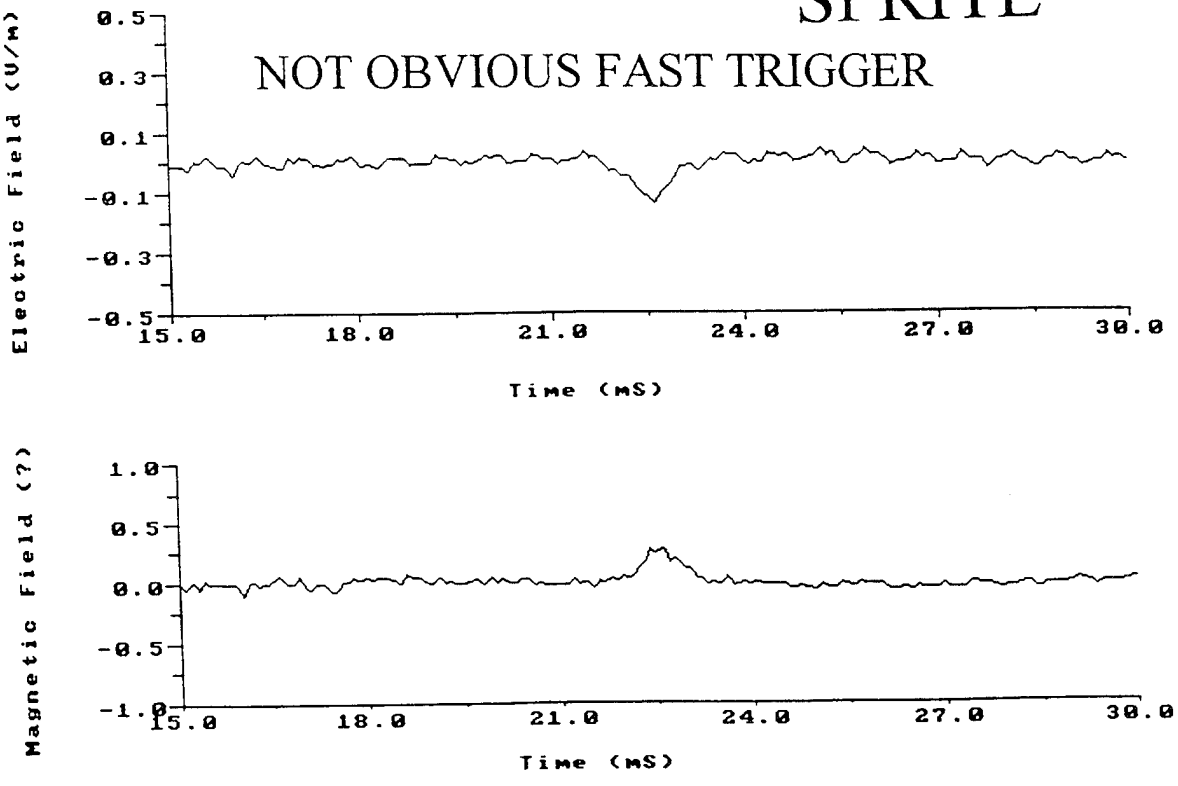
"SPRITE"



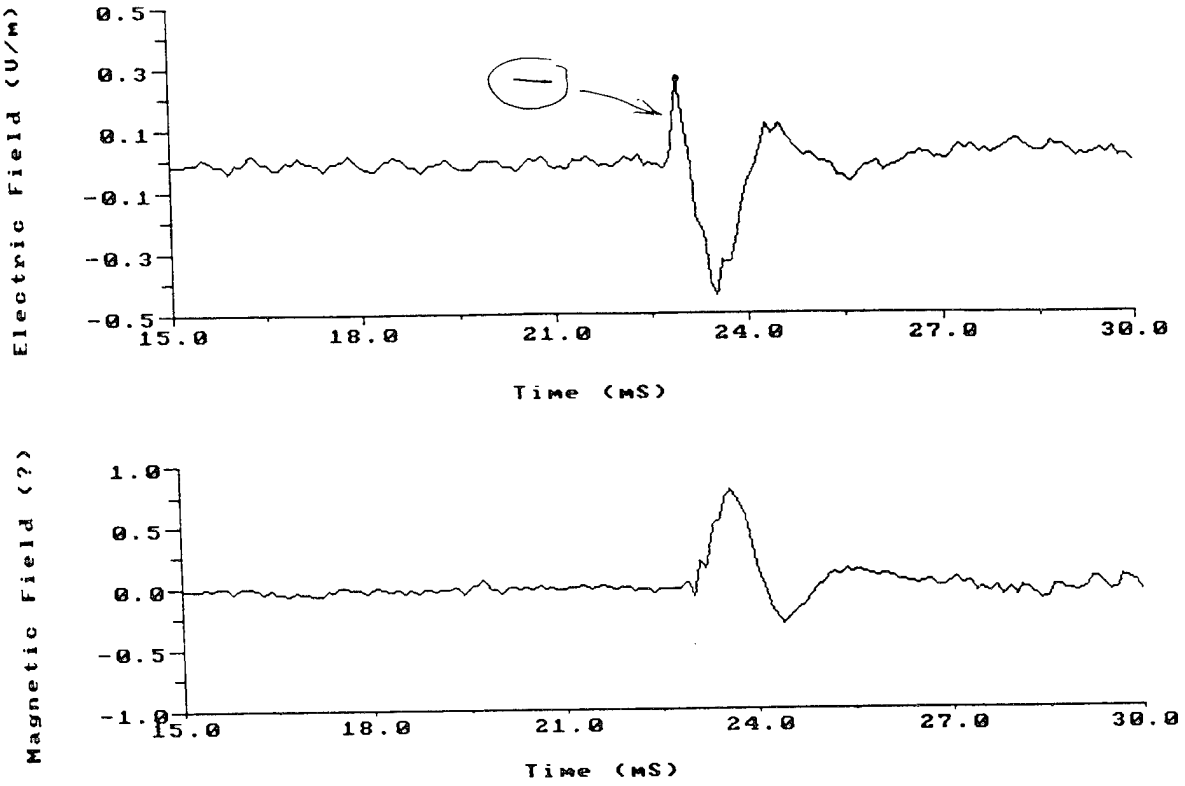
d:\rs724\080705.DAT

"SPRITE"

NOT OBVIOUS FAST TRIGGER

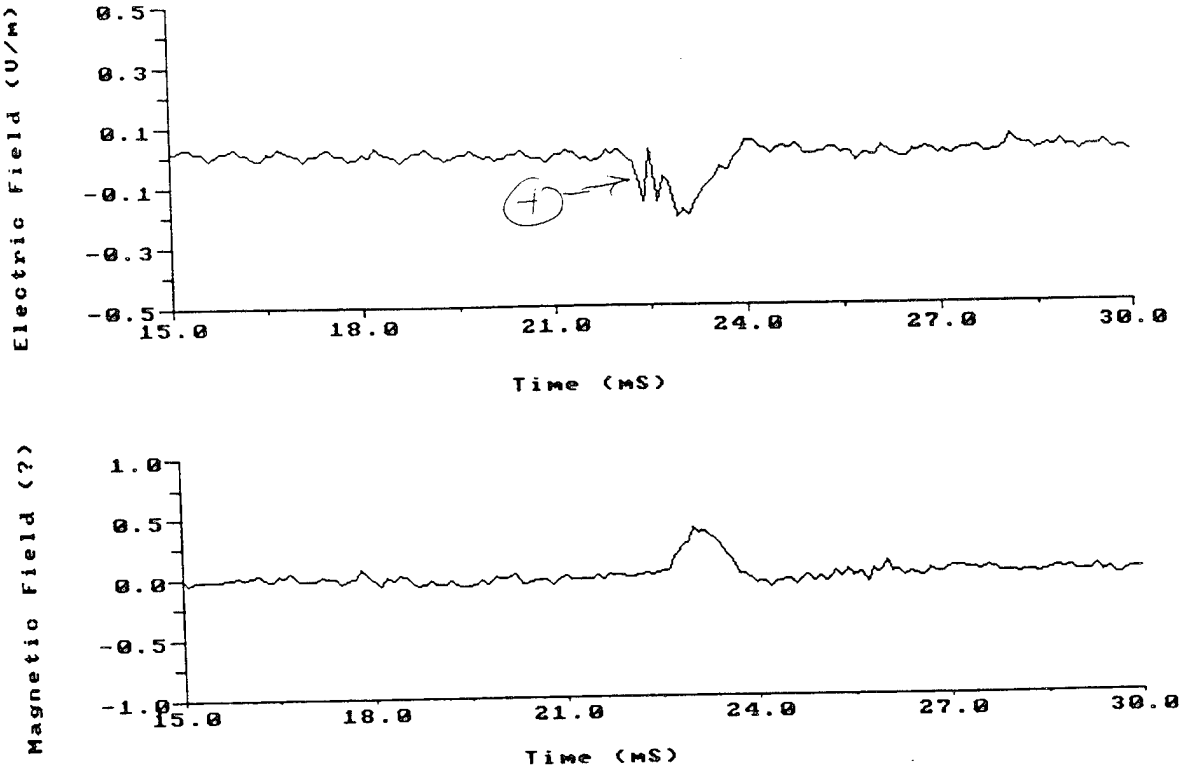


"SPRITE"

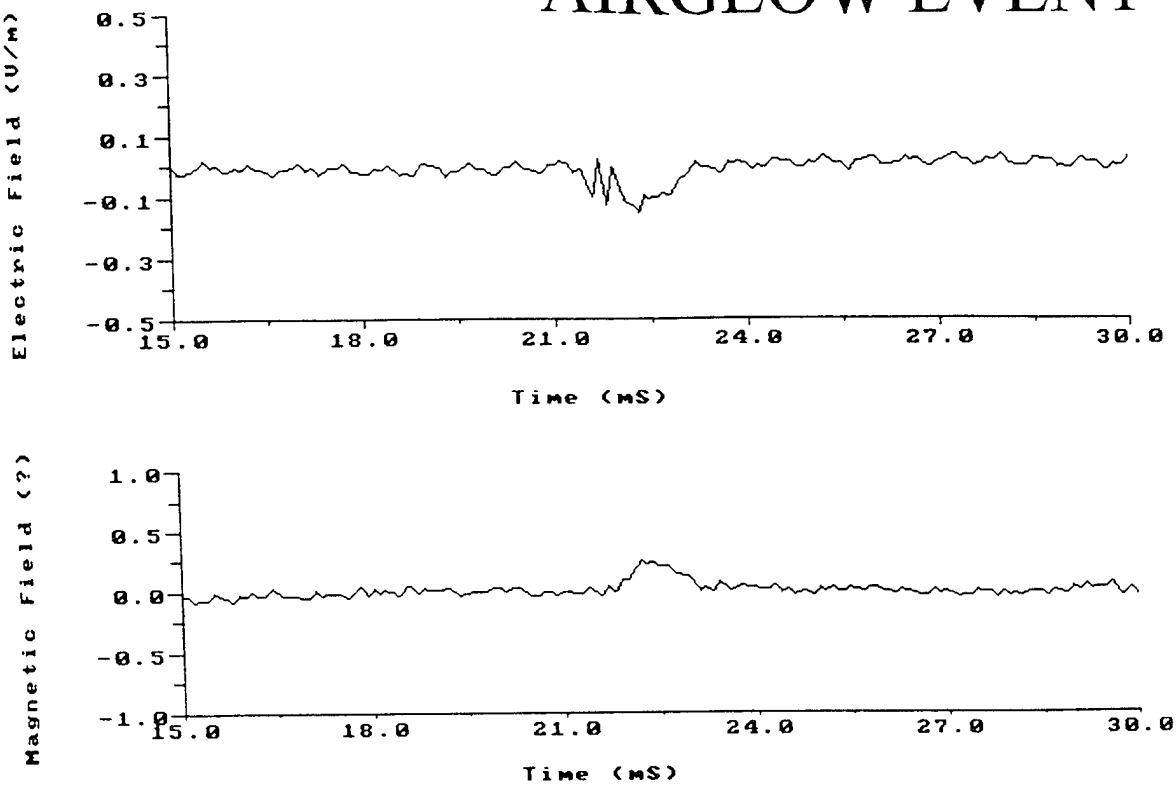


d:\rs724\083334.DAT

"SPRITE"

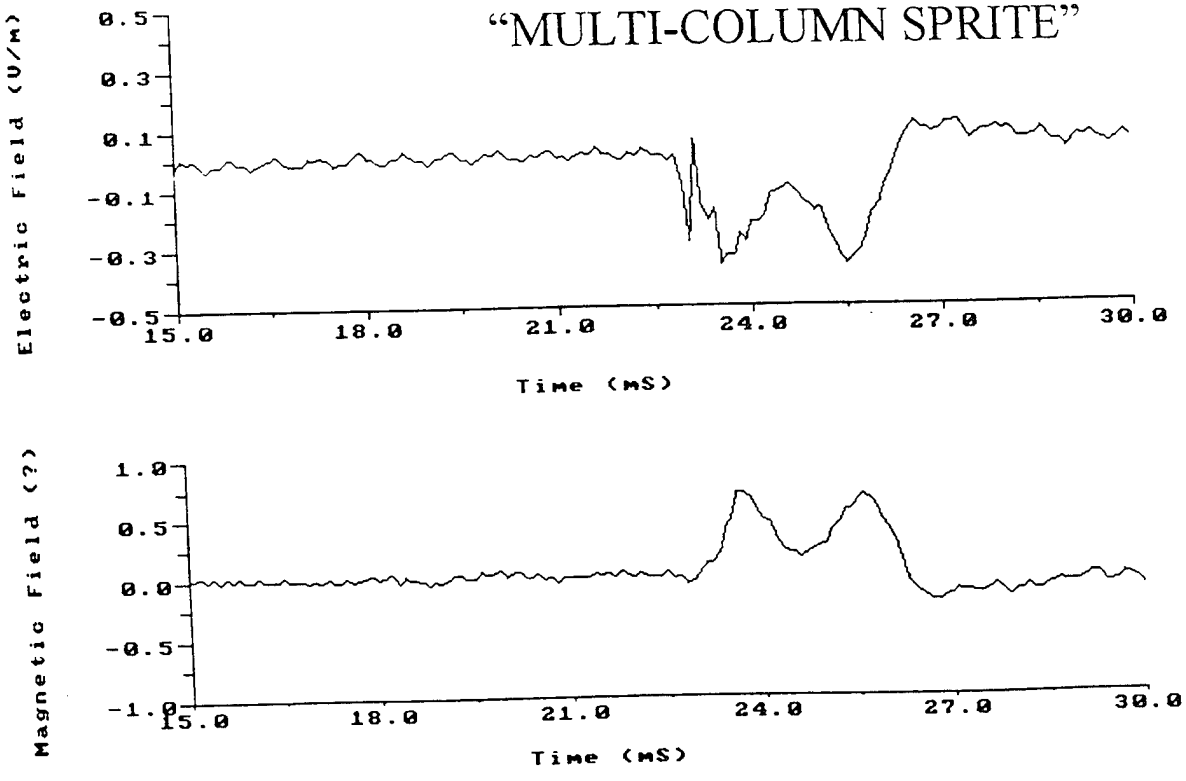


"AIRGLOW EVENT"

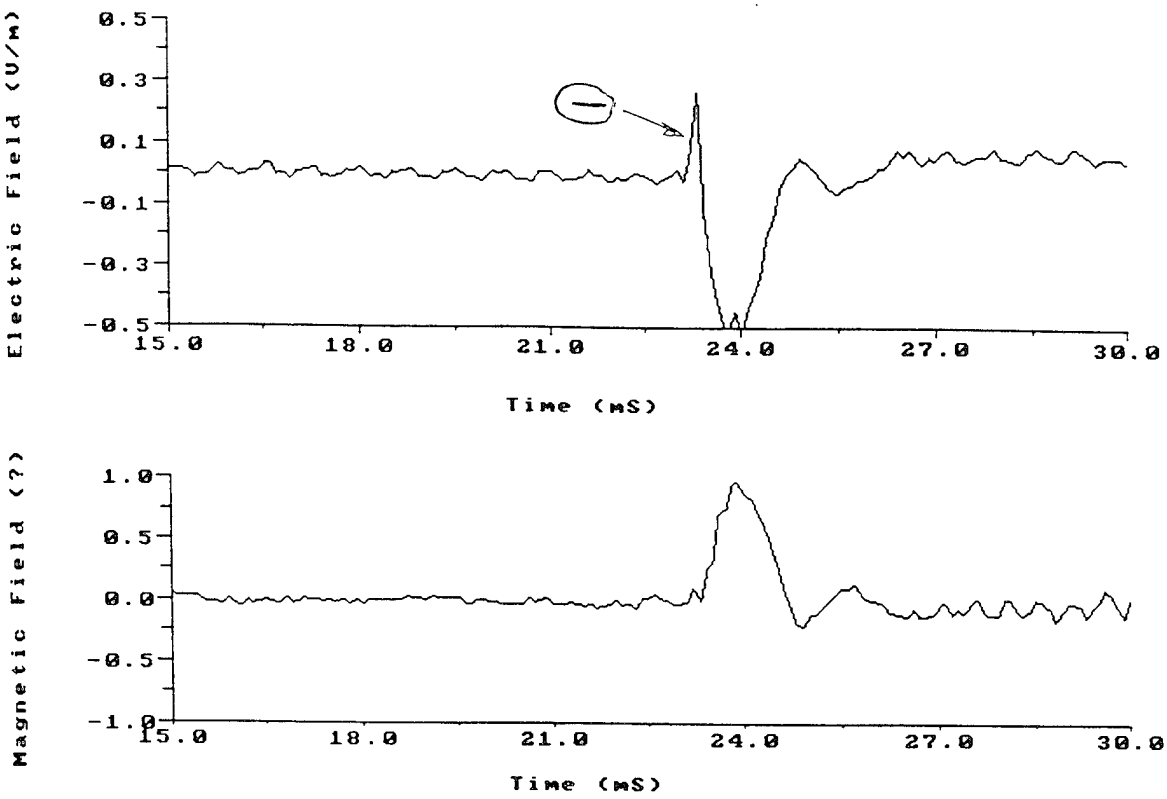


d:\rs724\081844.DAT

"MULTI-COLUMN SPRITE"

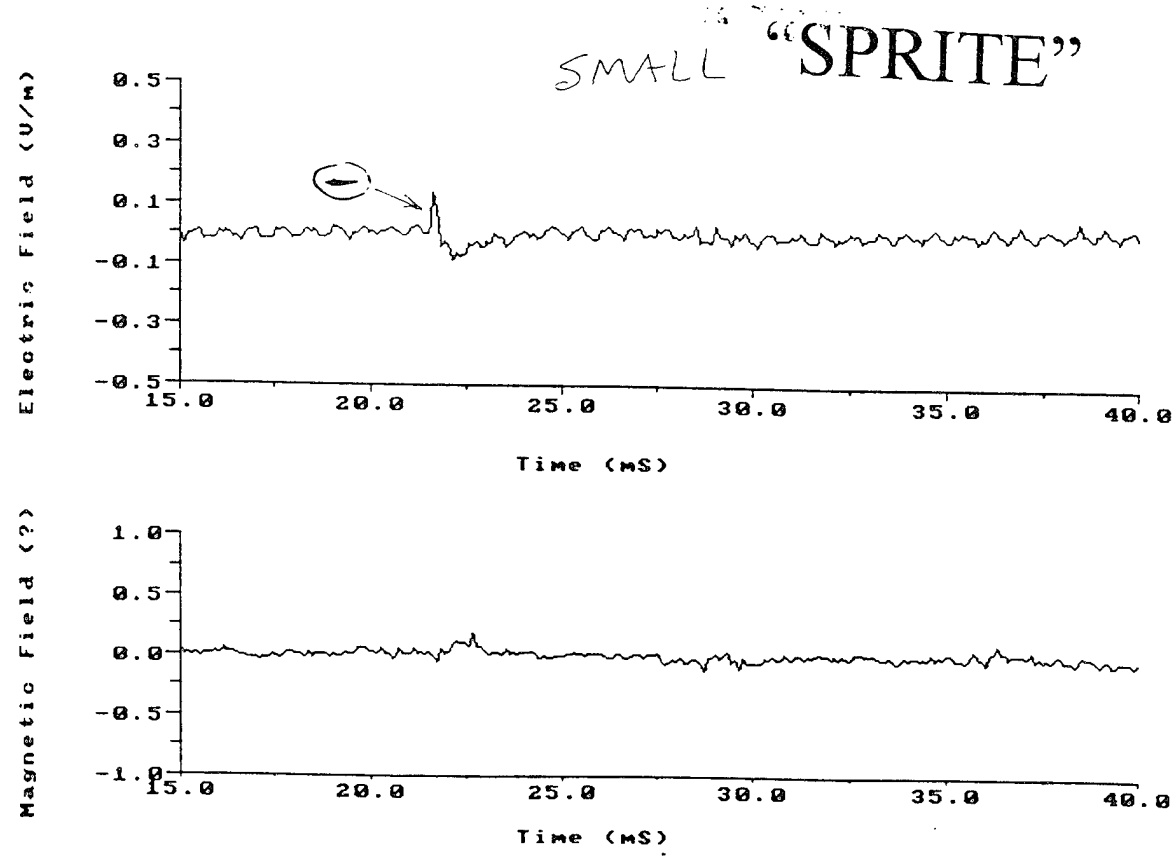


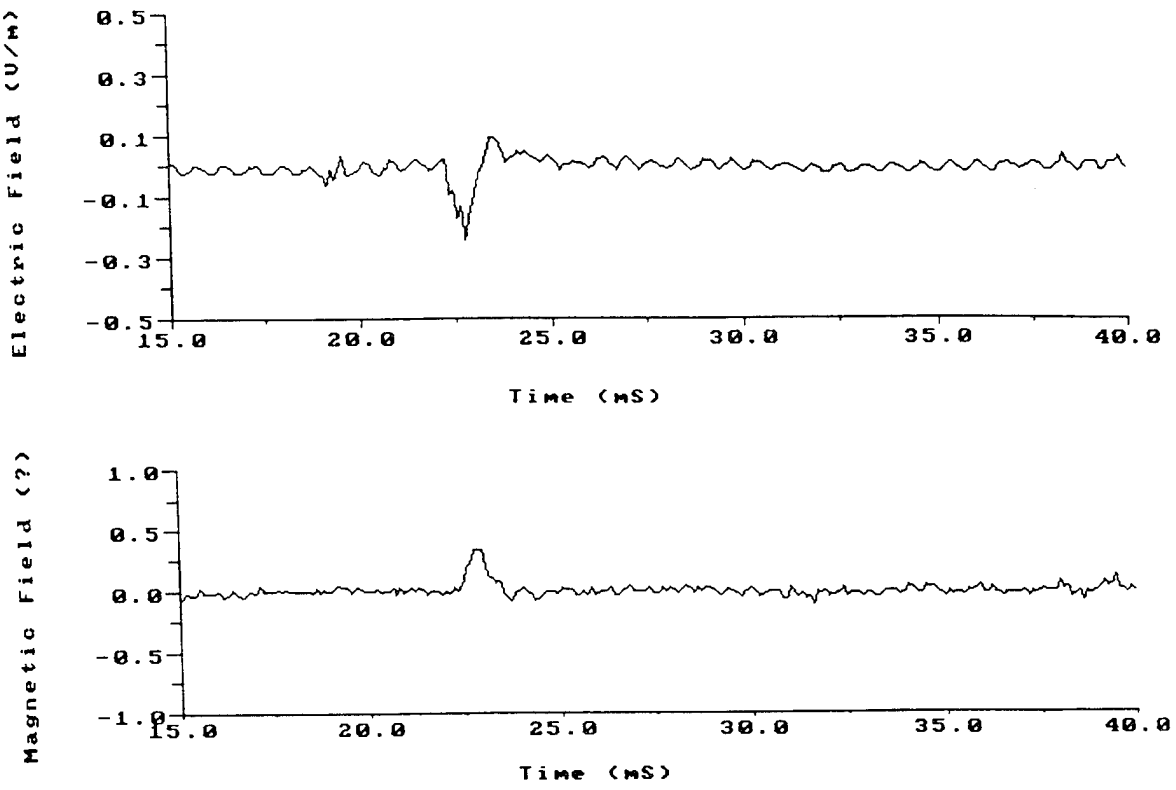
BIG "SPRITE"



d:\rs724\084111.DAT

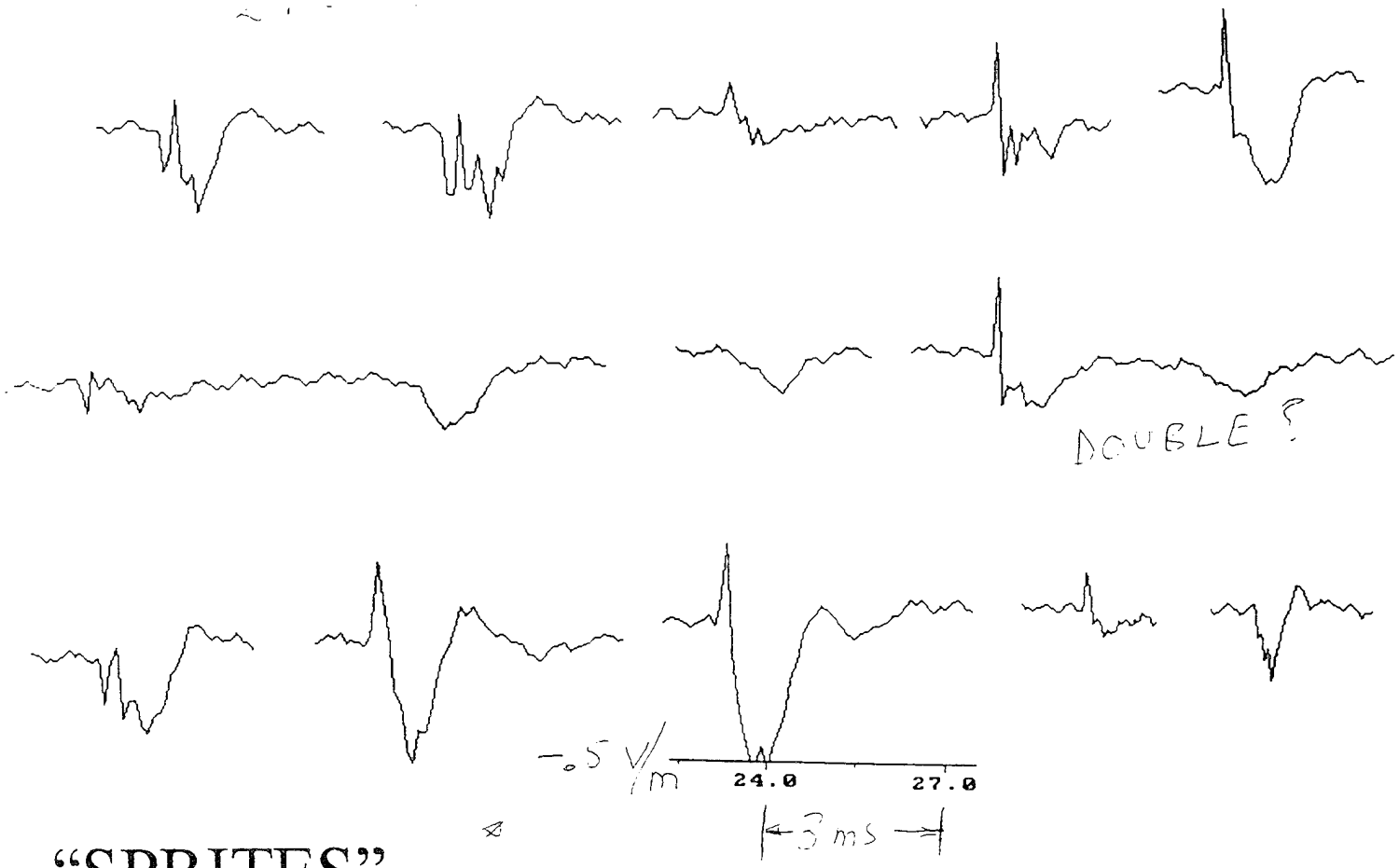
SMALL "SPRITE"



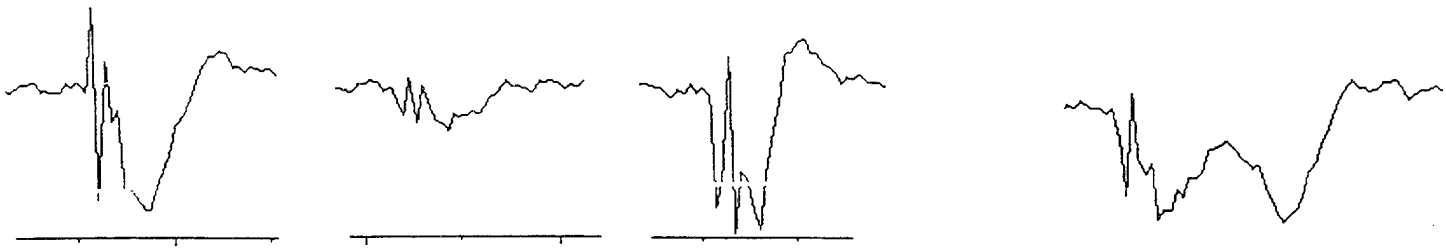


LAST SPRITE OF DAY IN E & M OBSERVATION IN PA.

ELECTRIC FIELD WAVEFORMS OF EVENTS IDENTIFIED BY WALT LYONS IN COLORADO - OBSERVED IN PENNSYLVANIA 24 JULY 1995 0640UT - 0910UT

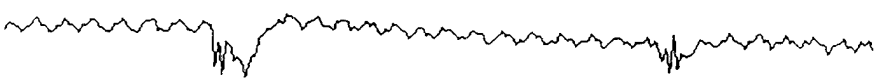


"SPRITES"



"AIRGLOW EVENTS"

"MULTI-COLUMN SPRITE"



"SPRITE AND AIRGLOW EVENT"

BANDWITH ~5kHz (RETURN STROKES IDENTIFIED BUT NOT RESOLVED)

CONCLUSIONS

1) VARIETY OF E & M SIGNALS FROM "SPRITES" AND "AIRGLOW EVENTS" WITH AND WITHOUT "FAST" EVENTS OF BOTH POLARITIES.

2) COMMON FEATURE: NEGATIVE GOING ELF WAVEFORM - POSSIBILITY TO COMBINE WITH LIGHTNING LOCATOR DATA FOR "SPRITE MAPPER".

3) ENERGY OF ELF SPRITE ~10^6 JOULES >> VISIBLE SPRITE.

4) ADVANTAGES OF E-FIELD MEASUREMENTS:
   - ◆ EASIER TO FIND QUIET LOCATION
   - ◆ EASIER TO MEASURE WIDE-BAND
   - ◆ OMNI-DIRECTIONAL

5) ADVANTAGES OF H-FIELD MEASUREMENTS:
   - ◆ POSSIBILITY OF DIRECTION-FINDING
   - ◆ LESS SENSITIVE TO LOCAL WEATHER

6) NEXT TIME: AT LEAST TWO LOCATIONS, ONE WITH OPTICS. 5 Hz TO 25kHz BANDWIDTH. COMPLETELY DIGITAL WITH TAPE BACKUP.

POSSIBLY UNPOPULAR CONCLUSION:

CONSISTENT "POSITIVE" LIGHTNING SIGNAL MAY BE FROM THE SPRITE ITSELF.

NOTE: This material was not considered sufficiently "new" to be published as a letter by a couple of journals, but may be of interest to some people not intimately familiar with the literature in this "field." Comments, including violent disagreement, are welcomed with enthusiasm. L.H.

ON THE COUPLING OF FIELDS, CURRENTS, AN ENERGY FROM LIGHTNING TO THE UPPER ATMOSPHERE AND IONOSPHERE: A "CURRENT" STATEMENT

Les Hale, CSSL/Penn State
University Park, PA 16802-2707
Tel: (814) 865-2361 e-mail: Les Hale@PSU.EDU

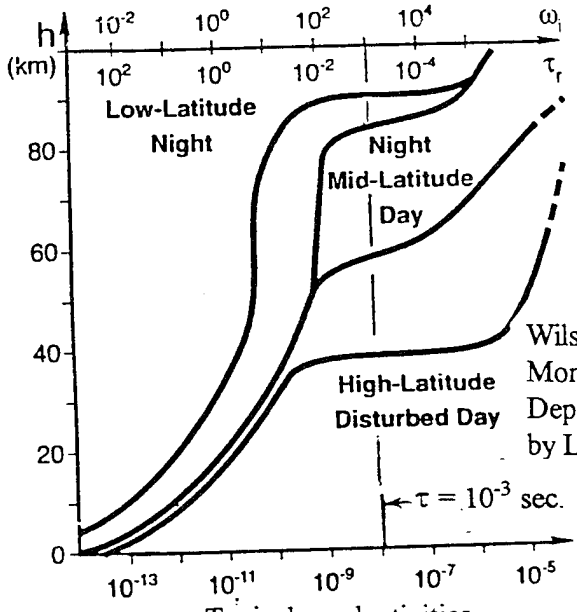
Stimulated by the "red-sprites" phenomenon, there has been a resurgence of interest in the coupling of E & M fields from tropospheric lightning to the "ionosphere." Many workers have concluded that the fields calculated using free space dipole moments (or, using superposition, multipole moments), e.g. radiation, induction or intermediate, and electrostatic, are inadequate to explain the mesospheric phenomenon of "red sprites." This communication is intended to collect some ideas which, while generally not new, may be relevant to the problem. While there appear to be some good theoretical treatments, for example the recent work of Sukorukov, such work tends to be somewhat mathematical, which is avoided in this discussion.

Free space dipole moments are not generally valid for lightning fields which are confined between the conducting earth and the generally more "fuzzy" ionospheric boundary. However, for a lightning return stroke current $i_L(t)$ which flows in less than about a millisecond, the "induction" and "radiation" fields incident on the upper atmosphere, due to i_L and di_L/dt, are valid as long as ground reflection is considered. This is not true for the "electrostatic" component, which is quite different from the free-space case. In the case of cloud-to-earth strokes this is usually handled by considering the effects of "Wilson monopoles," which are charge centers created by the time integral of the lightning currents. ("Dipoles" and more complex situations can be considered using the superposed fields of two or more such monopoles.) At large distances the monopoles can generally be considered to be point charges, persisting for the tens of seconds "relaxation time" of their tropospheric deposition altitude. They provide sources for calculating the time dependent "quasi-static" fields associated with the lightning. Although this is a very complex problem in an atmosphere with continuously varying conductivity, generally requiring a computer solution of the complete Maxwell's equations, in some cases simplifying assumptions may enable estimation of the fields and currents. In particular, in the "quiet" nighttime mesosphere, there are essentially zero free electrons and the electrical conductivity σ remains as low as 10^{-10} to 10^{-9} S/m up to a "ledge" at 80 to 85 km, which defines the effective height of the transient solution which persists for a time ϵ_o/σ of up to tens of milliseconds after a lightning stoke. This gives rise to a virtually free-space "electrostatic" solution for the fields involving upper and lower conducting boundaries and a Wilson monopole following a cloud-to-earth return stroke. The solution of this electrostatic problem is well known, and involves an infinite Bessel series. A result of interest to the sprites problem is that the electric field just below the "ledge" directly above the monopole is nearly double that calculated without considering the presence of the ionospheric boundary. Thus whatever lightning charge would be necessary to initiate "breakdown" just below the ledge (generally estimated at over 200 C using the "free-space-monopole-plus-earth-image" model) can be reduced by about half.

Although sufficient to create the electric fields that initiate breakdown, a purely "electrostatic" solution couples little energy and cannot sustain the discharge for the observed duration of several milliseconds. This requires substantial current in the discharge region, which can be generated in different ways. The first is direct excitation by a portion of the source lightning current $i_L(t)$. Although the electric fields are complex, the ratio of the electric flux is given by a fraction f (typically ~ 0.1) equal to the simple distance ratio h_m/h_i, where h_m is the altitude of the monopole and h_i is the effective height of the ionosphere. This means that for current pulses of milliseconds or longer, for which a quasi-static solution is valid a current of $fi_L(t)$ is coupled directly to the ionosphere. As the width of the current pulse is decreased to the millisecond range and below, it is found by a computer solution of the complete Maxwell's equation that the current pulse to the ionosphere does not continue to decrease accordingly, but remains about a millisecond. This is interpreted as the time required to establish the initial "quasi-static" solution, which is controlled by the round-trip propagation delay between the lightning and the upper boundary. In this limit the peak current is found to be several hundred amperes per coulomb of lightning-separated charge [Hale and Baginski, Nature 329, 814, 1987], and the writer believes that this is the most likely candidate for producing the brightest portion of the sprite discharge (which may be what is currently being called an elf).

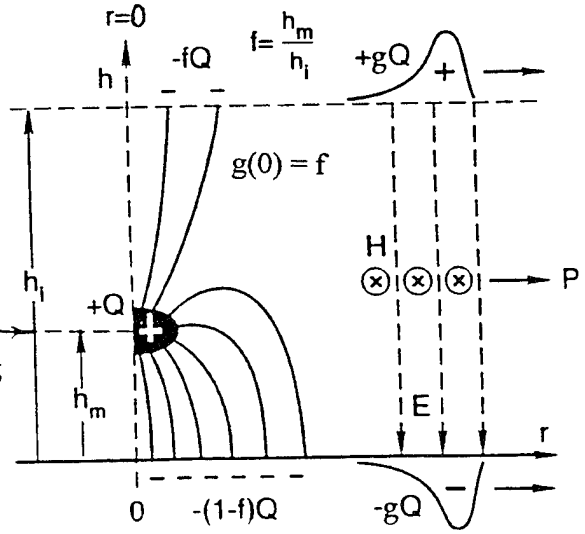
Another mechanism which produces a current to the ionosphere is due to the conductivity gradient $\nabla\sigma$. This mechanism was suggested by C. and P. Greifinger [JGR 81, 2237, 1976], who also gave an interesting physical interpretation, a post-stroke downward moving boundary between regions dominated by conduction current (above) and displacement current (below), which has been termed a "variable capacitor" model by Sukorukov. This mechanism dominates at ULF frequencies, but is much weaker than the "millisecond" ELF pulse, which has been shown by computer modelling to be dominant even in situations where the conductivity varies continuously, with no obvious "ledge." This mechanism could be important to the sprites situation if the discharge originated at or more likely propagated rapidly to very much lower altitudes (with a velocity of 10^7 m/sec or greater), causing a substantial change in the ionospheric boundary height on the millisecond time scale.

These post-stroke currents to the ionosphere give rise to radial TEM (zero mode) wavelets which are easily observed at a distance of thousands of kilometers as slow tails, although their waveshape will appear modified, both by local effects of the earth's magnetic field [Hale, JGR 99, 21089, 1994] and dispersion and attenuation, which will be much greater in the daytime than nighttime. The best diagnostics will probably be done by E & M measurements extending from about 5 Hz to 50 kHz to pass all of the highest energy parts of the E & M signal. The principal unknown quantity continues to be the actual pre-existing conductivity profile associated with "red sprites."



Typical conductivities under various conditions

Radial TEM Wavelet Launched to Satisfy Post-stroke Electrostatic Boundary Conditions:



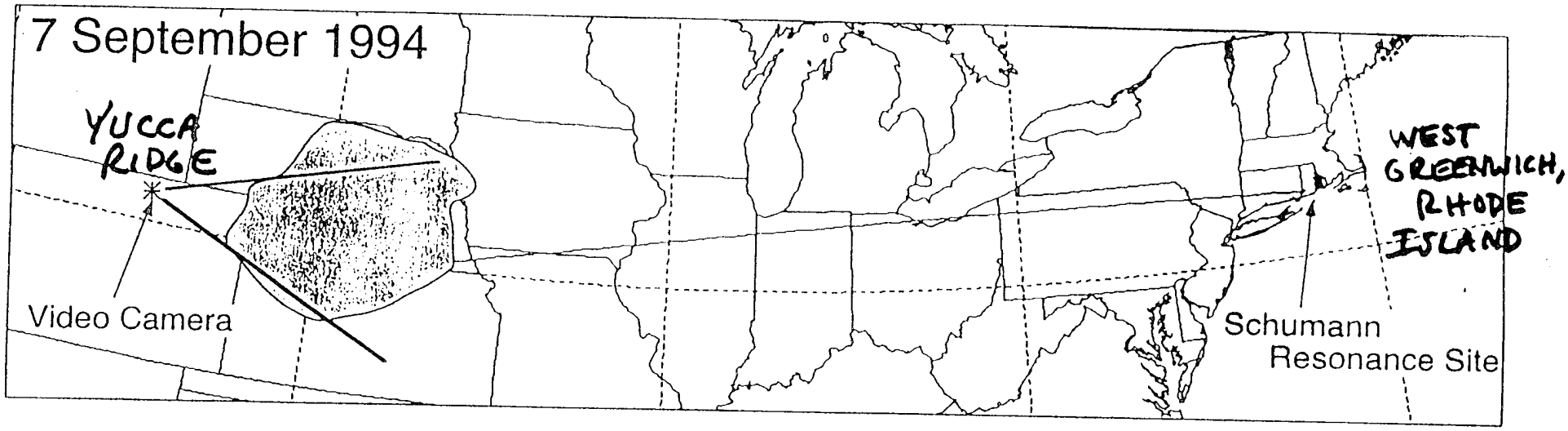
"Electrostatic" solution

Resulting wavelet

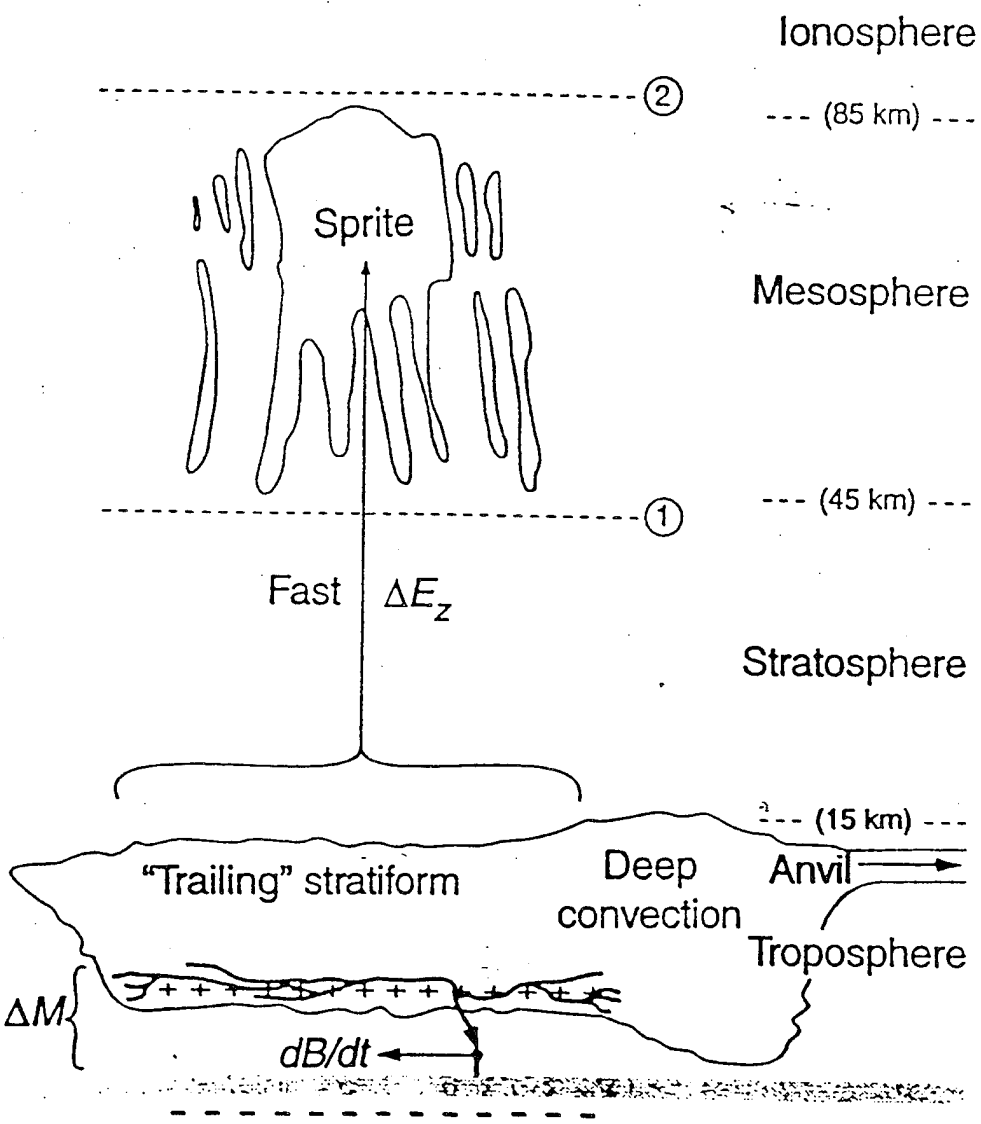
Mesoscale Origin of Sprites
and
Schumann Resonance Methods for their Location on a Global Scale

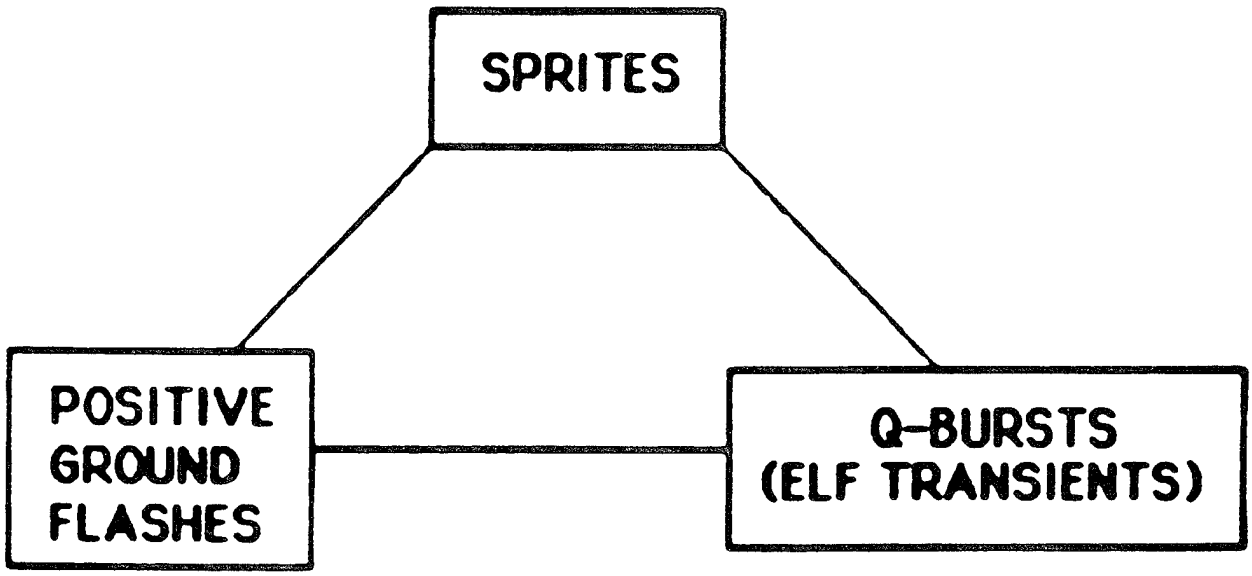
Earle Williams

Massachusetts Institute of Technology



WORKING HYPOTHESIS (BOCCIPPIO et al 1995)





1. WHY ONLY POSITIVES?

2. EXPLORATION OF SOURCE WITH SCHUMANN RESONANCE METHODS

SPRITES ARE ASSOCIATED ALMOST EXCLUSIVELY BY POSITIVE CG's.

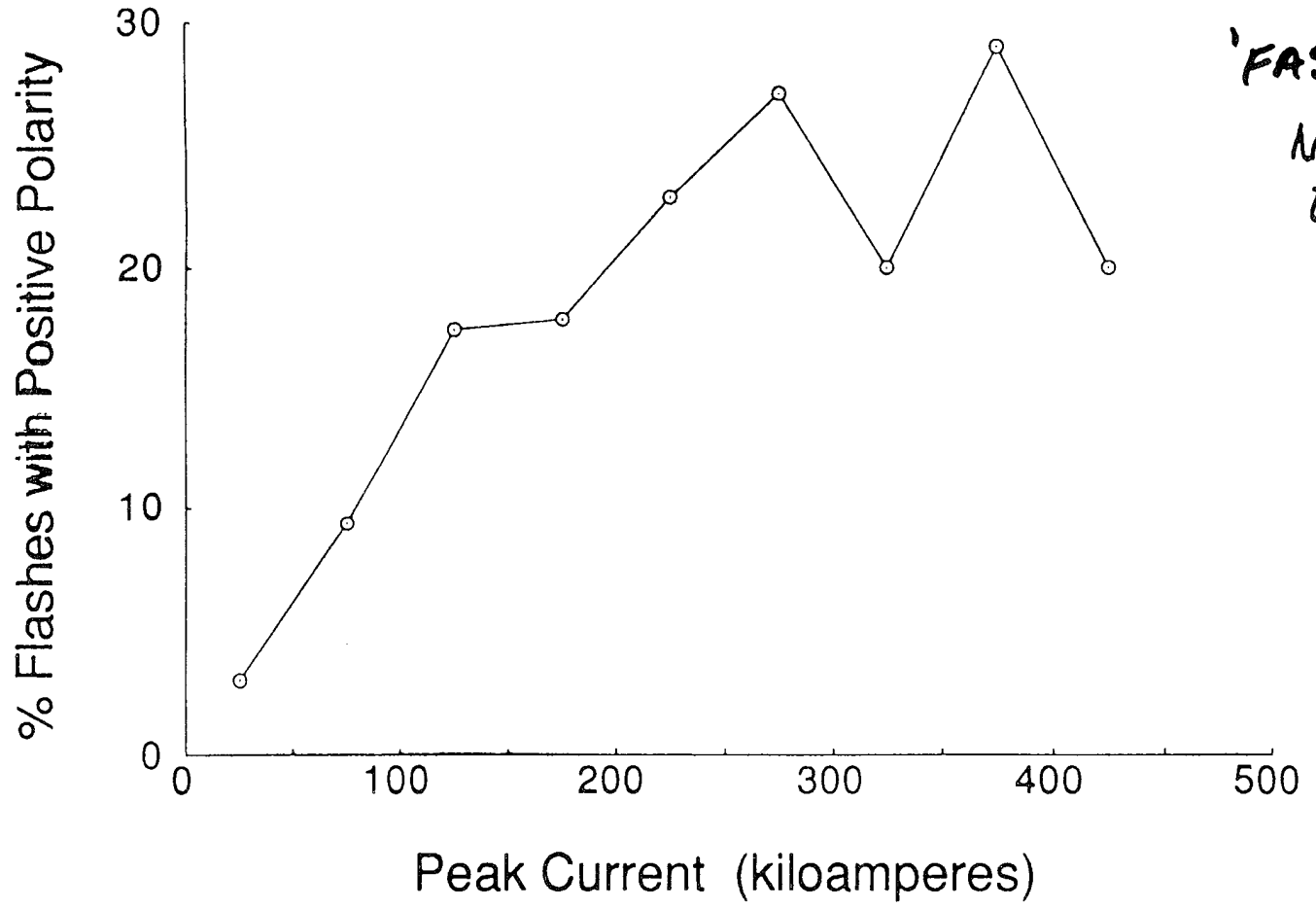
WHY CAN'T NEGATIVES DO IT?

ONE NEARLY BLACK-AND-WHITE DISTINCTION ALREADY KNOWN:

- THE MOST COMMON NEGATIVE CG IS A SINGLE STROKE CG BUT < 6% HAVE CONTINUING CURRENT

- THE MOST COMMON POSITIVE CG IS A SINGLE STROKE CG BUT > 85% HAVE LARGE CONTINUING CURRENT

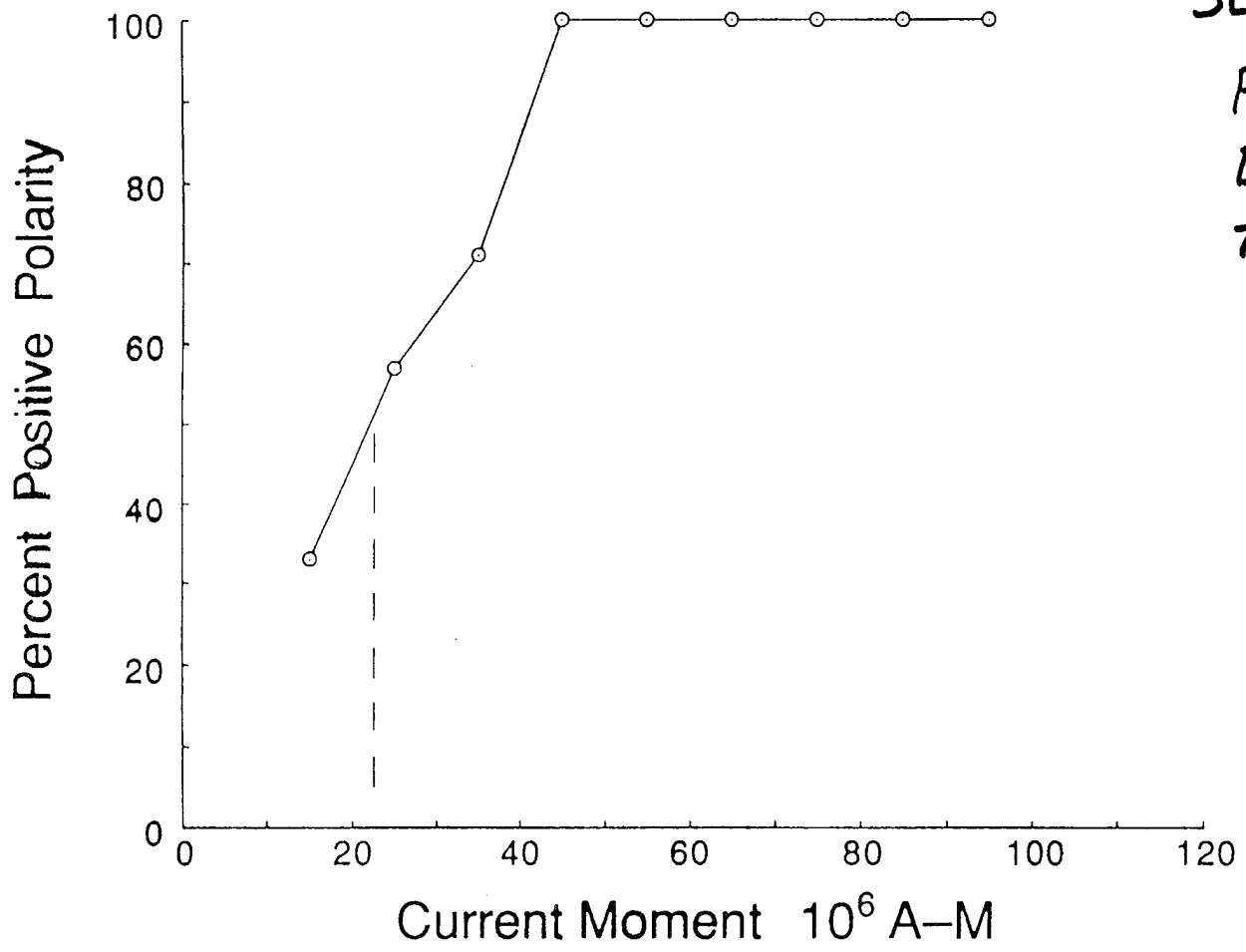
PERCENTAGE OF GROUND FLASHES WITH POSITIVE POLARITY vs. PEAK CURRENT All events for 1992 NLDN



'FAST' CURRENTS.

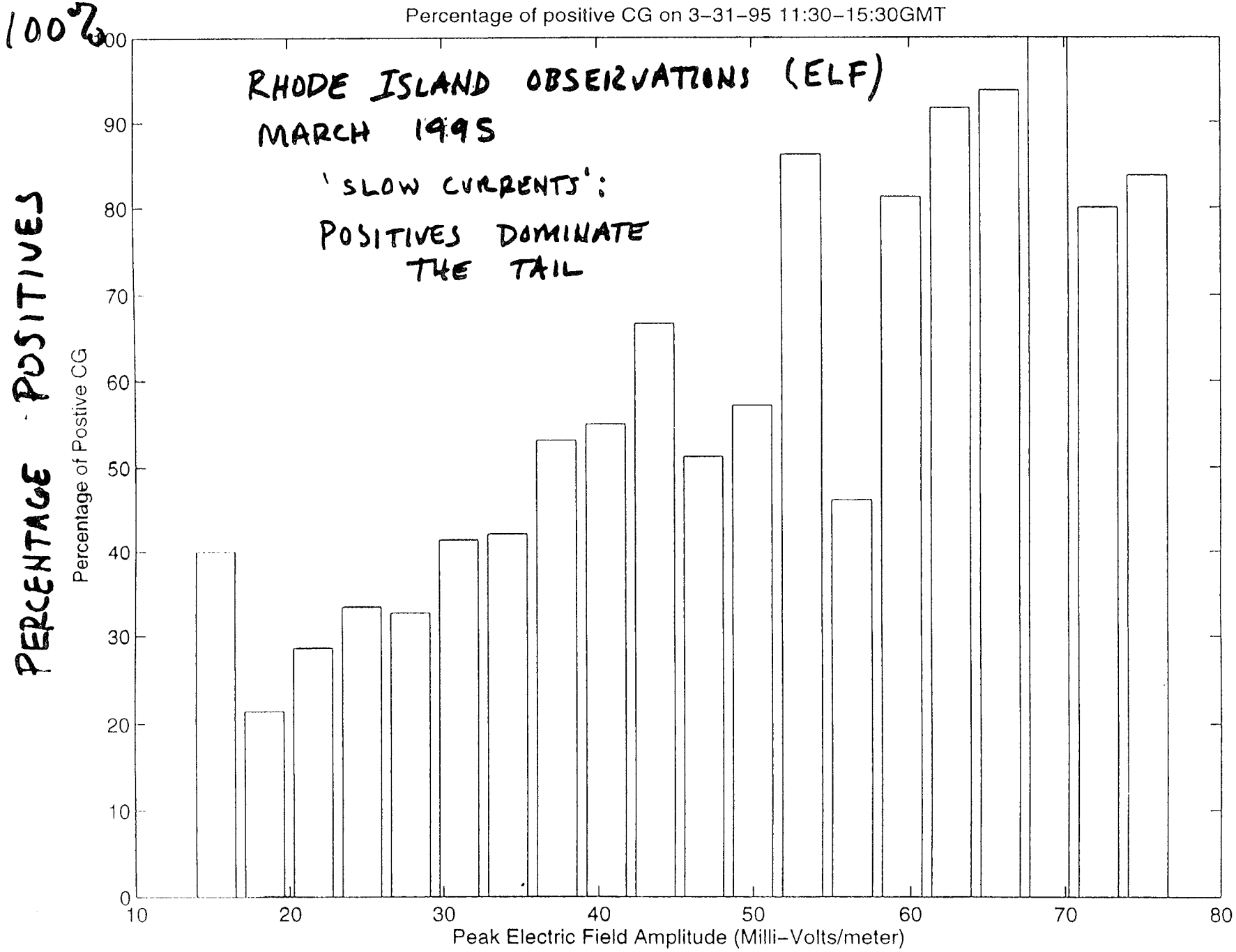
NEGATIVES DOMINATE THE TAIL

FRACTION OF EVENTS WITH POSITIVE POLARITY
Burke and Jones (1995)
274 events total



'SLOW' CURRENT

POSITIVES DOMINATE THE TAIL


100%
PERCENTAGE POSITIVES
Percentage of positive CG on 3-31-95 11:30-15:30GMT
RHODE ISLAND OBSERVATIONS (ELF)
MARCH 1995
'SLOW CURRENTS':
POSITIVES DOMINATE
THE TAIL
Percentage of Postive CG
0
10
20
30
40
50
60
70
80
90
100
10
20
30
40
50
60
70
80
Peak Electric Field Amplitude (Milli-Volts/meter)

NORMAL MODE EQUATIONS

(FINDING SPRITES WITH SCHUMANN RESONANCE

ELECTRIC FIELD

$$E(\omega) = i \frac{I\, ds(\omega)\, \nu\, (\nu+1)\, P_\nu^0\, (-\cos\theta)}{4\pi a^2 e_0\, \omega h \sin(\pi\nu)}$$

MAGNETIC FIELD

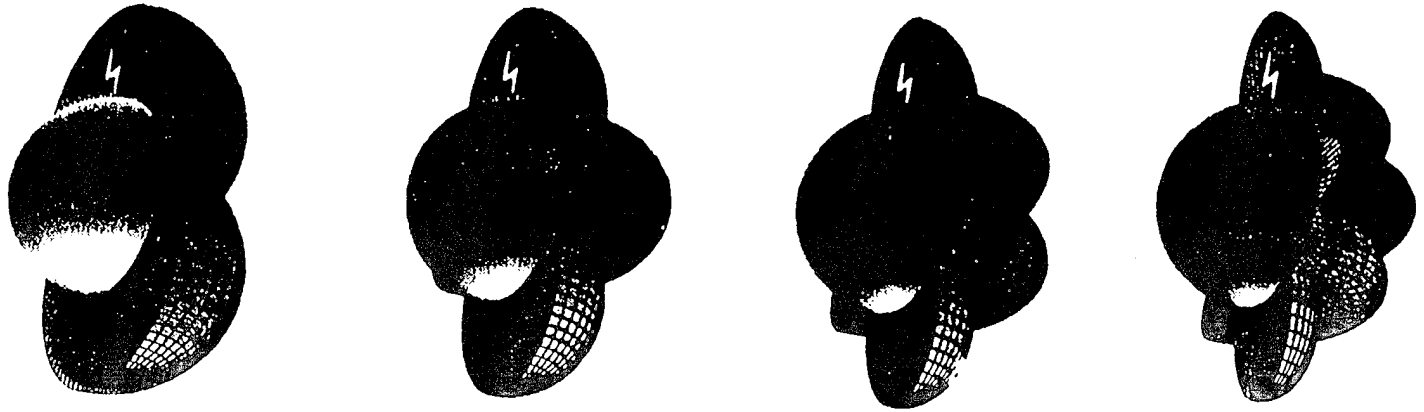
$$H(\omega) = \frac{-I\, ds(\omega)\, P_\nu^1\, (-\cos\theta)}{4ah \sin(\pi\nu)}$$

WAVE IMPEDENCE

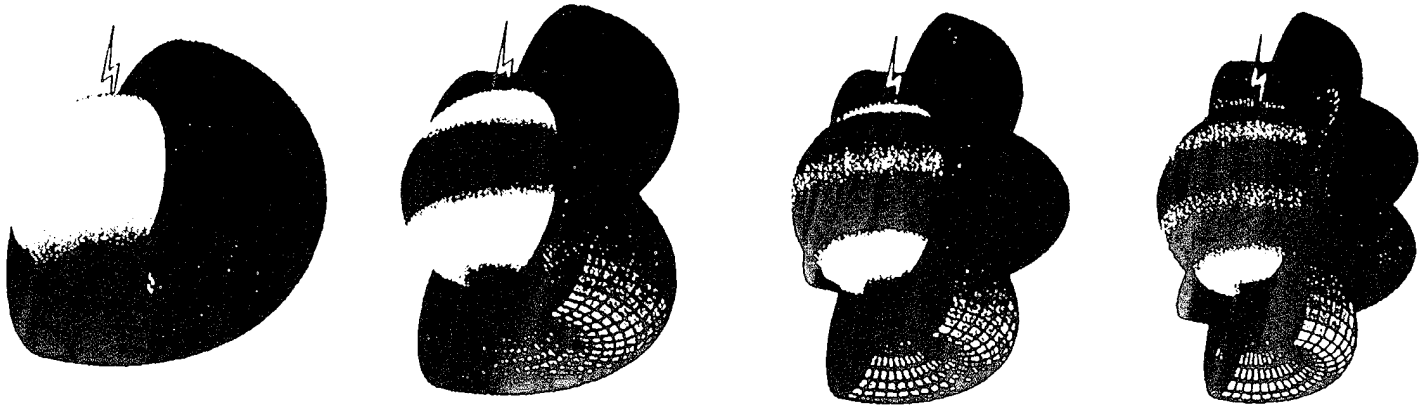
$$Z(\omega) = \frac{E(\omega)}{H(\omega)} = -i \frac{\nu\, (\nu+1)\, P_\nu^0\, (-\cos\theta)}{a\varepsilon_0 \omega\, P_\nu^1\, (-\cos\theta)}$$

Angular Distributions of Schumann Resonance Modes

Electric



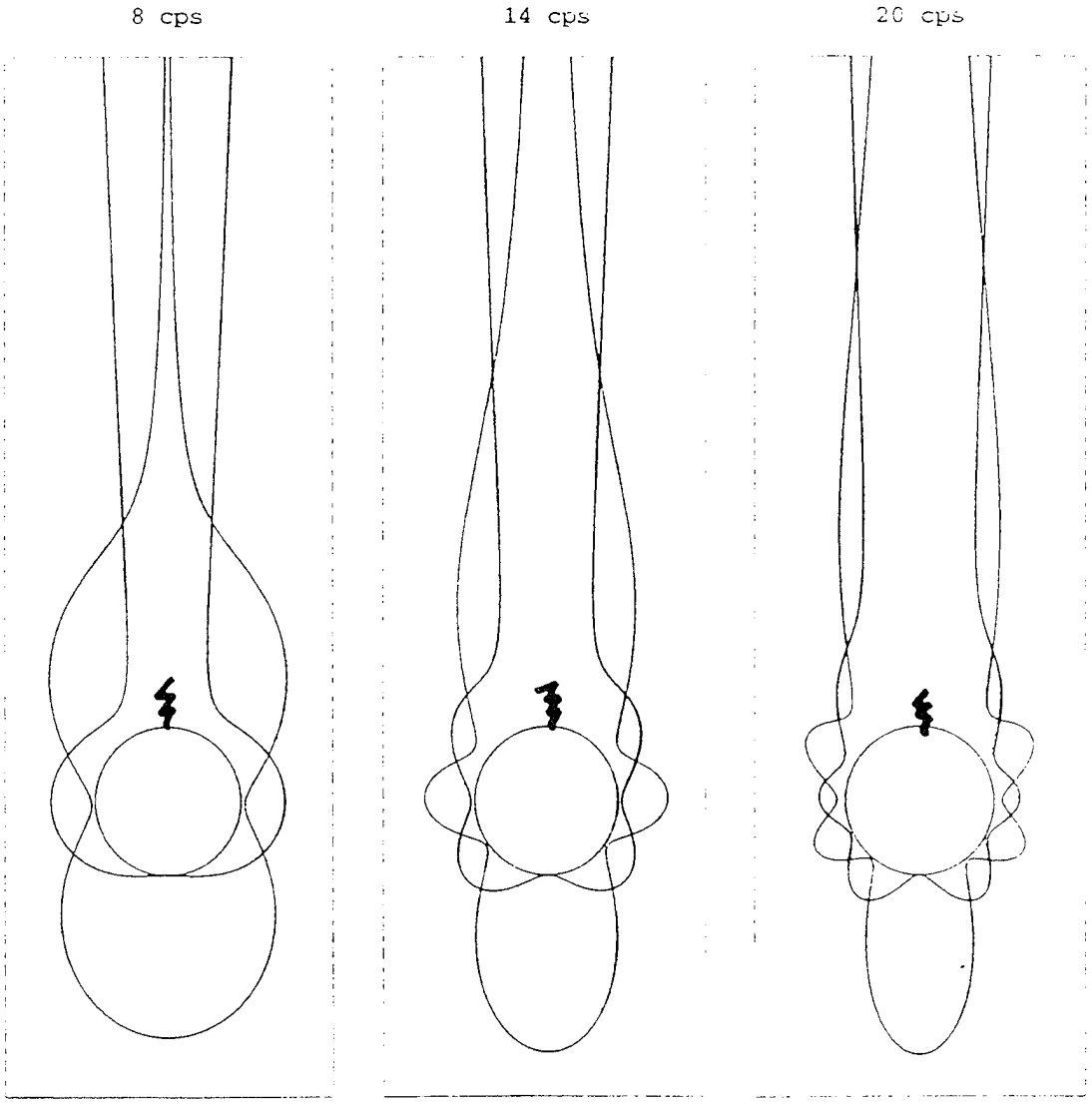
n=1 n=2 n=3 n=4



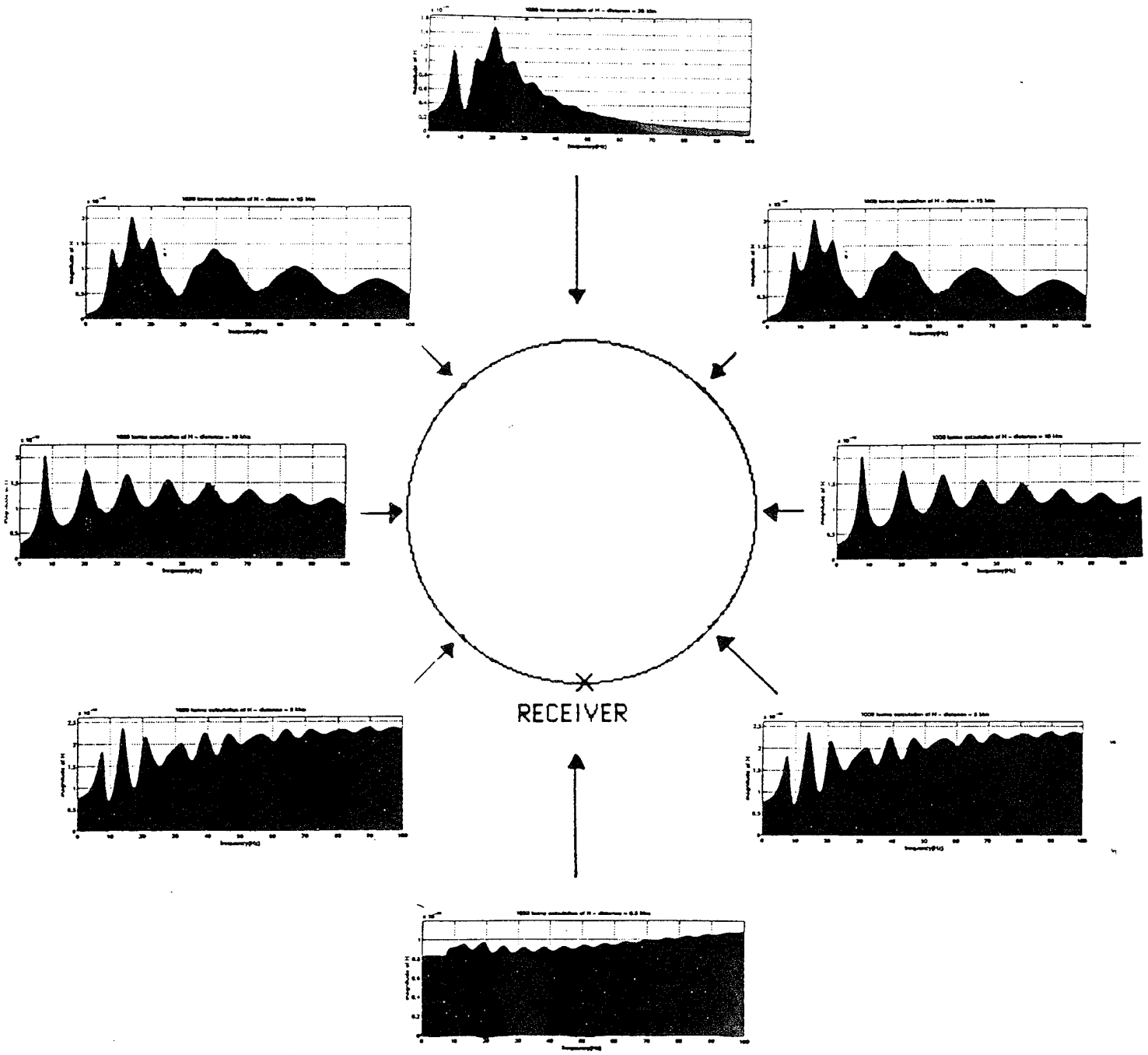
Magnetic

8 Hz 14 Hz 20 Hz 26 Hz

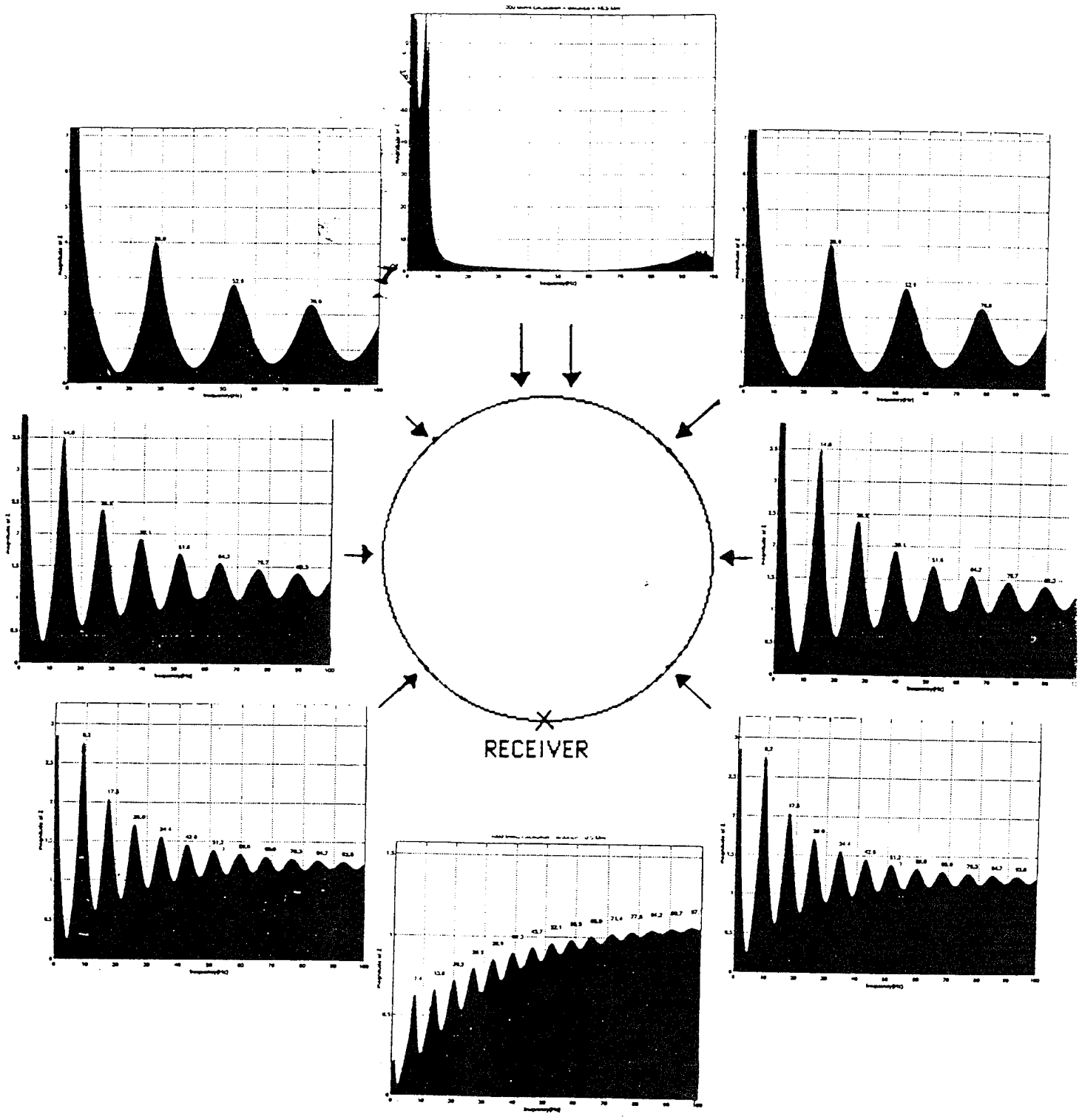
SR MODE STRUCTURE (WITH REALISTIC ATTENUATION) FOR POINT SOURCE



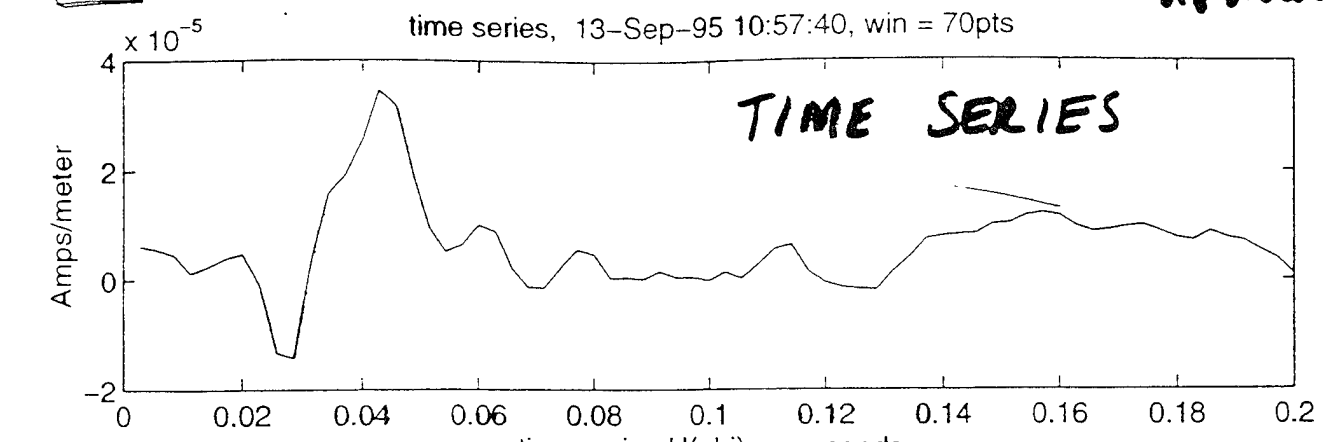
MAGNETIC FIELD SPECTRA

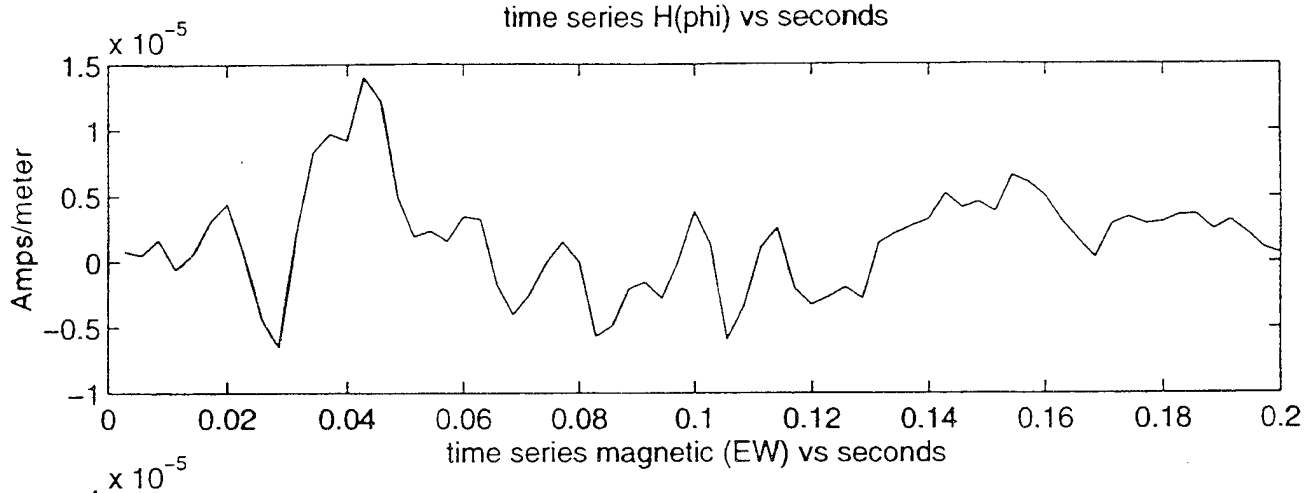


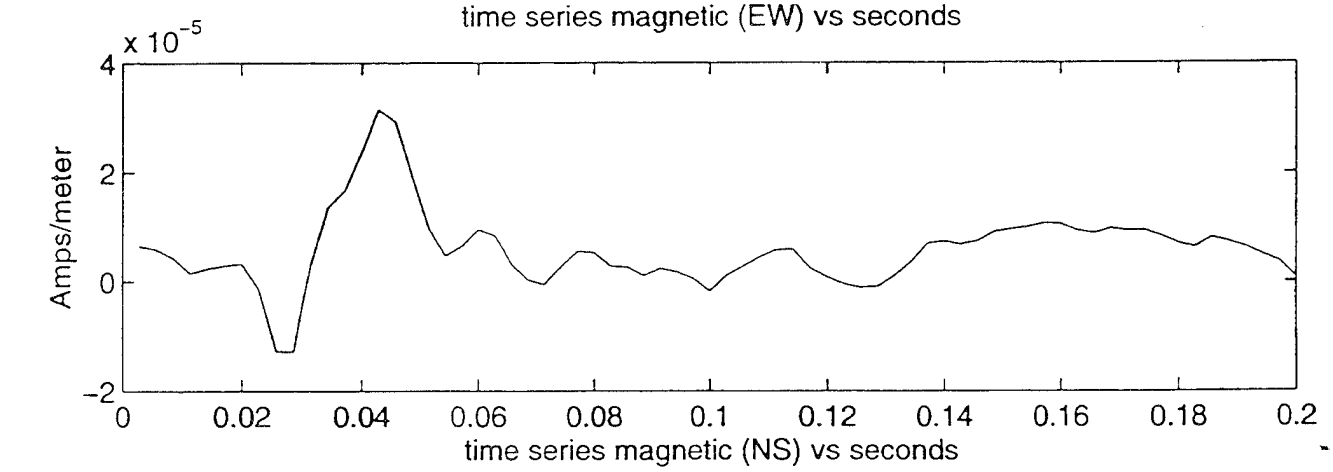
IMPEDANCE SPECTRA

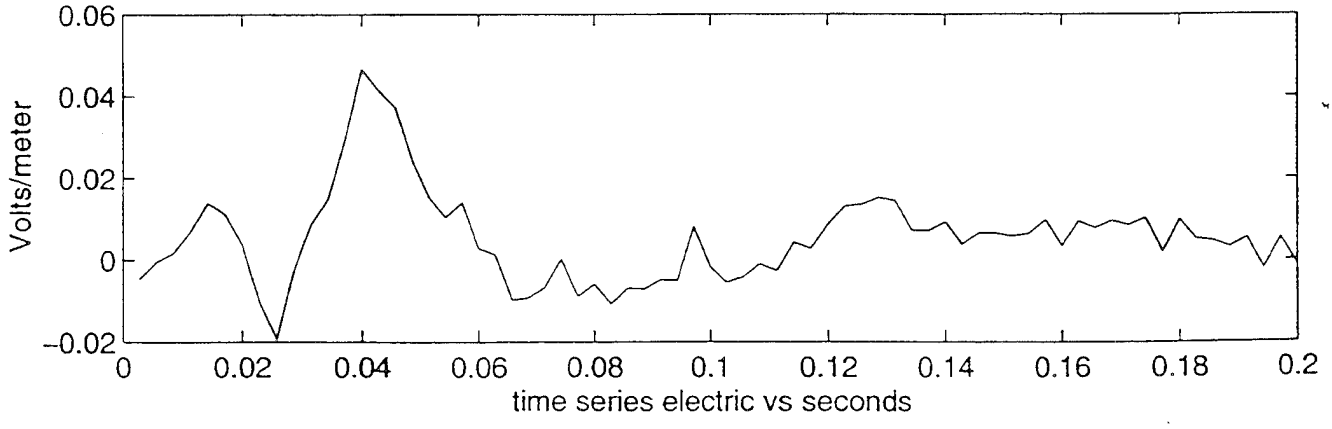


AFRICA

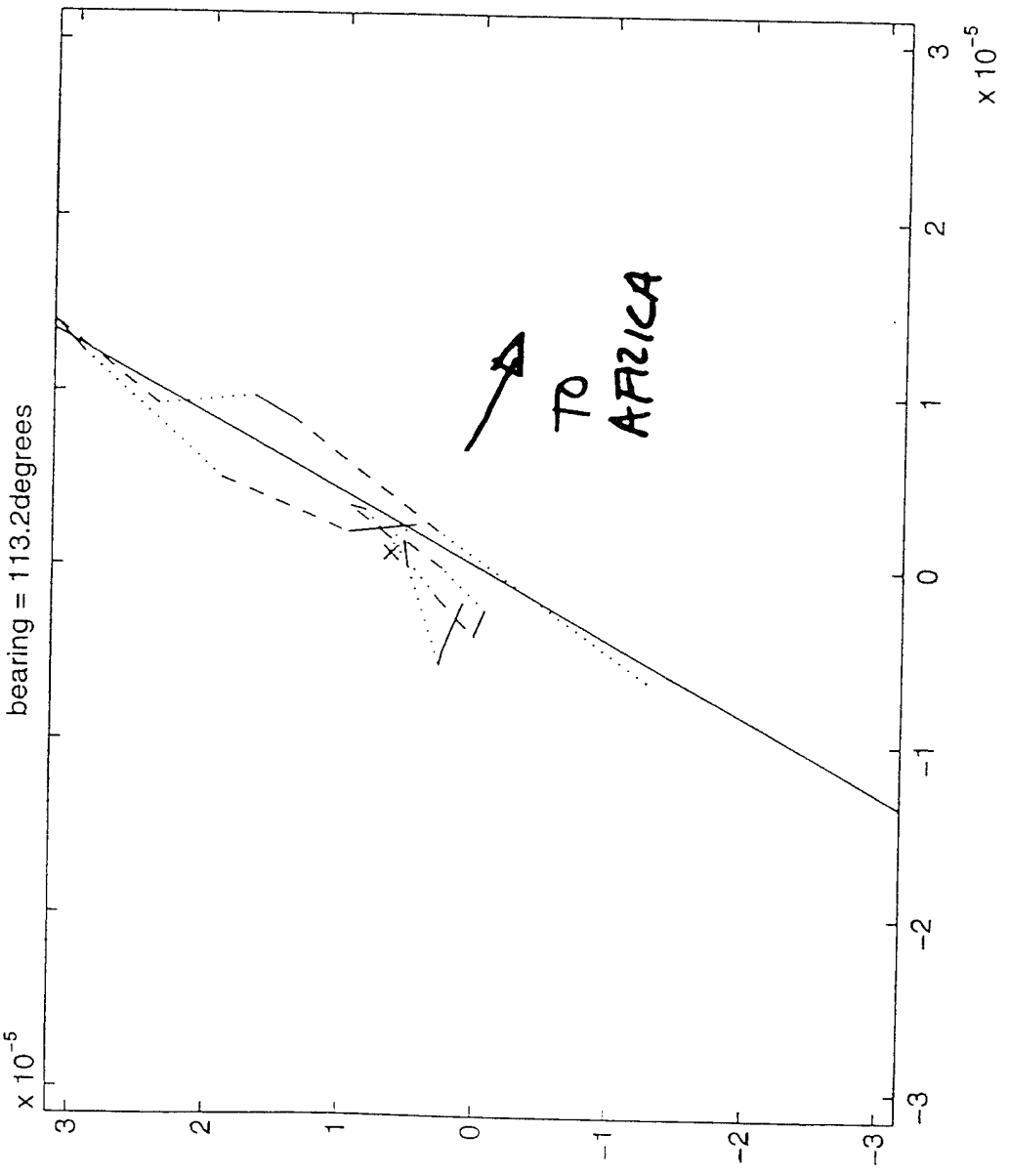

time series, 13-Sep-95 10:57:40, win = 70pts
x 10^-5
Amps/meter
TIME SERIES
time series H(phi) vs seconds

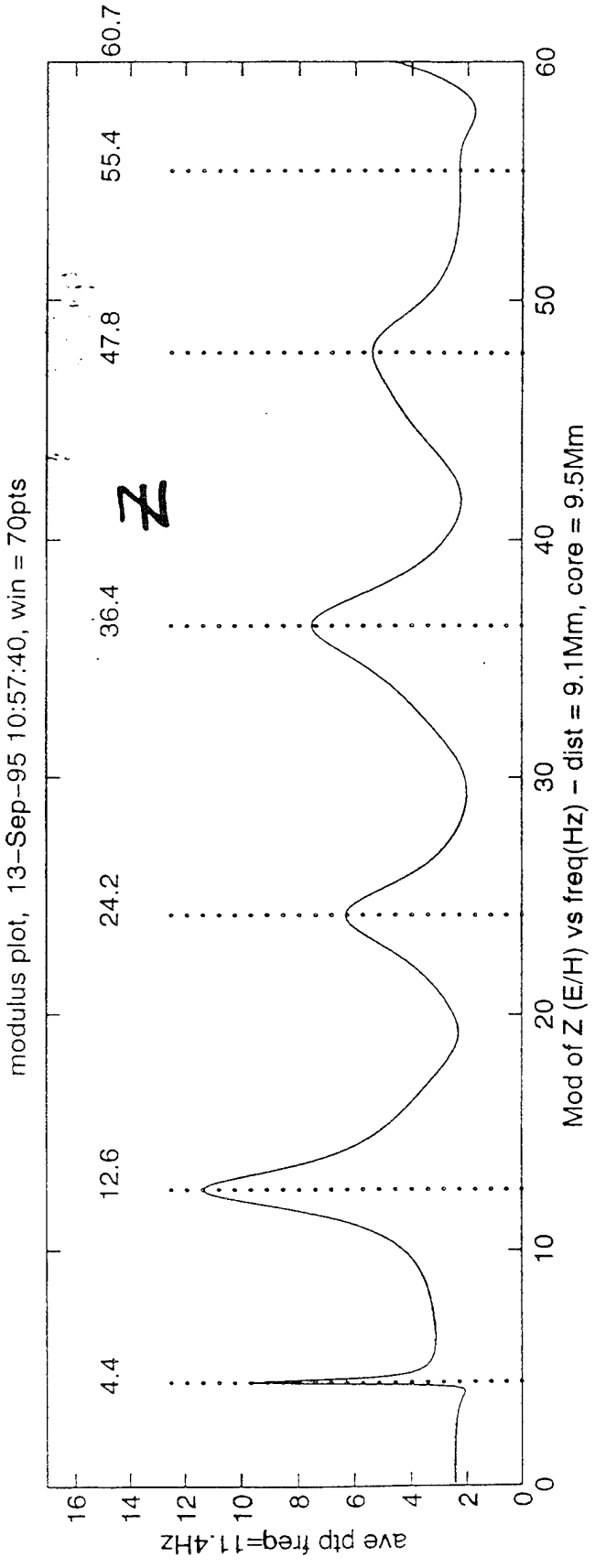

x 10^-5
Amps/meter
time series magnetic (EW) vs seconds

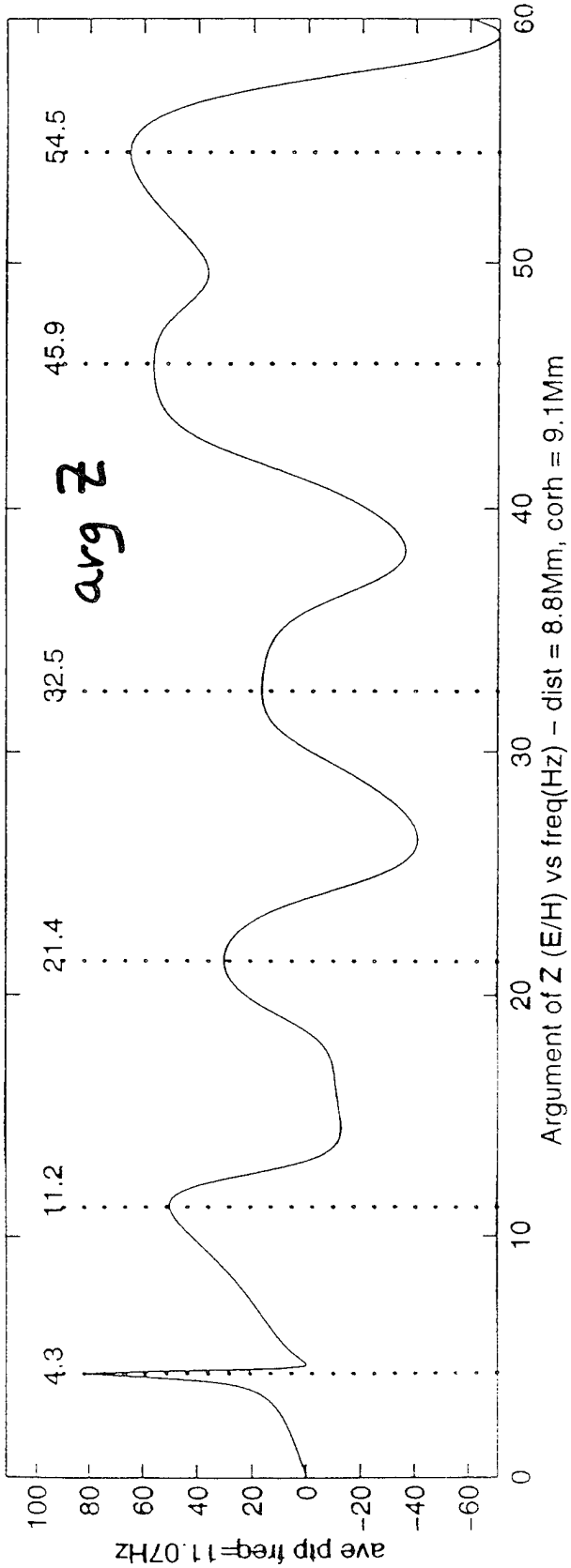

x 10^-5
Amps/meter
time series magnetic (NS) vs seconds

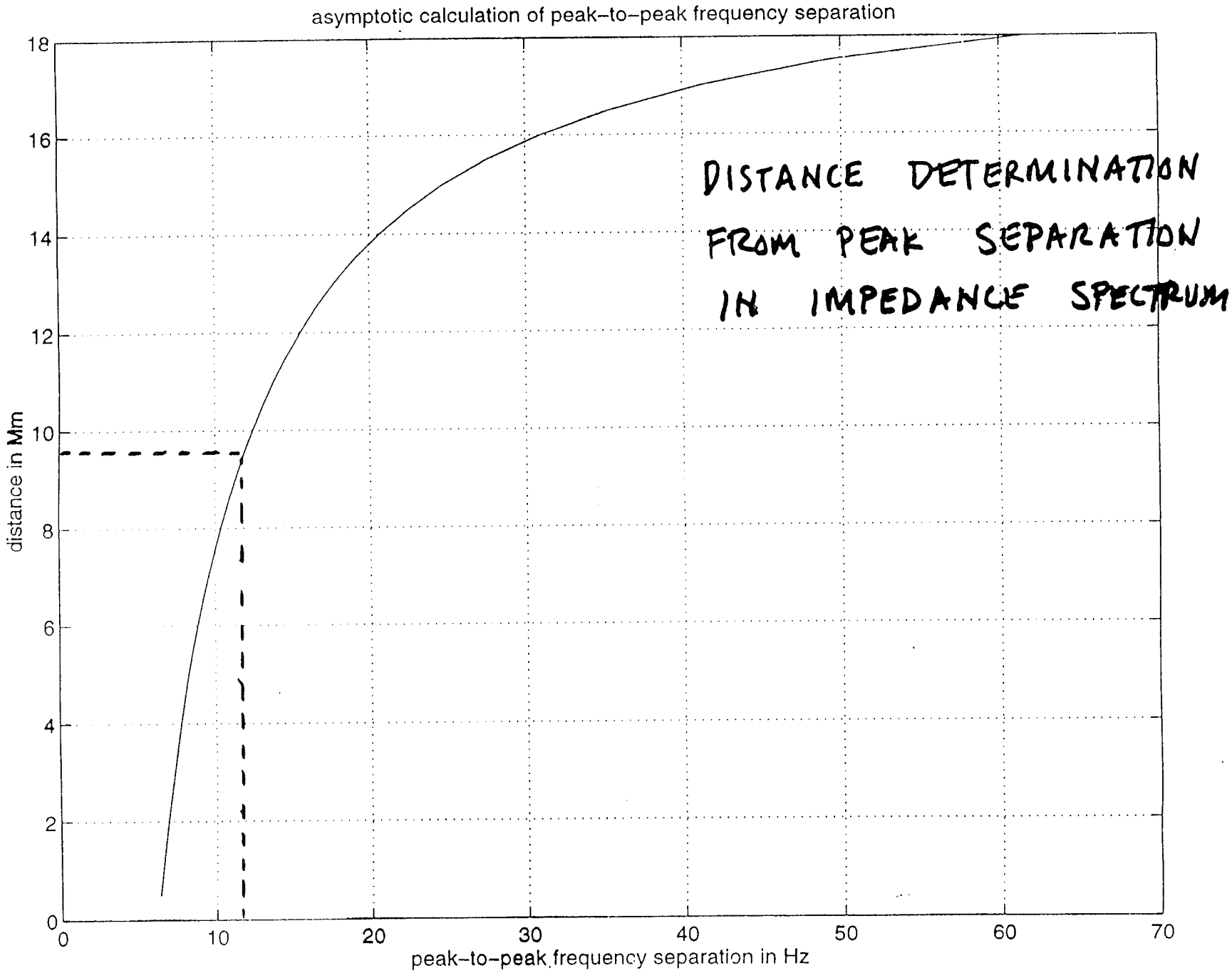

Volts/meter
time series electric vs seconds

AFRICA

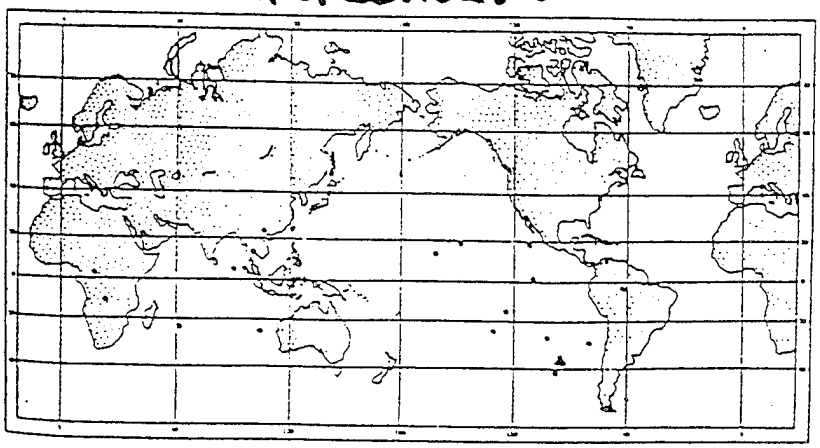



modulus plot, 13-Sep-95 10:57:40, win = 70pts
Z
4.4
12.6
24.2
36.4
47.8
55.4
60.7
ave pip freq=11.4Hz
Mod of Z (E/H) vs freq(Hz) - dist = 9.1Mm, core = 9.5Mm

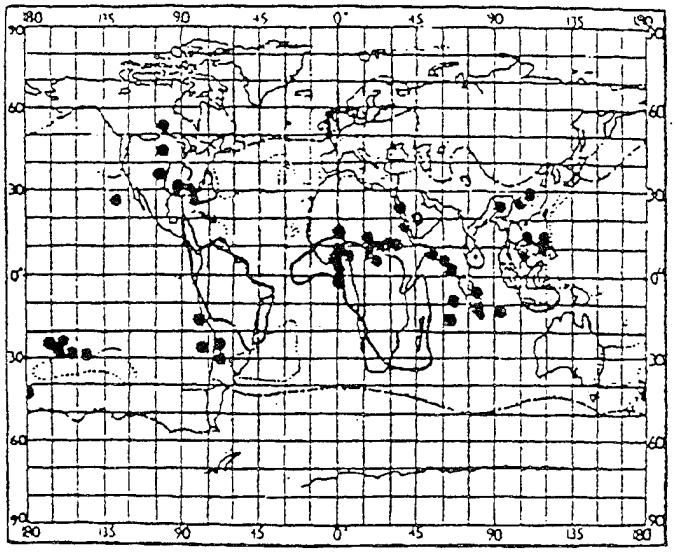

arg Z
4.3
11.2
21.4
32.5
45.9
54.5
ave pip freq=11.07Hz
Argument of Z (E/H) vs freq(Hz) - dist = 8.8Mm, corh = 9.1Mm


asymptotic calculation of peak–to–peak frequency separation
distance in Mm
peak–to–peak frequency separation in Hz
0
2
4
6
8
10
12
14
16
18
0
10
20
30
40
50
60
70
DISTANCE DETERMINATION
FROM PEAK SEPARATION
IN IMPEDANCE SPECTRUM

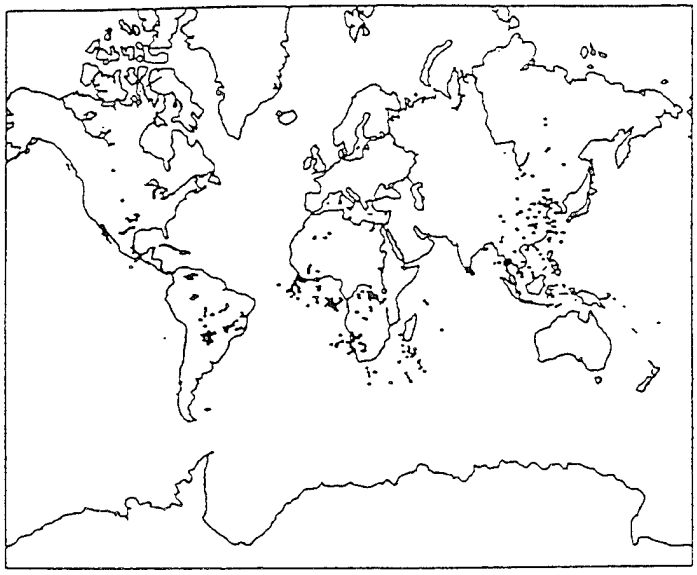
NICKOLAENKO



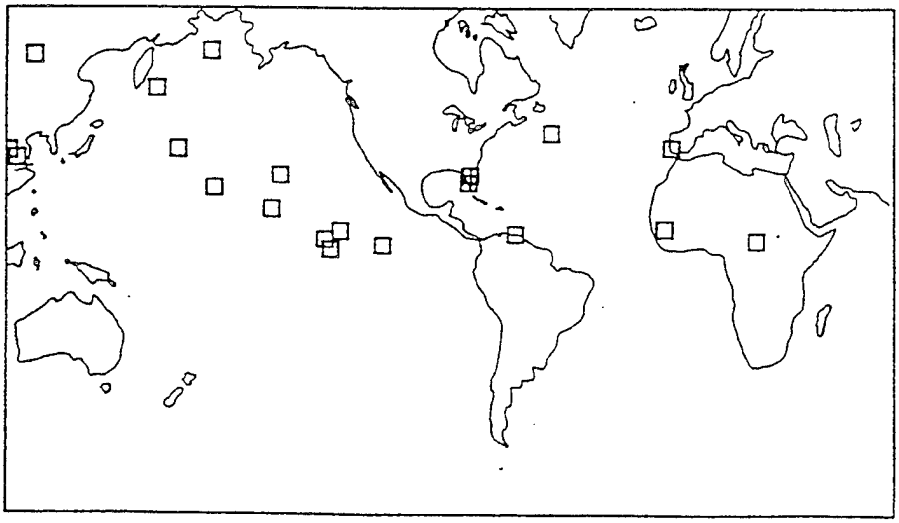
KEMP



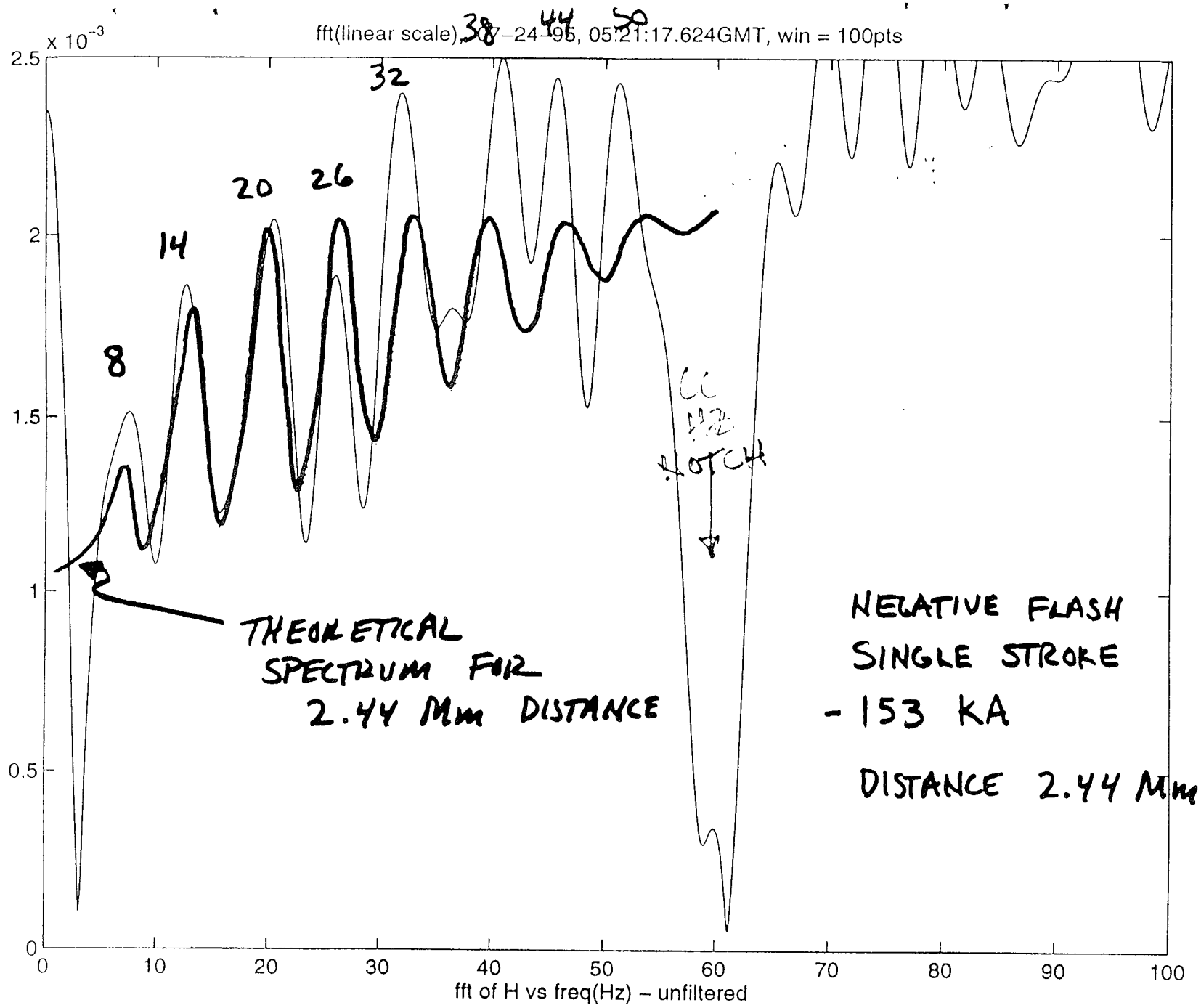
BURKE AND JONES

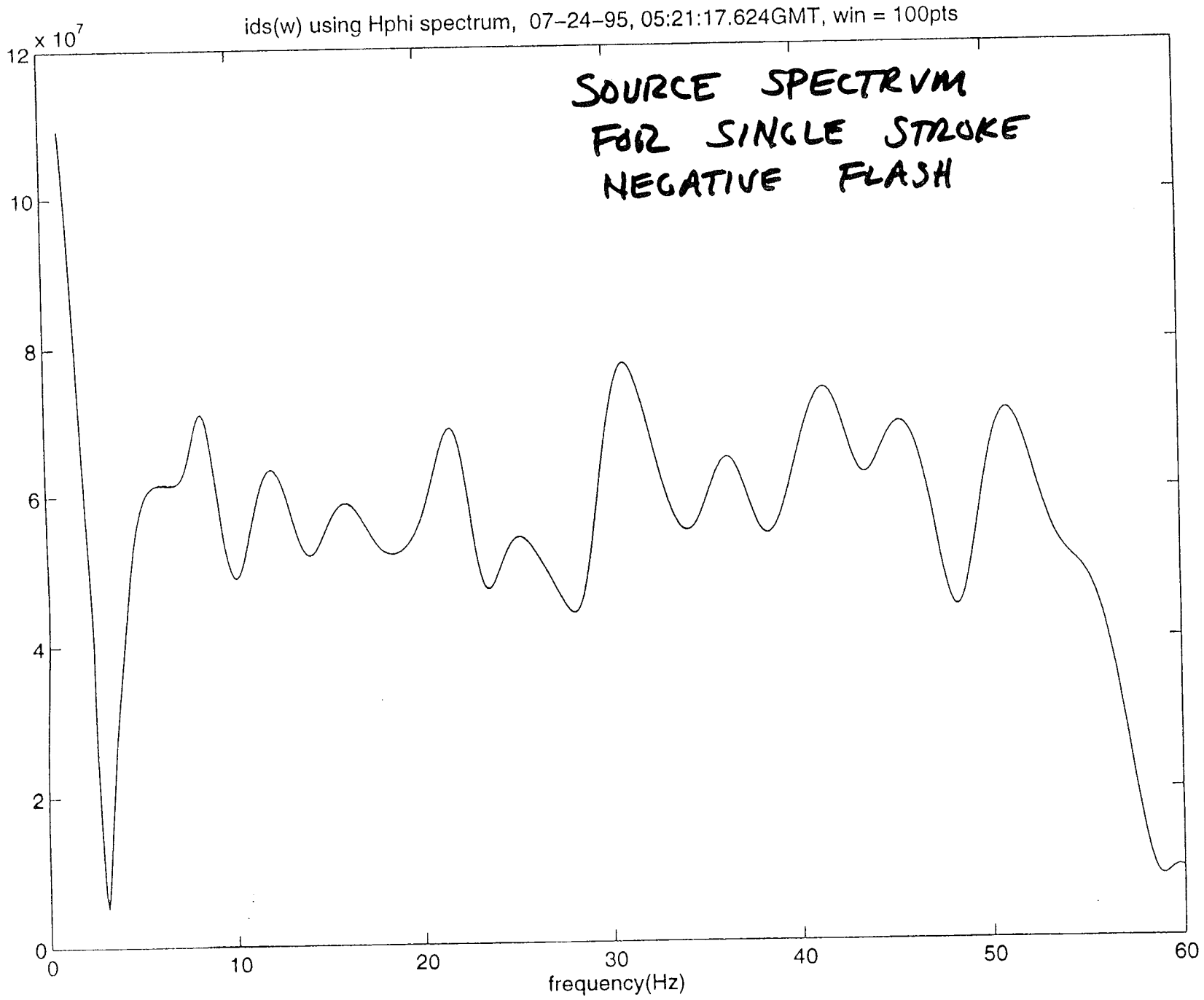


SCHMIDT

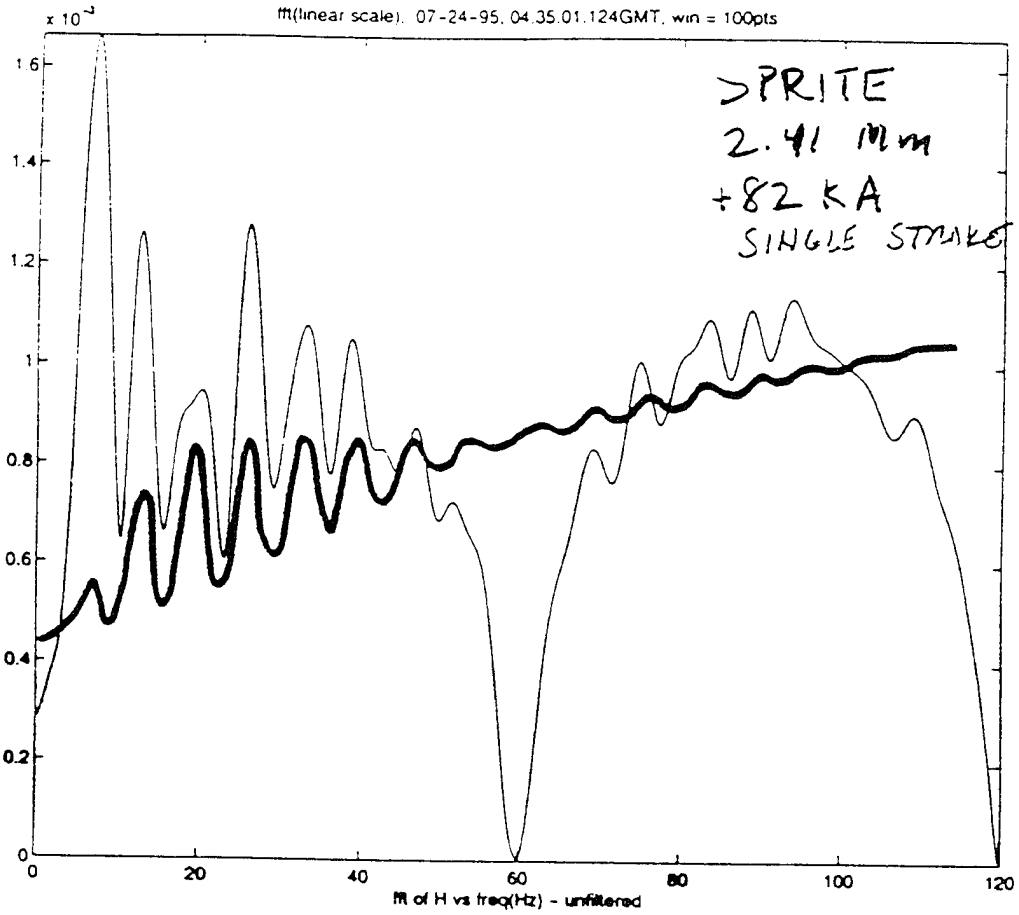


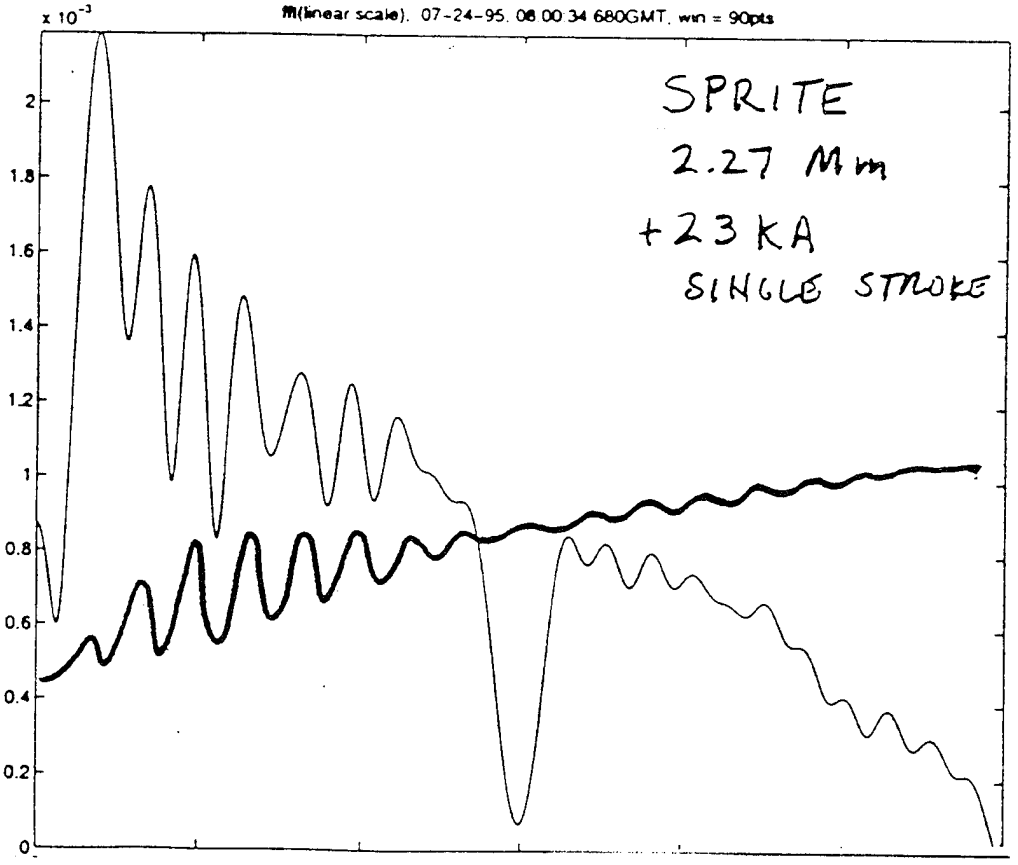
Q-BURST MAPS


fft(linear scale), 7-24-95, 05:21:17.624GMT, win = 100pts
x 10^-3
2.5
2
1.5
1
0.5
0
0
10
20
30
40
50
60
70
80
90
100
fft of H vs freq(Hz) – unfiltered
8
14
20
26
32
38
44
50
CC
NOTCH
THEORETICAL
SPECTRUM FOR
2.44 Mm DISTANCE
NEGATIVE FLASH
SINGLE STROKE
-153 KA
DISTANCE 2.44 Mm

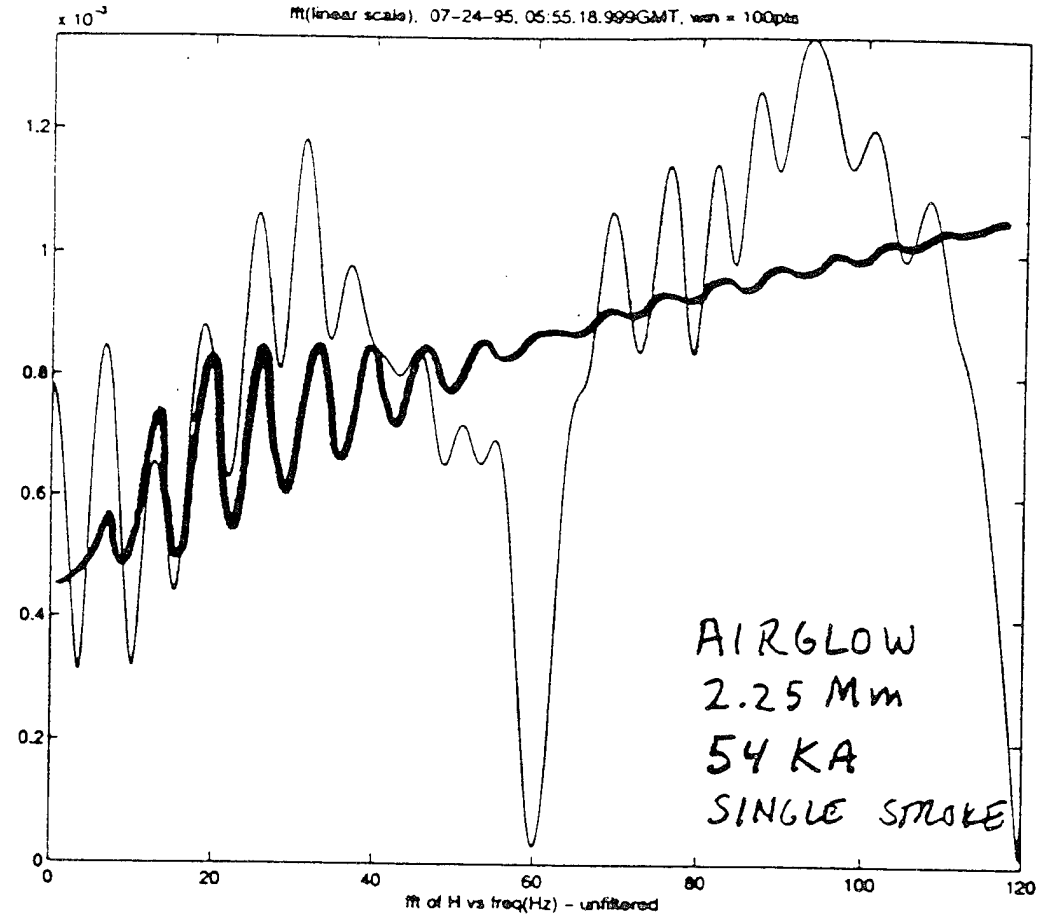

ids(w) using Hphi spectrum, 07-24-95, 05:21:17.624GMT, win = 100pts
x 10^7
12
10
8
6
4
2
0
0
10
20
30
40
50
60
frequency(Hz)
SOURCE SPECTRUM
FOR SINGLE STROKE
NEGATIVE FLASH

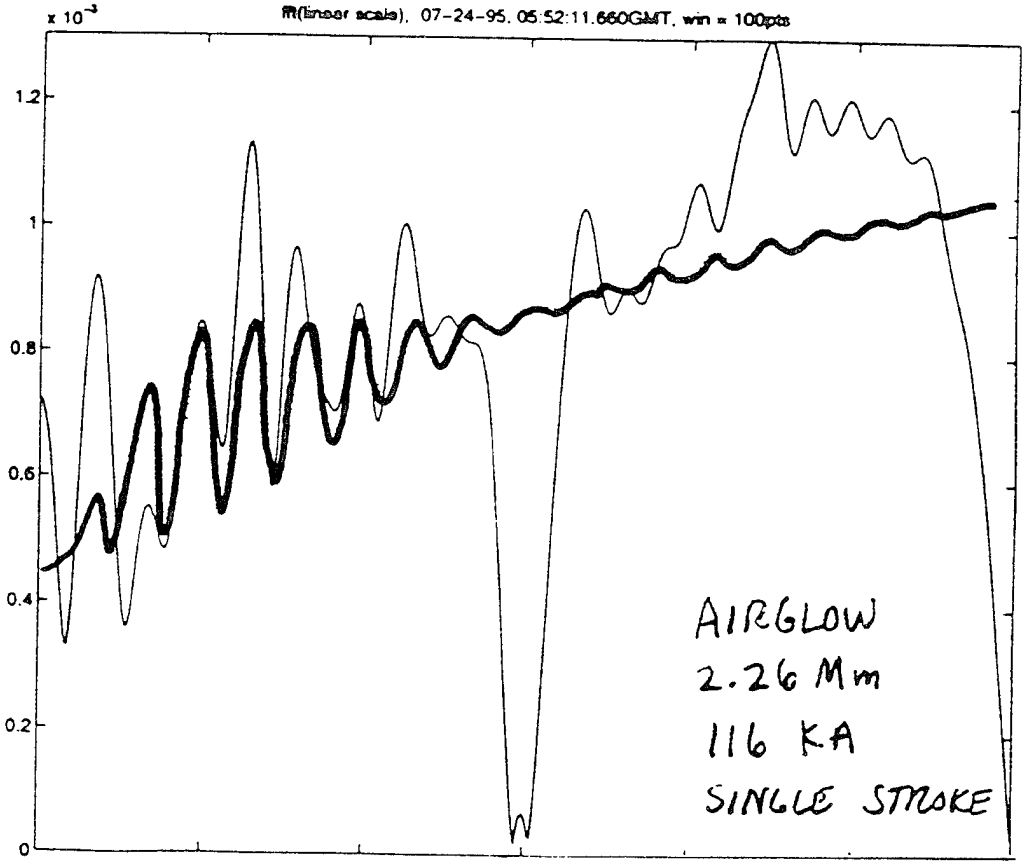
SPRITES


fft(linear scale), 07-24-95, 04:35:01.124GMT, win = 100pts
x 10^-3
>PRITE
2.41 Mm
+82 kA
SINGLE STROKE
fft of H vs freq(Hz) - unfiltered

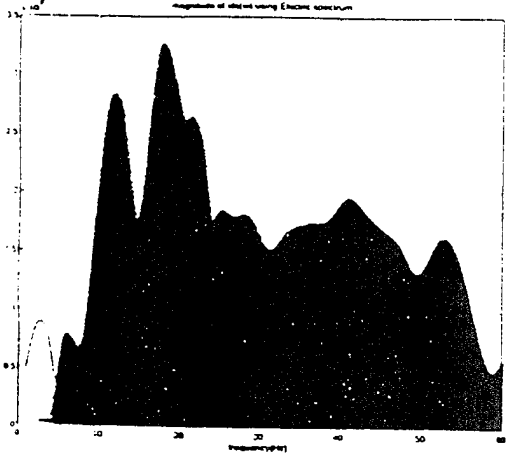

fft(linear scale), 07-24-95, 08:00:34.680GMT, win = 90pts
x 10^-3
SPRITE
2.27 Mm
+23 kA
SINGLE STROKE

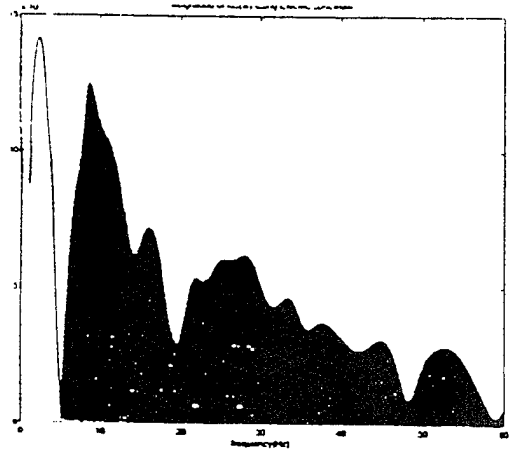
ELVES!

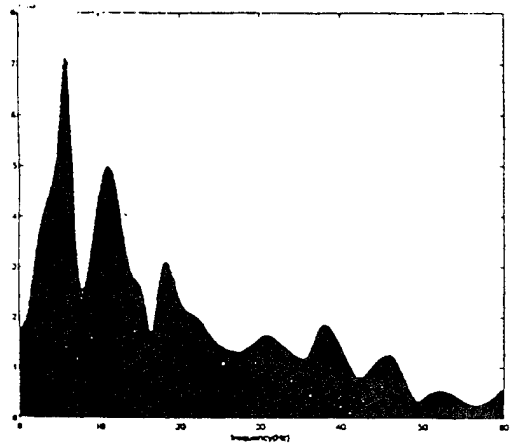

x 10^-3
fft(linear scale), 07-24-95, 05:55:18.999GMT, win = 100pts
1.2
1
0.8
0.6
0.4
0.2
0
0
20
40
60
80
100
120
fft of H vs freq(Hz) - unfiltered
AIRGLOW
2.25 Mm
54 KA
SINGLE STROKE

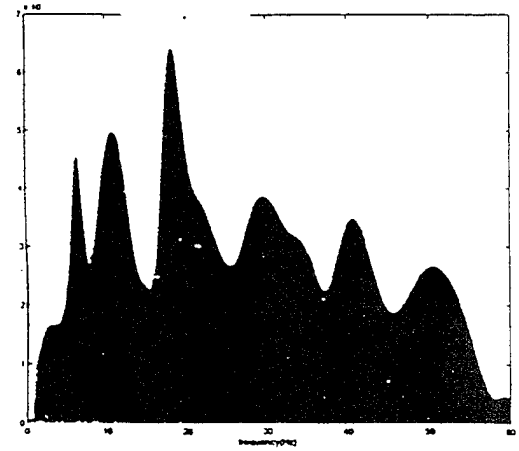

x 10^-3
fft(linear scale), 07-24-95, 05:52:11.660GMT, win = 100pts
1.2
1
0.8
0.6
0.4
0.2
0
AIRGLOW
2.26 Mm
116 KA
SINGLE STROKE

POSITIVE CG's

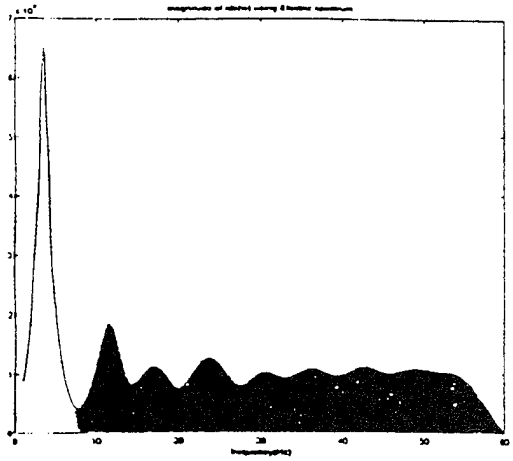


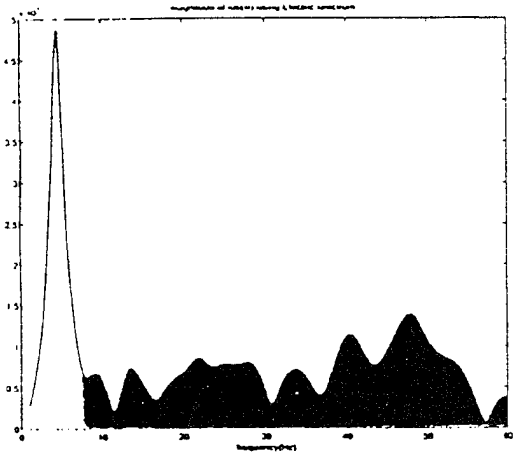


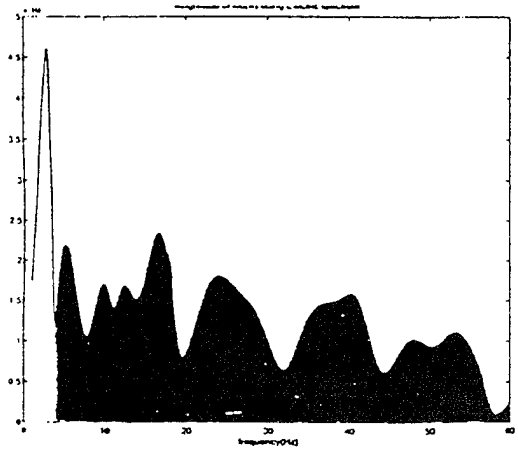


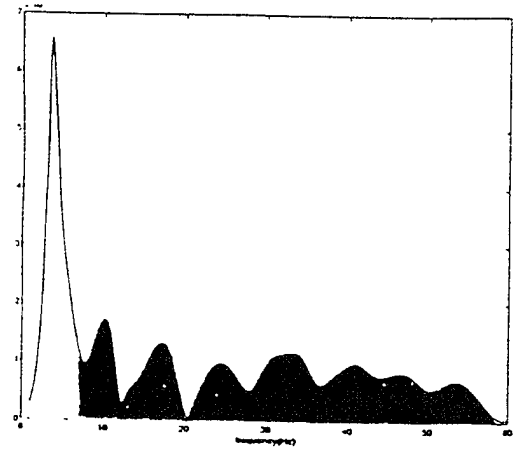


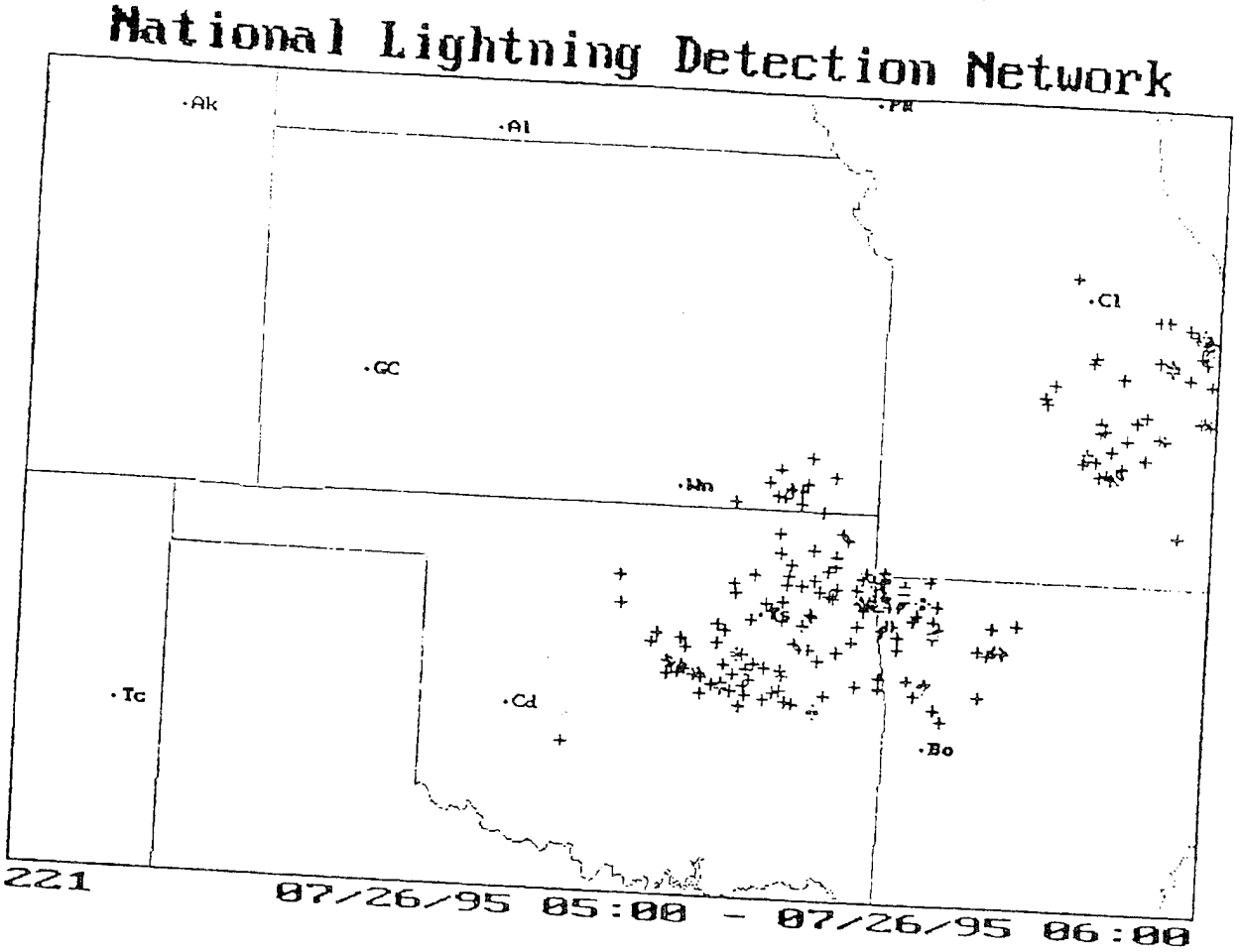
NEGATIVE CG's











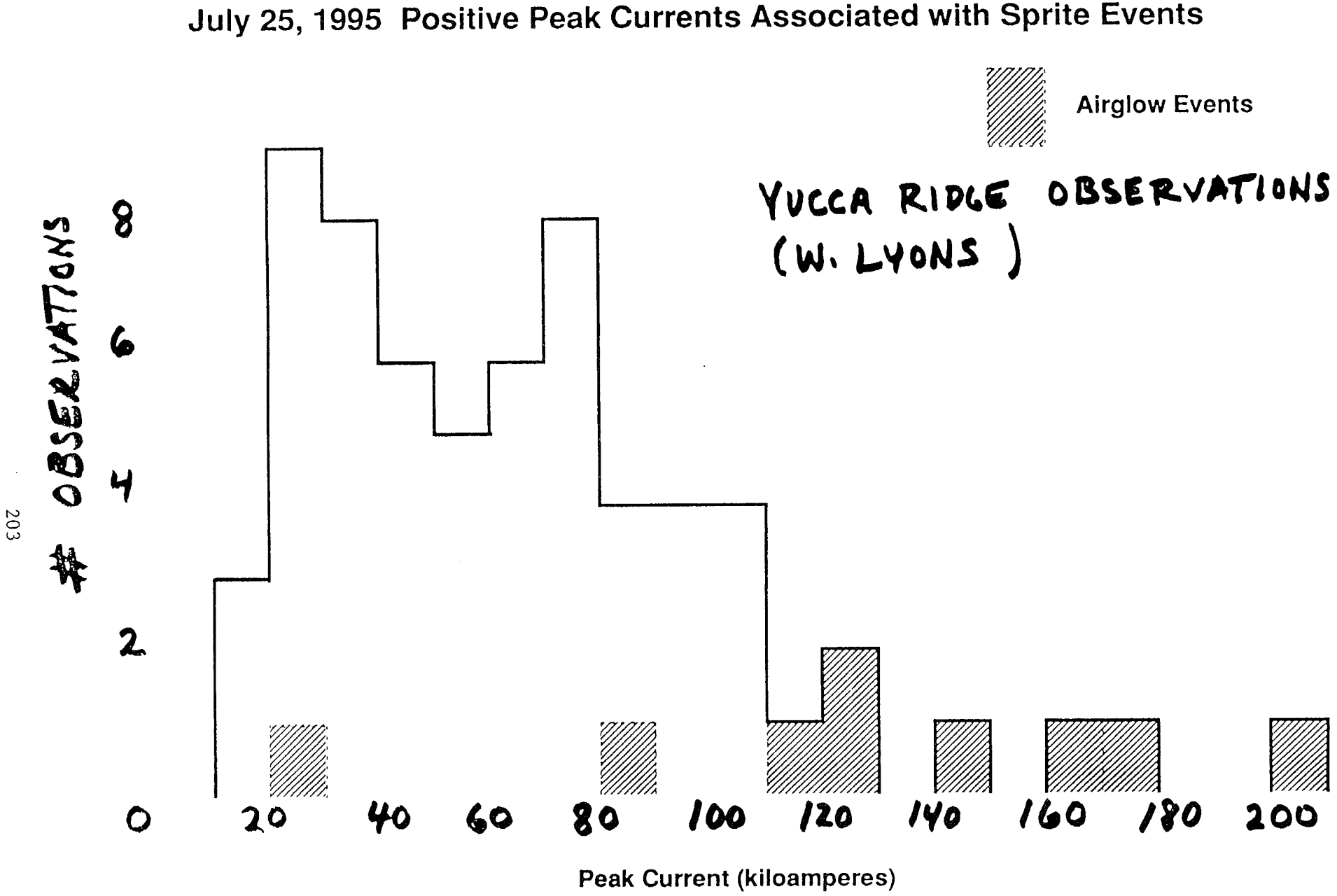
"last hour" -

Positives only -

POSITIVE GROUND FLASHES

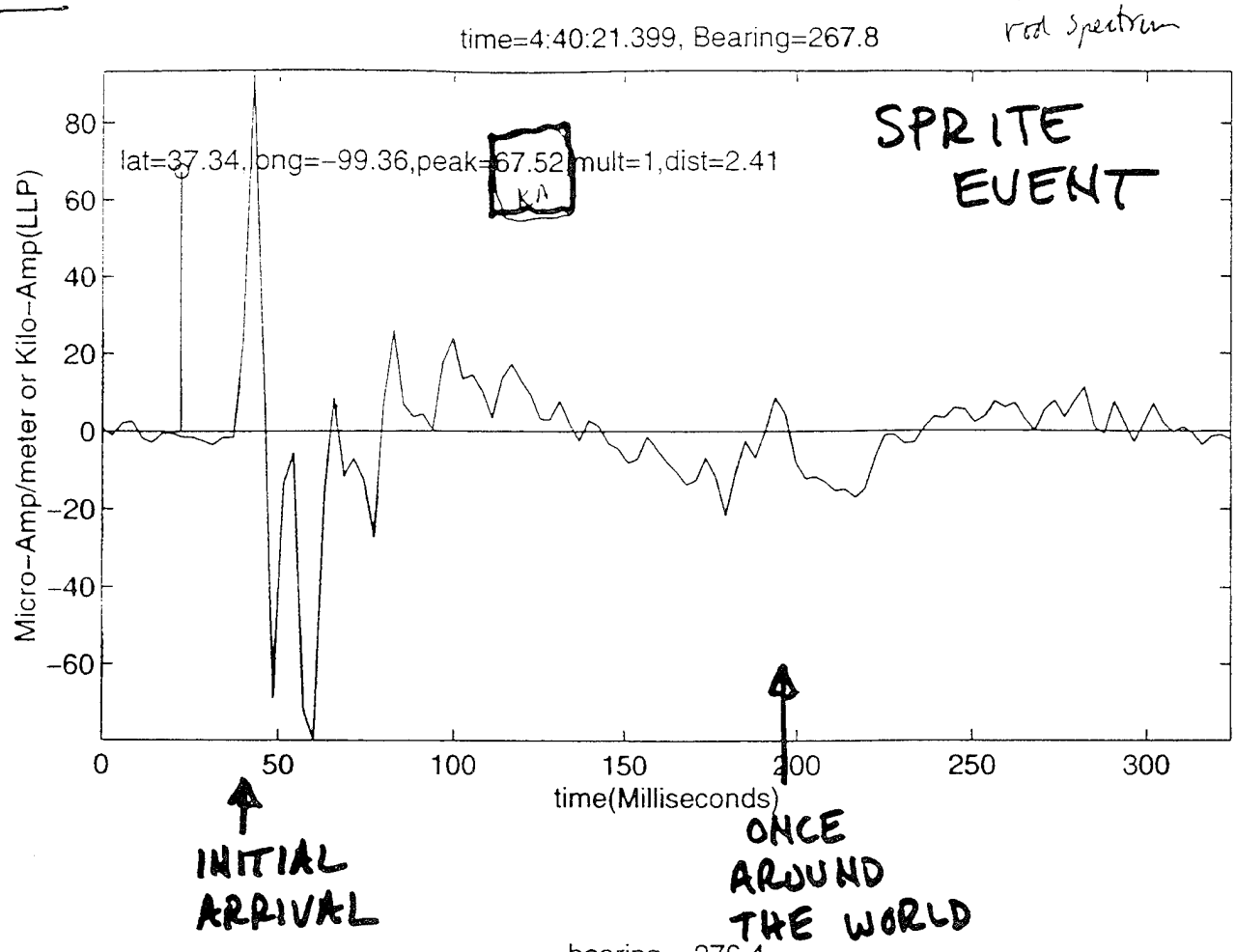
SPRITES FROM YUCCA RIDGE

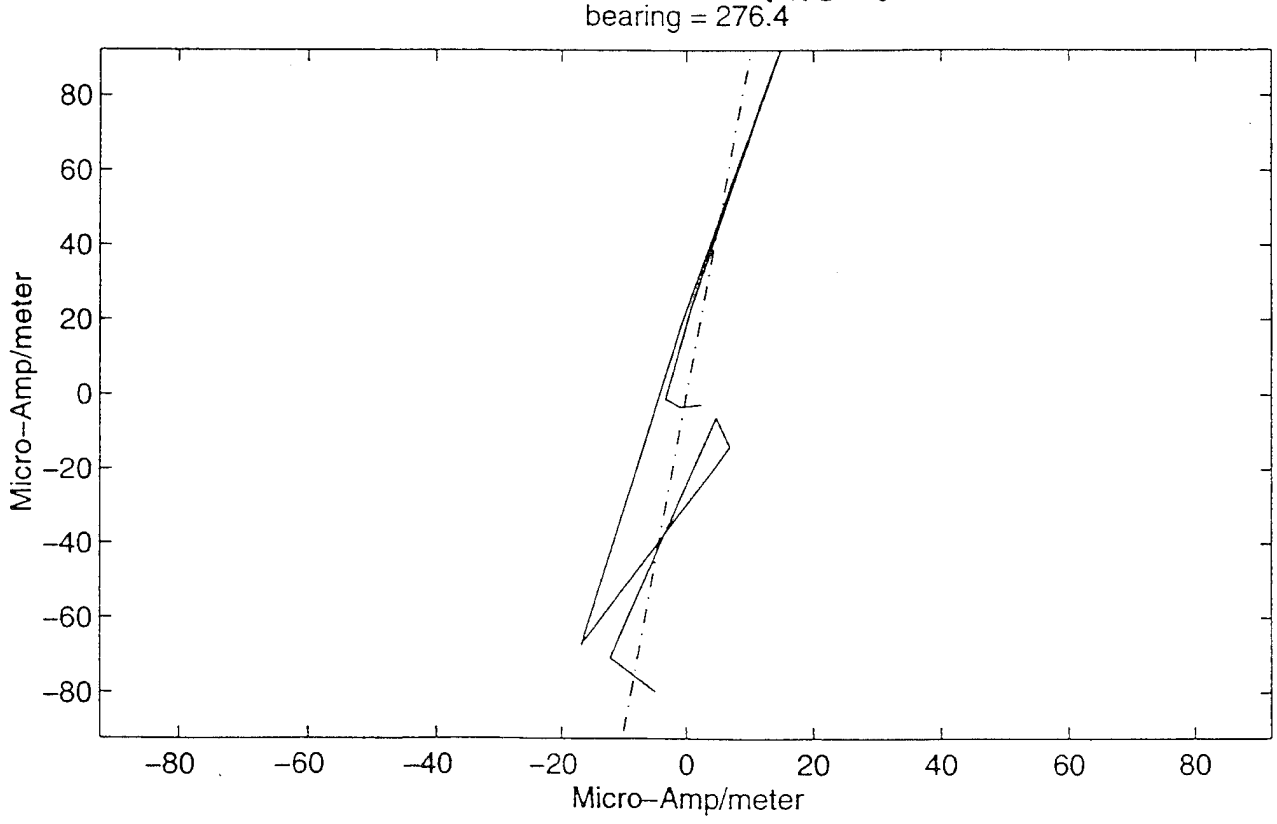
Q-BURSTS IN RHODE ISLAND

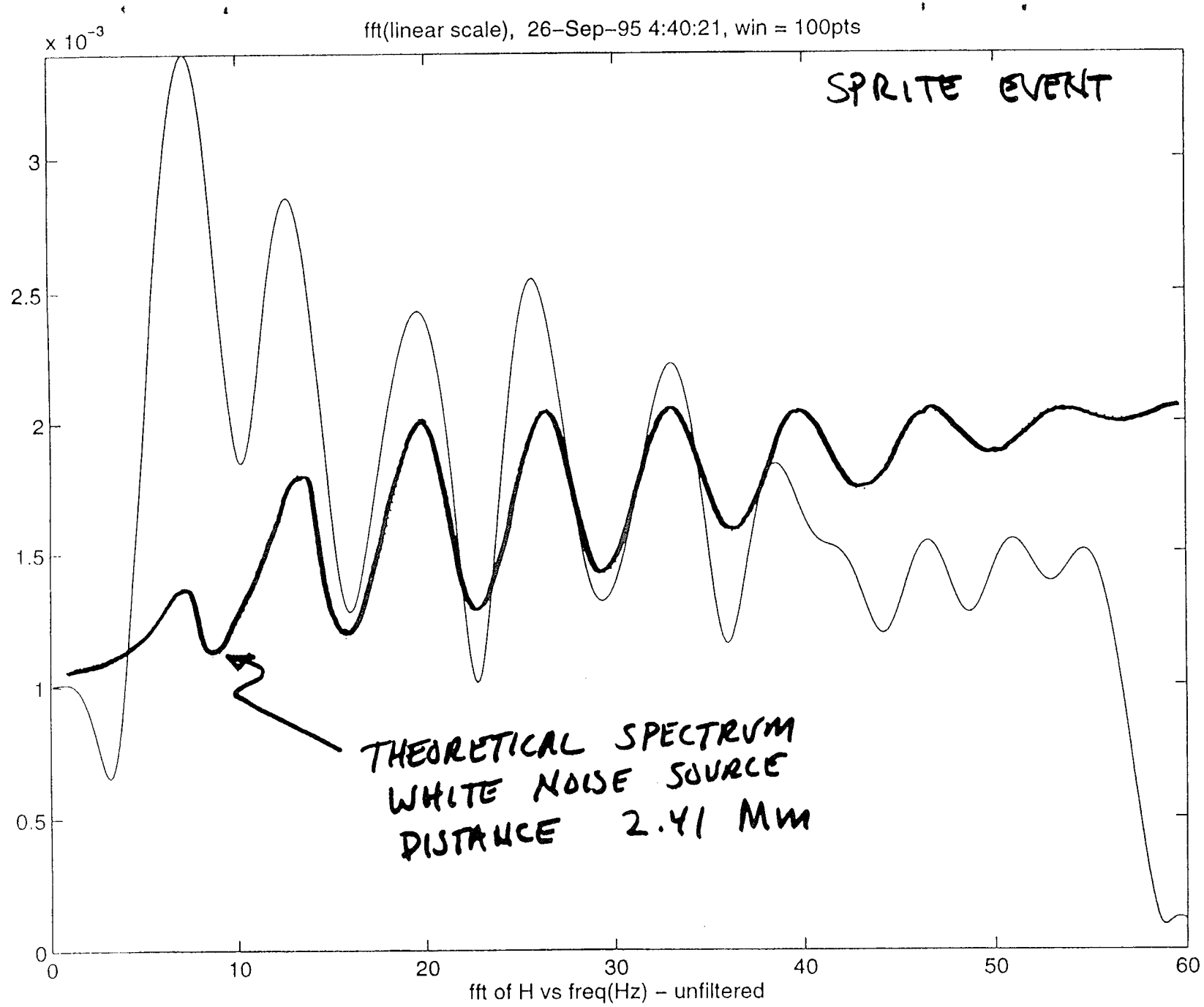

July 25, 1995 Positive Peak Currents Associated with Sprite Events
Airglow Events
YUCCA RIDGE OBSERVATIONS
(W. LYONS)
OBSERVATIONS
0
2
4
6
8
0
20
40
60
80
100
120
140
160
180
200
Peak Current (kiloamperes)

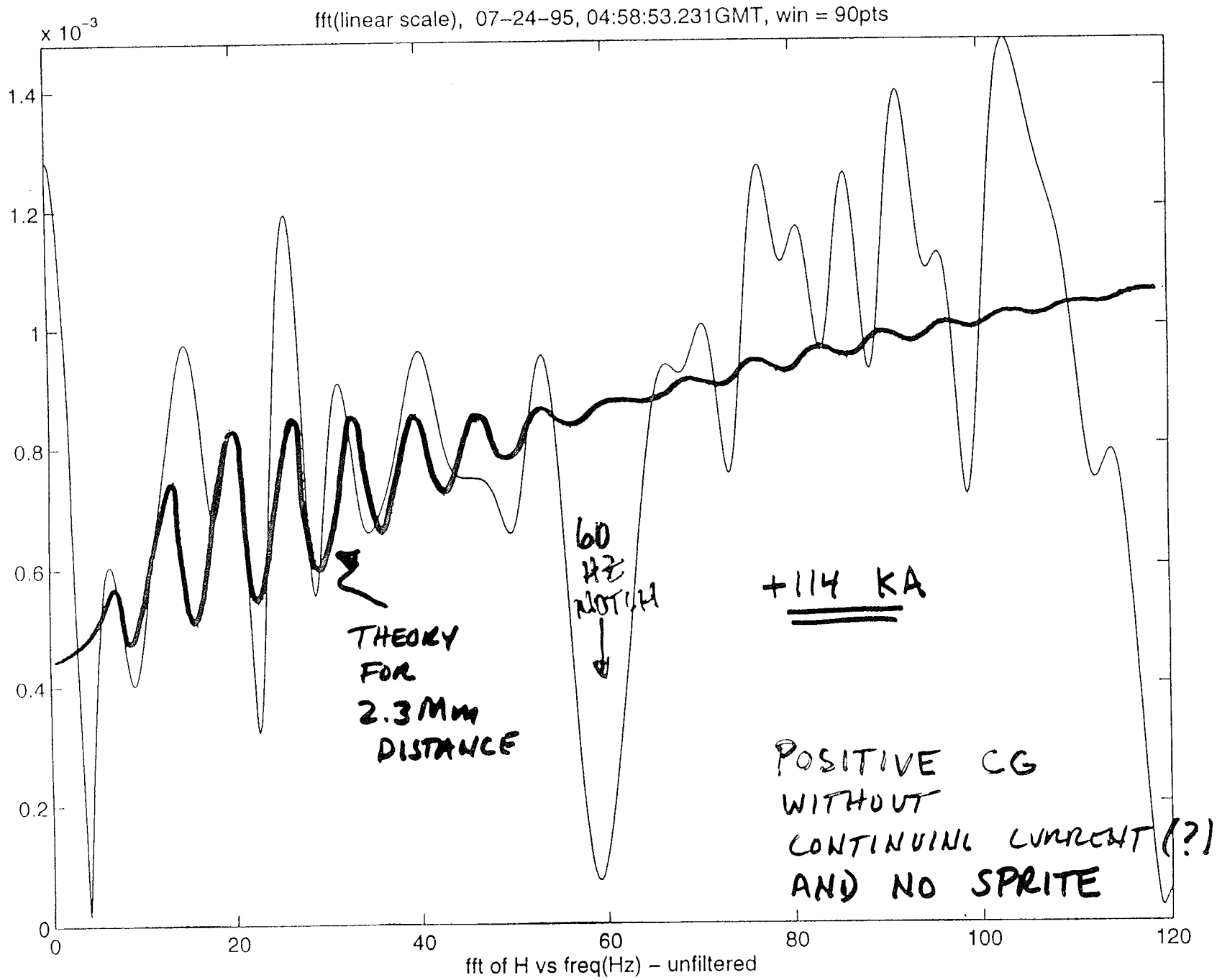
LLP = 291/s = 01:24

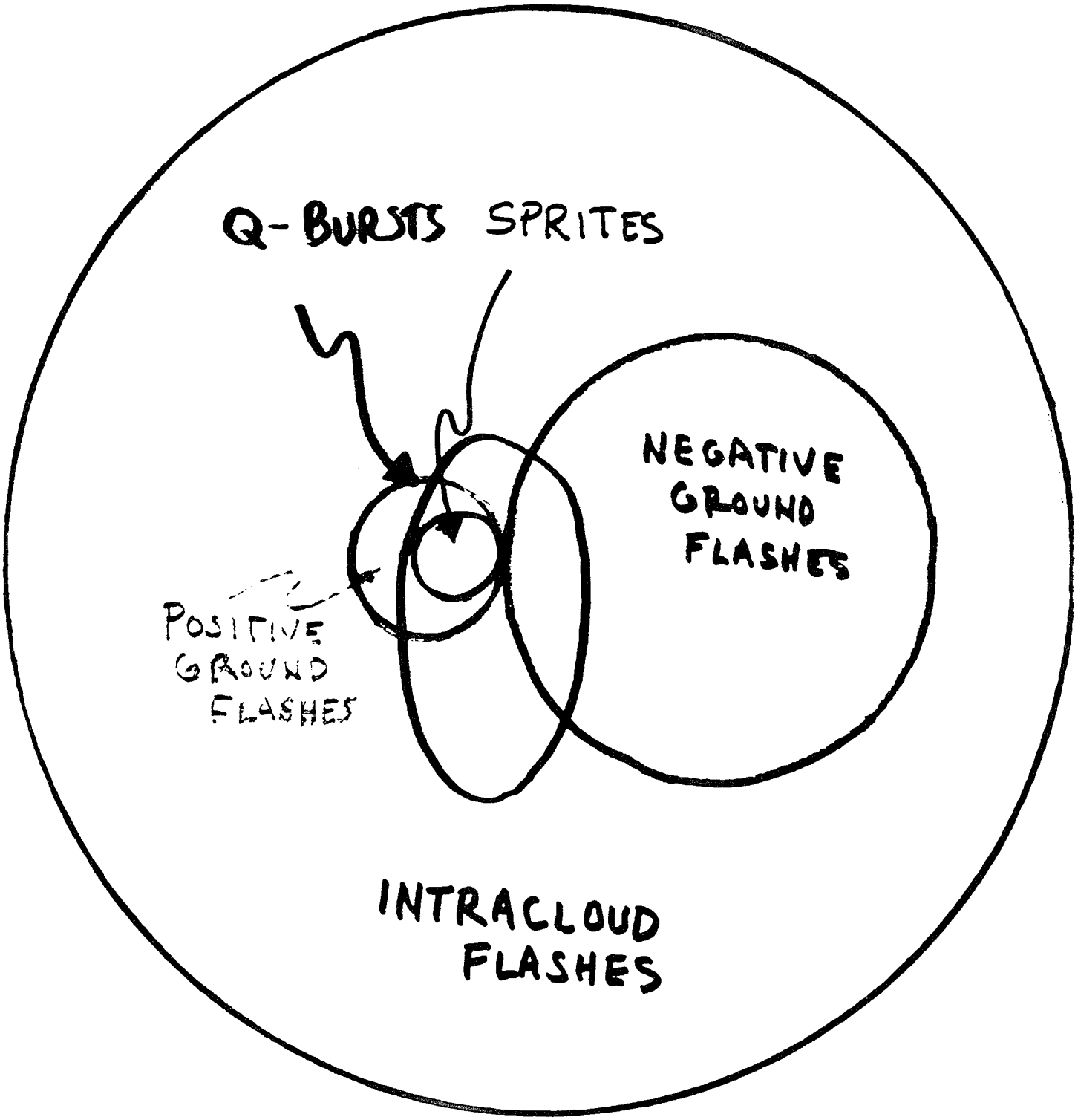
Sprite event
rod spectrum



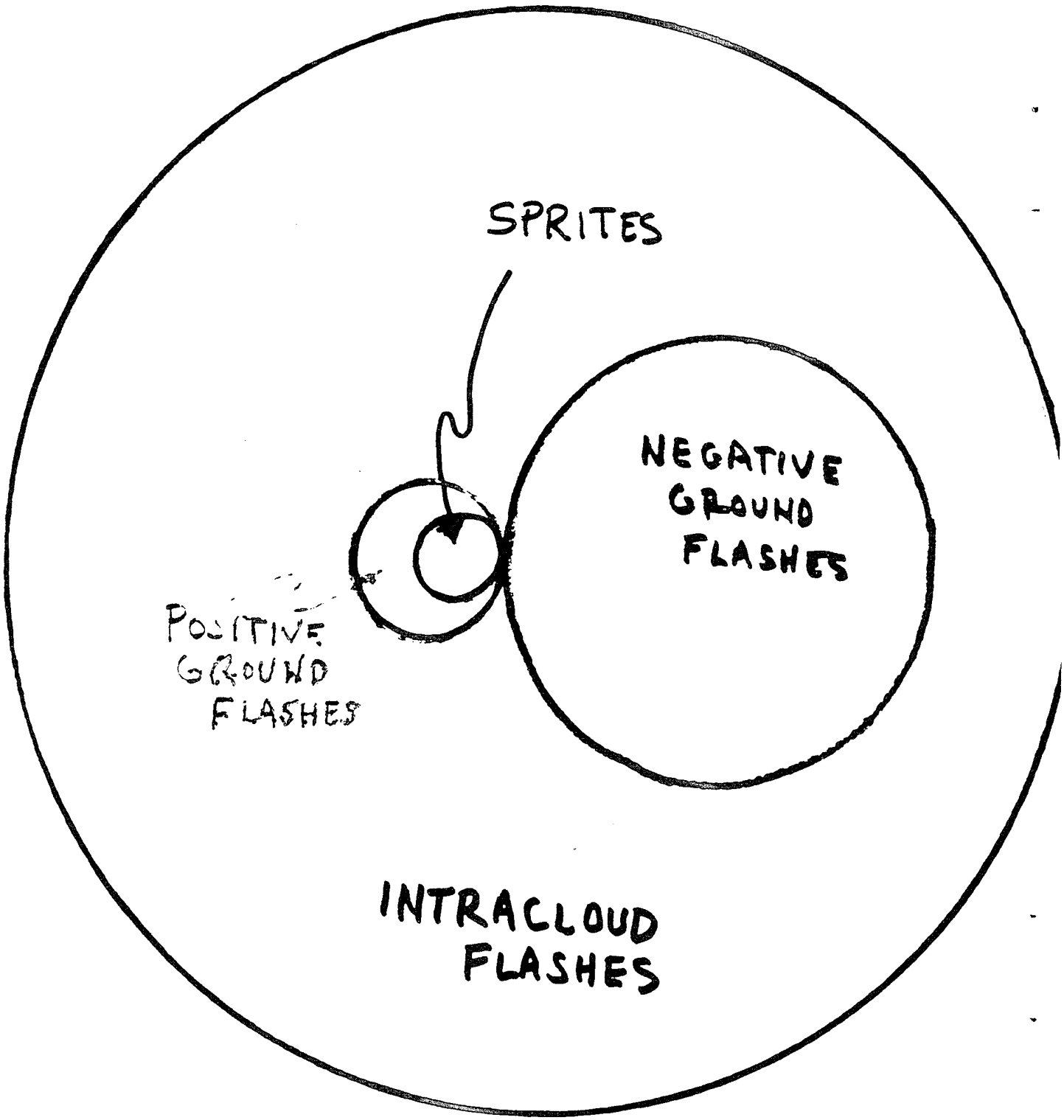



fft(linear scale), 26–Sep–95 4:40:21, win = 100pts
x 10^-3
SPRITE EVENT
3
2.5
2
1.5
1
0.5
0
0
10
20
30
40
50
60
fft of H vs freq(Hz) – unfiltered
THEORETICAL SPECTRUM
WHITE NOISE SOURCE
DISTANCE 2.41 MM


fft(linear scale), 07–24–95, 04:58:53.231GMT, win = 90pts
x 10^-3
1.4
1.2
1
0.8
0.6
0.4
0.2
0
0
20
40
60
80
100
120
fft of H vs freq(Hz) – unfiltered
THEORY FOR 2.3 Mm DISTANCE
60 Hz NOTCH
+114 KA
POSITIVE CG WITHOUT CONTINUING CURRENT (?) AND NO SPRITE



VENN DIAGRAM FOR LIGHTNING



VENN DIAGRAM FOR LIGHTNING

RELAXATION TIME HALE (1985)

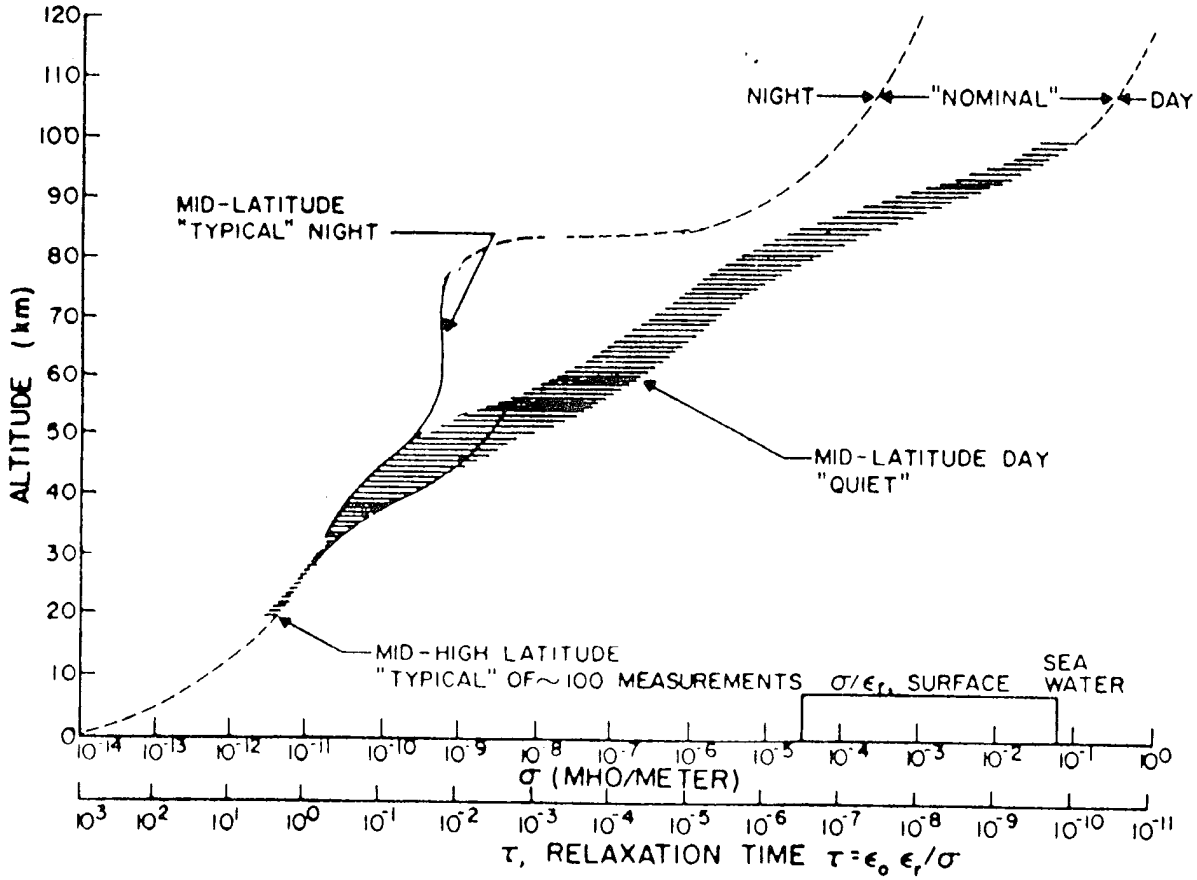
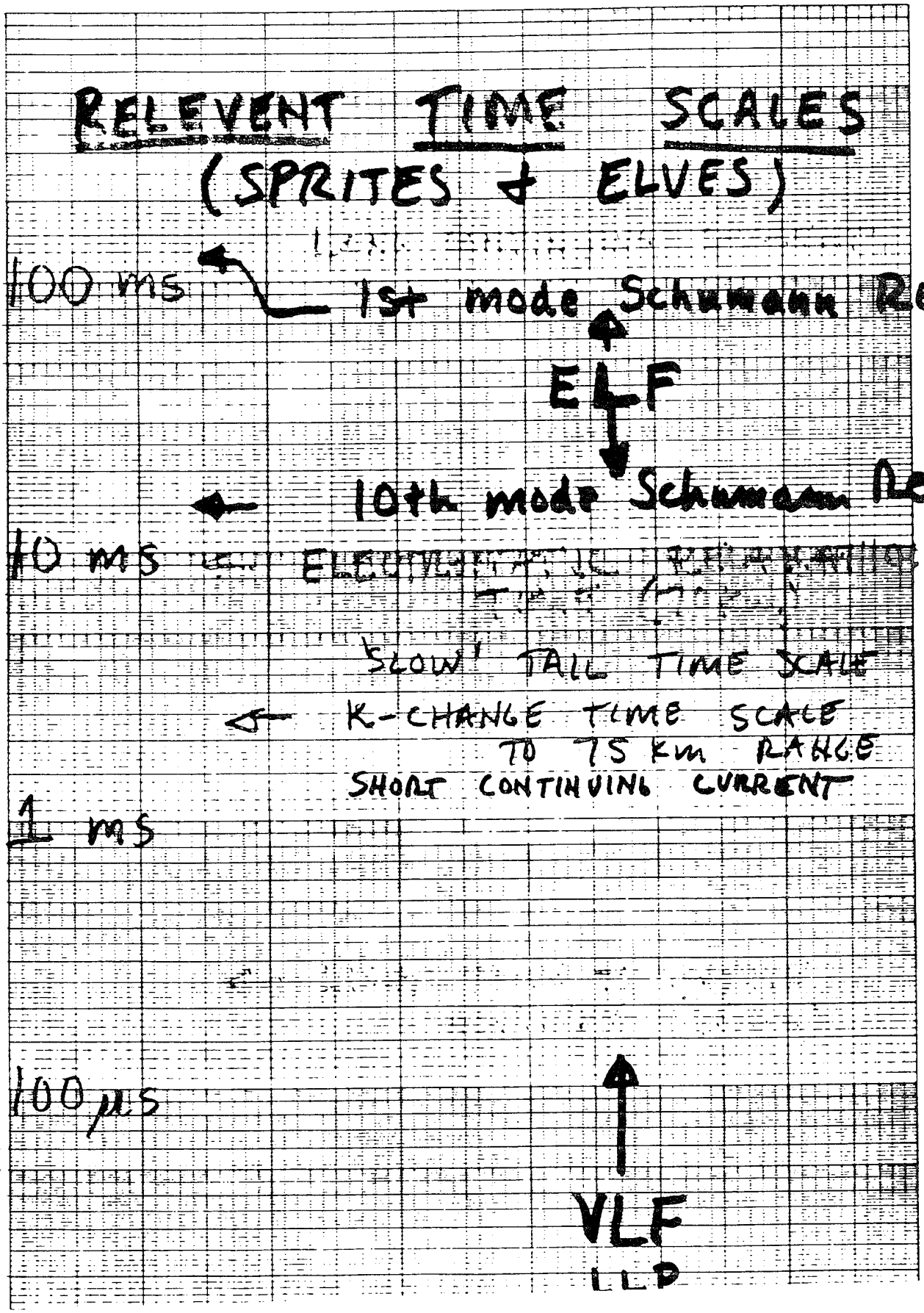


Fig. 3. Total conductivity and corresponding relaxation time under a variety of conditions.



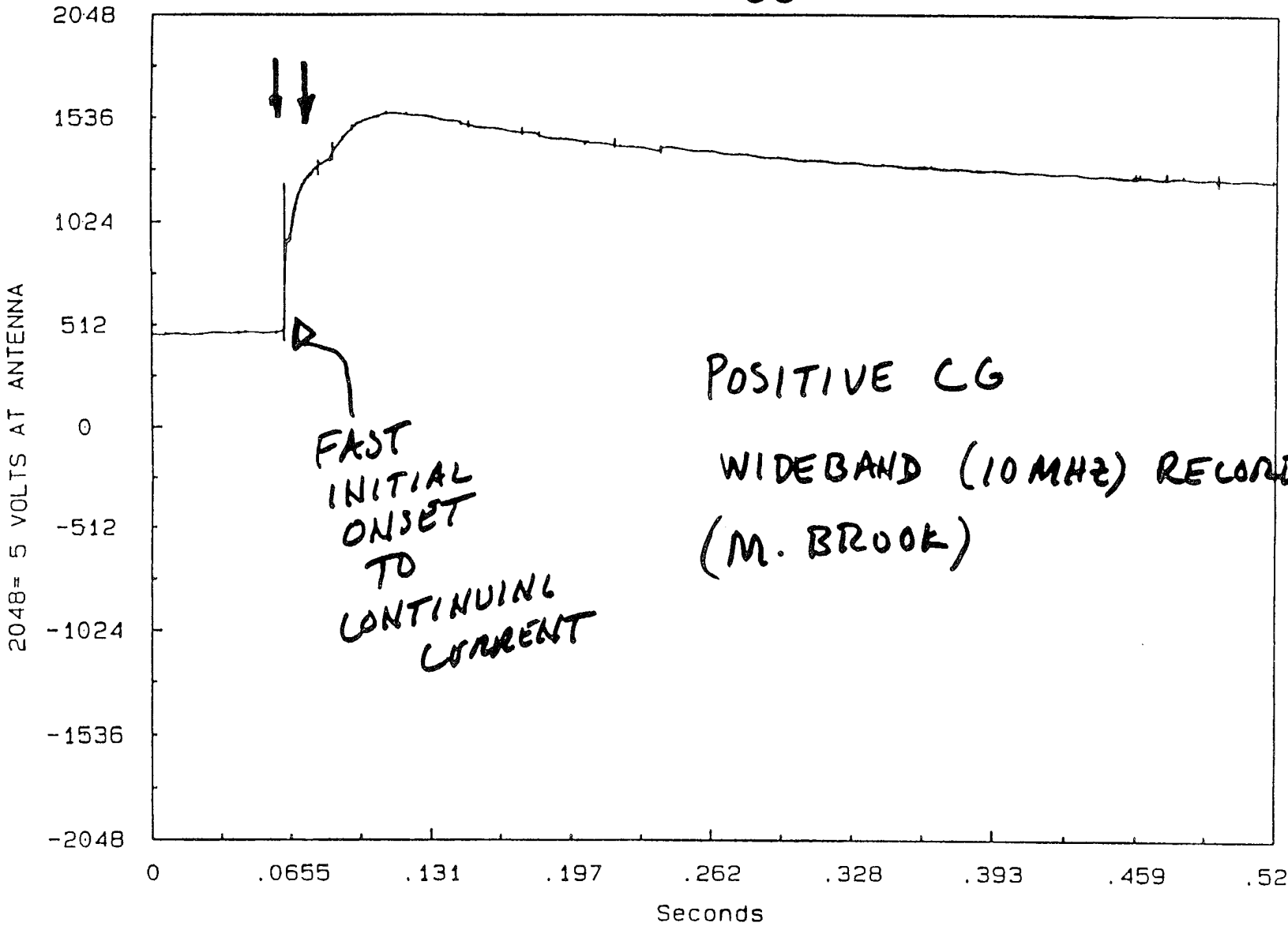
46 6210
K·E SEMI-LOGARITHMIC 5 CYCLES X 70 DIVISIONS
KEUFFEL & ESSER CO

SUMMARY

SPRITE EVENTS	POSITIVE CG's	'RED' SPECTRA
AIRGLOW	POSITIVE CG's	'PINK' SPECTRA
NON SPRITE	NEGATIVE CG SINGLE STROKE	WHITE SPECTRUM
NON SPRITE	POSITIVE CG NO CONT. CURRENT	WHITE SPECTRUM

COMPACTED PLOT

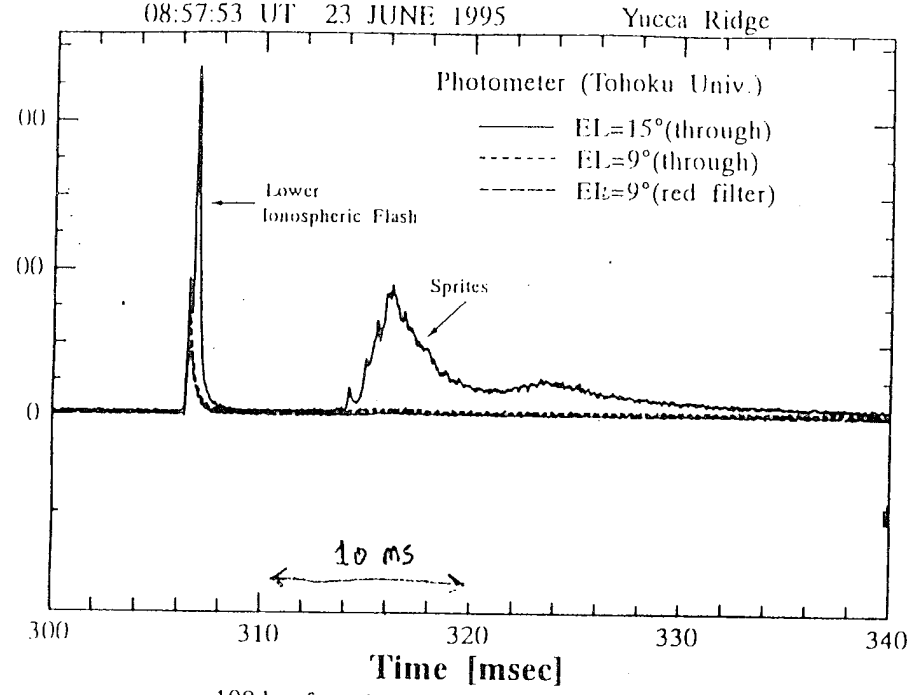
1990 139 57 21 27 29 3 64 5 2000 Trigger Time 21:27:29

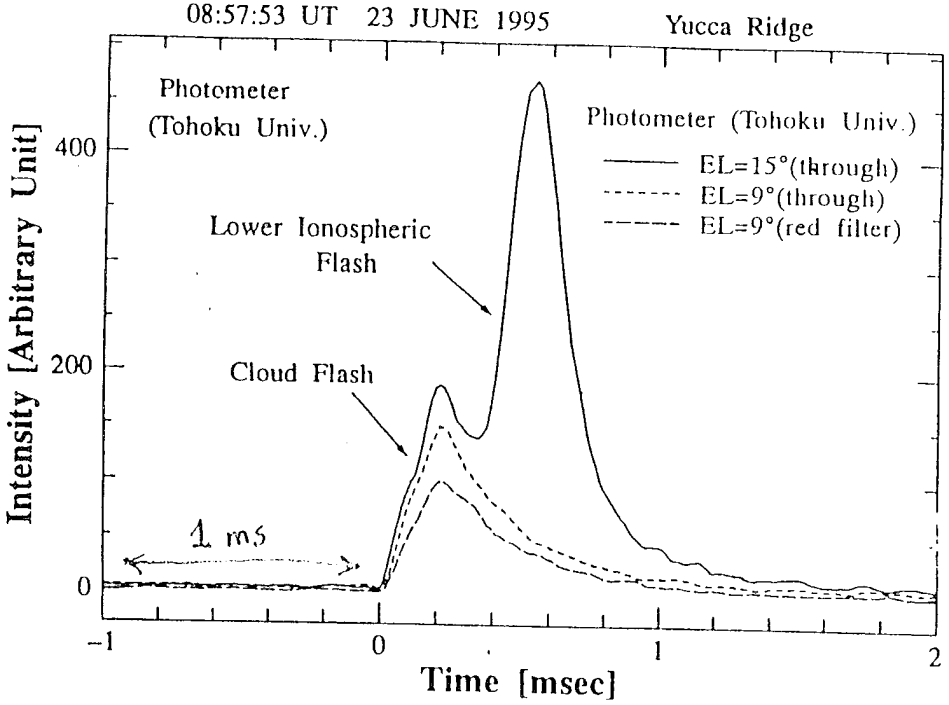


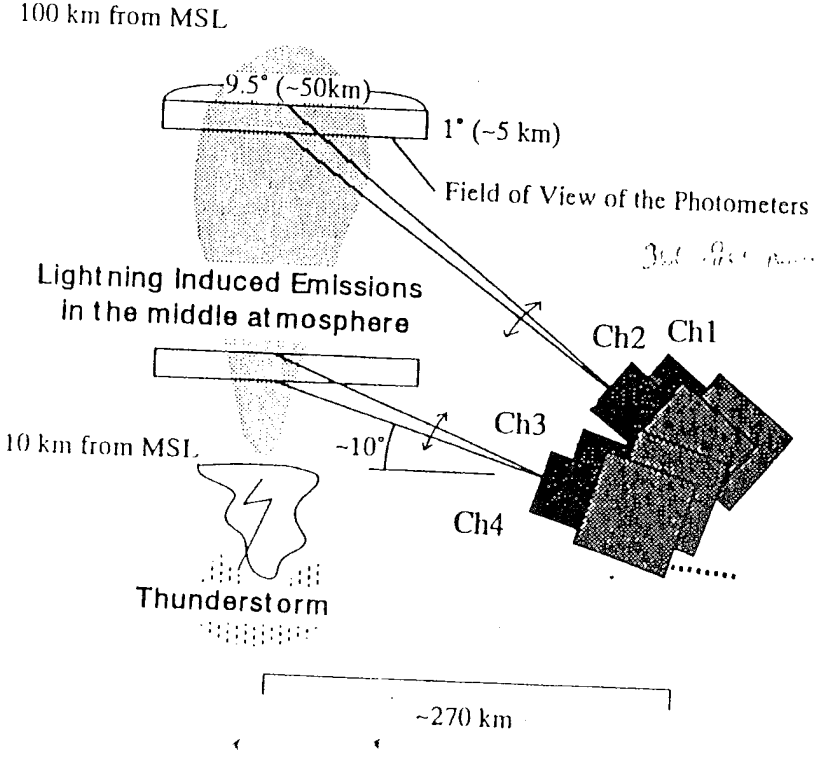
358°
96.4 km
+411 LLP
1 Str.

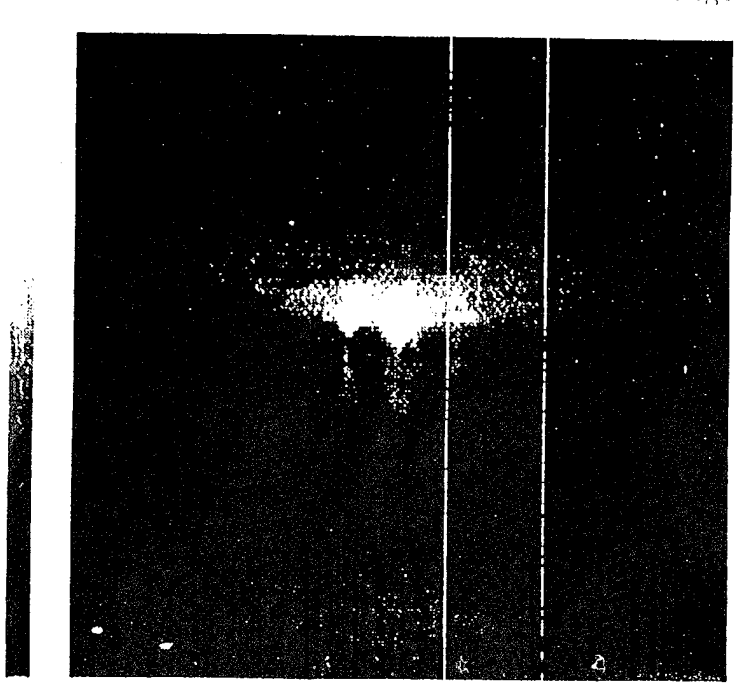
Sprites, Blue Jets, and High Altitude Optical Flashes Produced by Quasi-Electrostatic Thundercloud Fields and Lightning EMP

U.S. Inan
Stanford University



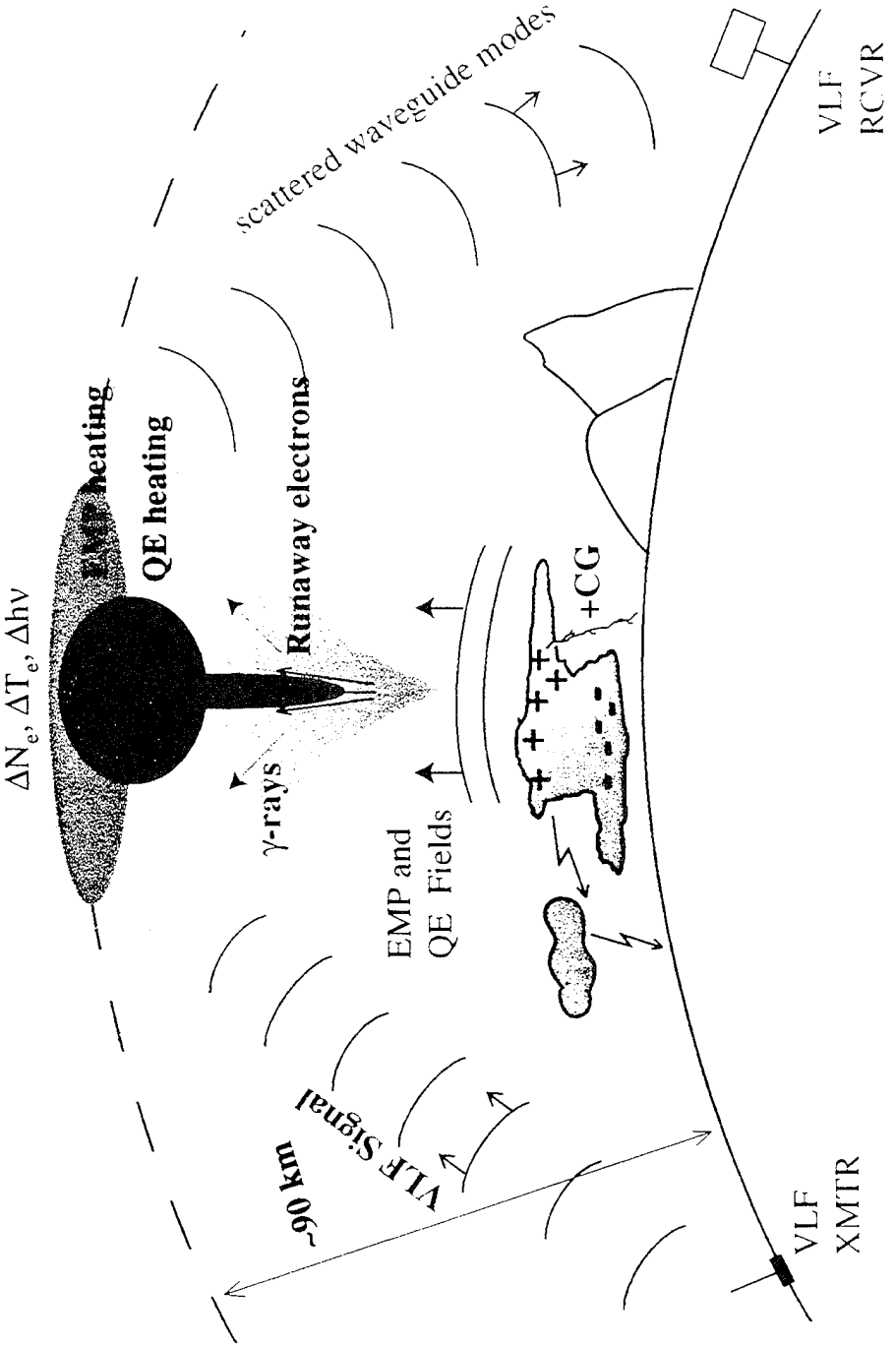






Description of the experiments of Fukunishi et al., carried out at Yucca Ridge during Summer 1995

Illustration of different mechanisms operating at different altitude ranges and detection of the disturbances via the VLF-scattering method



VLF remote sensing of transient ionospheric disturbances
from [Inan, Bell, Pasko, Sentman, Wescott,Lyons, in review at GRL, 1995]

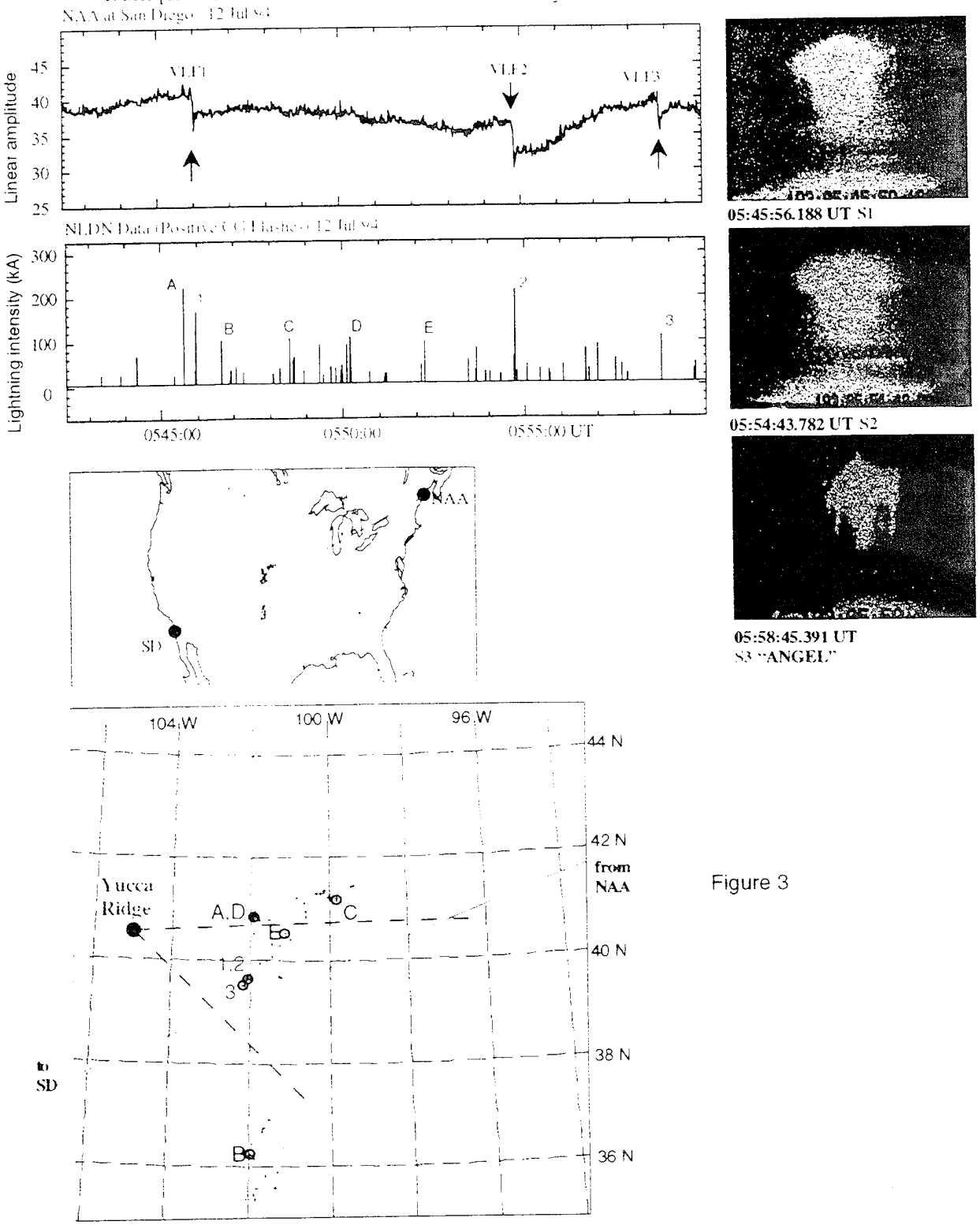
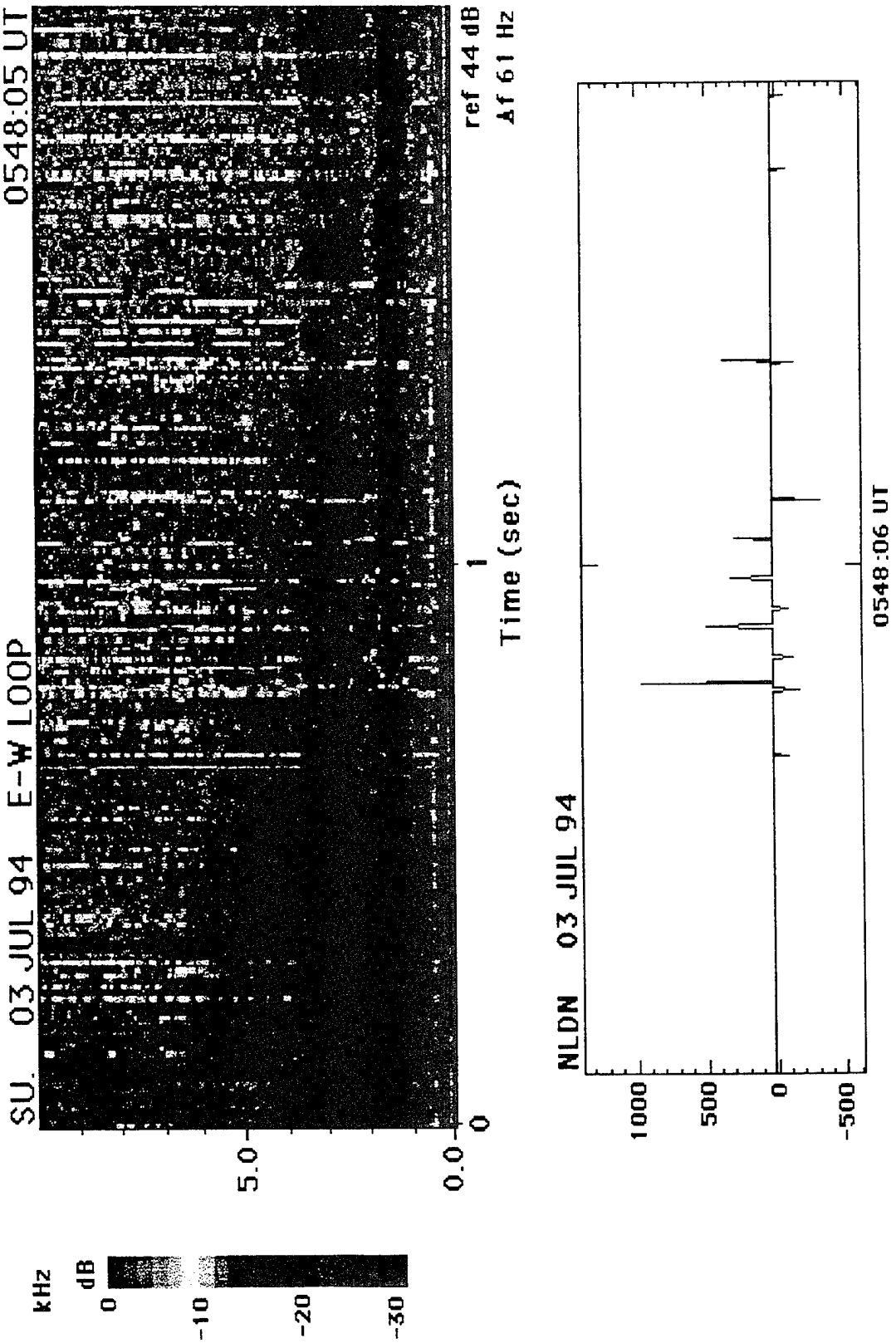
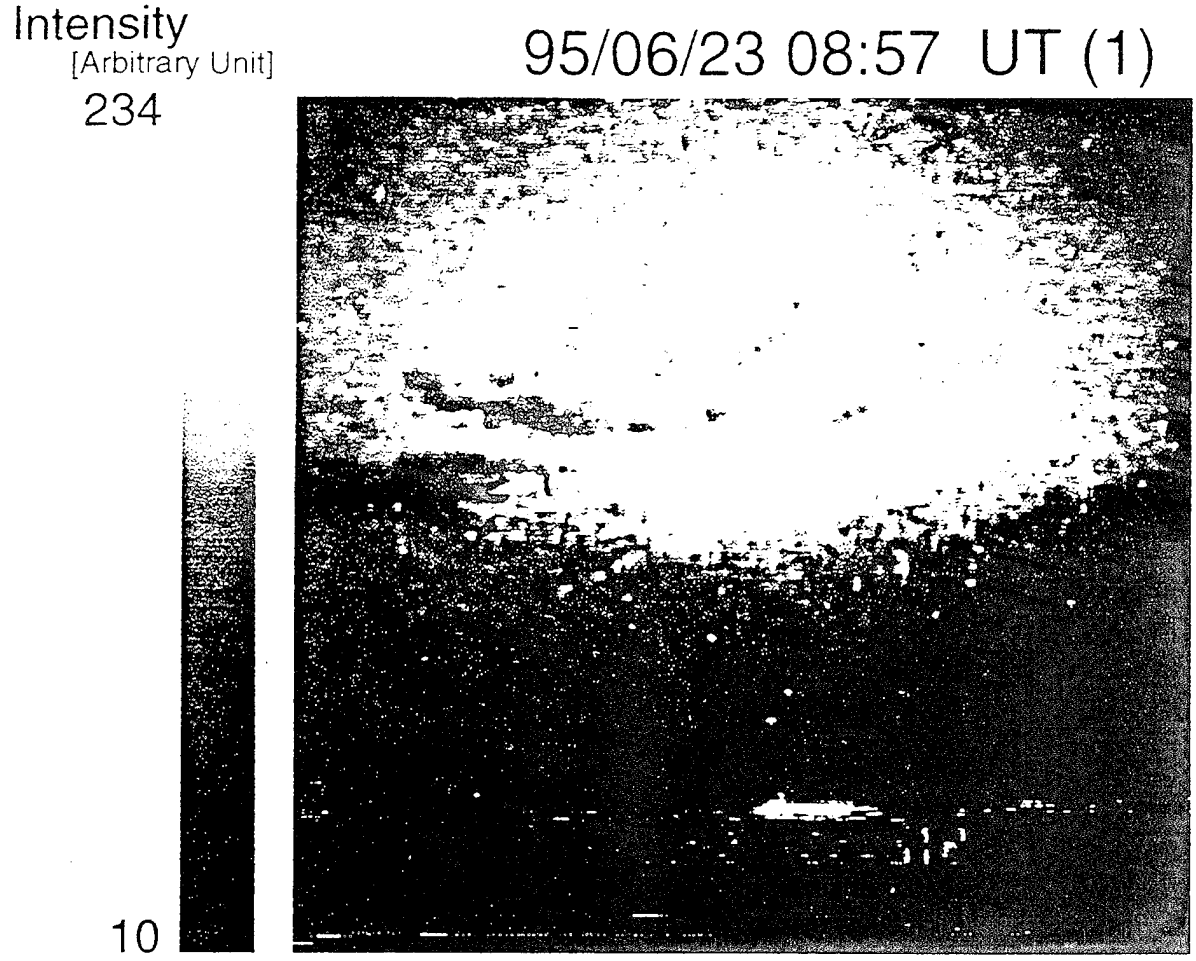
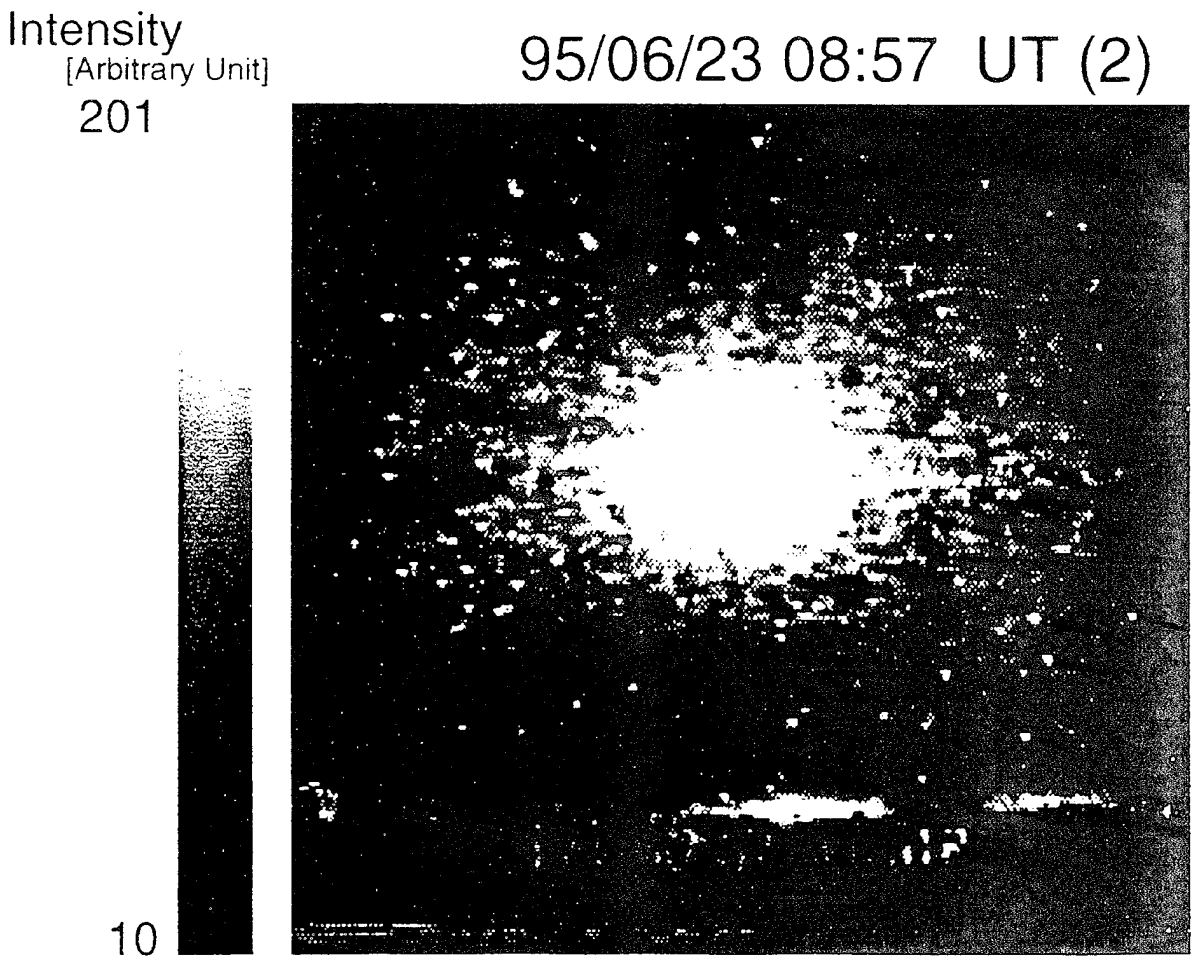


Figure 3

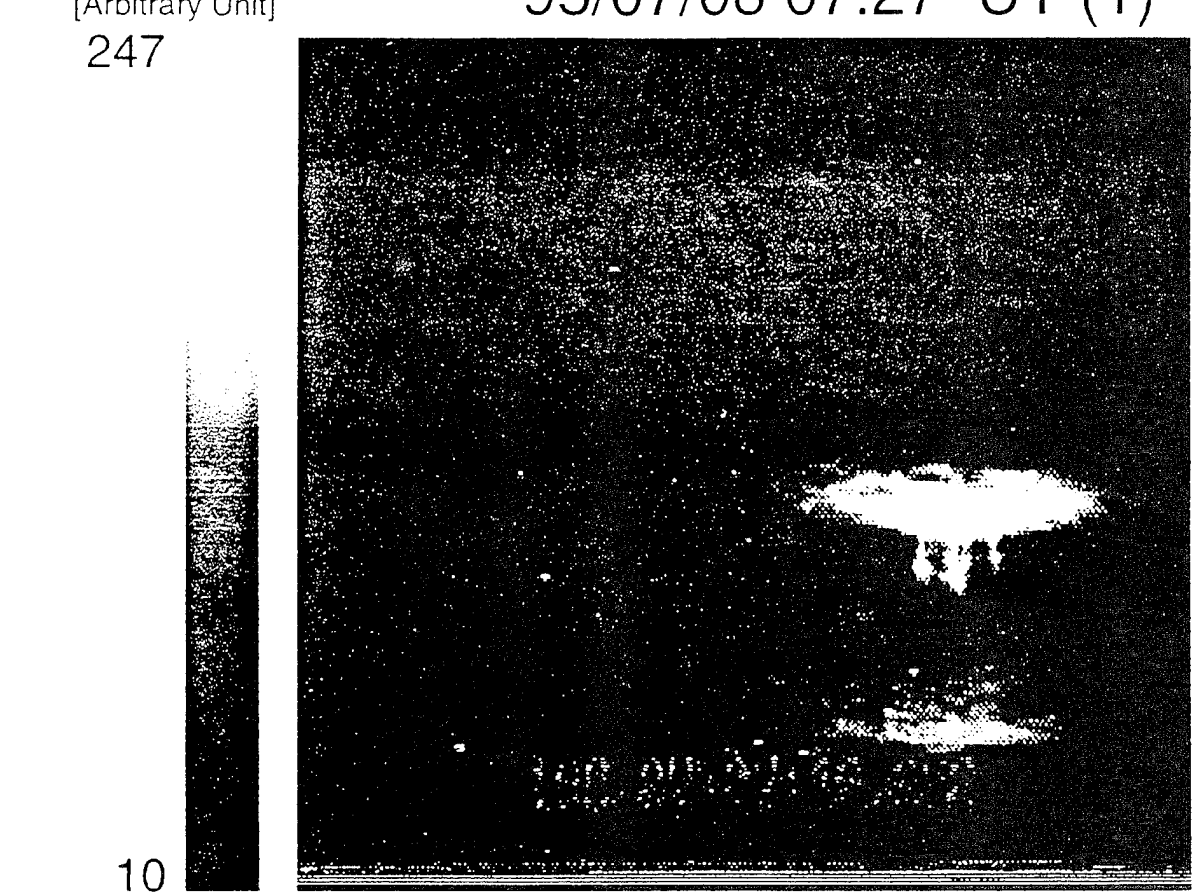
Characteristics of ELF/VLF sferics of CG lightning discharges producing sprites from [Reising, Inan, Bell, to be presented at Fall AGU Meeting]

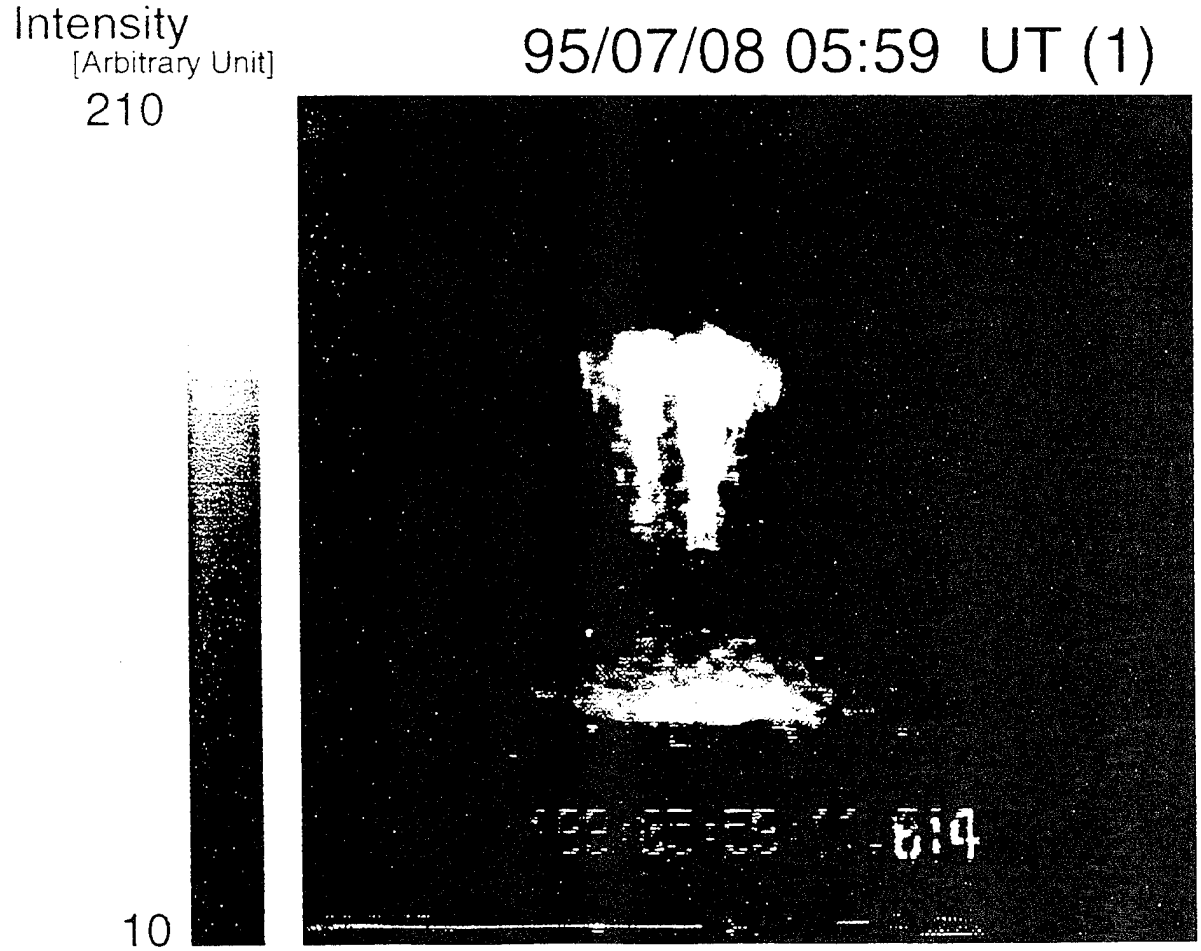






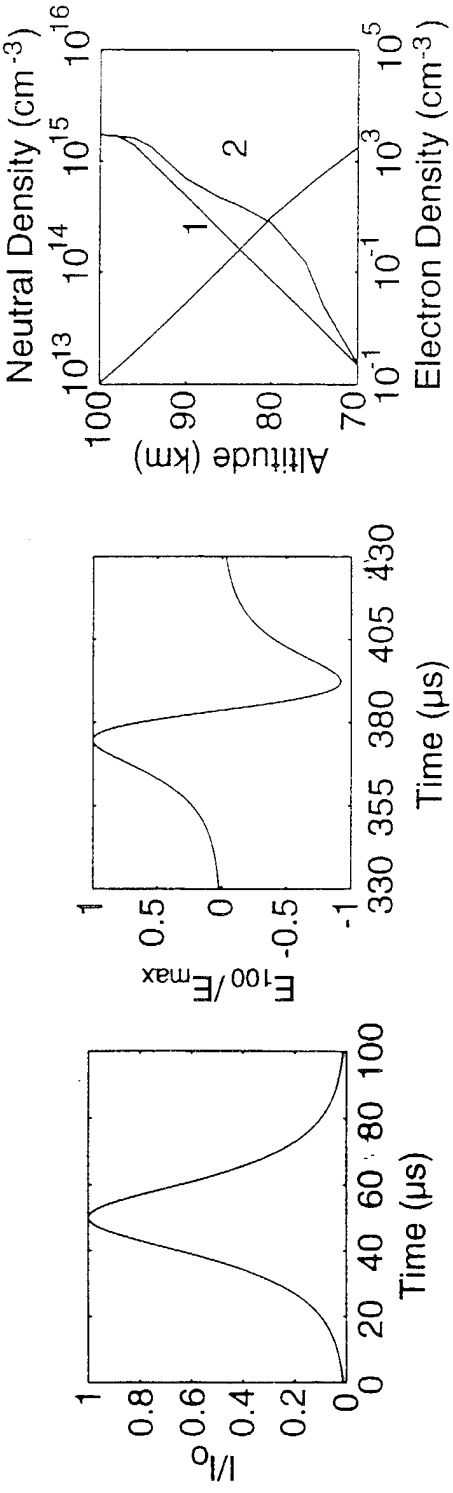
Images of lower ionospheric flashes (elves) and sprites
from Fukunishi et al. [1995, paper in preparation for submission to Nature]



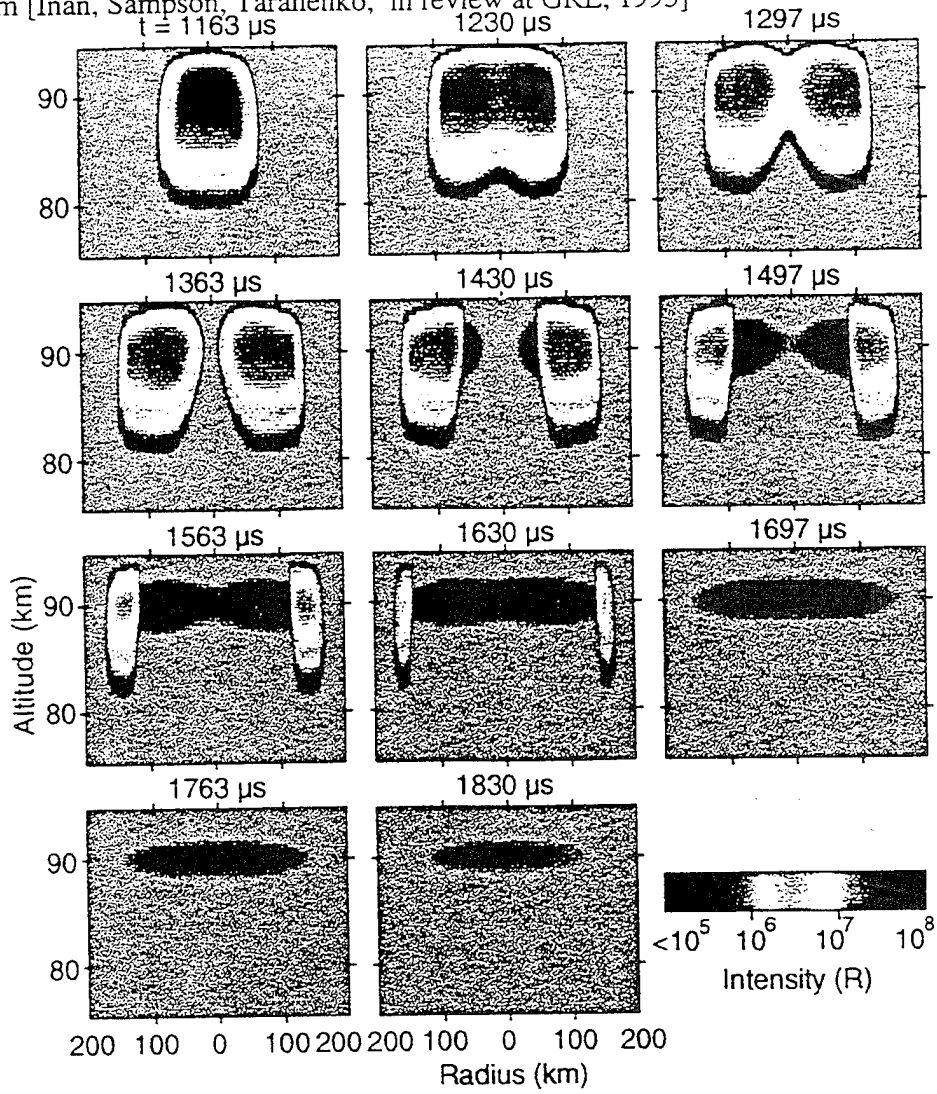


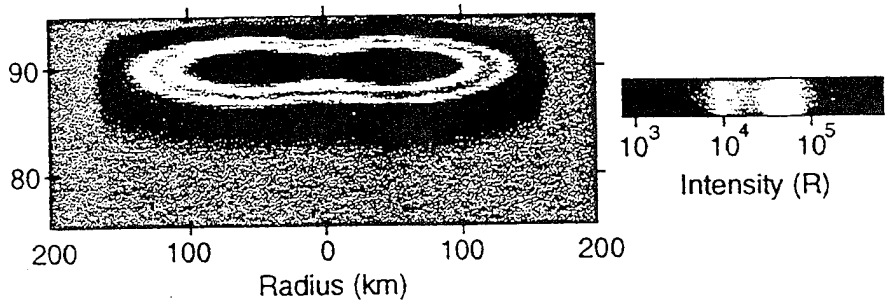
Images of lower ionospheric flashes (elves) and sprites from Fukunishi et al. [1995, paper in preparation for submission to Nature]

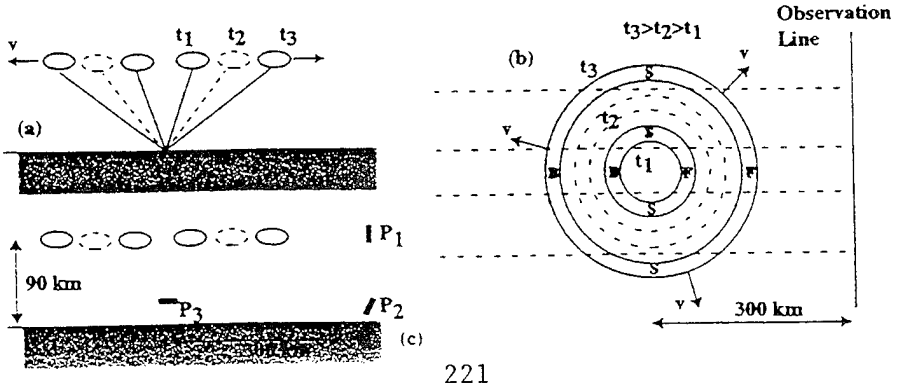
Results of a new 2-D model of EMP-ionosphere interaction
[Inan, Sampson, Taranenko, in review at GRL, 1995]

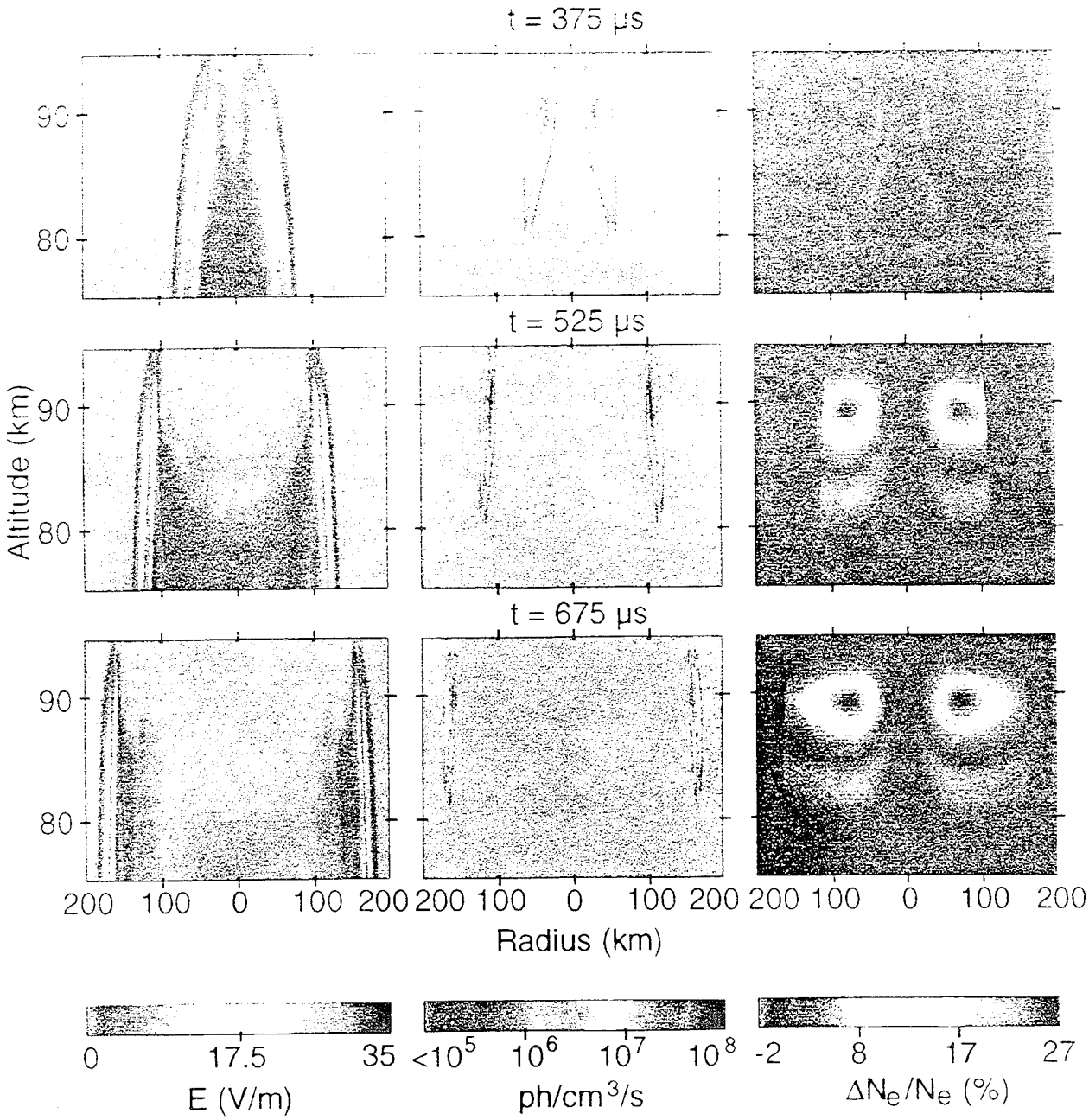


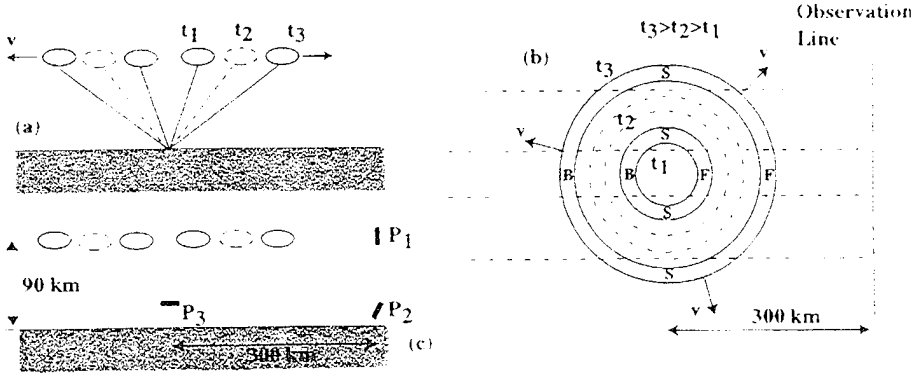
"A light show in the sky" produced by the interaction of the EMP with the ionosphere from [Inan, Sampson, Taranenko, in review at GRL, 1995]



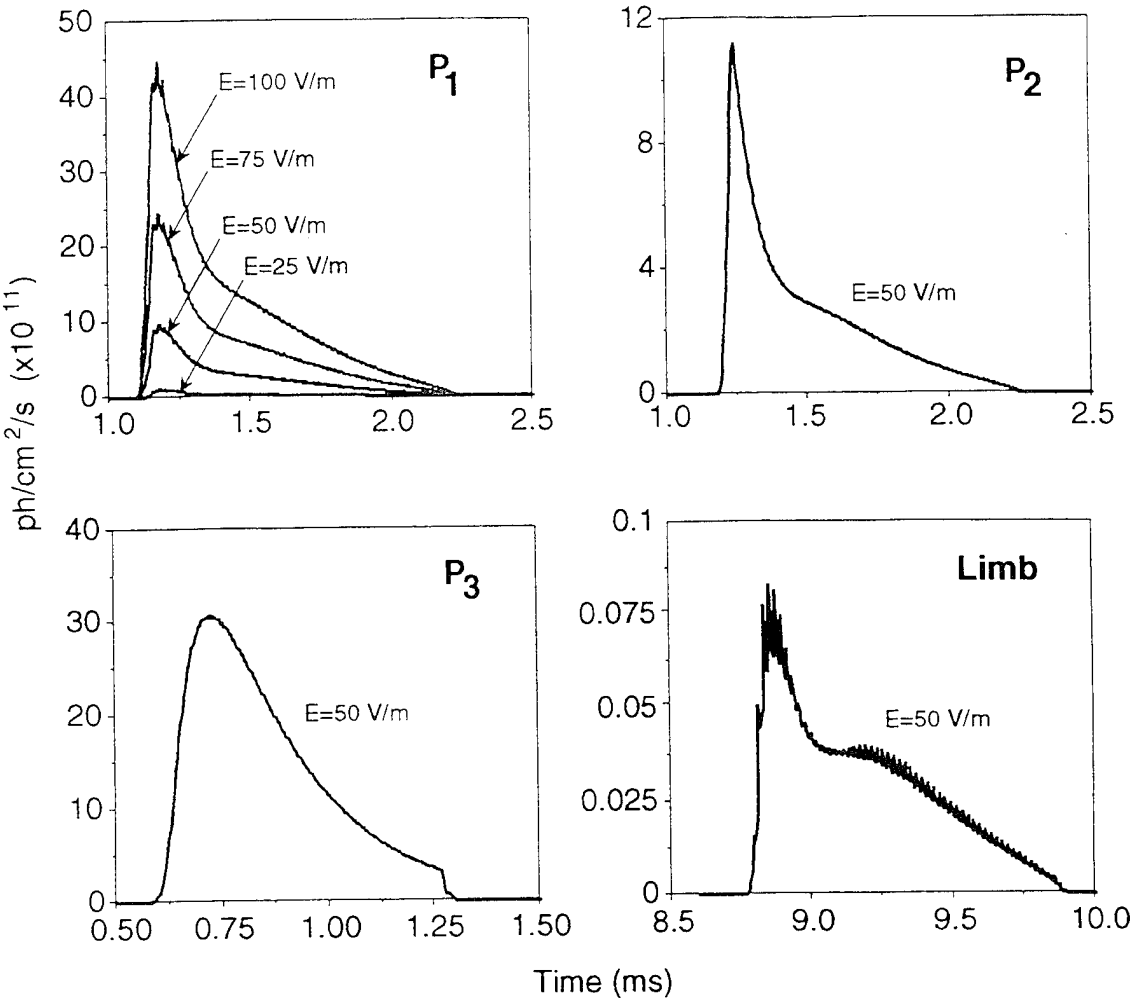


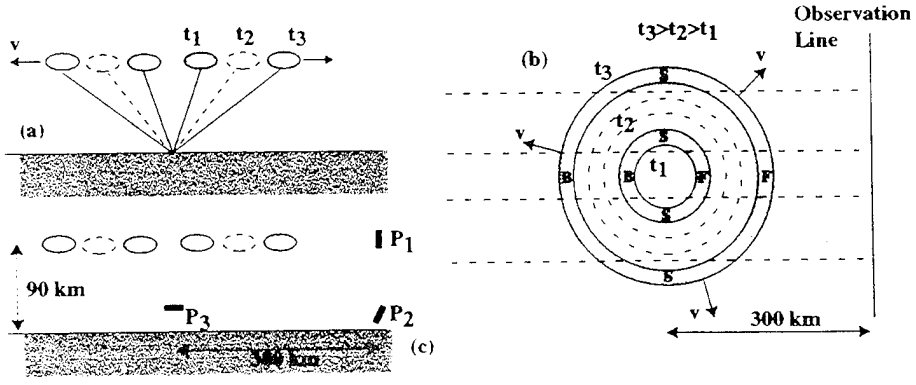



t = 375 μs
t = 525 μs
t = 675 μs
Altitude (km)
90
80
200 100 0 100 200
Radius (km)
0 17.5 35
E (V/m)
<10^5 10^6 10^7 10^8
ph/cm^3/s
-2 8 17 27
ΔNe/Ne (%)


v
t1 t2 t3
(a)
P1
90 km
P3
P2
300 km
(c)
(b)
t3>t2>t1
Observation Line
S
B
F
300 km

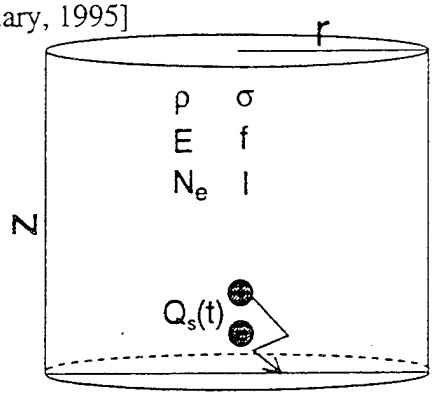
Theoretical predictions for photometric measurements from different vintage points from [Inan, Sampson, Taranenko, in review at GRL, 1995]

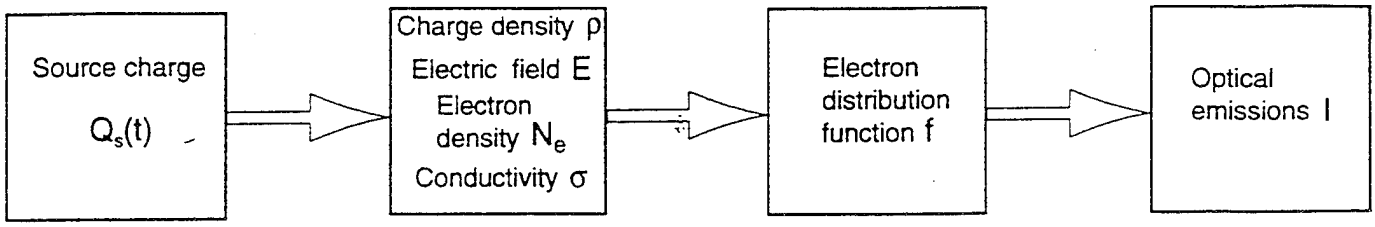




2-D Quasi-Electrostatic Model [Pasko et al., GRL, February, 1995]

2-D QE Model

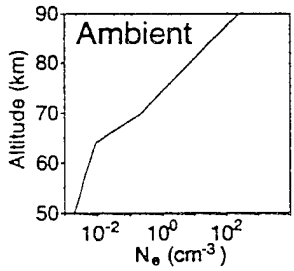


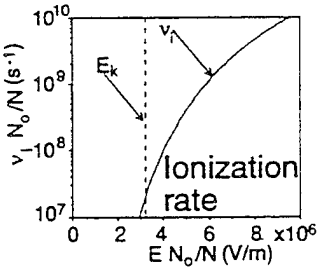


1. Charge density ρ : $\frac{\partial \rho}{\partial t} + \frac{\sigma}{\varepsilon_o}\rho + \nabla\sigma\cdot\vec{E} = 0$

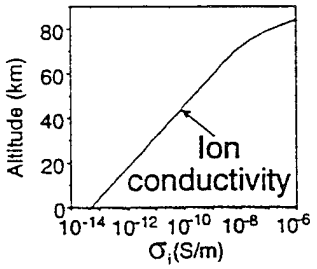
2. Electric field E : $\nabla\cdot\vec{E} = (\rho + \rho_s)/\varepsilon_o$

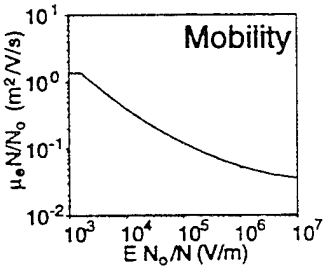
3. Electron number density N_e : $\frac{dN_e}{dt} = \nu_i N_e - \alpha N_e^2$



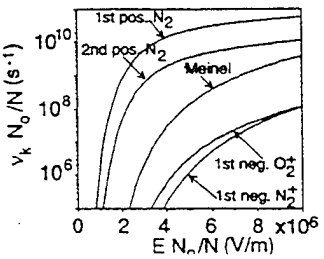


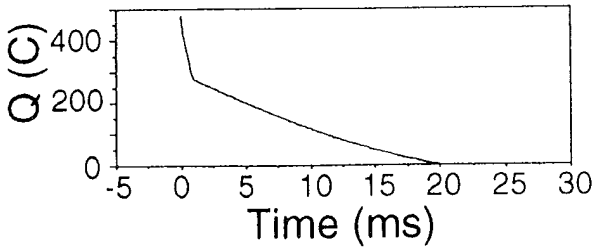
4. Conductivity σ : $\sigma = \sigma_i + \sigma_e$; $\sigma_e = \mu_e N_e e$

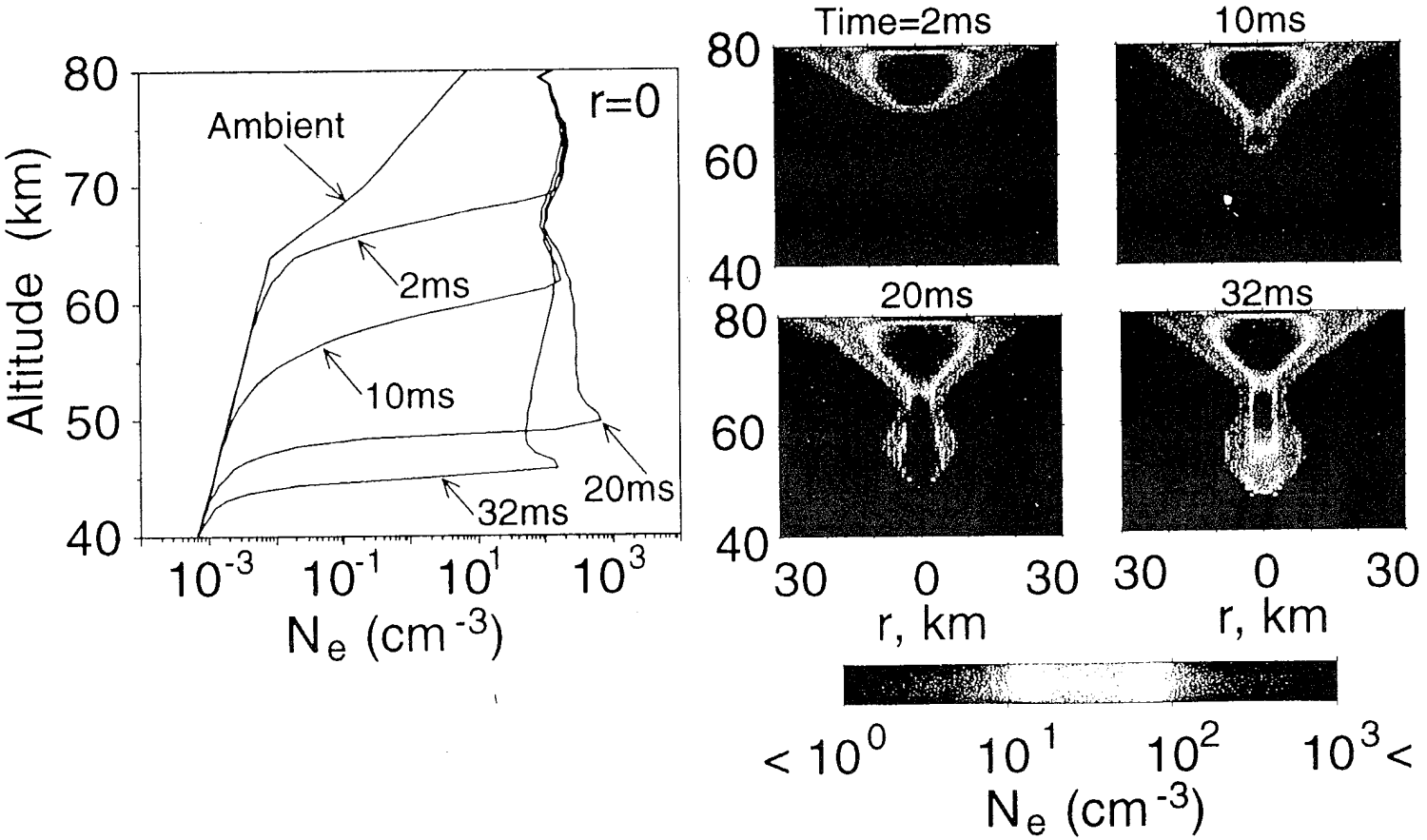




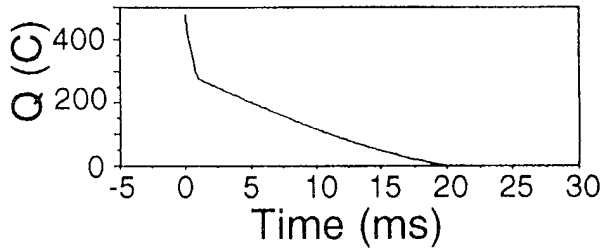
5. Optical emissions:

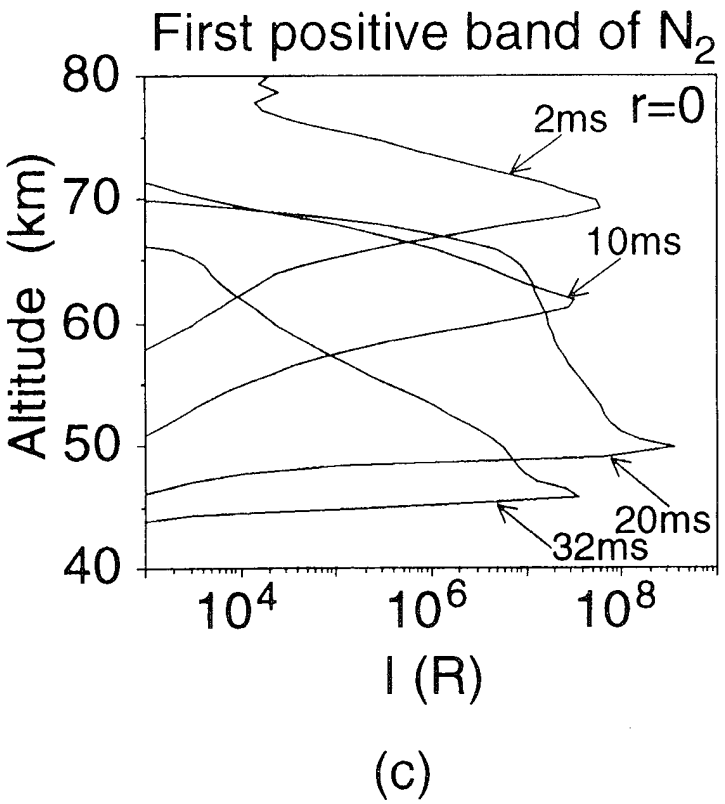




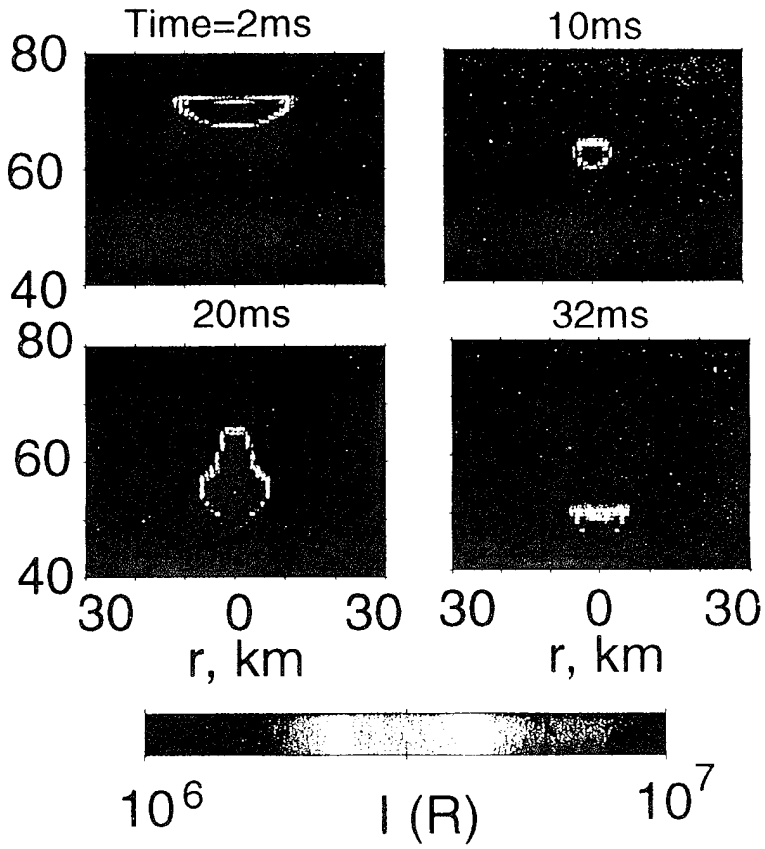


Predictions of a new paper on the formation of ionization columns and carrot-like structures [Pasko et al., 1995, in review at GRL]



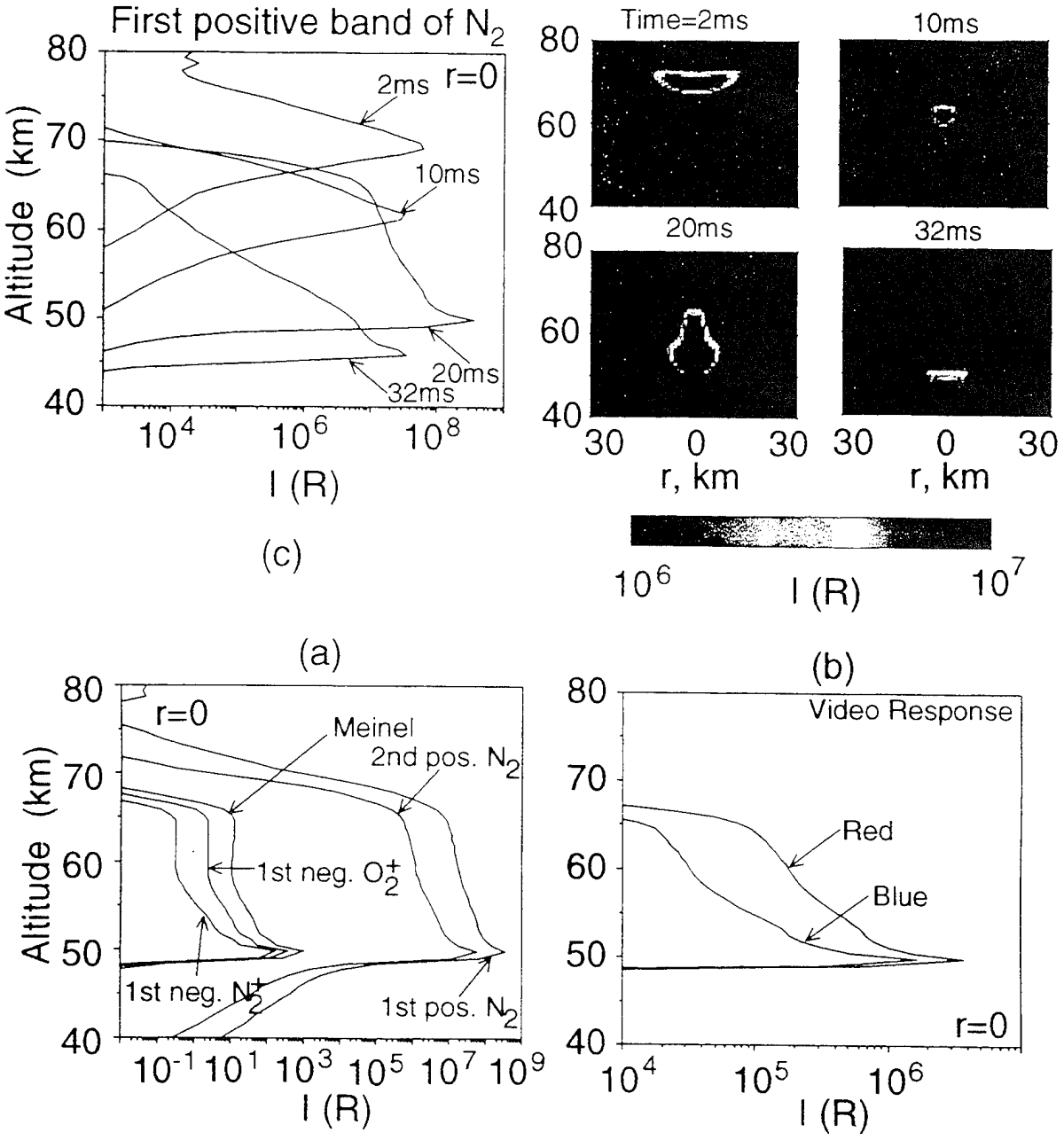


(c)

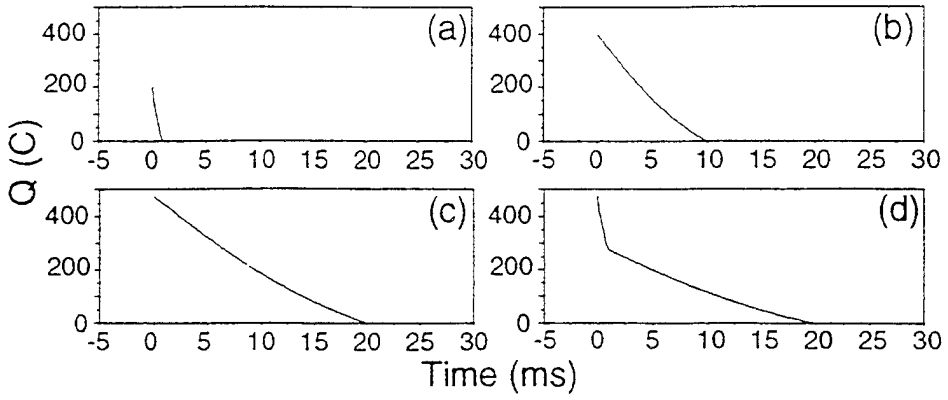


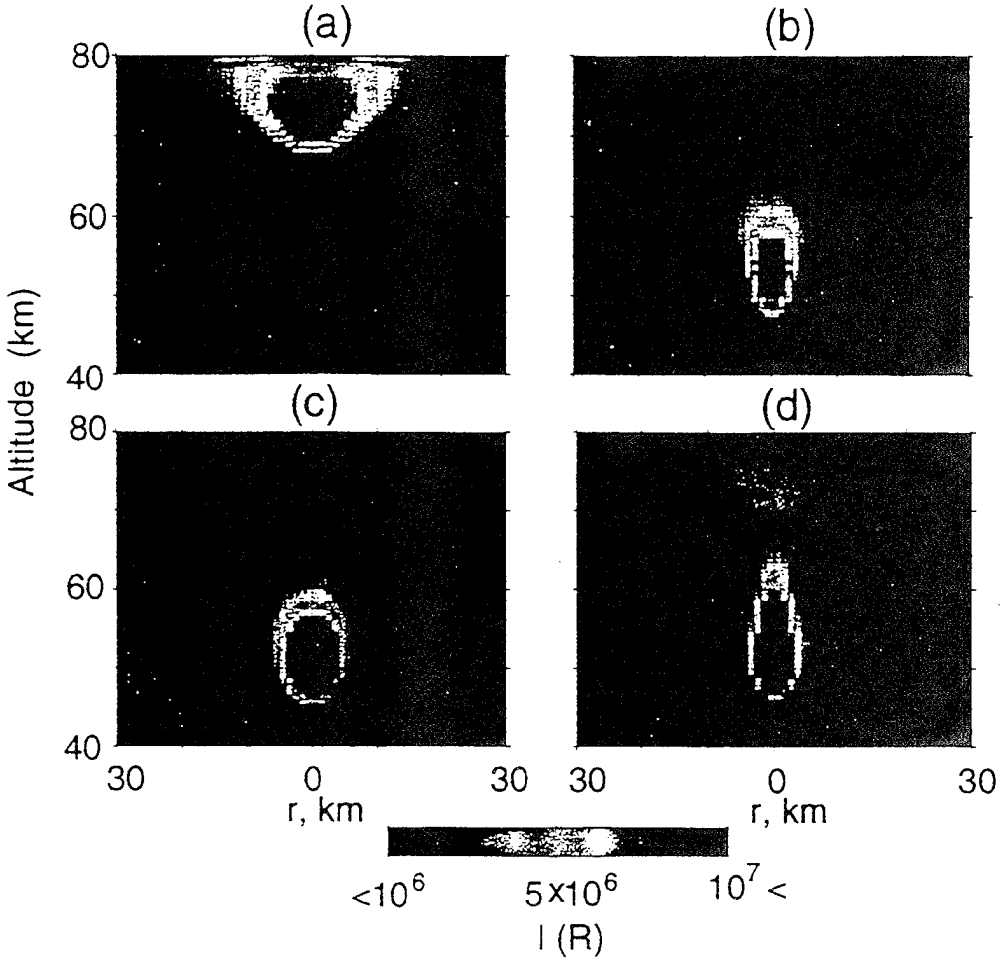
Predictions of a new paper on the formation of ionization columns and carrot-like structures [Pasko et al., 1995, in review at GRL]

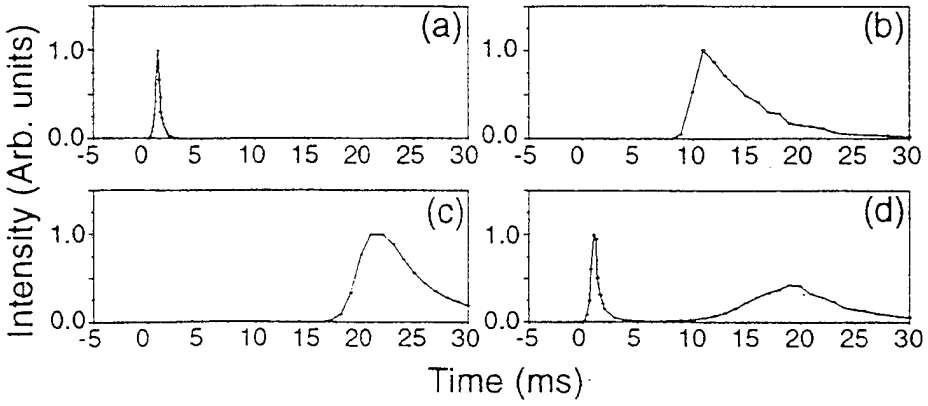
Predictions of a new paper on the formation of ionization columns and carrot-like structures [Pasko et al., 1995, in review at GRL]



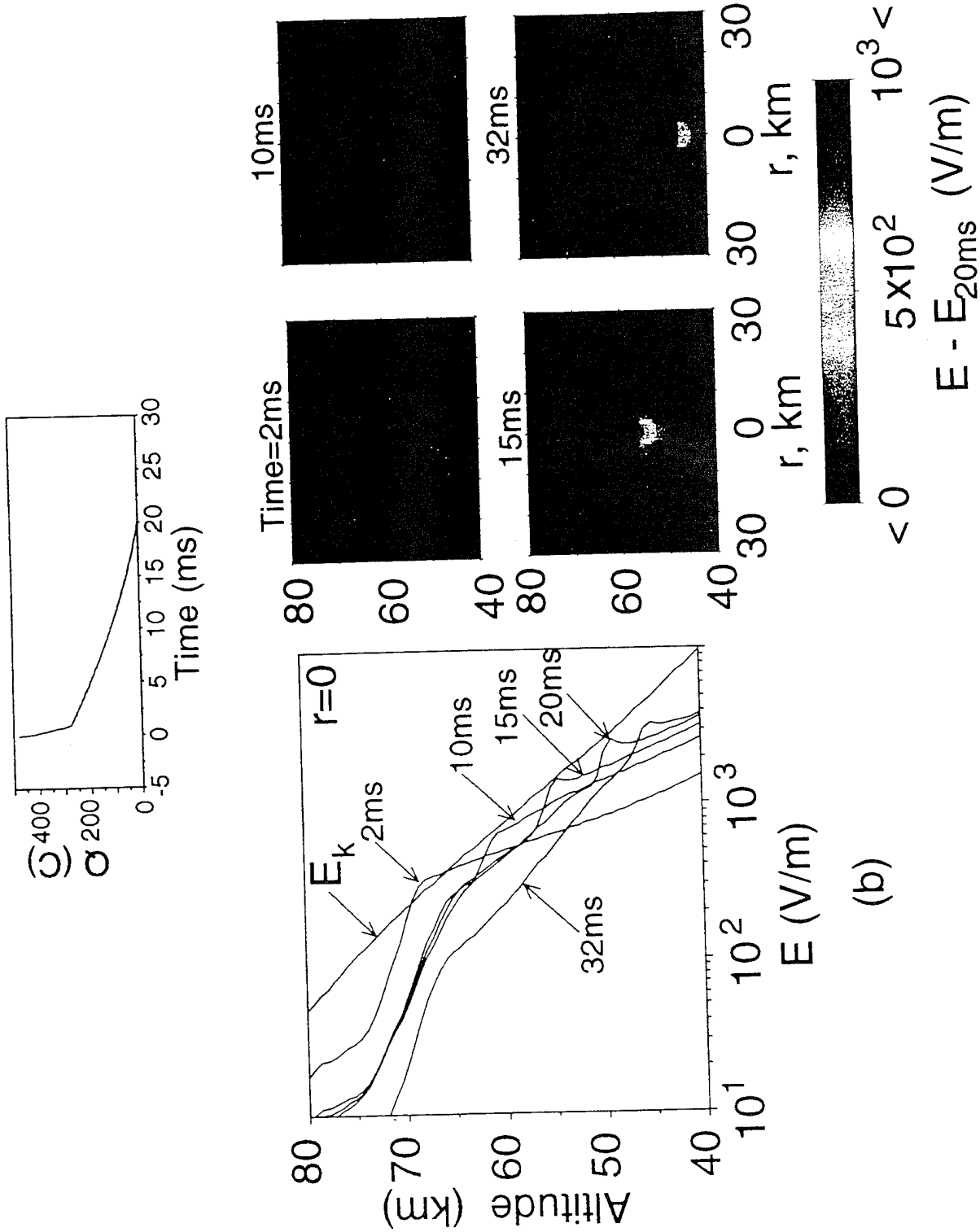
Dependence of the sprite structure and "delay" on the rate of removal of charge from [Pasko et al., 1995, in review at GRL]







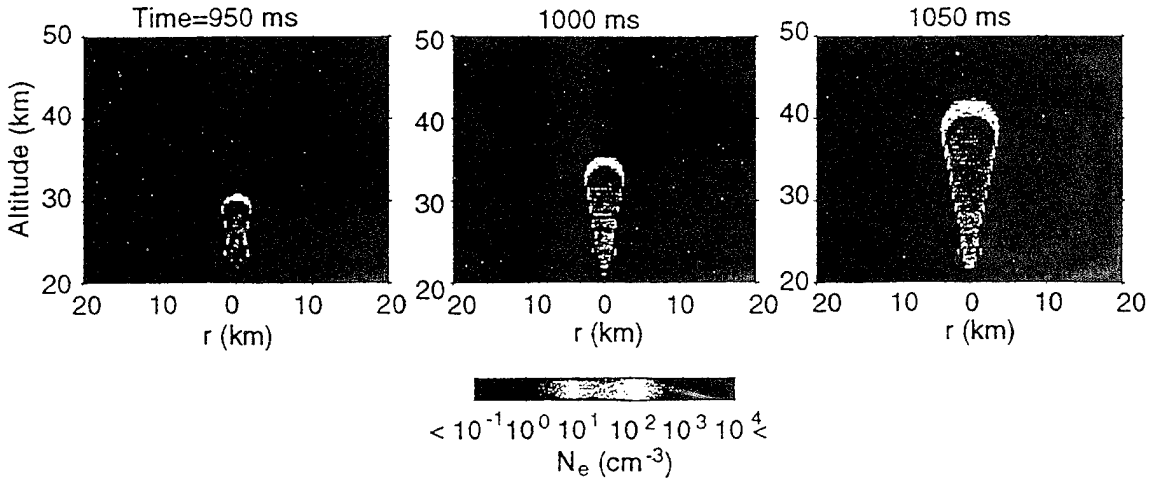
Predictions of a new paper on the formation of ionization columns and carrot-like structures [Pasko et al., 1995, in review at GRL]



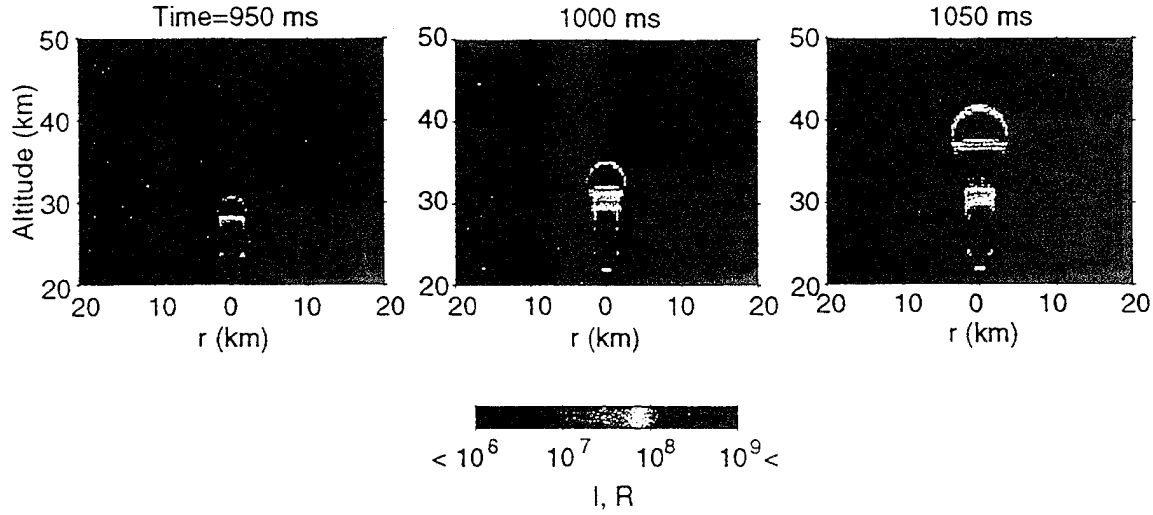
from an upcoming Fall AGU paper
[Pasko et al., 1995]

Blue Jets

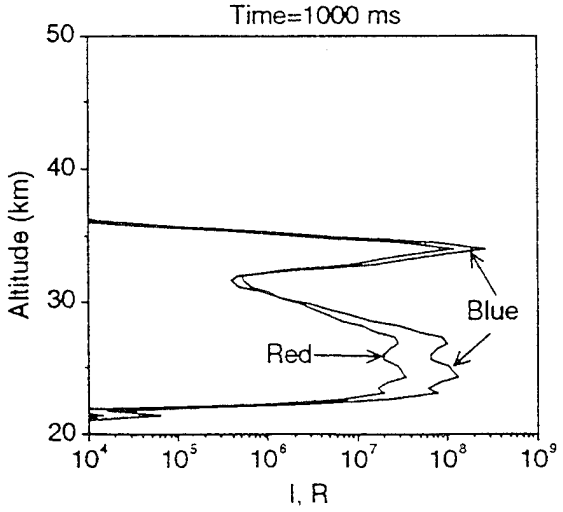
Electron number density

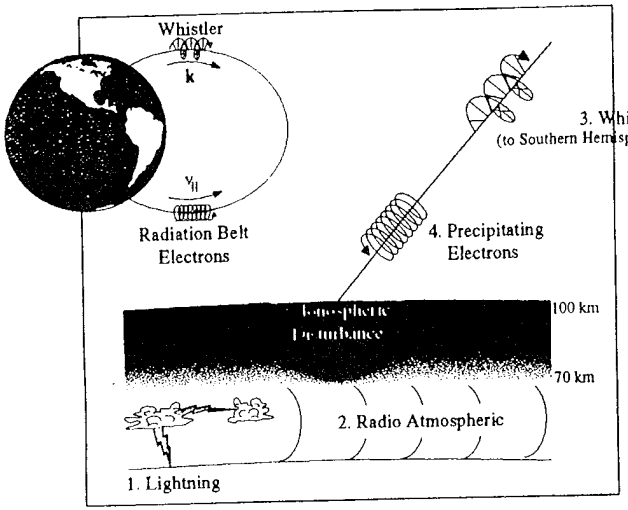


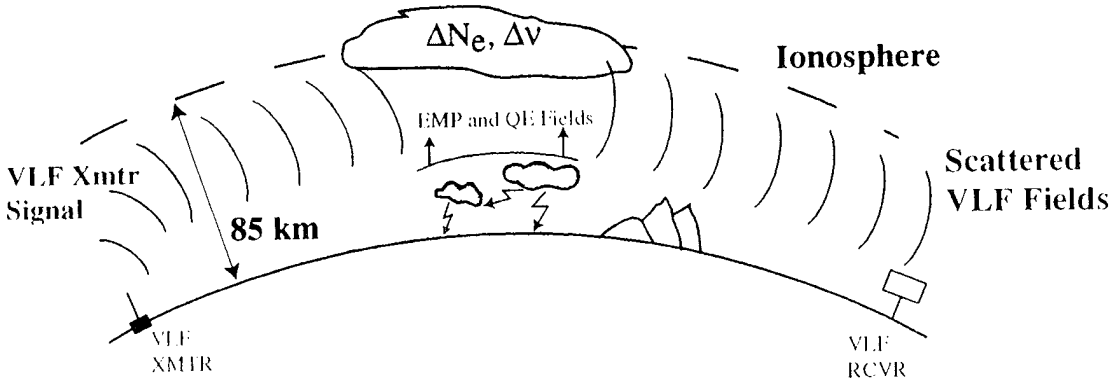
2nd positive band of N_2

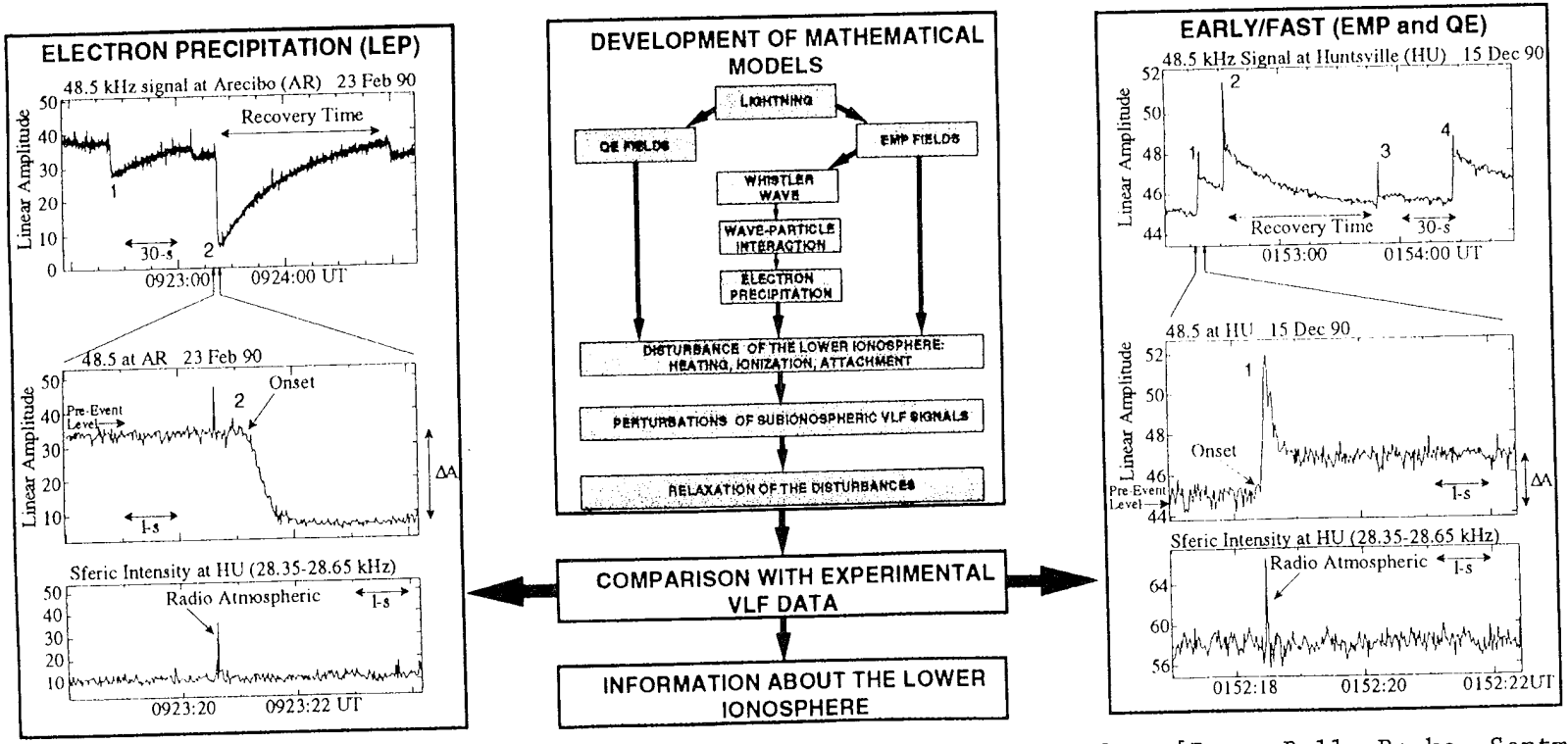


Video respose



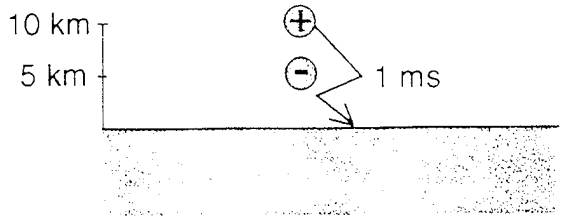


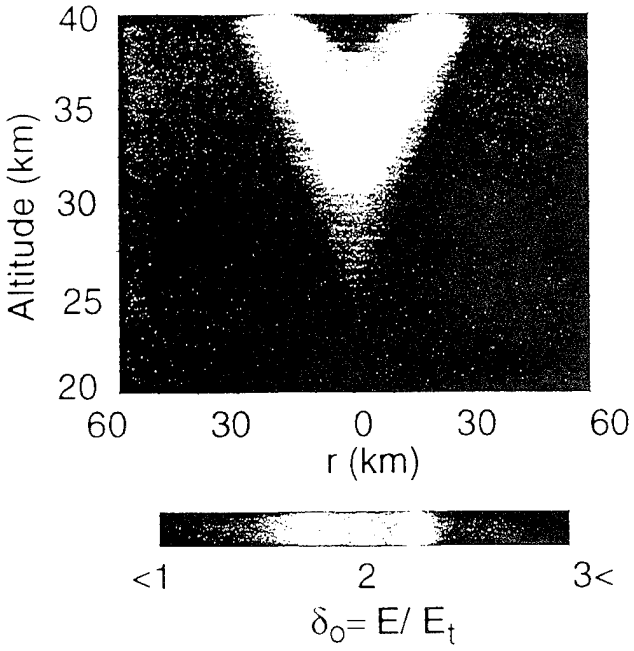




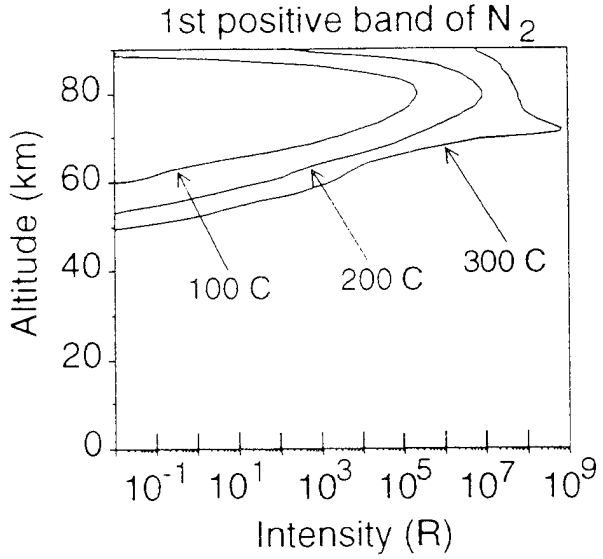
VLF remote sensing of transient ionospheric disturbances from [Inan, Bell, Pasko, Sentman, Wescott, Lyons, in review at GRL, 1995]

Essentials of the runaway breakdown model [Bell et al., GRL, August, 1995]

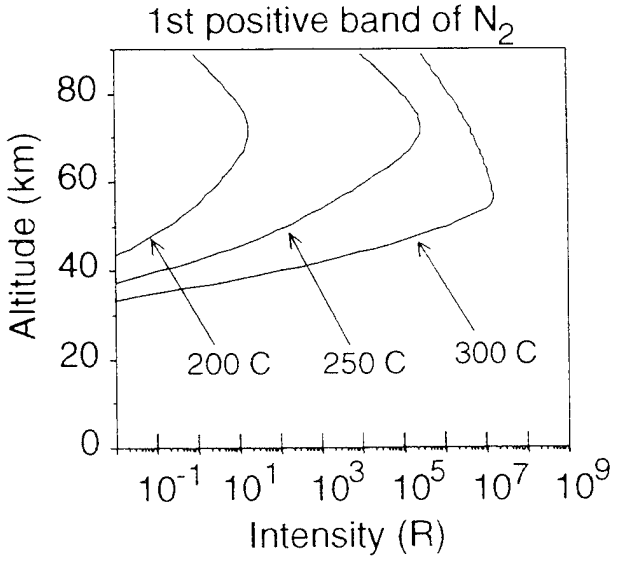




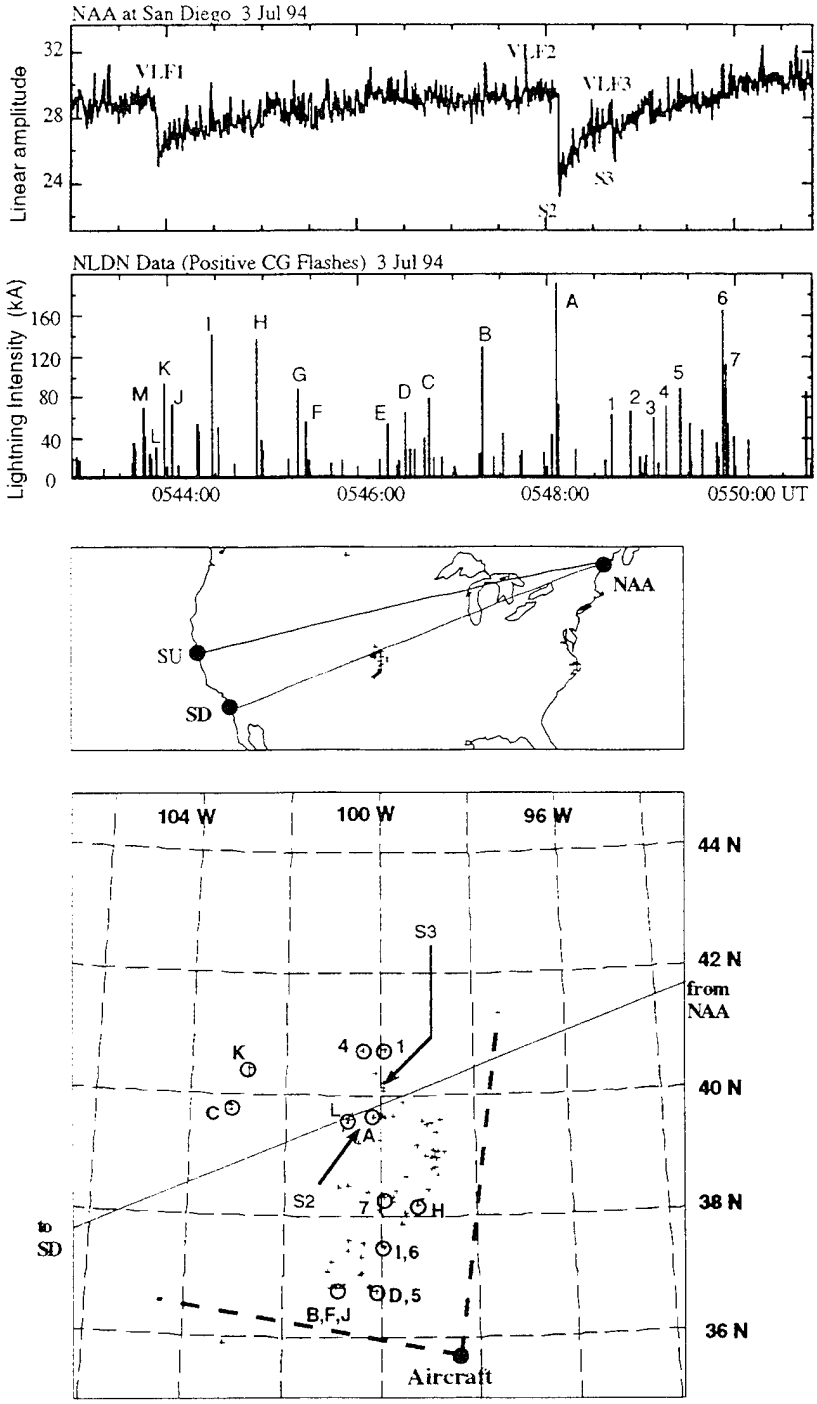
Quasi-electrostatic model

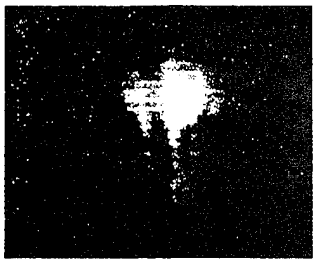


Runaway model

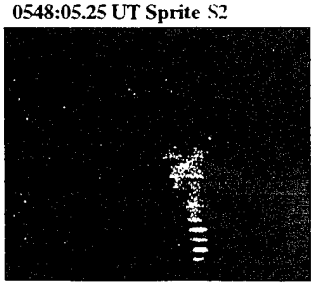


VLF remote sensing of transient ionospheric disturbances
from [Inan, Bell, Pasko, Sentman, Wescott,Lyons, in review at GRL, 1995]





0548:05.25 UT Sprite S2



0548:40.16 UT Sprite S3

Figure 1

VLF remote sensing of transient ionospheric disturbances
from [Inan, Bell, Pasko, Sentman, Wescott,Lyons, in review at GRL, 1995]

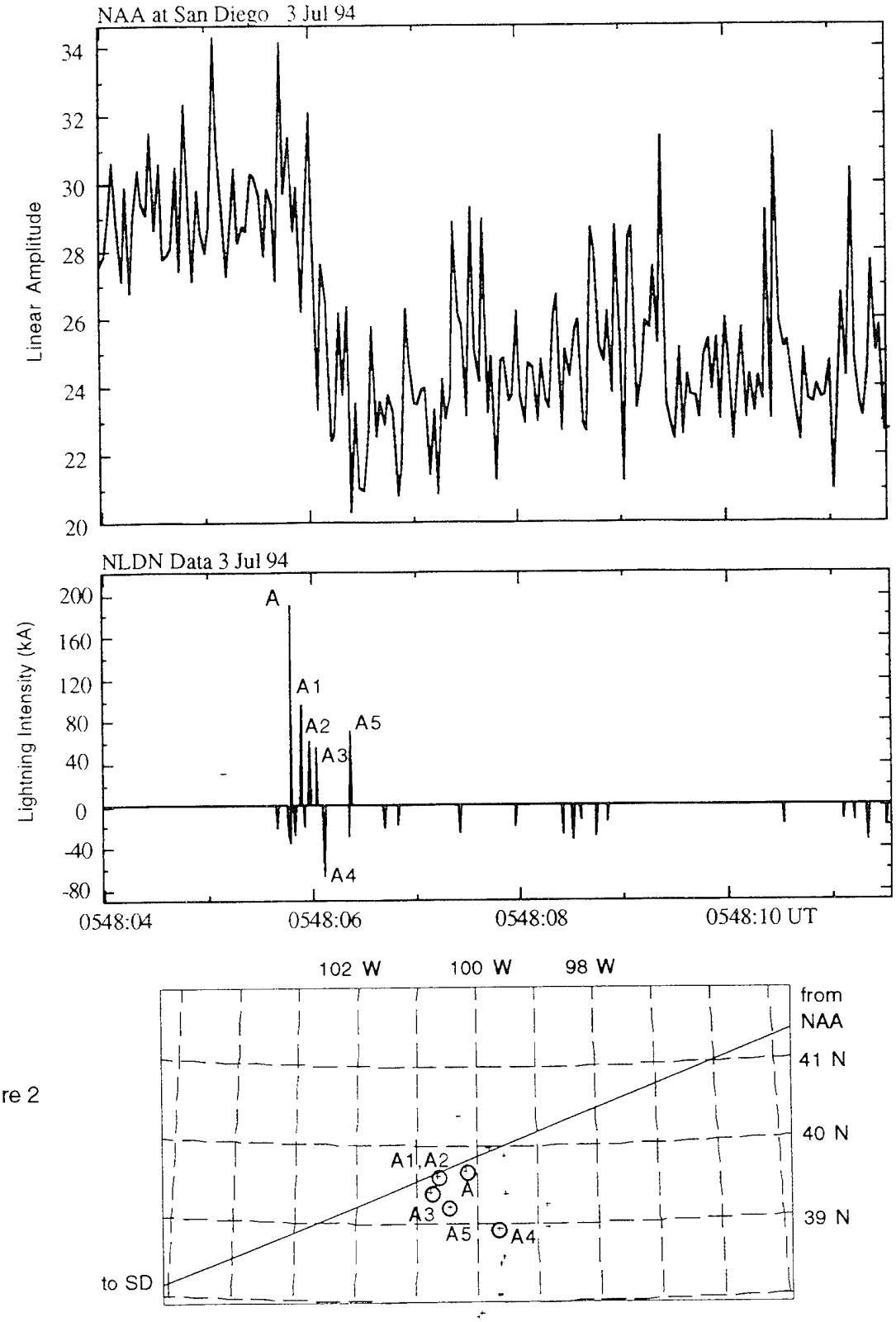
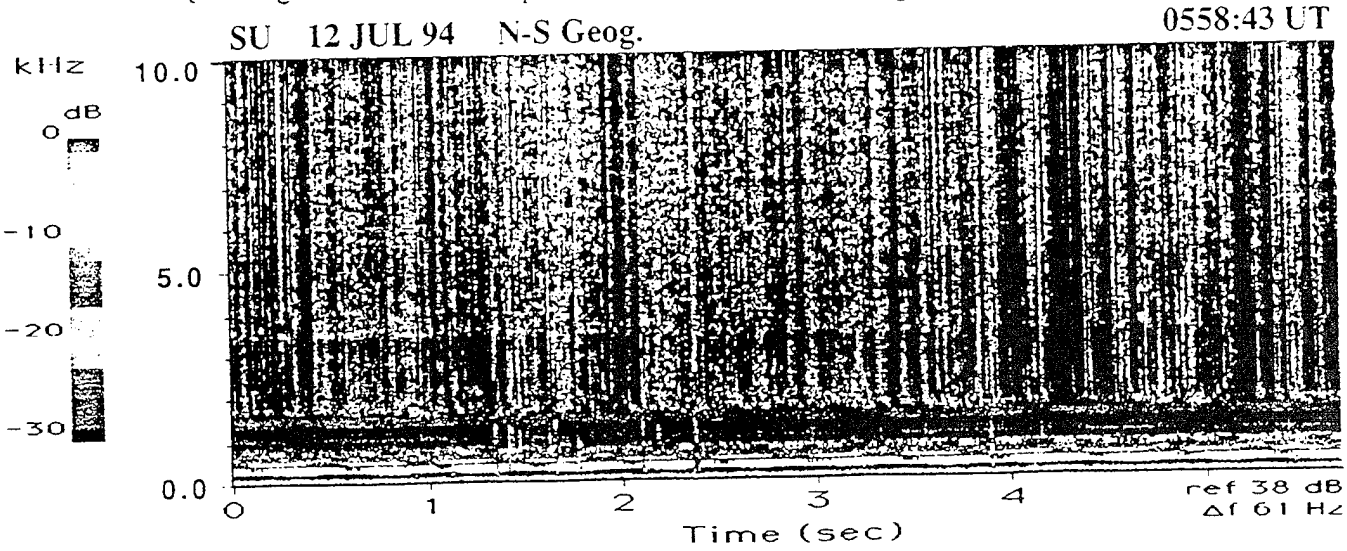
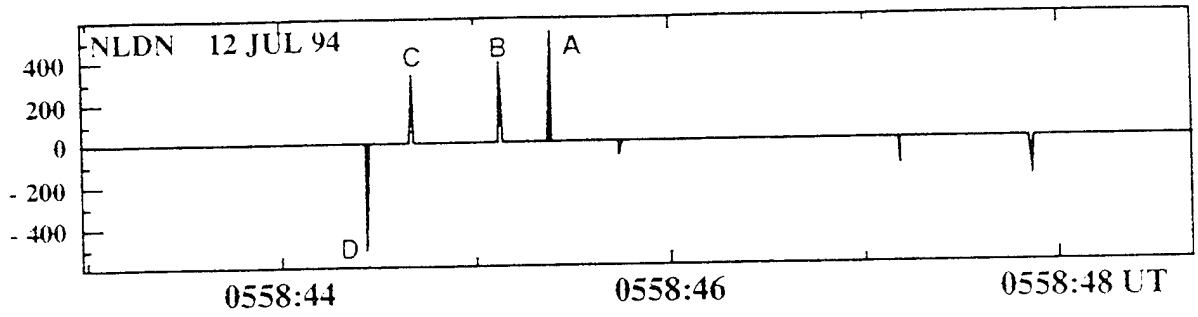


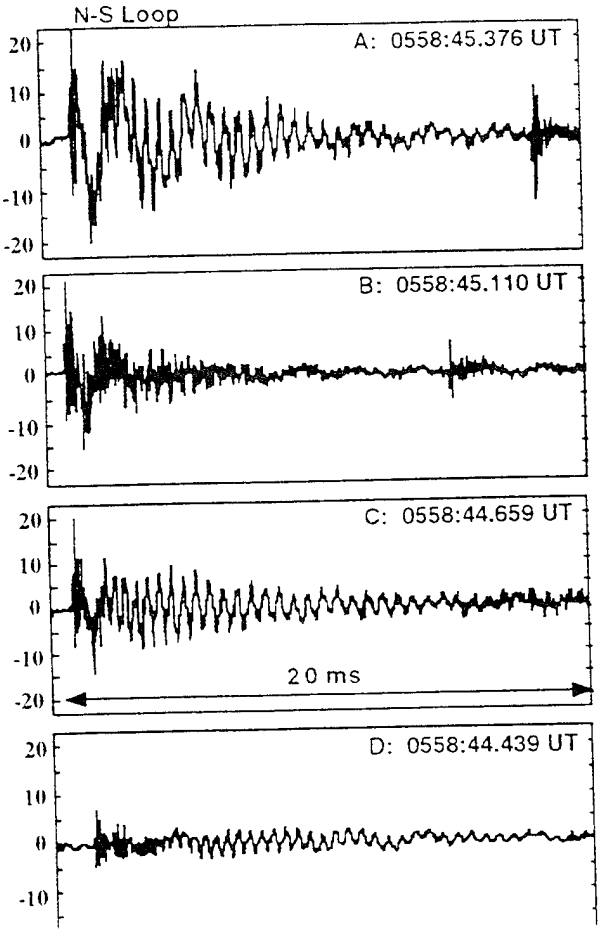
Figure 2

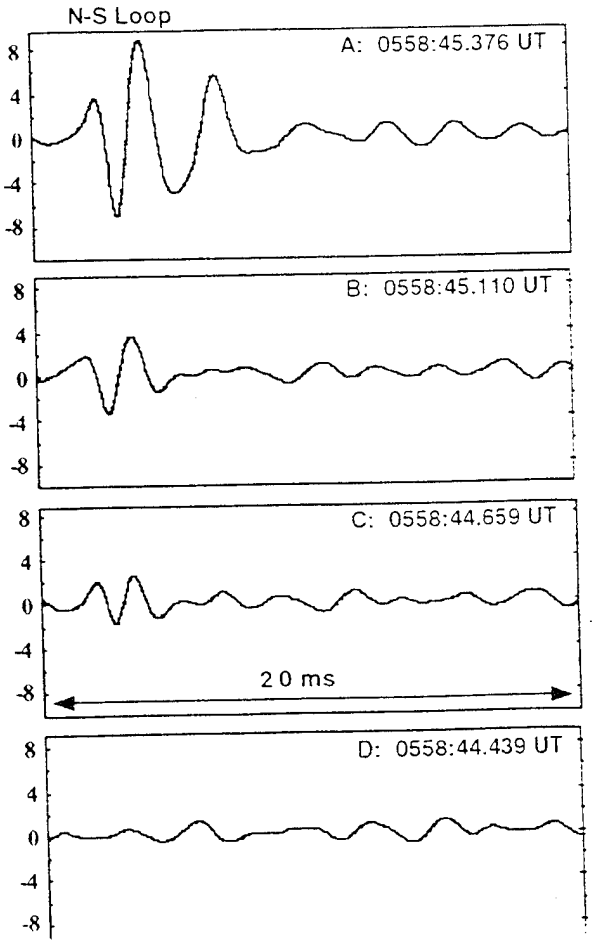
Characteristics of ELF/VLF sferics of CG lightning discharges producing sprites
from [Reising, Inan, Bell, to be presented at Fall AGU Meeting]



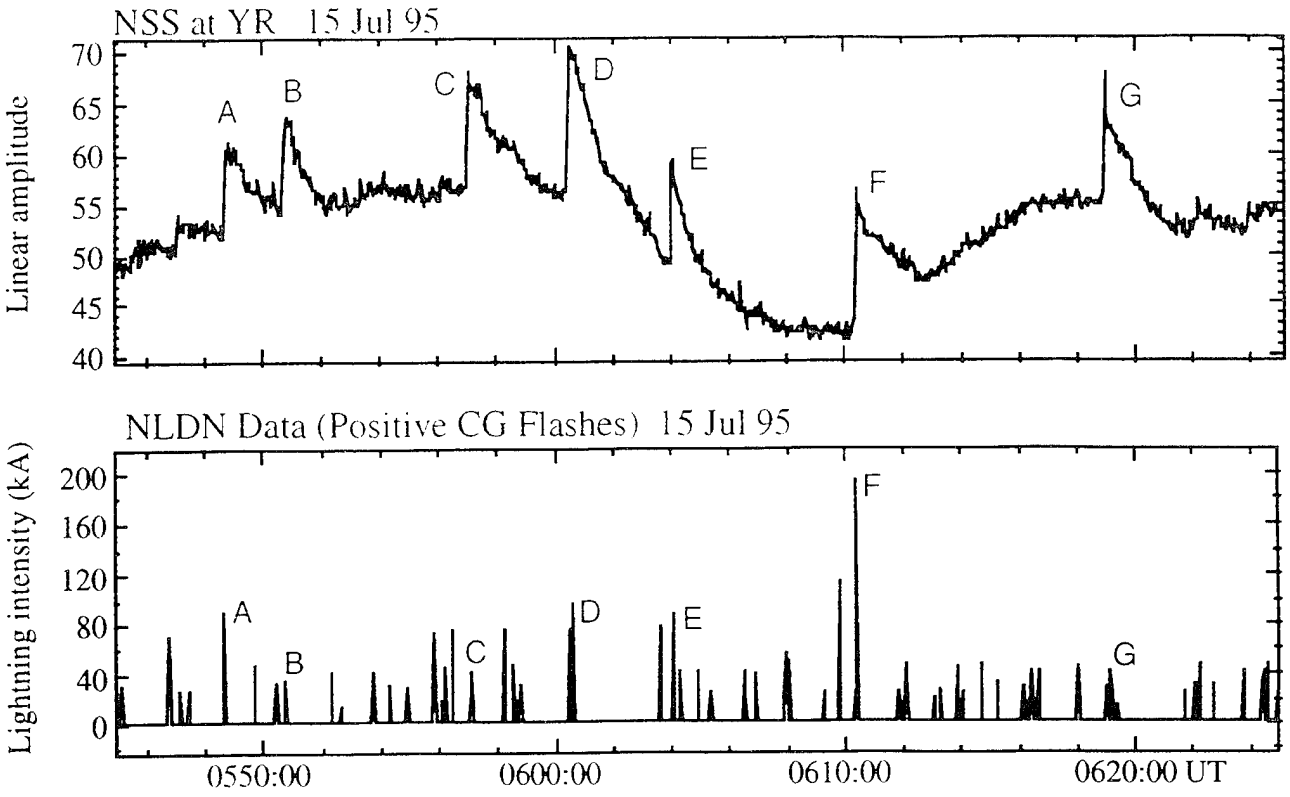


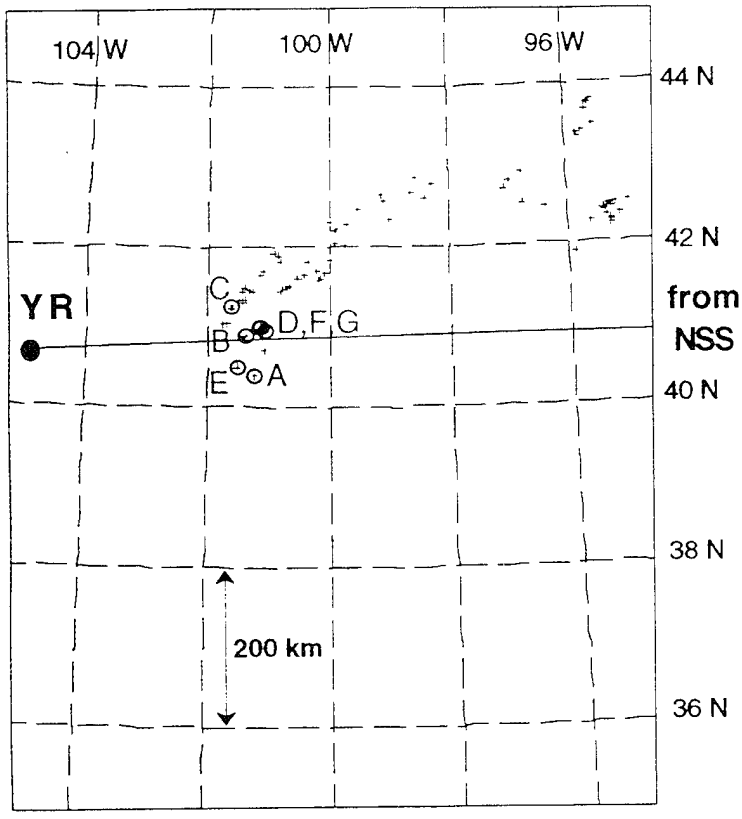






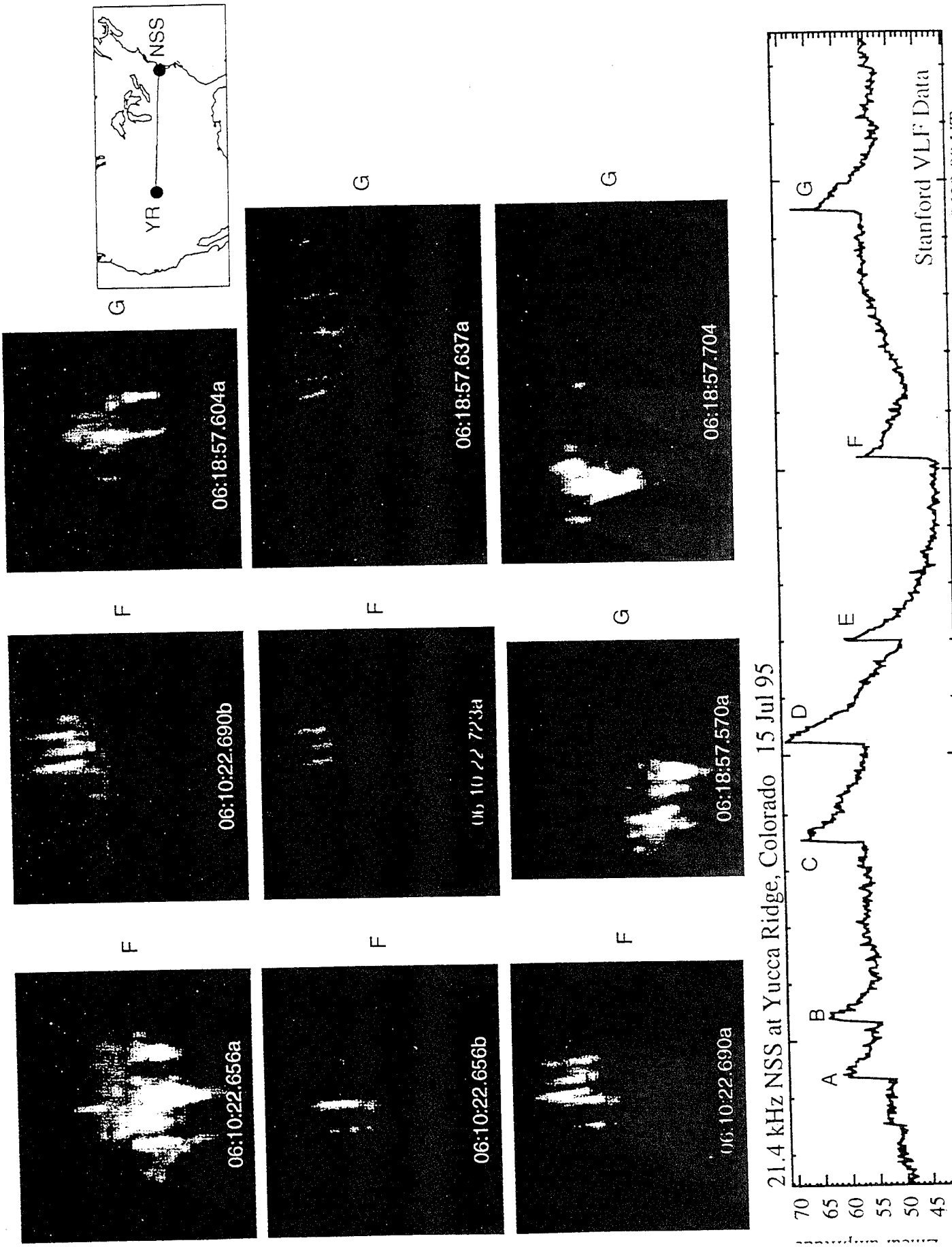
A spectacular example of association of VLF events and sprites
from [Inan, Reising, Lyons, to be presented at Fall AGU, 1995]



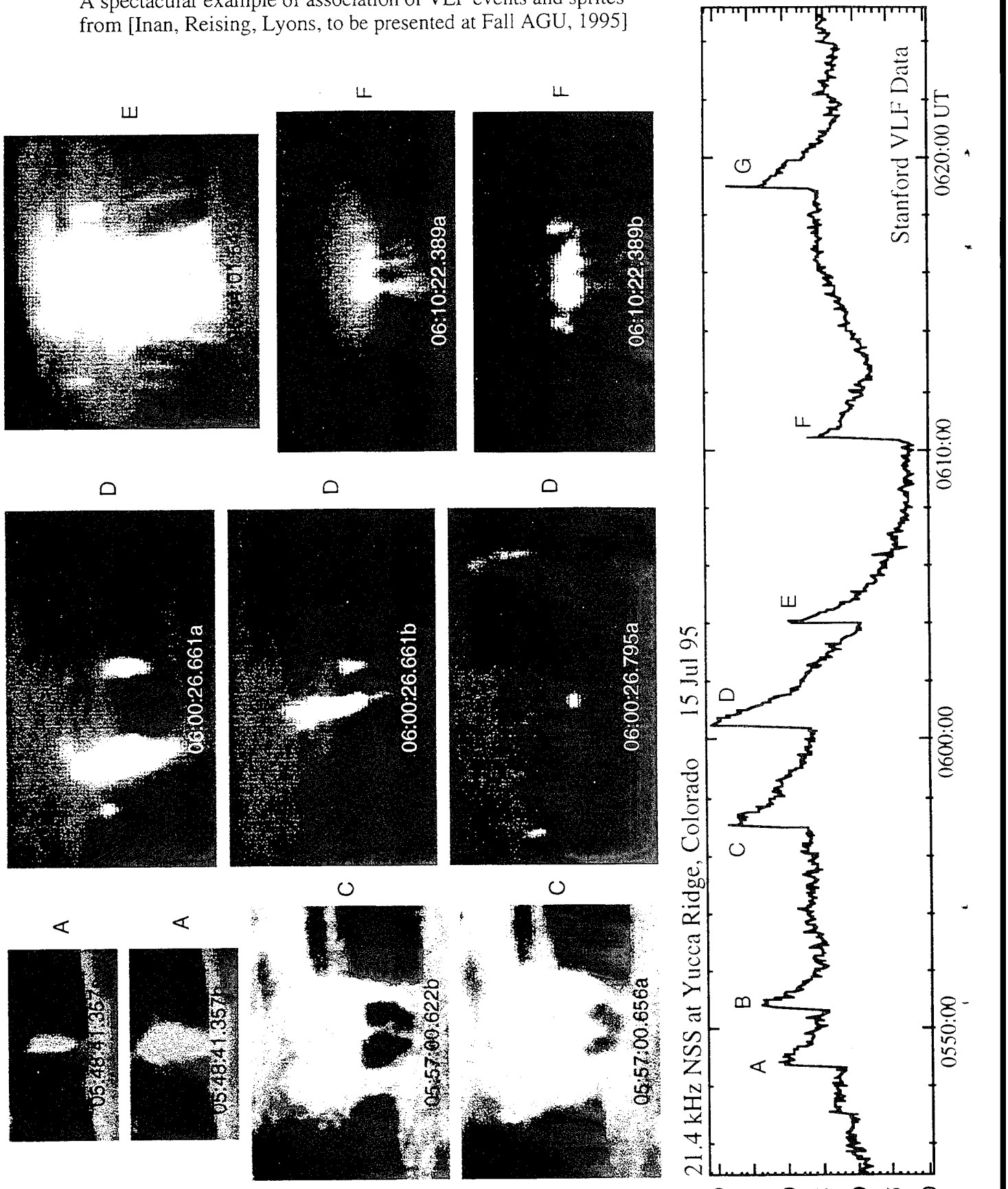


At least 6 of the 7 VLF perturbation events shown in the top panel were accompanied by well-defined, bright Sprites, as confirmed by optical ground measurements by the W. Lyons group. This figure shows the detailed association of VLF events observed on the NSS-YR signal with CG lightning discharges. The top panel shows the amplitude of the NSS (21.4 kHz) signal observed at Yucca Ridge showing seven large (> 1dB) amplitude perturbations. The positive CG flashes from this storm are shown in the middle panel. The CG flashes associated with the seven VLF events are denoted on the NLDN data, and the locations are shown on the map below.

A spectacular example of association of VLF events and sprites
from [Inan, Reising, Lyons, to be presented at Fall AGU, 1995]

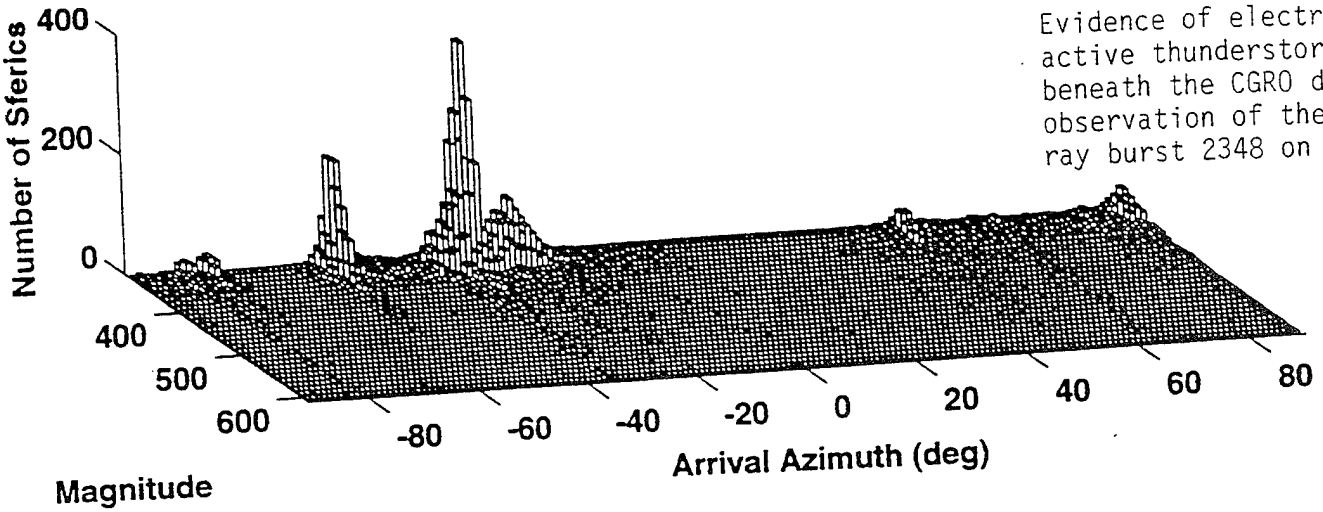


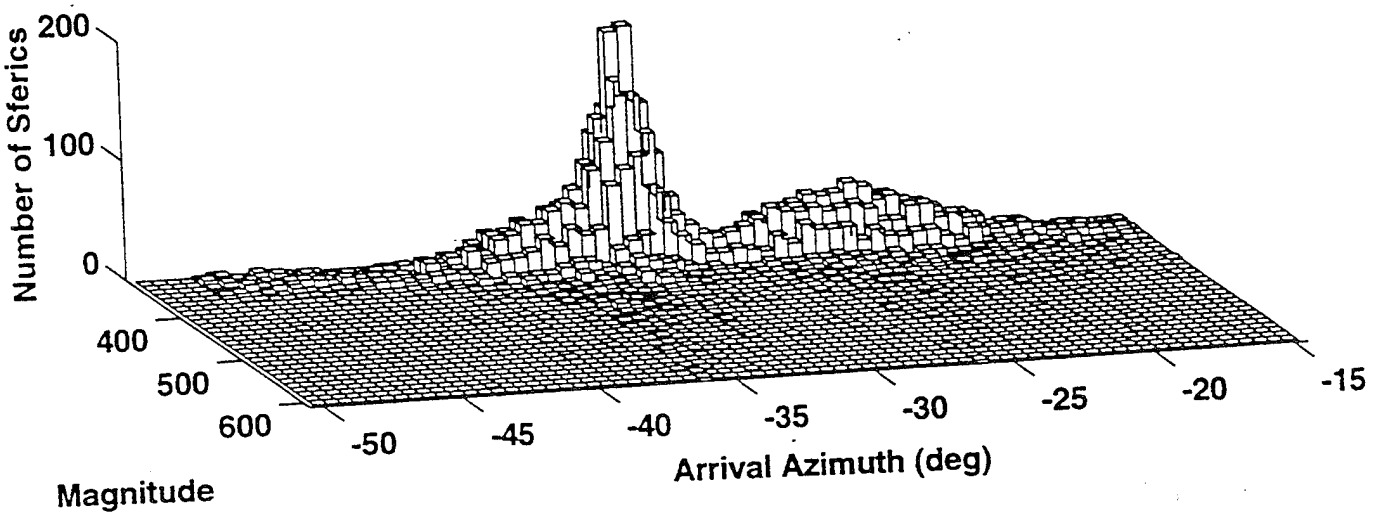
A spectacular example of association of VLF events and sprites
from [Inan, Reising, Lyons, to be presented at Fall AGU, 1995]

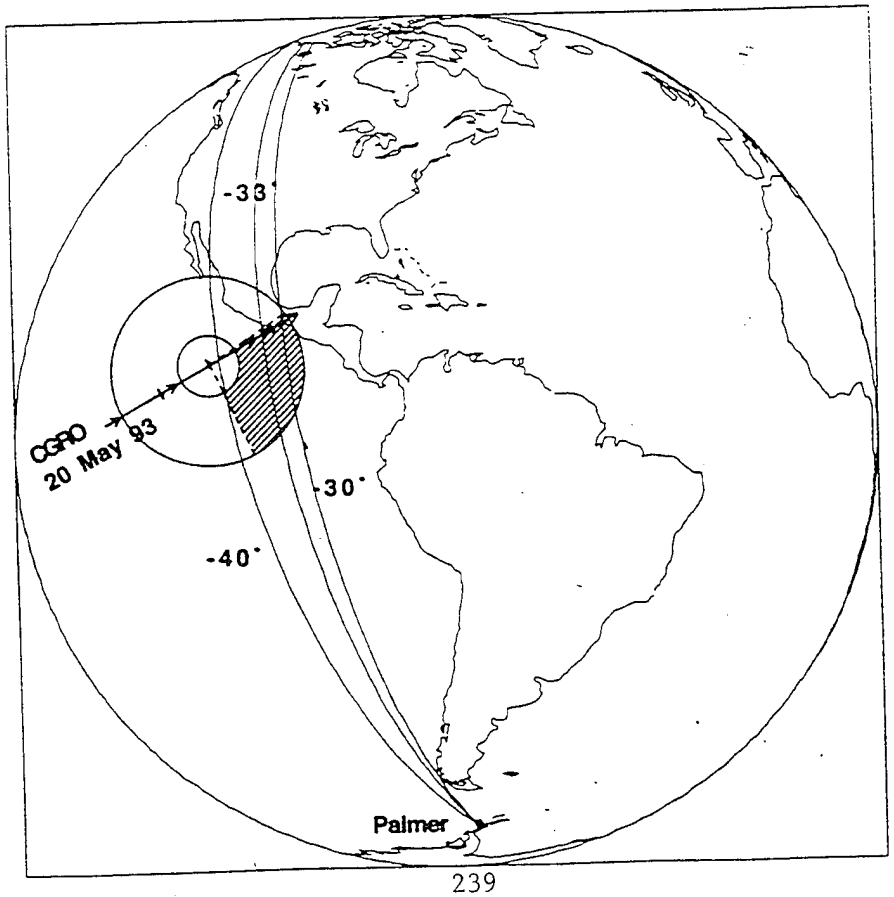


Sferic Histogram for PA, 20 May 93 0150-0220 UT, v. 3.2

Evidence of electrically active thunderstorm beneath the CGRO during the observation of the gamma ray burst 2348 on 5/20/93.

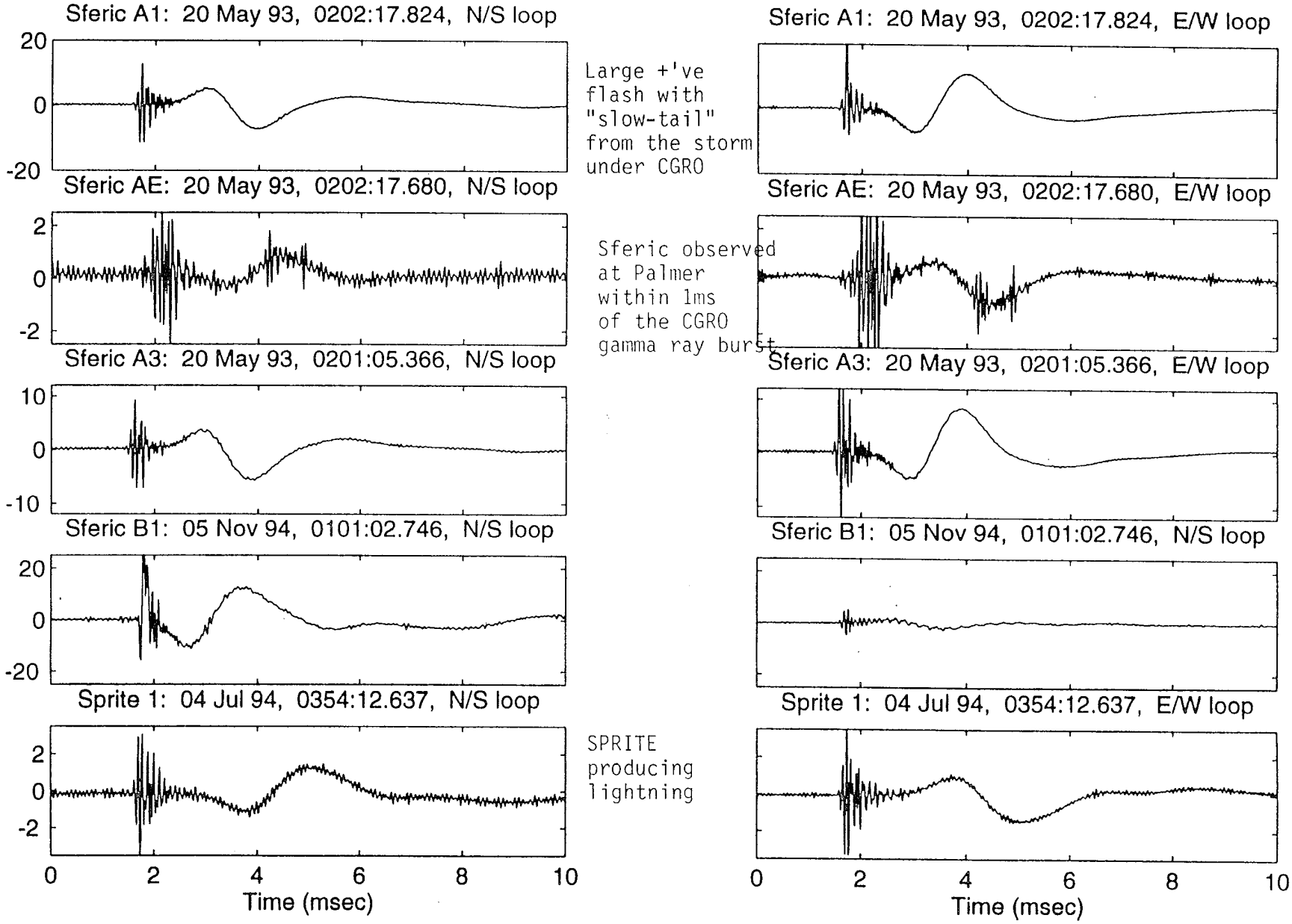






The "smoking-gun" evidence of terrestrial gamma ray burst-lightning-sprite connection

"Slow-tail" feature of these sferics as observed at PALMER STATION, ANTARCTICA indicates long enduring continuing currents



AFOSR/PL WORKSHOP ON
SPRITES AND BLUE JETS
18-19 October 1995

RF Measurements of Lightning-induced Ionospheric Effects

K. M. Groves, J. V. Rodriguez, P. J. Erickson[1]
J. M. Quinn, T. Arce[2] and M. Cox[1]

Ionospheric Effects Division,Phillips Laboratory
Hanscom AFB, MA 01731

[1]MIT Haystack Observatory, Westford MA 01886

[2]Eng. and Theory Ctr, Cornell Univ., Ithaca NY 14853

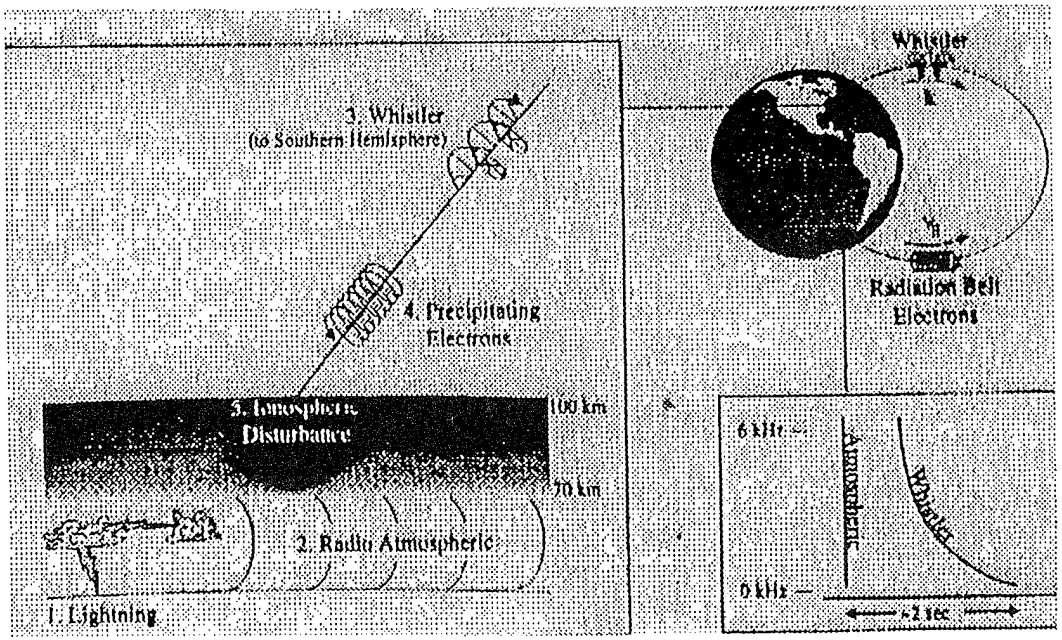
GROVES18OCT95

Outline

- **Background Motivation**
  - Recent Developments in Atmospheric Electricity ("Direct" interactions; Sprites, etc.)
- **Measurement Techniques**
  - Multi-Diagnostics Observations
    - UHF Incoherent Scatter Radar
    - VLF Receiver, VHF Radar, Others
- **Preliminary Results**
- **Summary**

Conventional Understanding of Lightning-Ionosphere Interaction

VLF Wave Generation, Whistler Wave Propagation, Subsequent Interaction and Electron Precipitation



Recent Evidence of "Direct" Interactions

- Upward Discharges (Sprites, Blue Jets)
- *D*-Region VLF Signatures: Heating, Ionization
- *F*-Region Wave Turbulence (Heating, E-fields, Irreg.)
- Excited Optical Emissions
- Link to Large Scale Structuring (e.g. Spread F)



[Sentman et al., 1995]

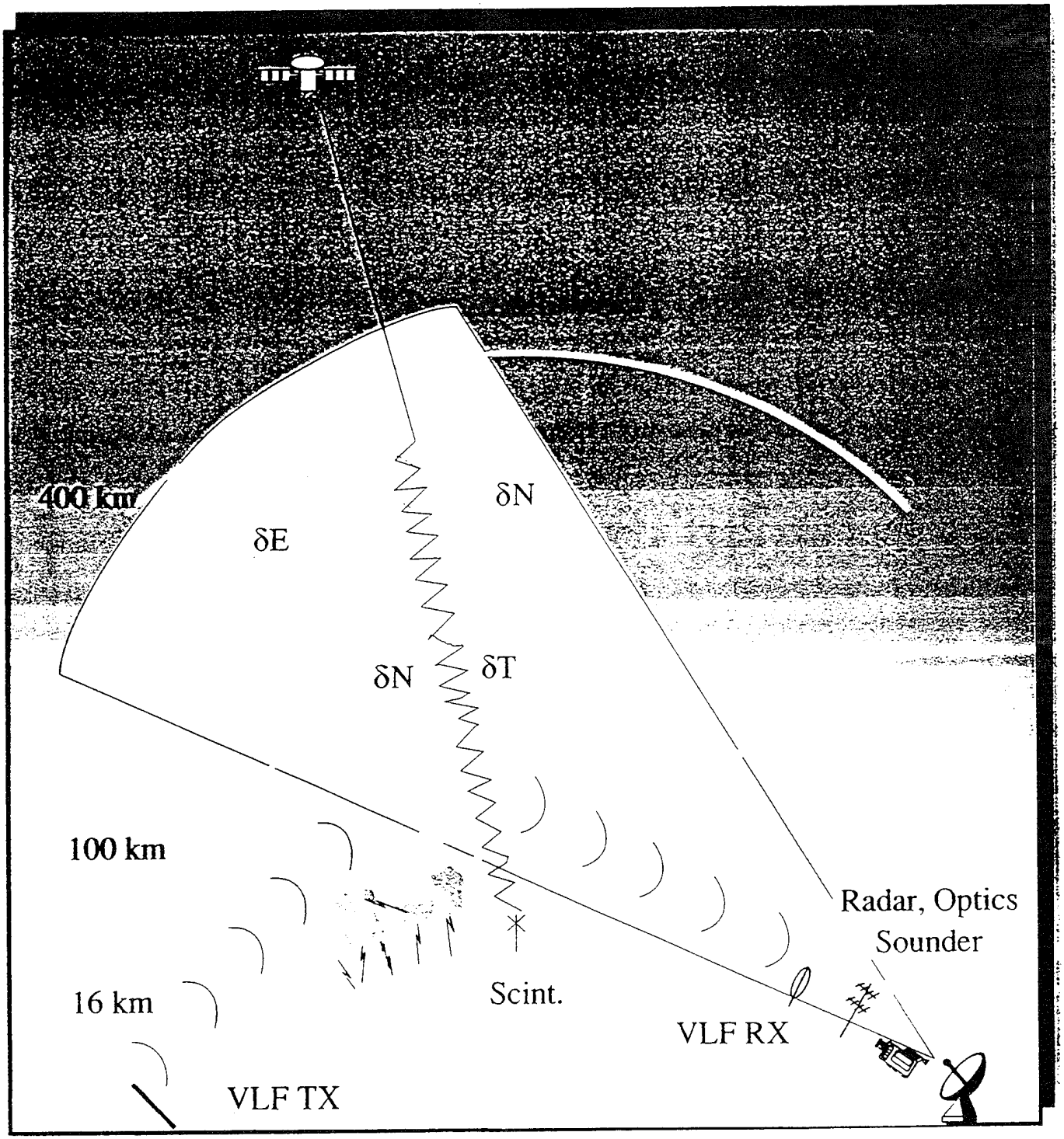
Potential Lightning-Induced "Direct" Ionospheric Effects

Effect	Estimated		Region Affected	Diagnostic(s)
	Magnitude	Duration		
Heating	10s-100s K	1-1000 ms	D, E, F	VLF, Radar
Ionization	10^2-10^4 /cc	> 10 sec	D	VLF, Radar
Plasma Waves	10s mV/m	1-10 ms	E, F	Radar
Optical Emission	10-50 kR	1-5 ms	D	low-light video
Irreg. Formation	???	>100 sec	F	Scintillation
Spread F	???	>100 sec	F	Digisonde
Accel. Part.	> 10 eV	1-1000 ms	D, E, F	DMSP

Lightning-induced Ionospheric Effects (TRUTH95) Diagnostics

- **Millstone Hill 440 MHz Incoherent Scatter Radar**
  - 2.5 MW Peak Power; 150' Steerable Dish (43 dB gain)
  - *D, E, F* region Plasma Parameters
- **VLF Receiver System**
  - *D* region Perturbations
  - Three Channel Phase/Amplitude; Multiple Simultaneous Paths
- **PL 50 MHz Coherent Backscatter Radar**
  - 50 kW Peak Power; Fixed Yagi Antenna Array (17 dB gain)
- **Additional Diagnostics**
  - Low-light Video; Digisonde; National Lightning Detection Network (NLDN)

TRUTH95
Measurements Concept



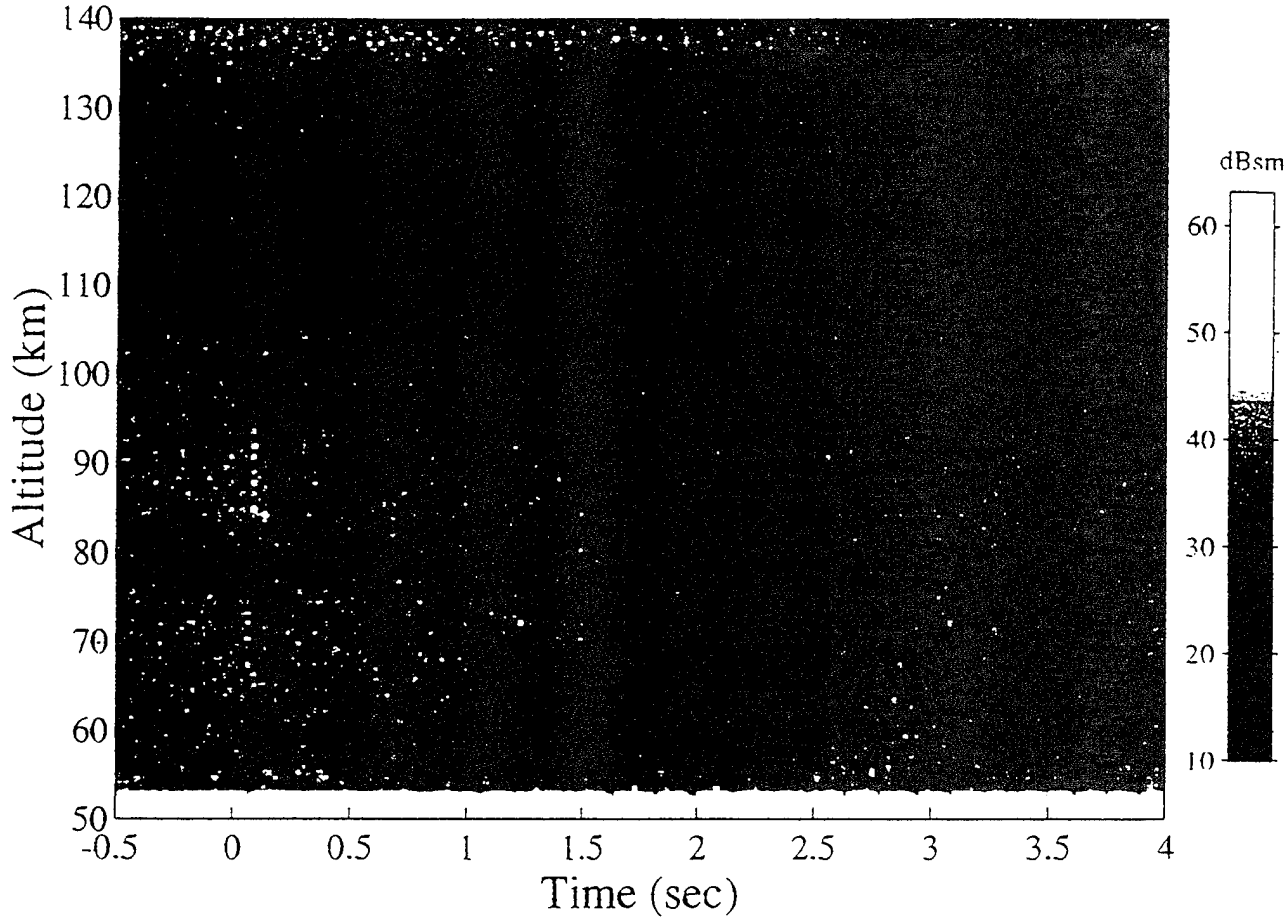
TRUTH95
Preliminary Results

- MHR Data Collected on 8 Days; 3 Days Analyzed
  - 39 Positive CG Events observed with UHF Radar to date
  - Satellites/ambiguous returns
  - Peak currents below nominal Sprites threshold (~50 kA)

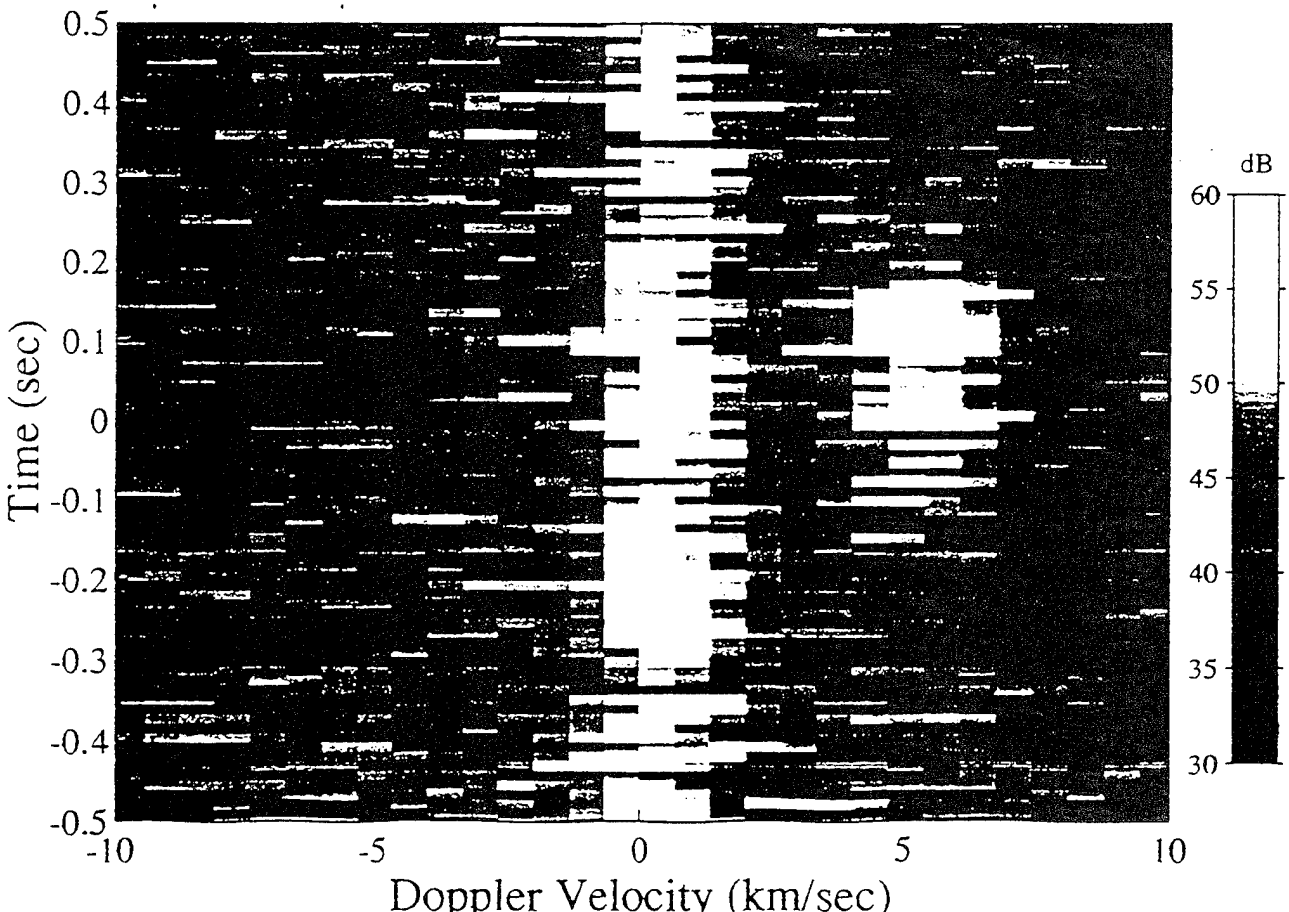
- VLF Signatures Confirm Direct Lightning Interactions

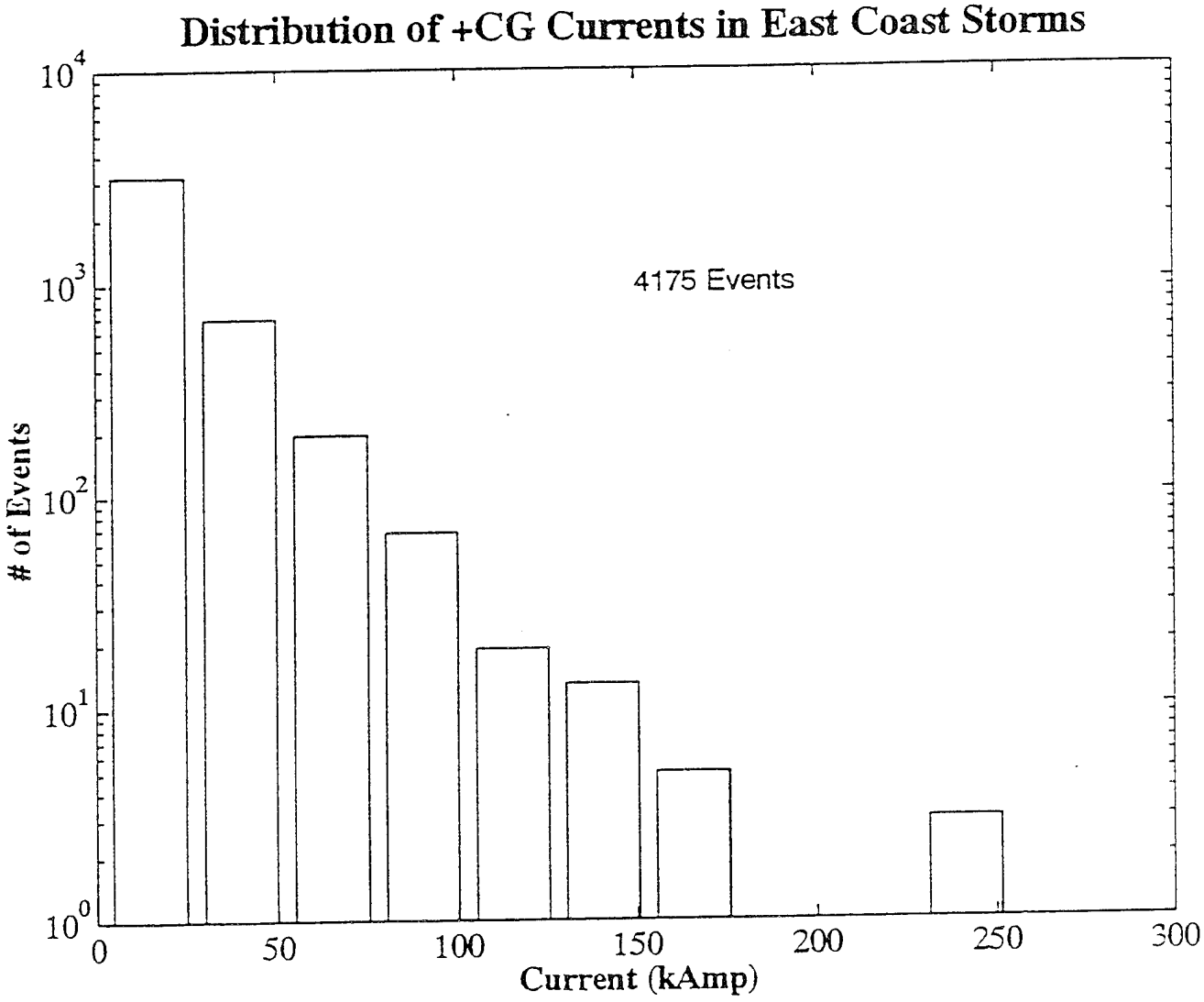
- Interference Issues with VHF Radar
  - Effective noise floor increased by ~6dB

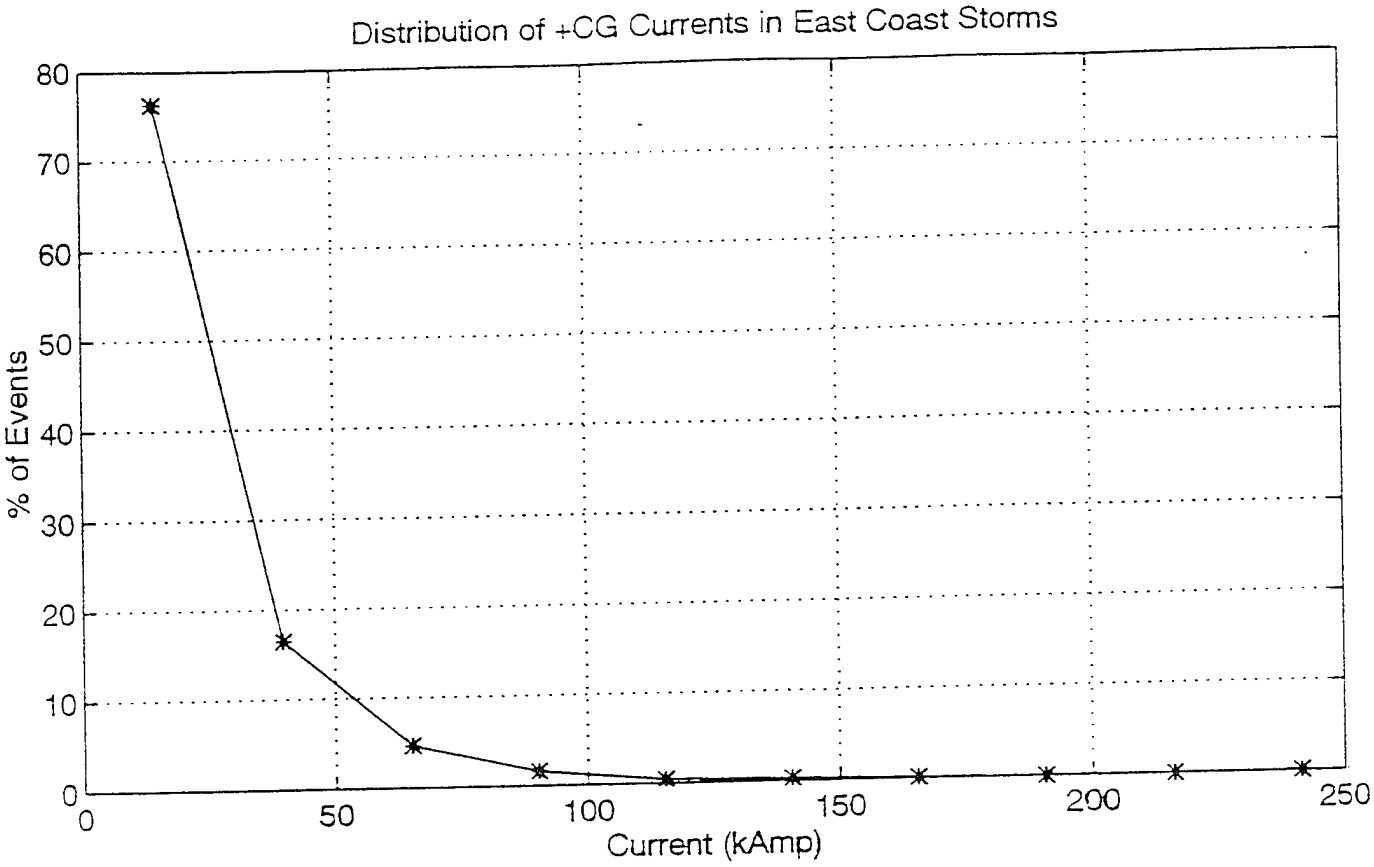
Millstone UHF 27 July 1995

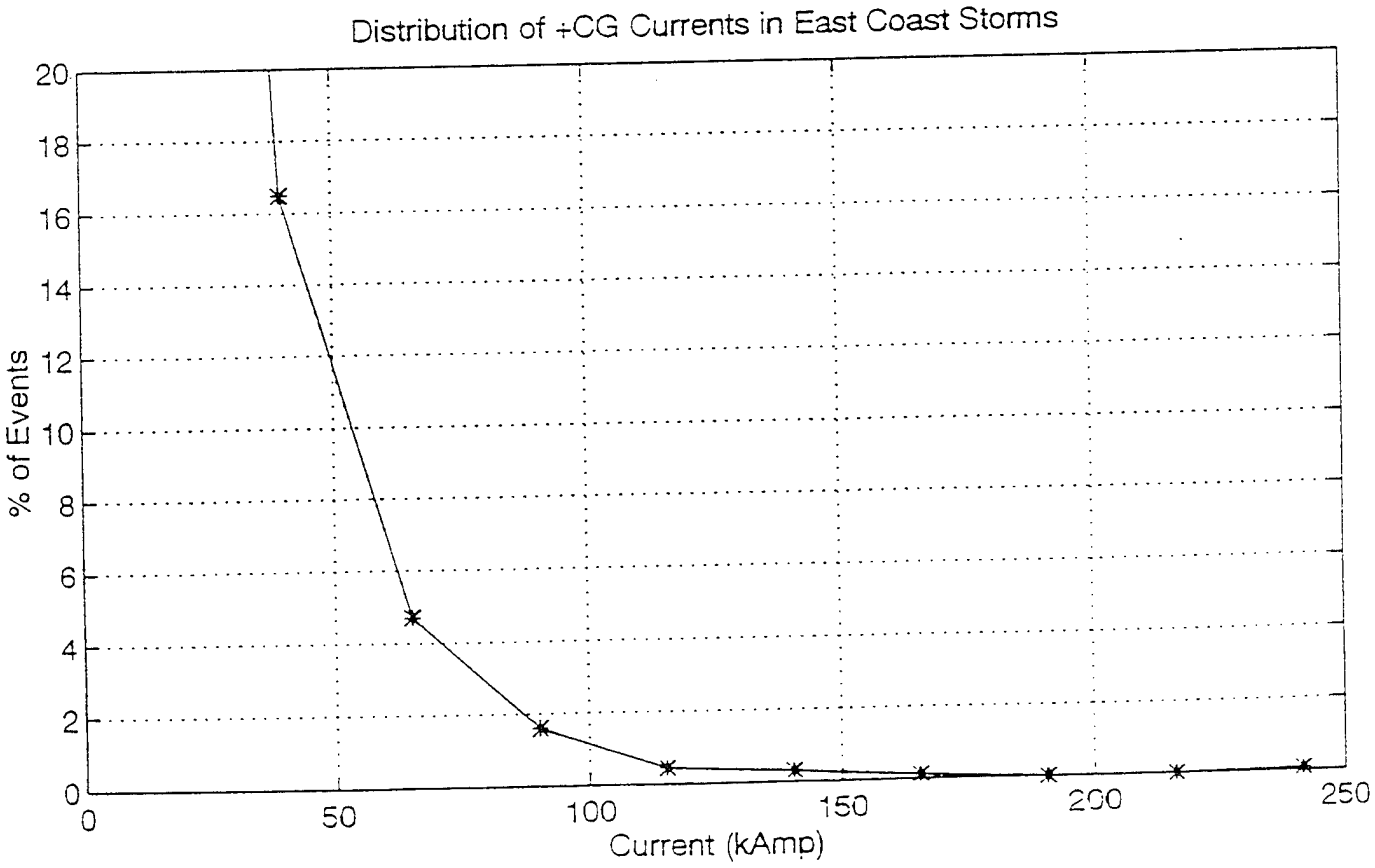


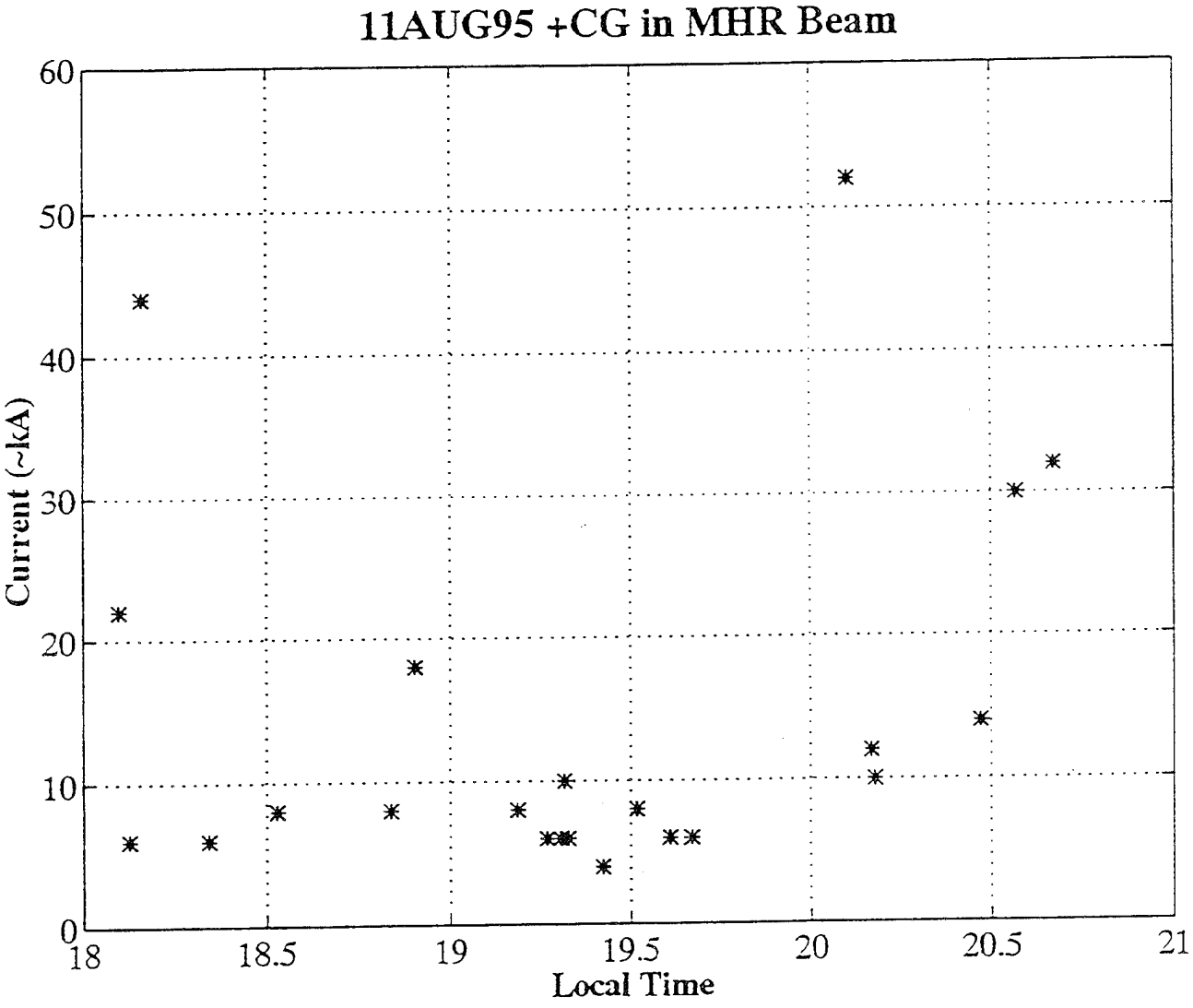
27JUL95 MHR UHF 23:16:47.8 UT

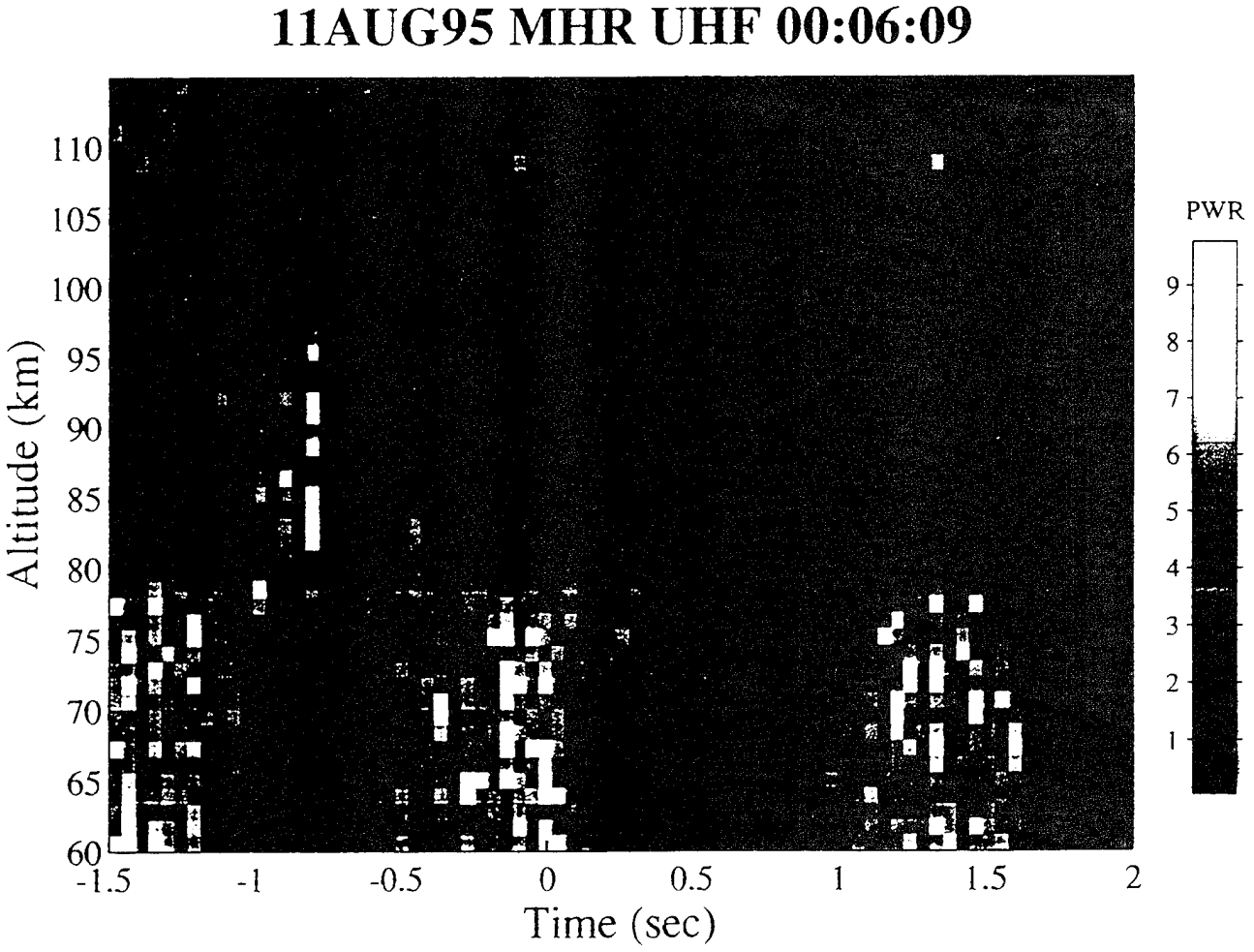



Distribution of +CG Currents in East Coast Storms
4175 Events
# of Events
Current (kAmp)
10^4
10^3
10^2
10^1
10^0
0
50
100
150
200
250
300

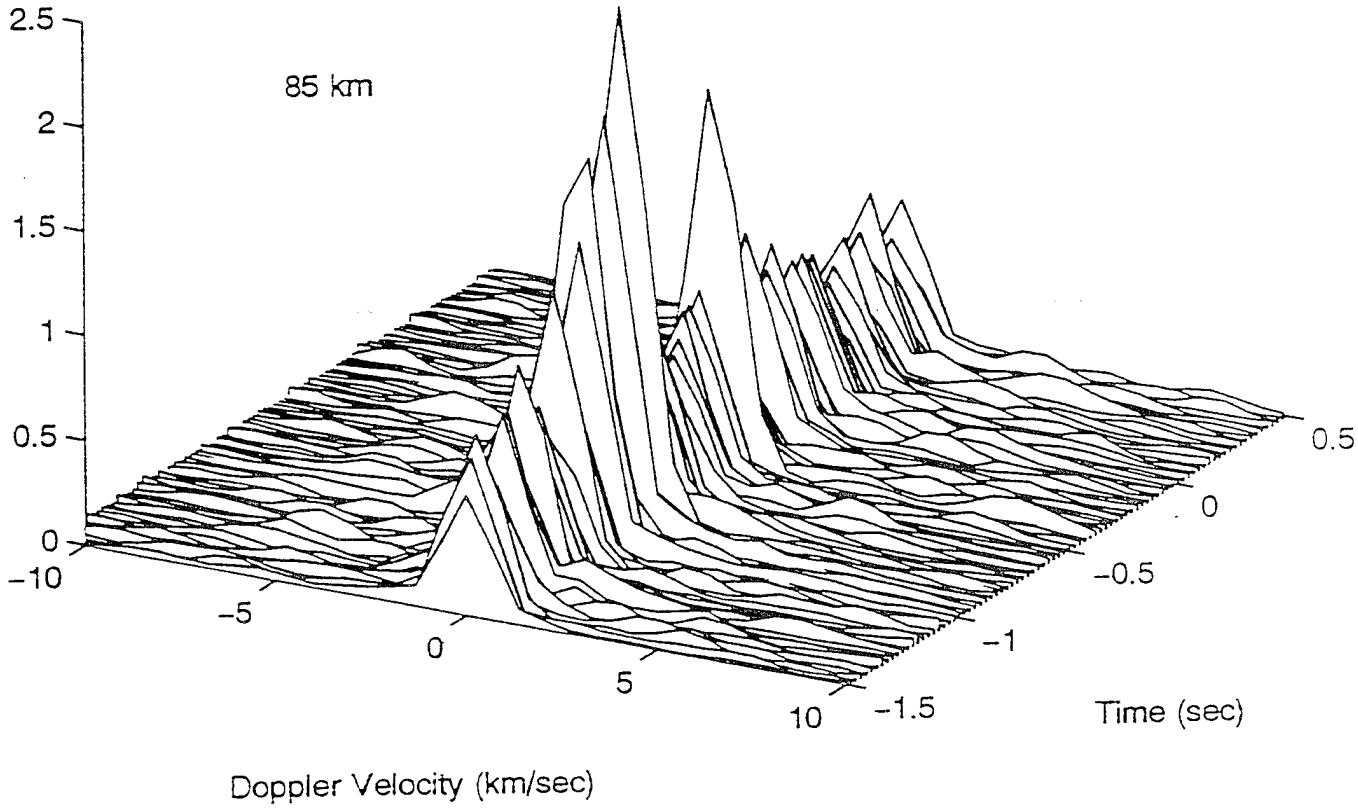

Distribution of +CG Currents in East Coast Storms
% of Events
Current (kAmp)
0
10
20
30
40
50
60
70
80
0
50
100
150
200
250


Distribution of +CG Currents in East Coast Storms
% of Events
Current (kAmp)
0
2
4
6
8
10
12
14
16
18
20
0
50
100
150
200
250


11AUG95 +CG in MHR Beam
Current (~kA)
Local Time
0
10
20
30
40
50
60
18
18.5
19
19.5
20
20.5
21


11AUG95 MHR UHF 00:06:09
Altitude (km)
110
105
100
95
90
85
80
75
70
65
60
-1.5
-1
-0.5
0
0.5
1
1.5
2
Time (sec)
PWR
9
8
7
6
5
4
3
2
1

11AUG95 MHR UHF 00:06:09 UT



Summary

- Preliminary RF Study of Sprites and Associated Phenomena
  - UHF observations of weak +CG events ambiguous
  - VLF signatures confirmed
  - East Coast storms are suitable for investigation

    MORE ANALYSIS AND DATA NEEDED

- Effort Contributes to Expanded Investigation in 1996/97
  - Emphasize "Common Volume" Measurements
  - Systematic *D*, *E*, and *F* Region Observations
  - Bi-Static Measurements Planned
  - Need "Proof of Sprites" Data

PULSED RADAR INVESTIGATIONS OF RED SPRITES

Roland T. Tsunoda
Geoscience and Engineering Center
SRI International
Menlo Park, CA 94025

- Sponsored by National Science Foundation, Aeronomy Section
- Experiment: Yucca Ridge Field Station, Colorado
  Last week in July 1995
- Rationale

  (1) Ionization anomalies associated with red sprites (e.g., VLF propagation effects)

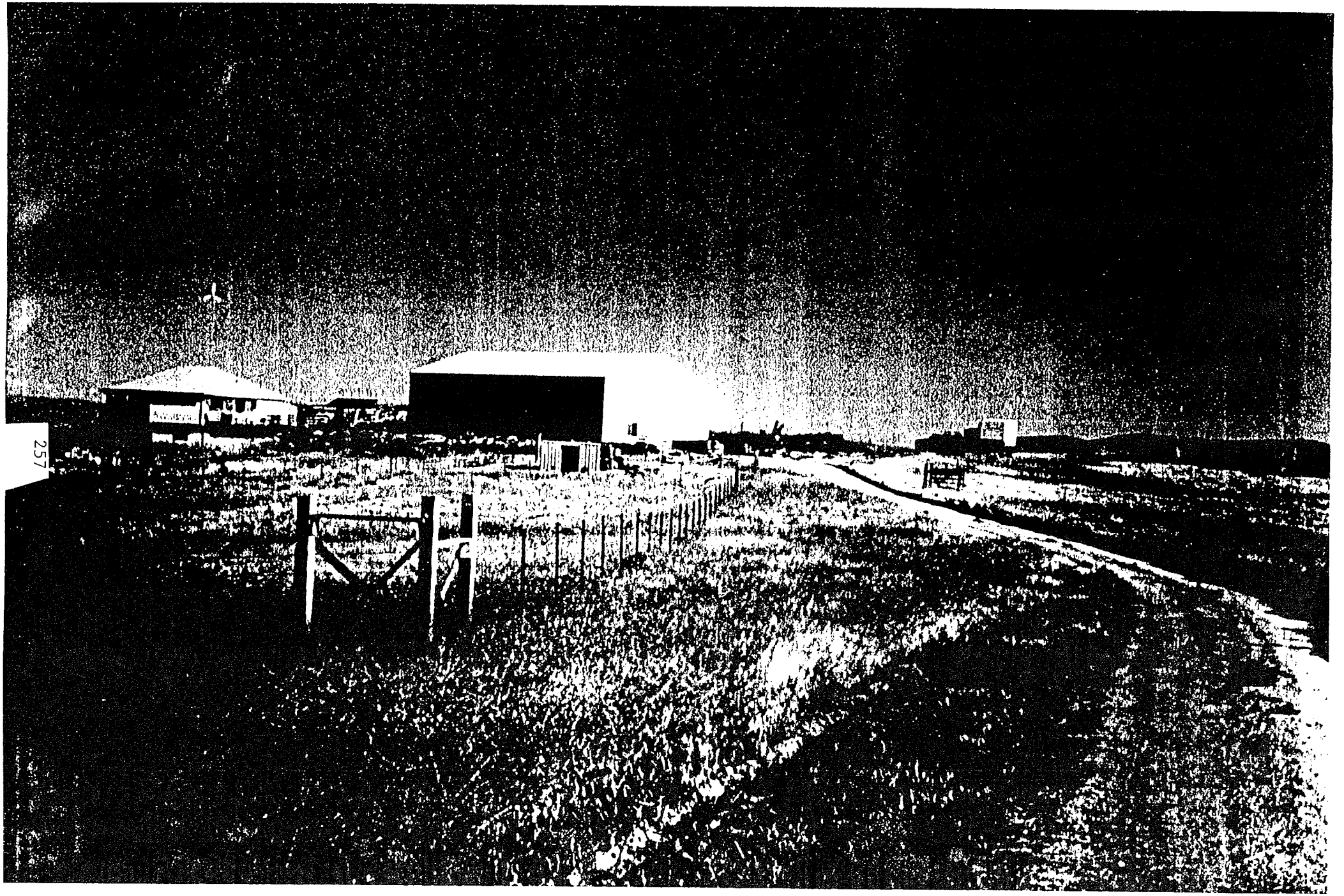
  (2) Increase in average ionization is likely to be small (e.g., $N \leq 10^4$ el/cm^3)

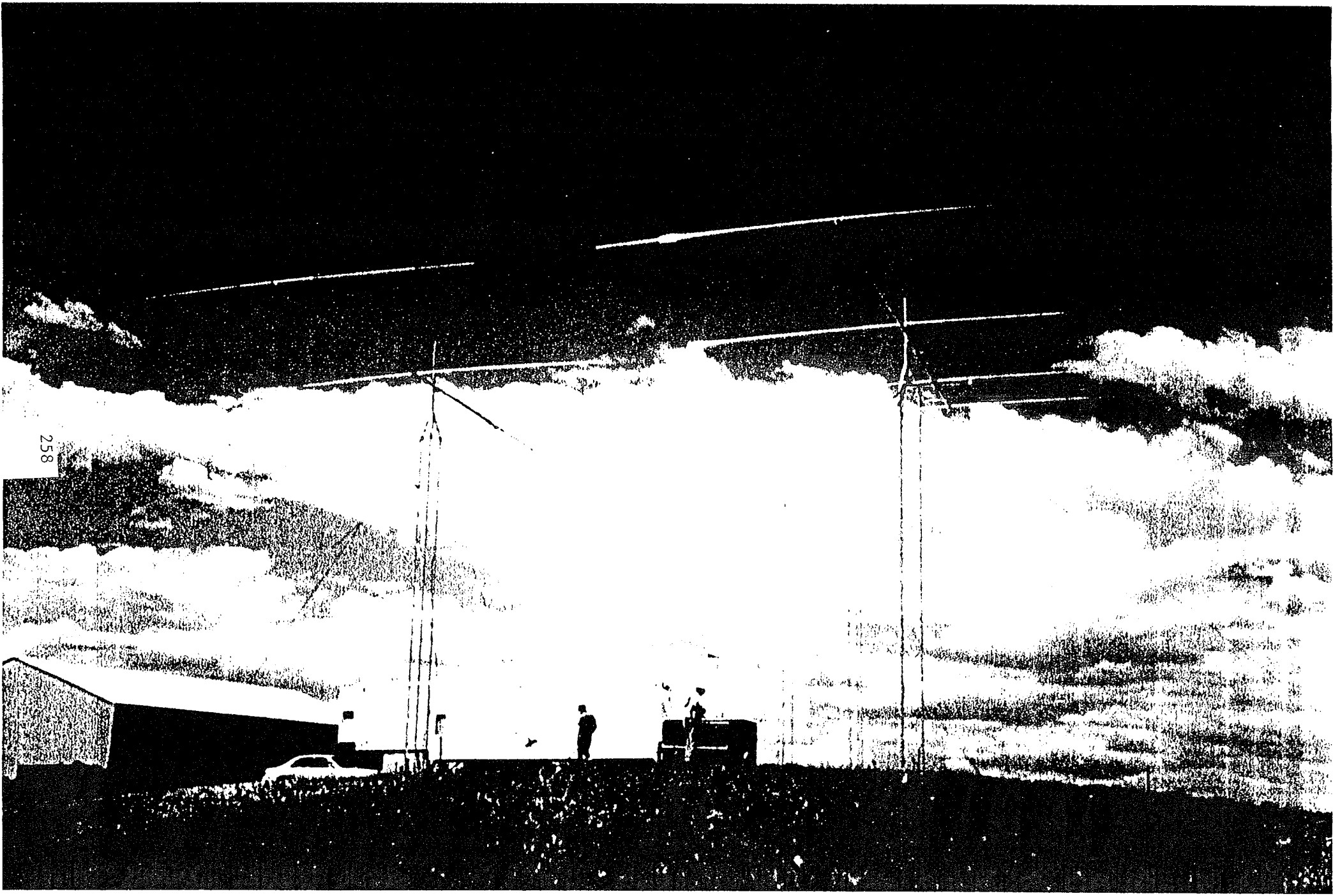
  (3) Ionization/electron heating likely to be impulsive and structured. Therefore, refractive index fluctuations could be large → Radar Backscatter

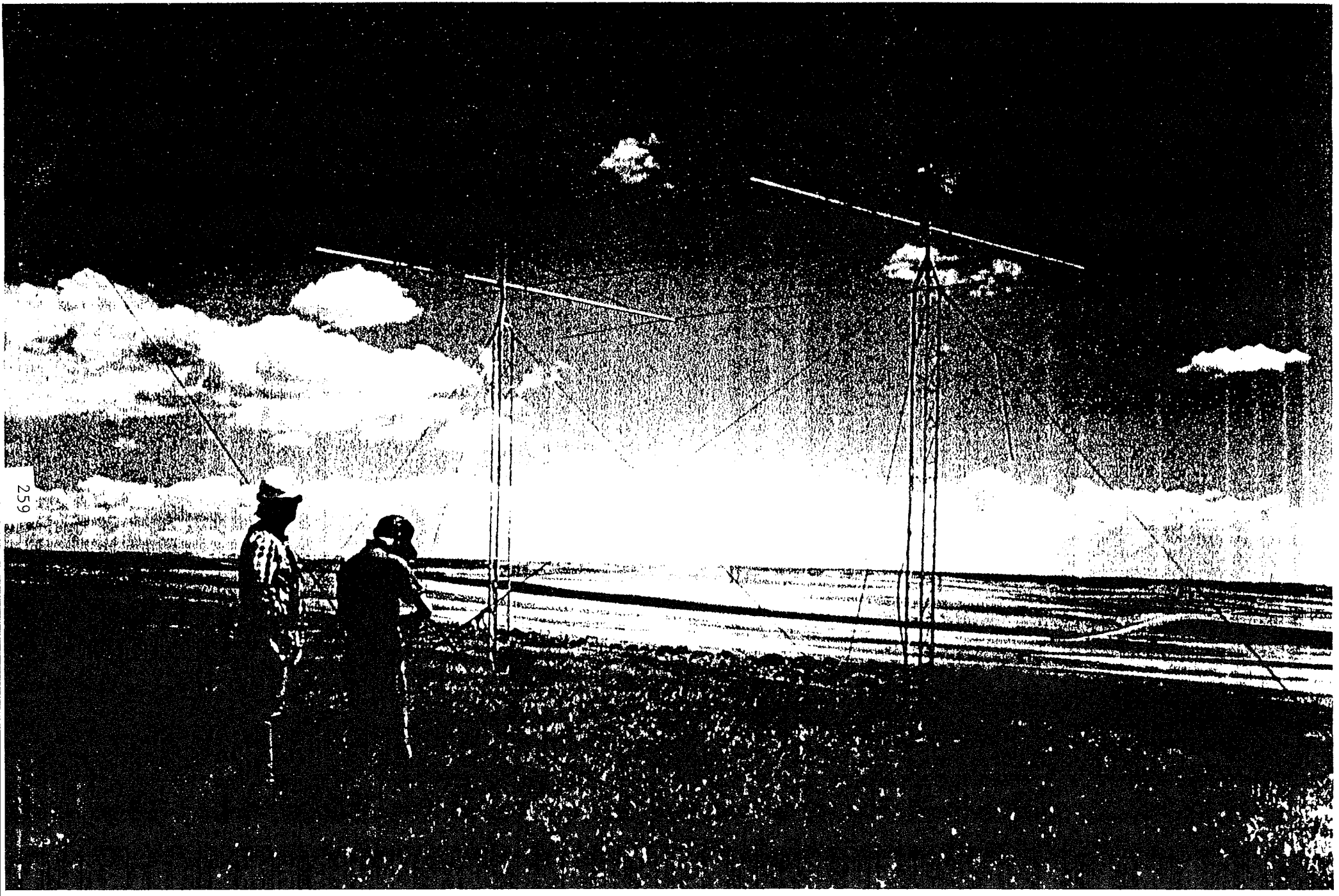
  (4) If measurable, backscatter characteristics could shed light on plasma physics associated with red sprites.

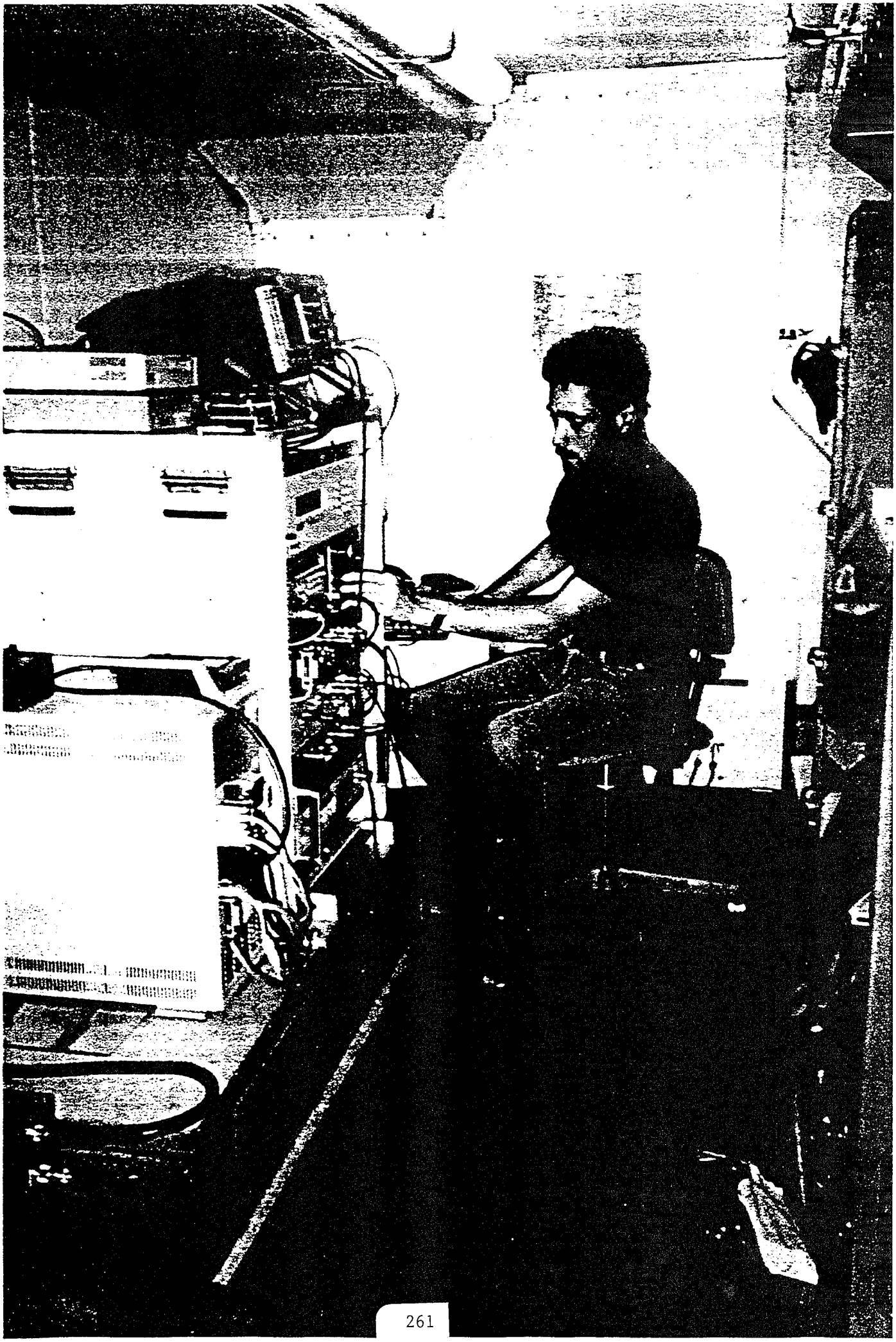
EXPERIMENTAL APPROACH

- Use SRI High-Power Frequency-Agile Radar (FAR)
  - -- Pulsed system
  - -- Frequency range: 2 to 32 MHz
  - -- Peak power: 4 × 30 kW (120 kW total)
  - -- Maximum duty cycle: 5 percent
- Reproduce Results by *Rumi* [1957]
- Make Measurements with Optical Sensors
  - -- compare and correlate radar echoes with red sprites







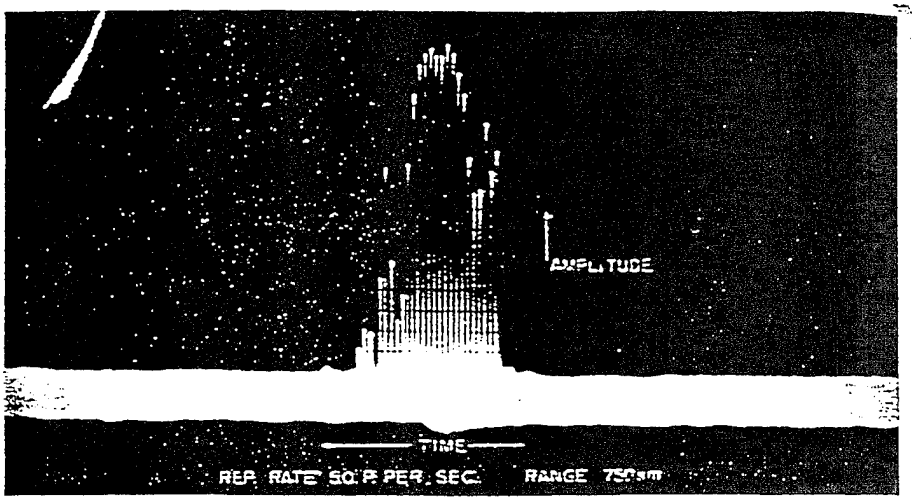


Pulsed Radar Investigations of Red Sprites

Radar Parameters	***Rumi* [1957]**	**SRI**
Radar frequency (MHz)	27.85	24.515
Peak power (kW)	200	30
Pulse width (μs)	40	60
PRF (s^{-1})	50	100
Antenna	Vee	two 4-element Yagi

Radar Echo Characteristics obtained by *Rumi* [1957]

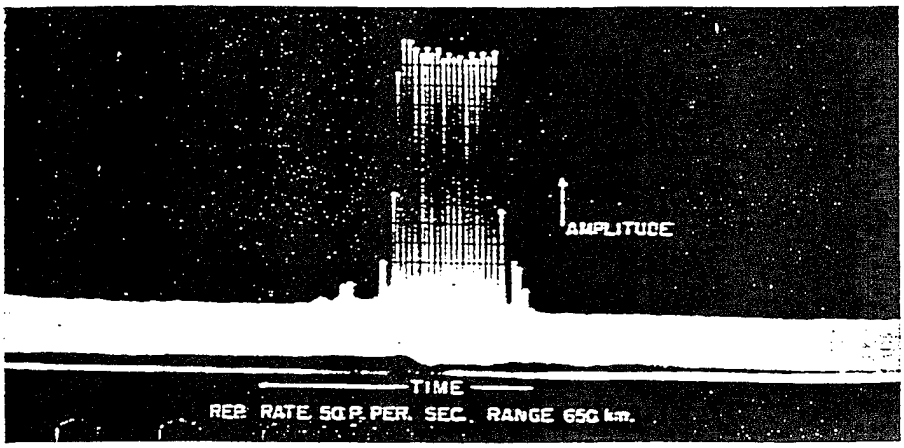
- Echoes are discrete and last less than 0.5 s
- Echoes show no preferred range, out to 900 km
- Rise times (noise level to maximum) in 40 ms
- Decay times (from at least 7 dB SNR) in 100 ms; not exponential
- Sometimes have tendency to recur at the same range
- Occurrence favored ±1 hour around midnight
- As many as 400 echoes occurred in 1 hour
- Occurred on more than half the nights during September-November 1955 (very few occurred in December)
- No correlation found with any known phenomena was established



Range = 750 km
PRF = 50 s^{-1}

ECHO 156—Radar echo obtained at Ithaca, New York, on 27.55 Mc/sec, October 21, 1955, 2310-2415 hours EST

Echo 150 is typical, not only for the steep rise, but also for the very flat horizontal top. It has to be emphasized that no saturation is limiting the amplitude. Indeed, the little rise at the left of the top indicates that there is still a possibility of increasing amplitude. Furthermore, a comparison with Echo 156 will show that larger pips with the same noise level can be recorded.



Range = 650 km
PRF = 50 s^{-1}

ECHO 150—Radar echo obtained at Ithaca, New York, on 27.55 Mc/sec, October 21, 1955, 2310-2415 hours EST

from Rumi [1957]

QUICK-LOOK RESULTS

- RADAR ECHOES WERE OBSERVED THAT SEEM TO BE SIMILAR TO THOSE REPORTED BY RUMI [1957].

  1) Echo strength $\lesssim 10$ dB (SNR)

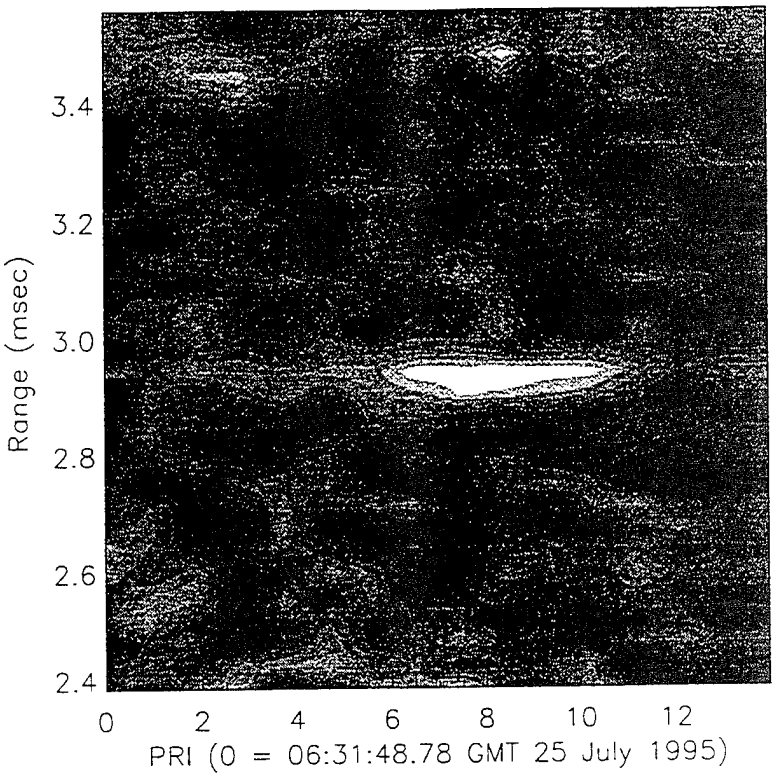
  2) Range extent $\sim 80\ \mu s$

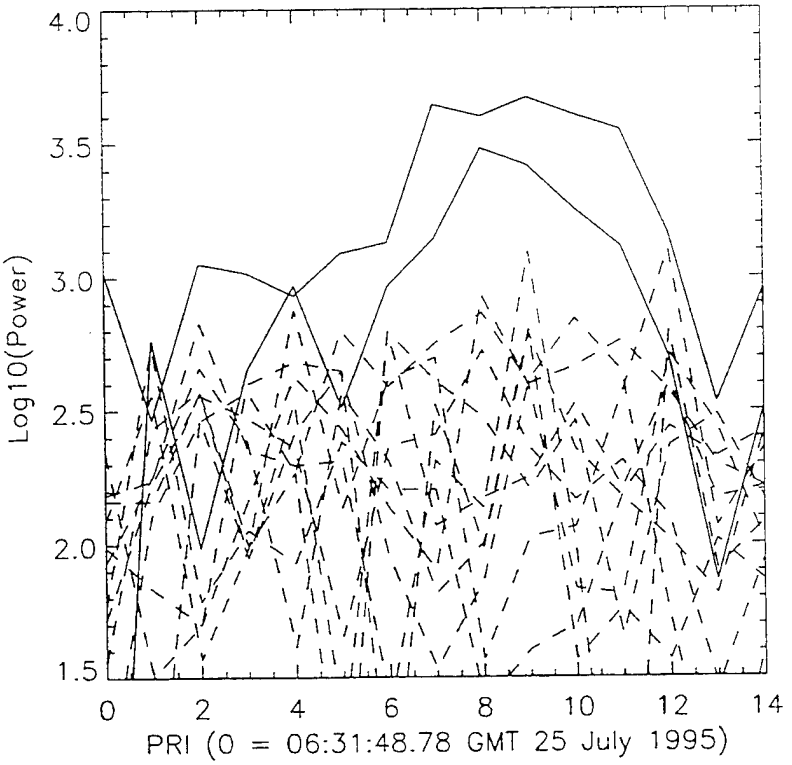
  3) Rise/fall times ~ 20 ms

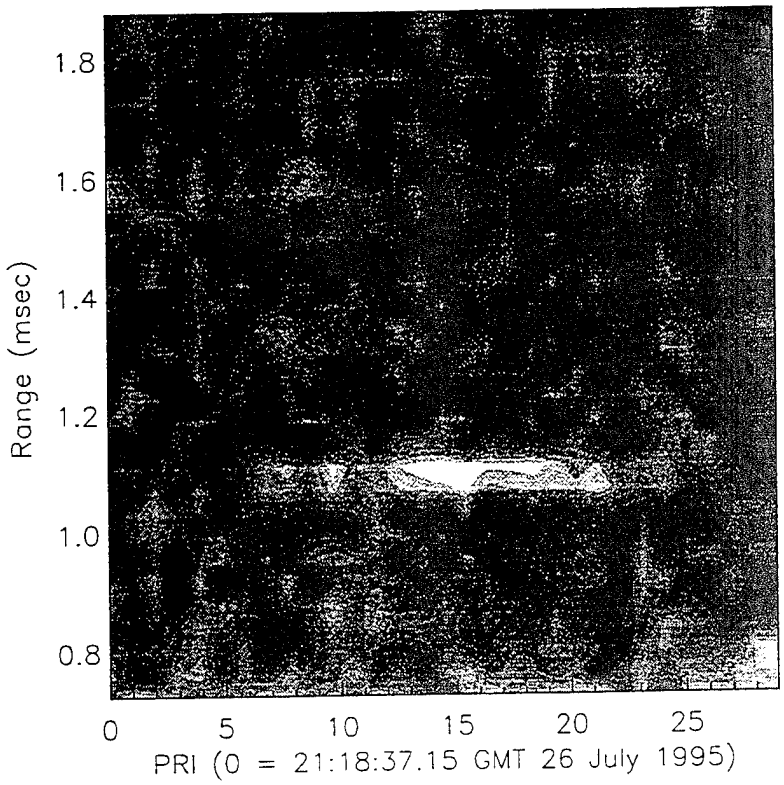
  4) Amplitude $\sim$ constant

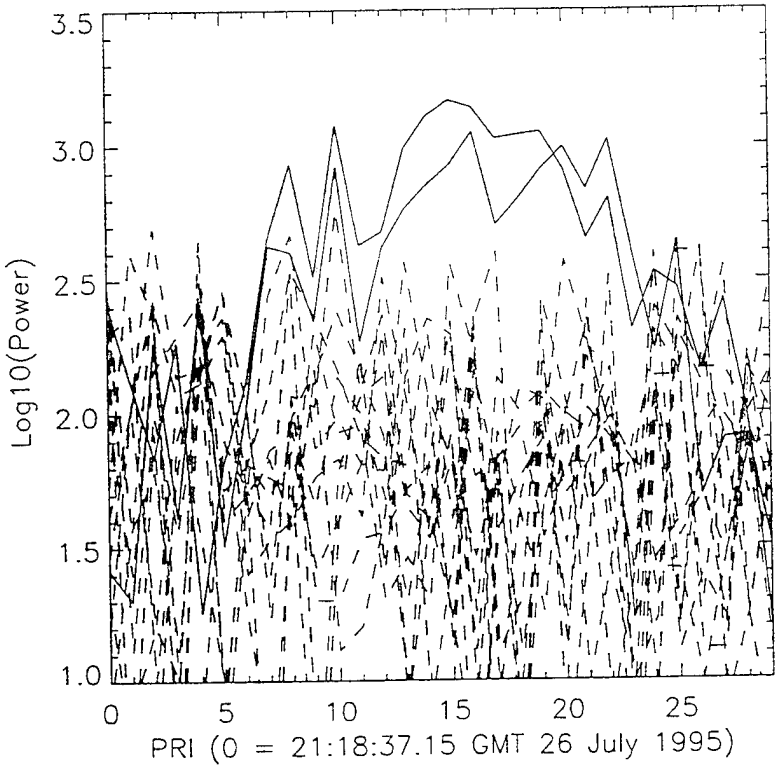
  5) Time duration: 70 - 200 ms

- RESULTS SUGGEST PRESENCE OF IONIZATION AND ROLE FOR ΔT_e


Range (msec)
3.4
3.2
3.0
2.8
2.6
2.4
0
2
4
6
8
10
12
PRI (0 = 06:31:48.78 GMT 25 July 1995)


Log10(Power)
4.0
3.5
3.0
2.5
2.0
1.5
0
2
4
6
8
10
12
14
PRI (0 = 06:31:48.78 GMT 25 July 1995)


1.8
1.6
1.4
1.2
1.0
0.8
Range (msec)
0
5
10
15
20
25
PRI (0 = 21:18:37.15 GMT 26 July 1995)


3.5
3.0
2.5
2.0
1.5
1.0
Log10(Power)
0
5
10
15
20
25
PRI (0 = 21:18:37.15 GMT 26 July 1995)

RADAR BACKSCATTER FROM RED SPRITES

In the absence of magnetic-field effects, the refractive index (magneto-ionic theory) is given by

$$(\mu - i\chi)^2 = 1 - \frac{X}{1 - iZ} \tag{1}$$

where μ and χ are the real and imaginary parts,

$$X = \frac{\omega_p^2}{\omega^2} \qquad \text{and} \qquad Z = \frac{\nu_e}{\omega} \tag{2}$$

where ω_p is the plasma frequency, ω is the angular radio wave frequency, and ν_e is the electron collision frequency. We can rewrite the real part of (1) as

$$\mu^2 = \frac{1}{2}\left\{\left[(1 - pX)^2 + (pXZ)^2\right]^{1/2} + 1 - pX\right\} \tag{3}$$

where $p = \dfrac{1}{1 + Z^2}$

For the case $X << 1$ and $Z^2 >> 1$, we have $p \approx Z^{-2}$ and $pX << 1$, and (3) becomes

$$\mu^2 \approx 1 + \frac{1}{4}\left[\frac{X}{Z}\right]^2 \tag{4}$$

Differentiating (4)

$$\Delta\mu \approx \frac{1}{2\mu}\frac{\omega_p^2}{\nu_e \omega}\left[\frac{\Delta N}{N} - \frac{\Delta\nu_e}{\nu_e}\right] \tag{5}$$

where $\omega_p^2 = 80.6N$ and N is the electron density. And from *Bostrom* [1964]

$$\nu_{en} = 1.5\times10^{-11} n_n T_e^{1/2} \tag{6}$$

$$\Delta\nu_{en} = 1.5\times10^{-11} n_n T_e^{-1/2} \Delta T_e \tag{7}$$

$$\frac{\Delta\nu_{en}}{\nu_{en}} = \frac{\Delta T_e}{T_e} \tag{8}$$

Substituting (6) and (8) into (5)

$$\Delta\mu \approx \frac{40.3}{1.5\times10^{-11} n_n} \frac{N}{T_e^{1/2}\omega}\left[\frac{\Delta N}{N} - \frac{\Delta T_e}{T_e}\right] \tag{9}$$

For the Yucca Ridge experiment, $f \approx 25$ MHz or $\omega = 1.57\times10^8$. If we assume that $N \approx 10^{10}$ m^{-3} and $n_n \approx 10^{20}$ m^{-3}, (9) becomes

$$\Delta\mu \approx \frac{1.7\times10^{-6}}{T_e^{1/2}}\left[\frac{\Delta N}{N} - \frac{\Delta T_e}{T_e}\right] \tag{10}$$

We also note that $X \approx 3.2\times10^{-5}$ and $Y \approx 4.5\times10^{-2}$ for $B = 0.4$ G.

To DO -- DATA ANALYSIS

- EXAMINE/ANALYZE LARGER DATA BASE.
- COMPARE RADAR ECHOES W/ RED SPRITES
- DETERMINE DOPPLER VELOCITIES

To DO -- NEXT EXPERIMENT

- MORE TIME OVERLAP W/ OPTICAL SENSORS
- OBTAIN ANGLE OF ARRIVAL INFORMATION
  - -- azimuth: sprite direction
  - -- elevation: altitude of echo
- TWO OR MULTI-FREQUENCY MEASUREMENTS
  - -- characterize scattering mechanism
- POSSIBLY INCREASE SENSITIVITY (i.e., Power-aperture product)

On Runaway Breakdown and Upward Propagating Discharges

Robert Roussel-Dupré, Yuri Taranenko

Space and Atmospheric Sciences
Los Alamos National Laboratory
Los Alamos, NM 87545

and

Alex Gurevich

P.N. Lebedev Institute of Physics
Moscow 117924
Russia

Los Alamos
Space & Atmospheric Sciences

Outline

- ⇨ Runaway Breakdown
- ⇨ Ingredients for an Upward Discharge
- ⇨ Models
- ⇨ Emissions
  - Optical
  - γ-ray
  - VHF Radio
- ⇨ Summary

Runaway Air Breakdown

- ⇨ Initiated by energetic (> 100 keV) electron produced by cosmic rays
- ⇨ Avalanche proceeds when $E > 218\ (N/N_0)$ kV/m
- ⇨ Formation of collimated electron beam
- ⇨ Spatial scales at high altitudes
  - Avalanche lengths ~ > 100 m - kms
  - Beam diameter ~ > 1 km - tens of kms
- ⇨ Temporal Scales
  - Beam growth ~ > 3 μs - 100 μs
  - Discharge duration ~ 100 - 150 μs

Ingredients for Upward Discharge

⇨ **Thunderstorm**

- Large Mesoscale Convective system
- High flash rate (50-60 / minute)

⇨ **Lightning stroke**

- Intracloud or Positive cloud-to-ground
- High currents (> 100 kA)
- Large charge neutralization (> 100 C)

⇨ **Low upper atmospheric conductivity**

- Electrical relaxation time > 10 ms up to 70 km altitude

Models of Upward Discharges

- 2-d hydrodynamic model
  - Primary electrons, secondary electrons, negative ions, positive ions
  - Avalanche of runaway electrons (based on kinetic calculations)
  - Ionization, recombination, attachment
  - Swarm model for secondary electrons
  - Quasi-electrostatic field model plus runaway and secondary currents
- Semi-empirical model
  - Use optical observations to constrain total energy in electron beam
  - Develop model of single equivalent discharge
  - Quasi-electrostatic field model, parameterization of beam in terms of δ_0

NORMALIZED ELECTRIC FIELD

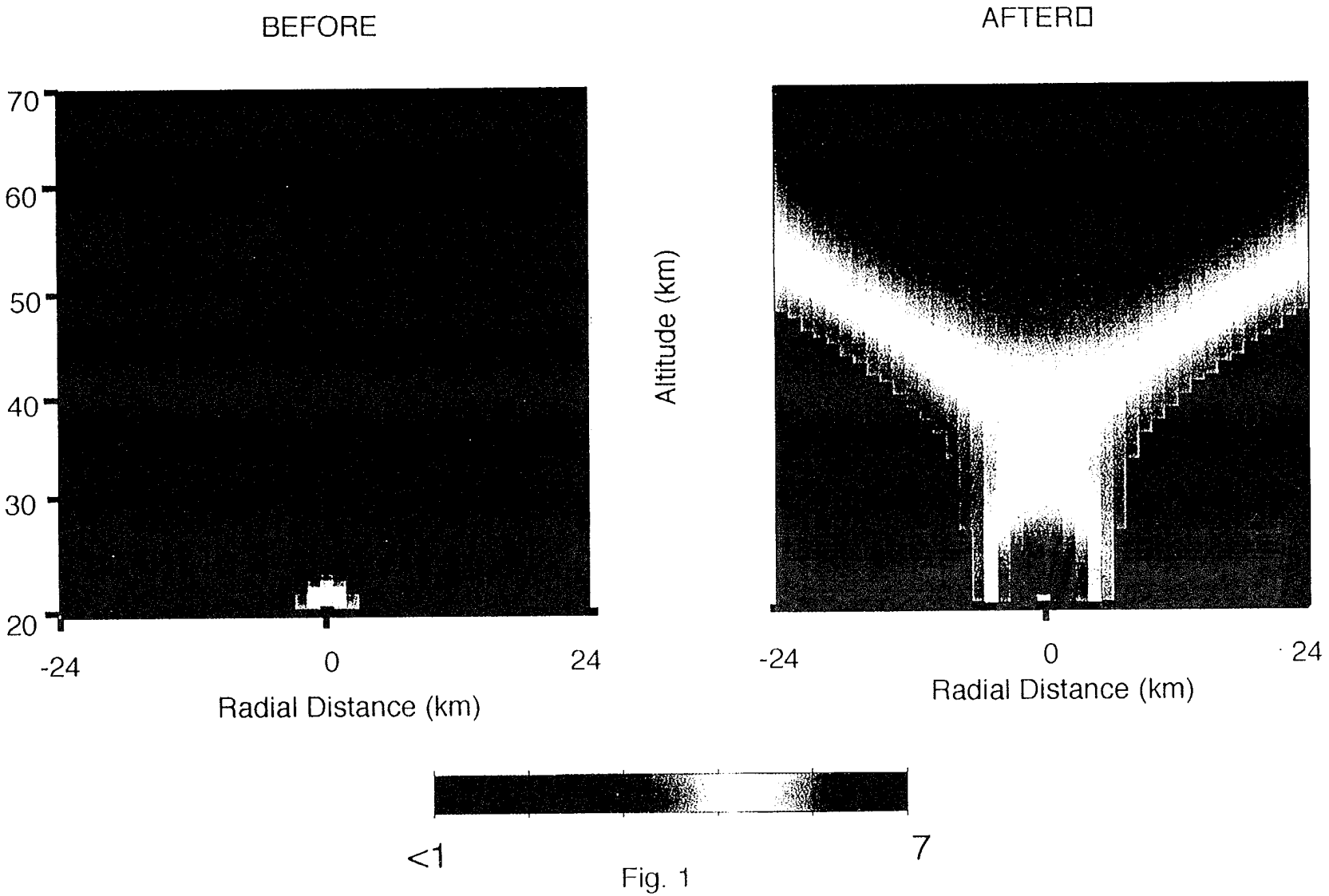


Fig. 1

NORMALIZED ELECTRIC FIELD

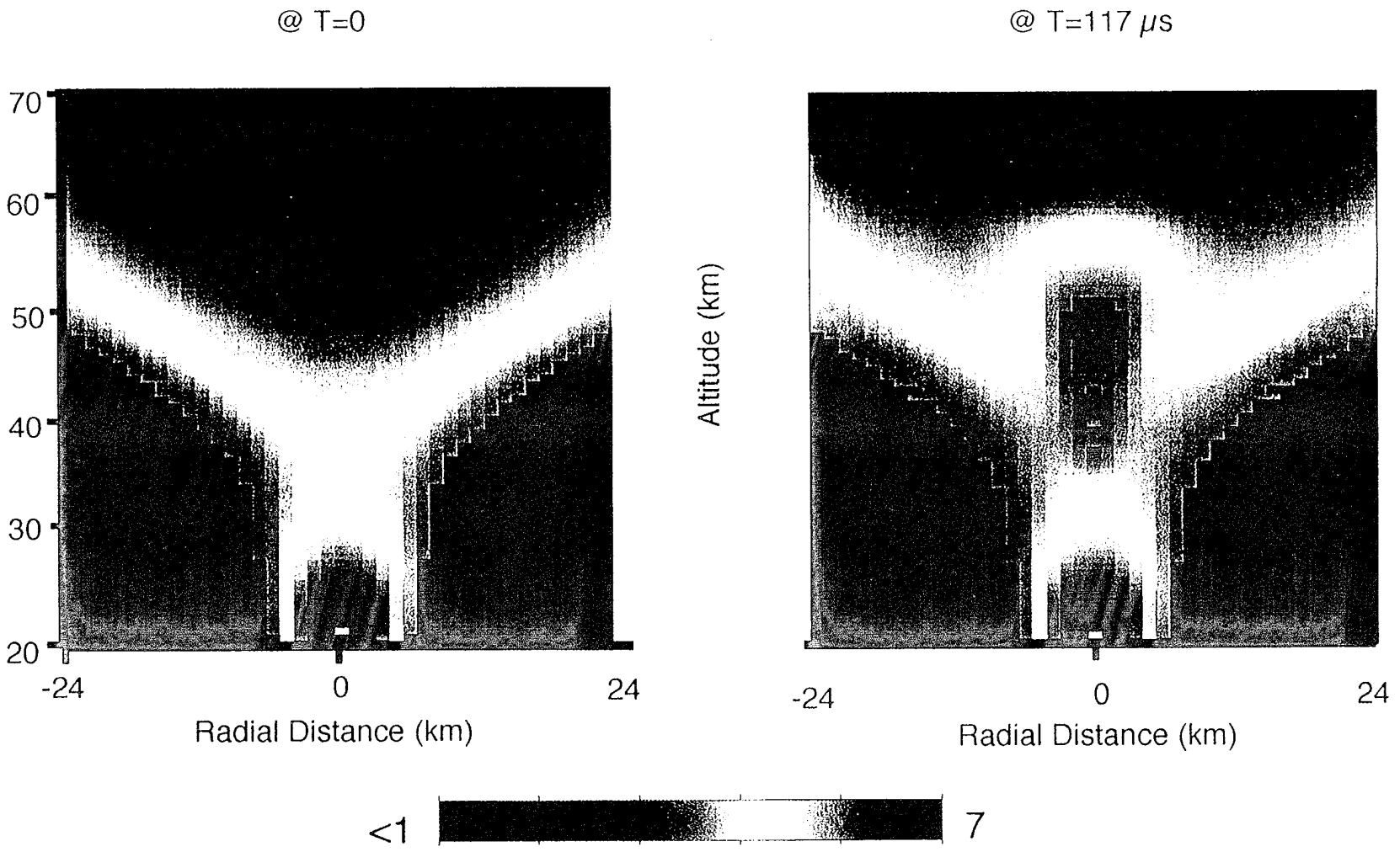


Fig. 5

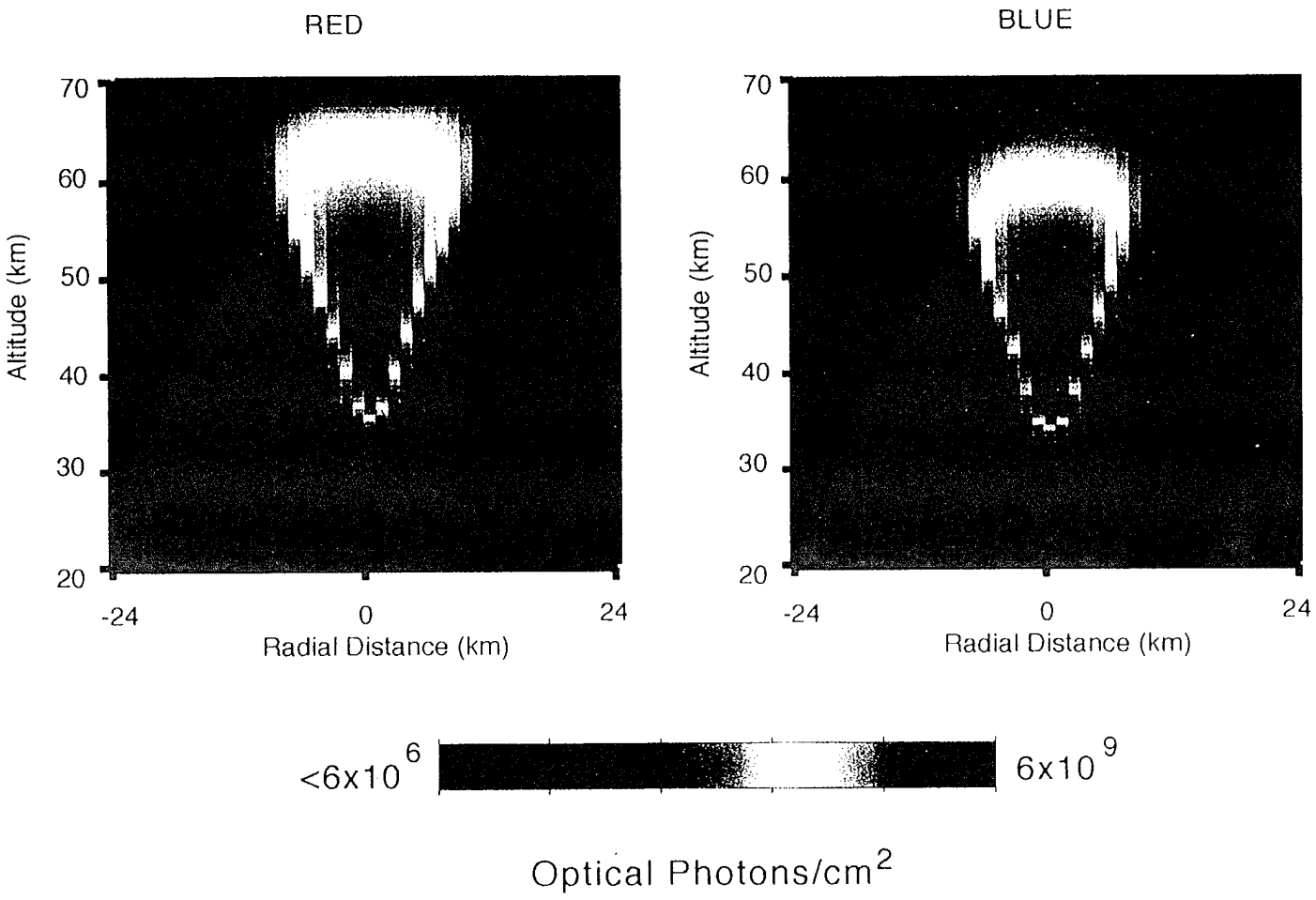
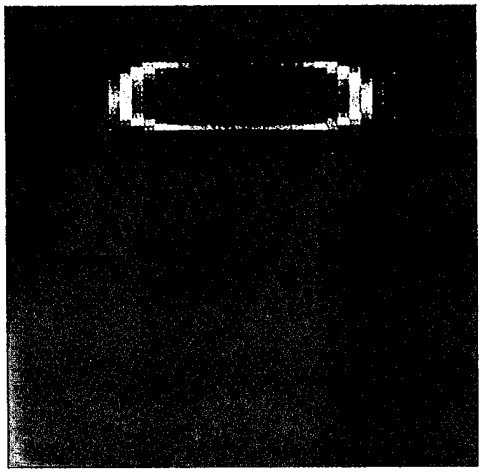

RED
BLUE
70
60
50
40
30
20
Altitude (km)
-24
0
24
Radial Distance (km)
<6x10^6
6x10^9
Optical Photons/cm^2

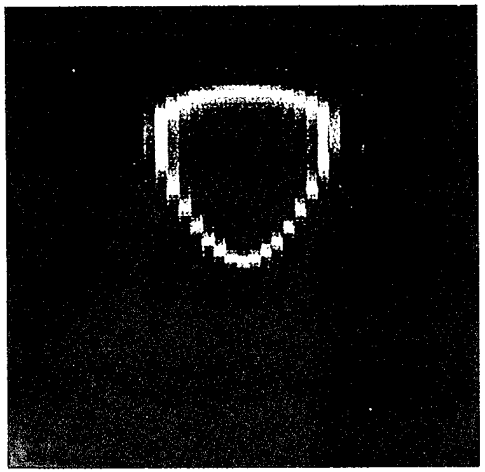
Fig. 4

PARTICLES @ T=117μs

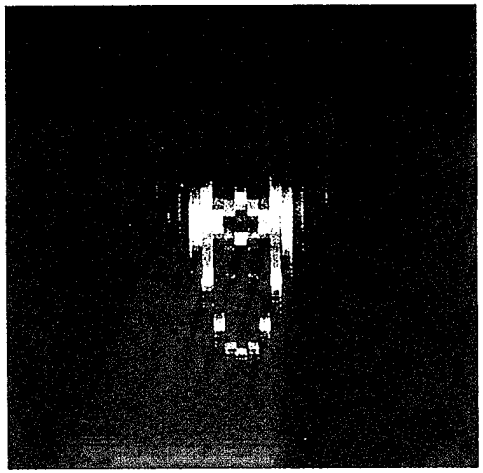
PRIMARIES



SECONDARIES



TOTAL CHARGES



SIGN OF CHARGE

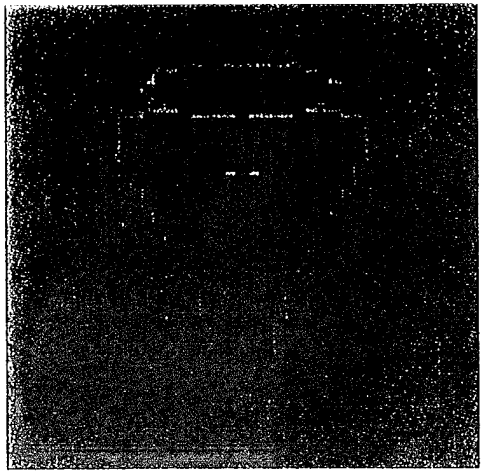
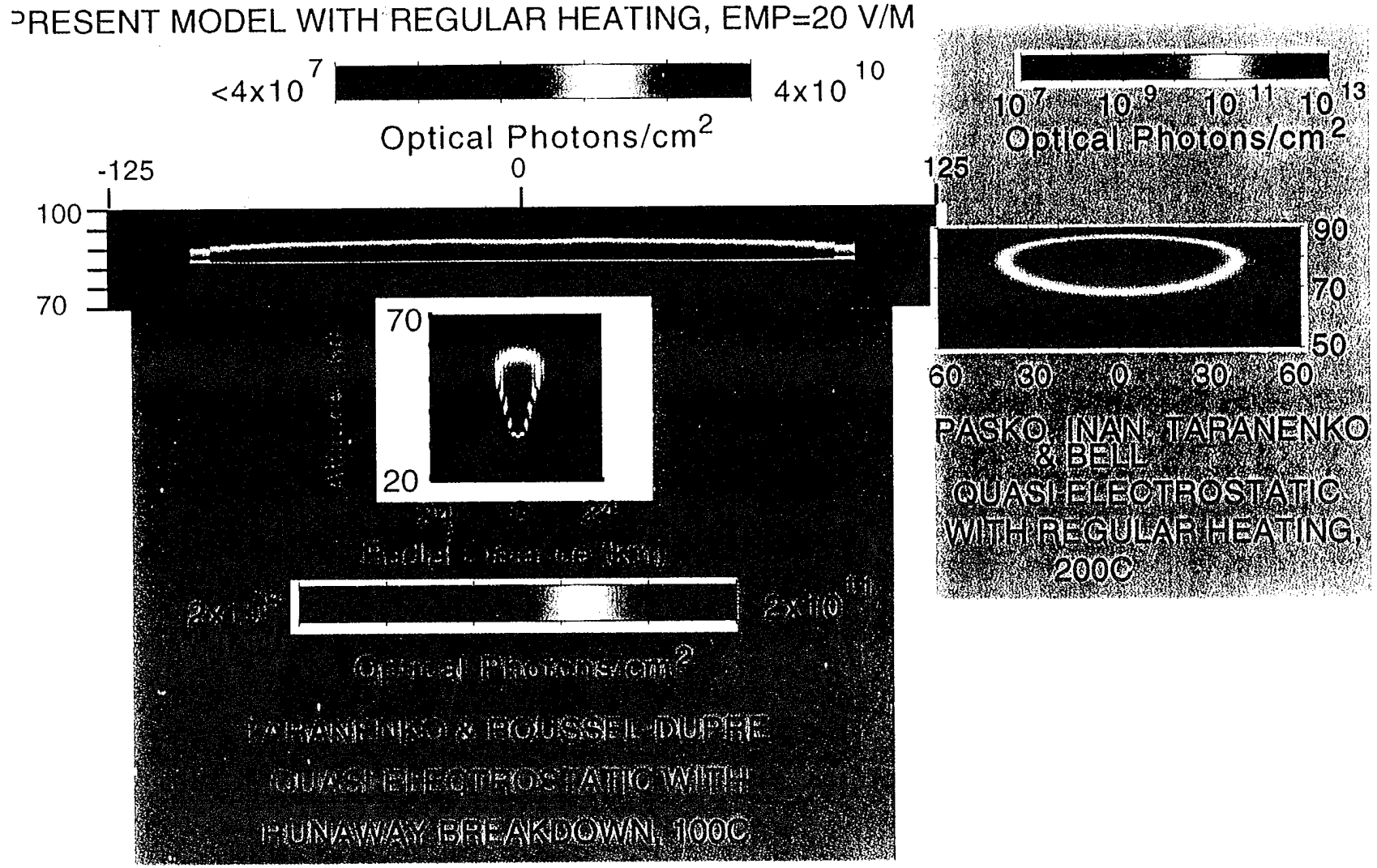


Fig. 4

OPTICAL EMISSIONS OF DIFFERENT MODELS



Emissions

		Model	Observations
Optical	Total Energy	~ 480 J	100 J - several kJ
	Intensity	~ 1 MR	~ 1 MR
	Spectrum	Red above 60 km and blue below	Red above 60 km and blue below
	Maximum Diameter	18 km	10 - 50 km
	Source Region	30 - 70 km	25 - 90 km
γ-rays	Count Rate	~800 counts / burst	~400 counts / burst
	Rise-time	~ 0.15 ms	~ 0.1 ms
	Duration	~ 0.3 ms	~ 1-5 ms
VHF above 25 MHz	VHF Flux	~ 1.1×10^{-14} J/m^2	median of 1×10^{-14} J/m^2
	Pulse Separation	tens of μs	mean of 51 μs
	Duration	several μs	mean of 5 μs

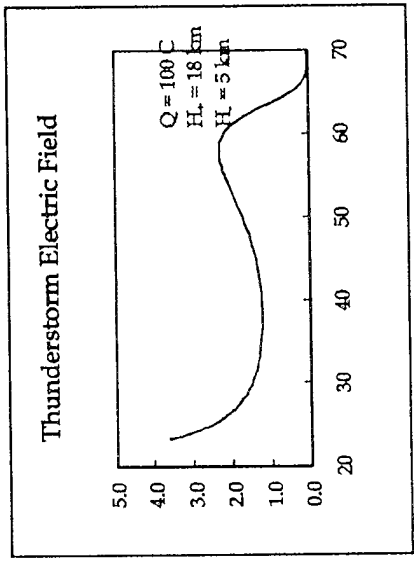
Satellite Measurements of TIPPs

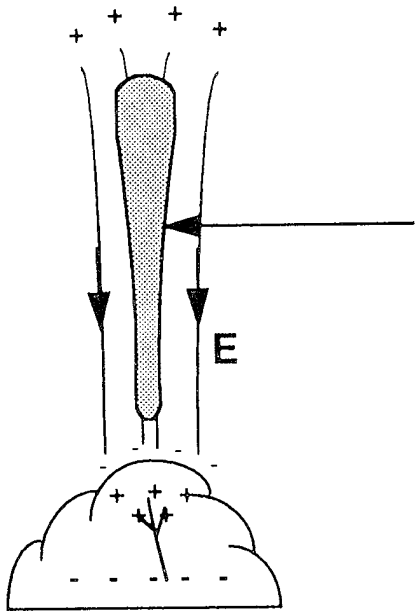
As seen from Blackbeard (low earth orbiting satellite in circular orbit at 800 km altitude and 70^0 inclination) in 25-75 MHz band

- ⇨Intense pairs of pulses
- ⇨Duration ranged from 0.5-14 μs with a mean of 5 μs and a median of 3.8 μs
- ⇨Separation ranged from 7.5-102 μs with a mean of 51 μs and a median of 52 μs
- ⇨Fluence ranged from 2.5-170 x 10^{-15} Joules/m^2 with a median of 10 x 10^{-15}.

TIPPs AND UPWARD DISCHARGES

Ionosphere



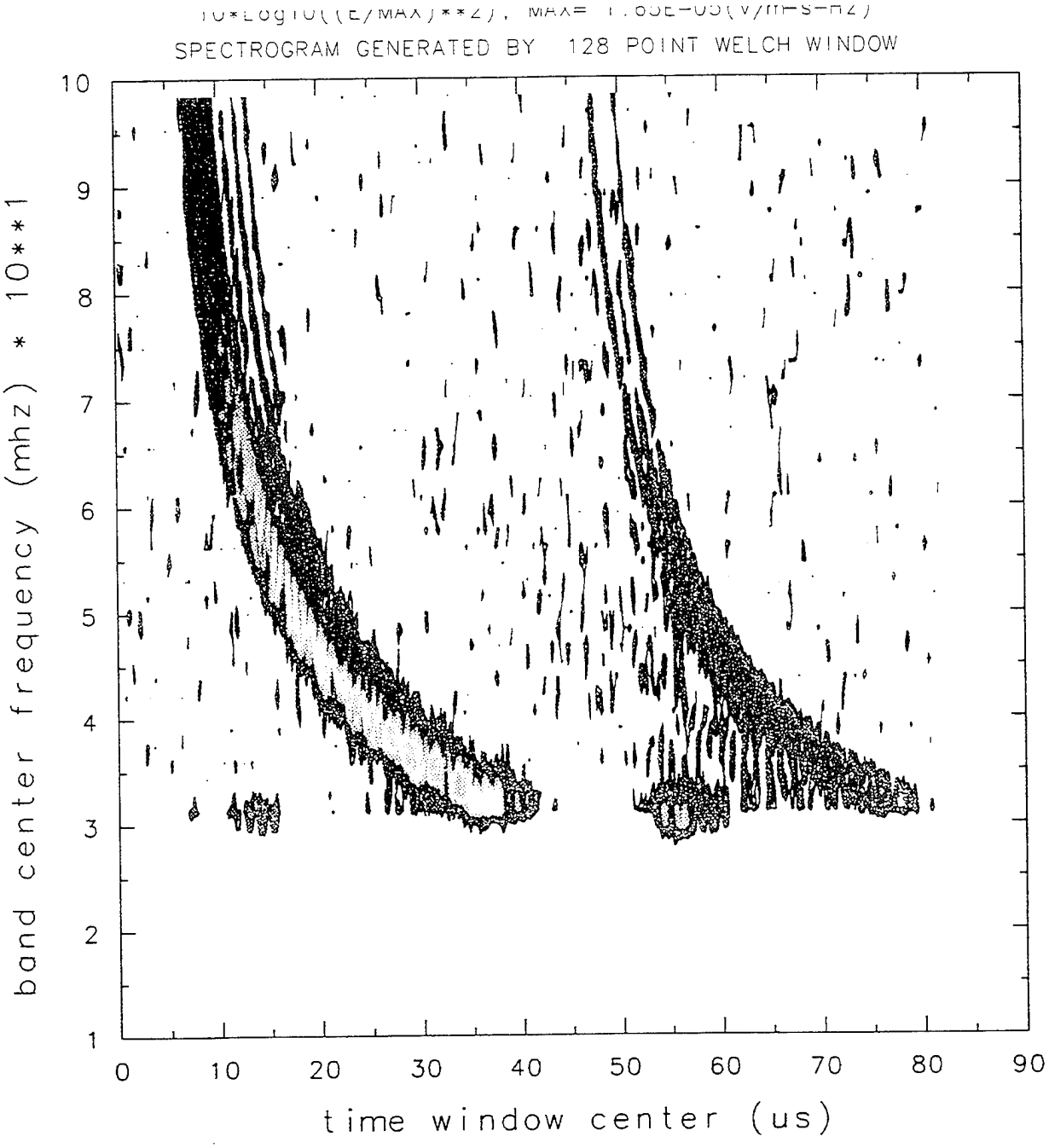


70 km

UPWARD-PROPAGATING BEAM

25 km

15 km


10*LOG10((E/MAX)**2), MAX= 1.65E-05(V/M-S-HZ)
SPECTROGRAM GENERATED BY 128 POINT WELCH WINDOW
band center frequency (mhz) * 10**1
time window center (us)
10
9
8
7
6
5
4
3
2
1
0
10
20
30
40
50
60
70
80
90

Summary

- **Runaway breakdown models reproduce**
  - optical observations of upward discharges
  - γ-ray measurements of BATSE
  - TIPP events measured by BLACKBEARD
- **Needed Measurements**
  - Simultaneous optical, γ, and rf
  - Atmospheric conductivity profiles
  - Thunderstorm electric fields, currents, and charge distribution
  - Energetic particle measurements
  - Experiment to validate theory of runaway breakdown

Numerical Simulations of Lower Ionospheric Breakdown Caused by Lightning Generated Electric Fields

Harvey Rowland, Richard Fernsler,
Carl Siefring and Paul Bernhardt

Naval Research Lab

Sprite Workshop, Phillips Lab.
Oct. 18, 1995

Model

The code uses Maxwell's equations with the currents calculated by Ohm's law, $\mathbf{j} = \sigma \mathbf{E}$, where

$$\sigma = \begin{vmatrix} \sigma_P & \sigma_H & 0 \\ -\sigma_H & \sigma_P & 0 \\ 0 & 0 & \sigma_\parallel \end{vmatrix} \quad (1)$$

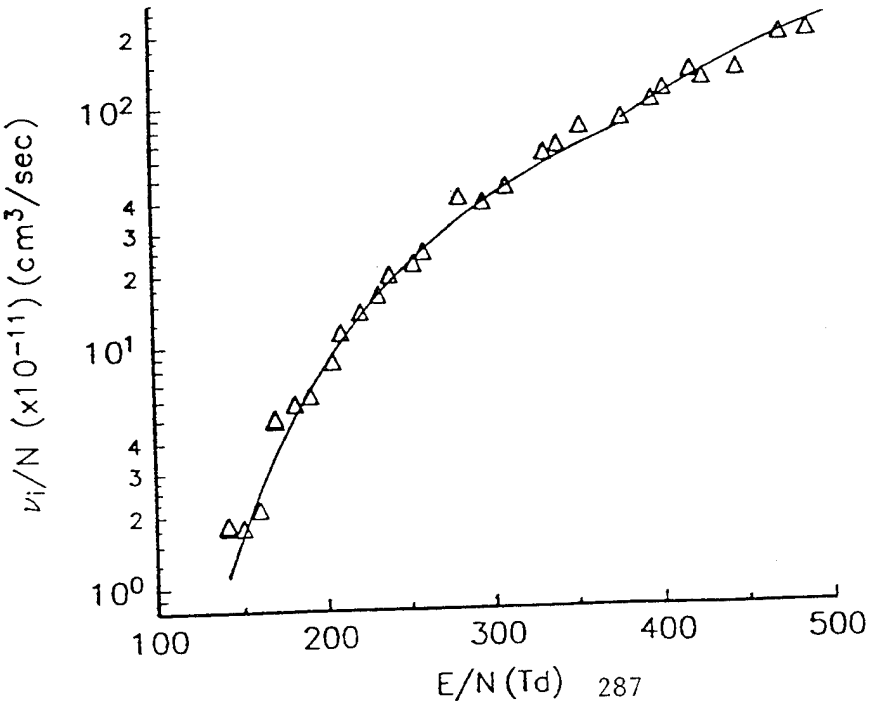
The conductivities are the Pedersen (σ_P), Hall (σ_H) and parallel ($\sigma_\parallel$). The code has two spatial dimensions and the currents (x, z, j_x, j_y, and j_z). The earth's magnetic field is in the z direction.

Ionization and Breakdown

We use a fit to laboratory data of ionization of air for the appropriate range of E/N values.

$$\nu_i \simeq \begin{cases} 5\times10^{-8}\, N \exp(-1550N/E_{eff}) & E_{eff}/N > 370 \\ 10^{-8}\, N \exp(-960N/E_{eff}) & E_{eff}/N < 370 \end{cases} \quad (2)$$

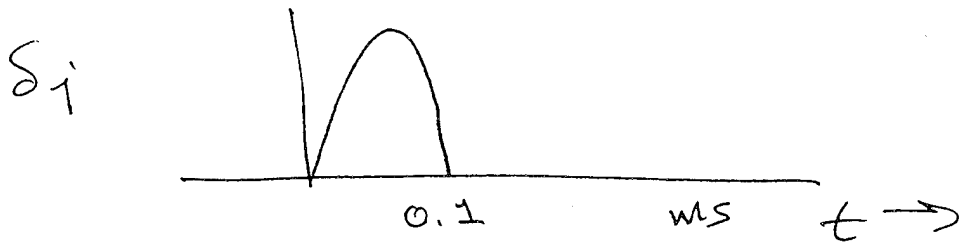
where the gas density N is in cm^{-3}, ν_i is in sec^{-1}, and E_{eff}/N is expressed in Td (1 Td = 10^{-17} V-cm^2). the ionization rate is then used to update the conductivities.



EMP Driven Breakdown

$$E_{EMP} \propto \frac{I}{r} \quad \text{while} \quad E_{QS} \propto \frac{Q}{r^3}$$

Use a discharge with large I_{max} but no continuing current -- EMP dominates (Rowland, et al., GRL, 361, 1995).



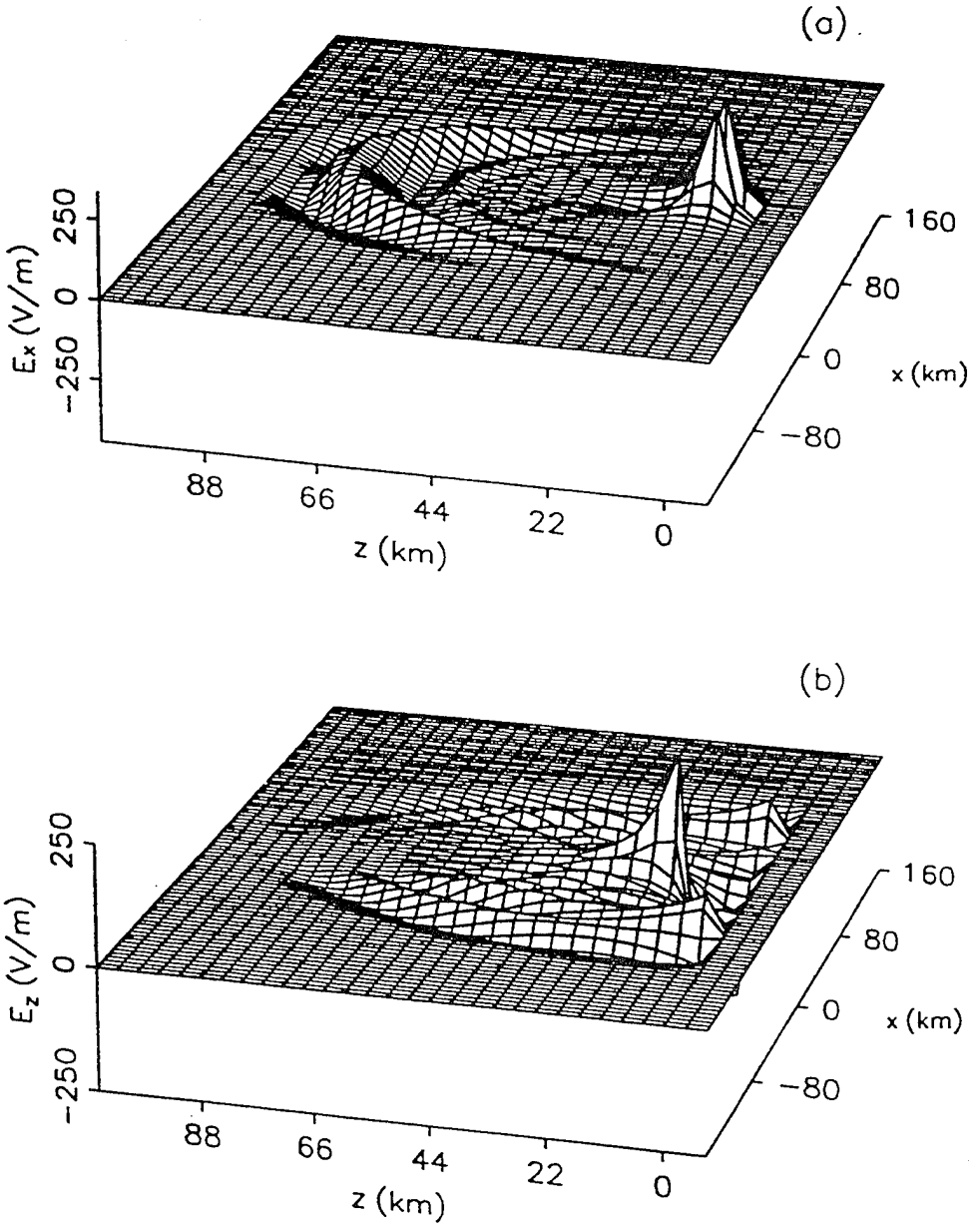


Figure 1. The electric fields generated by (a) a horizontal and by (b) a vertical discharge at 300 μsec after the start of the discharge.

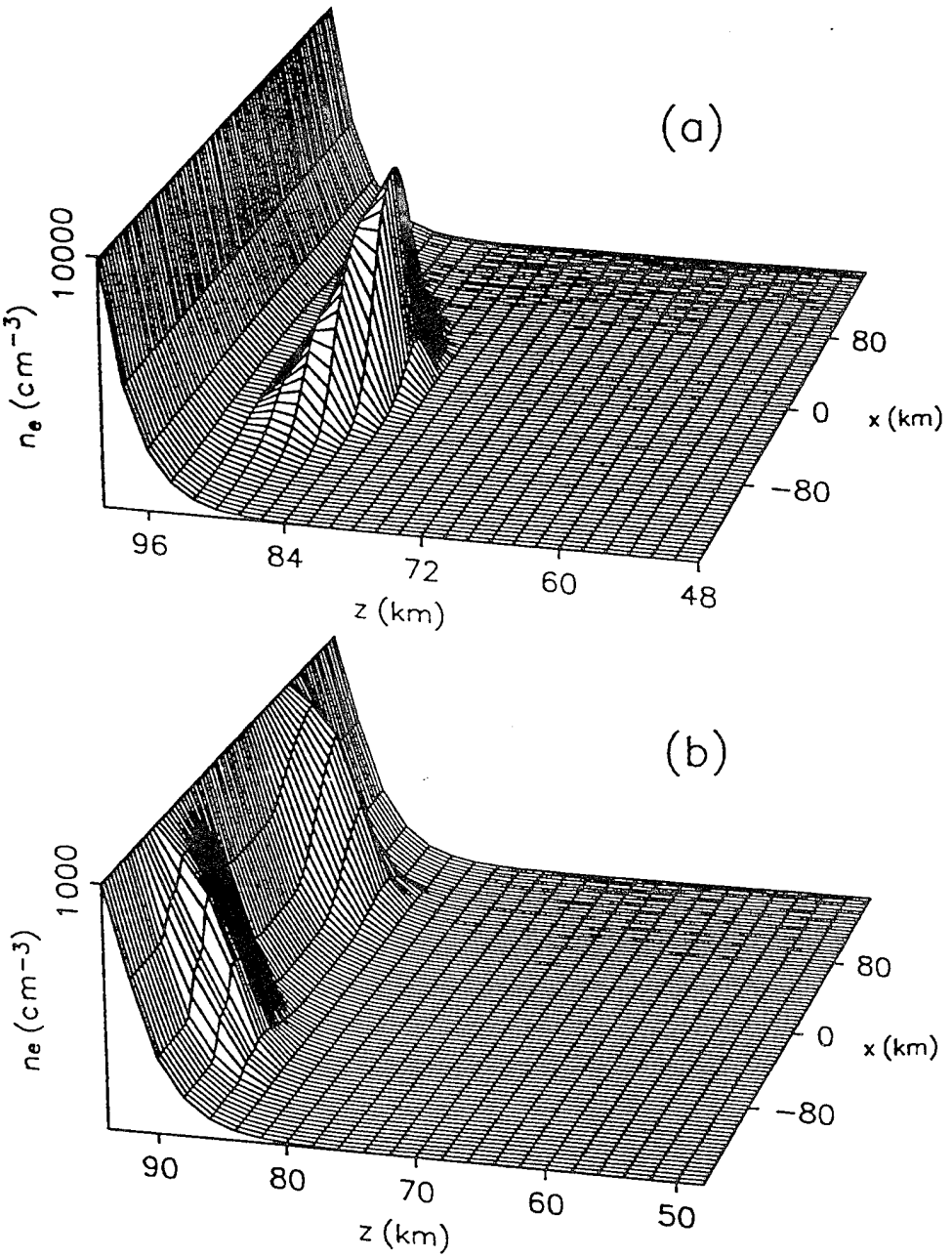
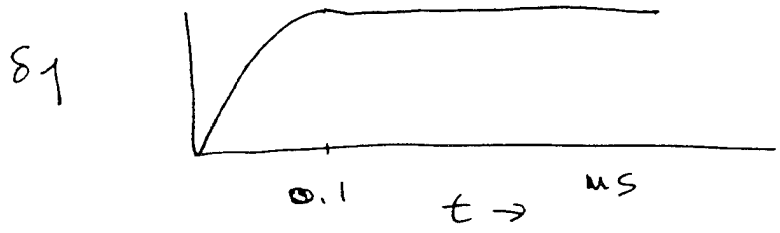


Figure 2. The ionospheric plasma density at 400 μsec after the start of the discharge (a) for a horizontal and (b) for a vertical discharge with E_{100}=55 V/m.

Breakdown due to combined EMP and QS fields

$$E_{EMP} \propto \frac{I}{r} \quad \text{while} \quad E_{QS} \propto \frac{Q}{r^3} \quad \text{where } Q = \int I\,dt$$

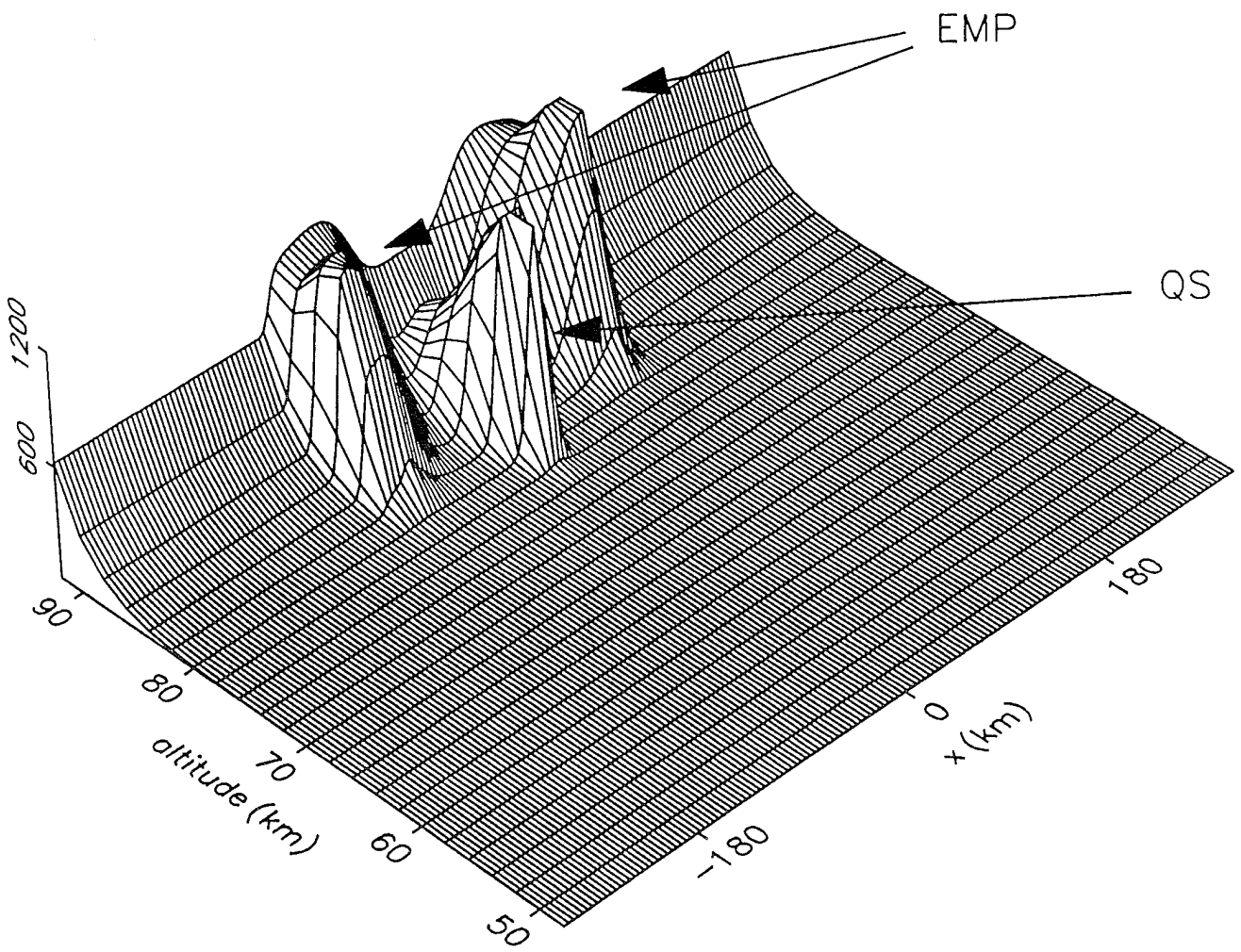


The same I_{max} as in previous simulation but with a continuing current. When Q ≈ 60C, breakdown from QS ≈ EMP. As Q becomes larger, maximum ionization moves to lower altitude.

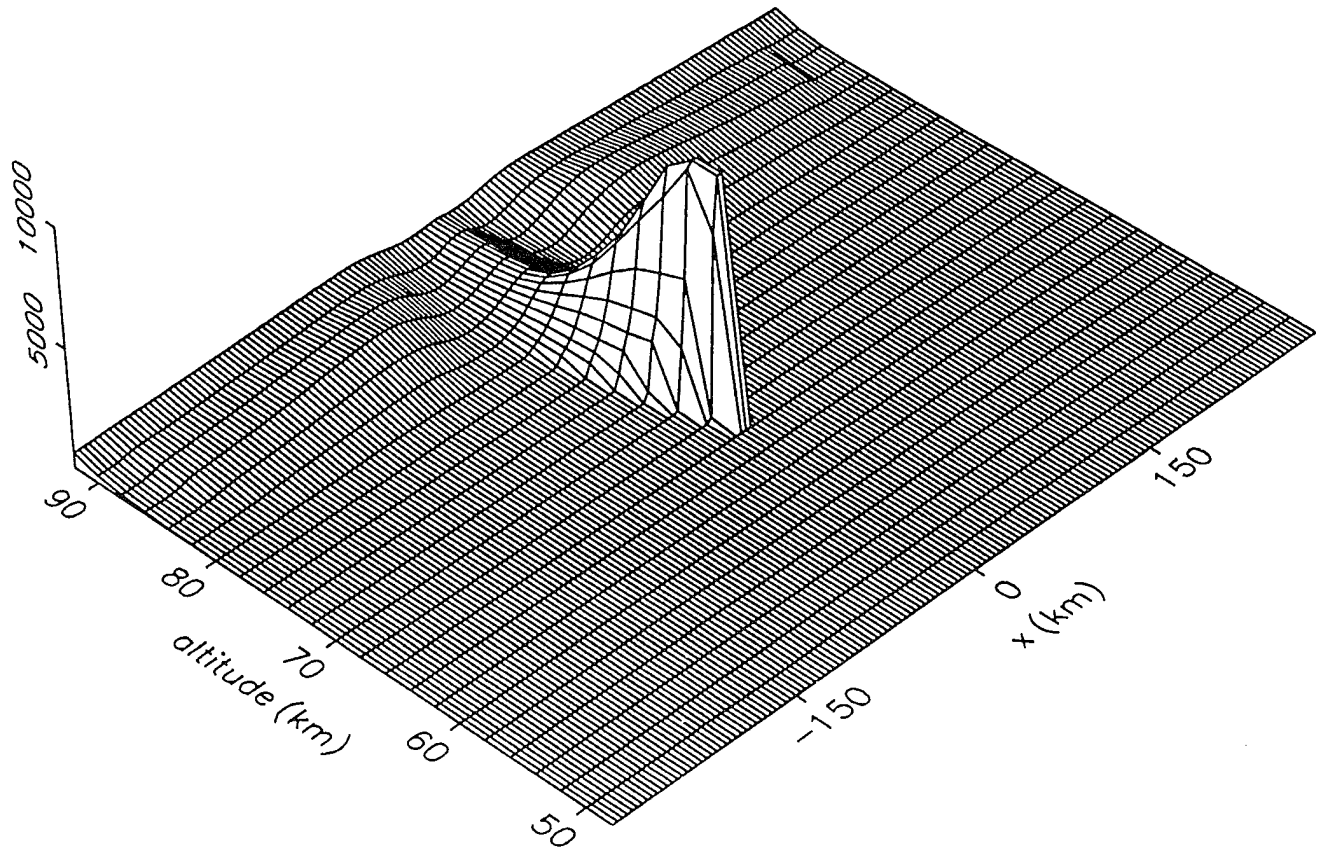
First, the EMP forms the broad (100's km), high altitude (70-90 km), sub-ms flash --ELVES.

The QS can then form the narrow (10- 50 km), lower altitude (55-90 km), several msec flash --- SPRITES.

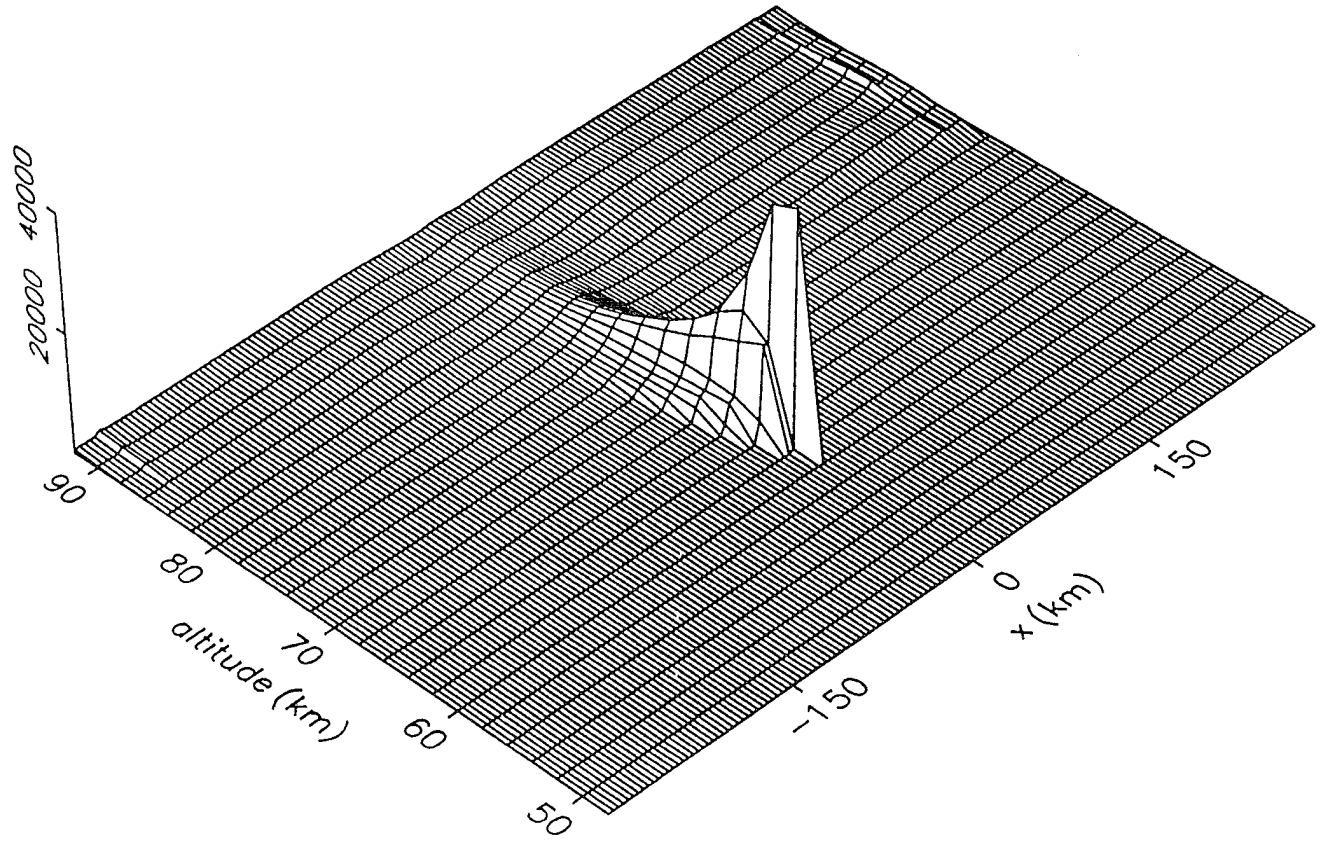
Raising the top of the discharge, increases ionization and lowers its altitude for same Q.


electron density
E100 = 110 V/m;t = 0.5 msec; Q = 60 C
EMP
QS
1200
600
90
80
70
60
50
altitude (km)
-180
0
180
x (km)

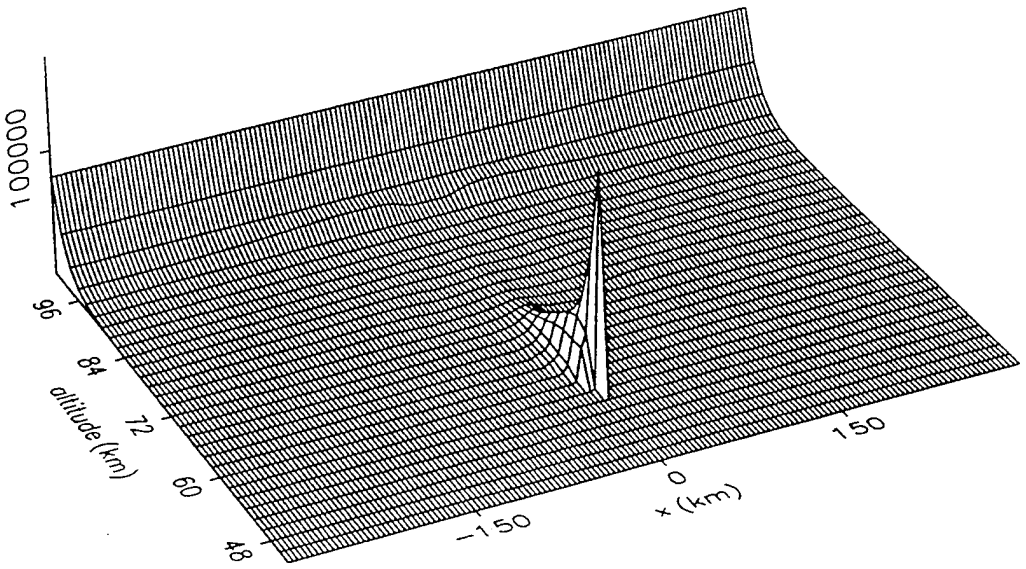
electron density
E_{100} = 110 V/m; t = 1 msec; Q = 210 C

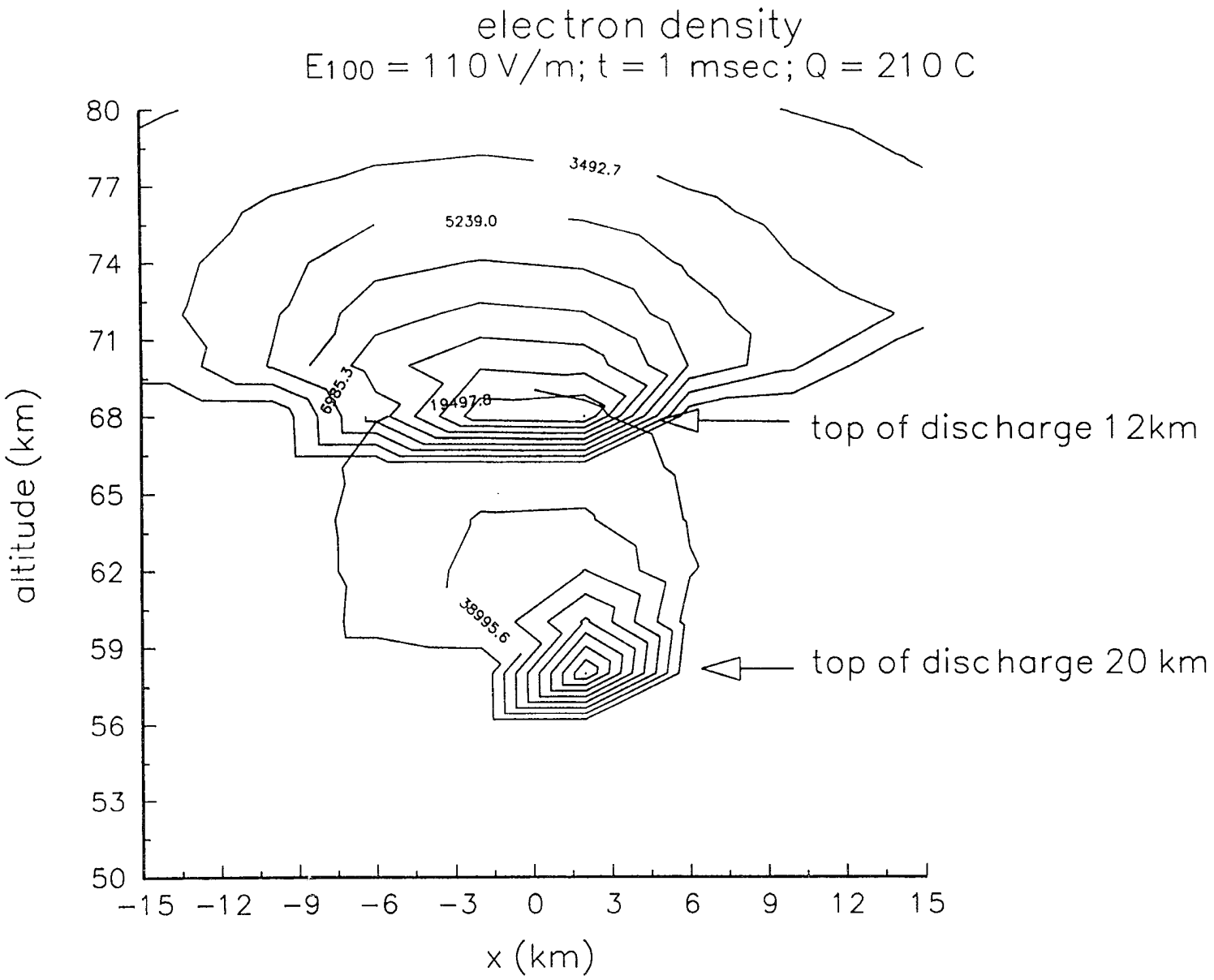


electron density
E_{100} = 110 V/m; t = 1.5 msec; Q = 360 C



n_e
continuing current; t = 1 msec; Q = 210 C




electron density
E100 = 110 V/m; t = 1 msec; Q = 210 C
altitude (km)
80
77
74
71
68
65
62
59
56
53
50
3492.7
5239.0
6985.3
19497.8
38995.6
top of discharge 12km
top of discharge 20 km
−15 −12 −9 −6 −3 0 3 6 9 12 15
x (km)

Effects on the EMP and the QS fields

Breakdown modifies the conductivity and thus the propagation of the EMP. Fig. 5, 3, and 6 are for the horizontal discharge shown in Fig. 2a. By turning off ionization, one can compare the interaction with only the ambient, unmodified ionosphere.

Figure 7 and 8 show the effects of breakdown on the QS field for a cloud-to-ground discharge by comparing a simulation with breakdown to one with a fixed ambient ionosphere. The top figure shows the time history of the vertical electric field at 70 km directly above the discharge. As the ionization patch moves downward, the vertical field is initially enhanced. As it sweeps past, the increased conductivity shorts out the field. The bottom figure shows the spatial distribution of the vertical electric field at 1 msec. The bottom of the ionization is at 70 km at this time. In comparison to the simulation with a fixed ionosphere, the field is enhanced below 70 kilometers and reduced above.

Figure 9 shows a 2 D plot of the time integrated E_{rms} for the c-g discharge with no ionization (top) and ionization (bottom). This shows only the high altitude fields. The central fields are the QS fields and the left and right structures are the EMP. There is an absorbing strip along the left and right boundaries. One can see the notch cut into the QS fields by the ionization patch.

The enhanced E vertical is due to-

- focusing of the field because of the pointed shape of the ionization patch in the horizontal direction and,

- lowering theeffective ionosphere bring closer together the charge at the top of the cloud and its image charge in the ionosphere.

The 50% enhancement is important, since this lowers the Q needed for breakdown.

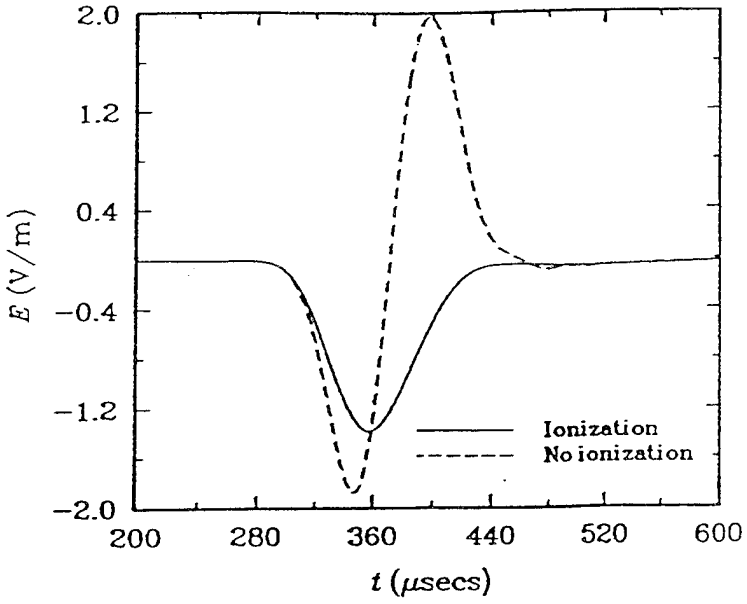


Figure 5. E versus time at 100 km altitude with ionization (solid line) and without ionization (dashed line). Only the leading edge propagates to higher altitude when an ionization patch forms.

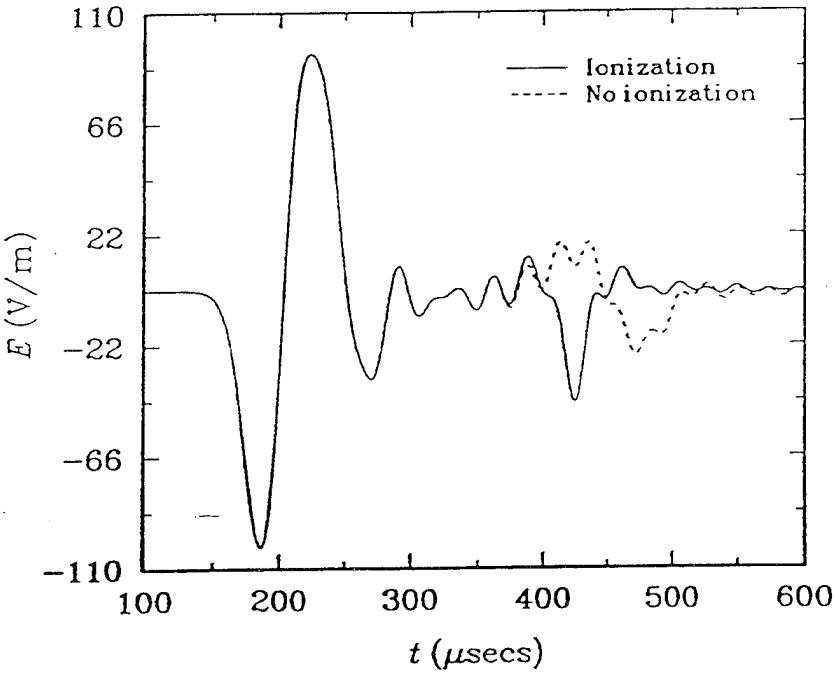


Figure 3. E_x versus time at 46 km altitude above the lightning discharge with (solid line) and without (dashed line) self consistent ionization. Enhanced ionization causes a strong reflected pulse from the trailing edge of the EMP.

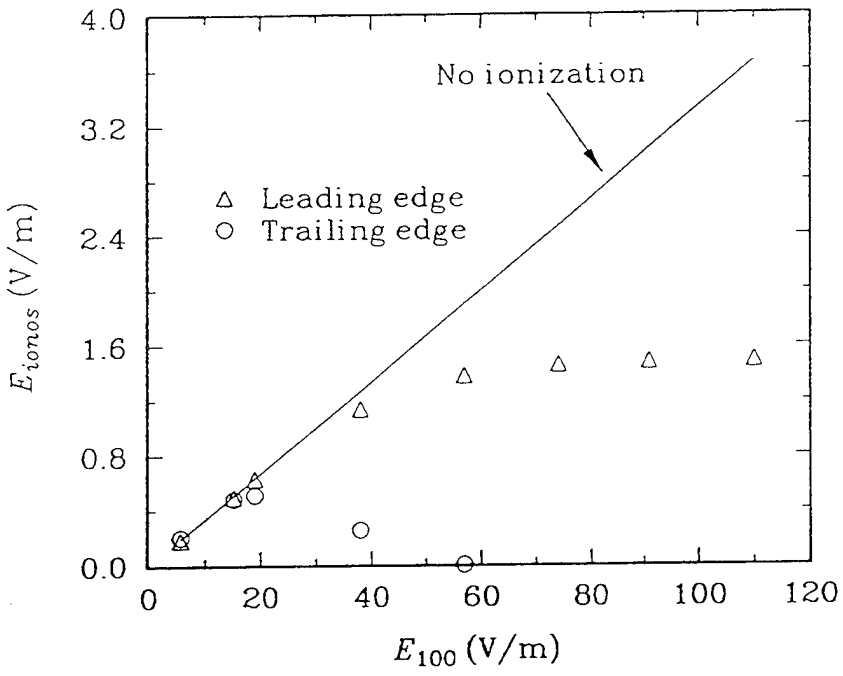


Figure 6. The amplitude of the leading edge of the EMP pulse (triangles) and the trailing edge (circles) as a function of normalized pulse strength. The straight line shows amplitude of the pulse with only initial ambient ionosphere. As the EMP exceeds breakdown threshold, first the trailing edge is reduced and then the leading edge reaches a maximum.

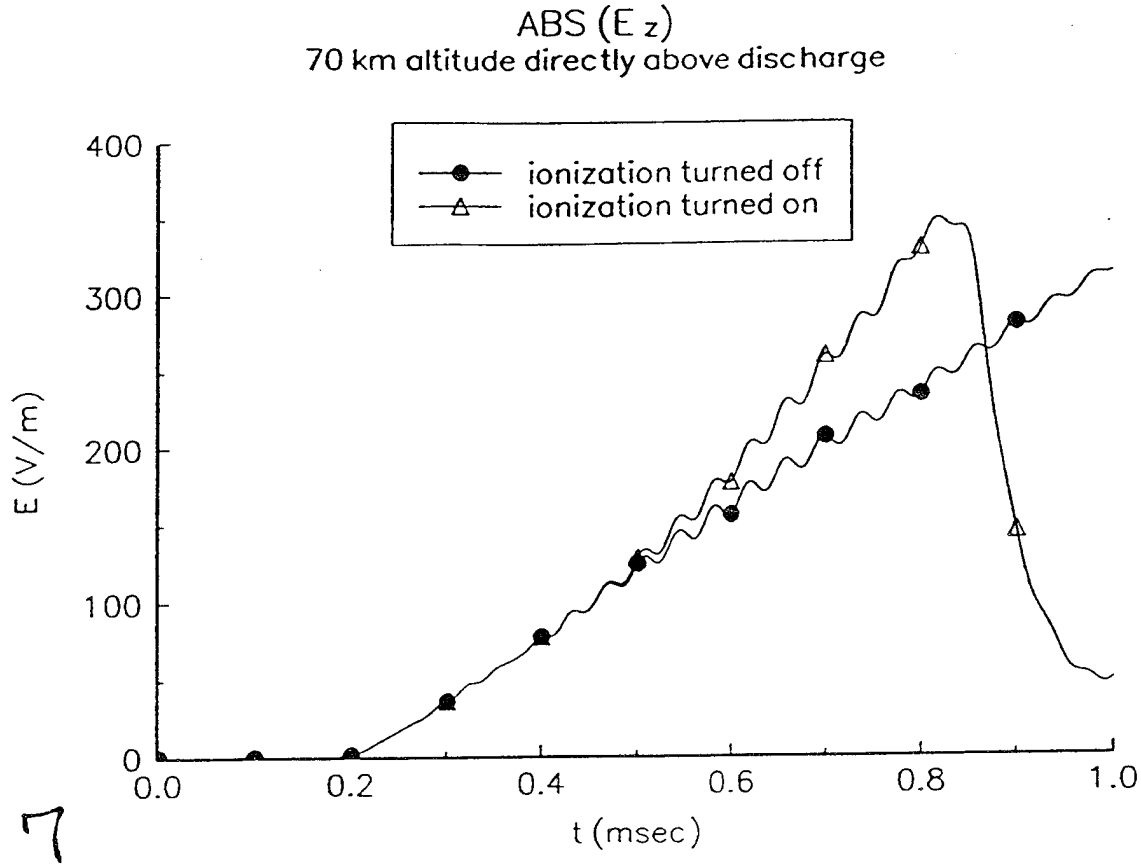

ABS (E z)
70 km altitude directly above discharge
ionization turned off
ionization turned on
E (V/m)
400
300
200
100
0
0.0
0.2
0.4
0.6
0.8
1.0
t (msec)

Fig 7

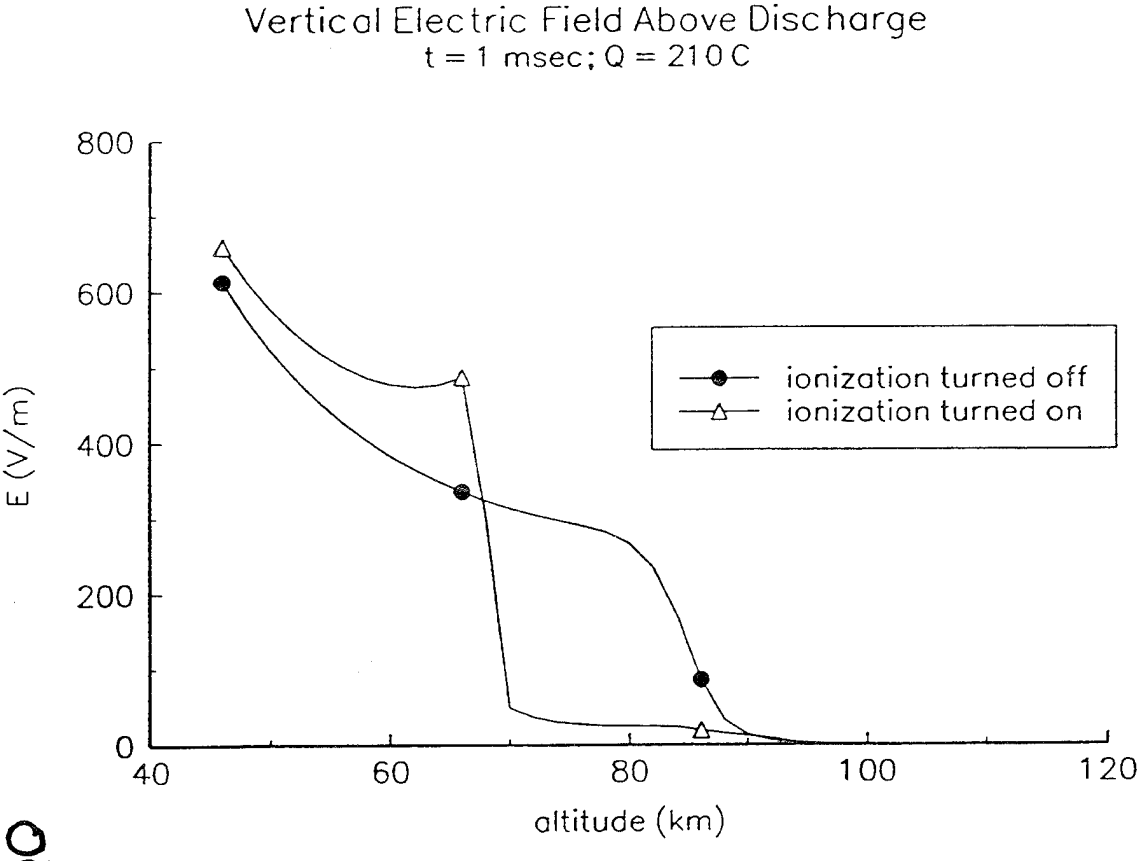
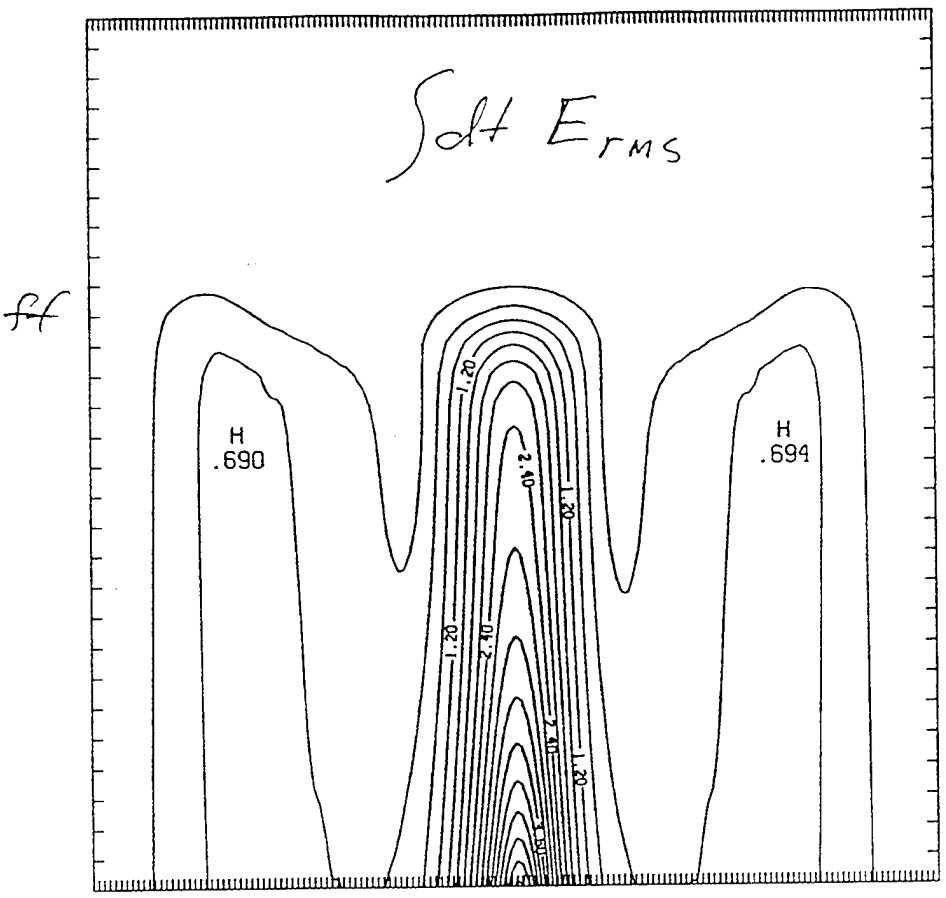

Vertical Electric Field Above Discharge
t = 1 msec; Q = 210 C
ionization turned off
ionization turned on
E (V/m)
800
600
400
200
0
40
60
80
100
120
altitude (km)

Fig 8

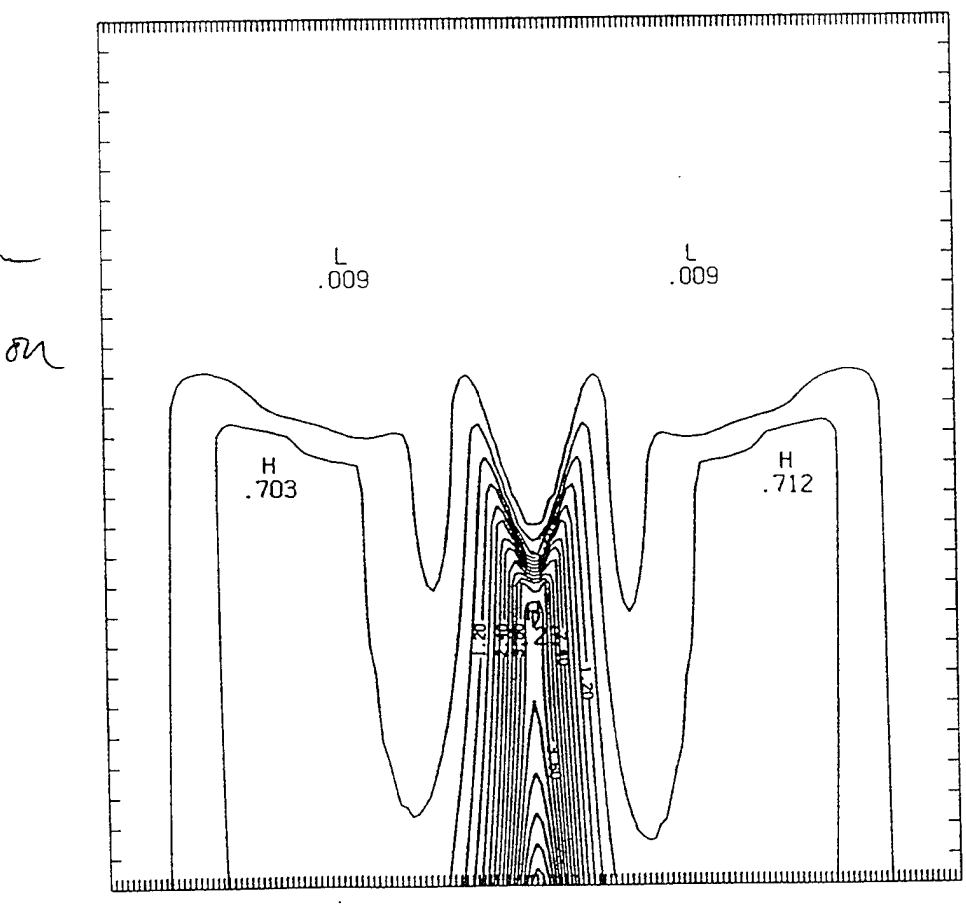


ionization turned off

-300km

+ 300 km

X



ionization turned on

Fig 9

- 300 km

+300 km

X

Neutral density fluctuations

The ionization rate is sensitive to the neutral density. The ionization depends exponentially on the ionization rate which will amplify any neutral density variation. Therefore one possible source of the structure seen in elves and sprites may gravity waves. The following figure (Rowland, et al. submitted JGR, 1995) shows how a gravity wave (modelled as a horizontal sine wave) changes the ionization shown in 2a. The wavelength is determined by the wavelength of the gravity wave. For this example a 10% variation in the neutral density cause a variation between 3 and 4 in the ionized density .

dne
1000
0
90
80
70
60
50
z(km)
x (km)
0
-80
80

Conclusions

1) The EMP of the pulse forms ionization patches that are wide (100's km) in the horizonal direction and restricted in altitude between 70- 90 km (Rowland, et al. GRL, 361, 1995; Rowland, et al., submitted JGR, 1995). These characteristics fit ELVES.

Since the airglow only exists while the electric field is present, they are brief (0.1 msec). Because of the short lifetime, breakdown must occur to explain the strength of the airglow.

2) The QS fields grow if there is a continuing current. When Q > 60 C, the maximum ionization due to the QS can become greater than that due to the EMP. The altitude of the QS ionization can extend slightly above the EMP ionization. As Q increases, the region of ionization extends to lower altitudes (55 km) and becomes narrower in the horizontal direction. In the simulations, the widths decrease to the cell size. The vertical altitude extends from 90 to 55 km. The horizontal size goes from 50 km at 80 km altitude down to a few km at 55 km altitude. These characteristics fit SPRITES.

As with the ELVES airglow, strong SPRITE airglow requires an E field. Since the enhanced conductivity shorts out the field internal to the SPRITE, it could be only the outer shell that radiates.

3) To form ELVES requires a large I_{max}. This favors positive-to-ground discharges. Even if negative-to-ground and positive- to- ground discharges have the same $\partial I/\partial t$, the positive EMP will be longer in time and cause more ionization. Horizontal currents have a threshold current roughly half of that required for a vertical discharge. For a SPRITE to form requires a continuing current that can generate a large Q. This favors a positive-to-ground, vertical discharge.

Depending upon I_{max} , the duration of the continuing current, and the orientation of the discharge, one can observe an ELF and a SPRITE or one and not the other. If both are present the ELF should appear first.

Runaway Breakdown in the Presence of Magnetic Field

A.V. Gurevich*, J. A. Valdivia, G. M. Milikh, and K. Papadopoulos

Departments of Physics and Astronomy
University of Maryland
College Park, Maryland 20742

9 October 1995

*On leave from P.N. Lebedev Institute of Physics, Moscow 117924, Russia

—Observed γ-ray fluxes associated with runaway breakdown due to:

(i) Laminar electric fields following lightning discharges (Taranenko et al., 1993; Roussel-Dupre et al., 1994; Pasko et al., 1995)

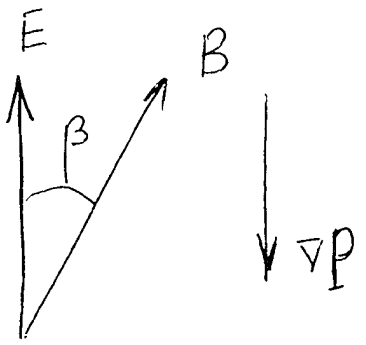
(ii) AC fields due to intracloud lightning discharges (Milikh et al., 1995; Rowland et al., 1995)

—Analysis up to day neglected the presence of B, and atmospheric density gradients.

—At high altitude the geomagnetic field could sufficiently influence the runaway process, since **the gyrofrequency of high energy electrons becomes higher than their collision frequency**.

—We present here analysis that includes the role of B. Restrict to-day to laminar fields. Analysis of AC fields ongoing.

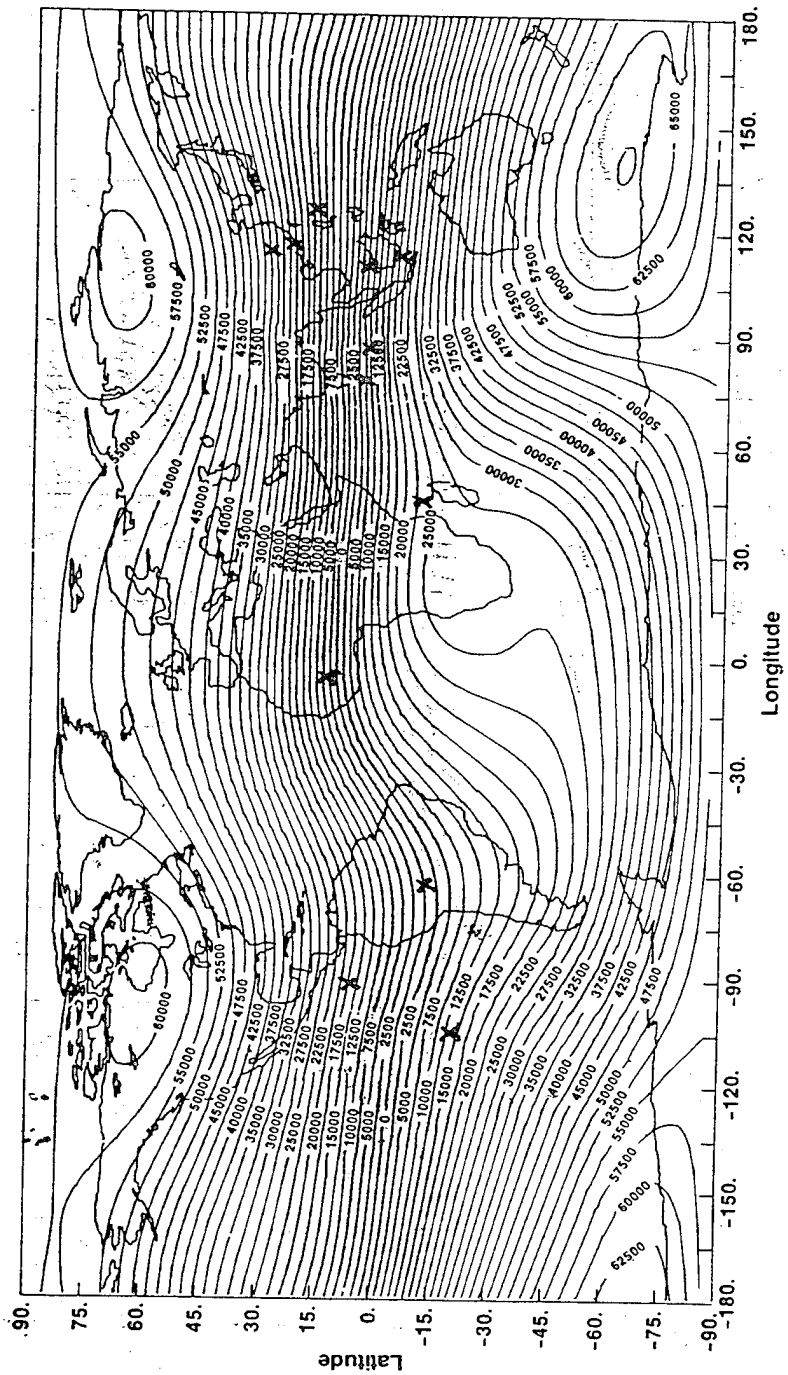
Main Results



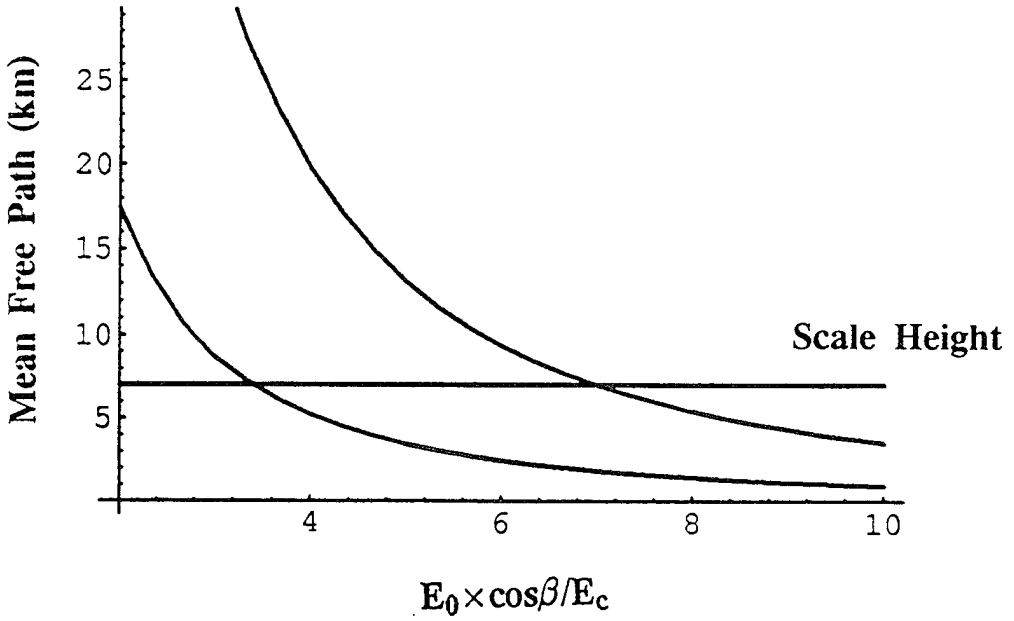
—For $80^o < \beta \leq 90^o$ the magnetic confinement occurs.
Runaway threshold is defined by the magnetic field.
Process is independent on density gradient.

—For $0 \leq \beta \leq 60^o$ the discharge is driven by the $E \times \cos\beta$ component.
The magnetic field reduces cross-field diffusion of runaway electrons.
Filaments along E field could appear.

—For $60^o < \beta \leq 80^o$ is the transient range.


Latitude
Longitude
90.
75.
60.
45.
30.
15.
0.
-15.
-30.
-45.
-60.
-75.
-90.
180.
150.
120.
90.
60.
30.
0.
-30.
-60.
-90.
-120.
-150.
-180.

Role of ∇N on $0 < \beta \leq 60^\circ$ case



Inhomogeneity increases threshold of the runaway breakdown at ≥ 7/50km

Runaway Acceleration

The equation of motion

$$\frac{d\underline{p}}{dt} = e\underline{E} - \underline{F}_D \qquad B = 0$$

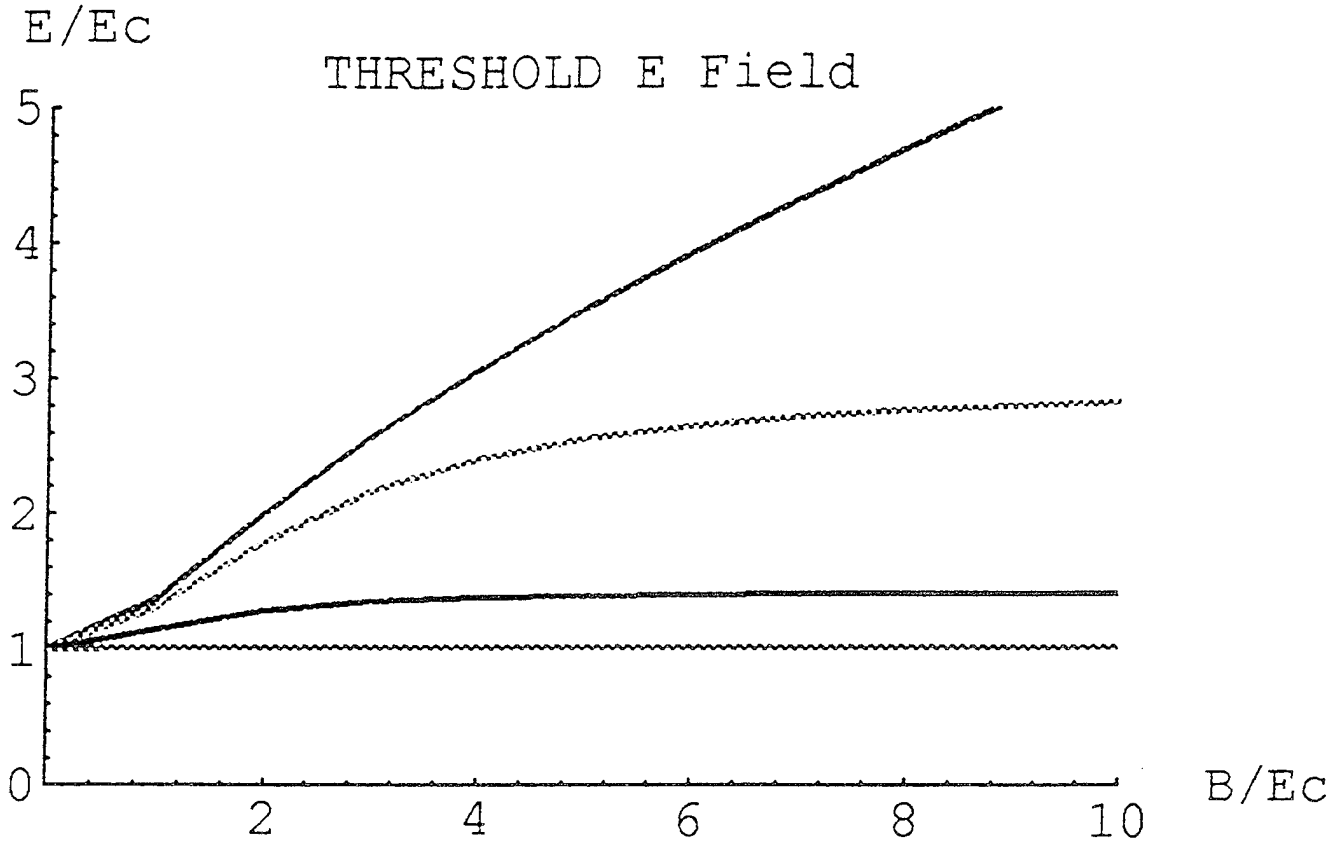
$$\frac{d\underline{p}}{dt} = e\underline{E} + \frac{e}{mc\gamma}(\underline{p} \times \underline{B}) - \underline{F}_D, \qquad B \neq 0$$

$$\nu = F_D/p$$

—Obtain stationary solution and runaway threshold.

—Study phase space to find regions of runaway acceleration.

—Find ionization rate for runaway electrons.



The height at which the runaway breakdown increses to the point of conventional breakdown.

This happens when the value of the critical electric field $\delta_{c0}(\eta_0)$ reaches the threshold of the conventional air breakdown $\delta_{c0}(\eta_0)\simeq 10$.

For instance, in E⊥B fields it corresponds to magnetic field B/Ec $\simeq$27. In Gaussian units:

$$\frac{9\,kV/m \times B/0.3\,G}{220\,kV/m \times P(atm)} = 27.$$

For a middle latitude B$\simeq$0.3 G, this gives p=1.5×10^{-3} atm.

Thus at z > 65 km the conventional breakdown dominates over the runaway if β > 80°.

3. The Electron Runaway Boundary

Equation of the electron motion:

$$\frac{d\tilde{p}_x}{d\tau} = \delta_0 + \frac{\eta_0}{\gamma}\tilde{p}_y \sin\beta - \frac{\Phi(\gamma)}{\sqrt{\gamma^2-1}}\tilde{p}_x,$$

$$\frac{d\tilde{p}_y}{d\tau} = -\frac{\eta_0}{\gamma}\tilde{p}_x \sin\beta + \frac{\eta_0}{\gamma}\tilde{p}_z \cos\beta - \frac{\Phi(\gamma)}{\sqrt{\gamma^2-1}}\tilde{p}_y,$$

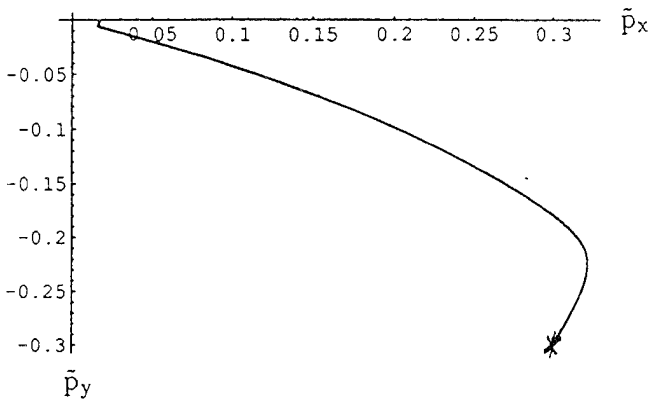
$$\frac{d\tilde{p}_z}{d\tau} = -\frac{\eta_0}{\gamma}\tilde{p}_y \cos\beta - \frac{\Phi(\gamma)}{\sqrt{\gamma^2-1}}\tilde{p}_x,$$

$$\gamma = \sqrt{1+\tilde{p}_x^2+\tilde{p}_y^2+\tilde{p}_z^2},$$

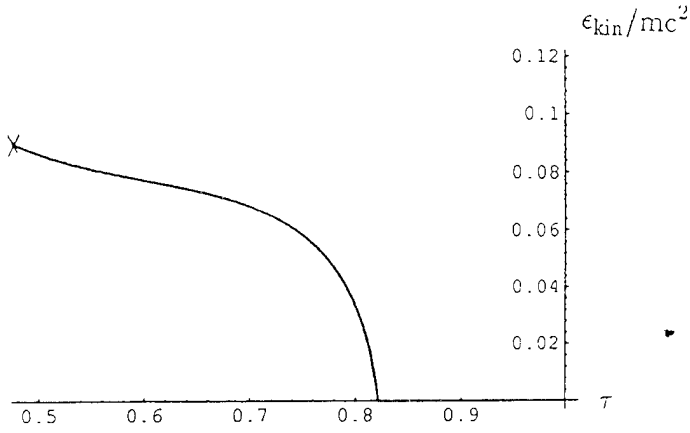
The dimensionless momentum $\tilde{p}_{x,y,z} = p_{x,y,z}/mc$, τ is the dimensionless time and β is the angle between **E** and **B**.

Equations were integrated numerically. Results of the computation are discussed separately for:

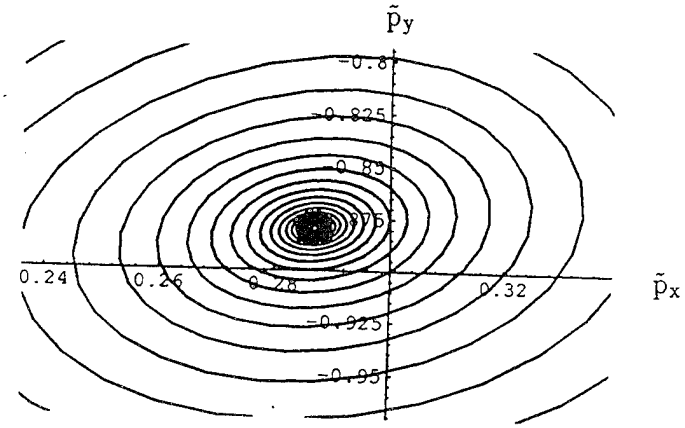
1. E⊥B, i.e. β=90°. In this case the momentum is fading along the axes z, so essentially electrons are moving in the x-y plane.
2. E ∥ B, i.e β=0.
3. Arbitrary β.


$\tilde{p}_x$
0.05
0.1
0.15
0.2
0.25
0.3
-0.05
-0.1
-0.15
-0.2
-0.25
-0.3
$\tilde{p}_y$

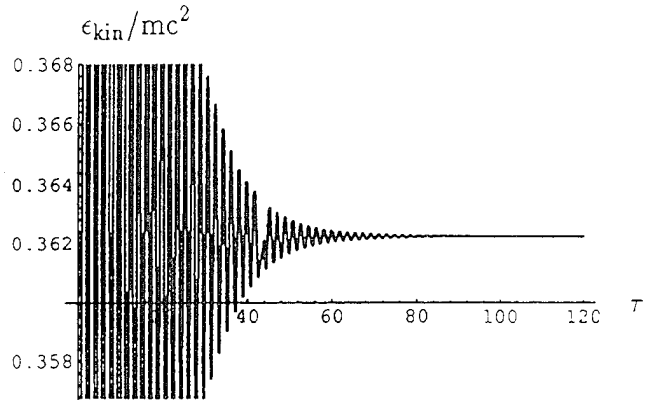
a)


ϵ_{kin}/mc^2
0.12
0.1
0.08
0.06
0.04
0.02
0.5
0.6
0.7
0.8
0.9
τ

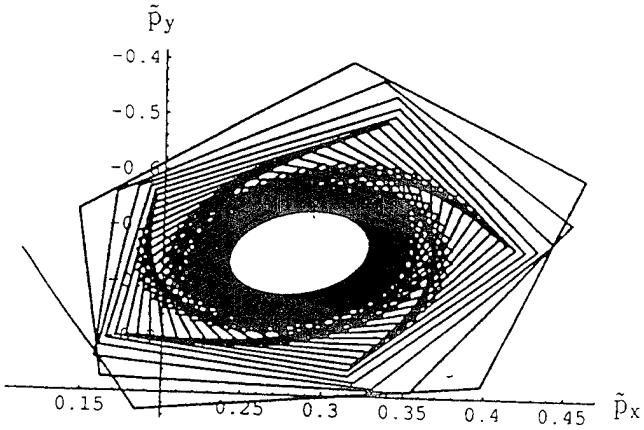
b)


$\tilde{p}_y$
-0.8
-0.825
-0.85
-0.875
-0.9
-0.925
-0.95
0.24
0.26
0.28
0.32
$\tilde{p}_x$

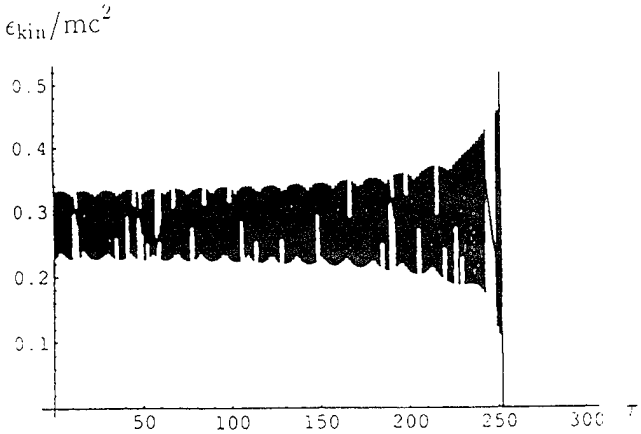
a)


ϵ_{kin}/mc^2
0.368
0.366
0.364
0.362
0.358
40
60
80
100
120
τ

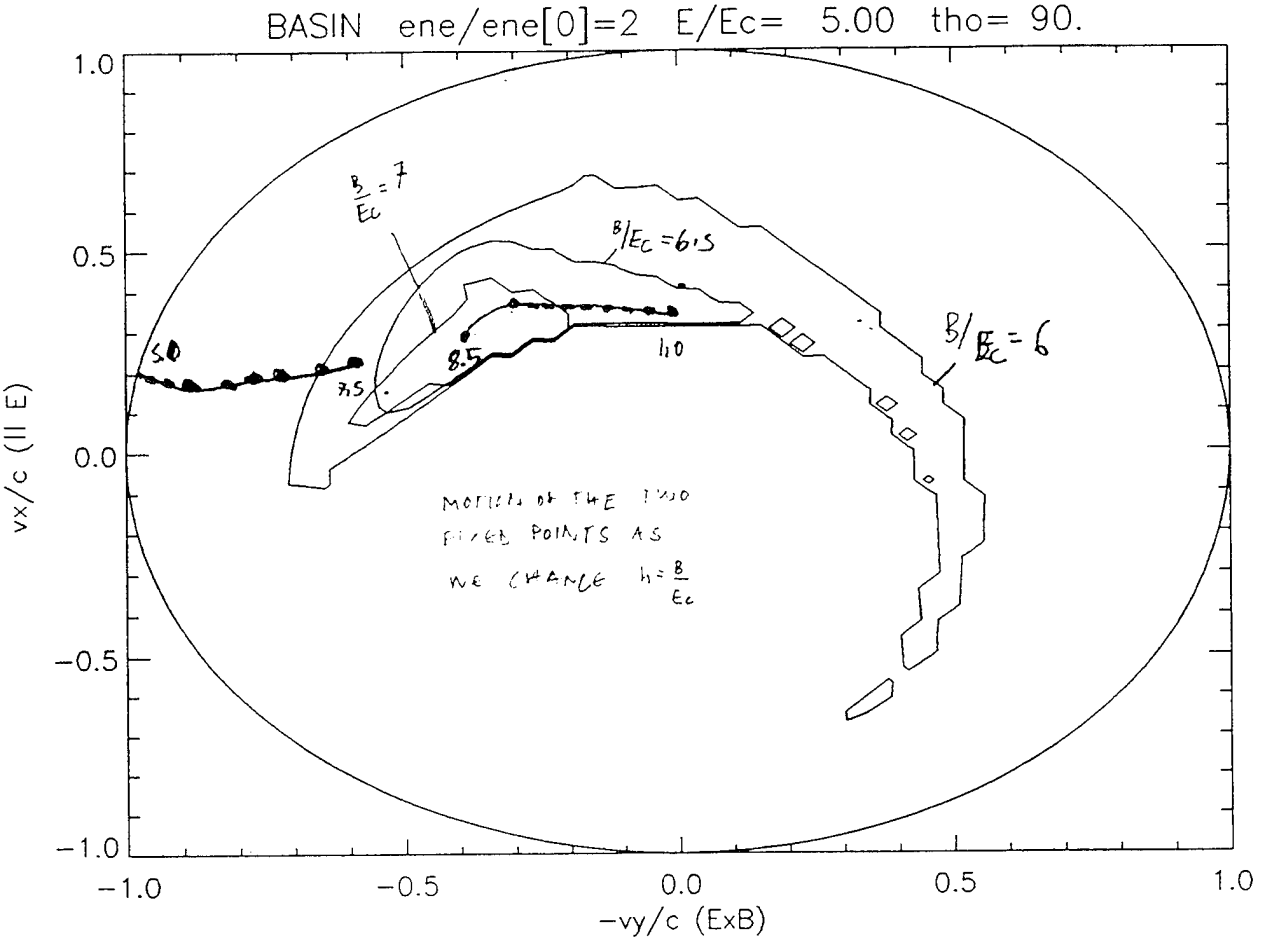
b)

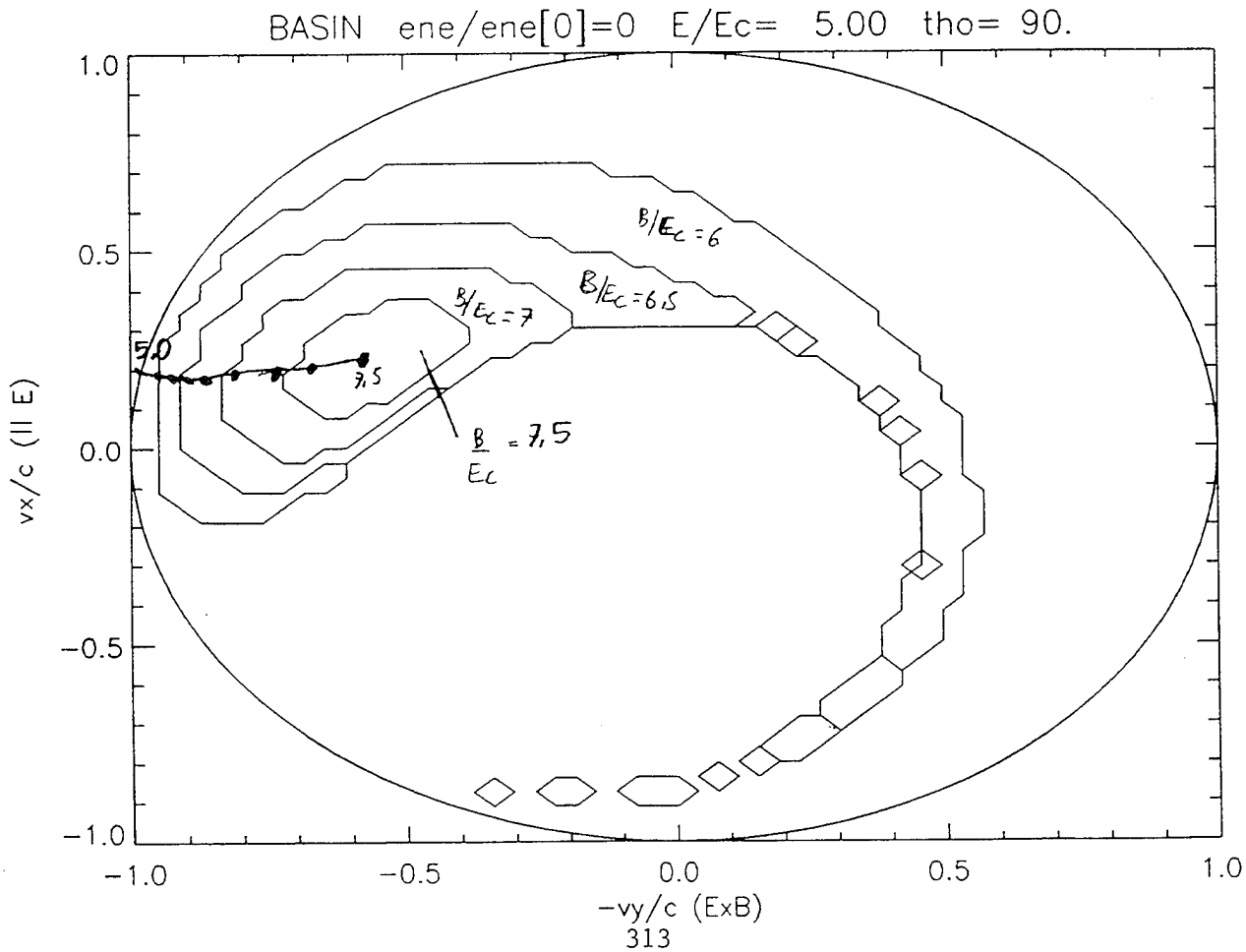

$\tilde{p}_y$
-0.4
-0.5
0.15
0.25
0.3
0.35
0.4
0.45
$\tilde{p}_x$

a)


ϵ_{kin}/mc^2
0.5
0.4
0.3
0.2
0.1
50
100
150
200
250
300
τ

b)


BASIN ene/ene[0]=2 E/Ec= 5.00 tho= 90.
B/Ec = 7
B/Ec = 6.5
B/Ec = 6
5.0
7.5
8.5
11.0
MOTION OF THE TWO FIXED POINTS AS WE CHANGE h = B/Ec
vx/c (II E)
-vy/c (ExB)
1.0
0.5
0.0
-0.5
-1.0


BASIN ene/ene[0]=0 E/Ec= 5.00 tho= 90.
B/Ec = 6
B/Ec = 6.5
B/Ec = 7
B/Ec = 7.5
5.0
7.5
vx/c (II E)
-vy/c (ExB)
1.0
0.5
0.0
-0.5
-1.0

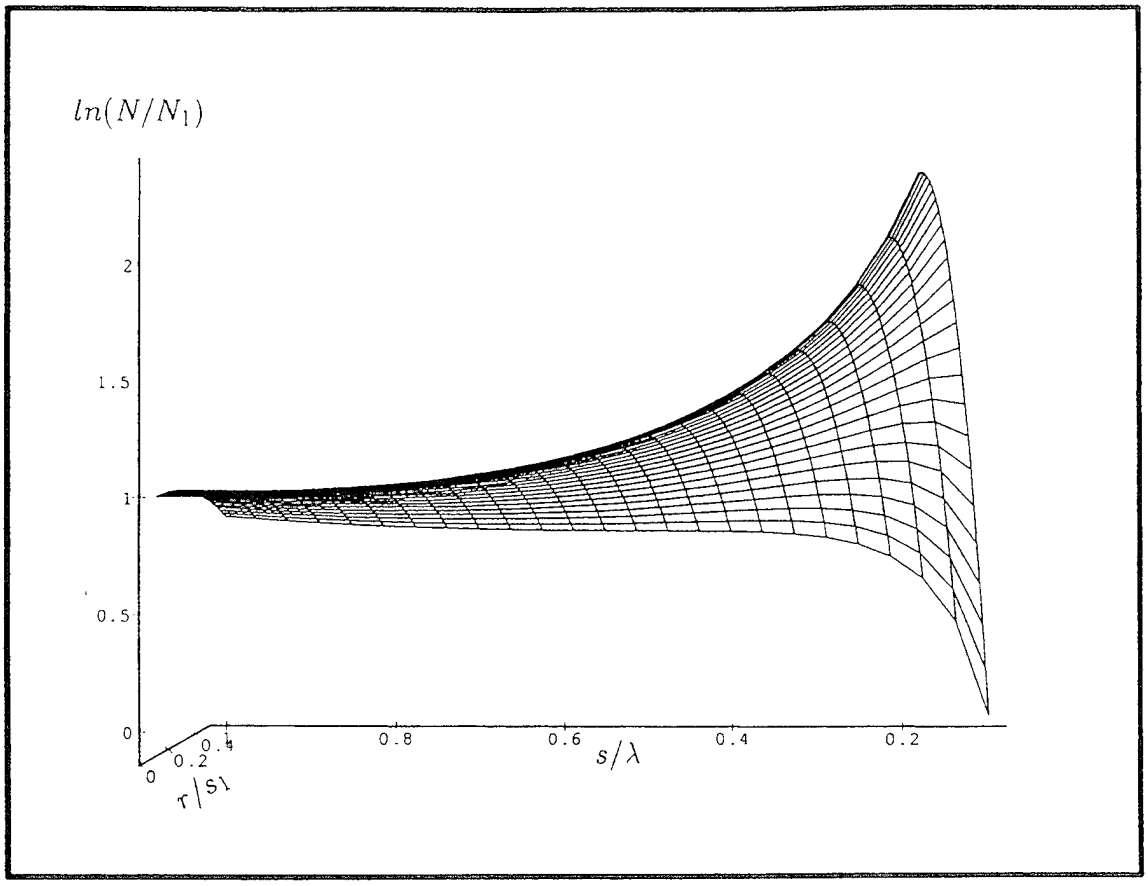
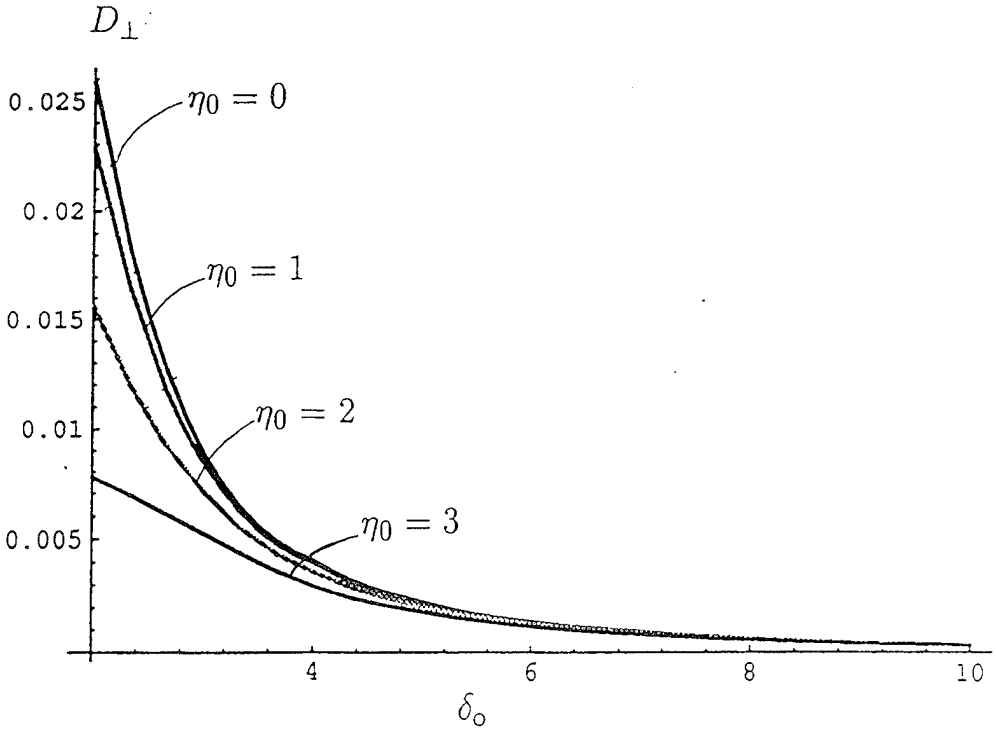
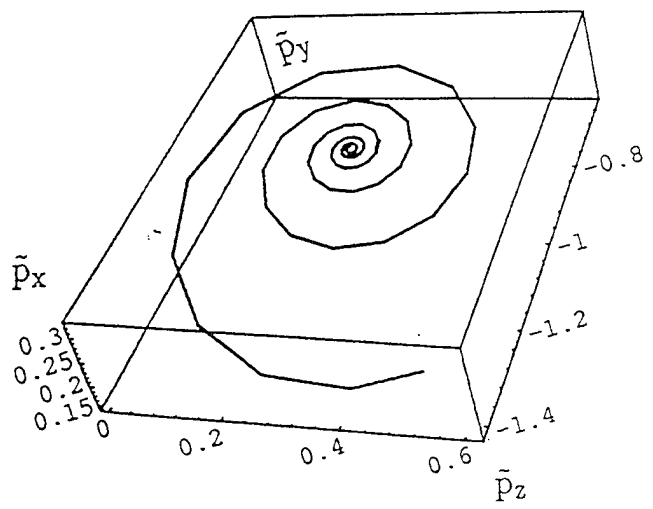

$ln(N/N_1)$
2
1.5
1
0.5
0
0.8
0.6
0.4
0.2
s/λ
0.2
0
$r/s\lambda$

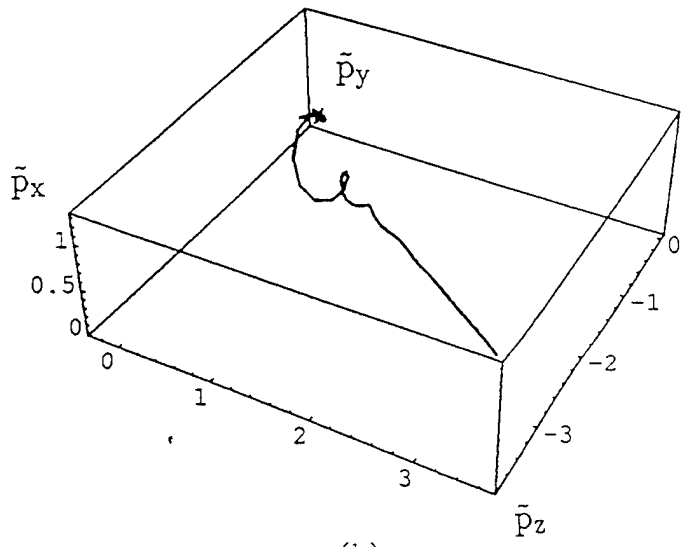
Fig 7


$D_\perp$
0.025
0.02
0.015
0.01
0.005
$\eta_0 = 0$
$\eta_0 = 1$
$\eta_0 = 2$
$\eta_0 = 3$
4
6
8
10
δ_o



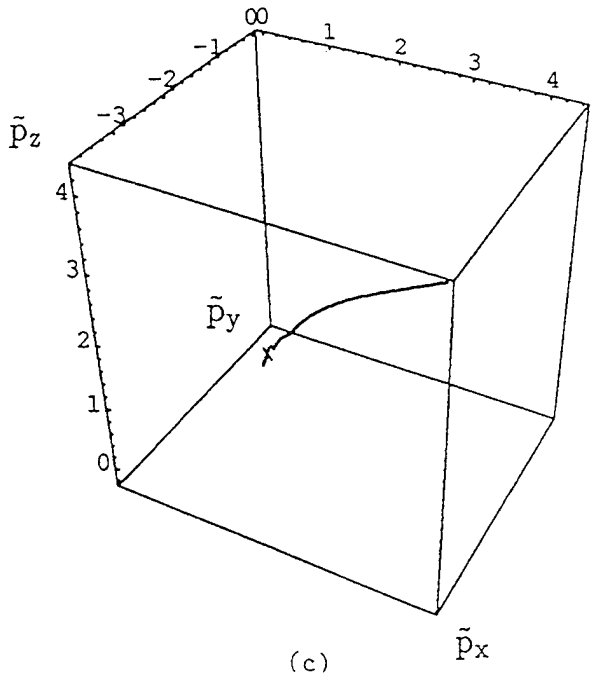
(a)

$\beta = 85^\circ$



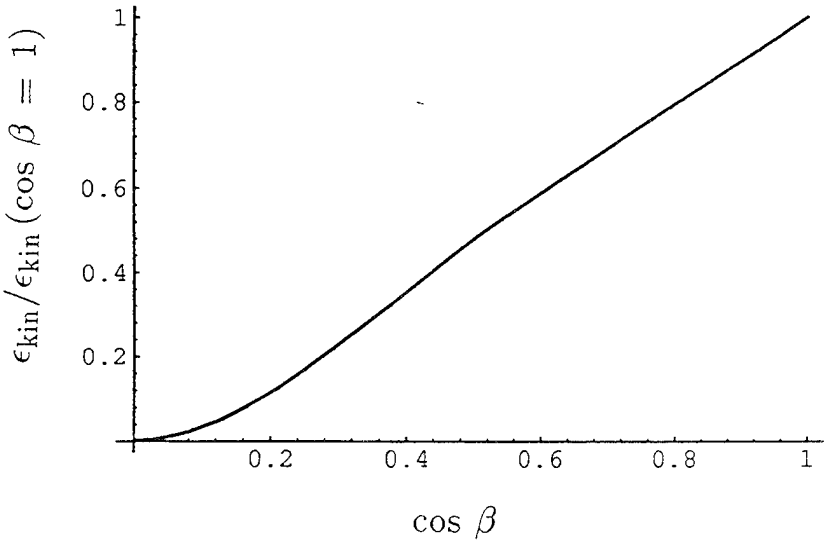
(b)

$\beta = 80^\circ$



(c)

$\beta = 60^\circ$



Conclusions

• Physics of the runaway discharge in laminar E, B fields is determined by the angle β between E and B, and by their ratio E/B.

• Three different ranges of the angle β were distinguished:

$80° < \beta \leq 90$ the runaway discharge develops only if the ratio E/B is less than a certain critical value; the runaway electrons reach a steady state. At high altitude the runaway discharge emerges into conventional breakdown.

$0° < \beta \leq 60°$ the electrons moving along the direction of the magnetic field driven by a $E \times \cos\beta$ component of the electric field, and gain the energy unlimitedly. The magnetic field manifests itself by pitching the runaway discharge.

$60° < \beta \leq 80°$ is the transient range. Electron trajectories are twisted by the magnetic field at low energy range. Electron then gains energy along a straight trajectory.

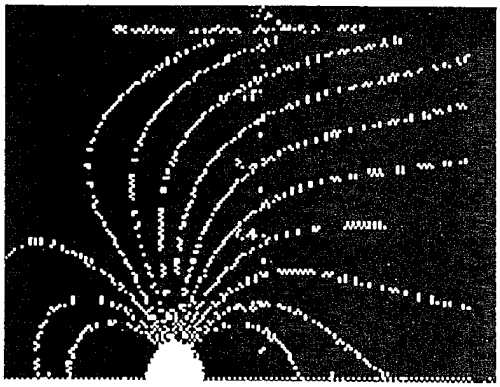
• Runaway separatrix is obtained, which separates momentum space into two regimes: those electrons which possess trajectories that take them into higher energies, and other electrons which possess trajectories leading to zero energy.

• Characteristic time required for the creation of a secondary runaway electron and the mean free path of the runaway electron are found.

On the Structure of the Red Sprites Lightning as a fractal antenna

J. Valdivia, K. Papadopoulos, G. M. Milikh

SPACE AND PLASMA PHYSICS



Dept. of Physics
Dept. of Astronomy

UNIVERSITY OF MARYLAND, College Park, MD 20742

Supported by NSF grant

HIGH ALTITUDE LIGHTNING

OBSERVATIONS —> SPRITES!!

- Sentman et al. [1995]
- Winckler et al. [1994]

- Extreme structures
- Multiple scale lengths
- Resembles a fractal

THEORY —> SPRITES!!

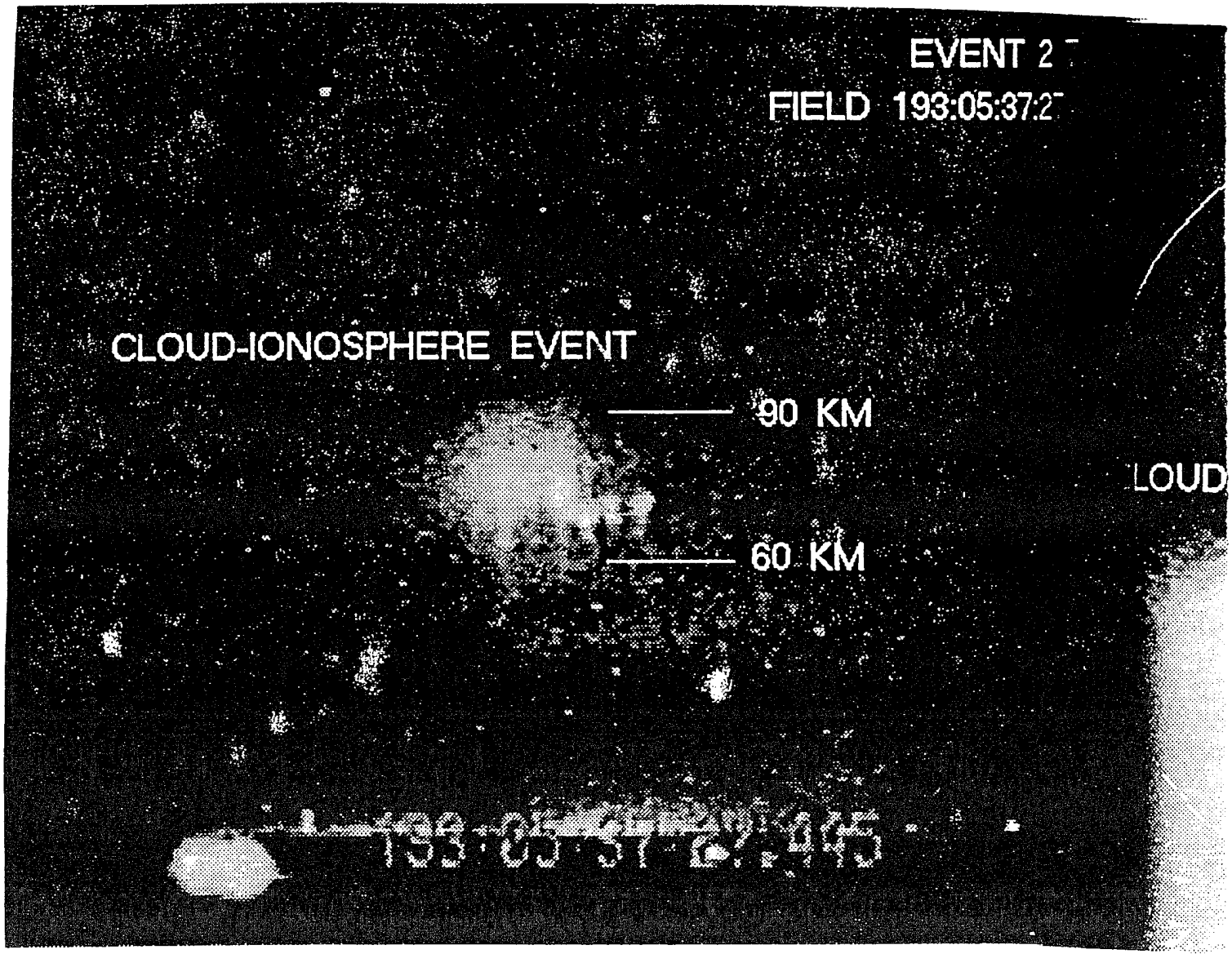
G. Milikh, K. Papadopoulos, C. Chang, et al [1995]

- Energetic tails of D-Region electrons

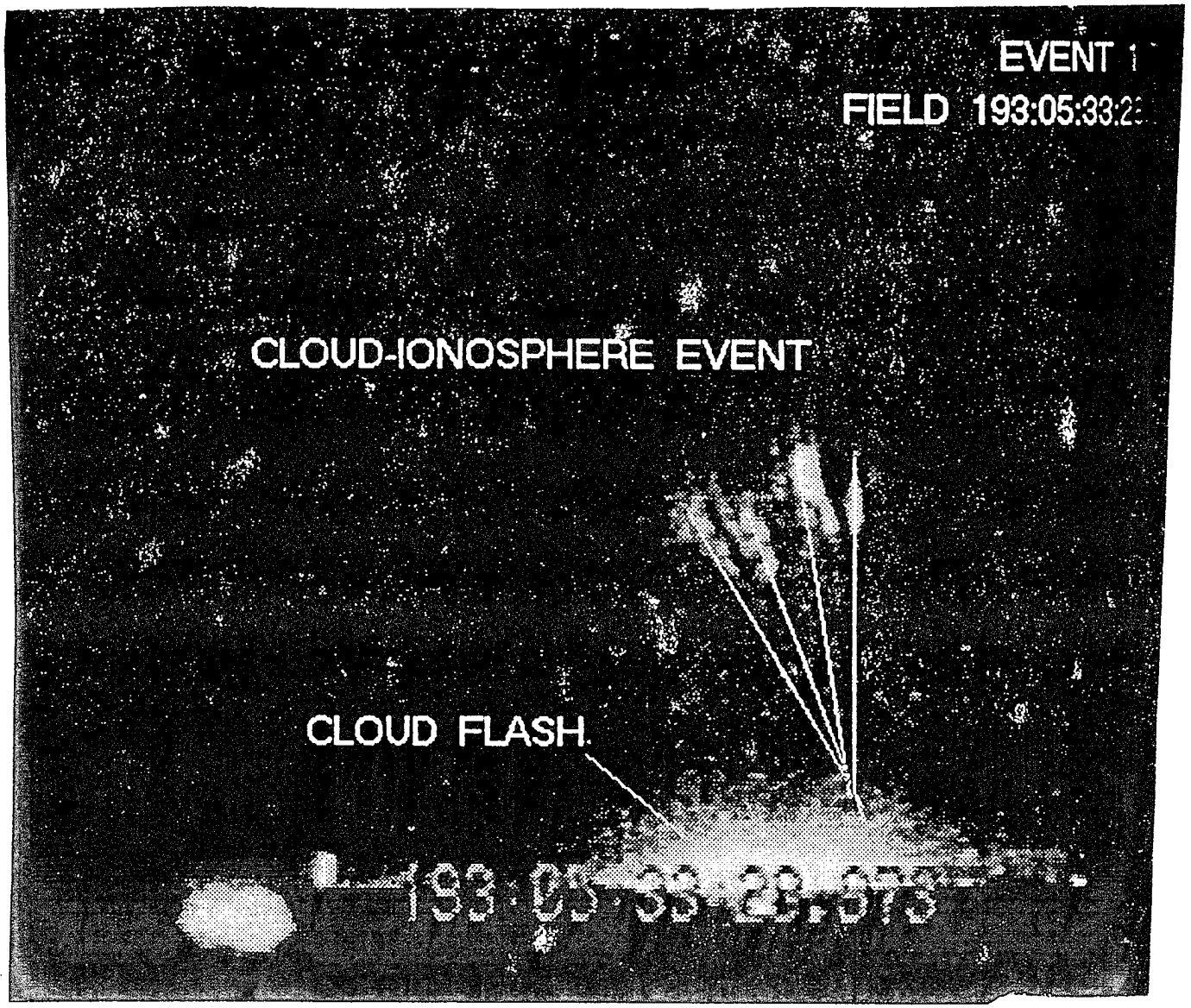
- Created by EMP fields due to

—> Horizontal intercloud discharge!!

(TWO CASES OF SPRITES)



- Winckler et al. [1994]



- Winckler et al. [1994]

HORIZONTAL DISCHARGES

- Spider Lightning

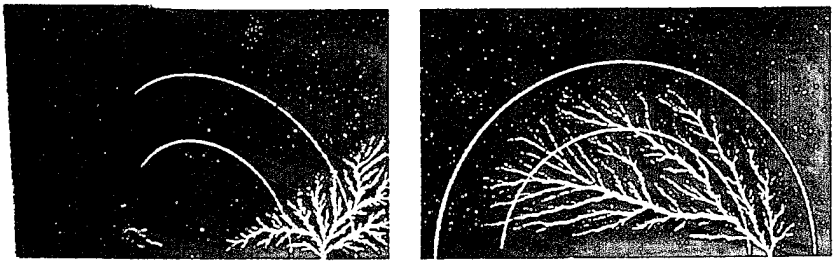
- Resemble Lichtenberg patterns

    —> Dielectric discharges

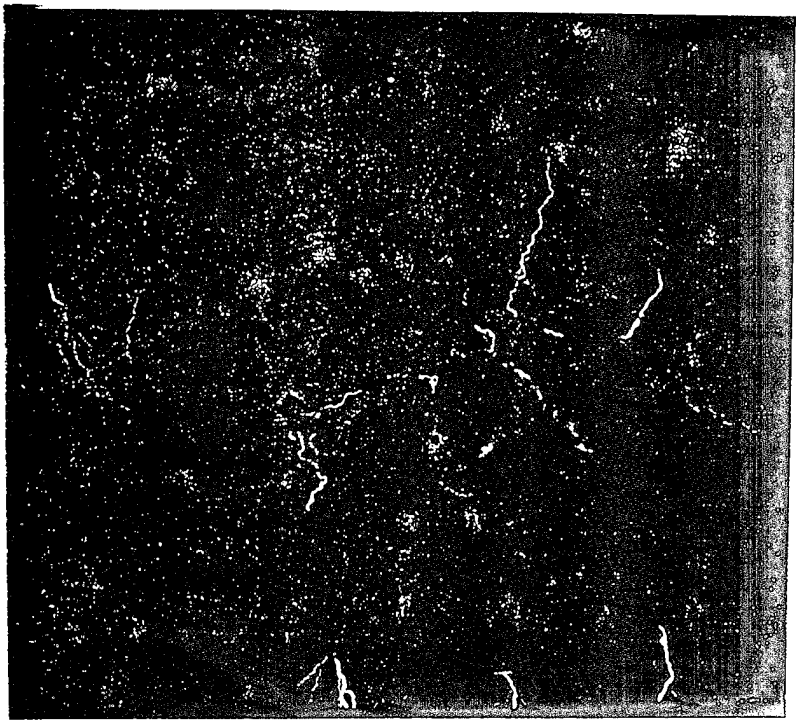
    —> Fractal with space filling properties

    —> Dimension ~ 2

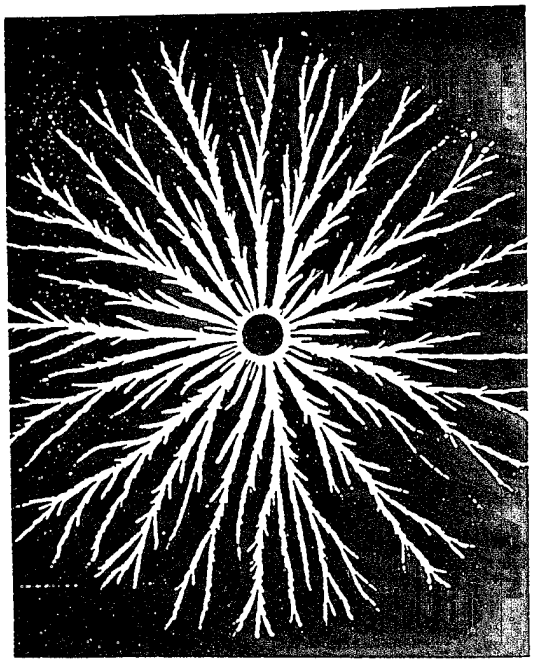
(LICHTENBERG PATTERN and LIGHTNING)



- Williams [1988]



- Williams [1988]



LICHTENBERG

What is the RELATION to cloud discharge?

- Discharge as a FRACTAL antenna array
- Characterization by a fractal dimension
- Radiation pattern depends on Dimension

  Important gain

  Fine scale structure

RADIATION PATTERN

- Use hertz vector !

$$\Pi(x,w) = \sum_{\{\theta_o\}} \frac{i}{w} \int_0^L I(s,w) \frac{e^{ik\|x-r_r-l\|}}{\|x-r_r-l\|} dl \qquad (1)$$

$$I(s,w) = I(w) e^{i\frac{w}{c}(r+l)}$$

$$B = -ik \nabla \mathrm{x} \Pi(x,w)$$
$$E = \nabla \mathrm{x} \nabla \mathrm{x} \Pi(x,w) \qquad (2)$$

- Compute far field !

- Make a CANTOR set out of a ring $\{\theta_o\}$

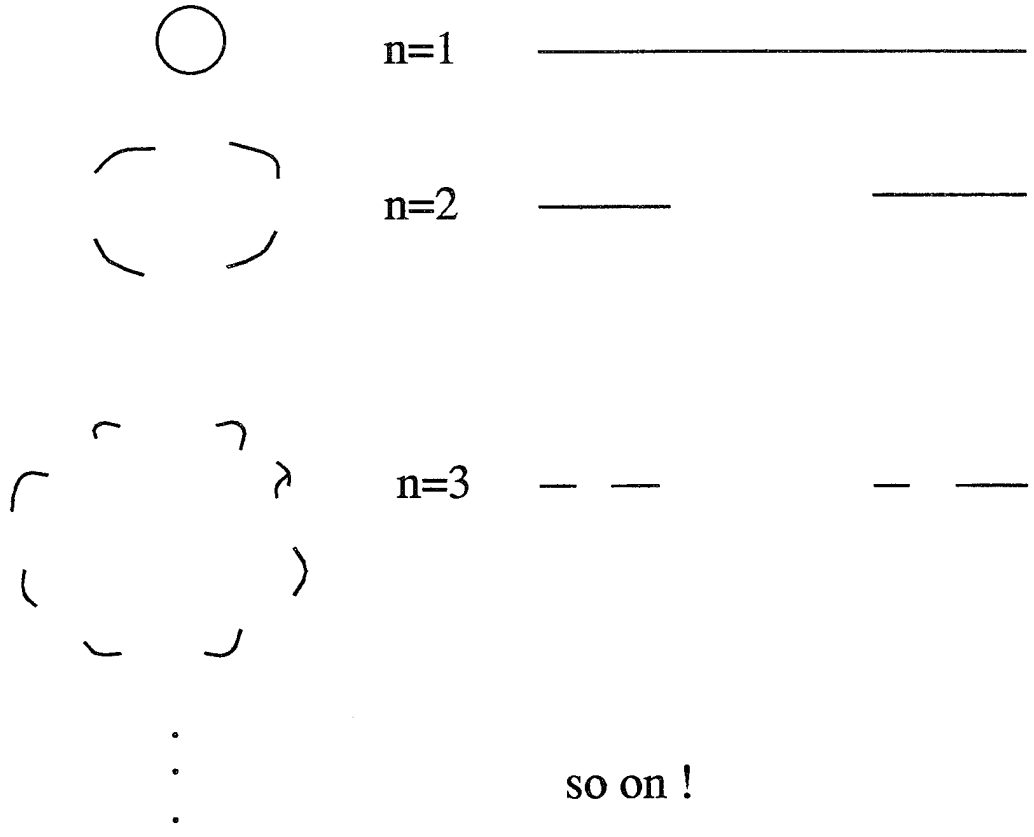
  Specifies the dimension

  Radially "peel" the cantor set

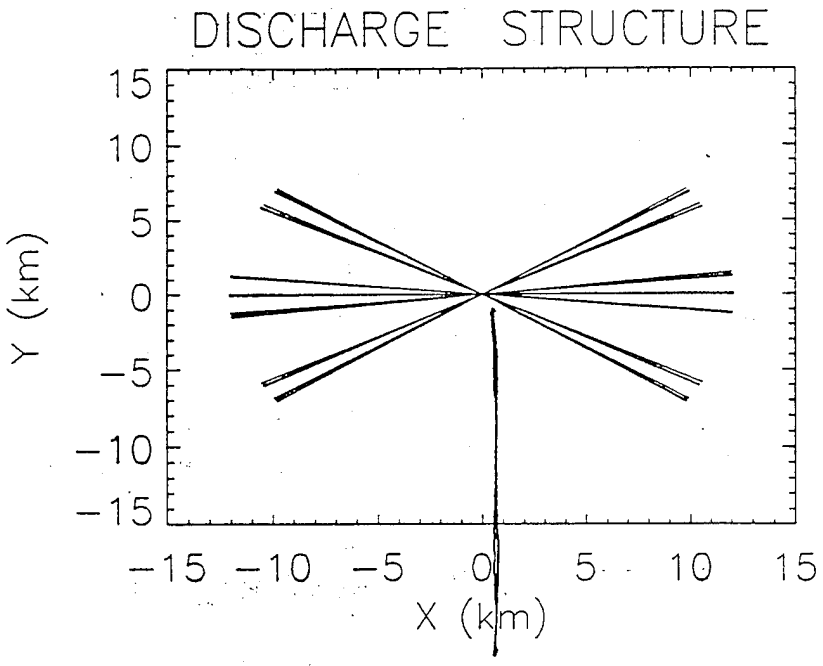
(CANTOR SET AND PEELING)

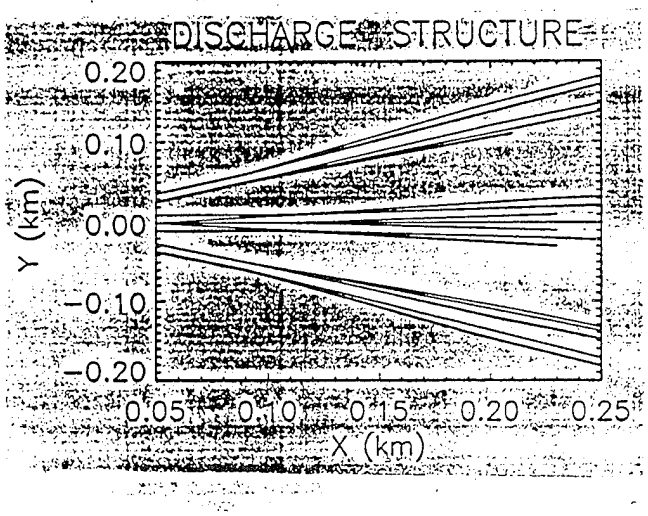


Line elements -> Fractal pattern
Werner et al. [1995]

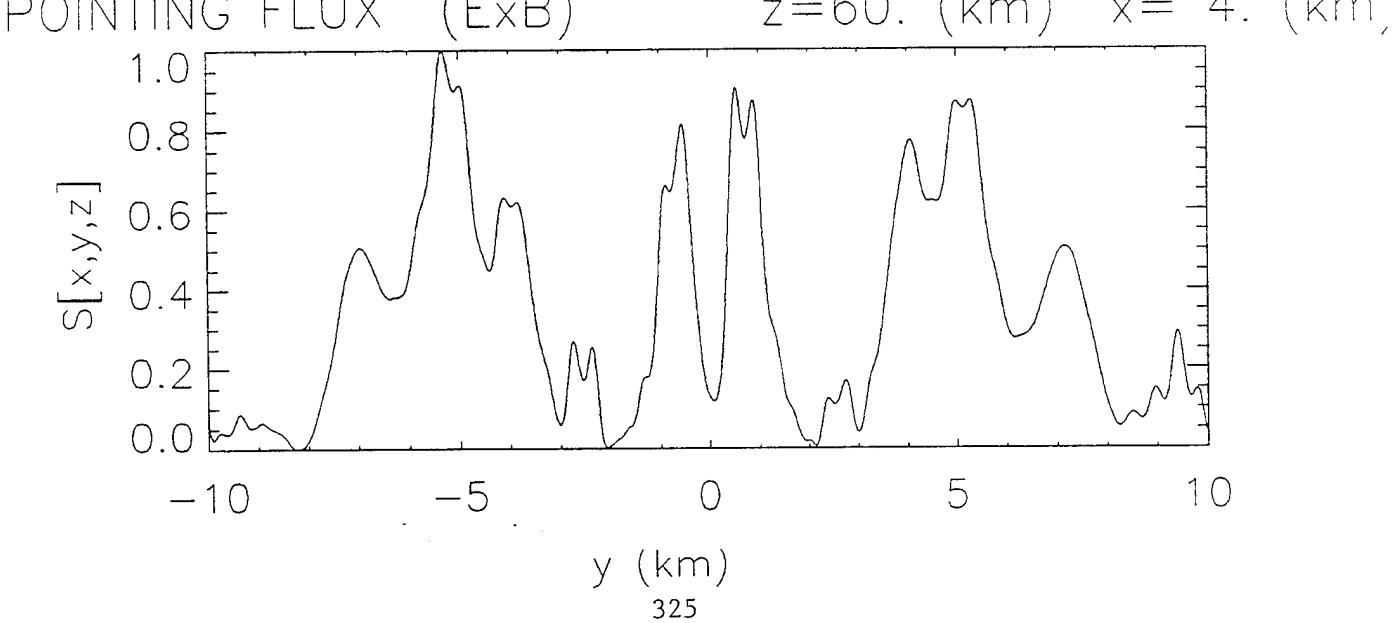


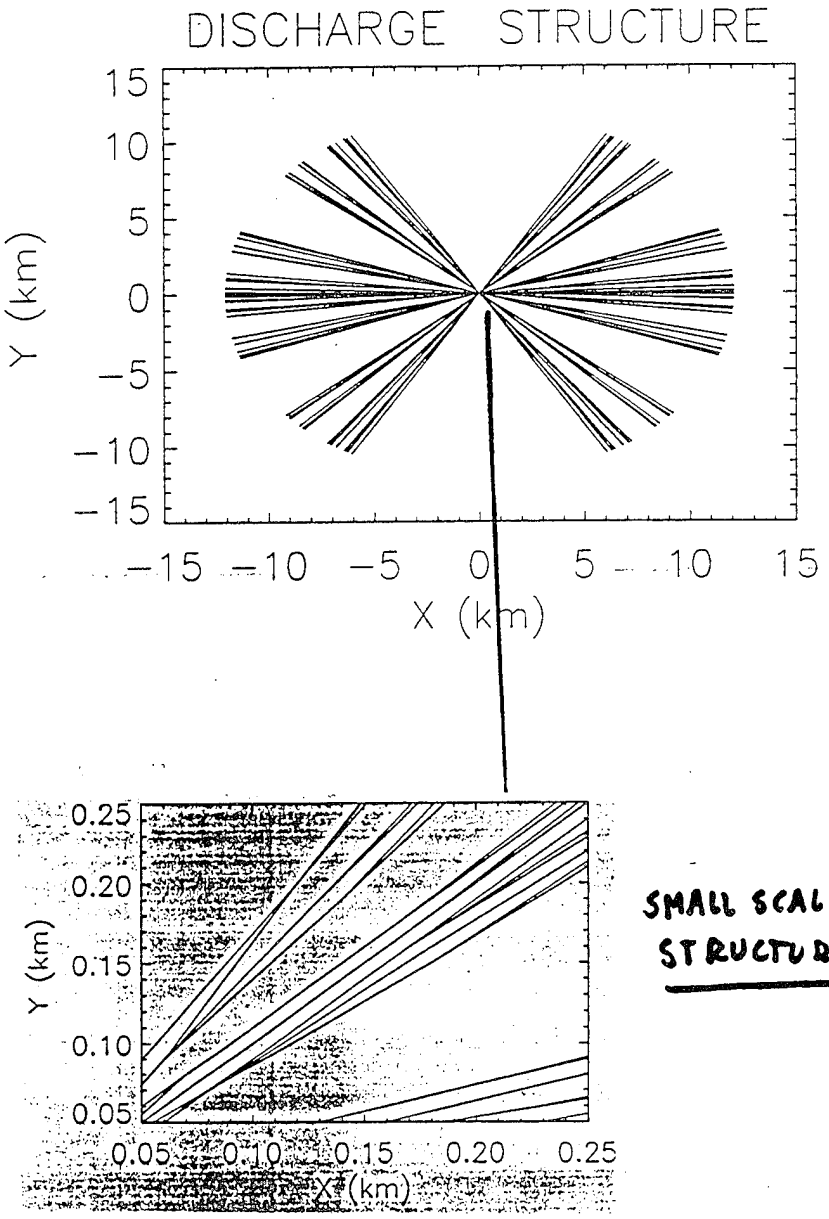
$\nu = 5/2$



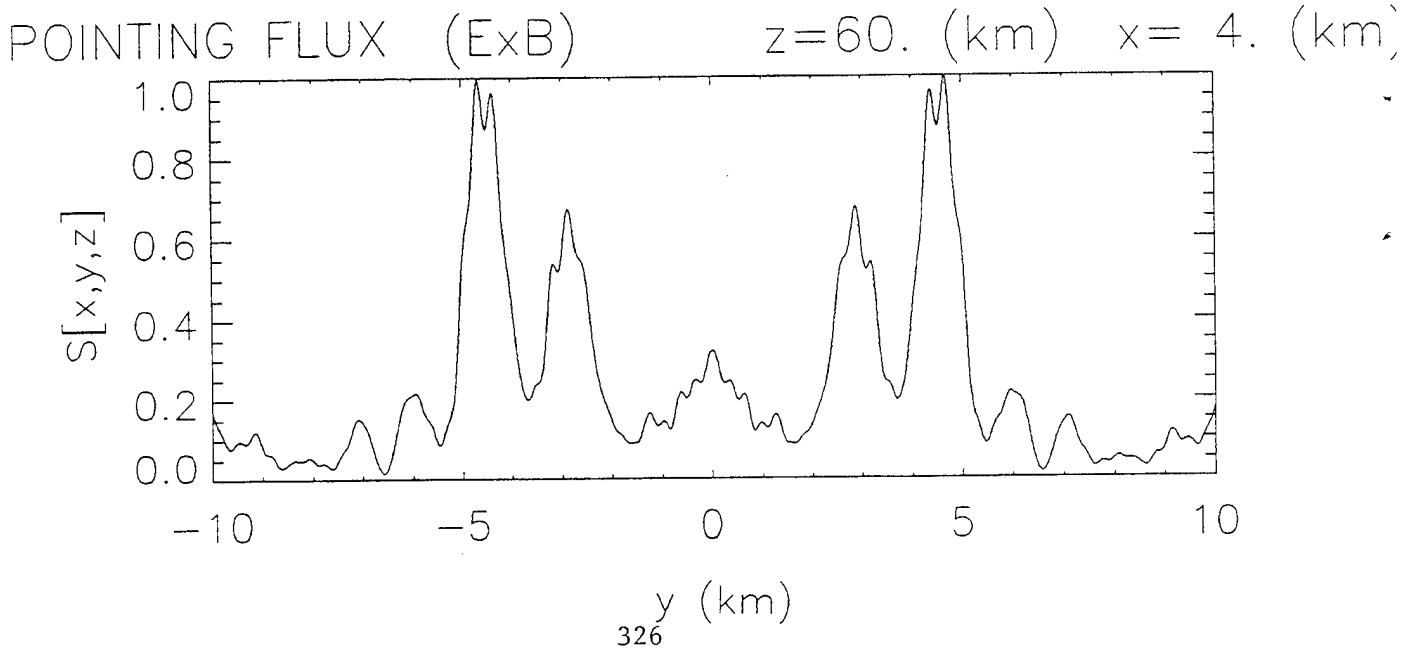


SMALL SCALE STRUCTURE





SMALL SCALE STRUCTURE.



DEPENDENCE ON DIMENSION

- Power density depends on dimension

- Gain depends on dimension

  Large gain can be obtained

- Structure depends on dimension

  Large scale

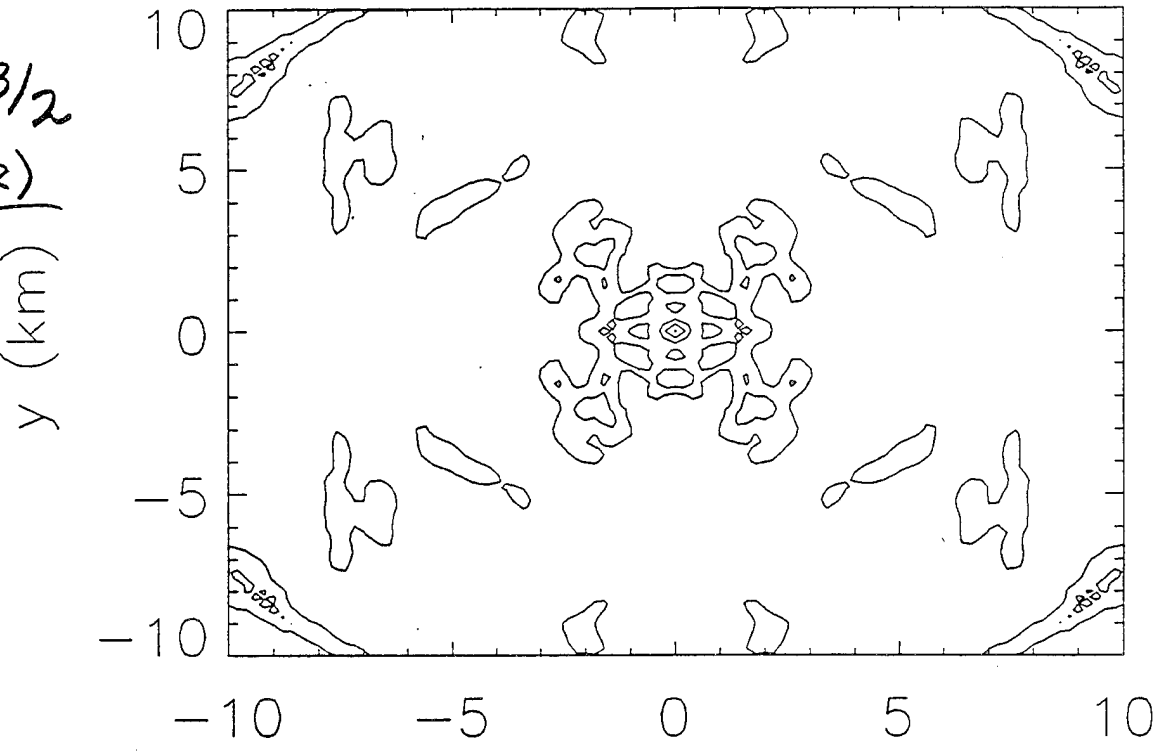
  Small scale

- Large scale structure insensitive to details
- Controlled mainly by dimension

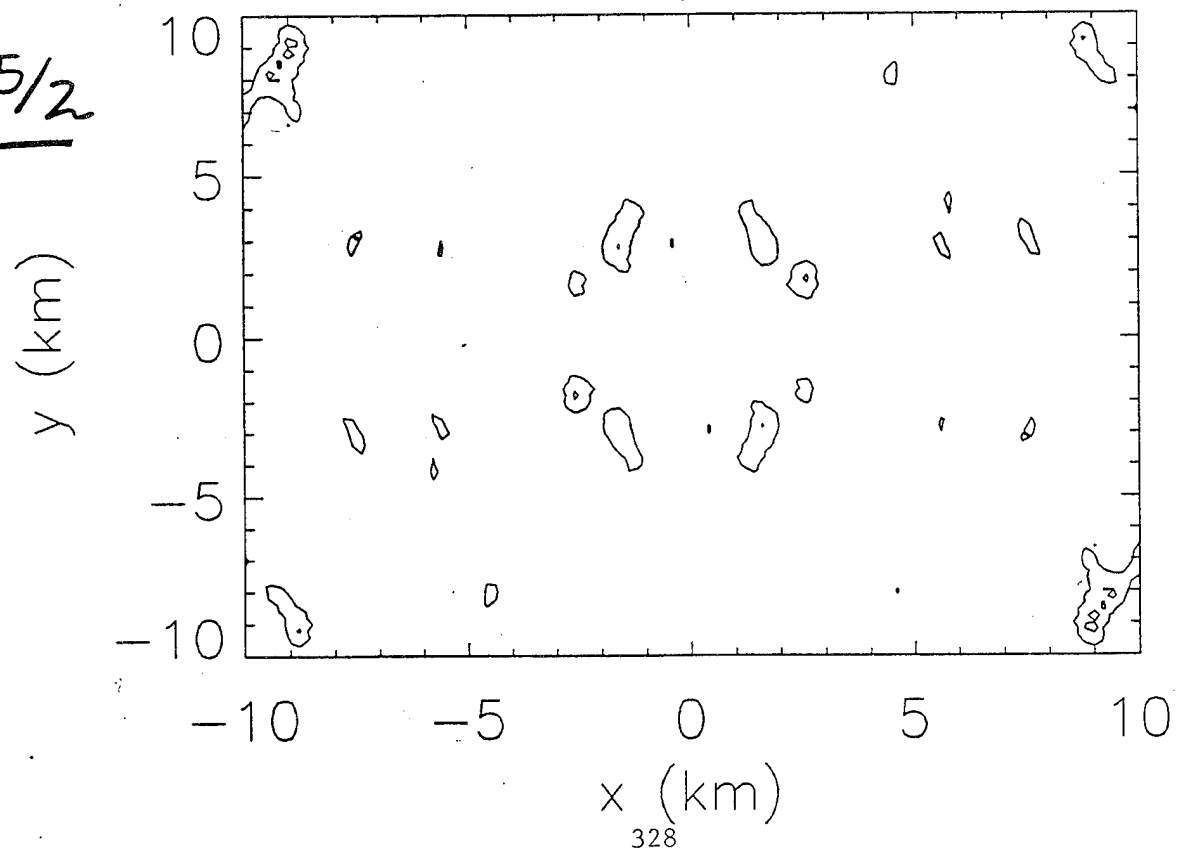
  —> General result !!

(CASES OF 2 DIMENSIONS with discharges)

$\alpha = 3/2$ (CANTOR)



$\alpha = 5/2$



HOW TO PROBE INTERCLOUD DISCHARGE?

- Direct correspondence between

  Dimension of discharge
  radiation pattern that causes sprites

- Connection can be made concrete!!

FURTHER STUDY —> As a general problem

- study full spatio-temporal structures
- Match for near field also!
- Applications in communications

CONCLUSIONS

- Radiation pattern due to horizontal discharge
- Associate with Sprites

- Dimension of discharge controls

  Power gain

  Large scale structure

- Large scale structure insensitive to details

- Only depends mainly on dimension

- Can be used as a probe to intercloud discharge

Nonequilibrium Infrared Radiative Modeling - Application to Sprites

R.H. Picard, J.R. Winick, W.A.M. Blumberg, Phillips Laboratory / Geophysics, Bedford, Mass., USA

P.P. Wintersteiner, ARCON Corporation, Waltham, Mass., USA

R.A. Armstrong, J.A. Shorter, Mission Research Corporation, Nashua, N.H., USA

AFOSR / PL Workshop on Sprites & Blue Jets

Hanscom AFB

18-19 Oct 1995

Nonequilibrium Infrared Radiative Modeling - Application to Sprites

R H Picard, J R Winick, W A M Blumberg (Phillips Laboratory, Geophysics Directorate, Hanscom AFB, MA 01731)
P P Wintersteiner (ARCON Corporation, Waltham, MA 02154)
R.A. Armstrong, J.A. Shorter (Mission Research Corporation, Nashua, NH 03062)

Estimating infrared emission from atmospheric high-altitude lightning is complicated by the transient nature of the excitation process and by the multidimensionality of the ensuing radiative transfer. This is especially true for the 4.3-μm CO_2 ν_3-mode rovibrational emission, due to a combination of the strength of the transitions, resulting in large opacities, and the slowness of the vibrational energy transfer to CO_2 from the large N_2 vibrational energy reservoir.. Photon trapping occurs due to the self-absorption, lengthening the effective lifetimes of the radiating vibrationally-excited states and broadening the excitation region. As a result, the magnitude, the shape, and the effective relaxation time of the CO_2 vibrational response vary strongly with altitude. We review briefly the nonequilibrium infrared radiative transfer problem in the quiescent and the disturbed atmosphere. Then we show how the ARC (Atmospheric Radiance Code) transient radiative model has been applied successfully to auroral emission data and indicate how it can be modified to predict 4.3-μm emission from sprites. We discuss the input requirements to the radiative model, from data or from discharge models, and make preliminary predictions of 4.3-μm spectral observations relevant to the forthcoming 1996 Summer Campaign.

Outline -

- Background
  - Infrared radiance models / codes
  - The nonequilibrium radiative transfer problem
  - CO_2 4.3–μm nonequilibrium radiance model
- Steady-state line-by-line model for quiescent atmosphere: CIRRIS-1A earthlimb spectra
- Time-dependent band model for aurora - RBFWI auroral data
- Toward a sprites 4.3-μm radiance model
  - Preliminary results
  - Implications for 1996 Summer Campaign
  - Model input needs
- Discussion / conclusions

Application to Sprites

- IR radiation modeling for sprites must deal with several complications:
  - Excitation process *transient*
  - *Multidimensional radiative transfer* (optically thick bands)
- These factors are most stressing for 4.3-μm $CO_2(\nu_3)$ emission
  - Slow vibrational energy transfer from $N_2(v)$ reservoir to $CO_2(\nu_3)$
  - Large transition strength ---> large optical depths
- Consequences for 4.3-μm sprites:
  - Time-dependent (*transient*) effects important
    - Steady-state band model (SSBM) not adequate
  - *Radiative transfer* affects both excitation & loss
    - Optically thin, opaque, & escape-function approximations (EFA) not adequate

IR Emission from High-Altitude Discharges

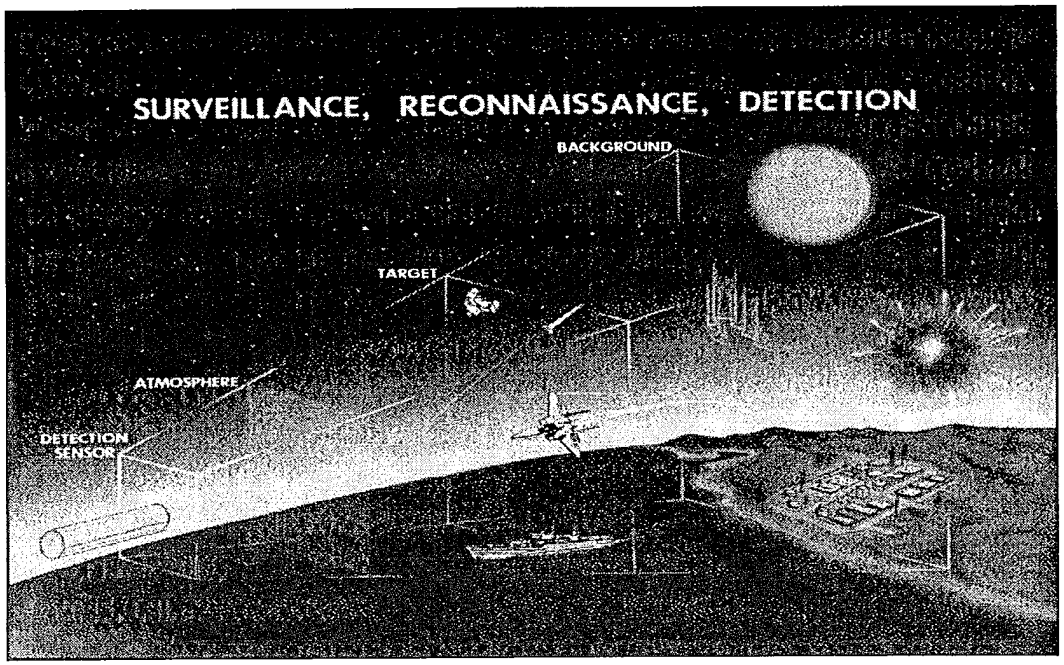
- Phillips Lab / Geophysics has extensive library of state-of-the-art IR radiation models/codes

- Models extensively validated against data for
  - LTE (local thermodynamic equilibrium) atmosphere
  - non-LTE quiescent atmosphere
  - non-LTE energetic-electron-disturbed atmosphere
    - aurora
    - artificial aurora

- These non-LTE models ideally suited to calculate IR radiance from sprites

PL Atmospheric and Celestial Background Effects Code Program

Code Overview



- 1-D Spectral Radiance Codes
  - MODTRAN 3.0
  - MOSART 1.4
  - SHARC 3.0
  - SAMM 1.0
  - FASCODE 3.0
- 2-D Radiance Structure Codes
  - SHARC 4.0
  - SASS 1.0
  - SAMM 2.0
  - CBSD 2.0
- Integrated Codes
  - PLEXUS 2.0

Non-LTE Models / Codes

- ARC (Atmospheric Radiance Code) - First-principles non-LTE line-by-line (LBL) model, quiescent atmosphere
- AARC (Auroral Atmospheric Radiance Code) - First-principles non-LTE auroral radiance model
  - Line-of-sight radiance: LBL model
  - Radiative excitation: Simple band model, several varieties
- AARC-EFA (Escape-function approximation) - Emitted photons either reabsorbed locally or escape to space, no radiative coupling
- AARC-SSBM (Steady-state band model) - Solve rate equations in steady-state
- AARC-TDBM (Time-dependent band model) - Time-dependent solution of rate equations

The Nonequilibrium (Non-LTE) Radiative Transfer Problem

- Solve coupled equations for monochromatic specific intensity of radiation and species / level population densities

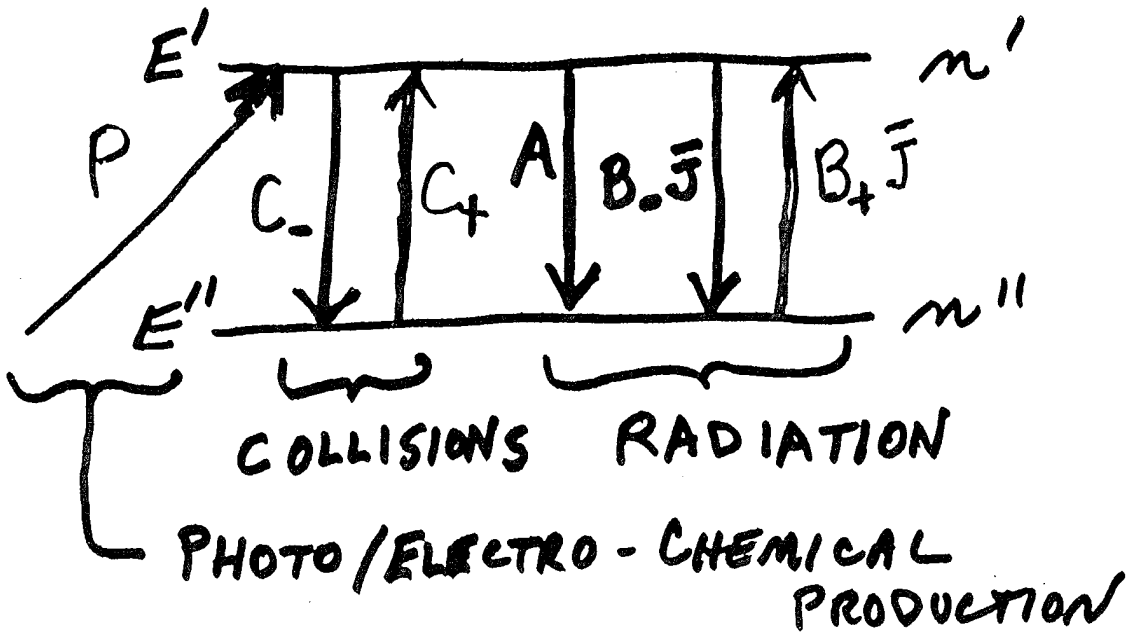
  - Equation of transfer:

$$\frac{dI(\nu)}{d\tau_\nu} = S(\nu) - I(\nu)$$

  - Source function:

$$S = \frac{\frac{n'}{n''}A}{B_+ - \frac{n'}{n''}B_-}$$

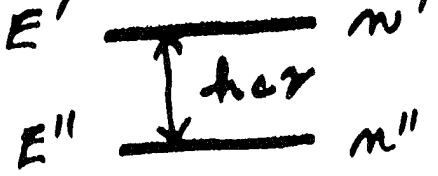
  - Rate equation:



$$\frac{dn'}{dt} = P + (C_+ + B_+\bar{J})\,n'' - (C_- + A + B_-\bar{J})\,n'$$

J = integrated mean intensity = average of I(ν) over absorption line and over solid angle

CONCEPT OF VIBRATIONAL TEMPERATURE T_{vib}



POPULATION RATIO

$$\frac{n'}{n''} = \frac{g'}{g''} e^{-\frac{E'-E''}{k_B T_{vib}}}$$

LTE : $T_{vib} = T$ COLLISIONS DOMINATE

Non-LTE: $T_{vib} \neq T$

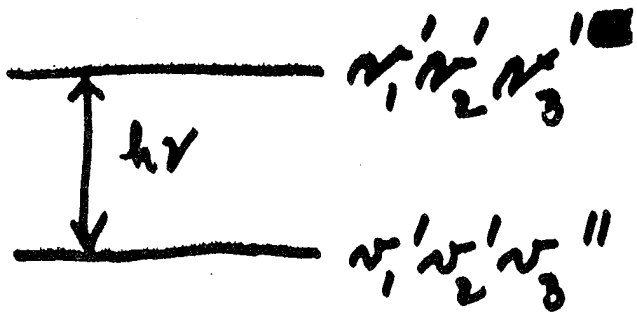
$T_{vib} < T \Longrightarrow$ NON-COLLISIONAL LOSS

$T_{vib} > T \Longrightarrow$ NON-COLLISIONAL PRODUCTION

Production & Loss Processes - $CO_2(\nu_3)$

-Radiative (4.3 μm)

$$CO_2(v'_1v'_2v'_3) \overset{A}{\underset{Bj}{\Leftrightarrow}} CO_2(v'_1v'_2v''_3) + h\nu$$



(solar and earthshine pumped; strong diurnal variation)

-Collisional (V-T)

$$CO_2(v'_1v'_2v'_3) + M \overset{k}{\underset{k'}{\Leftrightarrow}} CO_2(v'_1v'_2v''_3) + M$$

(M=N_2, O_2, O)

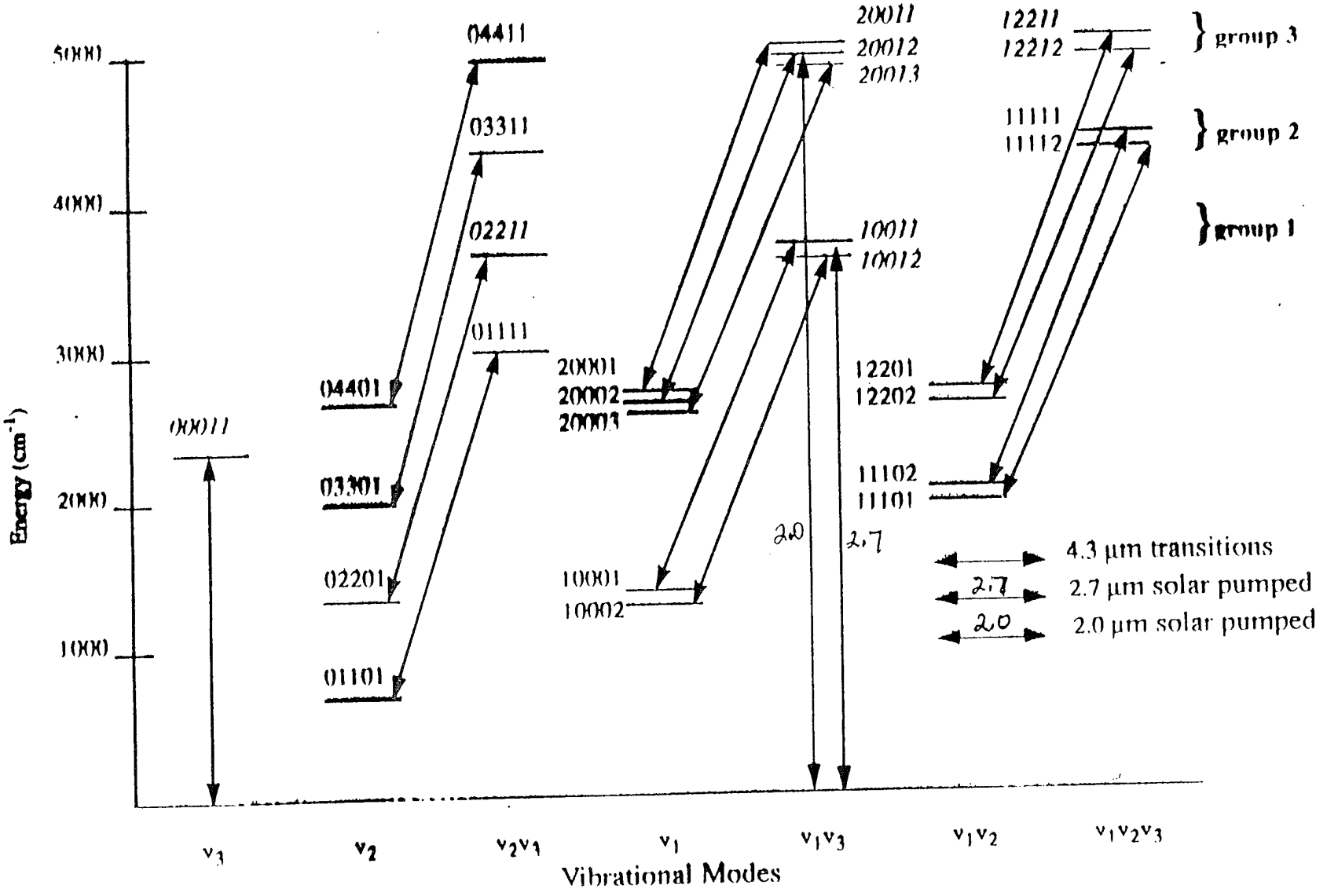
-Vibrational transfer (V-V)

$$CO_2(v'_1v'_2v'_3) + N_2 \overset{k_v}{\underset{k'_v}{\Leftrightarrow}} CO_2(v'_1v'_2(v'_3-1)) + N_2(v=1)$$

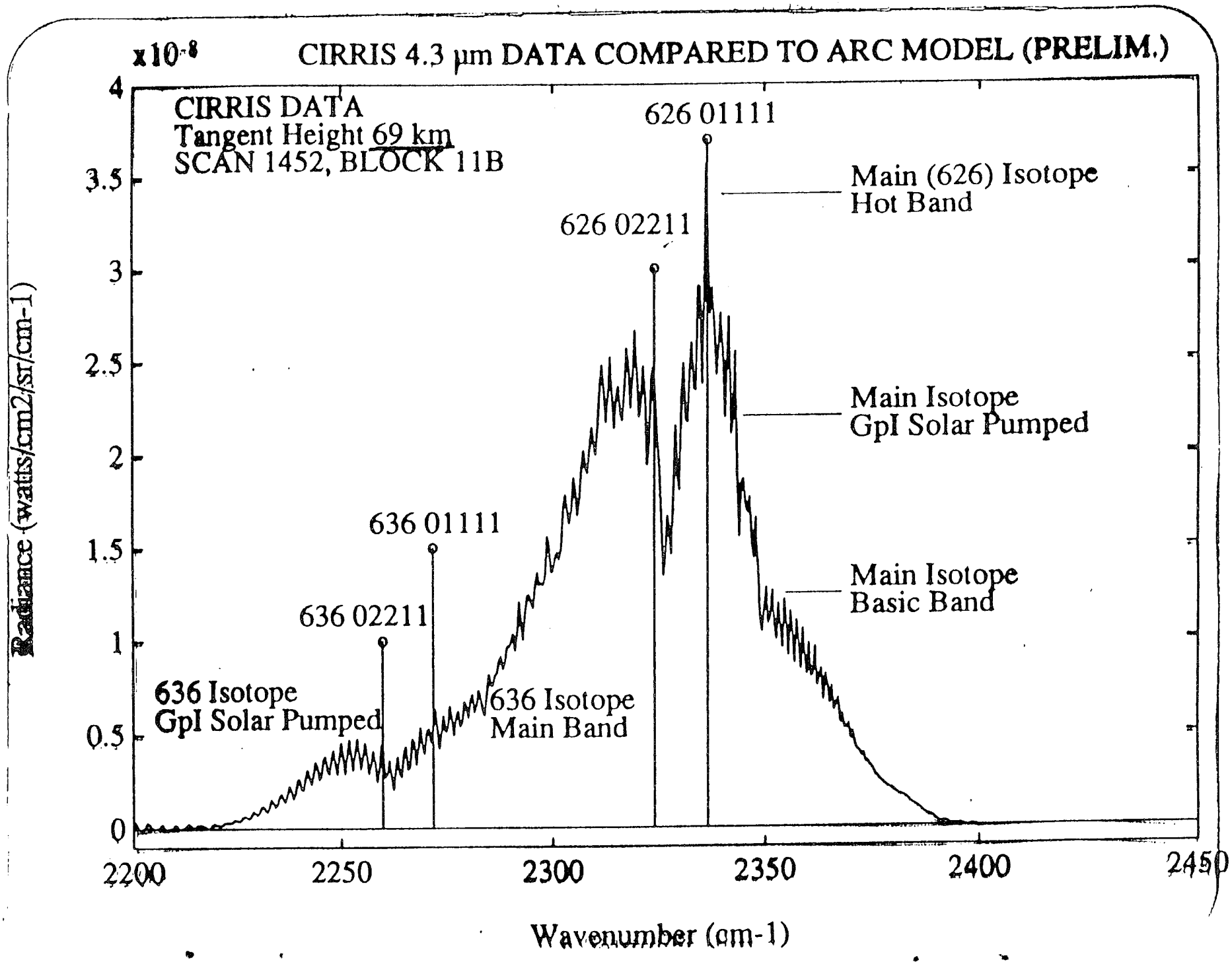
ΔE=19.2 cm^{-1}; $k_v = 5.0 \times 10^{-13}(300/T)^{0.5}$

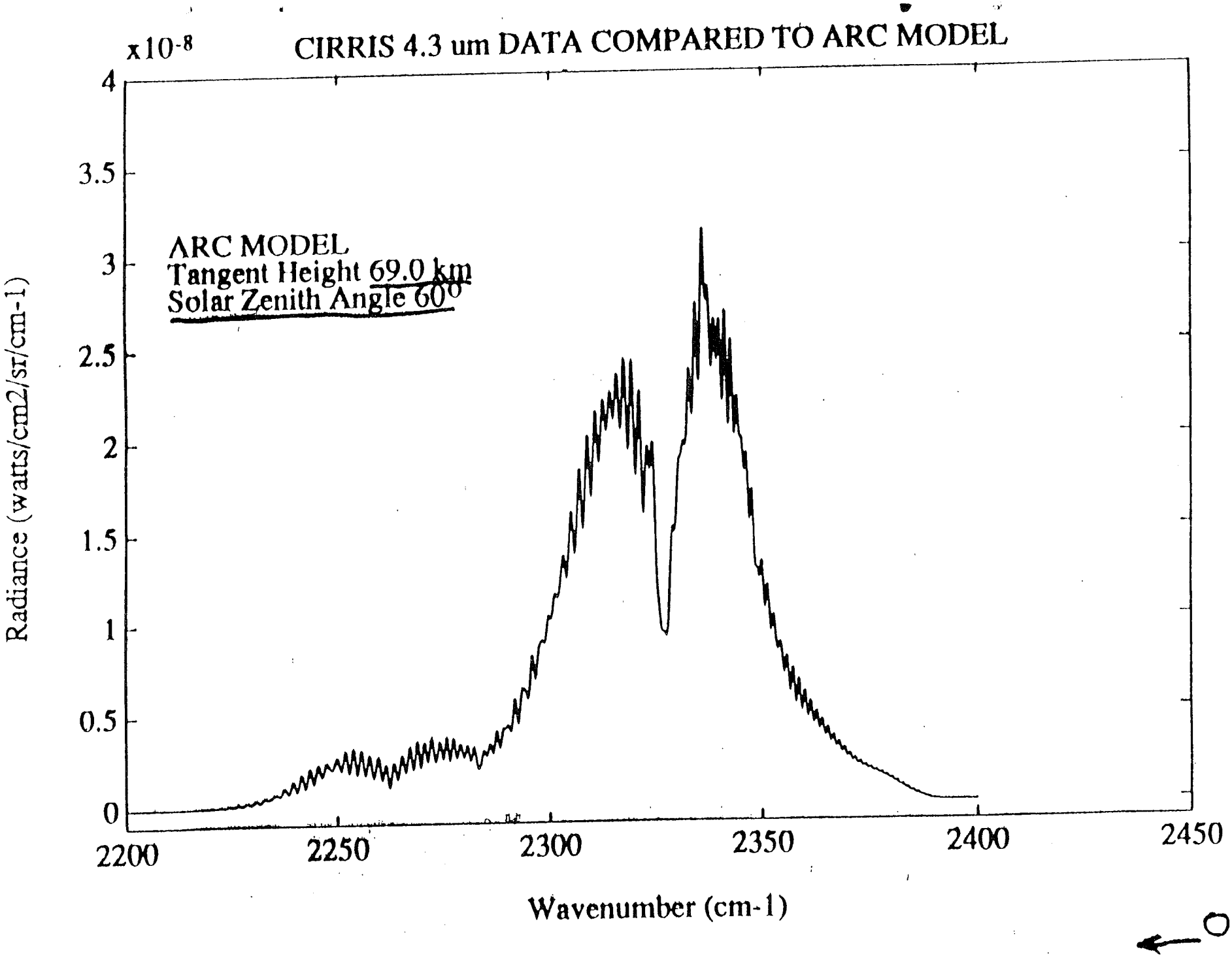
- Electron excitation: $e + N_2 \rightarrow N_2(\nu)$ (INDIRECT)
  $e + CO_2 \rightarrow CO_2(\nu_3)$

CO_2 Energy Diagram of 4.3 μm States



Fig


x10⁻⁸
CIRRIS 4.3 μm DATA COMPARED TO ARC MODEL (PRELIM.)
CIRRIS DATA
Tangent Height 69 km
SCAN 1452, BLOCK 11B
626 01111
626 02211
636 01111
636 02211
Main (626) Isotope
Hot Band
Main Isotope
GpI Solar Pumped
Main Isotope
Basic Band
636 Isotope
GpI Solar Pumped
636 Isotope
Main Band
Radiance (watts/cm2/sr/cm-1)
Wavenumber (cm-1)
4
3.5
3
2.5
2
1.5
1
0.5
0
2200
2250
2300
2350
2400
2450


CIRRIS 4.3 um DATA COMPARED TO ARC MODEL
x10-8
4
3.5
3
2.5
2
1.5
1
0.5
0
ARC MODEL
Tangent Height 69.0 km
Solar Zenith Angle 60°
Radiance (watts/cm2/sr/cm-1)
2200
2250
2300
2350
2400
2450
Wavenumber (cm-1)

Time-Dependent Band Model (TDBM) Assumptions (Currently)

- Plane-parallel atmosphere - *no horizontal radiative transport*
- Weak Isotopic and hot bands assumed to have same vibrational temperature as main band
- No coupling to OH(v) and H_2O(v)
- Includes correctly:
  - neutral collisional excitation / loss (V-T)
  - electron collisional excitation
  - radiative excitation / loss (--> *vertical radiative diffusion*)
  - N_2-CO_2 resonant V-V transfer
  - transient (time-dependent) effects

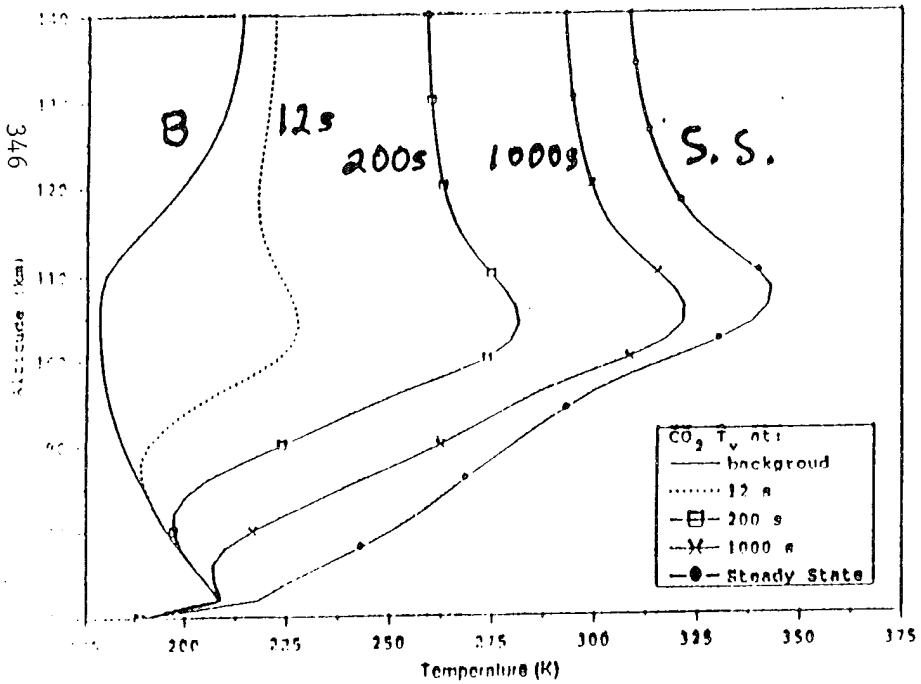
Applications of TDBM

- 4.3-μm aurora -
  - IBC III aurora, sudden initiation, constant dosing
  - IBC II$^+$ aurora - RBFWI data
    - Only 1.3 kR 427.8 nm N_2^+ 1N at time of measurement, significant predosing 190 s earlier peaking at 8 kR 427.8 nm (52 kR 557.7 nm)
    - Moderately hard spectrum: Peak electron energy ~11 keV, altitude of peak dosing 103 km
- 4.3-μm sprite
  - Vertical extent - 40-90 km
  - Horizontal extent - 40 km
  - Electron spectrum - Gaussian, Intensity 10^8 eV/cm^{3}s, E_o~2.5 eV, $\Delta E/E_o$~0.4, Gaussian

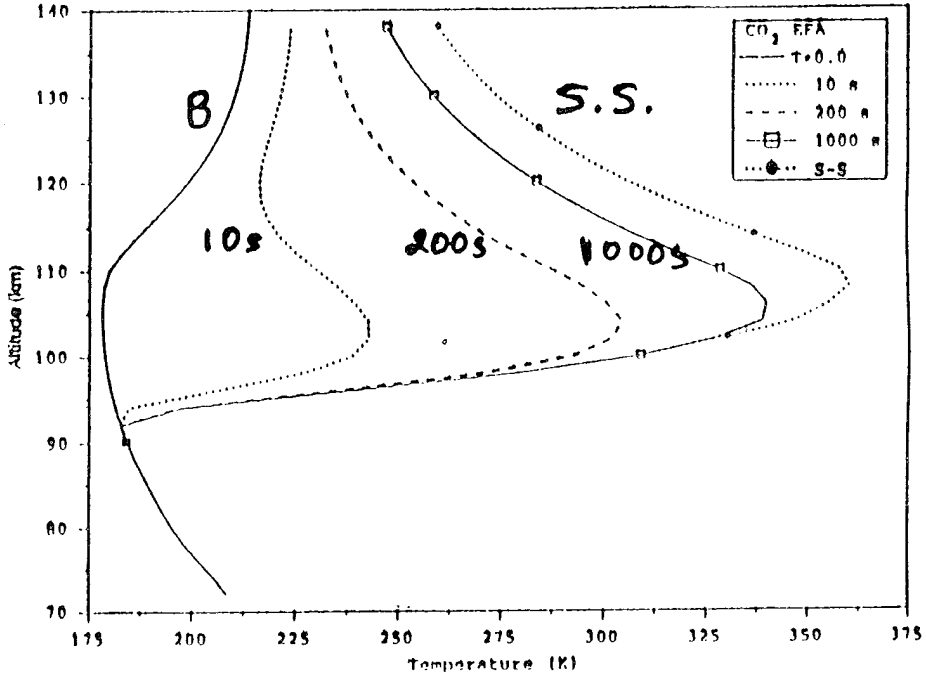
COMPARISON OF CO_2 (00011) VIBRATIONAL TEMPERATURES FOR CONSTANT STRONG AURORA STARTING AT TIME=0 USING AARC-TDBM AND AARC-EFA

IBC III

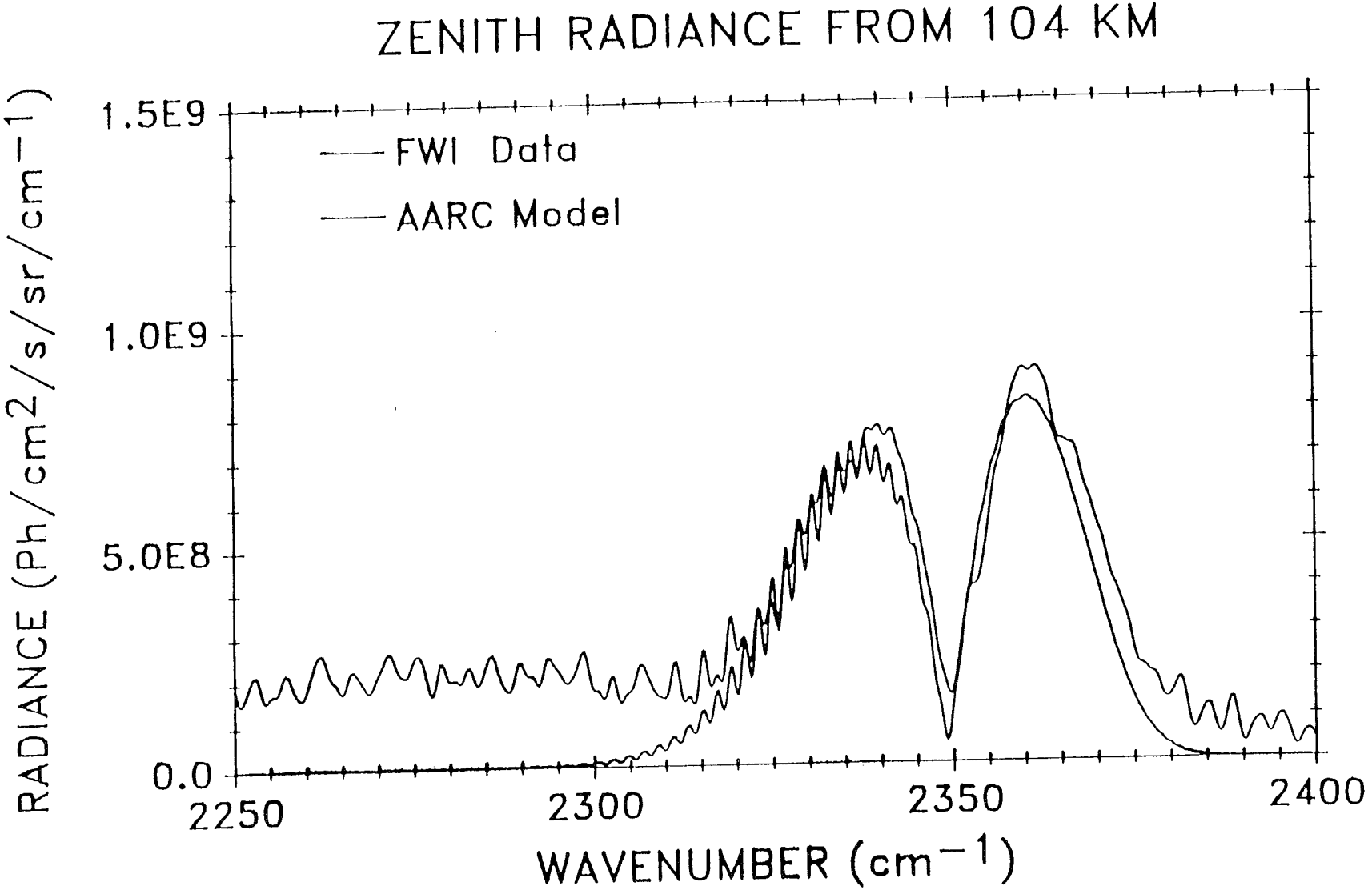
AARC-TDBM

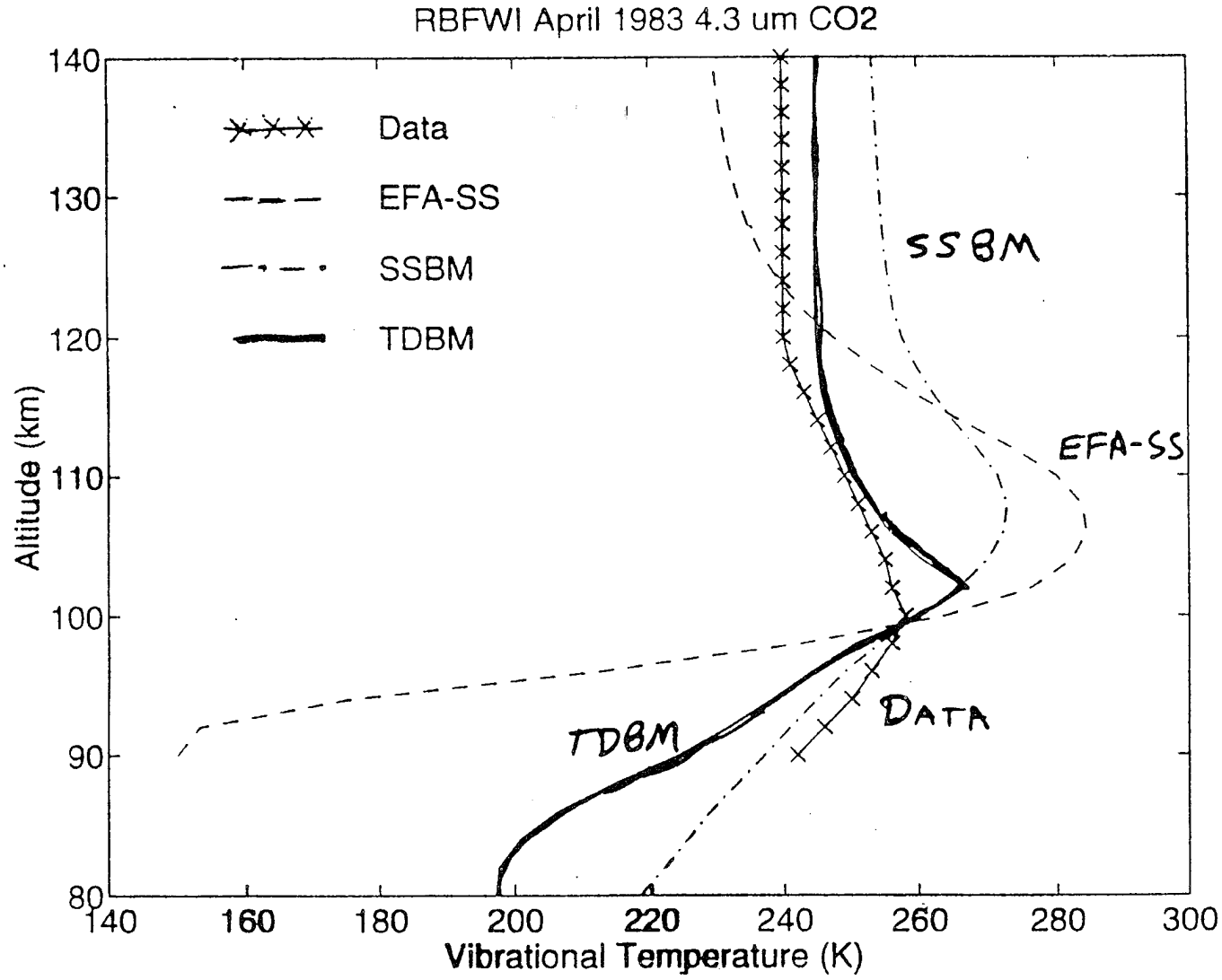


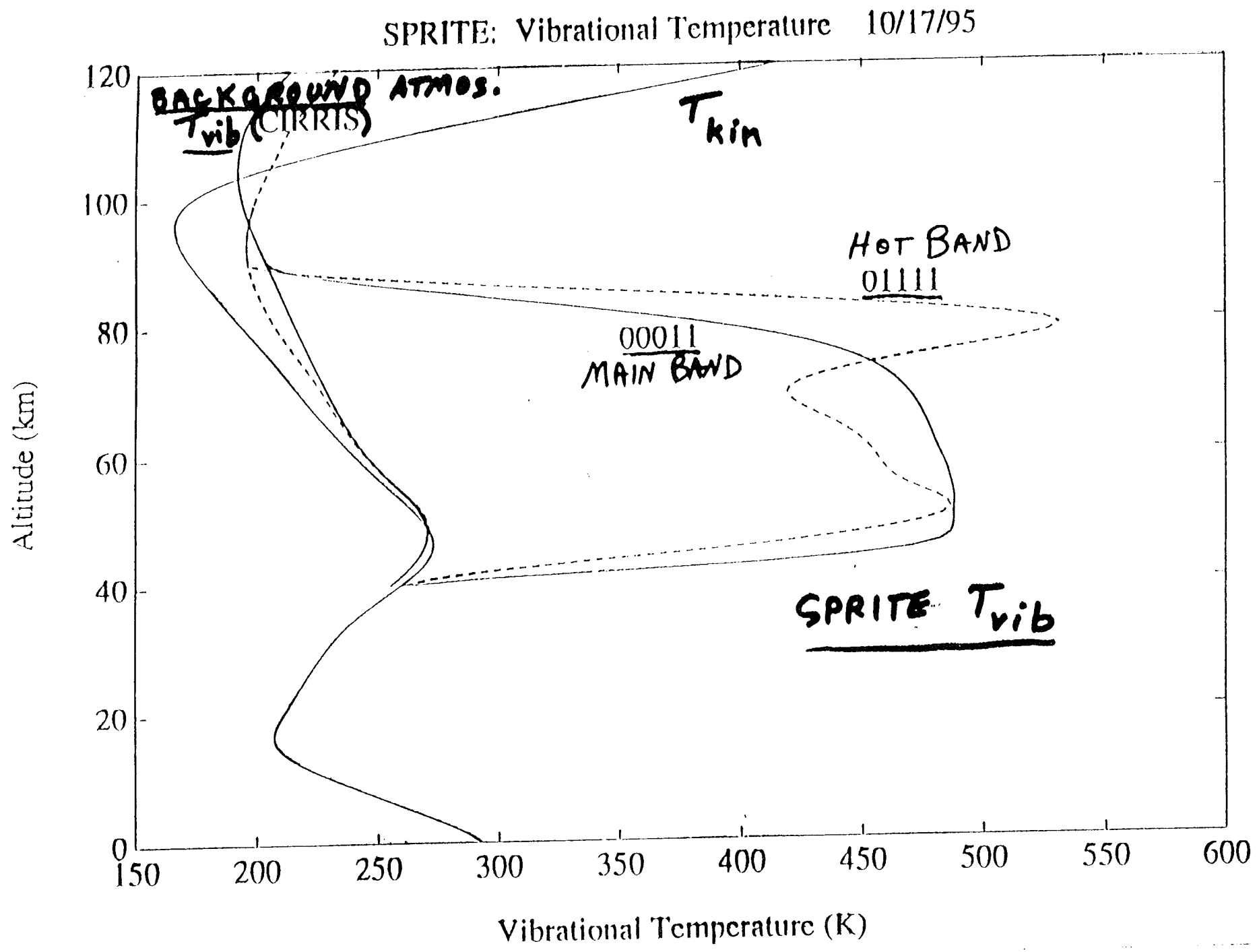
AARC-EFA

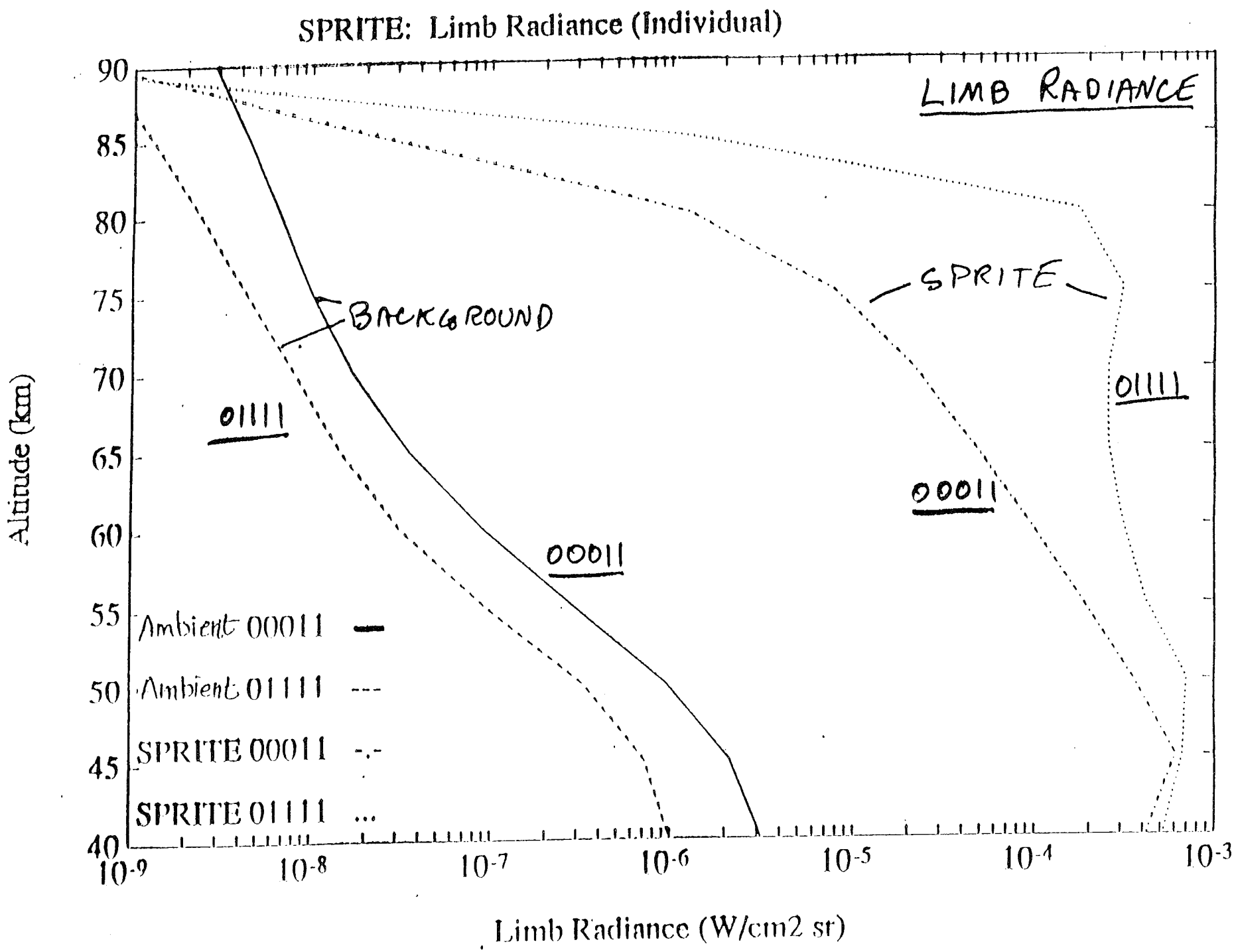


WRL 8204


ZENITH RADIANCE FROM 104 KM
FWI Data
AARC Model
1.5E9
1.0E9
5.0E8
0.0
2250
2300
2350
2400
RADIANCE (Ph/cm2/s/sr/cm-1)
WAVENUMBER (cm-1)

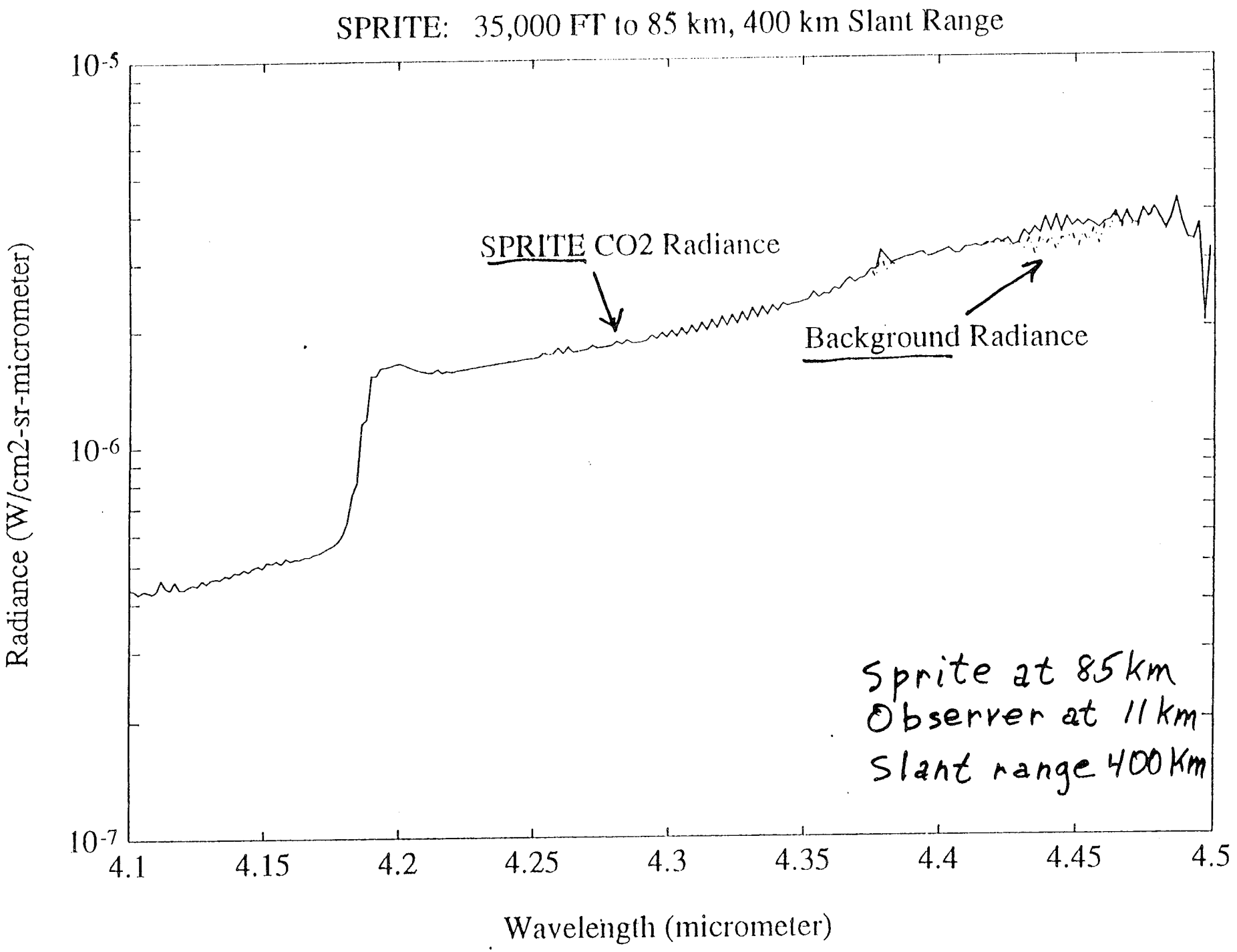

RBFWI April 1983 4.3 um CO2
Data
EFA-SS
SSBM
TDBM
SSBM
EFA-SS
DATA
TDBM
Altitude (km)
Vibrational Temperature (K)
140
130
120
110
100
90
80
140
160
180
200
220
240
260
280
300

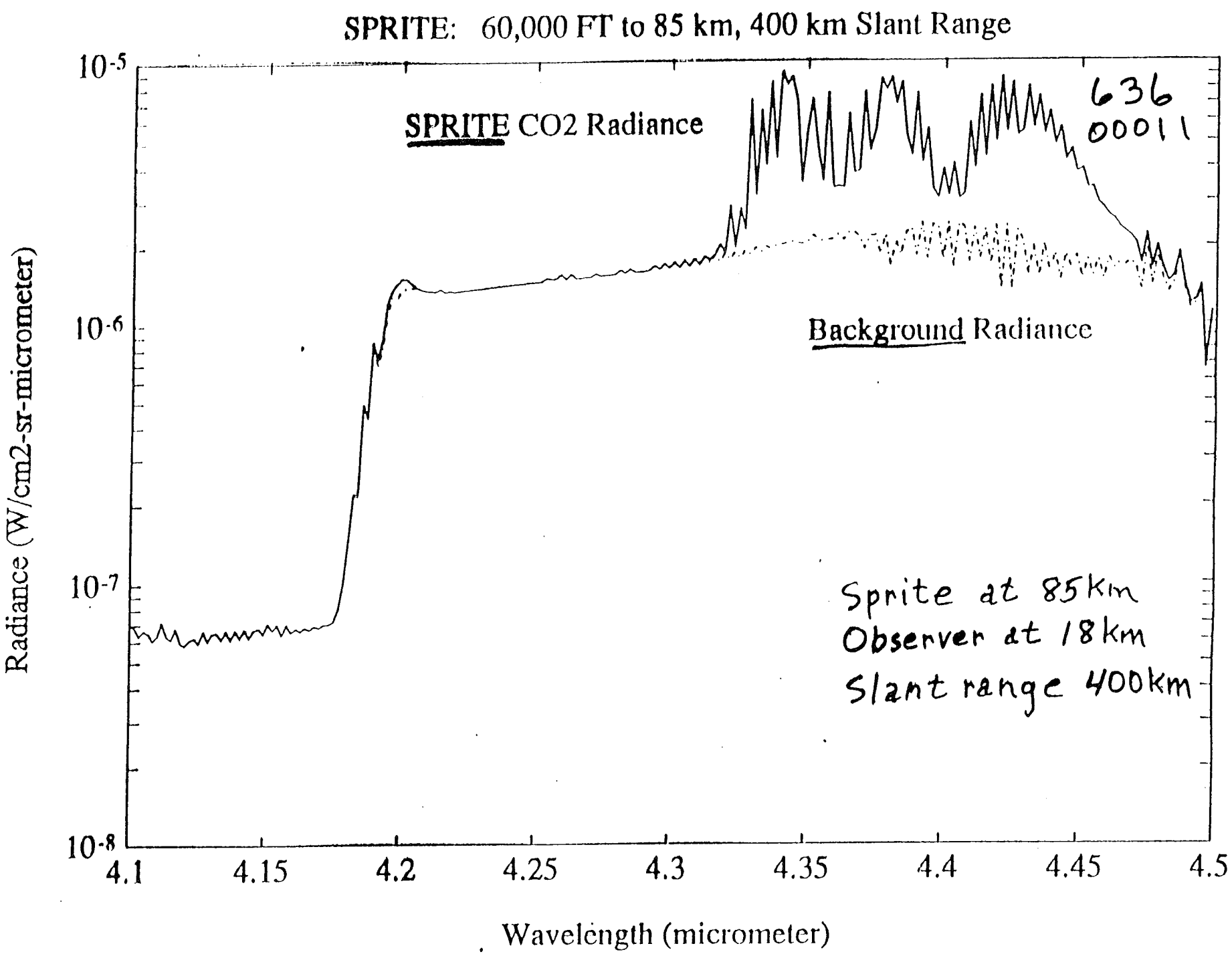

SPRITE: Vibrational Temperature 10/17/95
BACKGROUND ATMOS.
T_{vib} (CIRRIS)
T_{kin}
HOT BAND
01111
00011
MAIN BAND
SPRITE T_{vib}
120
100
80
60
40
20
0
150
200
250
300
350
400
450
500
550
600
Altitude (km)
Vibrational Temperature (K)

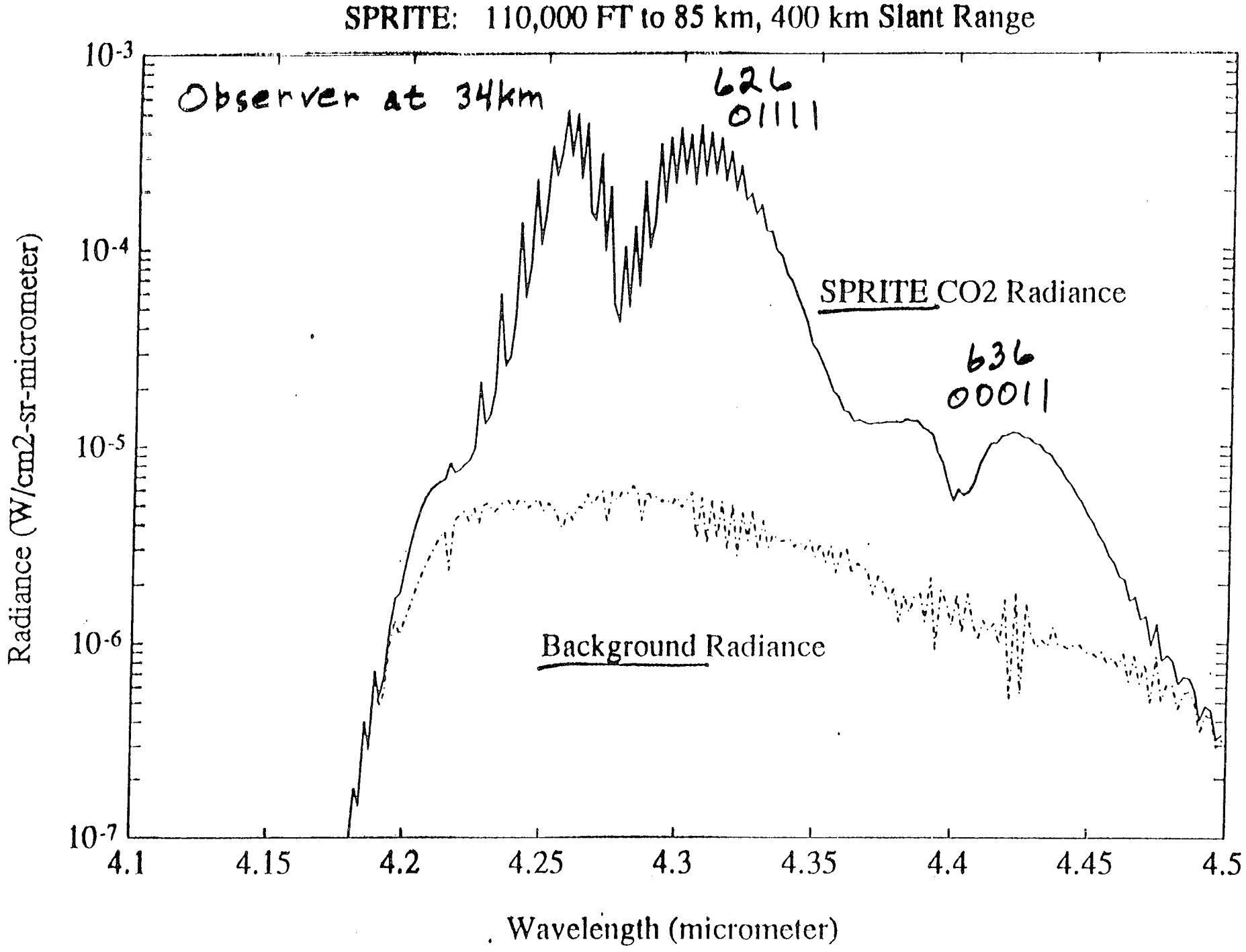

SPRITE: Limb Radiance (Individual)
LIMB RADIANCE
SPRITE
BACKGROUND
01111
00011
01111
00011
Ambient 00011
Ambient 01111
SPRITE 00011
SPRITE 01111
Altitude (km)
90
85
80
75
70
65
60
55
50
45
40
10-9
10-8
10-7
10-6
10-5
10-4
10-3
Limb Radiance (W/cm2 sr)

Observation of 4.3 μm CO_2 Radiance in Sprites from Ground-based and Airborne Platforms - Case Study

- Observation conditions-
  - Observer platform at ground (0 km), 35 kft (11 km), 60 kft (18 km), 110 kft (34 km)
  - Line-of-sight intercepts sprite at 85 km altitude
  - Slant range 400 km
- Sprite model
  - Horizontal extent - 40 km
  - Electron spectrum Gaussian - Flux 10^8 eV/cm^{3}s, E_o~2.5 eV, $\Delta E/E_o$~0.4
- Result
  - Sprite only observable at 4.3 μm from stratospheric aircraft and balloon platforms


SPRITE: 35,000 FT to 85 km, 400 km Slant Range
SPRITE CO2 Radiance
Background Radiance
Sprite at 85km
Observer at 11km
Slant range 400km
Radiance (W/cm2-sr-micrometer)
Wavelength (micrometer)
10-5
10-6
10-7
4.1
4.15
4.2
4.25
4.3
4.35
4.4
4.45
4.5


SPRITE: 60,000 FT to 85 km, 400 km Slant Range
SPRITE CO2 Radiance
Background Radiance
636
00011
Sprite at 85km
Observer at 18km
Slant range 400km
Radiance (W/cm2-sr-micrometer)
10-5
10-6
10-7
10-8
4.1
4.15
4.2
4.25
4.3
4.35
4.4
4.45
4.5
Wavelength (micrometer)


SPRITE: 110,000 FT to 85 km, 400 km Slant Range
Observer at 34km
626
01111
636
00011
SPRITE CO2 Radiance
Background Radiance
Radiance (W/cm2-sr-micrometer)
10-3
10-4
10-5
10-6
10-7
4.1
4.15
4.2
4.25
4.3
4.35
4.4
4.45
4.5
Wavelength (micrometer)

IR Radiative Model Needs

- Input:
  - Spatial map of electron spectrum as a function of time required from *data* or from *model - most critical need.*
    - Use to calculate production rate of $CO_2(\nu_3)$ from e on CO_2 and of $N_2(v)$ from e on N_2
  - Background atmosphere: $[N_2]$, $[O_2]$, $[O]$, $[CO_2]$, T versus altitude (from data or model)
- Validation:
  - Spectral measurements of monochromatic specific intensity of radiation from sprites in *well-characterized* atmosphere
    - Ancillary measurements of atmosphere and discharge important
    - At 4.3 μm airborne platform appears necessary

Trapping & Diffusion Effects - Sprites

- Radiation transport: Repeated absorption & reemission

  ---> radiation *trapping* - *Increases effective radiative lifetime to many times isolated* $CO_2(\nu_3)$ *lifetime of 2.5 ms*

  ---> radiative *diffusion* - Extends **production** outside region of discharge, vertically & **horizontally**

- Resonant transfer: V-V transfer $N_2(v)$ <--> $CO_2(\nu_3)$

  -Increases effective overall time constant because (a) not all N_2 collisions of $CO_2(\nu_3)$ --> quenching, (b) $N_2(v)$ does not radiate → Energy storage mechanism

Conclusions - IR Radiation Models

- Auroras & sprites can both lead to large enhancements in the 4.3–μm emission from $CO_2(\nu_3)$ above ambient
- Available tools, including transient radiative models, can model the IR radiation from the quiescent atmosphere, from aurora, and, somewhat modified, also from sprites
- A simple time-dependent band model (TDBM) is capable of accounting quantitatively for 4.3-μm RBFWI auroral data
- Space-time maps of electron spectra are required for input to the TDBM to model IR sprites radiance
- Bright sprites emission at 4.3 μm should be visible in satellite earthlimb observations & from high-altitude aircraft or balloon platforms

Future Work - IR Radiative Models for Sprites

- Incorporate diffusion model for horizontal transport into AARC-TDBM
- *Obtain better electron spectral input to model*
- *Investigate how radiative transfer effects broaden the $CO_2(\nu_3)$ excitation region*
- Investigate how radiative transfer and resonant V-V trapping lengthen the effective lifetime of $CO_2(\nu_3)$



AFOSR-PL Program



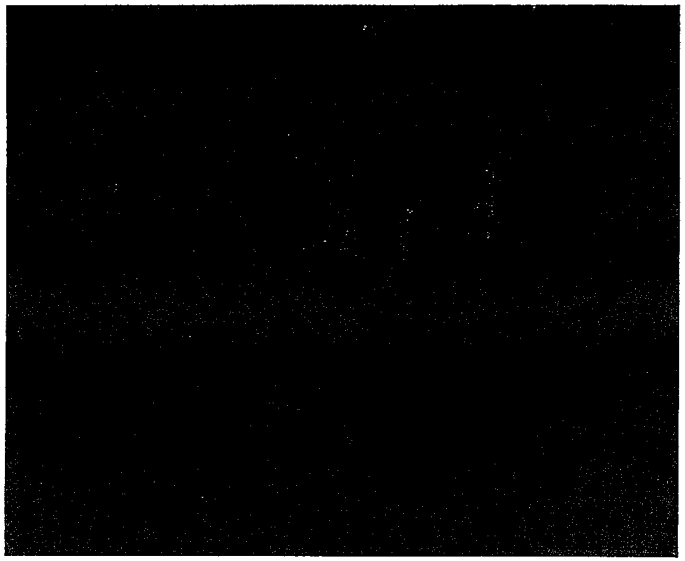
Infrared and Optical Signatures of High-Altitude Atmospheric Discharges

Presented To
AFOSR-PL Workshop
on Sprites and Blue Jets

Briefer
Dr. Laila S. Jeong
Phillips Laboratory
Geophysics Directorate

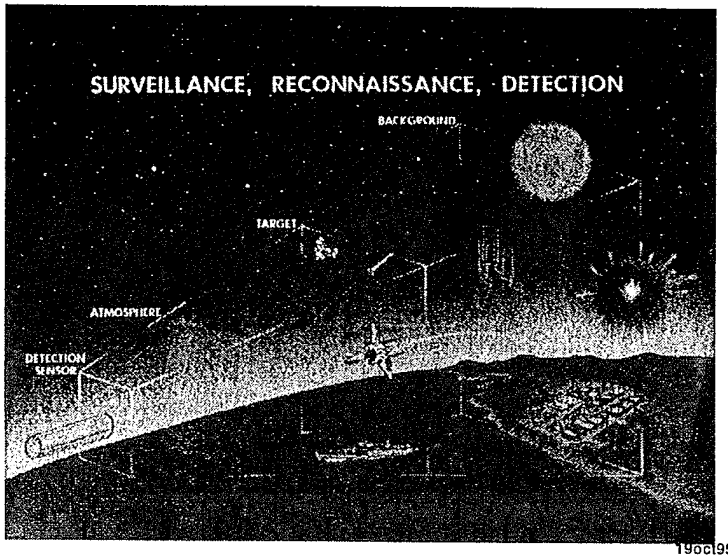
19 October 1995

Motivation



- Anomalous events observed by AF satellites
- Improved optical discrimination capability required for enhanced AF system performance

- Potential new source of persistent IR emission signatures
- Impact assessment required for next generation AF surveillance and tracking systems



Objectives

- Characterize enhancements in atmospheric radiance due to transient high-altitude atmospheric discharges
- Predict IR/UV/VIS signatures of elves, sprites, and blue jets
- Transition technical base to AF operational users

361

Products and Payoffs

- Measured IR, UV, and VIS backgrounds from atmospheric discharge events
- Integrated Sprites Atmospheric Radiance Code (SPARC)
  - Electrodynamics/Chemistry/Radiation Transport
- Tailored capability to determine discharge-induced atmospheric background impacts in AF system simulations to optimize system performance

Current Knowledge of High-Altitude Discharge Optical Emissions

- Sprite morphology determined (Sentman & Westcott)

- Sprite red emission identified as N_2 First Positive (Sentman & Westcott, Mende)

- Sprite and blue jet ranges of brightness determined from image data (Sentman & Westcott)

- Sprite blue emission measured at 427.8 nm due to N_2^+ First Negative (Armstrong)

- Ultra-bright precursor flash (elf) identified (Fukunishi, Lyons)

Key Technical Deficiencies

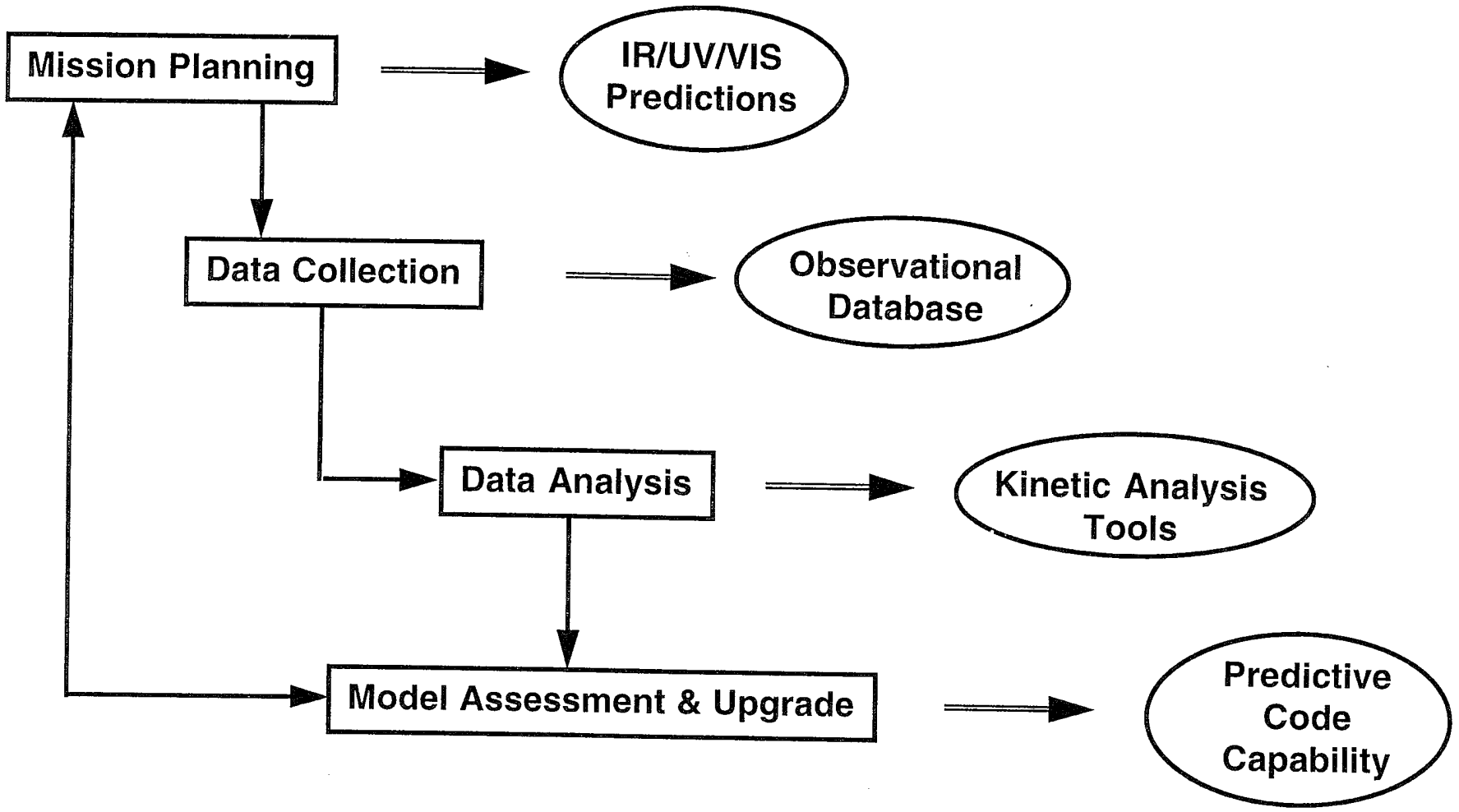
- Spectral/spatial/temporal data of enhanced background emissions

IR	UV/VIS
CO_2 4.3 micron band	N_2^+ First Negative
NO 2.7 micron band	(391.4 nm, 427.8 nm)

- Electron density/energy distribution
  - Temporal dependence
  - Altitude dependence

- Fundamental understanding of discharge dynamics (electro-, chemical)

Overall Approach



Mission Planning

- Review current database and define technical baseline

  - October '95 Workshop

- Conduct kinetic analysis of new data from Summer '95 Campaign

  - Spectral Fitting
  - Kinetic Assessments

- Develop modeling tools to predict UV/VIS/IR signatures for data collects

  - Modified high-altitude atmospheric radiance code

Mission Planning

- Predict UV/VIS/IR signatures to optimize data collects for Summer '96 Campaign

  - Radiance calculations for aircraft sensor bands and viewing geometries

- Define aircraft data collection requirements and mission operations

  - Aircraft mission requirements document and mission operations plan

- Identify satellite data collection events for sprite measurements

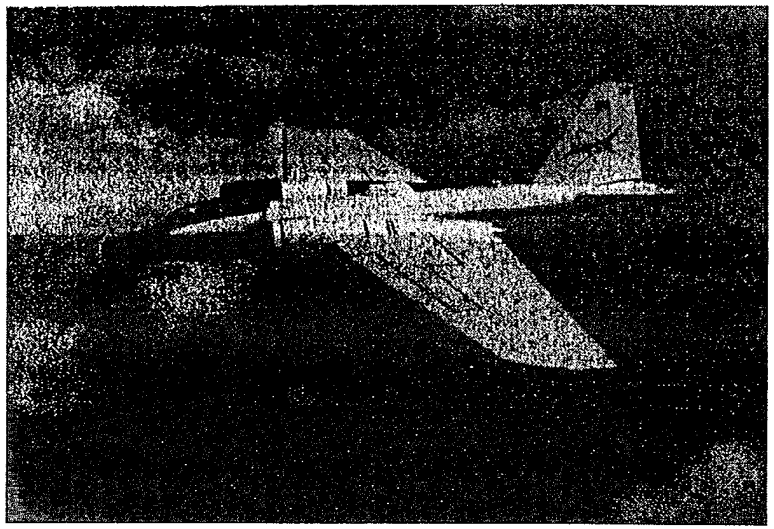
  - Add-on to automated data processing software to flag atmospheric discharge events and analyze emissions

Data Collection

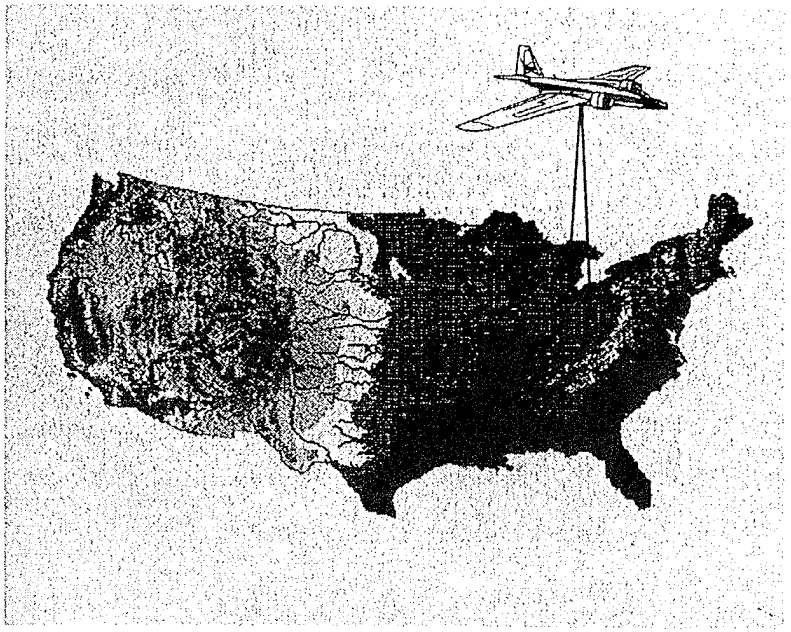
Platform	IR Signature Measurements	UV/VIS Signature Measurements	Radar Measurements
ARES Aircraft (SAFSP)	Radiometer Imaging Spectrometer IR Camera	Visible Cameras	
MSX Satellite (BMDO)	Radiometer Interferometer	Imaging Spectrometer	
MSTI-3 Satellite (SMC)	Imaging Radiometer		
Ground-Based (PL)		Radiometer	Portable Radar Millstone Hill

- Data Reduction ---> Calibrated Data Sets

Airborne Remote Earth Sensing (ARES)



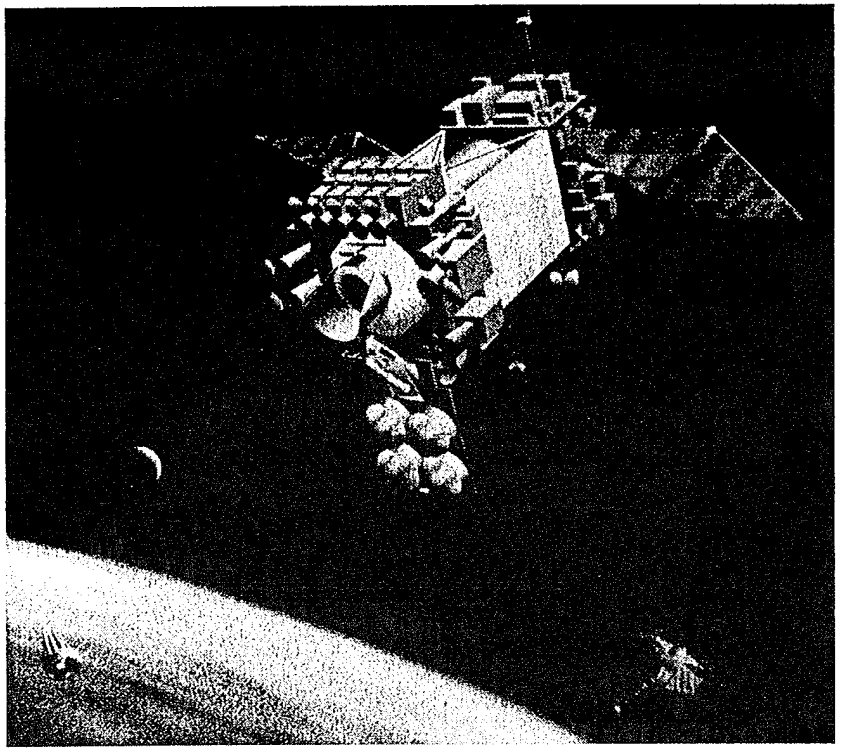
- RESPO Controllling Agency
- RB-57F Aircraft
- 65 kft Altitude
- 2,500 NM Range



- Two Visible Cameras
- IR Camera (2.0 x 3.2 microns)
- 4-Band Radiometer (2.2 - 4.6 microns)
- Imaging Spectrometer (2-6 microns)

Midcourse Space Experiment (MSX)

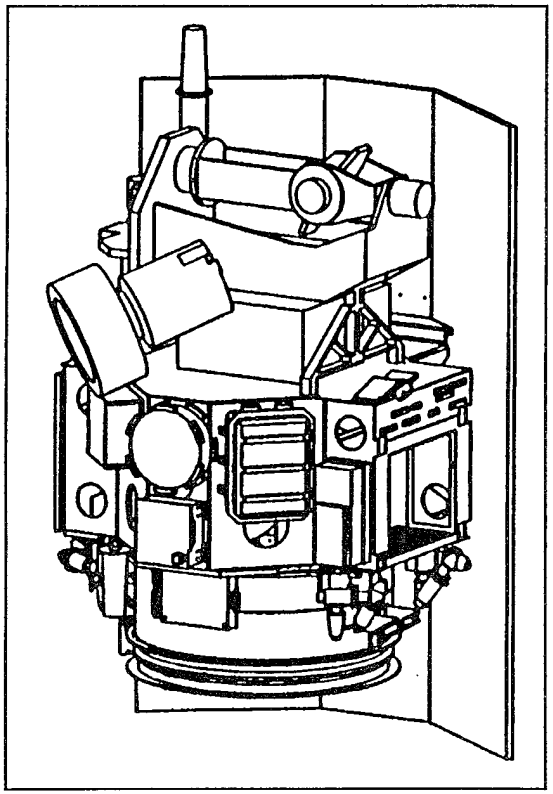
Provide multi-band and multi-LOS scene data of earth, earthlimb, and celestial backgrounds



- Sun-synchronous polar orbit at 800 km altitude
- Spatial Infrared Imaging Telescope (SPIRIT III) covering MWIR-VLWIR:
  - 5-band scanning radiometer
  - 6-channel Fourier transform spectrometer
- UV/VIS Imaging and Spectrographic Imaging Sensor System covering far UV to near IR:
  - 5 spectrographic imagers
  - 4 imagers
- March '96 launch date

Miniature Sensor Technology Integration (MSTI-3)

Provide high-spatial resolution SWIR/MWIR imagery of atmospheric backgrounds



- Sun-synchronous polar orbit at 425 km altitude
- Suite of three sensors
  - MWIR camera with 7 narrow-band filters
  - SWIR camera with 7 narrow-band filters
  - VIS imager
- April '96 launch date

Ground-Based Optical and Radar Measurements

Objective

- Characterize ionization enhancements in high-altitude discharge glows

Approach

- Characterize spectral/spatial/temporal UV/VIS emissions using co-aligned imaging spectrometer/radiometer

- Determine D-region effects using 28 and 50 MHz portable radar systems

- Determine D-F region effects using UHF (430 MHz) incoherent scatter radar and other diagnostics at Millstone Hill

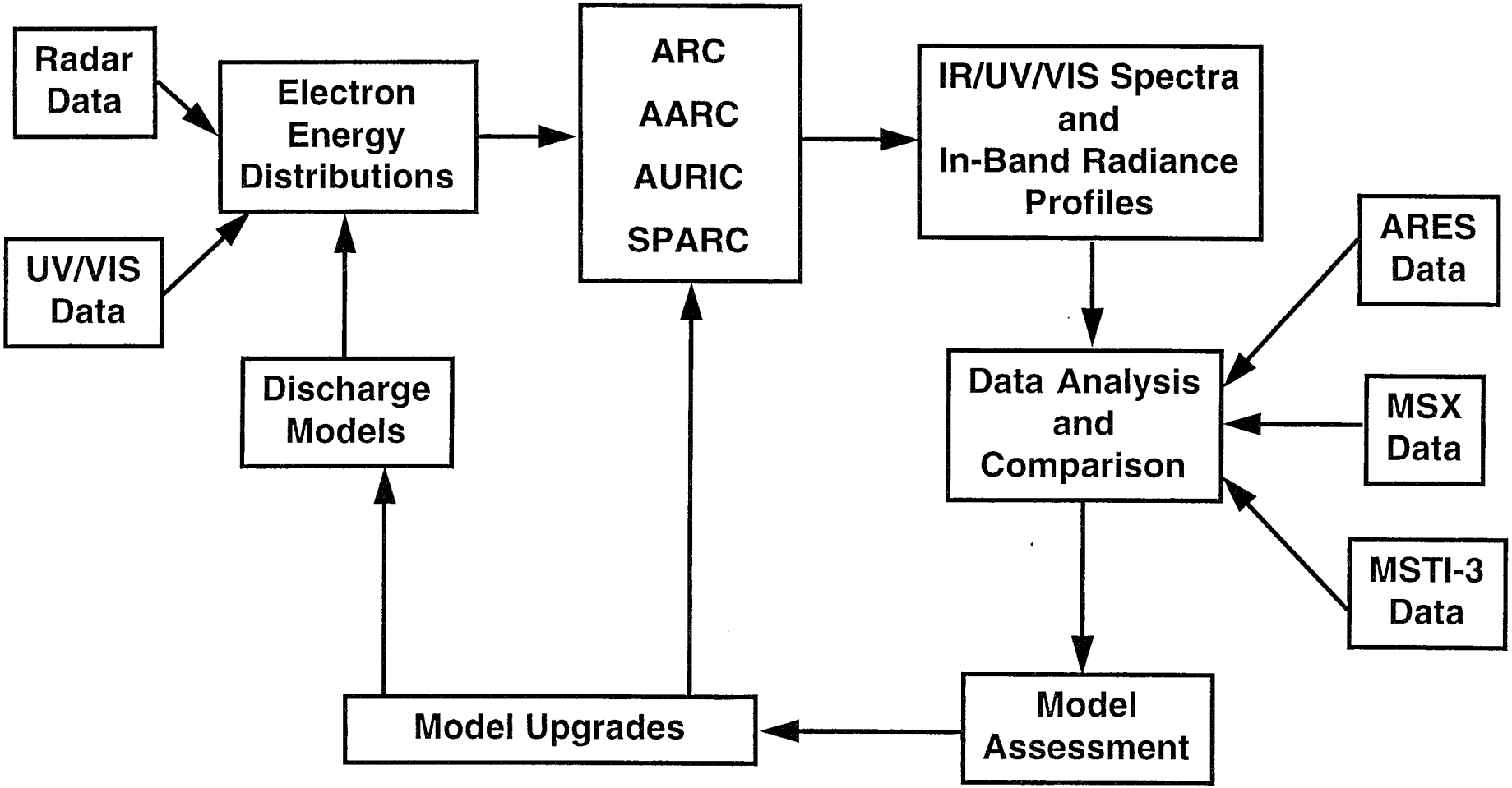
Infrared and Optical Background Measurement Data Analysis

- Spectral Fitting
  - Determine excited-state species number density
  - Interband comparisons
- Kinetic Analysis
  - Model excited-state excitation and relaxation dynamics

Atmospheric Background Model Assessment





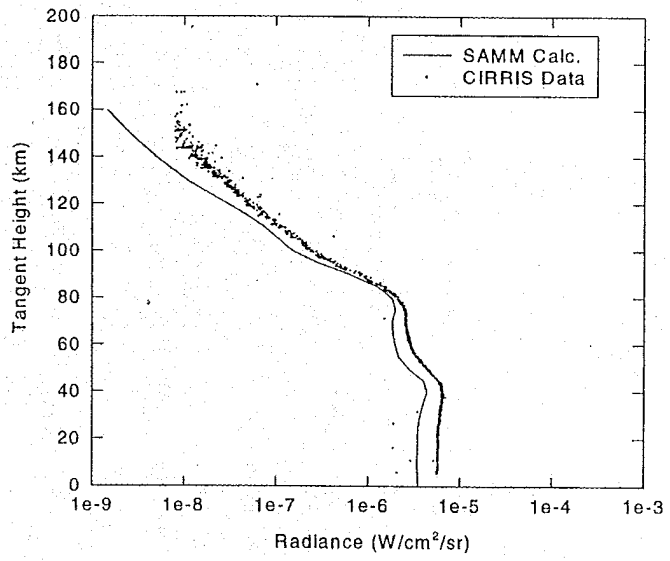


High-Altitude Atmospheric Radiance Codes

- ARC - Quiescent IR Backgrounds
- AARC - Auroral IR Backgrounds
- AURIC - UV/VIS Backgrounds

Capabilities

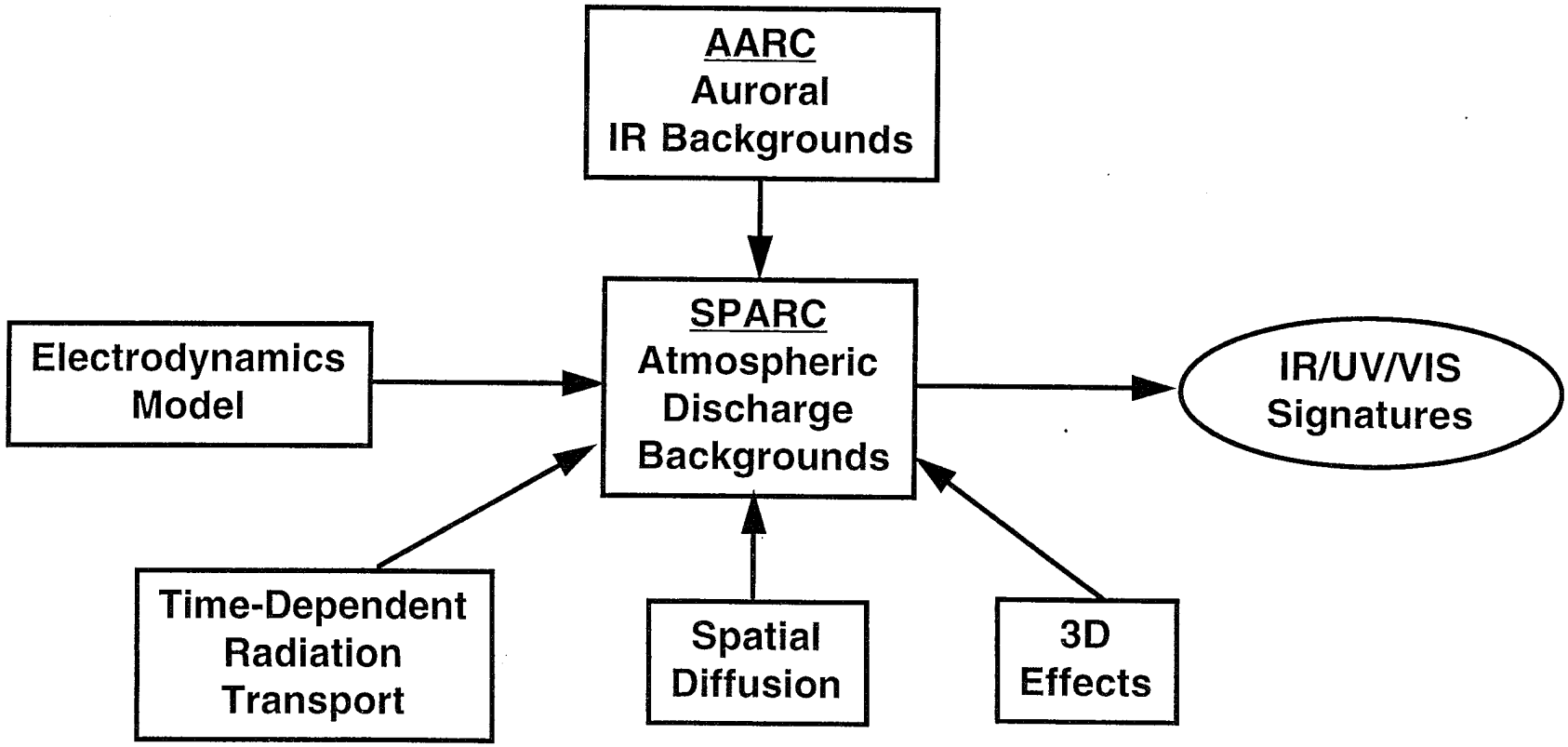
- Calculate high-altitude atmospheric radiance backgrounds
- Model NLTE atmospheric emission and photoexcitation processes
- Support arbitrary viewing geometries
- Extensively validated using field data



4.3 Micron Band Radiance Pofiles

Sprites Atmospheric Radiance Code (SPARC)

New Modeling Capability for High-Altitude Atmospheric Discharge Backgrounds



Summary

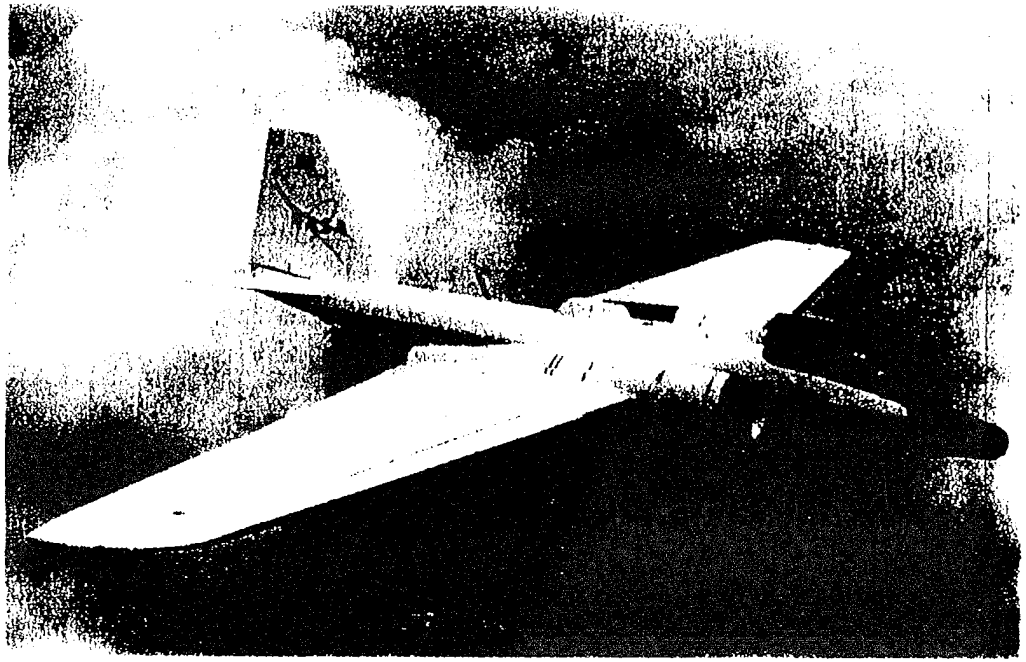
- Focused research program to measure and model IR/UV/VIS signatures of high-altitude atmospheric glow discharges

- Goal to integrate Air Force program with other agency programs to support coordinated Summer '96 Campaign with multiple assets

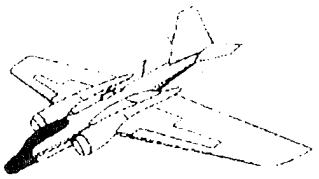
AN AIRBORNE IMAGING SPECTROMETER IN OPERATION AND AVAILABLE FOR COLLECTIONS

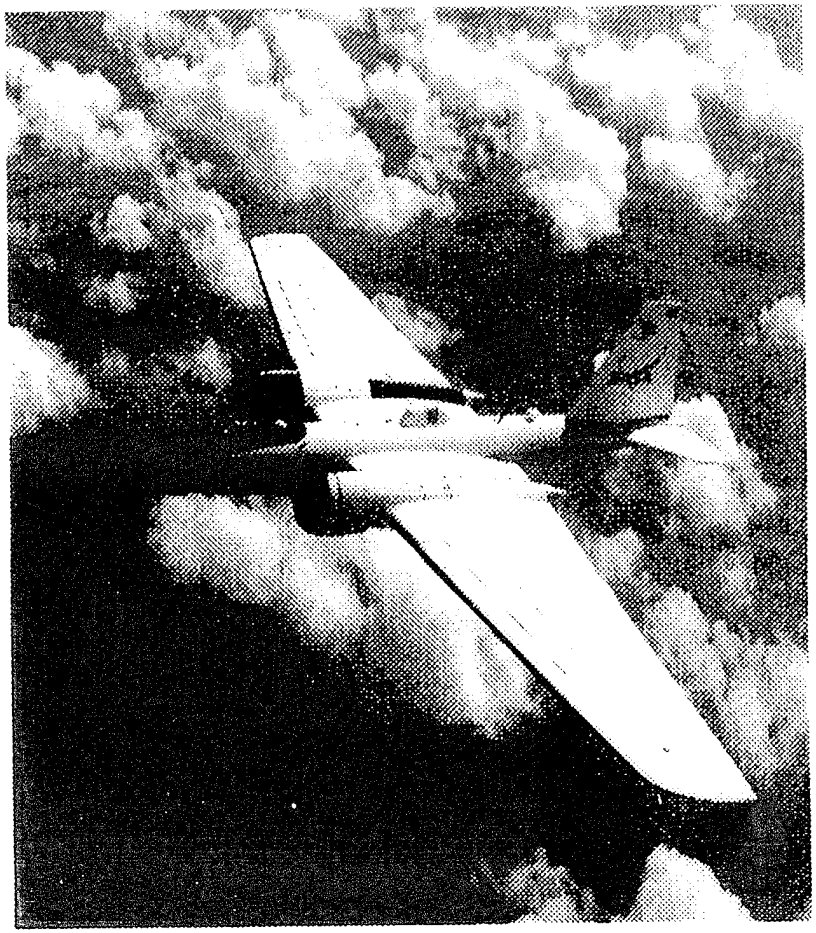
P. Kupferman
Aerospace Corporation

- AIRBORNE REMOTE EARTH SENSING PROGRAM (ARES)
- NASA WB-57F AIRCRAFT PLATFORM
- 75 CHANNEL IMAGING SPECTROMETER
- UPLOOK AND DOWNLOOK CONFIGURATIONS
- PROGRAM MANAGED BY DoD REMOTE EARTH SENSING PROGRAM OFFICE, CAPT. TILTON
- EXPERIENCED TEAM (10+ YEARS) PROVIDES MISSION PLANNING, OPERATIONS, ANALYSIS AND DATA DISTRIBUTION



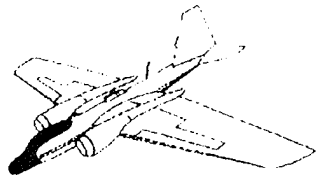
ARES PROGRAM



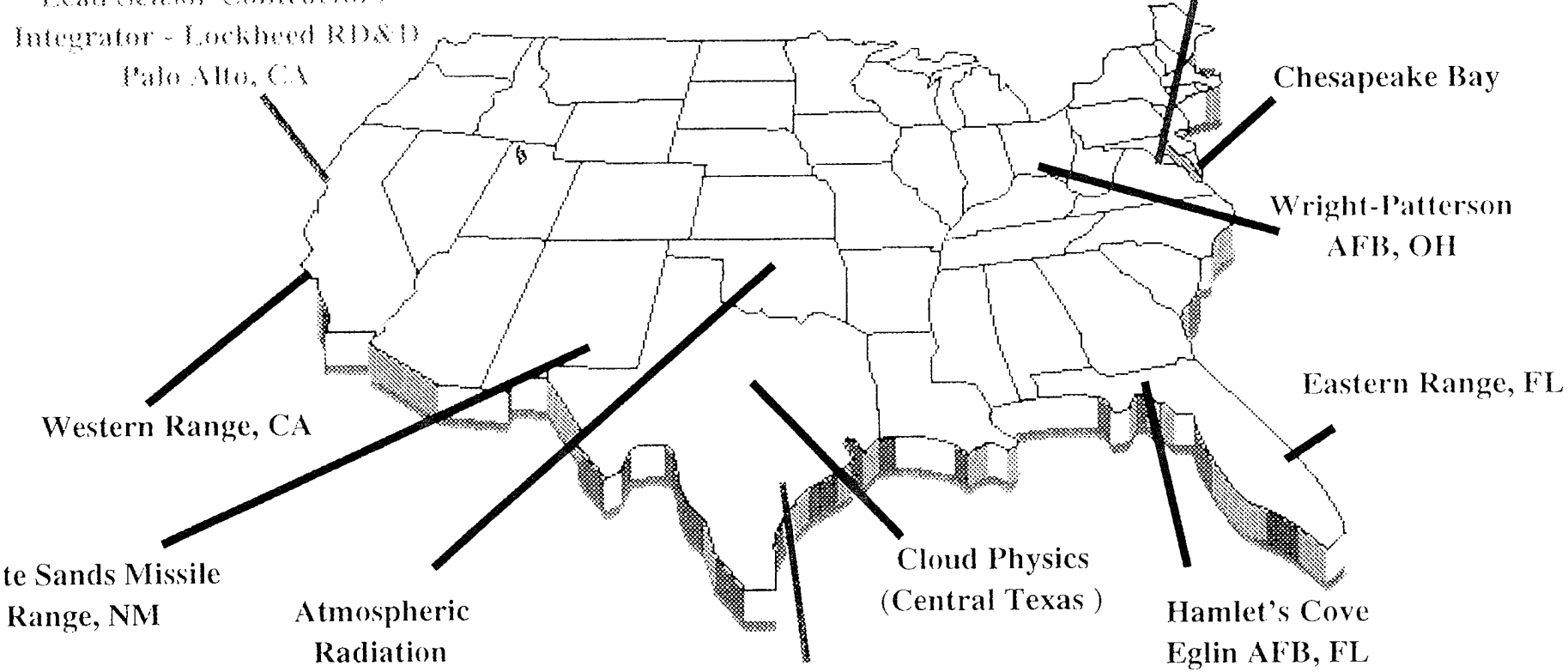


- PROVIDES HIGHLY CALIBRATED RADIOMETRIC AND SPECTROMETRIC S/MWIR DATA (2-6 μm)
- CONTINUE DATA COLLECTION TO SUPPORT:
  - SPACEBORNE IR SYSTEM CONCEPT DEFINITION
  - DEVELOPMENT OF IMAGERY FOR REFINEMENT OF MULTISPECTRAL EXPLOITATION TECHNIQUES
  - NATIONAL SECURITY REQUIREMENTS
  - MILITARY REQUIREMENTS
  - ENVIRONMENTAL COMMUNITY RESEARCH REQUIREMENTS

Location of ARES Program Facilities and Operation Sites



Also Planning FY 95 continental measurement series for NSF from 70° S to 70° N latitiude



SAFSP/RESPO
Headquarters
Fairfax, VA

Lead Sensor Contractor /
Integrator - Lockheed RD&D
Palo Alto, CA

Chesapeake Bay

Wright-Patterson
AFB, OH

Eastern Range, FL

Western Range, CA

White Sands Missile
Range, NM

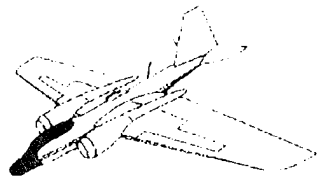
Atmospheric
Radiation
Measurements (ARM)
Program Site
Lamont, OK

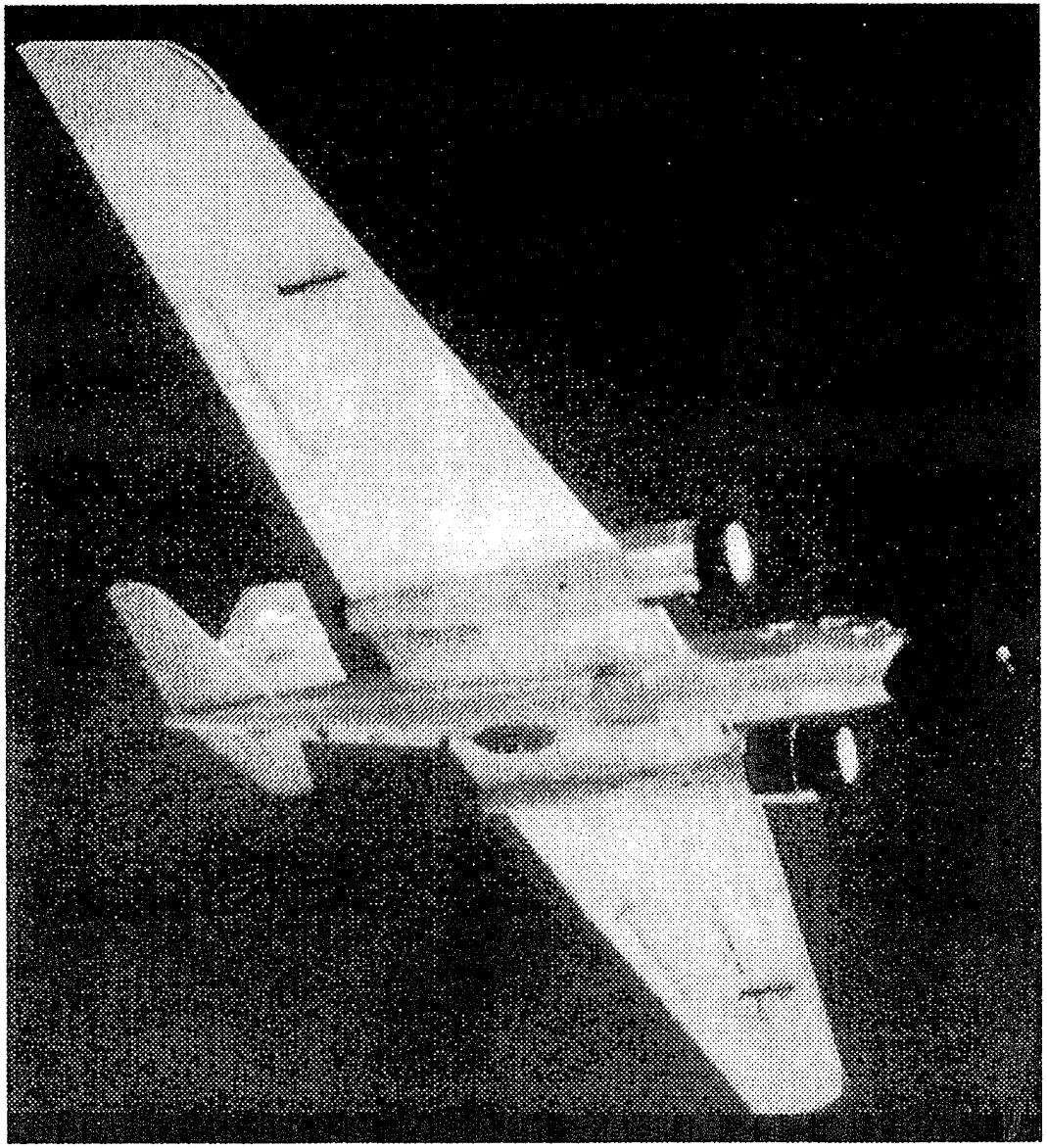
Cloud Physics
(Central Texas)

Aircraft Hangar Facilities /
Flight Operations Headquarters
Houston, TX

Hamlet's Cove
Eglin AFB, FL

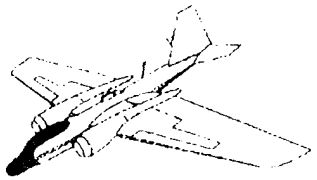
RB-57F

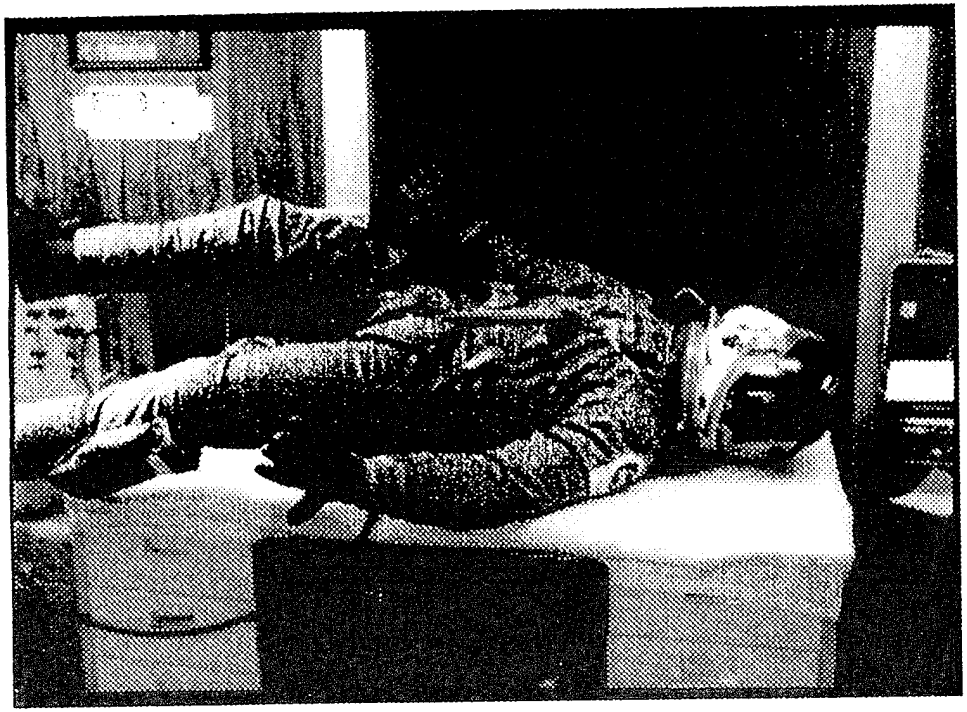


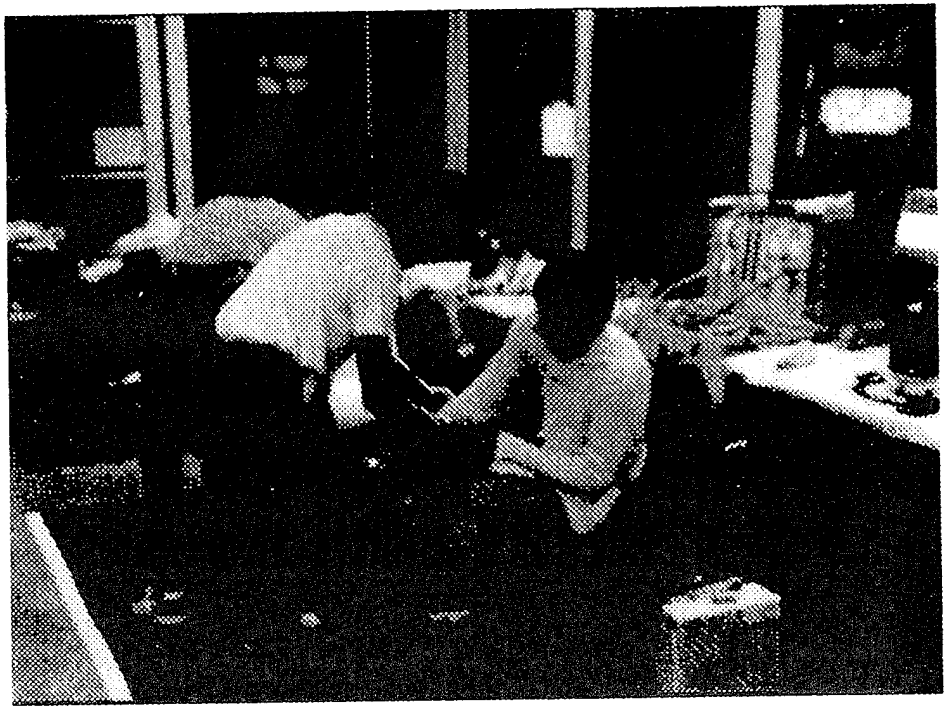


ALTITUDE	65,000 FT+
RANGE	2,500 NM
ENDURANCE	6 HOURS+
PAYLOAD	4,000 LB+
VOLUME	250 FT^3
POWER	40 KVA/GENERATOR
SPEED	400 KTS
RUNWAY	6,000 FT
CROSSWIND	15 KTS
NAVIGATION	INS/ONS/LORAN

PRESSURE SUITS FOR HIGH ALTITUDE

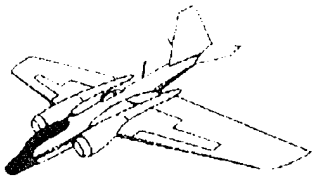


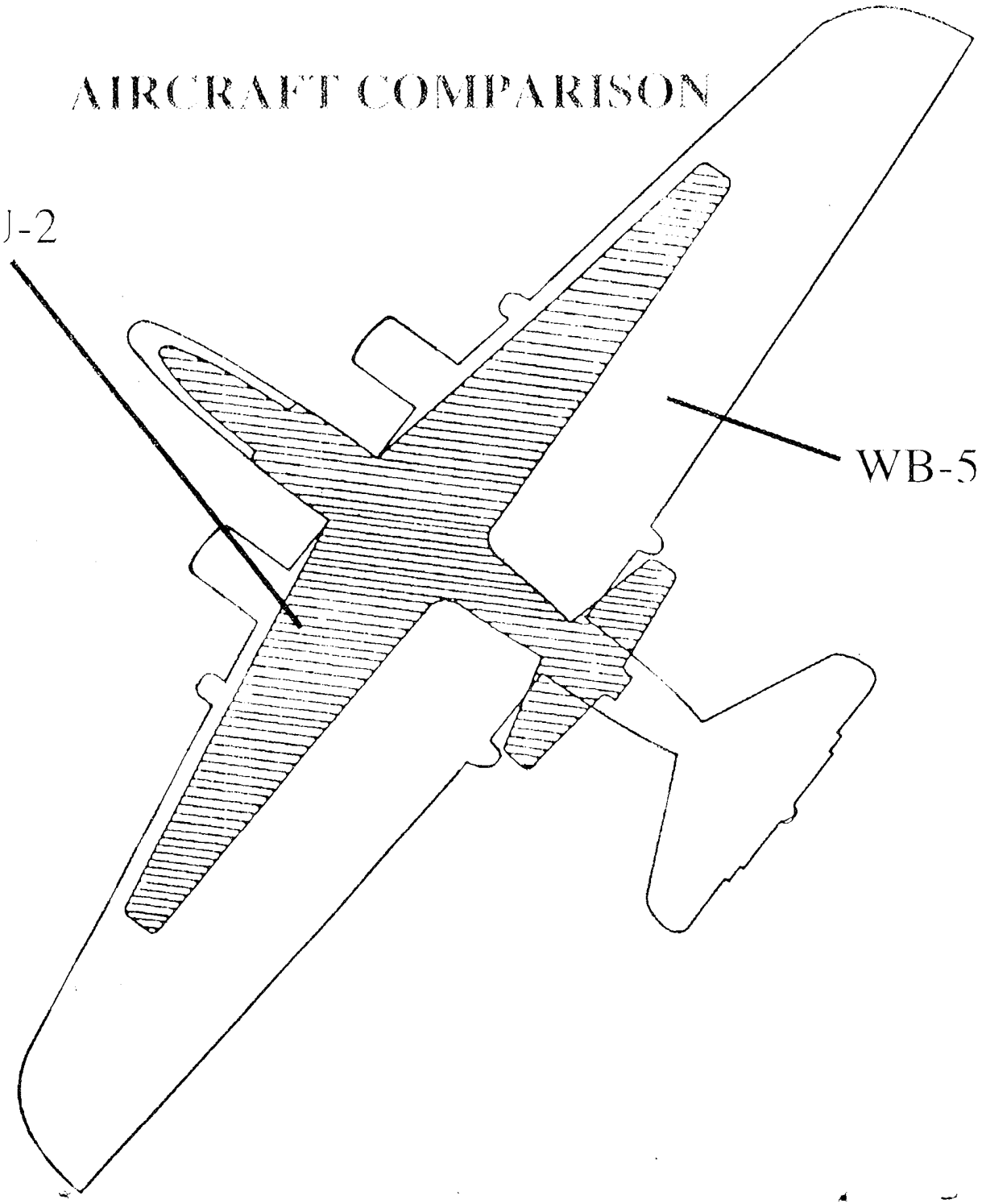




Program Fully compliant with DoD and FAA regulations for High Altitude Flight

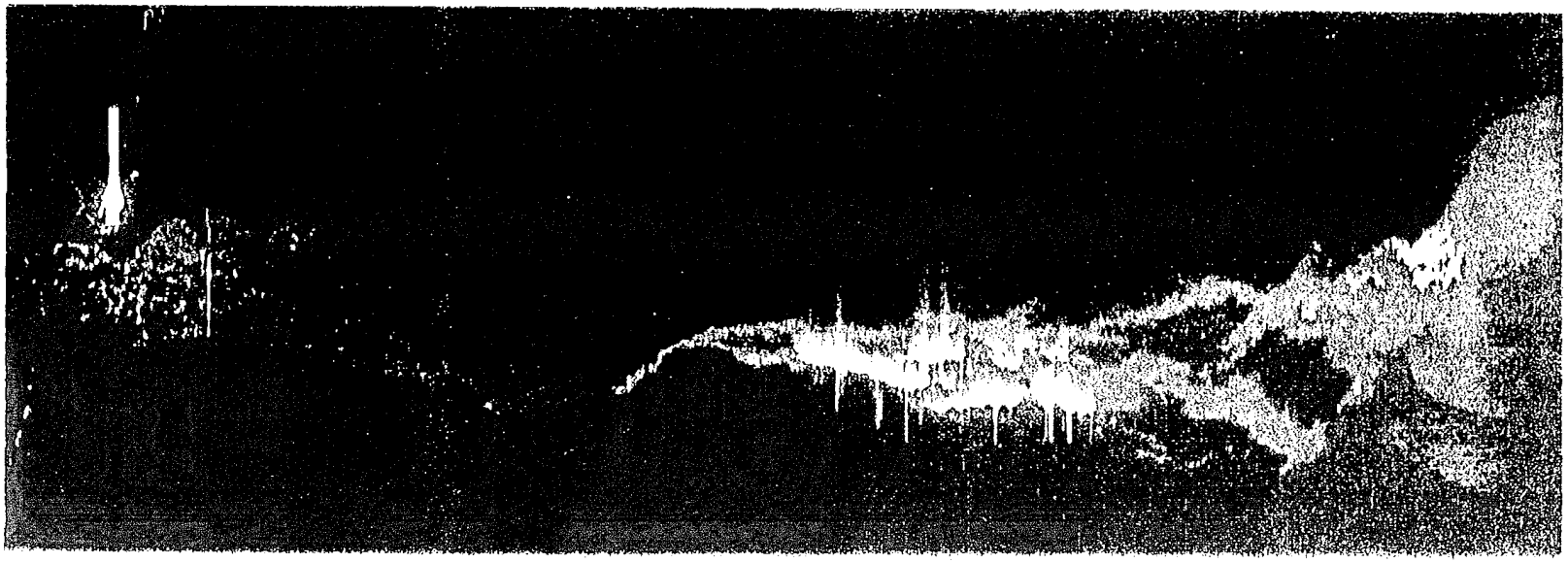
AIRCRAFT COMPARISON





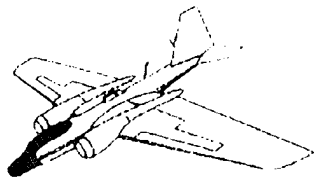
Sample Data Collection

Geology (Vulcanology)



4.5 km x 12.5 km mosaic image formed from seven multispectral flightlines over Kilauea volcano (Hawaii), depicting extensive subsurface lava tube network, ocean thermal plumes.

PAYLOAD INSTRUMENTS



TWO VISIBLE CAMERAS

FOV 1	10.4^{o} x 7.5^{o}	CAN BE UTILIZED WITH TRACKER (CENTROID/ EDGE/CORRELATION)
FOV 2	1.6^{o} x 1.9^{o}	

IR CAMERA

FOV	1.8^{o} x 1.4^{o}	
BANDPASS	2.0 X 3.2 μm	

IR FPA 45 X 45 FIELD OF REGARD 2.6^{o} x 2.6^{o} PIXEL RESOLUTION: 1.0 mrad x 1.0 mrad
20m x 20m @ 20KM

-- RADIOMETER:

BANDS	FULL WIDTH - HALF MAX (μm)
	2.205 – 2.259
	2.716 – 2.972
	3.723 – 3.843
	4.406 – 4.553

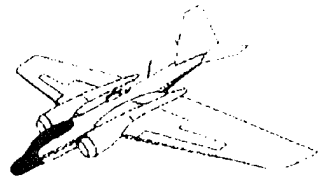
-- SPECTROMETER: IMAGING SLIT FOV 2.6^{o} x 0.36^{o} 20 m x 2.8m @ 20KM
2.0 - 6.0 μm/75 CHANNELS BANDPASS RANGE 26 - 69 NM

RECORDERS: TWO 12 BIT A & D (ALL FPA DATA DIGITALLY RECORDED)
(ALL INS DATA DIGITALLY RECORDED)
56 MINUTES TOTAL DATA RECORDING TIME

THREE VHS FLIGHT RECORDERS COCKPIT VIDEO MONITOR (INCLUDES AUDIO)
IR CAMERA
REAL TIME DISPLAY SYSTEM (RTDS)

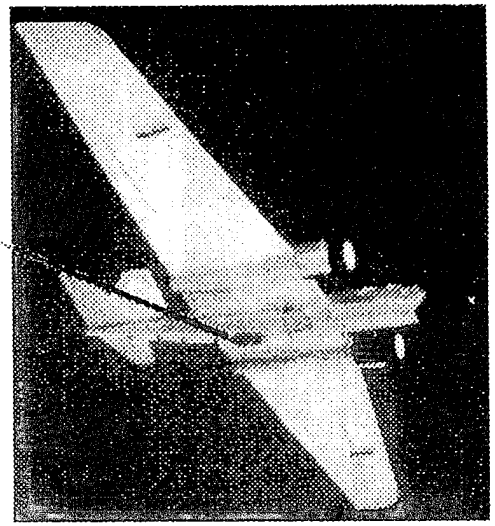
PAYLOAD INSTALLATION

WB-57F



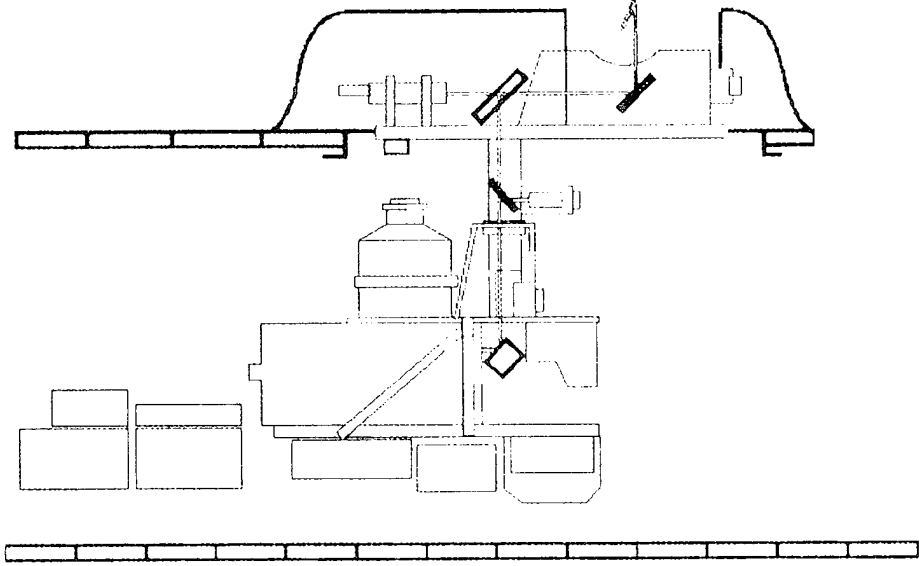


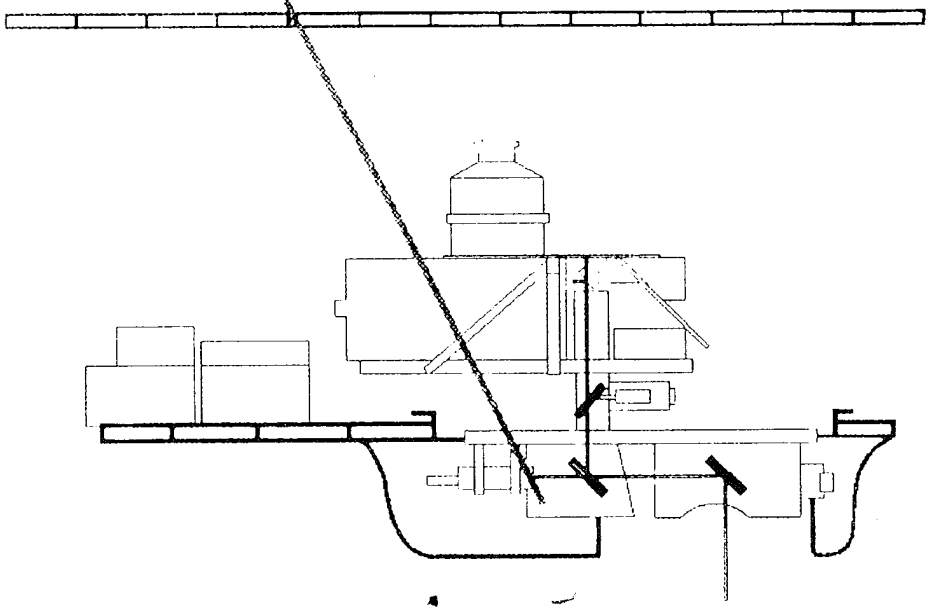
Telescope port



(Up-Look Configuration)

(Down Look Configuration)





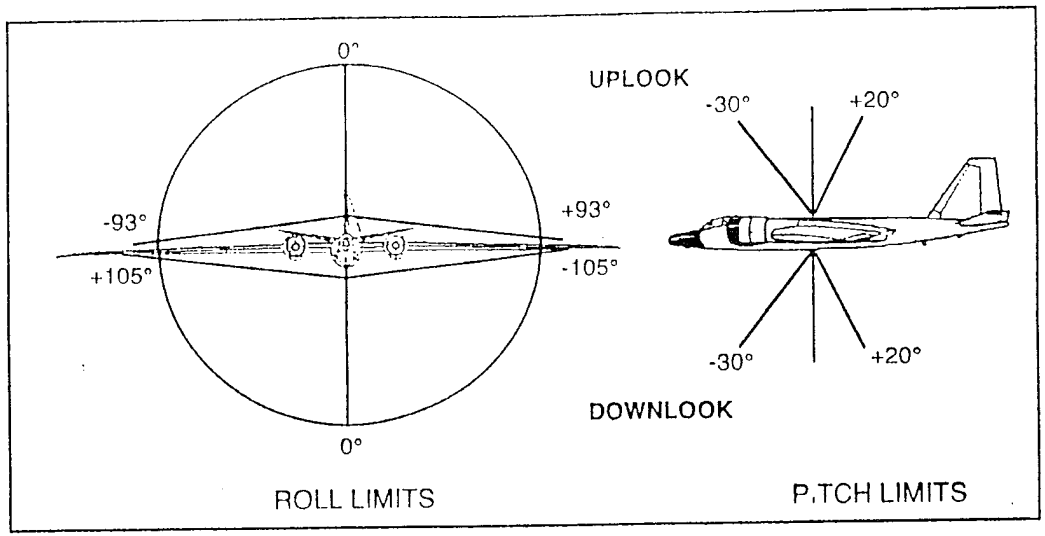
Sensor Basic Capabilities
- Continued -

- Total Spectral Bandwidth: 2.0 - 6.5μm (Optics Limited)

- Resolution
  - Spectral: 25 - 70nm
  - Spatial: 1.17mrad
  - Temporal: 10 - 80Hz

- Field- of-View: 53mrad Square, 53mrad x Scan/Sweep

- Field-of-Regard



Sensor Basic Capabilities (Currently Available)

- Optics
  - 2.0" Aperture
  - Multi-Element 3.8" Focal Length Imager (F1.9)
  - Afocal Reflective Slit Spectrometer Telescope
  - 2 Element Ge-MgO Prism Assembly
  - Two 5 - Position Motor Driven Filter Wheels
  - Internal Optics Vacuum/Cryo-Cooled (77° K)
  - External Scanning Mirror System
  - External Pointing Mirror
  - On-Board Blackbody Cal Sources (3)

- Pointing and Tracking Capabilities
  - Accuracy: .25° - .5°
    - » Within 4x4 Pixels in Radiometer Mode; Total - 45x45 Pixels
  - Types of pointing: Computer, Manual
  - Types of tracking: Correlation, Edge, Centroid

SENSOR BASIC CAPABILITIES
- Continued -

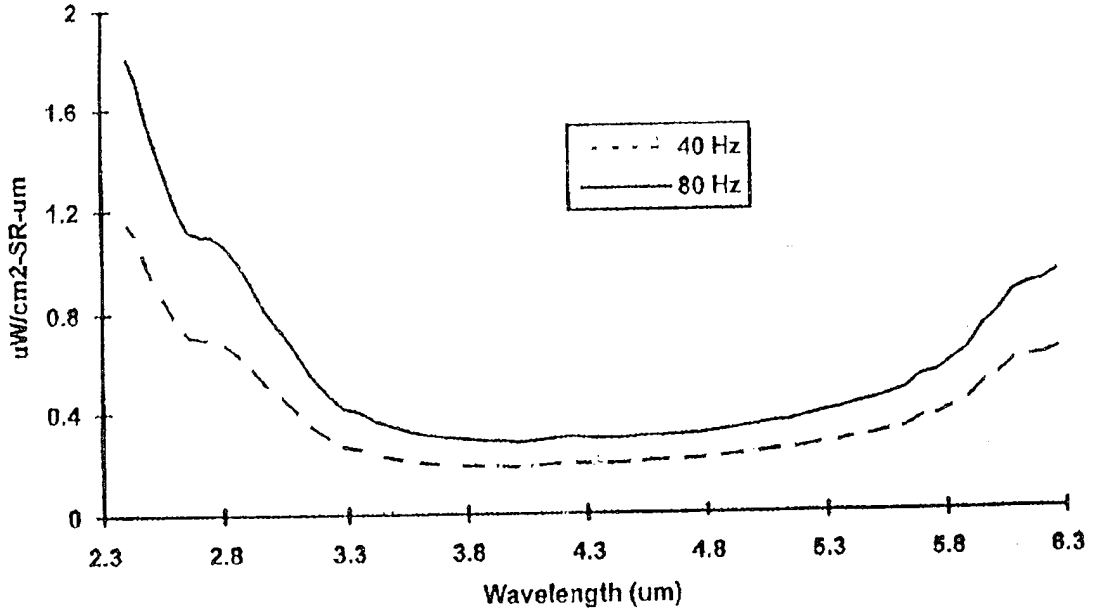
- Detector Characteristics
  - 45 x 90 Element 2-D Array
  - Si:In Photoconductive Detector Material
  - Hybrid w/ Si CCD Readout Structure
  - Spectral Range 2 - 7μm
  - Selectable 10 - 80Hz Integration Time
  - Vacuum/Cryo-Cooled to 24° K
  - 12-Bit A/D Conversion
  - Readout Noise: 1 Count out of 4096
  - 100μm Detector Pitch

- Dynamic Range
  - 12 Bit Digital (Selectable Dynamic Range Over 3 Orders of Magnitude Using IL Filter Wheel)

- Calibration Accuracy
  - <10% Absolute Traceable to NIST Standards
  - <2% Relative Spectrometric Accuracy Band-to-Band
  - <1% Relative Radiometric Accuracy w/in a Spectral Band

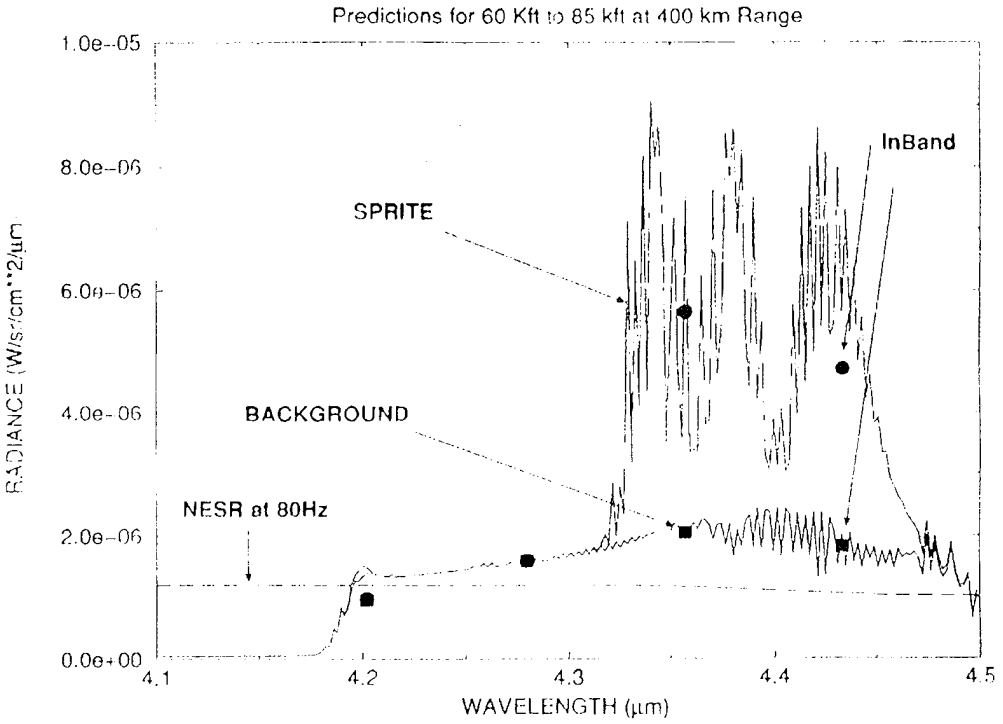
SENSOR BASIC CAPABILITIES
- Continued -

- Data handling
  - Recording: Digital
  - Reduction
  - Distribution/Archival: Archival Package @ LMSC
- Stereoscopic Imaging Capability
- Sensitivity



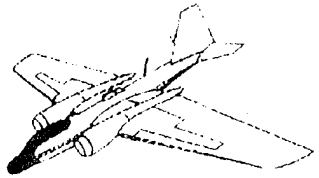
SENSITIVITY OF ARES SPECTROMETER SUFFICIENT FOR SPRITE MEASUREMENTS

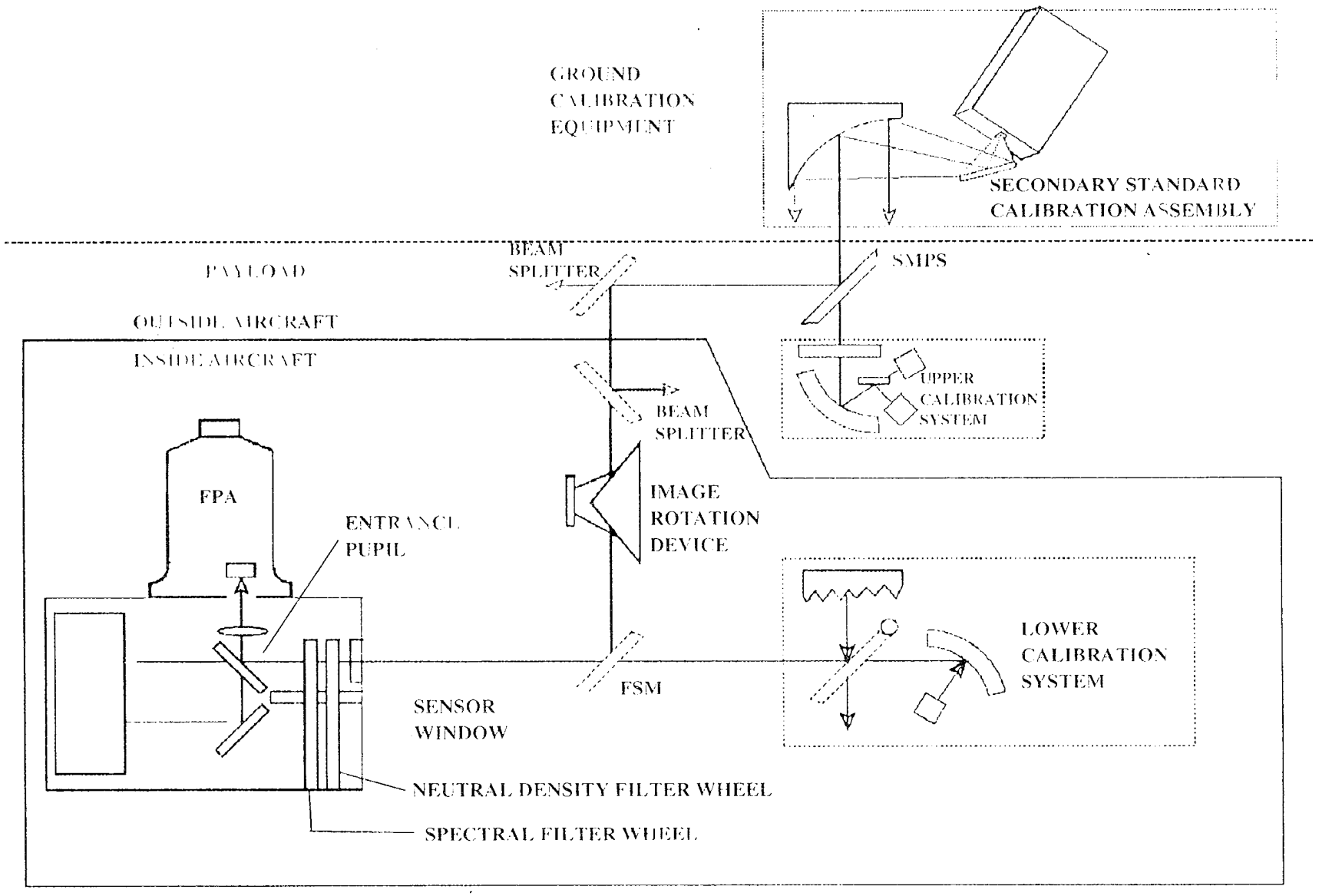
- PREDICTIONS PROVIDED BY L. JEONG, 10/13/95
- PREDICTIONS INTEGRATED INTO SAMPLE ARES SPECTRAL BANDS
- NESR FROM PREVIOUS OPERATION AND SHOULD IMPROVE
- SPECTROMETER OPERATION AT 40, 20, OR 10 Hz WILL IMPROVE NESR, DEPENDING ON SPRITE DURATION



101695 JJL

CALIBRATION SCHEMATIC



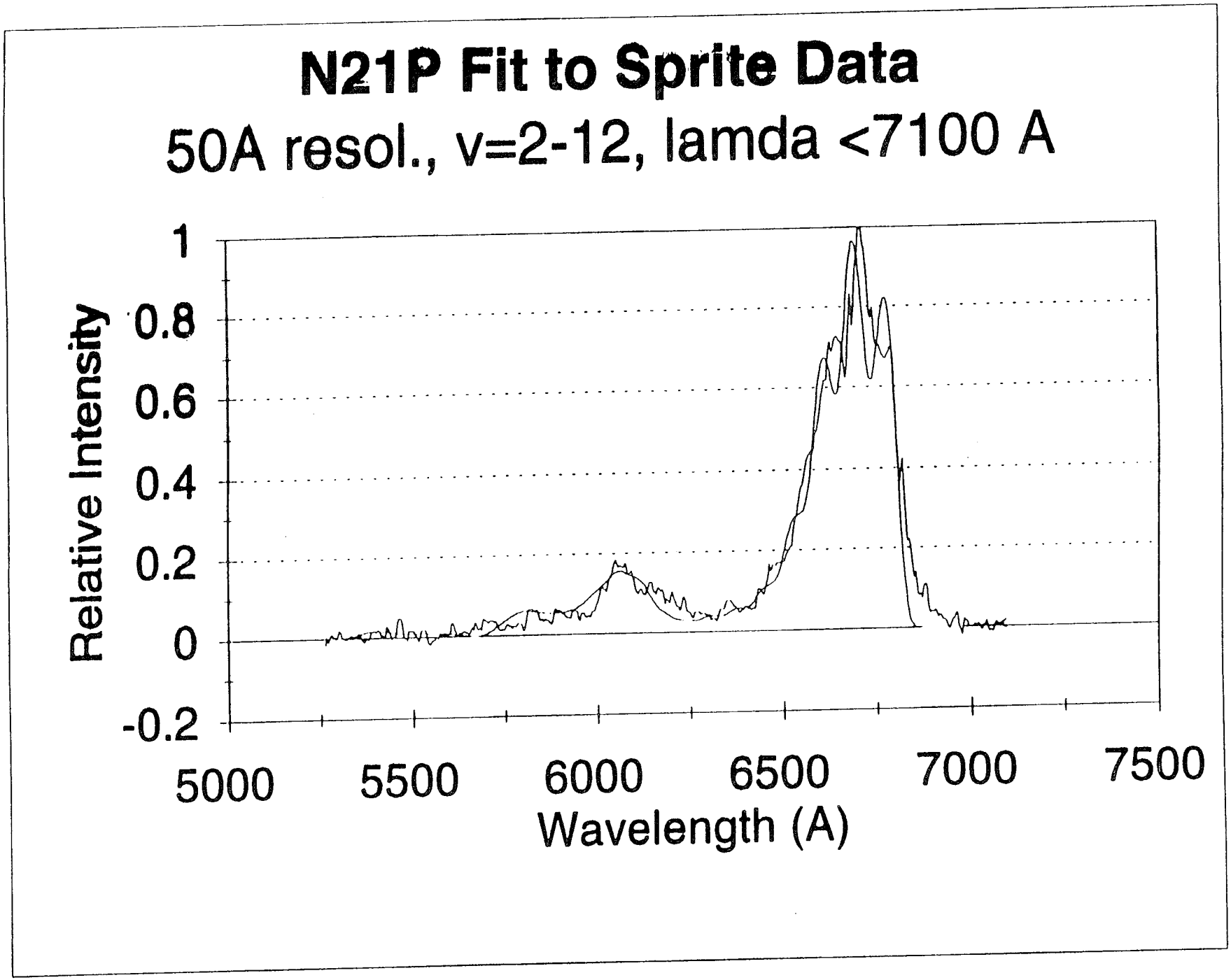


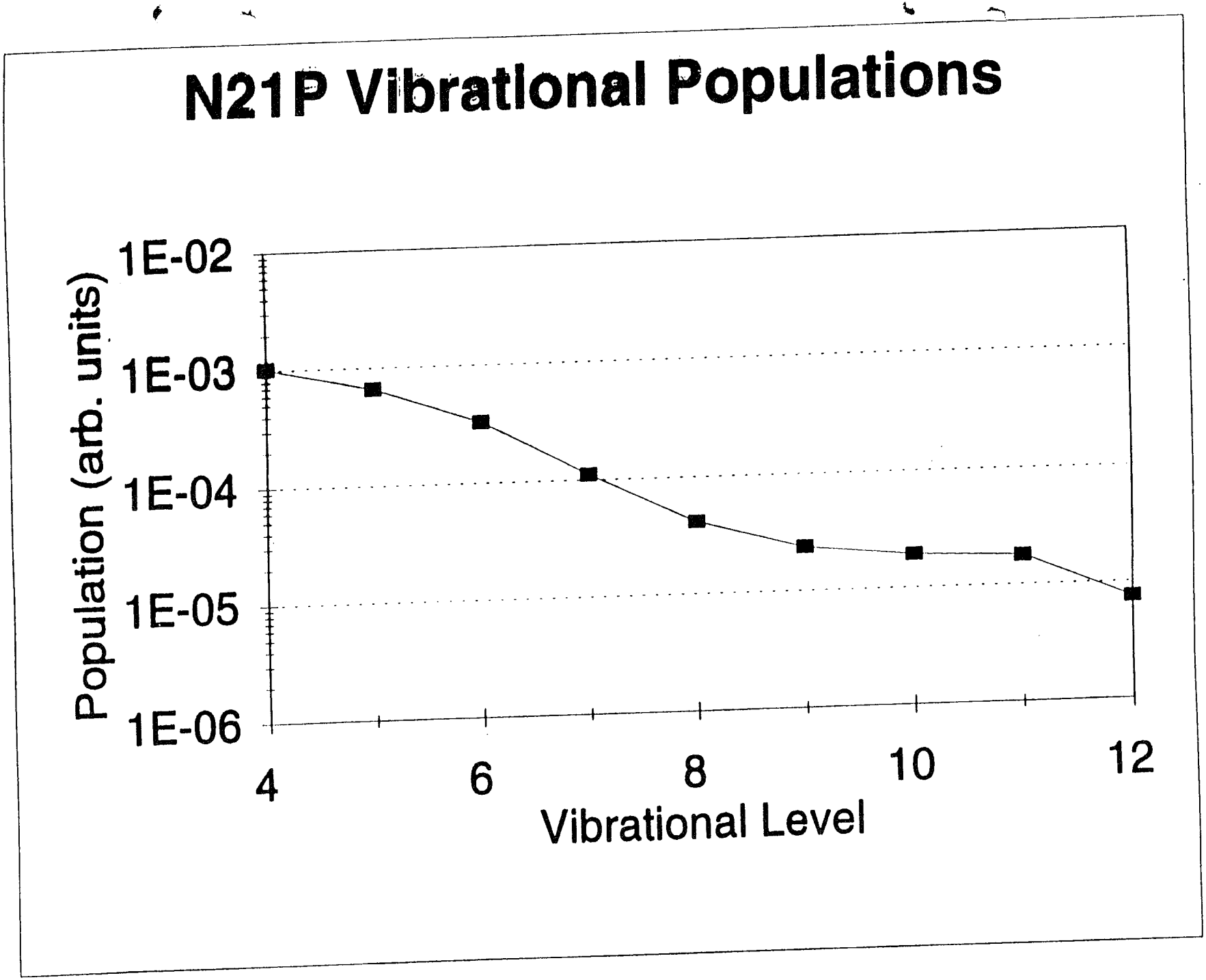
SPECTRAL FITTING OF MENDE's SPRITE SPECTRUM

MARK FRASER, DAVID GREEN AND TERRY RAWLINS
PHYSICAL SCIENCES INC.
ANDOVER MA 01810

PH: 508-689-0003 FAX; 508-689-3232 EMAIL: green@psicorp.com

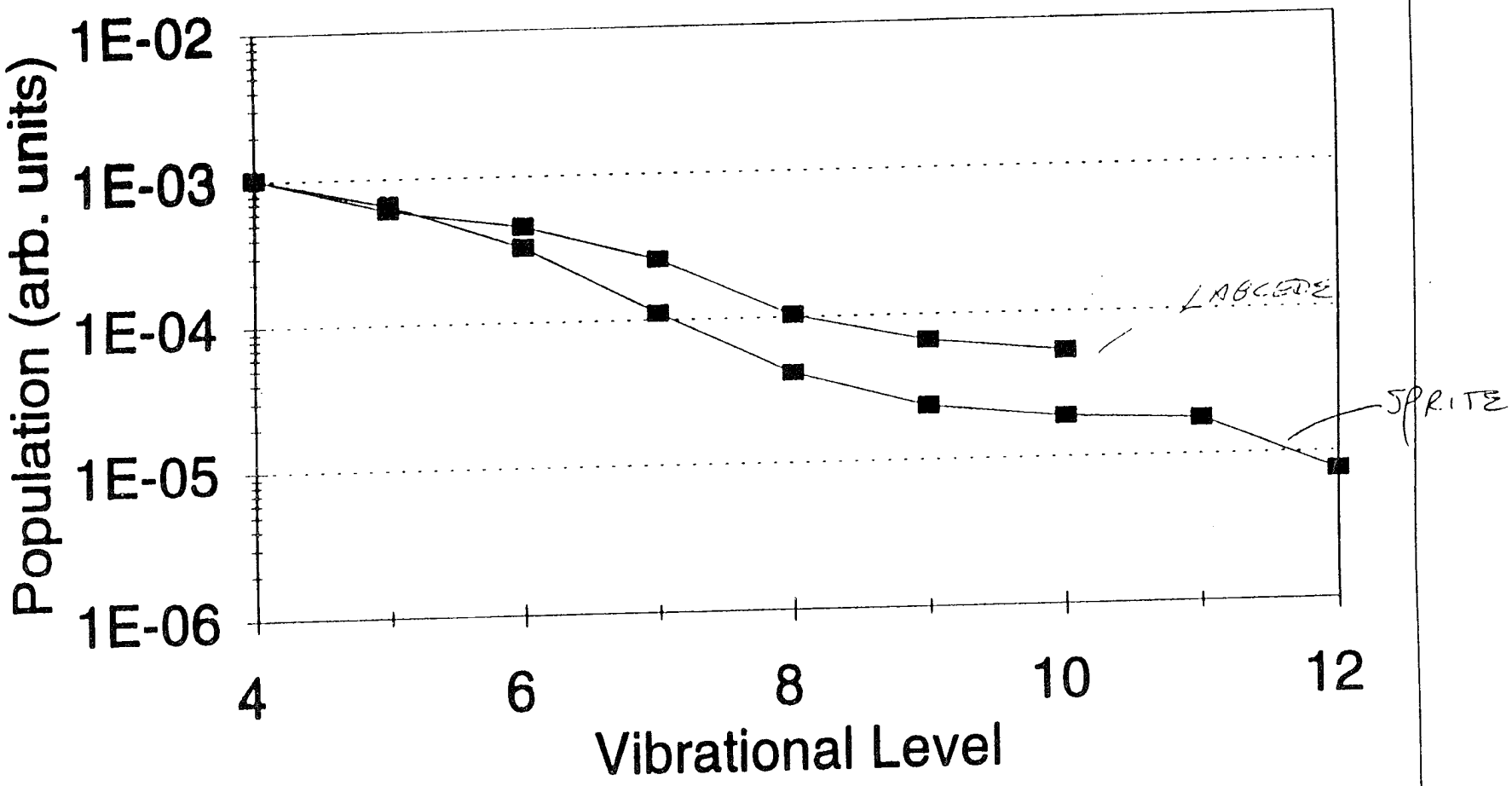
PRESENTED AT THE SPRITES WORKSHOP AT PL GEOPHYSICS
19 OCTOBER 1995


N21P Fit to Sprite Data
50A resol., v=2-12, lamda <7100 A
Relative Intensity
1
0.8
0.6
0.4
0.2
0
-0.2
5000
5500
6000
6500
7000
7500
Wavelength (A)


N21P Vibrational Populations
Population (arb. units)
1E-02
1E-03
1E-04
1E-05
1E-06
4
6
8
10
12
Vibrational Level

N21P Vibrational Populations

v=4-10 Labcede 68 km Data



STATED CONCLUSIONS

- DATA NOT RESPONSE CORRECTED SO CONCLUSIONS VERY PRELIMINARY

- OBSERVE N_2 B STATE LEVELS UP TO DISSOCIATION LIMIT
  - 15 eV ELECTRONS REQUIRED TO PRODUCE THESE STATES
  - ATOMS LIKELY FORMED
  - AT IONIZATION POTENTIAL, WITHIN FEW eV OF THRESHOLD
  - * ATOMS AND IONS TURN ON CHEMISTRY

- RELATIVE BRIGHTNESS OF N_2^+ 1st NEGATIVE TO N_2 1st POSITIVE PROVIDES INSIGHT INTO ELECTRON ENERGY DISTRIBUTION

- OBSERVED SPRITE DISTRIBUTION VIBRATIONALLY COLDER THAN THAT OBSERVED IN LAB keV ELECTRON IRRADIATED N_2 AT PRESSURES CORRESPONDING TO 68km

- IF THIS CONCLUSIONS HOLDS UP IN RESPONSE CORRECTED DATA, IMPLIES EXCITATION ELECTRONS LESS ENERGETIC THAN AURORAL, LESS THAN 100 eV

- OPTICAL EMISSIONS CAN PROVIDE INSIGHT INTO MECHANISMS AND THRESHOLDS VIA ELECTRON ENERGY SPECTRUM

Discussion of Major Research Issues and Experiments for Sprites '96 Campaign

- Altitude-dependent measurements of $N_2^+(1N)/N_2(1P)$ ratio
- Gamma rays (local)
  - High-altitude balloons
- Horizontal Luminosity
  - Temporal/spatial structure (neutral)
  - Gravity wave coupling
  - Elf-Gravity wave
  - Discharge dynamics
  - Coupling to neutrals
- Atmospheric monitoring of jets
  - Optical/IR spectra
- High frame rate optical measurements (2000 frames/second)
  - Add multi-spectral
- High-speed photometers (<0.5 ms)
  - NIR (atomic, ion lines)
- Co-aligned photometer/spectrometer
- Low-light cameras
  - Blue sensitive
- UHF/VHF
  - Compare with TIPPS
- Causative lightning
  - Optical
  - RF
  - new NLDN sensors (waveforms)
- Additional optical stations
  - Triangulation
- VLF/ELF signals
  - GPS clock
  - Sync with "anomalous events"
- 20 km balloons
  - Electric fields/charge distributions

- Cosmic rays
- CO_2/NO characterization
  - Ground-based
- VLF remote sensing
  - Ionization
- Mesoscale structure of lightning
- Radar
  - Temperature data
  - Scattering data
  - Other possible outputs
- IR signatures
  - ARES measurements
- Relativistic electrons
  - Important?
- Threshold
  - Why not more sprites?
- Relationship to +CG's
- Correlations with ELF
- Potential Locations/Dates
  - Last week June - Mid July
  - Midwest
  - Moon down (July 15 - new moon)
  - Local midnight
  - Coordinate with ARM, OK, and other sites
- Potential Aircraft/Balloon Platforms
  - FISTA
  - ARES (Petersen AFB, Tinker AFB)
  - NCAR (Jefferson County Airport)
  - NASA ER2
  - Balloons - LANL, OK
  - Sounding rockets
  - Drop sondes
- Potential Ground-Based Assets
  - NLDN
  - Chase vans
  - Electric field mills (MIT/LL)
  - Multiple sites ("long baseline") - NM, Univ. of Wyoming

Groups Interested in Sprites, Blue Jets, and Elves

Russ Armstrong
Mission Research Corporation
Atmospheric Sciences
One Tara Boulevard
Suite 302
Nashua, NH 03062-2801
Telephone: (603) 891-0070, Ext. 203
Fax: (603) 891-0088
Email: @lanl.gov:rarmstrong@mrcnh.com

Grant Aufderhaar
Aerospace
Telephone: (703) 318-5421.

Sunanda Basu
National Science Foundation
Division of Atmospheric Sciences
4201 Wilson Boulevard
Room 790
Arlington, VA 22230
Telephone: (703) 306-1529
Fax: (703) 306-0849
Email: sbasu@nsf.gov

William Beasley
University of Oklahoma
School of Meteorology
Norman, OK 73019-0470
Telephone: (405) 325-6561
Fax: (405) 325-7689
Email: wbeasley@uoknor.edu

Paul Bernhardt
Naval Research Laboratory
Beam Physics Branch
MC 4780 1PB
Washington, DC 20375-5320
Telephone: (202) 767-0196
Fax: (202) 767-0631
Email: bern@ppd.nrl.navy.mil

Dennis Boccippio
NASA Marshall Space Flight Center
ES44
Huntsville, AL 35812
Telephone: (205) 922-5909
Fax: (205) 922-5723
Email: djboccip@cirrus.mit.edu

William Boeck
Niagara University
Department of Physics
CIS
Niagara, NY 14109
Telephone: (716) 285-1212
Fax: (716) 286-8254
Email: boeck@niagara.edu

Bob Boldi
MIT/Lincoln Laboratory
Group 43
S1-613 (L Lab)
Lexington, MA 02173-9108
Telephone: (617) 981-2293
Email: bobb@ll.mit.edu

Eric Bucsela
Naval Research Laboratory
4555 Overlook SW
Washington, DC 20375
Telephone: (202) 767-6166
Email: bucsela@uap.nrl.navy.mil

Lin Callis
NASA Langley Research Center
Atmospheric Sciences Division
Hampton, VA 23681
Telephone: (804) 864-5843
Fax: (804) 864-6326
Email: lbc@jaguar.larc.nasa.gov

Hugh Christian
NASA Marshall Space Flight Center
Global Hydrology and Climate Center
977 Explorer Blvd.
ES 43, Room B210
Huntsville, AL 35806
Telephone: (205) 922-5828
Fax: (205) 922-5723
Email: hugh.christian@msfc.nasa.gov

Michael Desch
NASA Goddard Space Flight Center
LEP
Code 695
Greenbelt, MD 20771
Telephone: (301) 286-8222
Fax: (301) 286-1683
Email: ysmdd@lepmdd.gsfc.nasa.gov

Capt. David Desrocher
National Test Facility
730 Irwin Ave.
NTF/WE
Falcon AFB, CO 80912-7300
Telephone: (719) 567-9450
Fax: (719) 567-9464
Email: ddesroch@inet.ntf1.af.mil

Eric Dors
University of New Hampshire
Space Science Center - 254 Morse Hall
39 College Road
Durham, NH 03824
Telephone: (603) 862-3751
Email: eric.dors@unh.edu

Frank Djuth
GeoSpace Research Inc.
550 North Continental Blvd.
Suite 110
El Segundo, CA 90245
Telephone: (310) 322-1160
Fax: (310) 322-2596

Ken Eack
University of Oklahoma
Department of Physics and Astronomy
Norman, OK 73019
Email: keack@uoknor.edu

Philip Erickson
MIT Haystack Observatory
Atmospheric Science Group
Westford, MA 01886
Telephone: (617) 981-5769
Email: pje@hyperion.haystack.edu

Jim Ernstmeyer
Massachusetts Institute of Technology & RL
Department of Electrical Engineering
Telephone: (617) 377-8977
Email: imjay@mit.edu

Gerald Fishman
NASA Marshall Space Flight Center
Space Science Laboratory
Code ES81
Huntsville, AL 35812
Telephone: (205) 544-7691
Fax: (205) 544-5800
Email: fishman@ssl.msfc.nasa.gov

John Foster
MIT Haystack Observatory
Atmospheric Sciences
Route 40
Westford, MA 01886
Telephone: (617) 981-5621
Email: jef@hyperion.haystack.edu

Marv Frandsen
HQ AFTAC/TXC
Advanced Systems Directorate
1030 South Highway A1A
Patrick AFB, FL 32925-3002
Telephone: (407) 494-4178
Fax: (407) 494-5501
Email: frandsen@crusher.aftac.gov

Richard Goldberg
NASA Goddard Space Flight Center
Laboratory for Extraterrestrial Physics
Code 690
Greenbelt, MD 20771
Telephone: (301) 286-8603
Fax: (301) 286-1648
Email: goldberg@nssdca.gsfc.nasa.gov

Steve Goodman
NASA Marshall Space Flight Center
Global Hydrology and Climate Center
977 Explorer Blvd.
ES-43, Room C11
Huntsville, AL 35806
Telephone: (205) 922-5891
Fax: (205) 922-5723
Email: steven.goodman@msfc.nasa.gov

Dave Green
Physical Sciences Inc.
20 New England Business Center
Andover, MA 01810
Telephone: (508) 689-0003
Fax: (508) 689-3232
Email: green@psicorp.com

John Ground
Phillips Laboratory
PL/SX
3550 Aberdeen Ave. SE
Kirtland AFB, NM 87117-5776
Email: groundj@plk.af.mil

Leslie Hale
Pennsylvania State University
Communications and Space Sciences
Laboratory
316 Electrical Engineering East
University Park, PA 16802-2707
Telephone: (814) 865-2361
Fax: (814) 863-8457
Email: leshale@psu.edu

Bob Harris
NASA Headquarters
Code YS
300 E Street S.W.
Washington, DC 20546-0001

Al Hurd
Visidyne Inc.
10 Corporate Place
South Bedford St.
Burlington, MA 01803
Telephone: (617) 273-2820

Dan Holden
Los Alamos National Laboratory
Mail Stop D466
Los Alamos, NM 87545
Telephone: (505) 667-3406
Fax: (505) 665-7395
Email: dh@transio.lanl.gov

Rick Howard
NASA Headquarters
Space Physics
300 E Street S.W.
Code SS
Washington, DC 20546-0001
Telephone: (202) 358-0898
Fax: (202) 358-3987
Email: rhoward@hq.nasa.gov

Robert Huffman
Phillips Laboratory
GP Representative at PL/KAFB
29 Randolph Road
PL/GPI
Hanscom AFB, MA 01731-3010
Telephone: (505) 846-0298
Fax: (505) 846-2282
Email: huffman@plk.af.mil

Umran Inan
Stanford University
Department of Electrical Engineering
STAR Laboratory
Durand 321, MC-4055
Stanford, CA 94305
Telephone: (415) 723-4994
Fax: (415) 723-9251
Email: inan@nova.stanford.edu

Laila Jeong
Phillips Laboratory
Optical Environment Division
29 Randolph Road
PL/GPOS
Hanscom AFB, MA 01731-3010
Telephone: (617) 377-3671
Fax: (617) 377-8900
Email: jeong@plh.af.mil

Dikshitulu Kalluri
Univ. of MA at Lowell
Electrical Engineering Department
1 University Avenue
Lowell, MA 01856
Telephone: (508) 934-3318
Fax: (508) 934-3027
Email: kallurid@woods.uml.edu

Craig Kletzing
University of New Hampshire
Space Science Center - Morse Hall
39 College Road
Durham, NH 03824
Telephone: (603) 862-3187
Fax: (603) 862-1915
Email: kletzing@unhedi2.unh.edu

Maj James Kroll
Air Force Office of Scientific Research
110 Duncan Avenue
Bolling AFB, DC 20332-0001
Telephone: (202) 767-7900
Fax: (202) 404-7496
Email: kroll@afosr.af.mil

Peter Kupferman
Aerospace Corp.
Hallmark Bldg.
13873 Park Ct Rd.
Herndon, VA 22071
Telephone: (703) 318-1659
Fax: (703) 318-5409
Email: peter.n.kupferman@aero.org

Min-Chang Lee
Massachusetts Institute of Technology
Plasma Fusion Center (NW 16-240)
167 Albany Street
Cambridge, MA 02139
Telephone: (617) 253-5956
Fax: (617) 253-0448
Email: mclee@pfc.mit.edu

Carl Lennon
NASA JFK Space Center
TE-CID-3
Kennedy Space Center, FL 32899
Telephone: (407) 867-4042
Fax: (407) 867-2848

Walter Lyons
ASTER Division/Mission Research Corporation
Yucca Ridge Field Station
46050 Weld County Road 13
Ft Collins, CO 80524
Telephone: (970) 568-7664
Fax: (303) 482-8627
Email: lyonsccm@csn.org

Sam Makhlouf
Utah State University
Stewart Radiance Laboratory
139 Great Road
Bedford, MA 01730
Telephone: (617) 377-4903
Email: makhlouf@pldac.plh.af.mil

Lee Marshall
Penn State
Electrical Engineering
332 EE East
State College, PA 16802
Telephone: (814) 865-2361
Email: lhm100@psu.edu

Stephen Mende
Lockheed Martin Palo Alto Research Laboratory
Dept. 91 20 Bldg. 255
3251 Hanover St.
Palo Alto, CA 94304
Telephone: (415) 424-3282
Fax: (415) 424-3333
Email: mende@sag.space.lockheed.com

Gennady Milikh
University of Maryland
Department of Physics and Astronomy
College Park, MD 20850
Telephone: (301) 405-1558
Fax: (301) 405-9966
Email: milikh@avl.umd.edu

John Molitoris
Lawrence Livermore National Laboratory
Regional Atmospheric Sciences Division
700 East Ave.
P.O. Box 808, L-262
Livermore, CA 94551-9900
Telephone: (510) 423-3496
Fax: (510) 422-5844
Email: molitoris1@llnl.gov

Jeff Morrill
Naval Research Laboratory
4555 Overlook SW
Code 760
Washington, DC 20375-5352
Telephone: (202) 404-7826
Fax: (202) 767-5636

Dean Morss
Creighton University
Department of Atmospheric Sciences
Omaha, NE 68178-0114
Telephone: (402) 280-5759
Fax: (402) 280-1731
Email: damorss@creighton,edu

K. Papadopoulos
University of Maryland
Department of Physics and Astronomy
College Park, MD 20742
Telephone: (301) 454-6810
Fax: (301) 314-9067
Email: kp@astro.umd.edu

Larry Radke
NCAR
P.O. Box 3000
Boulder, CO 80397-3000
Telephone: (303) 497-1032
Fax: (303) 497-1092
Email: radke@atd.ucar.edu

Terry Rawlins
Physical Sciences Inc.
20 New England Business Center
Andover, MA 01810
Telephone: (508) 689-0003
Fax: (508) 689-3232
Email: rawlins@psicorp.com

Jean Reazer
NAIC/DXDR
4115 Hebble Creek Rd.
Suite 6
Wright Patterson ARB, OH 45433-5610
Telephone: (513) 257-0992
Fax: (513) 257-9888

Bill Roder
45th Weather Sq
1201 Minuteman St.
Patrick AFB, FL 32925-3238

Robert Roussel-Dupre
Los Alamos National Laboratory
Space and Atmospheric Sciences Group
NIS-1, Mail Stop D466
Los Alamos, NM 87545
Telephone: (505) 667-9228
Email: rroussel-dupre@lanl.gov

Harvey Rowland
Naval Research Laboratory
Plasma Physics
4555 Overlook SW
Washington, DC 20375
Telephone: (202) 767-6644
Email: rowland@ppd.nrl.navy.mil

David Rust
National Severe Storms Lab
1313 Halley Circle
Norman, OK 73069
Telephone: (405) 366-0404
Fax: (405) 366-0472
Email: rust@nssl.uoknor.edu

Phil Schwartz
Naval Research Laboratory
4555 Overlook SW
Washington, DC 20375

Davis Sentman
University of Alaska
Geophysical Institute
903 Koyukuk Drive
P.O. Box 757320
Fairbanks, AK 99775-7320
Telephone: (907) 474-6442
Fax: (907) 474-7290
Email: rocket@geewiz.gi.alaska.edu

Orr Sheperd
Visidyne Inc.
10 Corporate Place
South Bedford St.
Burlington, MA 01803
Telephone: (617) 273-2820
Fax: (617) 272-1068
Email: sheperd@bur.visidyne.com

Jeff Shorter
Mission Research Corporation
One Tara Boulevard
Nashua, NH 03062
Telephone: (603) 891-0070
Fax: (603) 891-0088

Carl Siefring
Naval Research Laboratory
Plasma Physics Division
4555 Overlook SW
Space Experiments Section/Code 6755
Washington, DC 20375
Telephone: (202) 767-2467
Fax: (202) 404-7082
Email: siefring@nrlfs1.nrl.navy.mil

Tom Slanger
SRI International
333 Ravenswood Avenue
Menlo Park, CA 94025-3493
Telephone: (415) 859-2764
Fax: (415) 859-6196
Email: slanger@mplvax.com

Cdr Steve Smolinski
Naval Research Laboratory
4555 Overlook SW
Washington, DC 20375
Email: smolinsk@sgate.com

Dick Spalding
Sandia Laboratory
ORG 5909
MS 0978
Albuquerque, NM 87185
Telephone: (505) 844-5934
Fax: (505) 844-2057
Email: respald@sandia.gov

Eugene Symbalisty
Los Alamos National Laboratory
NIS-1
Los Alamos, NM 87545
Telephone: (505) 667-9670
Fax: (505) 665-7398
Email: esymlalisty@lanl.gov

Yuri Taranenko
Los Alamos National Laboratory
Space and Atmospheric Sciences Group
MS D466
Los Alamos, NM 87545
Fax: (505) 665-3332
Email: ytaranenko@lanl.gov

Micheal Taylor
Utah State University
Science Division
Space Dynamics Laboratory
Engineering Building, Room 241
Logan, UT 84322-4145
Telephone: (801) 797-3919
Fax: (801) 797-4044
Email: taylor@psi.sci.sdl.usu.edu

Barry Tilton
SAFSP/RESPO
11782 Lee-Jackson Hwy
Oakwood Center, Suite 500
Fairfax, VA 22033
Telephone: Pager: (800) 759-8255 (PIN: 2832955)

Roland Tsunoda
SRI International
Geoscience and Engineering Center
333 Ravenswood Avenue
Menlo Park, CA 94025-3493
Telephone: (415) 859-3124
Fax: (415) 322-2318
Email: tsunoda@unix.sri.com

James Ulwick
Stewart Radiance Laboratory
Utah State University
139 Great Road
Bedford, MA 01730
Telephone: (617) 275-8273
Fax: (617) 271-0535
Email: ulwick@plh.af.mil

Otha Vaughan, Jr.
NASA Marshall Space Flight Center
Global Hydology & Climate Center
977 Explorer Blvd.
ES-44
Huntsville, AL 35812
Telephone: (205) 922-5893
Fax: (205)922-5723
Email: skeet@sferic.msfc.nasa.gov

Susan Voss
Los Alamos National Laboratory
NIS-1 Space and Atmospheric Science
MS D466
Los Alamos, NM 87545
Telephone: (505) 665-5520
Fax: (505) 665-7395
Email: svoss@lanl.gov

Mark Weber
MIT/Lincoln Laboratory
244 Wood Street
Lexington, MA 02173-9108
Telephone: (617) 981-7434
Fax: (617) 981-0632

Jeff West
Phillips Laboratory
PL/SX
3550 Aberdeen Ave. SE
Kirtland AFB, NM 87117-5776
Telephone: (505) 846-1411
Fax: (505) 846-4143

Gene Wescott
University of Alaska
Geophysical Institute
903 Koyukuk Drive
P.O. Box 757320
Fairbanks, AK 99709
Telephone: (907) 474-7576
Fax: (907) 474-7290
Email: rocket@giuaf.gi.alaska.edu

Earl Williams
Massachusetts Institute of Technology
Parsons Lab
77 Massachusetts Ave.
MIT 48-211
Cambridge, MA 02139-4307
Telephone: (617) 253-2459
Fax: (617) 253-6208
Email: earlew@ll.mit.edu

Jack Winckler
University of Minnesota
School of Physics and Astronomy
Minneapolis, MN
Telephone: (612) 624-5086
Fax: (612) 624-4578

Peter Wintersteiner
ARCON Corp.
260 Bear Hill Rd.
Waltham, MA 02154
Fax: (617) 890-5189
Email: winters@arcon.com

Charles Wong
Massachusetts Institute of Technology
77 Massachusetts Ave.
Cambridge, MA 02139-4307